

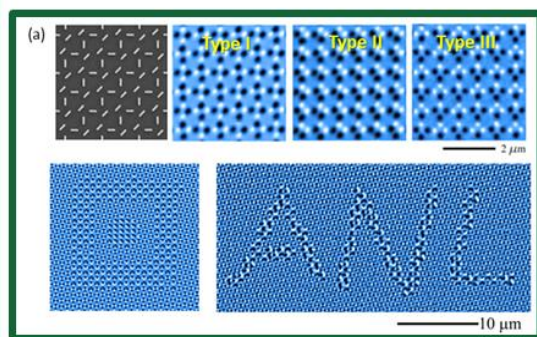
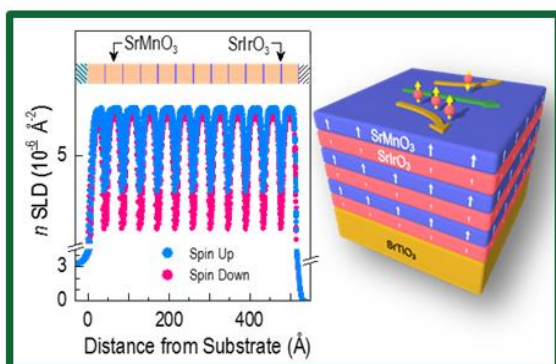
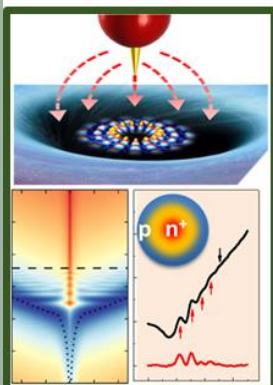
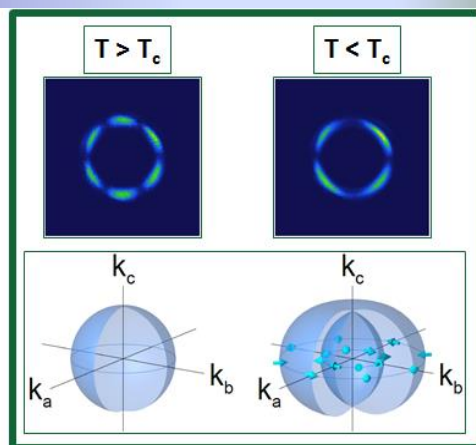
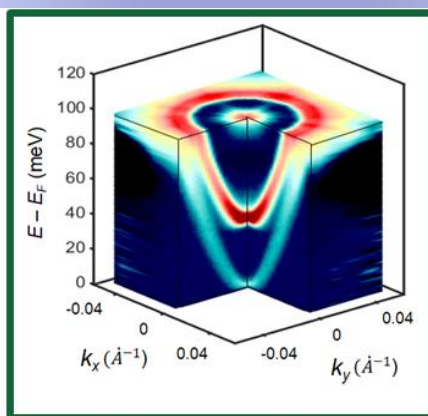
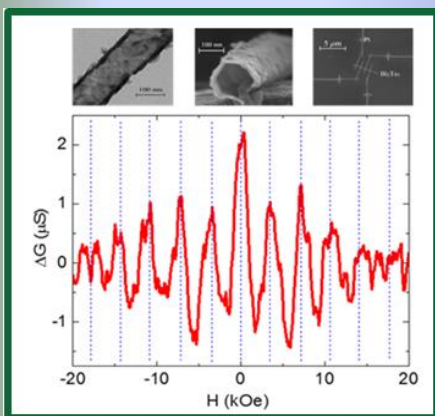
Experimental Condensed Matter Physics

Principal Investigators' Meeting–2017

September 11–13, 2017

Marriott Washingtonian, Gaithersburg, MD

Co-Chairs: Judy Cha (Yale), John Mitchell (ANL)



On the Cover

1	2	3
4	5	6

Figures are from selected highlight slides submitted to the ECMP PI Meeting.

1. Topological Insulator and Induced Topological Superconductivity in Bi₂Te₃ Nanotubes. Qi Li, PI. Penn State University.
2. Momentum and Energy Resolved Tunneling Spectroscopy. Ray Ashoori, PI. Massachusetts Institute of Technology.
3. New Class of 3D “Quantum Liquid Crystals” Discovered. David Hsieh, PI. California Institute of Technology.
4. Tuning a Circular p-n Junction From Quantum Confinement to Optical Guiding. Eva Andrei, PI. Rutgers University.
5. Anomalous Hall Effect Discovered in a Quantum Oxide Heterostructure. Ho Nyung Lee, lead PI. Oak Ridge National Laboratory.
6. Controlling Vortex Matter with Artificial Charge Ice. Wei Kwok, lead PI. Argonne National Laboratory.

This document was produced under contract number DE-SC0014664 between the U.S. Department of Energy and Oak Ridge Associated Universities.

The research grants and contracts described in this document are supported by the U.S. DOE Office of Science, Office of Basic Energy Sciences, Materials Sciences and Engineering Division.

Foreword

This book contains abstracts for presentations made at the 2017 Experimental Condensed Matter Physics (ECMP) Principal Investigators' Meeting sponsored by the Materials Sciences and Engineering Division of the US Department of Energy, Office of Basic Energy Sciences (DOE-BES). The meeting convenes scientists supported within ECMP by the DOE-BES to present the most exciting, new research accomplishments and proposed future research directions in their BES supported projects. The meeting also affords PIs in the program an opportunity to see the full range of research currently being supported. We hope the meeting fostered a collegial environment to 1) stimulate the discussion of new ideas and 2) provide unique opportunities to develop or strengthen collaborations among PIs. In addition, the meeting provides valuable feedback to DOE-BES in its assessment of the state of the program and in identifying future programmatic directions. The meeting was attended by approximately 100 ECMP supported scientists.

The Experimental Condensed Matter Physics Program covers a broad range of research activities supporting experimental research with the goal to fundamentally understand of the relationships between intrinsic electronic structure and the properties of complex materials. The program focus is largely on systems whose static and dynamic behavior derives from strong electron correlation effects, competing or coherent quantum interactions, effects of interfaces, defects, anisotropy and reduced dimensionality. Scientific themes include superconductivity, magnetism, low dimensional electron systems, and nanoscale systems. The program also supports studies of materials under extreme conditions such as ultra-low temperatures and ultra-high magnetic fields. In the last few years the program has increased support for research in the areas of quantum materials, spin physics, topological materials, materials far from equilibrium and highly anisotropic materials to provide new insights into the evolution of correlated electron behavior in condensed matter systems. Improving understanding of the electronic behavior of complex materials on the atomic, nano and mesoscopic scales is relevant to the DOE mission, as these materials offer enhanced properties potentially leading to dramatic improvements in wide-ranging technologies needed for efficient energy generation, conversion, storage, delivery, and use.

The meeting was organized into nine oral and two poster sessions covering the range of activities supported by the program. Co-chairs were introduced for the first time in the meeting and I express my appreciation to John Mitchell and Judy Cha for their invaluable help in organizing the meeting. One session featuring a panel discussion was also introduced, with this year's topic entitled, "*Opportunities in ECMP Basic Research for Next Generation Quantum Systems and Devices*". We thank all the participants for their investment of time and for their willingness to share their ideas with each other and with BES. We also want to gratefully acknowledge the excellent support provided by Ms. Linda Severs of the Oak Ridge Institute for Science and Education and by Ms. Teresa Crockett of BES, for their efforts in organizing the meeting.

Dr. Michael (Mick) Pechan
Program Manager, Condensed Matter and Materials Physics
Division of Materials Sciences and Engineering
Basic Energy Sciences

Table of Contents

Foreword	i
Agenda	xi
Session 1	
Spontaneous and Field-Induced Symmetry Breaking in Low Dimensional Nanostructures <i>Chun Ning (Jeanie) Lau and Marc Bockrath</i>	3
Correlated Quasiparticles in Graphene <i>Philip Kim</i>	7
Polaritons in van der Waals Materials <i>Dimitri N. Basov</i>	11
Quantum Electronic Phenomena and Structures <i>Wei Pan</i>	14
Transient Studies of Nonequilibrium Transport in Two-Dimensional Semiconductors <i>Jonathan Bird</i>	18
Session 2	
Novel Temperature Limited Tunneling Spectroscopy of Quantum Hall Systems <i>Raymond Ashoori</i>	25
Magneto-transport in GaAs Two-Dimensional Hole Systems <i>Monsour Shayegan</i>	29
Understanding and Controlling Phases with Topological and Charge Order in the Two-Dimensional Electron Gas <i>Gabor Csathy and Michael Manfra</i>	33
Engineering Topological Superconductivity towards Braiding Majorana Excitations <i>Leonid P. Rokhinson</i>	37
NV-Centers in Diamond for Non-invasive Optical Sensing and Quantum Spin Studies <i>R. Prozorov, N. M. Nusran, V. Mkhitarian, Kyuil Cho, M. A. Tanatar, M. Tringides, M. Hupalo, J. Wang, Y. Lee, Liqin Ke, and D. Vaknin</i>	41

Session 3

Panel Discussions and Report on Quantum Materials BRN Workshop (Collin Broholm)	47
--	----

Session 4

Correlated Materials – Synthesis and Physical Properties <i>Ian R. Fisher, Theodore H. Geballe, Aharon Kapitulnik, Steven A. Kivelson, and Kathryn A. Mo</i>	51
Novel and Unconventional Superconductors: Quantum Criticality and Possible Field-Induced Superconducting States <i>Luis Balicas</i>	55
Emerging Materials <i>John F. Mitchell, D. Phelan, and H. Zheng</i>	59
Dynamics of Electronic Interactions in Superconductors and Related Materials <i>Dan Dessau</i>	63
Electron Spectroscopy <i>Peter D. Johnson, Chris Homes, and Tonica Valla</i>	67

Session 5

Interface-Driven Chiral Magnetism in Ultrathin Metallic Ferromagnets: Towards Skyrmion Spintronics <i>Geoffrey Beach</i>	73
Magnetic Thin Films <i>Axel Hoffmann, J. S. Jiang, V. Novosad, and J. E. Pearson</i>	74
Quantum Order and Disorder in Magnetic Materials <i>Thomas F. Rosenbaum</i>	78
Topological Materials with Complex Long-Range Order <i>James Analytis</i>	82
Emergent Collective Phenomena in Artificial Spin Ice <i>Peter Schiffer and Nitin Samarth</i>	87
Spintronics Based on Topological Insulators <i>John Xiao, Branislav Nikolic, Matt Doty, and Stephanie Law</i>	91

Session 6

Search for 3D Topological Superconductors using Laser-Based Spectroscopy <i>David Hsieh</i>	99
Study of Topological Superconductivity in Nanoscale Structures <i>Qi Li</i>	103
Superconducting In-doped SnTe Topological Crystalline Insulator Nanowires <i>Judy J. Cha</i>	107
Non-Centrosymmetric Topological Superconductivity <i>Johnpierre Paglione</i>	111
Nanostructure Studies of Strongly Correlated Materials <i>Douglas Natelson</i>	115

Session 7

Epitaxial Complex Oxides <i>Ho Nyung Lee, G. Eres, T. Z. Ward, C. M. Rouleau, and H. M. Christen</i>	121
Atomic Engineering Oxide Heterostructures: Materials by Design <i>Harold Y. Hwang, Y. Hikita, J.-S. Lee, and S. Raghu</i>	125
Novel Synthesis of Quantum Epitaxial Heterostructures by Design <i>Chang-Beom Eom</i>	129
The Investigation of Oxygen Vacancies in Magnetic-Ferroelectric Heterostructures <i>Mikel Holcomb and Aldo Romero</i>	133
Novel Regimes of Spin Transport: Pure Spin Currents in Antiferromagnets and Time-Resolved Studies of Spin Dynamics <i>Fengyuan Yang and Ezekiel Johnston-Halperin</i>	137

Session 8

Electrical Generation of Valley Magnetization in 2D Transition Metal Dichalcogenides <i>Kin Fai Mak</i>	145
Quantum Transport in 2D Semiconductors <i>James Hone and Cory Dean</i>	146

Van der Waals Heterostructures: Novel Materials and Emerging Phenomena <i>Feng Wang</i>	150
Spectroscopic Investigations of Novel Electronic and Magnetic Materials <i>Janice L. Musfeldt</i>	154
Probing Linewidths and Biexciton Quantum Yields of Single Cesium Lead Halide Nanocrystals in Solution <i>Moungi G. Bawendi</i>	158

Session 9

Experimental Studies of Magnetism, Correlations, and Quantum Criticality in a 2D Electron System with Point Defects <i>Eva Y. Andrei</i>	165
Symmetries, Interactions and Correlation Effects in Carbon Nanotubes <i>Gleb Finkelstein</i>	169
Novel sp^2-Bonded Materials and Related Nanostructures <i>Alex Zettl, Marvin Cohen, Michael Crommie, Alessandra Lanzara, and Steven Louie</i>	173
Charge and Energy Transfer in Molecular Superconductors and Molecular Machines <i>Saw Wai Hla</i>	177

Session 10

Quantum Materials <i>Joseph Orenstein, R. J. Birgeneau, E. Bourret, A. Lanzara, D. H. Lee, J. E. Moore, and R. Ramesh</i>	183
Science of 100 Tesla <i>Neil Harrison</i>	187
Probing Competing Chemical, Electronic, and Spin Correlations for Materials Functionality <i>Athena S. Sefat, David Parker, and Zheng Gai</i>	191
Magneto-optical Study of Correlated Electron Materials in High Magnetic Fields <i>Dmitry Smirnov and Zhigang Jiang</i>	195
Vortex Lattice and Vortex Core Structure in $HgBa_2CuO_{4+\delta}$ Single Crystals <i>W. P. Halperin</i>	199

Poster Sessions

Poster Session I205

Poster Session II.....207

Poster Abstracts

Spin Effects in Low Dimensional Correlated Systems
Philip W. Adams211

Digital Synthesis: A Pathway to New Materials at Interfaces of Complex Oxides
Anand Bhattacharya215

Raman Spectroscopy of Pnictide and Other Unconventional Superconductors
Girsh Blumberg219

Complex States, Emergent Phenomena, and Superconductivity in Intermetallic and Metal-Like Compounds
Paul Canfield, Sergey Bud'ko, Yuji Furukawa, David Johnston, Adam Kaminski, Vladimir Kogan, Makariy Tanatar, and Ruslan Prozorov.....223

Cold Exciton Gases in Semiconductor Heterostructures
Leonid Butov.....227

Towards a Universal Description of Vortex Matter in Superconductors
Leonardo Civale and Boris Maierov.....230

Spin Polarized Tunneling in Aluminum Nanoparticles
Dragomir Davidovic.....235

LaCNS: Building Neutron Scattering Infrastructure in Louisiana for Advanced Materials
J. F. DiTusa, D. Zhang, J. Zhang, W. A. Shelton, R. Jin, V. T. John, R. Kumar, Z. Mao, E. Nesterov, E. W. Plummer, S. W. Rick, G. J. Schneider, D. P. Young, P. T. Sprunger, and M. Khonsari.....239

THz Plasmonics and Topological Optics of Weyl Semimetals
H. Dennis Drew and Andrei Sushkov248

High Magnetic Field Microwave Spectroscopy of Two-Dimensional Electron Systems in GaAs and Graphene
Lloyd W. Engel.....252

Electronic Structure and Spin Correlations in Novel Magnetic Structures <i>George G. Hadjipanayis, David J. Sellmyer; and Ralph Skomski</i>	256
Non-equilibrium Magnetism: Materials and Phenomena <i>Frances Hellman, Jeff Bokor, Peter Fischer, Steve Kevan, Sayeef Salahuddin, Lin-Wang Wang</i>	260
Spin-Coherent Transport under Strong Spin-Orbit Interaction <i>Jean J. Heremans</i>	264
APS Conferences for Undergraduate Women in Physics <i>Theodore Hodapp</i>	268
Proximity Effects and Topological Spin Currents in van der Waals Heterostructures <i>Ben Hunt</i>	271
Bose-Einstein Condensation of Magnons <i>J. B. Ketterson</i>	272
Spectroscopy of Degenerate One-Dimensional Electrons in Carbon Nanotubes <i>Junichiro Kono</i>	273
Nanoscale Magnetic Josephson Junctions and Superconductor/Ferromagnet Proximity Effects for Low-Power Spintronics <i>Ilya Krivorotov and Oriol T. Valls</i>	277
Superconductivity and Magnetism <i>W.-K. Kwok, U. Welp, A. E. Koshelev, V. Vlasko-Vlasov, Z. L. Xiao, and Y. L. Wang</i>	281
Non-Coulombic Frictional Drag Currents in Coupled LaAlO₃/SrTiO₃ Nanowires <i>Jeremy Levy and Patrick Irvin</i>	285
Spin-Polarized Current Injection Induced Magnetic Reconstruction at Oxide Interface <i>F. Fang, Y. W. Yin, Qi Li, and G. Lüpke</i>	289
Observation of spin and charge stripes in La_{2-x-y}Eu_ySr_xCuO₄ <i>Gregory MacDougall, Peter Abbamonte, Lance Cooper, Eduardo Fradkin, and Dale Van Harlingen</i>	293
Superconductivity and Magnetism in <i>d</i>- and <i>f</i>-Electron Materials <i>M. Brian Maple</i>	297

Controlling Superconductivity via Tunable Nanostructure Arrays <i>Nadya Mason, Raffi Budakian, and Taylor Hughes</i>	301
Exploring Superconductivity at the Edge of Magnetic or Structural Instabilities <i>Ni Ni</i>	305
Experimental Study of Novel Relativistic Mott Insulators in the 2-Dimensional Limit <i>Claudia Ojeda-Aristizabal</i>	309
A Gap-Protected Zero-Hall Effect State in the Quantum Limit of the Nonsymmorphic Metal KHgSb <i>N. Phuan Ong</i>	313
Understanding and Manipulating Quantum Spin Exchange Interactions in Colloidal Magnet Based Nanostructures by Ultrafast Light <i>Min Ouyang</i>	315
Investigation of Structural and Electronic Properties of Topological Heusler Thin Films <i>C. J. Palmstrøm and A. Janotti</i>	317
Effects of Lateral Broken Crystal Symmetries on Spin-Orbit Torques and Magnetic Anisotropy <i>Daniel Ralph</i>	321
Tuning Quantum Fluctuations in Low-Dimensional and Geometrically Frustrated Magnets <i>Arthur P. Ramirez</i>	325
Correlated and Complex Materials <i>B. C. Sales, L. A. Boatner, D. Mandrus, A. F. May, M. A. McGuire, and J.-Q. Yan</i>	329
Nanostructured Materials: From Superlattices to Quantum Dots <i>Ivan K. Schuller</i>	333
Dynamics of Emergent Crystallinity in Photonic Quantum Materials <i>J. Simon</i>	337
Spin-Polarized Scanning Tunneling Microscopy Studies of Nanoscale Magnetic and Spintronic Nitride Systems <i>Arthur R. Smith</i>	338
Understanding and Controlling Conductivity Transitions in Correlated Solids: Spectroscopic Studies of Electronic Structure in Vanadates <i>Kevin E. Smith</i>	342

Understanding (Mostly) Iron Based Superconductors <i>G. R. Stewart</i>	346
Nanoscale Electrical Transfer and Coherent Transport Between Atomically-Thin Materials <i>Douglas R. Strachan</i>	349
Fermi Gases in Bichromatic Superlattices <i>John E. Thomas</i>	353
Designing Metastability: Coercing Materials to Phase Boundaries <i>T. Zac Ward</i>	356
Charge Inhomogeneity in Correlated Electron Systems: Charge Order or Not <i>Barrett O. Wells</i>	360
Imaging Electrons in Atomically Layered Materials <i>Robert M. Westervelt and Philip Kim</i>	364
Quantum Hall Systems In and Out of Equilibrium <i>Michael Zudov</i>	368
Author Index	375
Participant List	381

Experimental Condensed Matter Physics Principal Investigators' Meeting Agenda

Monday, September 11, 2017

- 7:30–8:15am *****Breakfast*****
- 8:15–8:40am *BES – Welcome*
Mick Pechan, Department of Energy
- Session I** Chair: **Ben Hunt**, Carnegie Mellon University
- 8:40–9:05am **Jeanie Lau**, University of California, Riverside
Spontaneous and field-induced symmetry breaking in low dimensional nanostructures
- 9:05–9:20am **Philip Kim**, Harvard University
Correlated electrons in graphene at the quantum limit
- 9:20–9:35am **Dimitri Basov**, Columbia University
Electronic and photonic phenomena of graphene, boron nitride and graphene/boron nitride heterostructures
- 9:35–9:50am **Wei Pan**, Sandia National Laboratories
Quantum electronic phenomena and structures
- 9:50–10:05am **Jonathan Bird**, University at Buffalo
Nonlinear transport in mesoscopic structures in the presence of strong many-body phenomena
- 10:05–10:35am *****Break*****
- Session II** Chair: **Michael Zudov**, University of Minnesota
- 10:35–11:00am **Ray Ashoori**, Massachusetts Institute of Technology
Novel temperature limited tunneling spectroscopy of quantum Hall systems
- 11:00–11:15am **Mansour Shayegan**, Princeton University
Magneto-transport in GaAs two-dimensional hole systems
- 11:15–11:30am **Gabor Csathy**, Purdue University
Novel sample structures and probing techniques of exotic states in the 2nd Landau level
- 11:30–11:45am **Leonid Rokhinson**, Purdue University
Engineering topological superconductivity towards braiding Majorana excitations
- 11:45–12:00pm **Ruslan Prozorov**, Ames Laboratory
Magnetic nanosystems: making, measuring, modeling, and manipulation
- 12:00–1:25pm ***** Lunch*****
DMSE Overview
Linda Horton, Department of Energy

Session III	Chair: Tom Rosenbaum , Caltech
1:25–1:30pm	Mick Pechan , Department of Energy <i>Panel introduction: "Opportunities in ECMP basic research for next generation quantum systems and devices"</i>
1:30–1:45pm	Collin Broholm , Johns Hopkins University <i>Report on Quantum Materials BRN Workshop</i>
1:45–2:00pm	<u>Panel 1: Topological / 2D / Spin-orbit coupling</u> Judy Cha , Yale University Philip Kim , Harvard University
2:00–2:15pm	<u>Panel 2: Quantum magnetism</u> Axel Hoffmann , Argonne National Laboratory Arthur Ramirez , University of California—Santa Cruz
2:15–2:30pm	<u>Panel 3: Strongly correlated materials</u> Gabor Csathy , Purdue University Johnpierre Paglione , University of Maryland
2:30–3:15pm	Q&A
3:15–3:45pm	***Break***
Session IV	Chair: Wai Kwok , Argonne National Laboratory
3:45–4:10pm	Aharon Kapitulnik , SLAC National Accelerator Laboratory <i>Correlated materials – synthesis and physical properties</i>
4:10–4:25pm	Luis Balicas , Florida State University <i>Novel and unconventional superconductors: quantum critically and possible field-induced superconducting states</i>
4:25–4:40pm	John Mitchell , Argonne National Laboratory <i>Emerging Materials</i>
4:40–4:55pm	Dan Dessau , University of Colorado <i>Dynamics of electronic interactions in superconductors and related materials</i>
4:55–5:10pm	Peter Johnson , Brookhaven National Laboratory <i>Electron spectroscopy</i>
5:10–5:30pm	Poster Session I Introductions
5:30–5:40pm	***Break***
5:40–7:10pm	***Dinner***
7:10–9:10pm	Poster Session I

Tuesday, September 12, 2017

7:30–8:30am

Breakfast

Session V

Chair: **Ivan Schuller**, University of California, San Diego

8:30–8:55am

Geoff Beach, Massachusetts Institute of Technology
Interface-driven chiral magnetism in ultrathin metallic ferromagnets: towards skyrmion spintronics

8:55–9:10am

Axel Hoffmann, Argonne National Laboratory
Magnetic thin films

9:10–9:25am

Thomas Rosenbaum, Caltech
Quantum Order and Disorder in Magnetic Materials

9:25–9:40am

James Analytis, University of California, Berkeley
Topological materials with complex long-range order

9:40–9:55am

Peter Schiffer, University of Illinois, Urbana-Champaign
Thermalization of artificial spin ice and related frustrated magnetic arrays

9:55–10:10am

John Xiao, University of Delaware
Spintronics based on topological insulators

10:10–10:40am

Break

Session VI

Chair: **Phuan Ong**, Princeton University

10:40–11:05am

David Hsieh, Caltech
Search for novel topological phases in superconductors using laser-based spectroscopy

11:05–11:20am

Qi Li, Pennsylvania State University
Studies of multiband and topological superconductors

11:20–11:35am

Judy Cha, Yale University
Topological superconductor core-shell nanowires

11:35–11:50am

Johnpierre Paglione, University of Maryland
Non-centrosymmetric topological superconductivity

11:50–12:05pm

Douglas Natelson, Rice University
Nanostructure studies of strongly correlated materials

12:05–1:35pm

*** Lunch***

Session VII

Chair: **Anand Bhattacharya**, Argonne National Laboratory

1:35–2:00pm

Ho Nyung Lee, Oak Ridge National Laboratory
Epitaxial complex oxides

2:00–2:15pm	Harold Hwang , SLAC National Accelerator Laboratory <i>Atomic engineering oxide heterostructures: materials by design</i>
2:15–2:30pm	Chang-Beom Eom , University of Wisconsin, Madison <i>Novel synthesis of quantum epitaxial heterostructures by design</i>
2:30–2:45pm	Mikel Holcomb , West Virginia University <i>The investigation of oxygen vacancies in magnetic-ferroelectric heterostructures</i>
2:45–3:00pm	Fengyuan Yang , The Ohio State University <i>Novel regimes of spin transport: pure spin currents in antiferromagnets and time-resolved studies of spin dynamics</i>
3:00–3:30pm	***Break***
Session VIII	Chair: Jeremy Levy , University of Pittsburgh
3:30–3:55pm	Kin Fai Mak , Penn State University <i>Understanding topological pseudospin transport in van der waals' materials</i>
3:55–4:10pm	James Hone , Columbia University, New York City <i>Quantum transport in 2D semiconductors</i>
4:10–4:25pm	Feng Wang , Lawrence Berkeley National Laboratory <i>Van der Waals heterostructures: novel materials and emerging phenomena</i>
4:25–4:40pm	Janice Musfeldt , University of Tennessee <i>Spectroscopic investigations of novel electronic and magnetic materials</i>
4:40–4:55pm	Moungi Bawendi , Massachusetts Institute of Technology <i>Probing nanocrystal electronic structure and dynamics in the limit of single nanocrystals</i>
4:55–5:15pm	Poster Session II Introductions
5:15–5:35pm	***Break***
5:35–7:05pm	***Dinner***
7:05–9:05pm	Poster Session II

Wednesday, September 13, 2017

7:30–8:30am	***Breakfast***
Session IX	Chair: Doug Strachan , University of Kentucky
8:30–8:55am	Eva Andrei , Rutgers University <i>Experimental studies of correlations and topology in two dimensional hybrid structures</i>
8:55–9:10am	Gleb Finkelstein , Duke University <i>Symmetries, interactions and correlation effects in carbon nanotubes</i>

- 9:10–9:25am **Alex Zettl**, Lawrence Berkeley National Laboratory, UC Berkeley
Novel sp²-bonded materials and related nanostructures
- 9:25–9:40am **Saw Wai Hla**, Ohio University
Charge and energy transfer in molecular superconductors and molecular machines
- 9:40–10:10am *****Break*****
- Session X** Chair: **Nadya Mason**, University of Illinois, Urbana-Champaign
- 10:10–10:35am **Joseph Orenstein**, Lawrence Berkeley National Laboratory
Quantum materials
- 10:35–10:50am **Neil Harrison**, Los Alamos National Laboratory
Science of 100 Tesla
- 10:50–11:05am **Athena Sefat**, Oak Ridge National Laboratory
Tuning phase transformations for designed functionality
- 11:05–11:20pm **Dmitry Smirnov**, Florida State University
Magneto-optical study of correlated electron materials in high magnetic fields
- 11:20–11:35am **Bill Halperin**, Northwestern University
Antiferromagnetism and superconductivity
- 11:35–11:50am *BES – Conclusion*
Mick Pechan, Department of Energy
- 11:50am **Meeting Adjourns**

Session 1

Spontaneous and Field-Induced Symmetry Breaking in Low Dimensional Nanostructures

PI: Chun Ning (Jeanie) Lau

co-PI: Marc Bockrath

Department of Physics and Astronomy, University of California, Riverside, CA 92521

Department of Physics, The Ohio State University, Columbus, OH 43210

Program Scope

Electron-electron interactions can strongly modify the qualitative properties of low-dimensional materials. For example, one-dimensional (1D) systems exhibit Luttinger liquid behavior instead of Fermi liquid behavior, while two-dimensional (2D) systems exhibit the fractional quantum Hall effect. The goal of our current grant is to investigate and understand strongly correlated electron behavior using few-layer graphene, which has emerged as archetypal 2D nanostructures. This research program explore 3 key areas:

- (1). exploiting the instability of few-layer graphene to the formation of a correlated electron ground state[1-3] [4-6], due to the many competing symmetries. In particular, we will investigate the intrinsic gapped state and the related filling factor $\nu=0$ quantum Hall states at the charge neutrality point, by mapping their phase diagram and phase transitions as a function of electric field, perpendicular and parallel magnetic fields, charge density, disorder and temperature. Many of the phases are topological with quantized conductance.
- (2). the emergence of novel phenomena when it is in the proximity of other materials, such as the Hofstadter butterfly physics and topological bands in aligned BN/graphene superlattices[7-9], and inducing superconductivity via ionic liquid gating of suspended samples that allow ion accumulation on both surfaces.
- (3). realizing topological superconductivity with Majorana excitations, which is predicted to appear in superconductor-contacted graphene[10]. This project combines both of the above directions, as it takes advantage of graphene's tunable magnetic orders in the $\nu=0$ state – the crossover from antiferromagnetic to magnetic states is expected to accompany a transition from gapless to gapped Majorana excitations.

We will perform low temperature transport and nanoelectromechanical measurements, using ultra-clean devices that are either suspended or encapsulated by hexagonal BN. Taken together, these experiments will provide a comprehensive investigation of how electron-electron interactions affect the properties of these exciting materials, and how topological modes can emerge and be tuned in these systems. Successful implementation of the proposed experiments will be a major step forward in our fundamental knowledge of electron correlation and many-body physics in materials, which is important for physics, material science, engineering and energy science.

Recent Progress

In the past two years, we have made significant progress in our studies of ultra-clean low dimensional nanostructures, focusing on ultra-clean graphene devices that are either suspended or supported on hexagonal BN substrates. Some of the works are highlighted below.

1. Fractional Quantum Hall Effect in BLG

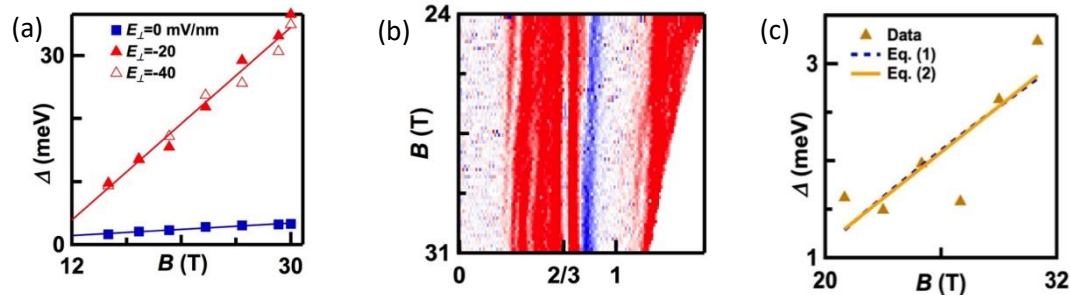


Fig. 1. Data from a bilayer graphene. (a). Measured LL gap $\Delta(B)$ for the $\nu=1$ state at out-of-plane electric field $E_{\perp}=0$ (blue) and $E_{\perp}=-20$ mV/nm and -40 mV/nm (red) respectively. The states have very different slopes at zero and finite electric field. (b). $G(B, \nu)$. The fractional QH state $\nu=2/3$ is visible as a vertical white stripe. (c). Landau level gap of $\nu=2/3$ state vs B .

Owing to the spin, valley, and orbital symmetries, the lowest Landau level in BLG exhibits multicomponent quantum Hall (QH) ferromagnetism. Using transport spectroscopy, we investigate the energy gaps of integer and fractional QH states in BLG with controlled layer polarization. The state at filling factor $\nu=1$ has two distinct phases: a layer polarized state that has a larger energy gap and is stabilized by high electric field, and a hitherto unobserved interlayer coherent state with a smaller gap that is stabilized by large magnetic field. In contrast, the $\nu=2/3$ QH state and a feature at $\nu=1/2$ are only resolved at finite electric field and large magnetic field (Fig. 2). These results underscore the importance of controlling layer polarization in understanding the competing symmetries in the unusual QH system of BLG. This work is published in *Physical Review Letters*.

2. Tunable Symmetries of Integer and Fractional Quantum Hall Phases in Multi-Dirac-Band Heterostructures

The co-presence of multiple Dirac bands in few-layer graphene leads to a rich phase diagram in the quantum Hall regime. Here we map the phase diagram of BN-encapsulated ABA-stacked trilayer graphene as a function charge density n , magnetic field B and interlayer displacement field E_{\perp} , and observe transitions among states with different spin, valley, orbital and parity polarizations. Such rich pattern arises from crossings between Landau levels from different subbands, which reflect the evolving symmetries that are tunable in situ. At $E_{\perp}=0$, we observe fractional quantum Hall (FQH) states at filling factors $2/3$ and $-11/3$. Unlike those in bilayer graphene, these FQH states are destabilized by a small interlayer potential that hybridizes the different Dirac bands. This work is published by *Physical Review Letters*.

3. Gate-Tunable Landau Level Filling and Spectroscopy in Coupled Massive and Massless Electron Systems

An interacting electron system's quasiparticle spectrum strongly influences its behavior. Here we study the interaction between coupled two-dimensional electron systems with different spectra where one is massive and the other massless, realized using a graphene monolayer (massless spectrum) in contact with a graphene bilayer (massive spectrum). We incorporate this system into a dual-gated transistor geometry and study its properties using transport measurements. Because of their close proximity, the interlayer interactions are strong, and the disparate spectra produce unique and novel behavior. As a result of the interlayer interactions, the monolayer's Dirac spectrum causes its capacitance to become nonlinear. Moreover, in a magnetic field we are able to perform spectroscopy on the Landau levels in the system, measuring the Fermi velocity in the monolayer and the effective mass in the bilayer. The value obtained for the mass is larger than that obtained for an isolated layer, suggesting that the interlayer interaction renormalizes the parameters of the band structure (Fig. 5). Finally, our work enables quantitative measurement of the band structure of layered systems, which may be applicable to the many novel systems under investigation such as topological insulators or other two-dimensional materials. This work published by *Physical Review Letters*.

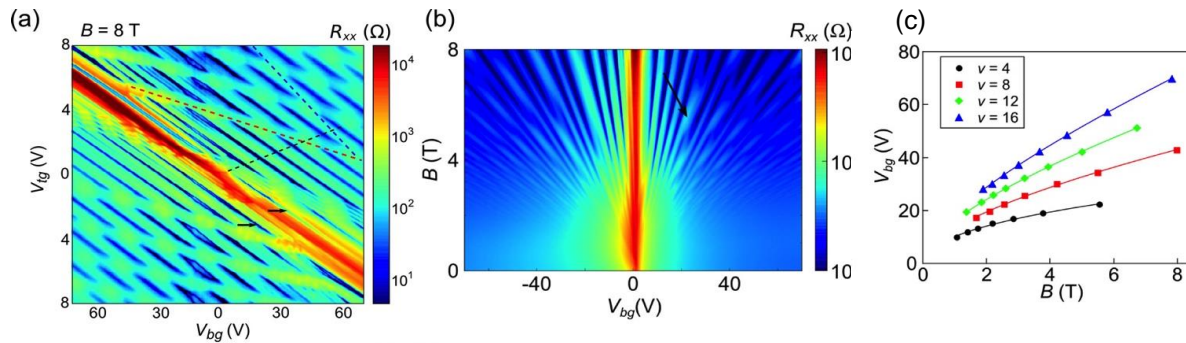


Fig. 2. (a) $R_{xx}(V_{bg}, V_{fg})$ at $B=8$ T. The red dashed line connects crossing point features for which the monolayer charge is constant, while the blue dashed line connects features where the bilayer charge is constant. (b) $R_{xx}(V_{bg}, B)$, at out-of-plane displacement field $D=0$. The arrow indicates a LL crossing point. (c) The gate voltage of the crossing points from a is plotted for several values of ν . The Fermi velocities obtained from the fits are 1.2, 1, 0.9, 0.9×10^6 m/s for $\nu=4, 8, 12$ and 16, respectively.

Future Plans

Apart from the general direction outlined in the first section, our immediate plans for the next year include

- the integer and fractional quantum Hall states in few-layer graphene,
- the phase diagram of trilayer and tetralayer graphene at the charge neutrality point
- transport of Cooper pairs in the filling factor $\nu=0$ state

References

- [1] M. Kharitonov, *Phys. Rev. Lett.* 109, 046803 (2012).
- [2] F. Zhang *et al.*, *Phys. Rev. Lett.* 106, 156801 (2011).
- [3] R. T. Weitz *et al.*, *Science* 330, 812 (2010).
- [4] P. Maher *et al.*, *Nat. Phys.* 9, 154 (2013).
- [5] A. F. Young *et al.*, *Nature* 505, 528 (2014).
- [6] J. Velasco *et al.*, *Nature Nanotechnol.* 7, 156 (2012).
- [7] B. Hunt *et al.*, *Science* 340, 1427 (2013).
- [8] C. R. Dean *et al.*, *Nature* 497, 598 (2013).
- [9] L. A. Ponomarenko *et al.*, *Nature* 497, 594 (2013).
- [10] P. San-Jose *et al.*, *Phys. Rev. X* 5, 041042 (2015).

Two-year Publications Supported by BES

1. B. Cheng, P. Wang, C. Pan, T. Miao, Y. Wu, T. Taniguchi, K. Watanabe, C. N. Lau and M. Bockrath, "Raman spectroscopy measurement of bilayer graphene's twist angle to boron nitride." *Applied Physics Letters*, 107, 033101 (2015).
2. P. Wang, B. Cheng, O. Martynov, T. Miao, L. Jing, T. Taniguchi, K. Watanabe, V. Aji, C. N. Lau, and Bockrath, "Topological Winding Number Change and Broken Inversion Symmetry in a Hofstadter's Butterfly." *Nano Letters* 15, 6395–6399 (2015).
3. Y. Lee, D. Tran, K. Myhro, J. V. Jr., N. Gillgren, Y. Barlas, J. M. Poumirol, D. Smirnov and C. N. Lau, "Multicomponent Quantum Hall Ferromagnetism and Landau Level Crossing in Rhombohedral Trilayer Graphene", *Nano Letters*, **16**, 227 (2016).
4. Y. Shi, Y. Lee, S. Che, Z. Pi, T. Espiritu, P. Stepanov, D. Smirnov, C.N. Lau and F. Zhang, "Energy gaps and layer polarization of integer and fractional quantum Hall states in bilayer graphene", *Physical Review Letters*, 116, 056601 (2016).
5. P. Stepanov, Y. Barlas, T. Espiritu, S. Che, K. Watanabe, T. Taniguchi, D. Smirnov, and C. N. Lau, "Tunable Symmetries of Integer and Fractional Quantum Hall Phases in Heterostructures with Multiple Dirac Bands", *Physical Review Letters* 117, 076807 (2016).
6. B. Cheng, Y. Wu, P. Wang, C. Pan, T. Taniguchi, K. Watanabe, and M. Bockrath, "Gate-Tunable Landau Level Filling and Spectroscopy in Coupled Massive and Massless Electron Systems", *Physical Review Letters* 117, 026601 (2016).
7. O. V. Martynov, and M. Bockrath, "Carbon nanotube stabilized single layer graphene cantilevers", *Applied Physics Letters* 110, 151901 (2017).
8. J. Hu, Z. J. Tang, J. Y. Liu, X. Liu, Y. L. Zhu, D. Graf, K. Myhro, S. Tran, C. N. Lau, J. Wei, and Z. Q. Mao, "Evidence of Topological Nodal-Line Fermions in ZrSiSe and ZrSiTe", *Physical Review Letters* 117, 016602 (2016).
9. C. Pan, Y. Wu, B. Cheng, S. Che, T. Taniguchi, K. Watanabe, C. N. Lau, and M. Bockrath, "Layer Polarizability and Easy-Axis Quantum Hall Ferromagnetism in Bilayer Graphene", *Nano Letters*, 17, 3416 (2017).

Correlated Quasiparticles in Graphene

Philip Kim, Department of Physics, Harvard University

Program Scope

Coulomb interactions between charge carriers in graphene often lead to exotic electronic states. A notable example of such systems is the Dirac fluid, which can be realized near the neutrality point where strong electron-electron interactions and electron-hole symmetry can decouple heat current from charge flow, blurring the existence of quasiparticles. Here, the thermally excited electron-hole plasma reveals hydrodynamics of quasi-relativistic fermions, which is an ideal candidate to show this exciting and exotic phenomenon. Under quantizing magnetic fields, strong Coulomb interaction can also lead to spontaneous symmetry breaking in the internal quantum degrees of freedom of correlated quasiparticles. Finally, creating a hybrid system of a superconductor (SC) and quantum Hall (QH) states can also create strongly-correlated quasiparticles in the mesoscopic sized graphene samples by proximity-induced superconductivity near the SC electrodes. In this project, we investigate the fundamental physics of correlated electronic systems realized in these three different ways. Our major proposed tasks are: (i) realization of controlled quantum Hall edge states using split local back gates for selective depletion; (ii) probing electronic thermal transport to investigate magneto-hydrodynamics; (iii) measurement of entropy in spontaneous symmetry-broken graphene quantum Hall ferromagnetism; (iv) exploration of superfluid magneto exciton condensation in double layers; (v) proximitizing quantum Hall edges for creation of non-Abelian quasiparticles; and, (vi) proximitizing bulk quantum Hall states for topological superconductivity.

Recent Progress

Dirac fluid and the breakdown of the Wiedemann-Franz law in graphene: We fabricated extremely clean graphene samples where electron-electron scattering is the dominant interaction, thus driving the system into the hydrodynamic transport regime. We used very sensitive Johnson noise thermometry, developed in the previous funding period [1] to measure the electronic contribution to thermal conductivity, and demonstrated a complete breakdown of the WF law (Fig. 1) at a finite temperature at the CNP. This is direct evidence for quasi-relativistic hydrodynamic flow of the quantum electronic fluid in graphene. Our results imply that electrons at the graphene's CNP is a nearly perfect fluid with extremely low viscosity. Our demonstration of an experimentally realizable Dirac fluid in graphene opens the way for follow up studies of strongly interacting relativistic many-body systems. Beyond a diverging thermal conductivity and an

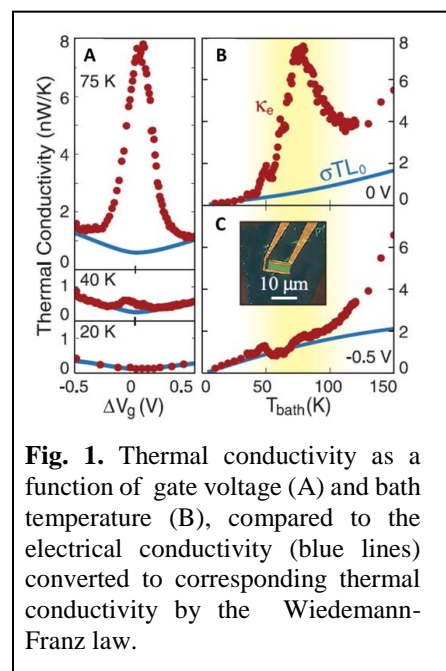


Fig. 1. Thermal conductivity as a function of gate voltage (A) and bath temperature (B), compared to the electrical conductivity (blue lines) converted to corresponding thermal conductivity by the Wiedemann-Franz law.

ultra-low viscosity, other peculiar phenomena are expected to arise in this strongly correlated quasi-relativistic plasma. The massless nature of the Dirac fermions is expected to result in a small kinematic viscosity, which may lead to hydrodynamic instability. Observable hydrodynamic effects have also been predicted to extend into the Fermi liquid regime [2].

Specular Andreev reflection in bilayer graphene: We demonstrate an extremely clean van der Waals interface between bilayer graphene (BLG) and the quasi 2-dimensional superconductor NbSe₂ (Fig. 2A). Utilizing the vdW interfaces, we realize a superconductor and

graphene interface, where the Fermi energy of normal channel can be smaller than the superconducting energy gap. In this unusual limit, the holes are expected to be reflected specularly at the superconductor-graphene interface due to the onset of intervalley- interband Andreev processes. We measure the conductance across the graphene-NbSe₂ interface searching a suppression when the Fermi energy is tuned to values smaller than the superconducting gap by gate voltage, a hallmark for the transition between intraband retro- and interband specular- Andreev reflections. In this experiment, we performed measurements of gate modulated Andreev reflections across the low disorder van der Waals interface formed between graphene and the superconducting NbSe₂. Indeed, we find that the conductance across the graphene-superconductor interface exhibits a characteristic suppression when the Fermi energy is tuned to values smaller than the superconducting gap, a hallmark for the transition between intraband retro-and interband specular- Andreev reflections (Fig. 2B). Our observation of gate tunable transitions between retro intraband and specular interband Andreev reflections opens a new route for future experiments that could employ gate control of the reflection angles, which can be continuously and independently altered with gate and bias voltages. Most importantly our finding helps to draw a general picture of the exact physical processes underlying Andreev reflection.

Crossed Andreev reflection and proximitizing quantum Hall edge states: For this experiment, we fabricated highly transparent NbN superconducting electrodes on a hexagonal boron nitride (hBN) encapsulated graphene sample (Fig. 3A). If the superconducting electrode is narrower than the superconducting coherence length, the incoming electron is correlated to the outgoing hole along the chiral edge state by the Andreev process across the SC electrode [3]. In order to realize this crossed Andreev conversion (CAC), it is necessary to fabricate highly transparent and nanometer-scale superconducting junctions to the QH system. In this experiment, we report the observation

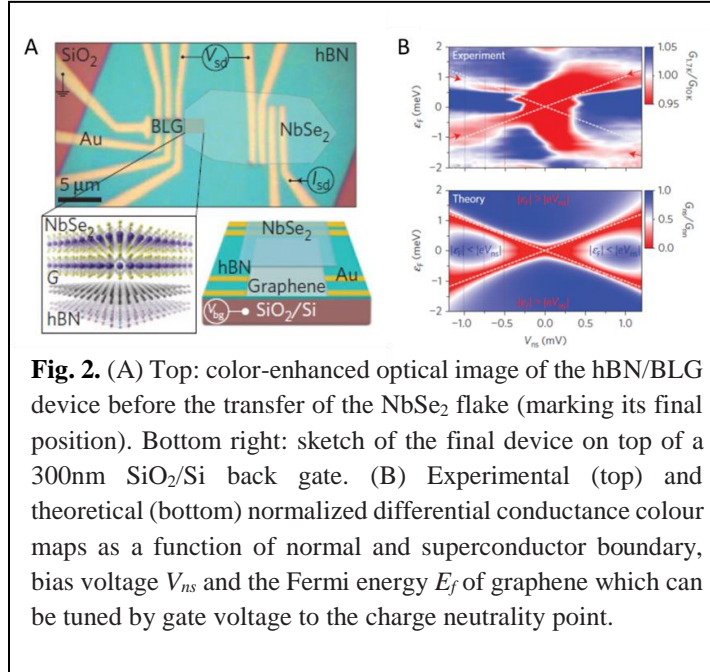


Fig. 2. (A) Top: color-enhanced optical image of the hBN/BLG device before the transfer of the NbSe₂ flake (marking its final position). Bottom right: sketch of the final device on top of a 300nm SiO₂/Si back gate. (B) Experimental (top) and theoretical (bottom) normalized differential conductance colour maps as a function of normal and superconductor boundary, bias voltage V_{ns} and the Fermi energy E_f of graphene which can be tuned by gate voltage to the charge neutrality point.

of CAC in a graphene QH system contacted with a nanostructured NbN superconducting electrode. The chemical potential of the edge states across the SC electrode exhibits a sign reversal, providing direct evidence of CAC. The result is a hallmark of crossed Andreev conversion and constitutes direct evidence of coupling of counter propagating quantum Hall edge states via Cooper pairing. This hybrid SC/QH system can be a novel route to create isolated non-Abelian anyonic zero modes in resonance with the chiral QH edge.

Quantized Hall drag and magneto exciton condensation in bilayer graphene; Using the strong Coulomb interaction across the atomically thin hBN separation layer, we realize the magneto-exciton BEC in bilayer graphene double layers whose transition temperature is an order of magnitude higher than that in GaAs quantum wells. Driving current through one graphene layer generates a quantized Hall voltage in the other layer, signifying coherent superfluid exciton transport. The wide-range tunability of densities and displacement fields enables exploration of a rich phase diagram of BEC across Landau levels with different filling factors and internal quantum degrees of freedom. The observed robust exciton superfluidity opens up opportunities to investigate various quantum phases of the exciton BEC and design novel electronic devices based on dissipationless transport.

Future Plans

To extend our success beyond our ongoing work, we propose a set of new research aims to explore novel physical phenomena stemming from the Correlated Quasiparticles in Graphene. In this renewal project, we set the following ambitious, yet experimentally feasible research goals to probe the emergent phenomena in the Dirac fermionic system:

- Engineering graphene edge depletion and gate geometry to improve controlled quantum Hall edge state formation
- Investigating electronic thermal transport measurement and magnetic hydrodynamics
- Developing measurement technique for measuring entropy and thermal conductance in quantum Hall ferromagnetism in bilayer graphene
- Exploring superfluid magneto exciton condensation in double layers

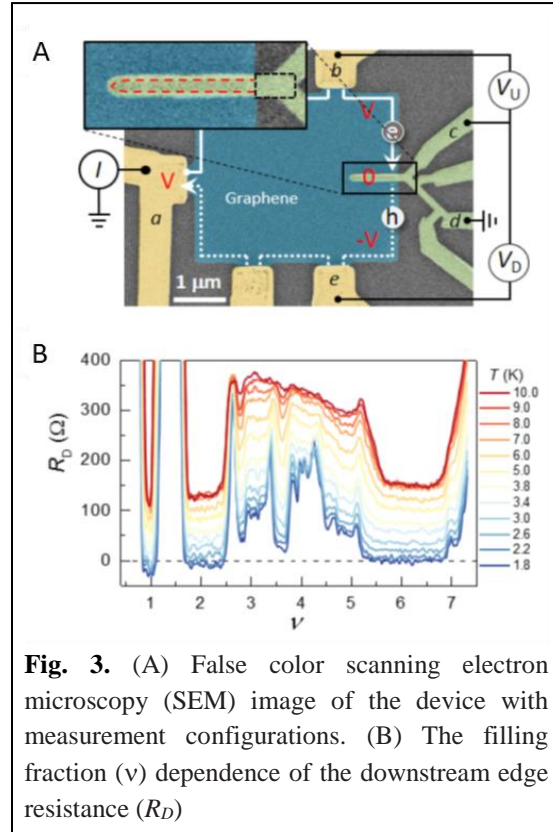


Fig. 3. (A) False color scanning electron microscopy (SEM) image of the device with measurement configurations. (B) The filling fraction (ν) dependence of the downstream edge resistance (R_D)

- Investigation of proximitized quantum Hall edges to create and control non-Abelian quasiparticles
- Studying proximitized superconducting orders competing with the quantum Hall states in order to create topological superconductivity

References

- [1] J. Crossno, X. Liu, T. Ohki, P. Kim, and K. C. Fong, “Development of high frequency and wide bandwidth Johnson noise thermometry,” *Appl. Phys. Lett.* **106**, 023121 (2015)
- [2] A. Principi, G. Vignale, M. Carrega, and M. Polini, “Bulk and shear viscosities of the 2D electron liquid in a doped graphene sheet,” *Phys. Rev. B* **93**, 125410 (2016).
- [3] D. Beckmann, H. B. Weber, and H. v. Löhneysen, “Evidence for Crossed Andreev Reflection in Superconductor-Ferromagnet Hybrid Structures,” *Phys. Rev. Lett.* **93**, 197003, (2004).

Publications

- J. Crossno, J. K. Shi, K. Wang, X. Liu, A. Harzheim, A. Lucas, S. Sachdev, P. Kim, T. Taniguchi, K. Watanabe, T. A. Ohki, K. C. Fong, “Observation of the Dirac fluid and the breakdown of the Wiedemann-Franz law in graphene,” *Science* **351**, 1058-1061 (2016);
- F. Ghahari, H.-Y. Xie, T. Taniguchi, K. Watanabe, M. S. Foster, P. Kim, “Enhanced Thermoelectric Power in Graphene: Violation of the Mott Relation By Inelastic Scattering,” *Phys. Rev. Lett.* **116**, 136802 (2016).
- D. K. Efetov, L. Wang, C. Handschin, K. B. Efetov, J. Shuang, R. Cava, T. Taniguchi, K. Watanabe, J. Hone, C. R. Dean, and P. Kim, “Specular Interband Andreev Reflections in Graphene,” *Nature Physics* **12**, 328–332 (2016)
- C. Chen, V. V. Deshpande, M. Koshino, S. Lee, A. Gondarenko, A. H. MacDonald, P. Kim and J. Hone, “Modulation of mechanical resonance by chemical potential oscillation in graphene,” *Nature Physics* **12**, 240–244 (2016).
- G.-H. Lee, K.-F. Huang, D. K. Efetov, D. S. Wei, S. Hart, T. Taniguchi, K. Watanabe, A. Yacoby, P. Kim, “Inducing Superconducting Correlation in Quantum Hall Edge States,” *Nature Physics* **13**, 693–698 (2017)
- X. Liu, L. Wang, K. C. Fong, Y. Gao, P. Maher, K. Watanabe, T. Taniguchi, J. Hone, C. Dean, P. Kim, “Frictional magneto-Coulomb drag in graphene double-layer heterostructure,” *Phys. Rev. Lett.* **119**, 056802 (2017)
- X. Liu, K. Watanabe, T. Taniguchi, B. I. Halperin, and P. Kim, “Quantum Hall Drag of Exciton Condensate in Graphene,” *Nature Physics* **13**, 746–750 (2017)

Polaritons in van der Waals materials

D.N. Basov, Columbia University

Program Scope

Our program is focused on the fundamental physics of graphene and other van der Waals materials. The emphasis of the proposed research is on the investigation of novel optical and electronic effects of hBN, graphene and their heterostructures. The PI implemented a novel approach to inquire into the electronic properties of complex materials based on nano-spectroscopy and nano-imaging of hybrid light matter modes referred to as polaritons [1].

Recent Progress

Experimental work carried out with DOE support over the last two years has resulted in 10 peer-reviewed articles published in *Science*¹, *Nature Materials*², *Nature Nanotechnology*³, *Nature Photonics*⁴, *Physical Review Letters*⁵, *Nano Letters*^{6,7,8}, *Physical Review B*⁹, and *Nature Communications*¹⁰.

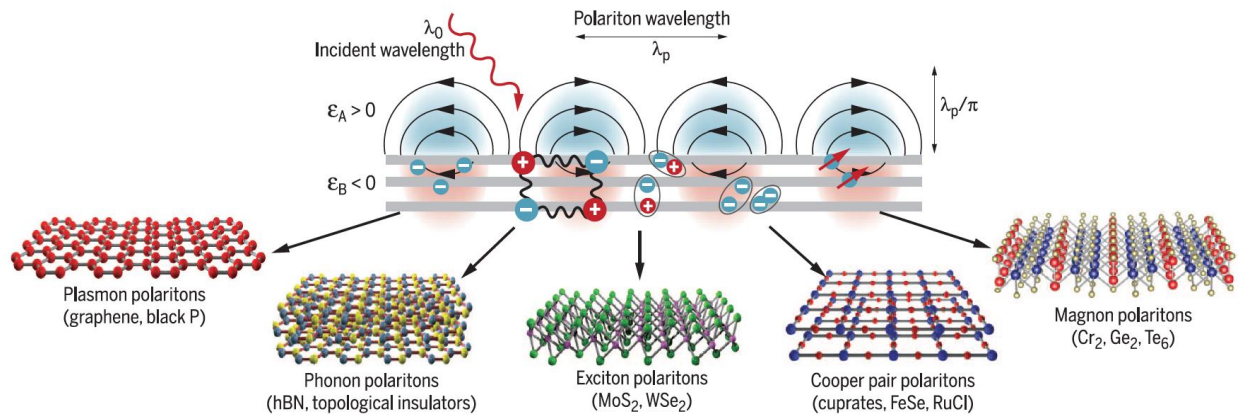


Figure 1. Polaritons in van der Waals (vdW) materials. Polaritons (hybrid light-matter oscillations) can originate from various physical phenomena: conduction electrons in graphene and topological insulators (surface plasmon polaritons), infrared-active phonons in boron nitride (phonon polaritons), excitons in dichalcogenide materials (exciton polaritons), superfluidity in FeSe- and Cu-based superconductors with high critical temperature T_c (Cooper-pair polaritons), magnetic resonances (magnon polaritons). All of these polaritons are supported by the family of vdW materials. The matter oscillation component results in negative permittivity ($\epsilon_B < 0$) of the polaritonic material, giving rise to optical-field confinement at the interface with a positive-permittivity ($\epsilon_A > 0$) environment. vdW polaritons exhibit strong confinement, as defined by the ratio of incident light wavelength λ_0 to polariton wavelength λ_p . Adapted from Ref.[1].

Focus area 1: physics of polaritons in graphene, boron nitride and other two-dimensional van der Waals materials. Publications [1,3,4,10]. Surface plasmon polaritons can be regarded as coupled oscillations of electron density and electromagnetic field. Yet there exist many other varieties of polaritons, including those formed by atomic vibrations in polar insulators, excitons in semiconductors, Cooper pairs in superconductors, and spin resonances in (anti) ferromagnets (Fig.1). Together, they span a broad region of the electromagnetic spectrum, ranging from microwave to ultraviolet wavelengths[1]. The PI has systematically investigated polaritons in two-dimensional materials; infrared nano-imaging has played a central role in these studies. Experimental observations augmented with modeling in collaboration with Prof. M.Fogler, have led to significant outcomes. This research established polaritonic imaging as a method of choice for investigating the physics of materials supporting polaritonic waves. Essentially, polaritonic imaging experiments carried out with broad-band tunable light sources constitute a new form of spectroscopy. Relevant information is contained in the dispersion of polaritonic modes, and can be directly extracted from near field nano-imaging of propagating polaritonic waves.

Focus area 2: intrinsic properties of graphene/hBN interfaces. Publications [2,4]. The PI has systematically investigated the interaction of nearly-matching hexagonal lattices of graphene and hBN, which results in a quasiperiodic moiré superlattice. The PI utilized polaritonic imaging methods to probe the dynamical response of the moiré graphene. The analysis of nano-IR data showed that the Dirac mini-bands produce two distinct contributions to the plasmonic response of the moire superlattice in graphene. This novel character of collective modes established by the PI is likely to be generic to other forms of moiré-forming superlattices, including van der Waals heterostructures. In a separate series of experiments [10], the PI has demonstrated that hyperbolic polaritons of hBN can be effectively modulated in a van der Waals heterostructure composed of monolayer graphene on h-BN. Tunability originates from the hybridization of surface plasmon polaritons in graphene with hyperbolic phonon polaritons in h-BN. The hyperbolic plasmon–phonon polaritons possess the combined virtues of surface plasmon polaritons in graphene and hyperbolic phonon polaritons in h-BN.

Future Plans

Currently on-going experiments exploit the unique capabilities of scanning plasmon interferometry to investigate previously unexplored physics of high-mobility electron liquid in high-mobility graphene. Specific research directions:

- i) Intrinsic electrodynamics of two-dimensional electron liquid in graphene that has remained elusive but is now within the experimental reach, due to the availability of high mobility graphene/hBN samples and the advent of technology allowing nano-optical experimentation at cryogenic temperatures;
- ii) Topological phenomena in bilayer graphene. Using plasmonic nano-imaging, the PI will investigate the electronic response associated with nano-scale stacking domains in bilayer samples, which are expected to show a rich variety of novel electronic properties governed by non-trivial topology and the electronic structure associated with the domain walls;

- iii) Properties of graphene/hBN interfaces that will be continuously tuned in reconfigurable devices will enable in-operando modification of the electronic and photonic phenomena by moire superlattice patterns.

Publications

- ¹ D.N. Basov, M.M. Fogler and F. J. Garcia de Abajo, “Polaritons in van der Waals materials,” *Science* 354, 195 (2016).
- ² G. X. Ni, H. Wang, J. S. Wu, Z. Fei, M. D. Goldflam, F. Keilmann, B. Özyilmaz, A. H. Castro Neto, X. M. Xie, M. M. Fogler, and D. N. Basov, “Plasmons in graphene moiré superlattices,” *Nature Materials* 14, 1217 (2015).
- ³ S. Dai, Q. Ma, M. K. Liu, T. Andersen, Z. Fei, M. D. Goldflam, M. Wagner, K. Watanabe, T. Taniguchi, M. Thiemens, F. Keilmann, G. C. A. M. Janssen, S-E. Zhu, P. Jarillo-Herrero, M. M. Fogler, and D. N. Basov, “Graphene on hexagonal boron nitride as a tunable hyperbolic metamaterial,” *Nature Nanotechnology* 10, 682 (2015).
- ⁴ G. X. Ni, L. Wang, M. D. Goldflam, M. Wagner, Z. Fei, A. S. McLeod, M. K. Liu, F. Keilmann, B. Özyilmaz, A. H. Castro Neto, J. Hone, M. M. Fogler, and D. N. Basov, “Ultrafast optical switching of infrared plasmon polaritons in high-mobility graphene,” *Nature Photonics* 10, 244 (2016).
- ⁵ K.W. Post, B. C. Chapler, M. K. Liu, J. S. Wu, H. T. Stinson, M. D. Goldflam, A. R. Richardella, J. S. Lee, A. A. Reijnders, K. S. Burch, M. M. Fogler, N. Samarth, and D. N. Basov, “Sum-Rule Constraints on the Surface State Conductance of Topological Insulators,” *Physical Review Letters* 115, 116804 (2015).
- ⁶ Yinming Shao, Kirk W. Post, Jih-Sheng Wu, Siyuan Dai, Alex J. Frenzel, Anthony R. Richardella, Joon Sue Lee, Nitin Samarth, Michael M. Fogler, Alexander V. Balatsky, Dmitri E. Kharzeev, and D. N. Basov, “Faraday Rotation Due to Surface States in the Topological Insulator $(Bi_{1-x}Sb_x)_2Te_3$,” *Nano Letters* 17, 980 (2017).
- ⁷ William S. Whitney, Victor W. Brar, Yunbo Ou, Yinming Shao, Artur R. Davoyan, D. N. Basov, Ke He, Qi-Kun Xue, and Harry A. Atwater, “Gate-Variable Mid-Infrared Optical Transitions in a $(Bi_{1-x}Sb_x)_2Te_3$ Topological Insulator,” *Nano Letter* 17, 255 (2017).
- ⁸ I. T. Lucas, A. S. McLeod, J. S. Syzdek, D. S. Middlemiss, C. P. Grey, D. N. Basov, and R. Kostecki, “IR Near-Field Spectroscopy and Imaging of Single Li_xFePO_4 Microcrystals,” *Nano Letter* 15, 1 (2015).
- ⁹ K. W. Post, Y. S. Lee, B. C. Chapler, A. A. Schafgans, Mario Novak, A. A. Taskin, Kouji Segawa, M. D. Goldflam, H. T. Stinson, Yoichi Ando, and D. N. Basov, “Infrared probe of the bulk insulating response in $Bi_{2-x}Sb_xTe_{3-y}Se_y$ topological insulator alloys,” *Physical Review B* 91, 165202 (2015).
- ¹⁰ S. Dai, Q. Ma, T. Andersen, A. S. McLeod, Z. Fei, M. K. Liu, M. Wagner, K. Watanabe, T. Taniguchi, M. Thiemens, F. Keilmann, P. Jarillo-Herrero, M. M. Fogler, and D. N. Basov, “Subdiffractive focusing and guiding of polaritonic rays in a natural hyperbolic material,” *Nature Communications* 6, 6963, 7963 (2015).

Project Title: Quantum Electronic Phenomena and Structures

Wei Pan, Sandia National Laboratories

Program Scope

The purpose of this project is to discover and to understand emergent quantum phenomena and states-of-matter in novel materials and nanostructures that are governed by the laws of quantum mechanics. The project includes research on quantum transport and ultrafast optical studies in low dimensional electron systems, and high quality materials synthesis. We will investigate new electron physics emerging at the nano and mesoscopic scales that occurs due to strong electron-electron and electron-disorder interactions. We will further explore quantum properties in topological materials where the spin-orbit coupling is strong. These research topics are at the frontier of condensed matter physics and will yield new discoveries and understanding of emergent quantum matter and behaviors.

The proposed research activities are categorized in two synergistically integrated areas: quantum transport in structured semiconductors and quantum properties in topological materials. Quantum transport and ultrafast optical measurements will be carried out to probe exotic quantum electronic properties and topological phase transitions in topological nanostructures. Computational modeling approaches will be developed to simulate non-equilibrium quantum transport in architectures composed of topological nanostructures, building on our established extensive experience in developing and implementing quantum transport approaches. Finally, the impact of disorder on topological states in quantum matters will be studied. We emphasize here the cutting-edge, highly integrated multidisciplinary approach involving high quality material growth, precise device fabrication, ultra-low temperature quantum transport measurement, and theoretical investigations and simulations.

Recent Progress

Berry phase of composite fermions (CFs) in HIGFETs

The interest in CFs [1-3] was recently reinvigorated in part from the realization of the significance of particle-hole symmetry [4-18]. Many of these studies predict a Berry phase of the composite Fermi liquid at $\nu=1/2$. These predictions are a significant new development, as this possibility has been overlooked in the past. Thus, an experimental detection of the Berry phase of CFs points towards the novel topological properties of CFs. Here, we present our results from examining the Berry phase of CFs via Shubnikov-de Haas (SdH) oscillations.

Experimentally, a π Berry phase can be demonstrated by a non-zero intercept of $-1/2$ in the Landau level fan diagram [19,20]. In the proposals using a Dirac model to treat CFs at finite densities [7-12] and considering CFs as neutral particles carrying vorticity [14] the CF density, $n_v = eB/2h$, is proportional to the external magnetic (B) field. Only at $\nu=1/2$ does n_v equal the underlying electron density (n_e). In conventional SdH measurements at a fixed n_e , both the CF density and its effective B field change with the varying external B field [14]. Thus, it is not possible to obtain a coherent Berry phase in SdH measurements for a fixed n_e . In order to reveal the Berry phase of CFs, one needs to measure SdH oscillations at a fixed B field (or fixed CF density) while varying electron density (or CF

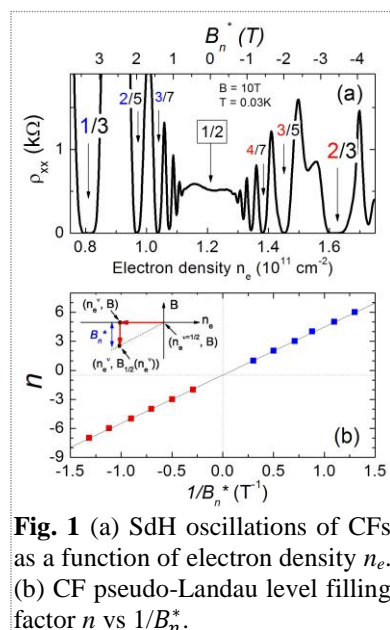


Fig. 1 (a) SdH oscillations of CFs as a function of electron density n_e . (b) CF pseudo-Landau level filling factor n vs $1/B_n^*$.

effective B field). The samples we used to measure the density-dependent SdH oscillations are specially designed heterojunction insulated-gate field-effect transistors (HIGFETs), in which the electron density can be tuned over a large range. The growth structure of a HIGFET and its unique, relevant aspects can be found in Ref. [21].

To look for signatures of the predicted Berry phase, we have measured density-dependent SdH oscillations in ρ_{xx} , around $\nu=1/2$ at various B fields in HIGFETs, as shown in Fig. 1a under a fixed B field of 10 Tesla (T). A series of well-defined FQHE states is observable as a function of electron density. In our analysis we first locate the densities corresponding to the FQHE states at the ρ_{xx} minima of the SdH oscillations. For the CFs at the $\nu = n/(2n+1)$, $n = \pm 1, \pm 2, \pm 3 \dots$ sequence of FQHE states, the effective magnetic field $B_n^* = B - 2hn_e/e$. In Fig. 1b, we plot the CF Landau level index n from the Jain sequence of FQHE states (n is chosen to be negative for the CF sequence for $\nu > 1/2$). An intercept of $-1/2$ at $1/B_n^* = 0$ is clearly seen in Fig. 1b. This result establishes the Berry phase of π for the CFs at $\nu = 1/2$, and can be understood within the framework of the recently proposed theoretical studies of CFs at the half-filled Landau level [7-12,14]. It follows that the experimental detection of the Berry phase of CFs in 2D electrons points towards the novel topological properties of CFs, which was not previously realized.

Terahertz Magneto-Optical Spectroscopy of Structured Semiconductors

We have developed the capability to do terahertz (THz) magneto-optical spectroscopy at temperatures as low as 1.3 K and in magnetic fields up to 8 T, using an amplified Ti:sapphire laser system producing 6 mJ, 50 femtosecond pulses at 800 nm (1.55 eV) to generate and detect THz pulses in ZnTe [22]. Recently, we have modified our system to optically photoexcite samples and measure the photoinduced changes in the transmitted THz pulse (optical-pump, THz-probe

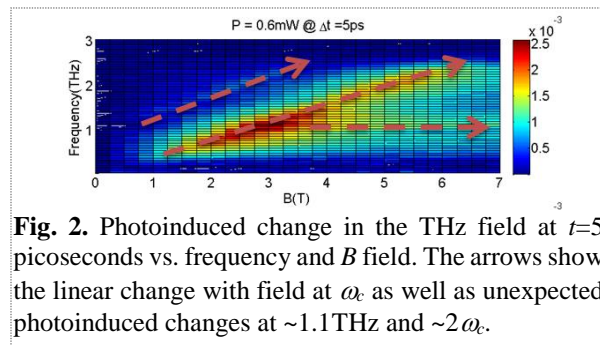


Fig. 2. Photoinduced change in the THz field at $t=5$ picoseconds vs. frequency and B field. The arrows show the linear change with field at ω_c as well as unexpected photoinduced changes at ~ 1.1 THz and $\sim 2\omega_c$.

(OFTP) spectroscopy) in a magnetic field. We plan to further improve our system to generate intense THz pulses (fields >25 kV/cm) at the sample position in the magnet [23]. These changes will enable us to examine topological electron dynamics in previously unexplored regimes, revealing a wide range of novel physical phenomena.

Using our improved OFTP system, preliminary B-field-dependent experiments on a 2DEG reveal that optical photoexcitation induces changes in the conductivity at the cyclotron frequency ω_c , as expected (Fig. 2). Moreover, we also observed an unexpected photoinduced conductivity change at 1.1 THz and at a higher frequency that is nearly twice ω_c . This unexpected conductivity change at $\sim 2\omega_c$ decays more rapidly than that at ω_c and depends on the excitation fluence and applied magnetic field. We believe that these additional photoinduced changes in the conductivity are due to internal hydrogen-like transitions of ionized donor atoms in the GaAs buffer layers within the 2DEG heterostructure. The capability to do OFTP in a high magnetic field is fairly unique worldwide and will enable us to perform a wide range of novel experiments, for example, in artificial graphene systems.

Future Plans

CFs Hall conductivity as a function of e-e interactions

In the large density or small r_s (r_s is the electron potential energy to kinetic energy ratio) limit, particle-hole symmetry (PHS) is preserved. As the 2D electron density is reduced, e-e interactions

and thus the Landau level mixing effect become stronger, eventually breaking PHS and causing the CFs to become Schrodinger-like particles. This phase transition can be revealed by examining the CF Hall conductivity (σ_{xy}) at $\nu=1/2$ as a function of electron density. In the limit of weak e-e interactions, $\sigma_{xy} \cong 1/2$ [4], in units of e^2/h . On the other hand, in the limit of strong e-e interactions or large Landau level mixing, σ_{xy} is expected to deviate from $1/2$.

To examine this transition, we will carry out precision measurements of the magneto-resistivity ρ_{xx} and Hall resistivity ρ_{xy} in high quality HIGFETs. σ_{xy} is then calculated via the formula $\sigma_{xy} = \rho_{xy}/(\rho_{xx}^2 + \rho_{xy}^2)$. In these measurements, the B field will be fixed while sweeping the electron density. To facilitate determining the position of the $1/2$ state, temperature (T) dependent measurements will be carried out. It is expected that the traces for different temperatures will cross exactly at $\nu=1/2$. A phase diagram of σ_{xy} as a function of electron density (or r_s) will be constructed. This should allow us to study the topological phase transition induced by interaction effects.

Optical measurements will be carried out to further examine this transition at 0.3K. Non-contact measurements of the B field and density-dependent conductivity at THz frequencies will be done in our THz magneto-optical spectroscopy system. By tracking the dependence of the cyclotron frequency and σ_{xy} on electron density at a fixed B field, we should gain additional insight into the topological phase transition of CFs. We can also measure photo-induced conductivity changes with femtosecond time resolution; by varying the excitation intensity, we will modify the transient non-equilibrium electron density and track the resulting changes in σ_{xy} with femtosecond time resolution, enabling us to shed new light on the timescale over which electron-electron correlations develop in these systems.

Impact of disorder on the linear density dependence of CF conductivity

While studying the Berry phase of CFs in HIGFETs, we made a surprising observation regarding the linear density dependence of the CF conductivity [21]. This result differs from the conductivity of Schrödinger electrons at $B = 0$ T, where a n_e^2 density dependence is normally observed. At present, the origin of this striking linear density dependence at $\nu = 1/2$ is not known. We plan to carry out the following experiments to gain a deeper understanding of the transport mechanisms governing the CF conductivity that may give rise to a linear density dependence. Based on the microscopic model in the Halperin-Lee-Read theory [3], the scattering of CFs is due to long-range gauge field fluctuations that are related to the modulation doping in a quantum well structure. In order to understand the impact of this long range potential fluctuation, we plan to study the CF conductivity in alloy disordered HIGFETs, where a controlled amount of random Al disorder can be introduced into the nearly ideal GaAs 2DEG in undoped heterostructures of $Al_xGa_{1-x}As/Al_{0.3}Ga_{0.7}As$ with $x < 3\%$. The 2DEG is capacitively induced by applying a gate voltage to a HIGFET nanofabricated out of a heterostructure, and is free of long-range potential fluctuations from modulation doping impurities. Instead, disorder in the 2DEG is predominantly from the neutral Al alloy impurities, which is short-range on atomic size scales, with a 1.1 eV scattering potential [24]. The sample, being highly uniform, can remain conducting for densities down to $\leq 1 \times 10^9/\text{cm}^2$. We will examine how this short-range disorder affects CFs, in particular whether the linear density dependence still exists. This should allow us to study how long-range and short-range disorder fluctuations affect the CF conductivity. In addition, by tuning the density in alloy disordered HIGFETs, the interplay between e-e interactions and e-disorder interactions will also be studied. Finally, THz magneto-optical measurements will enable us to directly measure τ^* in the time domain, allowing us to determine whether it depends linearly on n_ν or varies with $n_\nu^{1/2}$.

References

- [1] J.K. Jain, Phys. Rev. Lett. 63, 199 (1989).
- [2] A. Lopez and E. Fradkin, Phys. Rev. B 44, 5246 (1991).
- [3] B.I. Halperin, P.A. Lee, and N. Read, Phys. Rev. B 47, 7312 (1993).
- [4] S.A. Kivelson, D.-H. Lee, Y. Krotov, and J. Gan, Phys. Rev. B 55, 15552 (1997).
- [5] F.D.M. Haldane, Phys. Rev. Lett. 93, 206602 (2004).
- [6] D. Kamburov et al., Phys. Rev. Lett. 113, 196801 (2014).
- [7] D.T. Son, Phys. Rev. X 5, 031027 (2015).
- [8] D.F. Mross, A. Essin, and J. Alicea, Phys. Rev. X 5, 011101 (2015).
- [9] M.A. Metlitski and A. Vishwanath, Phys. Rev. B 93, 245151 (2016).
- [10] S.D. Geraedts et al., Science 352, 197-201 (2016).
- [11] A.C. Potter, M. Serbyn, and A. Vishwanath, Phys. Rev. X 6, 031026 (2016).
- [12] M. Barkeshli, M. Mulligan, and M.P.A. Fisher, Phys. Rev. B 92, 165125 (2015).
- [13] A.C. Balram, C. Toke, and J.K. Jain, Phys. Rev. Lett. 115, 186805 (2015).
- [14] C. Wang and T. Senthil, Phys. Rev. B 94, 245107 (2016).
- [15] C. Wang, N.R. Cooper, B.I. Halperin, and A. Stern, arXiv:1701.00007.
- [16] G. Murthy and R. Shankar, Phys. Rev. B 93, 085405 (2016).
- [17] Kun Yang, Phys. Rev. B 88, 241105(R) (2013).
- [18] M. Ippoliti, S.D. Geraedts, and R.N. Bhatt, Phys. Rev. B 95, 201104 (2017).
- [19] K.S. Novoselov et al., Nature (London) 438, 197 (2005).
- [20] Y. Zhang, Y.-W. Tan, H.L. Stormer, and P. Kim, Nature (London) 438, 201 (2005).
- [21] W. Pan, W. Kang, et al., arXiv:1702.07307, accepted to Nature Physics.
- [22] N. Kamaraju et al., Appl. Phys. Lett. 106, 031902 (2015).
- [23] T. Maag et al., Nature Phys. 12, 119 (2016).
- [24] Wanli Li, G.A. Csáthy, D.C. Tsui, L.N. Pfeiffer, and K.W. West, Appl. Phys. Lett. 83, 2832 (2003).

Publications (October'15 to September'17)

Publications intellectually led by this FWP:

1. S.K. Lyo and **W. Pan**, J. Appl. Phys. 118, 195705 (2015).
2. D. Laroche et al., and **T. M. Lu**, AIP Advances 5, 107106 (2015).
3. F. Leonard et al., and **G.T. Wang**, Nano Letters 15, 8129 (2015).
4. E. Song et al., **W. Pan**, **G.T. Wang**, and J.A. Martinez, Nanotechnology 27, 015204 (2016).
5. G. C. Dyer et al., **E. A. Shaner**, and **W. Pan**, Appl. Phys. Lett. 108, 013106 (2016)
6. **T. M. Lu**, **G.T. Wang**, **W. Pan** et al., Appl. Phys. Lett. 108, 063104 (2016).
7. **T. M. Lu** et al., Scientific Reports 6:20967 (2016).
8. M. Seo et al., and **R.P. Prasankumar**, Scientific Reports 6:21601 (2016).
9. D. Laroche et al., and **T. M. Lu**, Appl. Phys. Lett. 108, 233504 (2016).
10. B.V Olson et al., and **E.A. Shaner**, Applied Physics Letters 108, 252104 (2016).
11. B.V. Olson et al., and **E.A. Shaner**, Applied Physics Letters 109, 022105 (2016).
12. **W. Pan**, K.W. Baldwin, K.W. West, L.N. Pfeiffer, and **D.C. Tsui**, Phys. Rev. B 94, 161303(R) (2016).
13. W. Yu et al., and **W. Pan**, Scientific Reports 6:35357 (2016).
14. E. A. Kadlec et al., and **E. A. Shaner**, Appl. Phys. Lett. 109, 261105 (2016)
15. S. Boubanga-Tombet et al., **G. T. Wang**, and **R. P. Prasankumar**, ACS Photonics 3, 2237 (2016).
16. **T.M. Lu** et al., Scientific Reports 7:2468 (2017).
17. **W. Pan**, W. Kang, K.W. Baldwin, K.W. West, L.N. Pfeiffer, **D.C. Tsui**, arXiv:1702.07307, accepted to Nature Physics.

Collaborative publications:

18. O. Mitrofanov et al., Solid State Communications 224, 47 (2015).
19. X. Shi et al., J. Appl. Phys. 118, 133905 (2015).
20. Omri Wolf et al., Appl. Phys. Lett. 107, 151108 (2015).
21. B.V. Olson et al., Appl. Phys. Lett. 107, 183504 (2015).
22. B. V. Olson et al., Appl. Phys. Lett. 107, 261104 (2015).
23. Changyi Li et al., Nanoscale 8, 5682-5687 (2016).
24. Heather J. Haugan et al., Journal of Vacuum Science & Technology B 34, 02L104 (2016).
25. N. F. Brady et al., J. Phys. Cond. Matt. 28, 125603 (2016).
26. Y. Aytac et al., J. Appl. Phys. 119, 215705 (2016).
27. M. D. Goldflam et al., Appl. Phys. Lett. 109, 251103 (2016).
28. Qi Zhang et al., Nature Physics (2016), doi:10.1038/nphys3850.
29. Jian Li et al., Phys. Rev. Lett. 117, 046804 (2016).
30. Nikolai G. Kalugin et al., 2D Materials 4, 015002 (2017).
31. Heather J. Haugan et al., Opt. Eng. 56, 091604 (2017).
32. Y. Jiang et al., Phys. Rev. B 95, 045116 (2017).
33. P. Bowlan et al., Optica 4, 383 (2017).

Transient Studies of Nonequilibrium Transport in Two-Dimensional Semiconductors

Principal Investigator: Jonathan Bird, University at Buffalo, jbird@buffalo.edu

Program Scope

The overarching objective of this research is to apply time-dependent measurement techniques to investigate aspects of nonequilibrium transport in two-dimensional (2D) semiconductors. This work builds on progress made by the PI during the prior period of DOE support, utilizing nanosecond-duration electrical pulsing to reveal novel aspects of quantum transport in different mesoscopic devices. In comparison to conventional DC measurements, transient studies provide a time-resolved picture of carrier relaxation mechanisms, allowing many of the fundamental interactions that govern transport to be revealed. In the current period of support, the 2D semiconductor of interest is graphene, and transient pulsing is utilized in order to investigate several important aspects of its transport: 1. The search for negative differential conductance in graphene. 2. Probing fundamental relaxation processes in graphene in real time.

This research program yields significant impact in terms of our understanding of the fundamental condensed-matter physics of 2D semiconductors. Work on the search for negative differential conductance may open up a new field of experimental research, on the manifestations of high-field instabilities in 2D materials. It may also drive the development of new solid-state terahertz sources, which exploit the large drift velocities inherent to graphene to realize terahertz-frequency oscillators based on the driven motion of high-field domains. Additionally, the transient investigations of energy relaxation and dephasing in graphene yield important fundamental insight into the microscopic processes responsible for these processes.

Recent Progress

This project was initiated in November 2016, and in the intervening ten months we have made progress on a number of inter-related issues as we now describe below.

1. Nonlinear Differential Conductance of Graphene in the Presence of Quantum Corrections

In this work, we have been exploring the manner in which the nonlinear differential conductance of graphene is modified in the presence of quantum corrections to the conduction, most notably weak localization and electron-electron interactions. In our most recently published work [1], we have demonstrated the presence of a zero-bias anomaly in graphene that arises from these quantum-transport phenomena. Since the presence of this anomaly obscures the contributions to the resistivity due to other mechanisms, such as electron-impurity and electron-phonon scatter-

ing, we have developed a technique of “differential-conductance mapping” to suppress the influence of quantum corrections and to allow the study of the underlying classical resistivity terms.

Accompanying our experimental efforts, we have worked with Prof. Jonas Fransson of Uppsala University to develop a theoretical picture of the nonlinear suppression of the quantum corrections in graphene. In spite of all the work that has been done in recent decades, to understand the manner in which quantum corrections are manifested in the *linear* conduction of mesoscopic systems, we were surprised to find that the nonlinear counterpart of this problem had really attracted very little attention. In our theoretical study [2], we explore the manner in which the quantum correction due to weak localization is suppressed in weakly-disordered graphene, when it is subjected to the application of a non-zero voltage. Using a nonequilibrium Green function approach, we address the scattering generated by the disorder up to the level of the maximally crossed diagrams, capturing the interference among different, impurity-defined, Feynman paths. Our calculations of the charge current, and of the resulting differential conductance, reveal the logarithmic divergence typical of weak localization in linear transport. The main finding of our study is that the applied voltage suppresses the weak localization contribution in graphene, in a manner that is dependent upon the temperature (T). The latter parameter sets an effective scale ($k_B T/e$), below which the applied voltage has little noticeable effect on the localization correction. Once this threshold is exceeded, however, the suppression of localization is manifested directly as a logarithmic increase of the conductance. This behavior can be discussed in terms of a “self-averaging” of diffusing electron waves, which arises as they undergo multiple scattering events within the graphene layer. Our results appear consistent with prior experimental observations of the low-temperature differential conductance of mesoscopic graphene, and with our own more recent [1] observations.

2. Transient Investigations of Nonlinear Transport in Encapsulated Graphene/BN Devices

In this work, we have been extending our recent investigations of high field velocity saturation in graphene-on-SiO₂ devices [3,4], to explore the transient transport of hot carriers in graphene channels, fully encapsulated in hexagonal boron nitride. This work involves a collaboration with the group of Prof. Nobuyuki Aoki of Chiba University and is motivated by the potential of demonstrating negative differential conductance in this system. An example of one of the devices that we have studied is indicated in Fig. 1. In this optical micrograph, we clearly see the coplanar waveguides that provide (at left and right) the input and output signal lines of the device. The long, narrow structure shown at the center of the image is a 1- μ m wide finger gate that controls the carrier concentration in a graphene channel. This channel is fully encapsulated by BN, which may be identified as the two irregularly-shaped flake structures at the center of the image. In our experiments, we apply a scheme of repetitive pulsing, using transient pulses as short as just a few nanoseconds, as we have discussed previously for graphene-on-SiO₂ devices [3,4].

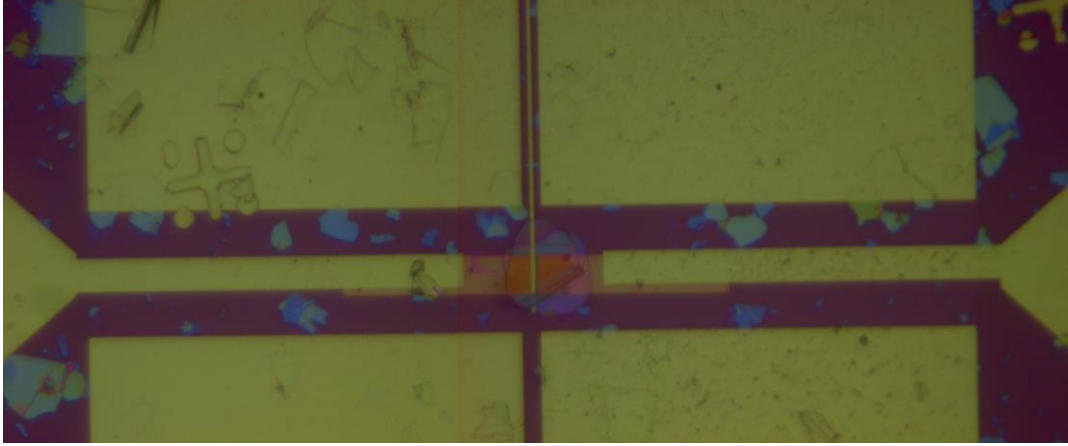


Fig. 1. Optical micrograph of a fabricated graphene/BN RF transistor. For further details please refer to the text above.

Our initial investigations of the transient transport in the hybrid graphene/BN devices indicate that this transport is essentially free of the influence of defect related carrier trapping, a phenomenon that plagues graphene-on-SiO₂ devices [3,4]. At the same time, we have also found that the influence of Joule heating is significantly suppressed in these devices. Using the top-gate to vary the carrier density in the graphene layer, we observe a transition from current saturation to linear I - V curves as the charge neutrality point is approached from either the conduction or valence bands. At present, we are working with Prof. Jong Han of the University at Buffalo to analyze this transition in terms of strong nonequilibrium carrier generation by Landau-Zener tunneling.

Future Plans

In future work we are planning to extend our current investigations on nonlinear transient transport in hybrid graphene/BN devices. Further studies, performed on additional devices with varying channel length, are required to confirm our recent observations in these structures. We are also interested in extending our measurements to explore nonequilibrium carrier processes in transition metal dichalcogenides, such as MoS₂ and WS₂, in which the very different bandstructure from graphene may lead to novel possibilities for transferred-electron effects (e.g. the Gunn effect).

References

1. R. Somphonsane, H. Ramamoorthy, G. He, J. Nathawat, C.-P. Kwan, N. Arabchigavkani, Y.-H. Lee, J. Fransson, and J. P. Bird, “*Evaluating the sources of graphene’s resistivity using differential conductance*”, *Sci. Rep.*, *accepted for publication* (2017).

2. J. Fransson, R. Somphonsane, H. Ramamoorthy, G. He, and J. P. Bird, “*Voltage-induced suppression of weak localization in graphene*”, Phys. Rev. B, *under review*.
3. H. Ramamoorthy, R. Somphonsane, J. Radice, G. He, C.-P. Kwan, and J. P. Bird, ““Freeing” graphene from its substrate: Observing intrinsic velocity saturation with rapid electrical pulsing”, Nano Lett. **16**, 399 – 403 (2016).
4. H. Ramamoorthy, R. Somphonsane, J. Radice, G. He, J. Nathawat, C.-P. Kwan, M. Zhao, and J. P. Bird, “*Probing charge trapping and joule heating in graphene field-effect transistors by transient pulsing*”, Semicond. Sci. Technol. **32**, 084005 (2017).

Publications

1. R. Somphonsane, H. Ramamoorthy, G. He, J. Nathawat, C.-P. Kwan, N. Arabchigavkani, Y.-H. Lee, J. Fransson, and J. P. Bird, “*Evaluating the sources of graphene’s resistivity using differential conductance*”, Scientific Reports, *accepted for publication* (2017).
2. M. Matsunaga, A. Higuchi, G. He, T. Yamada, P. Krüger, Y. Ochiai, Y. Gong, R. Vajtai, P. M. Ajayan, J. P. Bird, and N. Aoki, “*Nanoscale-barrier formation induced by low-dose electron-beam exposure in ultrathin MoS₂ transistors*”, ACS NANO **10**, 9730 – 9737 (2016).
2. G. He, H. Ramamoorthy, C.-P. Kwan, Y.-H. Lee, J. Nathawat, R. Somphonsane, M. Matsunaga, A. Higuchi, T. Yamanaka, N. Aoki, Y. Gong, X. Zhang, R. Vajtai, P. M. Ajayan, and J. P. Bird, “*Thermally-assisted nonvolatile memory in monolayer MoS₂ transistors*”, Nano Lett. **16**, 6445 – 6451 (2016).
3. S. Xiao, Y. Yoon, Y.-H. Lee, J. P. Bird, Y. Ochiai, N. Aoki, J. L. Reno, and J. Fransson, “*Detecting weak coupling in mesoscopic systems with a nonequilibrium Fano resonance*”, Phys. Rev. B **93**, 165435 (2016).
4. H. Ramamoorthy, R. Somphonsane, J. Radice, G. He, C.-P. Kwan, and J. P. Bird, ““Freeing” graphene from its substrate: Observing intrinsic velocity saturation with rapid electrical pulsing”, Nano Lett. **16**, 399 – 403 (2016).
5. D. K. Ferry, R. Somphonsane, H. Ramamoorthy, and J. P. Bird, “*Plasmon-mediated energy relaxation in graphene*”, Appl. Phys. Lett. **107**, 262103 (2015).
6. I. Rotter and J. P. Bird, “*A review of progress in the physics of open quantum systems: theory and experiment*”, Rep. Prog. Phys. **78**, 114001 (2015).
7. W. Gao, X. Wang, R. Chen, D. B. Eason, G. Strasser, J. P. Bird, and J. Kono, “*Electroluminescence from GaAs/AlGaAs heterostructures in strong in-plane electric fields: Evidence for k- and real-space charge transfer*”, ACS Photonics **2**, 1155 – 1159 (2015).
8. G. He, K. Ghosh, U. Singisetti, H. Ramamoorthy, R. Somphonsane, G. Bohra, M. Matsunaga, A. Higuchi, N. Aoki, S. Najmaei, Y. Gong, X. Zhang, R. Vajtai, P. M. Ajayan, and J. P. Bird, “*Conduction mechanisms in CVD-grown monolayer MoS₂ transistors: From variable-range hopping to velocity saturation*”, Nano Lett. **15**, 5052 – 5058 (2015).

Session 2

Novel Temperature Limited Spectroscopy of Quantum Hall Systems

Raymond Ashoori, MIT (Principal Investigator)

Program Scope:

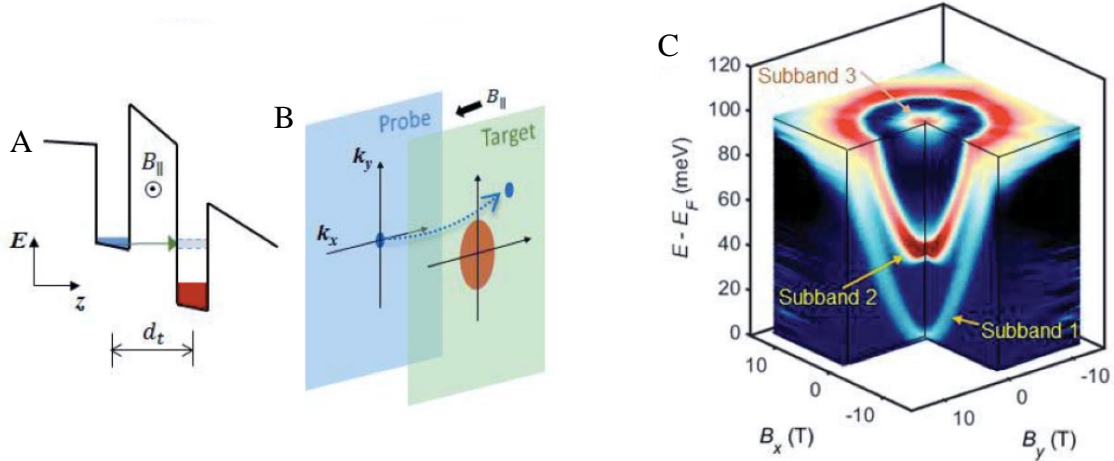
The “single-particle spectral function” obtained from techniques such as photoemission or tunneling spectroscopy is among the most fundamental quantities in theories of highly interacting systems, answering the question, “at which energies and momenta can electrons be added to (or removed from) the system?” Such spectra have provided central insights into phenomena such as superconductivity and Mott insulators. While scanning tunneling microscopy and other tunneling methods have provided partial spectral information, until now only angle-resolved photoemission spectroscopy (ARPES) has permitted a comprehensive determination of the spectral function of materials in both momentum and energy. However, both STM and ARPES operate only on metallic electronic systems at the material surface, and ARPES cannot work in the presence of applied magnetic fields. This excludes ARPES and STM from studying systems underneath surfaces such as the two-dimensional electron system 2DES in semiconductors, host to the remarkable quantum Hall effects (1985 and 1998 Nobel Prizes). The 2DES continues to produce fascinating results as scientists discover new ways in which electrons that strongly repel one another correlate their motions to minimize the energy of this repulsion, creating a plethora of new quantum states of matter. This proposal describes the development and use of two means for determining the spectral function inside of semiconductors and other material, each involving the application of hundreds of thousands of short electrical pulses to induce and track, via charge measurements, the motion of electrons across a tunnel barrier.

The first method not provide momentum resolution but yields extremely high resolution in energy (limited only by sample temperature). Recently, the use this pulsed capacitive tunneling spectroscopy with microvolt resolution and in a dilution refrigerator cooled to 8 mK led to the discovery of sharp resonance for tunneling into the 2D electronic system. Detailed study of the behavior of this resonance revealed that it originates from the vibrations of a long-range ordered electronic “Wigner Crystal”. We aim to extend this method to study other novel states of the 2D electronic system such as “stripe” and “bubble” phases by resolving the effects of their vibrations on tunneling spectra. The work also includes a broad study of intriguing quantum Hall states for new spectral features such as might arise from spin textures or fractionally charged quasiparticles. We are also working to use the pulsed tunneling method at the single electron level in a study of ultra-clean quantum dots.

The second method is called “Momentum and Energy Resolved Tunneling Spectroscopy” (MERTS). MERTS determines the full electronic spectral function of 2DES in both momentum and energy. It provides a direct high-resolution and high-fidelity probe of the dispersion and dynamics of the interacting 2D electron system. By ensuring the system of interest remains under equilibrium conditions, the technique can uncover delicate signatures of many-body effects involving electron-phonon interactions, plasmons, polarons, and has demonstrated a novel phonon analog of the vacuum Rabi splitting in atomic systems. Moreover, MERTS has the potential to reveal detailed crystallographic information on ordering of electrons in novel states such as the stripe and bubble phases described above.

Recent Progress: Momentum and Energy Resolved Tunneling Spectroscopy

We have succeeded at a long-standing goal, to produce a version of tunneling spectroscopy that yields a full determination of the momentum and energy resolved spectral function, with spectra comparable to those produced by angle resolved photoemission spectroscopy (ARPES). In contrast with ARPES, our momentum and energy resolved tunneling spectroscopy (MERTS) works underneath surfaces and even deep inside materials, it can work on systems that are electrically insulating and even in



systems with zero electron density, and it can function for 2D systems in high perpendicular magnetic fields.¹ MERTS has comparable energy and momentum resolution (and momentum reach) to laser-based ARPES systems,^{2,3} a capability that is critical for investigation of the subtle e-e interaction effects near the Fermi level.

Figure 1 | Schematics of tunneling device and principles of energy-momentum selection process. **A** The tunneling structure used in the experiment. Two GaAs QWs (width of 20 nm each) are separated by a $\text{Al}_{0.8}\text{Ga}_{0.2}\text{As}$ potential barrier (6 nm). Electrons in the left (probe) QW with nearly zero planar momentum probe electronic states in the right (target) QW. **B** The injection of an electron packet probes empty available states in the target layer. Diagram for explaining the momentum selection mechanism. The in-plane field creates a momentum boost in the tunneling process to displace the zero planar momentum into $k_{final} = eBd_t/\hbar$ in the bottom QW. **C** Measured spectra with B_{\parallel} along the crystallographic axis of [100] and [010] of GaAs. Multiple unoccupied QW subbands are visible.

In MERTS, we generate a collimated packet of electrons with precisely-defined energy and momentum from an adjacent 2D quantum well, and we use tunneling to inject the electrons into the unoccupied quantum states of the target 2D system to measure the target 2D system's spectral function. Electrons from this collimated beam can tunnel into the target 2D electron system only when unoccupied states are available with the same energy and momentum, resulting in E - k selectivity. The tunneling current reflects the spectral function for adding a particle into the 2D system. For high E - k resolution, we prepare electrons with a very small Fermi surface in the probe layer (containing a very

low density of electrons $n = 3 \times 10^{10} \text{ cm}^{-2}$ with $E_F \approx 1 \text{ meV}$ and $k_F = 0.004 \text{ \AA}^{-1}$; these numbers set the resolution of the technique) at $E = 0$ and $k = 0$ (Γ -point in the GaAs conduction band minimum), and translate the momentum of the packet using a magnetic field B_{\parallel} applied perpendicular to the tunneling direction giving electrons a momentum shift of $\Delta k_{x,y} = \frac{eB_{\parallel}d_t}{\hbar}$ in the tunneling process. Here, $\Delta k_{x,y}$ is the momentum translation of the tunneling electrons, and d_t is the tunneling distance (Fig. 1A). In previous studies⁴ double quantum well experiments involving large Fermi surfaces in both the probe and target wells, the tunneling measurements involved complicated convolutions of two systems and electrical conductivity through both layers, making it unfeasible to obtain direct spectral information. In MERTS we instead achieve full momentum and energy resolution by adapting our pulsed tunneling method^{5,6} that requires no direct electrical contact to the system of 2 quantum wells and does not rely on conductivity of the 2D systems. The method functions even if either or both of the 2D systems are electrically insulating. The pulsed tunneling has important elements that contributed to the success of MERTS by allowing us to **(i)** maintain the small Fermi surface of source electrons (probe layer) into nearly a single point and **(ii)** to eliminate lateral transport in either layer to ensure uniform tunneling at all points in the plane.

The results shown in Figure 1C are actual data – not a schematic drawing or a simulation. MERTS allows us to probe the high-energy spectrum of systems at very low temperature equilibrium. We achieve this by using short pulses with long wait times between pulses. MERTS has uncovered delicate signatures of many-body effects involving electron-phonon interactions, plasmons, polarons, and has demonstrated a novel phonon analog of the vacuum Rabi splitting in atomic systems. We are working to apply MERTS to explore a number of features in quantum Hall systems such as stripe and bubble phases and the Wigner crystals that we observed in previous non-momentum resolved tunneling studies.⁷

Future Plans:

The chief objectives of our work under this DOE proposal are:

- 1) To advance the use of our pulsed tunneling and MERTS techniques and develop them as a method for use in a wider range of quantum Hall systems.
- 2) To use pulsed tunneling and MERTS to examine spatially ordered structure within the 2D electronic system. We will perform crystallographic measurements on the Wigner Crystal and stripe and bubble phases.
- 3) To find the magnetoplasmon mode of the Wigner Crystal and use it as a means of studying the Wigner Crystal and other ordered structure when the magnetophonon mode is obscured by the magnetic field induced Coulomb gap.
- 4) To perform pulsed tunneling and MERTS in AIAs quantum wells and explore the effects of valley pseudospin for novel ordered states and for valley skyrmions.

References

1. Jang, J. *et al.* Full Momentum and Energy Resolved Spectral Function of a 2D Electronic System. *ArXiv170101684 Cond-Mat* (2017).
2. Okazaki, K. *et al.* Octet-Line Node Structure of Superconducting Order Parameter in KFe₂As₂. *Science* **337**, 1314–1317 (2012).
3. Damascelli, A., Hussain, Z. & Shen, Z.-X. Angle-resolved photoemission studies of the cuprate superconductors. *Rev. Mod. Phys.* **75**, 473–541 (2003).
4. Eisenstein, J. P., Gramila, T. J., Pfeiffer, L. N. & West, K. W. Probing a two-dimensional Fermi surface by tunneling. *Phys Rev B* **44**, 6511–6514 (1991).
5. Dial, O. E., Ashoori, R. C., Pfeiffer, L. N. & West, K. W. High-resolution spectroscopy of two-dimensional electron systems. *Nature* **448**, 176–179 (2007).
6. Dial, O. E., Ashoori, R. C., Pfeiffer, L. N. & West, K. W. Anomalous structure in the single particle spectrum of the fractional quantum Hall effect. *Nature* **464**, 566–570 (2010).
7. Jang, J., Hunt, B. M., Pfeiffer, L. N., West, K. W. & Ashoori, R. C. Sharp tunnelling resonance from the vibrations of an electronic Wigner crystal. *Nat. Phys.* **13**, 340–344 (2017).

Publications in the last two years acknowledging Federal support solely from DOE BES for Ashoori Group portion

1. Joonho Jang, Heun Mo Yoo, Loren Pfeiffer, Ken West, K.W. Baldwin, and Raymond Ashoori, “Full Momentum and Energy Resolved Spectral Function of a 2D Electronic System”, provisionally accepted to Science. (<https://arxiv.org/abs/1701.01684>)
2. Joonho Jang, Benjamin M. Hunt, Loren N. Pfeiffer, Kenneth W. West, and Raymond C. Ashoori, “Sharp tunnelling resonance from the vibrations of an electronic Wigner crystal” *Nature Physics*, published online 12 DECEMBER 2016 | DOI: 10.1038/NPHYS3979
3. B.M. Hunt, J.I.A. Li, A.A. Zibrov, L. Wang, T. Taniguchi, K. Watanabe, J. Hone, C. R. Dean, M. Zaletel, R.C. Ashoori, and A.F. Young, “Competing valley, spin, and orbital symmetry breaking in bilayer graphene”, in preparation for resubmission to *Nature Nanotechnology* (<https://arxiv.org/abs/1607.06461>)

Program Title: Magneto-transport in GaAs Two-dimensional Hole Systems

Principal Investigator: M. Shayegan

Mailing Address: Department of Electrical Engineering, Princeton University, Princeton, NJ, 08544

E-mail: shayegan@princeton.edu

Program Scope

Two-dimensional (2D) carrier systems confined to modulation-doped semiconductor heterostructures provide a nearly ideal testing ground for exploring new physical phenomena. At low temperatures and in the presence of a strong magnetic field, these systems exhibit fascinating, often unexpected, many-body states, arising from the strong electron-electron interaction. Examples include the fractional quantum Hall liquid, the Wigner solid, and the newly discovered striped and bubble phases in the higher Landau levels.

Much of the work on the clean 2D systems has been performed on 2D *electrons* confined to a remotely-doped GaAs quantum well. The goal of this project is to study the materials science and physics of 2D *holes* confined to such wells. Compared to the 2D electrons in GaAs, the 2D holes possess a more complex energy band structure which not only depends on the quantum well width and 2D hole density, but it can also be tuned via perpendicular electric field (gate bias), parallel magnetic field, and strain. These characteristics add new twists and allow for insight into fundamental phenomena in confined, low-disorder carrier systems.

In our project we study 2D hole samples which are grown via state-of-the-art molecular beam epitaxy, and use low-temperature magneto-transport measurements to explore their novel physics. Among the problems we are addressing are the shapes of Fermi contours of 2D holes and of flux-hole composite fermions as a function of parameters such as parallel magnetic field and/or strain. Also of interest are the fractional quantum Hall states, including the state at the even-denominator filling $\nu = 1/2$, in 2D hole systems confined to wide GaAs quantum wells. In our work, we collaborate closely with Prof. Roland Winkler (Univ. of Northern Illinois), who is an expert in calculating the energy band structure and Landau levels in 2D hole systems, and Dr. Loren Pfeiffer who is a world expert in molecular beam epitaxy.

Recent Progress

A hallmark of the GaAs 2D holes is their complex band structure. Thanks to the spin-orbit interaction, the 2D hole bands are often split at finite values of wave vector (k) and also become anisotropic as k grows in different in-plane directions. One goal of our proposed research is to quantitatively probe these dispersions, both experimentally and theoretically. Experimental determination of the 2D hole dispersions has long been a subject of interest. It continues to be a subject of active research, thanks partly to the interest in spintronic devices and also the possibility that holes in confined structures might have a long spin coherence time (because of the lack of overlap of holes' p -type wave function with the nuclei) and be useful in quantum computing. Here we describe our recent results in two areas, demonstrating how the complex band structure of 2D holes can in fact be utilized to learn exciting new physics.

A. Observation of an unusual, anisotropic Wigner crystal phase at Landau level filling factor $\nu = 1/2$ in hole systems confined to wide GaAs quantum wells:

In 2D hole systems confined to wide GaAs quantum wells, where the heavy- and light-hole states are close in energy, there is a very unusual crossing of the lowest two Landau levels as the sample is tilted in a magnetic field. The crossing leads to a weakening or disappearance of the commonly seen odd-denominator fractional quantum Hall states in the filling range $1/3 \leq \nu \leq 2/3$. But, surprisingly, a new fractional quantum Hall state at the even-denominator filling $\nu = 1/2$ comes to life at the crossing in samples with appropriate parameters (quantum well-width and density). In our recent work, we discovered yet another new correlated phase of 2D hole systems in slightly wider quantum wells near this crossing [10]. The phase is manifested by an *anisotropic insulating* behavior at low temperatures which appears in a large range of low Landau level fillings $1/3 < \nu < 2/3$ when the sample is tilted in magnetic field to an intermediate angle (see Fig. 1). The parallel field component (B_{\parallel}) leads to a crossing of the lowest two Landau levels, and an elongated hole wave function in the direction of B_{\parallel} . Under these conditions, the in-plane resistance exhibits an insulating behavior, with the resistance along B_{\parallel} about 10 times smaller than the resistance perpendicular to B_{\parallel} . We interpreted this anisotropic insulating phase as a two-component, striped Wigner crystal.

B. Transference of Fermi Contour Anisotropy to Composite Fermions:

There has been a surge of recent interest in the role of anisotropy in interaction-induced phenomena in 2D charged carrier systems. A fundamental question is how an anisotropy in the energy-band structure of the carriers at zero magnetic field affects the properties of the interacting particles at high fields, in particular of the composite fermions (CFs) and the fractional quantum Hall states. In our latest work we demonstrated tunable anisotropy for holes and hole-flux CFs confined to GaAs quantum wells, via applying in situ in-plane strain and measuring their Fermi wave vector anisotropy through geometric resonance measurements. For

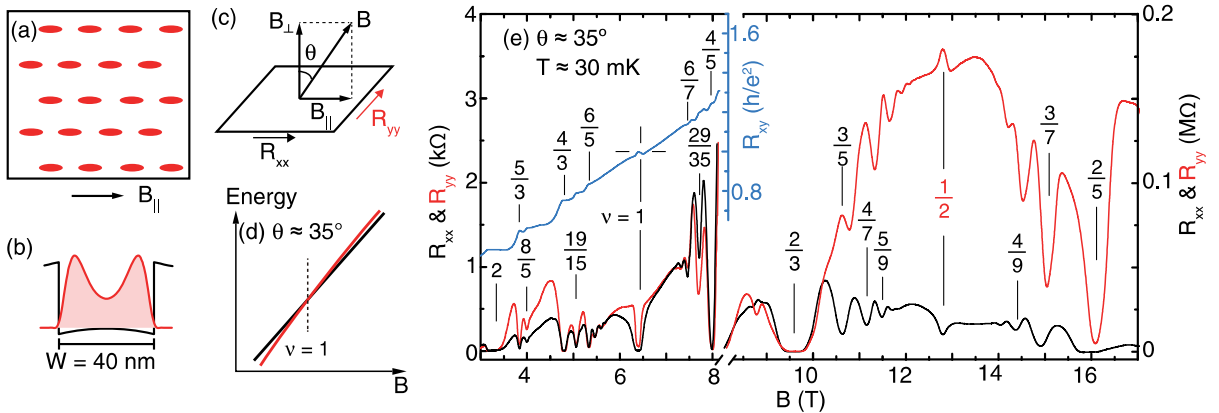


Fig. 1. (a) Conceptual rendition of an anisotropic (striped) Wigner crystal. (b) The charge distribution (red) and potential (black), from calculating the Schrodinger and Poisson's equations self-consistently at $B = 0$. (c) Experimental geometry: R_{xx} and R_{yy} denote the longitudinal magnetoresistance measured along and perpendicular to the parallel magnetic field (B_{\parallel}), respectively. (d) Schematic diagram, showing the crossing of the lowest two Landau levels at $\theta \approx 35^\circ$ near $\nu = 1$. (e) Magnetoresistance traces measured at tilt angle $\theta \approx 35^\circ$ for a 2D hole system with density $p = 1.28 \times 10^{11} \text{ cm}^{-2}$ and confined to a 40-nm-wide GaAs quantum well. Note the factor of 50 change in the scale for R_{xx} and R_{yy} for $B > 8$ T. We observe an anisotropic insulating phase in a large filling factor range, from $\sim 2/3$ to $\sim 1/3$; note also the competition with fractional quantum Hall states at several fillings. (After Ref. 10)

strains on the order of 10^{-4} we observed significant deformations of the shapes of the Fermi contours for both holes and CFs. The measured Fermi contour anisotropy for CFs at high magnetic field (α_{CF}) is less than the anisotropy of their low-field hole (fermion) counterparts (α_F), and closely follows a simple relation $\alpha_{CF} = (\alpha_F)^{1/2}$. The energy gap measured for the $\nu = 2/3$ fractional quantum Hall state, on the other hand, is nearly unaffected by the Fermi contour anisotropy up to $\alpha_F \sim 3.3$, the highest anisotropy achieved in our experiments. These are fascinating results, and are finding verification in numerical calculations.

Future plans

We plan to perform experiments on a novel bilayer hole system that allows us to directly probe the Wigner solid phase of 2D holes and its impact on a nearby layer containing hole-flux CFs. This will entail measuring the magneto-resistance of a bilayer hole system where one layer has a very low density and is in the Wigner crystal regime ($\nu \ll 1$), while the other (“probe”) layer is near $\nu = 1/2$ and hosts a sea of composite fermions. The data should exhibit commensurability features in the magneto-resistance of the composite fermion layer, induced by the periodic potential of Wigner crystal holes in the other layer. We can use such data to probe the symmetry of the Wigner crystal, its lattice constant, and melting.

Publications acknowledging DOE support; since 2015:

1. S. Hasdermir, Yang Liu, H. Deng, M. Shayegan, L.N. Pfeiffer, K.W. West, and K.W. Baldwin, “ $\nu = 1/2$ Fractional Quantum Hall Effect in Tilted Magnetic Fields,” *Phys. Rev. B* **91**, 045113 (2015).
2. M.A. Mueed, D. Kamburov, Y. Liu, M. Shayegan, L.N. Pfeiffer, K.W. West, K.W. Baldwin, and R. Winkler, “Composite Fermions with a Warped Fermi Contour,” *Phys. Rev. Lett.* **114**, 176805 (2015).
3. M.A. Mueed, D. Kamburov, M. Shayegan, L.N. Pfeiffer, K.W. West, K.W. Baldwin, and R. Winkler, “Splitting of the Fermi Contour of Quasi-2D Electrons in Parallel Magnetic Fields,” *Phys. Rev. Lett.* **114**, 236404 (2015).

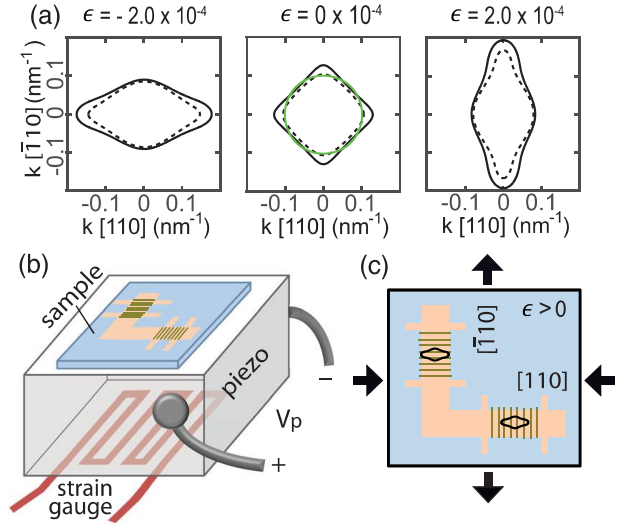


Fig. 2. (a) Calculated Fermi contours of GaAs holes at density $p = 1.8 \times 10^{11} \text{ cm}^{-2}$ as a function of strain ϵ along the $[1\bar{1}0]$ direction. Solid and dashed contours represent two spin-split_{SEP} subbands; the green circle with radius $k_0 = (2\pi p)^{1/2}$ shows a spin-degenerate, circular Fermi contour at the same density. (b) Schematic of the experimental setup showing a thinned GaAs wafer glued on a piezo-actuator. A strain gauge mounted underneath measures the strain along $[1\bar{1}0]$. (c) Sample fabricated to an L-shaped Hall bar has regions with electron-beam resist gratings on the surface. Thick arrows indicate the deformation of the crystal when a positive voltage V_P is applied to the piezo. The resulting deformed cyclotron orbits are shown in black; note that these are rotated by 90° with respect to the Fermi contours in reciprocal space. The shapes of the orbits and therefore the Fermi contours are determined via commensurability oscillations measurements.

4. M.A. Mueed, D. Kamburov, S. Hasdemir, M. Shayegan, L.N. Pfeiffer, K.W. West, and K.W. Baldwin, “Geometric Resonance of Composite Fermions Near the $\nu = 1/2$ Fractional Quantum Hall State,” *Phys. Rev. Lett.* **114**, 236406 (2015).
5. Yang Liu, S. Hasdemir, M. Shayegan, L.N. Pfeiffer, K.W. West, and K.W. Baldwin, “Unusual Landau Level Pinning and Correlated $\nu = 1$ Quantum Hall Effect in Hole Systems Confined to Wide GaAs Quantum Wells,” *Phys. Rev. B* **92**, 195156 (2015).
6. Yang Liu, S. Hasdemir, J. Shabani, M. Shayegan, L.N. Pfeiffer, K.W. West, and K.W. Baldwin, “Multicomponent Fractional Quantum Hall States with Subband and Spin Degrees of Freedom,” *Phys. Rev. B* **92** (Rapid Communications), 201101(R) (2015).
7. M.A. Mueed, D. Kamburov, S. Hasdemir, L.N. Pfeiffer, K.W. West, K.W. Baldwin, and M. Shayegan, “Anisotropic Composite Fermions and Fractional Quantum Hall Effect,” *Phys. Rev. B* **93**, 195436 (2016).
8. M.A. Mueed, Md. Shafayat Hossain, L.N. Pfeiffer, K.W. West, K.W. Baldwin, and M. Shayegan, “Reorientation of the Stripe Phase of 2D Electrons by a Minute Density Modulation,” *Phys. Rev. Lett.* **117**, 076803 (2016).
9. H. Deng, Yang Liu, I. Jo, L.N. Pfeiffer, K.W. West, K.W. Baldwin, and M. Shayegan, “Commensurability Oscillations of Composite Fermions Induced by the Periodic Potential of a Wigner Crystal,” *Phys. Rev. Lett.* **117**, 096601 (2016). [**Featured in *Physics*; Editor’s Suggestion.**]
10. Yang Liu, S. Hasdemir, L.N. Pfeiffer, K.W. West, K.W. Baldwin, and M. Shayegan, “Observation of an Anisotropic Wigner Crystal,” *Phys. Rev. Lett.* **117**, 106802 (2016).
11. Yang Liu, M. Mueed, Md. Shafayat Hossain, S. Hasdemir, L. Pfeiffer, K. West, K. Baldwin, M. Shayegan, “Morphing of 2D Hole Systems at $\nu = 3/2$ in Parallel Fields: Compressible, Stripe, and Fractional Quantum Hall Phases,” *Phys. Rev. B* **94**, 155312 (2016).
12. M.A. Mueed, D. Kamburov, L.N. Pfeiffer, K.W. West, K.W. Baldwin, and M. Shayegan, “Geometric Resonance of Composite Fermions near Bilayer Quantum Hall States,” *Phys. Rev. Lett.* **117**, 246801 (2016).
13. Insun Jo, Yang Liu, L.N. Pfeiffer, K.W. West, K.W. Baldwin, M. Shayegan, and R. Winkler, “Signatures of an Annular Fermi Sea,” *Phys. Rev. B* **95**, 035103 (2017).
14. M.A. Mueed, D. Kamburov, Md. Shafayat Hossain, L.N. Pfeiffer, K.W. West, K.W. Baldwin, and M. Shayegan, “Search for Composite Fermions at Filling Factor $5/2$: Role of Landau Level and Subband Index,” *Phys. Rev. B* **95**, 165438 (2017).
15. Insun Jo, K. A. Villegas Rosales, M. A. Mueed, L. N. Pfeiffer, K. W. West, K. W. Baldwin, R. Winkler, Medini Padmanabhan, and M. Shayegan, “Transference of Fermi Contour Anisotropy to Composite Fermions,” *Phys. Rev. Lett.* **119**, 016402 (2017).
16. Insun Jo, M. A. Mueed, L. N. Pfeiffer, K. W. West, K. W. Baldwin, R. Winkler, Medini Padmanabhan, and M. Shayegan, “Tuning of Fermi Contour Anisotropy in GaAs (001) 2D Holes via Strain,” *Appl. Phys. Lett.* **110**, 252103 (2017).
17. H. Deng, Y. Liu, I. Jo, L.N. Pfeiffer, K.W. West, K.W. Baldwin, and M. Shayegan, “Interaction-induced Interlayer Charge Transfer in the Extreme Quantum Limit,” *Phys. Rev. B* (Rapid Communications) **96**, 081102(R) (2017).

Understanding and controlling phases with topological and charge order in the two-dimensional electron gas

Principal Investigators: Gabor Csathy and Michael Manfra
Institution: Purdue University
Address: 525 Northwestern Ave., West Lafayette, IN 47907
E-mail of PIs: gcsathy@purdue.edu and mmanfra@purdue.edu

Program Scope

The development and the study of materials with the least possible disorder has been at the heart of contemporary condensed matter research. Among these materials GaAs/AlGaAs heterostructures have historically been important as they host the cleanest two-dimensional electron gases as measured by the record high mean free paths as high as 0.3 μm . Advances in the MBE technology have played a pivotal role in reaching the exquisite quality in this material system. As the quality of the system improved often times new correlated electron ground states have been observed. The discovery of such new ground states has strongly impacted our understanding of correlated electron physics.

Recently it was suggested that this system may support unusual ground states which harbor exotic particles with special topological properties. Specifically, some ground states are thought to behave as p -type superconductors and to support Abelian and non-Abelian quasiparticles of various kinds [a]. Prime examples of such unusual ground states in the two-dimensional electron gas are the fractional quantum Hall states at the quantum numbers $5/2$ and $12/5$. These ground states are not only of fundamental interest as they may manifest behavior not seen in any other physical system, but also may find technological utility in fault-tolerant schemes for quantum computation [b]. These exotic states are, however, fragile and hence they develop only under special conditions.

At Purdue University we pursue an experimental program targeting outstanding questions concerning the collective behavior of the correlated electronic ground states of the two-dimensional electron gas. Our primary focus is the study of the fractional quantum Hall states and exotic electronic solids. The goal of our program is to use state-of-the-art growth and incisive experimental measurement techniques to generate new insight into the nature of the exotic correlated states.

Recent Progress

Tuning the exotic states with hydrostatic pressure. One current focus of Csathy's research is the development of novel, incisive techniques probing the two-dimensional electron gas. Historically the most popular measurement technique used in investigations of this system is electronic transport. However, over the last decade or so it became increasingly clear that the probing of the new topologically ordered states requires more sophisticated techniques. Measurement of these systems at high hydrostatic pressures is one such techniques currently being used in Csathy's lab. At pressures of the order of 10,000 atmospheres one can tune many relevant quantities which are expected to impact numerous ground states.

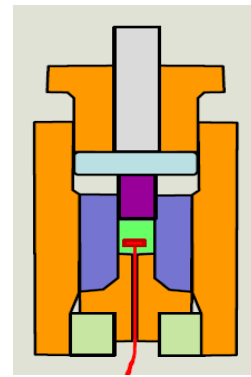


Fig. 1: Schematic of a pressure cell which generates 25 kbar at 12 mK and 10T.

While exploring the high pressure regime, we have recently discovered an **unexpected phase transition** from the $\nu=5/2$ fractional quantum Hall state to an electronic nematic phase. While both of these ground states were known to develop in our system, the nematic phase so far has only developed at the quantum number $\nu=9/2$ and other higher values. The stabilization of the nematic phase we observed at $\nu=5/2$ came as a surprise. The most interesting feature of this transition from the fractional state to the nematic phase is that these two phases belong to fundamentally distinct classes of phases: the former is a topologically ordered phase while the latter is a traditional broken symmetry phase. The phase transition we found is thus a very interesting example of rare phase transitions between a topological and traditional broken symmetry phases.

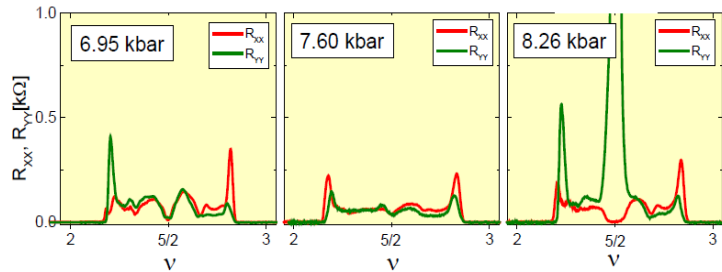


Figure 2: The evolution of the ground state at $\nu=5/2$ from a fractional quantum Hall state, to a Fermi liquid, to a nematic phase is shown with an increasing value of the pressure. Data are taken at ~ 12 mK. The signature of the nematic phase is a strong resistance anisotropy near $\nu=5/2$.

A particularly interesting aspect of our work is that the $\nu=5/2$ fractional quantum Hall state can be thought of as a topological superconductor. This is because the state forms as a result of the Cooper-like pairing of the composite fermions and the edge of the sample supports topological edge states. Owing to the spin-polarized nature of the $\nu=5/2$ fractional quantum Hall state, the superconducting pairing symmetry is thought to be of p -type. Our observations can therefore be interpreted as a result of a **competition of topological superconductivity and nematicity**. We are hopeful that, due to the simplicity and cleanliness of our system we can learn new physics with potential insight on the competition of superconductivity and nematicity in other systems, such as the high temperature superconductors, transition metal dichalcogenides, and He-3.

Isotropic to Nematic to Smectic Phase Transitions at Half-filling

In Manfra's laboratory direct isotropic to nematic to smectic phase transitions in a half-filled Landau level has been observed for the first time. At half-filling in high Landau levels theory has long predicted a series of possible ground states in which various spatial symmetries are broken. As temperature is decreased the electron system is expected to evolve from an isotropic Fermi liquid, into an ordered nematic phase that breaks rotational symmetry but preserves translational symmetry, then into a smectic phase that breaks both rotational and translational symmetry in one direction, and finally into a fully crystalline state. To date the existing data in GaAs has been most consistent with nematic order without evidence for smectic order, presumably limited by residual disorder and elevated temperature. Recently in an extremely high quality sample and at very low temperature we have recently observed three novel transport phenomena that indicate a change in symmetry beyond the nematic phase: a non-monotonic temperature dependence of sample resistance R_{xx} , dramatic onset of large time-dependent fluctuations in R_{xx} , and a sharp feature in differential resistance reminiscent of depinning. Taken together, these data suggest that smectic order prevails in the cleanest electron gases at lowest accessible temperatures.

In Fig. 3 we display three signatures of smectic ordering at $\nu=9/2$. In panel (a) non-monotonic temperature dependence of the resistance along the hard direction, R_{xx} , is clearly evident below $T=50$ mK. In panel (b) highly non-linear behavior in the differential resistance is observed and in panel (c) the onset of large scale temporal fluctuations in R_{xx} can be seen below 50 mK.

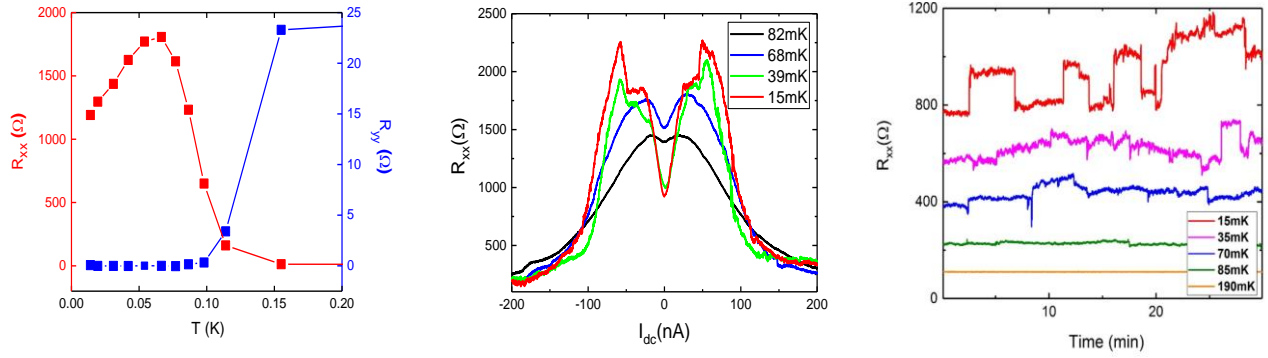


Fig. 3: (a) non-monotonic resistance vs. temperature at $\nu=9/2$. (b) non-linear I-V characteristics suggest depinning of charge-density-wave state (the smectic phase). (c) onset of noise at lowest temperatures at $\nu=9/2$.

Our data strongly indicate that exquisite new correlated electron motion continues to be uncovered as we continue to improve the quality of the GaAs system. Such novel behaviors continue to be the focus of the Csathy and Manfra collaborative growth and transport program.

Future Plans. Encouraged by our recent results, we will continue to study pressure effects and the nematic-smectic transition in the GaAs system. Specifically, we seek to elucidate the role played by the pressure in the observed topological-to-nematic phase transition. Furthermore, we plan to investigate the spin polarization effects in the exotic ground states. Such investigations are part of our long term effort aimed at exploring unconventional collective behavior in low-dimensional systems. In addition, we will continue our effort in studying disorder effects by expanding the energy gap measurements for new types of well-controlled disorder, such as charged disorder. We expect that disorder-specific information will guide us in further improvements of the growth process and may lead to new insight of the behavior of these systems.

References

- a) A. Stern, “Non-Abelian States of Matter”, *Nature (London)* **464**, 187 (2010)
- b) C. Nayak, S. Simon, A. Stern, M. Freedman, and S. Das Sarma, “Non-Abelian Anyons and Topological Quantum Computing”, *Review of Modern Physics*. **80**, 1083 (2008)

Publications acknowledging DOE BES support since 2015

1. K.A. Schreiber, N. Samkharadze, G.C. Gardner, R.R. Biswas, M.J. Manfra, and G.A. Csathy, “Onset of Quantum Criticality in the Topological-to-Nematic Transition in a Two-dimensional Electron Gas at Filling Factor $\nu=5/2$ ”, *Physical Review B* **96**, 041107 (2017), Rapid Communication
2. Q. Qian, J. Nakamura, S. Fallahi, G.C. Gardner, J.D. Watson, S. Luscher, J.A. Folk, G.A. Csathy, and M.J. Manfra, Quantum lifetime in ultrahigh quality GaAs quantum wells: Relationship to $\Delta_{5/2}$ and impact of density fluctuations,” *Physical Review B* **96**, 035309 (2017)
3. Q. Qian, J.R. Nakamura, S. Fallahi, G.C. Gardner, J.D. Watson, and M.J. Manfra, “High-temperature resistivity measured at $\nu=5/2$ as a predictor of two-dimensional electron gas quality in the $N=1$ Landau level,” *Physical Review B* **95**, 241304 (2017), Rapid Communication
4. X. Fu, Q.A. Ebner, Q. Shi, M.A. Zudov, Q. Qian, J.D. Watson, and M.J. Manfra, “Microwave-induced resistance oscillations in a back-gated GaAs quantum well,” *Physical Review B* **95**, 235415 (2017)

5. Q. Shi, M.A. Zudov, B. Fries, J. Smet, J.D. Watson, G.C. Gardner, and M.J. Manfra, “Apparent temperature-induced reorientation of quantum Hall stripes,” *Physical Review B* **95**, 161404 (2017)
6. Q. Shi, M.A. Zudov, Q. Qian, J.D. Watson, and M.J. Manfra, “Effect of density on quantum Hall stripe orientation in tilted magnetic fields,” *Physical Review B* **95**, 161303 (2017)
7. A.V. Rossokhaty, Y. Baum, J.A. Folk, J.D. Watson, G.C. Gardner, and M.J. Manfra, “Electron-Hole Asymmetric Chiral Breakdown of Reentrant Quantum Hall States,” *Physical Review Letters* **117**, 166805 (2017)
8. Q. Zhang, M. Lou, X. Li, J.L. Reno, W. Pan, J.D. Watson, M.J. Manfra, and J. Kono, “Collective non-perturbative coupling of 2D electrons with high-quality terahertz cavity photons,” *Nature Physics* **12**, 1005 (2016)
9. Q. Zhang, Y. Wang, W. Gao, Z. Long, J.D. Watson, M. J. Manfra, A. Belyanin, and J. Kono, “Stability of high-density two-dimensional excitons against a Mott transition in high magnetic fields probed by coherent terahertz spectroscopy,” *Physical Review Letters* **117**, 207402 (2016)
10. N. Samkharadze, K.A. Schreiber, G.C. Gardner, M.J. Manfra, E. Fradkin, and G.A. Csathy, “Observation of a Transition from a Topologically Ordered to a Spontaneously Broken Symmetry State,” *Nature Physics* **12**, 191 (2016)
11. S. Wang, D. Scarabelli, Y.Y. Kuznetsova, S.J. Wind, A. Pinczuk, V. Pellegrini, M.J. Manfra, G.C. Gardner, L.N. Pfeiffer, and K.W. West, “Observation of electrons states of small period artificial graphene in nano-patterned GaAs quantum wells,” *Applied Physics Letters* **109**, 113101 (2016)
12. G.C. Gardner, S. Fallahi, J.D. Watson, and M.J. Manfra, “Modified MBE hardware and techniques and the role of gallium purity for attainment of two-dimensional electron gas mobility $> 35 \times 10^6 \text{cm}^2/\text{Vs}$ in AlGaAs/GaAs quantum wells grown by MBE,” *Journal of Crystal Growth*, **441**, 71 (2016)
13. A.L. Levy, U. Wurstbauer, Y.Y. Kusnetsova, A. Pinczuk, K.W. West, L.N. Pfeiffer, M.J. Manfra, G.C. Gardner, and J.D. Watson, “Optical Emission Spectroscopy Study of Competing Phases in the Second Landau Level,” *Physical Review Letters* **116**, 016801 (2016)
14. Q. Shi, M.A. Zudov, L.N. Pfeiffer, K.W. West, J.D. Watson, and M.J. Manfra, “Resistively Detected Higher-order Magnetoplasmons in a High-quality Two-dimensional Electron Gas,” *Physical Review B* **93**, 165438 (2016)
15. Q. Shi, M.A. Zudov, J.D. Watson, G.C. Gardner, and M.J. Manfra, “Evidence for a New Symmetry Breaking Mechanism Reorienting Quantum Hall Nematics,” *Physical Review B* **93**, 121411 (2016)
16. Q. Shi, M.A. Zudov, J.D. Watson, G.C. Gardner, and M.J. Manfra, “Reorientation of Quantum Hall Stripes within a Partially Filled Landau Level,” *Physical Review B* **93**, 121404 (2016)
17. J.D. Watson, G.A. Csathy, and M.J. Manfra, “Impact of heterostructure design on transport properties in the second Landau level in in-situ back-gated two-dimensional electron gases,” *Physical Review Applied* **3**, 064004 (2015)
18. Tingxin Li, Pengjie Wang, Hailong Fu, Lingjie Du, Kate Schreiber, Xiaoyang Mu, Xiaoxue Liu, Gerard Sullivan, Gabor Csathy, Xi Lin, and Rui-Rui Du, “Observation of Helical Luttinger-Liquid in InAs-GaSb Quantum Spin Hall Edges,” *Physical Review Letters* **115**, 136804 (2015)
19. Q. Shi, P.D. Martin, A.T. Hatke, M.A. Zudov, J.D. Watson, G.C. Gardner, M.J. Manfra, L.N. Pfeiffer, and K.W. West, “Shubnikov–de Haas oscillations in a two-dimensional electron gas under subterahertz radiation,” *Physical Review B* **92**, 081405 (2015)
20. U. Wurstbauer, A.L. Levy, A. Pinczuk, K.W. West, L.N. Pfeiffer, M.J. Manfra, G.C. Gardner, and J.D. Watson, “Gapped Excitations of Unconventional Fractional Quantum Hall Effect States in the Second Landau Level,” *Physical Review B* **92**, 241407 (2015)
21. D. Scarabelli, S. Wang, A. Pinczuk, S.J. Wind, Y.Y. Kuznetsova, L.N. Pfeiffer, K. West, G.C. Gardner, M.J. Manfra, and V. Pellegrini, “Fabrication of Artificial Graphene in a GaAs Quantum Heterostructure,” *Journal of Vacuum Science and Technology B* **33**, 06FG03 (2015)
22. Z. Wan, A. Kazakov, M.J. Manfra, L.N. Pfeiffer, K.W. West, and L.P. Rokhinson, “Induced superconductivity in high-mobility two-dimensional electron gas in gallium arsenide heterostructures,” *Nature Communications* **6**, 7426 (2015)

Program Title: Engineering topological superconductivity towards braiding Majorana excitations

Principle Investigator: Leonid P. Rokhinson

Mailing Address: Department of Physics, Purdue University, West Lafayette, IN 47906

E-mail: leonid@purdue.edu

Program Scope

The goal of the program is to develop systems which support excitations with non-Abelian statistics and to study properties of these new unconventional states of matter. In such matter some quantum numbers of a many-particle condensate are encoded in the topology of the state and protected from small local perturbations. These protected degrees of freedom can be used to encode quantum information and are the basis of fault-tolerant topological quantum computer proposals, which presents a robust alternative to the conventional quantum computation where decoherence poses the major technological challenge.

With DOE support we explored different systems where topologically non-trivial phases can be realized and, most importantly, exchange statistics of non-Abelian excitations can be probed experimentally. The major objective of the proposed research was to develop quasi-one dimensional structures where non-Abelian statistics of topological excitations can be tested, and we proposed experiments to demonstrate a σ_x gate with a rotating magnetic field. Over the last year we made a substantial progress toward that goal. In parallel, we also studied superconductivity in topological insulator nanoribbons and looked for the signatures of topologically non-trivial superconductivity. Finally, we developed a new system where helical states with fractional charge excitations can be formed. These helical channels are precursors of a new class of topological superconductors where higher order non-Abelian excitations, such as parafermions, may be realized.

Recent Progress

A. Development of quasi-one dimensional topological superconductors.

One of the biggest challenges in accomplishing the main objective of the proposed research was inadequate quality of the available InSb material. Recently we started collaboration with Prof. Shabani from NYU who have grown several outstanding wafers for our project. The material is InAs capped with epitaxial layer of Al. Results of material characterization are shown in Fig. 1. The high quality of the material revealed in well defined weak localization dip at $B = 0$ and well pronounced quantum oscillations in high magnetic fields. Epitaxially grown layer of aluminum has high superconducting transition temperature $T_c = 1.5$ K. We developed fabrication of Josephson junction where electron density and critical current can be controlled by electrostatic gates, Fig. 1c shows an AFM image of a typical device where two JJs form a SQUID. At zero gate voltage superconductivity is induced in InAs from Al at low T, Fig 1e. Negative voltages deplete carriers and reduce critical currents, with pinch-off gate voltages in the range of -2 - -4 V

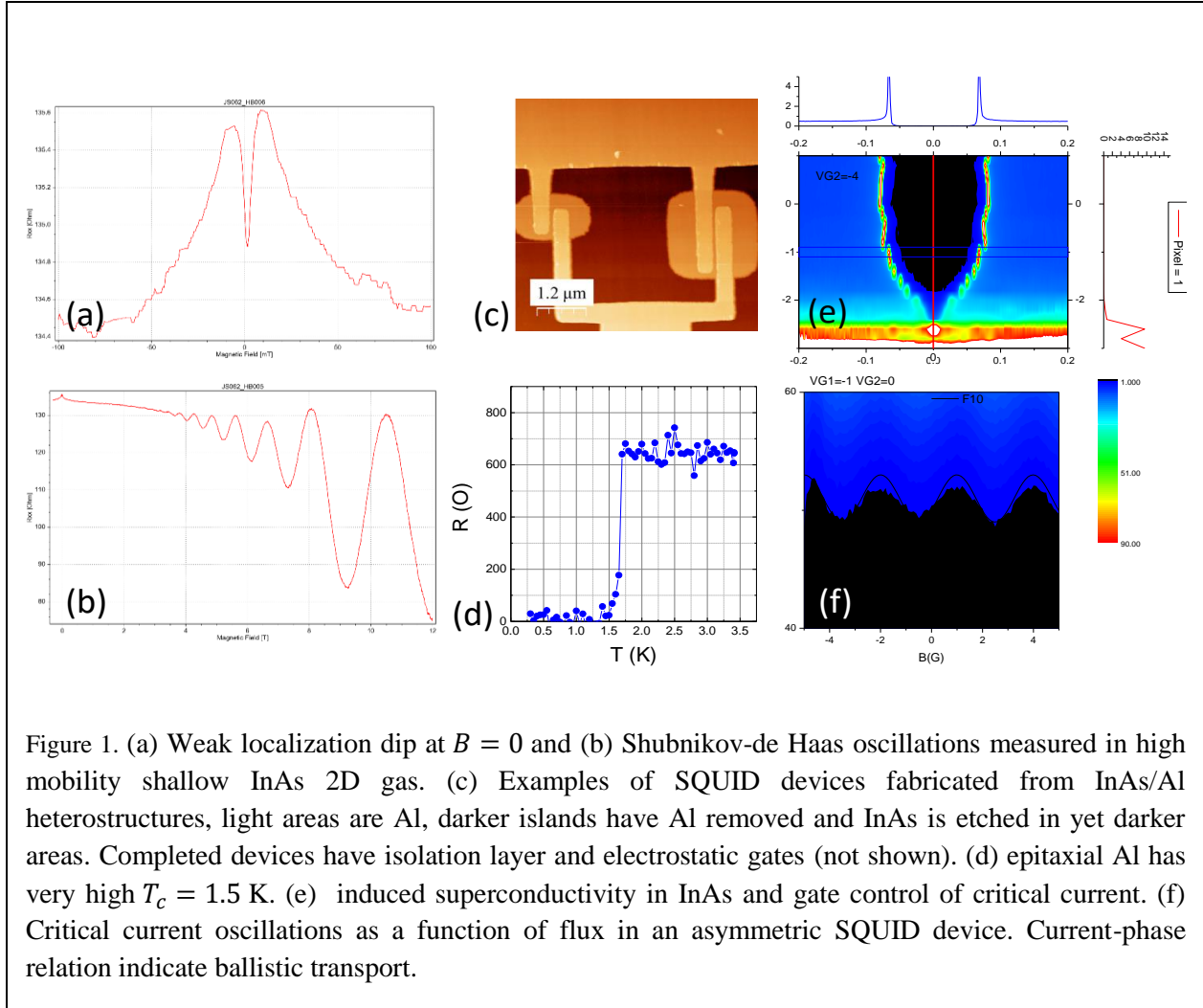


Figure 1. (a) Weak localization dip at $B = 0$ and (b) Shubnikov-de Haas oscillations measured in high mobility shallow InAs 2D gas. (c) Examples of SQUID devices fabricated from InAs/Al heterostructures, light areas are Al, darker islands have Al removed and InAs is etched in yet darker areas. Completed devices have isolation layer and electrostatic gates (not shown). (d) epitaxial Al has very high $T_c = 1.5$ K. (e) induced superconductivity in InAs and gate control of critical current. (f) Critical current oscillations as a function of flux in an asymmetric SQUID device. Current-phase relation indicate ballistic transport.

depending on the distance between Al leads. Recently measured current-phase relation of a JJs shows a high degree of anharmonicity, an indication of ballistic transport in our JJs. After finishing the preliminary material and device characterization we will start working on the devices along the lines of the original proposal.

B. Formation of helical channels in the fractional quantum Hall regime: development of a parafermion-supporting platform.

The original goal of the research was to develop a platform where Majorana excitations can be realized and manipulated. Recently we established a collaboration with Prof. Shabani from NYU who is growing outstandingly good material for our experiments. From the quantum information perspective, however, the Hilbert space available for Majorana fermions (MF) is rather restricted and MFs-based quantum gates have to be complemented by two operations outside the protected topological state or be approximated by a "distillation code" with a huge overhead. Parafermions - fractional MFs - have denser rotation group and their braiding enables two-qubit entangling gates. The holy grail of topological quantum computing will be a system which supports so-

called Fibonacci fermions with universal braiding statistics, where universal quantum computations will become possible entirely within the topologically protected subspace. It has been shown that due to the sparse symmetry group, factorization of a 128-bit prime number will be 10^9 -operations intensive with MFs, while it will take only 10^3 braiding operations with Fibonacci fermions. Over the last year our laboratory together with Loren Pfeiffer from Princeton University developed GaAs heterostructures where 1D helical channels with fractionalized charge excitation can be realized, these channels being precursors of topological superconductors with parafermionic excitations.

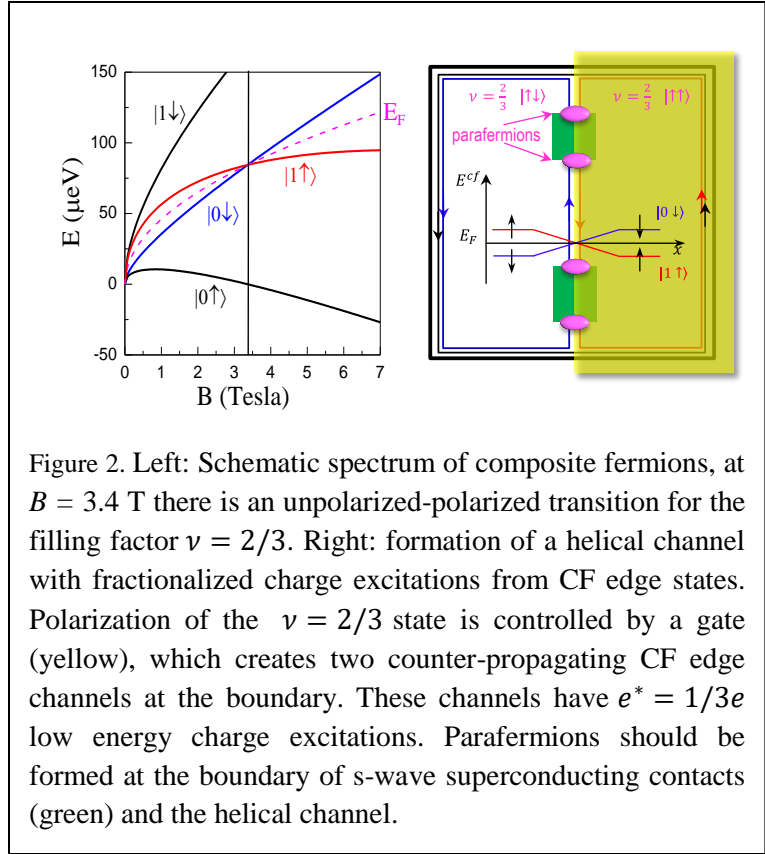


Figure 2. Left: Schematic spectrum of composite fermions, at $B = 3.4$ T there is an unpolarized-polarized transition for the filling factor $\nu = 2/3$. Right: formation of a helical channel with fractionalized charge excitations from CF edge states. Polarization of the $\nu = 2/3$ state is controlled by a gate (yellow), which creates two counter-propagating CF edge channels at the boundary. These channels have $e^* = 1/3e$ low energy charge excitations. Parafermions should be formed at the boundary of s-wave superconducting contacts (green) and the helical channel.

Helical channels are commonly associated with quantum spin Hall effect or two-dimensional topological insulators, where strong spin-orbit interactions introduce bulk band inversion and topologically protected helical modes are confined to the edges. In conventional quantum Hall setting the bulk is also gapped but topologically protected edge modes are *chiral* due to the broken time-reversal symmetry. However, we realized that an ability to gate-control quantum Hall ferromagnetic transitions should allow formation of synthetic helical edge channels. In Fig. 1 the concept is visualized for the filling factor $\nu = 2/3$ FQHE state. The $\nu = 2/3$ state can be viewed as a $p = 2$ integer quantum Hall state for composite fermions (CFs), composite particles consisting of an electron with two flux quanta attached. A filling factor for electrons and CFs are related via $\nu = p/(2p \pm 1)$ transformation, where \pm corresponds to the electron spin being parallel or antiparallel to the field direction. Energy levels for electrons and CFs have very different magnetic field dependences, and CF energy levels $|0\downarrow\rangle$ and $|1\uparrow\rangle$ cross at high field $B^* = 3.4$ T as shown in Fig. 1. Provided that B^* can be controlled electrostatically, two counter-propagating edge channels with fractional charge excitations (a helical domain wall) should be formed at the boundary, Fig. 2. Coupled to a s-wave superconductor such system should support parafermionic excitations.

The major progress for this part of the project during the last year was development of devices where a single helical domain wall (hDW) in the fractional quantum Hall effect regime can be investigated. Some number of wafers has been grown and we successfully demonstrated gate control of ferromagnetic transition at $\nu = 2/3$, see Fig. 3. Isolation of a single domain wall requires complicate 14 layers of lithography and takes 2-3 weeks to fabricate. Some aspects of such device has not been studied before, for example it was not known whether QHE, especially fragile fractional QHE states, will be formed in point contacts formed by ohmic contacts (usually point contacts are formed by electrostatic gates, which results in a very different confining potential profile and Fermi energy pinning). We found that indeed it is possible to tune contact formation conditions to obtain insulating states in FQHE regime between contacts as close as $2 \mu\text{m}$ with resistance $> \text{M}\Omega$. We confirmed that QHFm transition can be observed in both large areas and inside point contacts. The level of control is shown in Fig. 3c, where we demonstrate formation of a helical domain wall in a point contact. In that device we were able to see and tune QHFm transition on both sides of the point contact independently and to clearly identify 4 configurations $\uparrow\uparrow, \uparrow\downarrow, \downarrow\uparrow$, and $\downarrow\downarrow$.

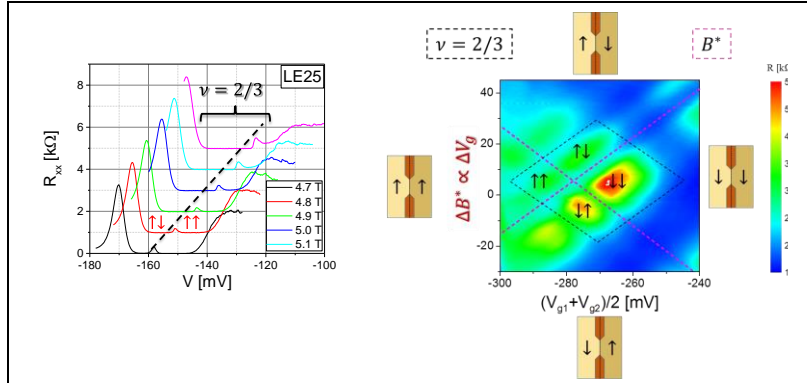


Figure 3: Left: Gate control of a ferromagnetic transition at $\nu = 2/3$. Dashed line marks the transition between $\uparrow\downarrow$ and $\uparrow\uparrow$ spin configurations. Right: full control of spin polarization and formation of helical channels in a point contact device.

Some aspects of such device has not been studied before, for example it was not known whether QHE, especially fragile fractional QHE states, will be formed in point contacts formed by ohmic contacts (usually point contacts are formed by electrostatic gates, which results in a very different confining potential profile and Fermi energy pinning). We found that indeed it is possible to tune contact formation conditions to obtain insulating states in FQHE regime between contacts as close as $2 \mu\text{m}$ with resistance $> \text{M}\Omega$. We confirmed that QHFm transition can be observed in both large areas and inside point contacts. The level of control is shown in Fig. 3c, where we demonstrate formation of a helical domain wall in a point contact. In that device we were able to see and tune QHFm transition on both sides of the point contact independently and to clearly identify 4 configurations $\uparrow\uparrow, \uparrow\downarrow, \downarrow\uparrow$, and $\downarrow\downarrow$.

Future Plans

For InAs-based devices our plans for the next year include (i) demonstration of ballistic devices (CPR), (ii) fabrication and characterization of QD charge sensors, (iii) Fabrication and characterization of lithographical nanowires (iv) work toward demonstration of Majorana braiding. **For parafermion-development platform** our goal is to characterize transport in helical channels and develop high transparency superconducting contacts to these structures.

Publications

George Simion, Tzu-ging Lin, John D. Watson, Michael J. Manfra, Gabor A. Csathy, Yuli Lyanda-Geller, and Leonid P. Rokhinson, "Theory of topological excitations and metal-insulator transition in reentrant integer quantum Hall effect" under review at PRL (2017); [arXiv:1705.05233](https://arxiv.org/abs/1705.05233)

NV-centers in diamond for non-invasive optical sensing and quantum spin studies

R. Prozorov, N. M. Nusran, V. Mkhitarian, Kyuil Cho, M. A. Tanatar, M. Tringides, M. Hupalo, J. Wang, Y. Lee, Liqin Ke, D. Vaknin, *Ames Laboratory, Ames, Iowa 50011*

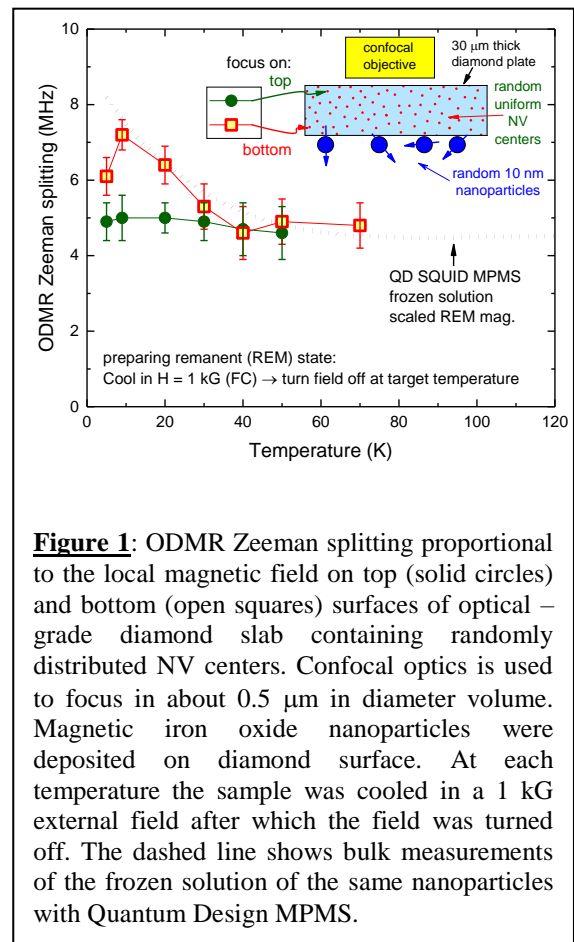
Program Scope

Magnetic NanoSystems: Making, Measuring, Modeling, Manipulation.

The scientific goal of this program is to study the effects of geometric confinement on electronic and magnetic properties, excitations, currents and coherence in quantum materials. Advanced experimental probes, such as NV-centers in diamond optical magnetic field sensor and spin - polarized scanning tunneling spectroscopy are used to obtain spatially - resolved maps of magnetic and electronic degrees of freedom, while x-ray magnetic circular dichroism and ultra-fast optical spectroscopies provide information on element - specific local moment and non-equilibrium charge and spin dynamics. Theoretical analysis of the collected data is used in the numerical calculations of spin - resolved electronic structure and simulation of quantum spin dynamics to obtain a fundamental understanding of quantum magnetism in the systems of interest at the microscopic level.

Recent Progress

Here we focus only on one aspect of our program – successful development of the novel sensing technique based on the nitrogen – vacancy (NV) - centers in diamond whose optical fluorescence levels are highly dependent on local magnetic fields. Other types of sensing (e.g., temperature or local NMR) are also possible. This technique is still under active development in several research labs worldwide. Each has its own “flavor” and unique in one aspect or another. For the description of the physical principles behind this technique, please see Refs. [1-3]. In this FWP, the NV – centers in diamond are used to probe local magnetic fields. Separately, they are used as a well – defined system to study spin coherence and spin dynamics. During past three years, we built functional NV - centers laboratory from ground up, implemented optical readout algorithms and data analysis. As a first step, we have successfully implemented magneto-sensing aspect, while quantum spin studies are planned for the near future. The magneto-sensing itself can be realized in two ways – with the ensembles of NV - centers randomly distributed in diamond crystal, as shown schematically in **Figure 1**, or as a scanning setup with the single NV-center in nano-diamond that is places at the end of an AFM tip. The former has larger signal to noise ratio, but lacks the spatial resolution of the latter, which can be better than 50 nm. The sensitivity in either approach is



about $50 \mu\text{T}/\sqrt{\text{Hz}}$ in DC mode and three orders of magnitude better in the more advanced AC mode. The sensing can be further improved by using novel quantum control methods (advanced microwave pulsed sequences, etc.). The low-temperature ensemble magneto - sensing is already operational with several research projects on the way, and the scanning sensing is nearing its critical phase where we fabricate diamond nano-pillars containing NV centers. This work is done at the Center for Nanoscale Materials at Argonne National Laboratory.

The nitrogen-vacancy (NV) center is a point defect in the diamond lattice that has a spin triplet, $S=1$, ground state. When excited to a higher energy level by a 532 nm green laser from the $m_S=0$ spin projection ground state, the relaxation back to $m_S=0$ proceeds through spin - conserving cyclic transitions emitting red photons. However, if excited from $m_S=\pm 1$ levels, the NV center mostly relaxes *via* the meta-stable (dark) states back to $m_S=0$ resulting a lesser red fluorescence rate. This spin - dependent fluorescence allows for optical detection of the magnetic resonance (ODMR) by sweeping frequency of low-intensity microwave radiation. When the frequency matches the energy difference between $m_S=0$ levels and $m_S=\pm 1$ levels, the fluorescence rate is minimal. Finally, the $m_S=\pm 1$ levels are Zeeman - split in a magnetic field resulting in a double - dip ODMR spectrum.

Figure 1 shows an example of sensing magnetic field produced by a dilute ensemble of iron oxide nanoparticles deposited directly on the diamond plate surface. By focusing either on the surface close or far from the nanoparticles layer using confocal optics, the measured ODMR changes when the sample is cooled below 50 K signifying so-called blocking transition of these superparamagnetic particles. This observation is very important, as it will allow studying collective effects in magnetic nanoparticle ensembles, separating them from the behavior of a single nanoparticle as high-resolution sensing mode becomes available.

Figure 2 demonstrates spatially - resolved imaging of a magnetic field across a superconducting sample. In a conventional Meissner effect, weak magnetic field is expected to be expelled from the sample, but many superconductors show quite different behavior. We studied several classes of superconducting materials and observed behavior ranging from expulsion to paramagnetic Meissner effect [4,5]. In **Fig.2**, stoichiometric iron-pnictide $\text{CaKFe}_4\text{As}_4$ is shown not to expel magnetic field at all, confirming its anomalous nature described previously by our group [6].

By focusing precisely near the edge of a well - shaped sample (as determined from SEM imaging) we can measure magnetic field at which Abrikosov vortices begin penetrating the sample. This field is related to the first critical field, which in turn depends on one of the fundamental parameters describing superconductors, - London penetration depth, which is notoriously difficult to measure precisely. **Figure 3 (a)** shows measurements of ODMR Zeeman splitting in $\text{Ba}(\text{Fe}_{1-x}\text{Co}_x)_2\text{As}_2$

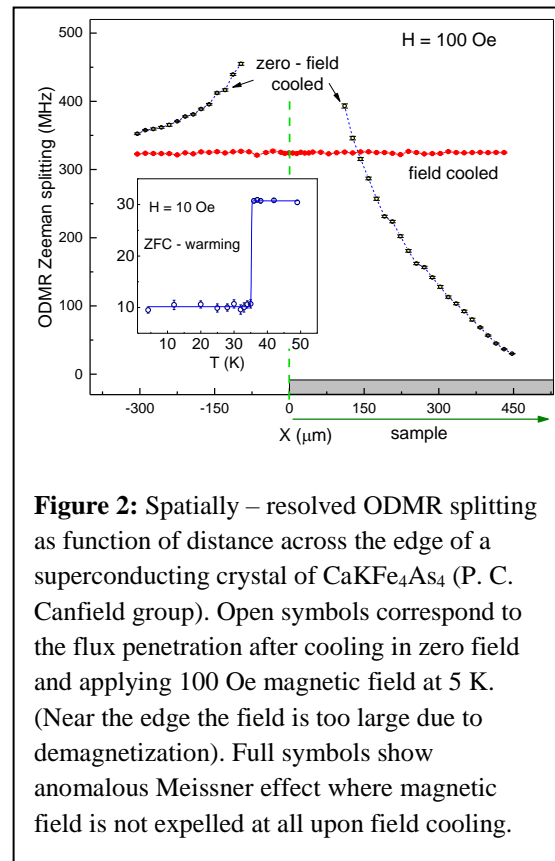
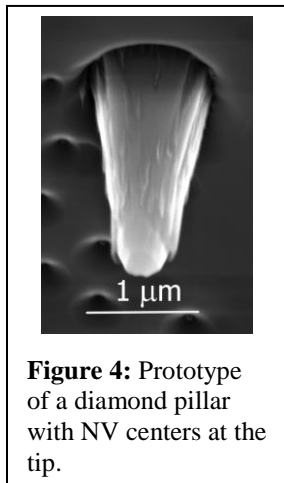
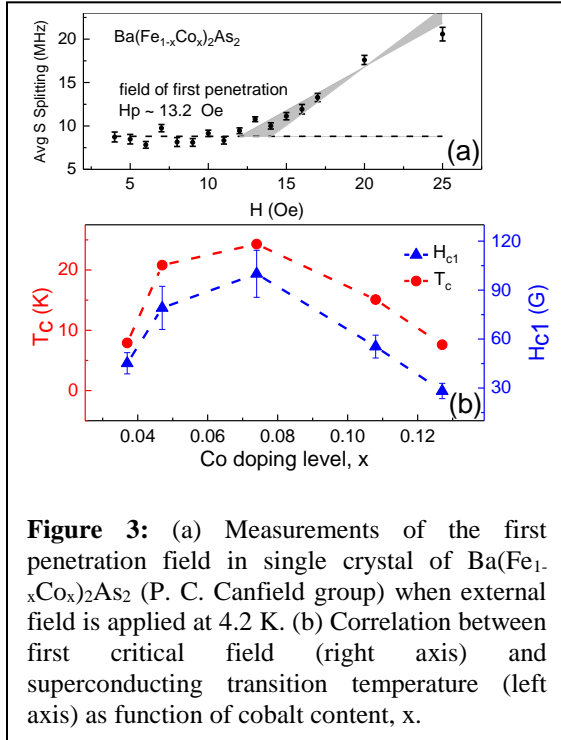


Figure 2: Spatially - resolved ODMR splitting as function of distance across the edge of a superconducting crystal of $\text{CaKFe}_4\text{As}_4$ (P. C. Canfield group). Open symbols correspond to the flux penetration after cooling in zero field and applying 100 Oe magnetic field at 5 K. (Near the edge the field is too large due to demagnetization). Full symbols show anomalous Meissner effect where magnetic field is not expelled at all upon field cooling.



Science: Advanced NV sensing will be used to map vector magnetic field and infer spin distribution in magnetic nanoislands and nanoparticles as function of the number of layers, capping and wetting layer, lateral size, etc. This information will be used to study correlation between atomic and magnetic structures comparing bulk and nanoscale objects, collective effects, and superparamagnetic blocking. We will determine current density distributions in superconductors and topological matter focusing on the effects of geometric confinement. We will hopefully prove experimentally spin-locked nature of non-dissipative currents in topological insulators. We will study fundamental properties of superconductors, such as first critical field, critical current density and vortex behavior as function of sample size, down to the nanoscale where exotic effects, such as parity – dependent gap, self-organization and paramagnetism are expected at the nanoscale. Study magnetic topological excitations such as skyrmions, magnetic domains, Abrikosov vortices comparing behavior of these excitations in

crystal near optimal composition.

The signal is measured as a function of applied external magnetic field in several locations inside the sample near the edge and then averaged. At approximately $H_p \sim 13.2$ Oe the signal starts to increase signaling penetration of vortices into the interior. The values of H_p obtained using this procedure in samples of different cobalt concentration, x , are converted into the first critical field, H_{c1} , from which the London penetration depth can be calculated directly. **Figure 3(b)** shows interesting direct correlation between superconducting transition temperature (left axis) and the values of the first critical field (right axis).

Future Plans

Technical: In the nearest future, we will start using single NV scanning mode to spatially resolve magnetism at the nanoscale. A prototype NV-functionalized diamond pillar is shown in **Fig.4**. We will develop non-invasive optical magnetic sensing with novel protocols for enhanced

sensitivity. Potential directions for achieving increased sensitivity include: employing dynamic-decoupling protocols to improve the NV spin coherence, and suppressing background fluorescence and/or continuous resonant driving of NV metastable states to enhance the signal contrast. In addition, we will attempt to develop/employ pulsed-ESR protocols on NV centers to study fluctuating local magnetic environments in various materials. Develop Rabi spectroscopy with NV centers to achieve vector magnetometry of EM fields. This will have a broad range of applications including MW technologies and metamaterials. Specific examples include systematic study of micron-scale electromagnetic resonators and superconducting split-ring resonators.

bulk and nanoscale systems. We will study the role of defects in these systems. Explore unconventional superconductivity driven by spin/magnetic/nematic fluctuations in the 3D \rightarrow 2D crossover regime (from bulk to monolayer films). We will elucidate and exploit spin coherence in materials lacking spin-orbit (SO) coupling, thus featuring long spin coherence times. While such materials provide suitable environment for spintronics purposes, the spin read-out by the traditional means (e.g., Faraday or Kerr rotation) appears to be challenging. Inclusion of NV centers is promising for providing the spin read-out, rendering these materials appealing for potential spintronics applications. Develop and explore ensembles of NV centers for collectively enhanced spontaneous emission (superradiance) behavior. One of the interests in superradiance study lies in its close connection with the physics of laser emission. Potential applications include magnetic field-controlled NV lasing and ultra-precise NV ensemble laser sensors, providing nanoscale resolution owing to the enhanced read-out signal contrast.

References

1. J. R. Maze *et al.*, *Nature* **455**, 644 (2008).
2. L. Rondin *et al.*, *Rep. Prog. Phys.* **77**, 056503 (2014).
3. D. Le Sage *et al.*, *Nature* **496**, 486 (2013).
4. P. Kostic *et al.*, *Phys. Rev. B* **53**, 12441 (1996).
5. S. Kumar *et al.*, *J. Phys. Condens. Matter* **27**, 295701 (2015).
6. R. Prozorov *et al.*, *Phys. Rev. B* **82**, 180513, (2010).

FWP Publications

- N. A. Anderson *et al.*, *J. Mag. Mag. Mater.* 435, 212 (2017)
 N. A. Anderson *et al.*, *J. App. Phys.* 121, 014310 (2017)
 H. F. Fotso and V. V. Dobrovitski, *Phys. Rev. B* 95, 214301 (2017)
 D. McDougall *et al.*, *Carbon* 108, 283 (2016)
 E. Kawakami *et al.*, *Proc. Nat. Acad. Sci.* 113, 11738 (2016)
 Q. P. Ding *et al.*, *Phys. Rev. B* 93, 140502 (2016)
 H. F. Fotso *et al.*, *Phys. Rev. Lett.* 116, 033603 (2016)
 X. Liu *et al.*, *Prog. Surf. Sci.* 90, 397-443 (2015)
 X. J. Liu *et al.*, *Nano Research* 9, 1434 (2016)
 V. V. Mkhitarian *et al.*, *Sci. Rep.* 5, 15402 (2015)
 J. Cui *et al.*, *Phys. Rev. B* 94, 085203 (2016)
 Q.-P. Ding *et al.*, *Phys. Rev. B* 93, 140502R (2016)
 D. Farfurnik *et al.*, *Spie-Int Soc Opt. Eng. Bellingham*, 2016, 99000n
 P. V. Klimov *et al.*, *Sci. Adv.* 1, 8 (2015)
 Y. Wu *et al.*, *Nat. Phys.* 12, 667 (2016)

Session 3

Session 3 — PANEL DISCUSSIONS

Mick Pechan, Department of Energy

Panel introduction: "Opportunities in ECMP basic research for next generation quantum systems and devices"

Collin Broholm, Johns Hopkins University

Report on Quantum Materials BRN Workshop

Panel 1: *Topological / 2D / Spin-orbit coupling*

Judy Cha, Yale University

Philip Kim, Harvard University

Panel 2: *Quantum magnetism*

Axel Hoffmann, Argonne National Laboratory

Arthur Ramirez, University of California—Santa Cruz

Panel 3: *Strongly correlated materials*

Gabor Csathy, Purdue University

Johnpierre Paglione, University of Maryland

Q&A

Session 4

Program Title: Correlated Materials - Synthesis and Physical Properties

Principle Investigators: Ian R. Fisher, Theodore H. Geballe, Aharon Kapitulnik, Steven A. Kivelson, and Kathryn A. Moler

Institution: Geballe Laboratory for Advanced Materials, and Departments of Applied Physics and Physics, Stanford University, and the Stanford Institute for Materials & Energy Science, SLAC National Accelerator Laboratory.

Emails: irfisher@stanford.edu, geballe@stanford.edu, aharonk@stanford.edu, kivelson@stanford.edu, kmoler@stanford.edu

PROGRAM SCOPE

The overarching goal of our research is to understand, and ultimately control, emergent behavior in strongly correlated quantum materials. Our research combines synthesis, measurement and theory to coherently address questions at the heart of these issues. We use cutting edge, often unique, experimental probes to uncover novel forms of electronic order in a variety of complex materials. Our theoretical work provides a framework to understand the rich variety of possible ordered states, and guides our ongoing measurements and synthesis efforts. Big questions that we collectively address include:

- What are the rules and organizing principles governing emergent behavior in quantum materials, particularly quantum critical points and their proximate phases. Examples include:
 - What are origins of pseudogap phases and what are their possible relations to quantum critical behavior?
 - Why so often a superconducting dome emerges around a quantum critical point?
 - What is the nature of the coexisting and competing phases in high temperature superconductors, and how do they determine/limit the maximum critical temperature?
 - How does disorder affect quantum phase transitions in strongly correlated materials?
 - How do we understand electrical and thermal transport in the quantum critical regime?
- Do we need a new set of paradigms to define metallic behavior?
 - How do we understand metals that emerge from “failed superconductors”?
 - Why some strongly correlated metals exhibit hydrodynamic transport?
 - What is the origin of “bad metals” where quasi-particles are no longer well-defined?

Our research addresses these challenging questions in the context of a range of complex quantum materials and artificial structures.

RECENT PROGRESS

1. The Superconductor-Insulator Transition and its proximate phases

The conventional picture of possible ground states in a two-dimensional electron gas (2DEG) system, at zero temperature and in the presence of disorder, allows only superconducting or insulating phases (and in magnetic field also quantum Hall liquid phases). Tuning the disorder and/or magnetic field between superconducting and insulating ground states -- the so called superconductor-insulator transition (SIT) -- has received acute attention because they led to

exploration of new ground states and appear to be broadly relevant to other quantum phase transitions (QPTs) and unsolved puzzles such as unconventional superconductivity in the high- T_c cuprates. In particular, detailed experimental studies of disordered superconducting thin-films near the magnetic-field tuned superconductor-insulator transition (SIT) have revealed several unexpected new ground states for films that otherwise superconduct at zero magnetic field. First, in weakly disordered films (with normal state resistivity small compared to the quantum of resistance, the superconducting state gives way to an anomalous metallic phase with a resistivity that extrapolates to a non-zero value as the temperature tends to zero [paper accepted to Science Advances. See point (2) below for further discussion]. Second, for highly disordered superconducting films with normal state resistance close to the quantum of resistance a direct SIT occurs at a field H_c , giving way to a boson-dominated insulator. In new experiments, where the longitudinal resistance is supplemented with Hall resistance data, additional striking results were obtained. These include: 1) the resistivity tensor at criticality approaches the universal value expected at a point of vortex-particle self-duality, 2) the critical exponents governing the quantum critical behavior appear to be the same as those observed at both the integer and fractional quantum Hall to Insulator transitions, and 3) the insulating phase proximate to the SIT appears to be a Hall insulator where in the limit of $T \rightarrow 0$, the longitudinal resistance tends to infinity while the Hall resistance is finite, approaching a simple value of $\sim H/nc$ [PNAS **113**, 280-285 (2016)]. These new results shade light on the nature of the SIT and bare important consequences to other QPT in two-dimensional systems.

2. Critical Review of Anomalous Metals - Failed Superconductors

A fundamental disjunction between theoretical prejudice and experimental reality concerns the existence of metallic ground states of a wide variety of two-dimensional electronic systems. Specifically, (in collaboration with B. Spivak) we have assembled and critically analyzed the experimental evidence of the existence of a new regime, which we call the "anomalous metal regime," in a diverse 2D superconducting systems driven through a quantum superconductor to metal transition (QSMT) by tuning a physical parameter such as magnetic field, the gate voltage in the case of systems with a MOSFET geometry, or, in some cases, the degree of disorder. The principle phenomenological observation is that in such systems, as a function of decreasing temperature, the resistivity first drops as if the systems were approaching a superconducting ground state, but then saturates at low temperatures to a value that can be many orders of magnitude smaller than the Drude value. The anomalous metal typically exhibits a giant positive magneto-resistance and, where it has been tested, a Hall resistance that is orders of magnitude smaller than its classical (Drude) value. Thus in a sense it can be considered as a "failed superconductor." This behavior is observed in a relatively broad range of parameters. We moreover exhibit, by controlled theoretical solution of a model of superconducting grains embedded in a metallic matrix, that such anomalous metallic behavior can occur in a well defined quantum critical domain in the neighborhood of a QSMT. However, we also argue that the robustness and ubiquitous nature of the observed phenomena are difficult to reconcile with any existing theoretical treatment [a review paper in preparation].

2. Current-phase relations in exotic Josephson-junctions

To control and characterize individual modes in junctions is long-standing challenge in mesoscopic superconductivity. This challenge is especially timely due to the great interest in exotic junctions for quantum computation. We measured the “current-phase relation” (CPR), the key defining property of any junction, of many superconducting rings interrupted by individual InAs nanowire junctions. We showed that the CPRs of these junctions are skewed, indicated high-quality transmission. Furthermore, they can be tuned, which is important for the control of Majorana modes. Many theorists have proposed using the CPR to dynamically read out the state of the Majorana mode, and this work represents a significant step towards that goal. (Nature Physics, appeared online on August 14, 2017).

4. Progress in the study of nematicity in strongly correlated materials

Our collaborative study, which involves synthesis, measurement and theory. First we used differential elastoresistance measurements [Rev. Sci. Instrum. **88**, 043901 (2017)] from five optimally doped iron-based superconductors to show that divergent nematic susceptibility appears to be a generic feature in the optimal doping regime of these materials. This observation motivates consideration of the effects of nematic fluctuations on the superconducting pairing interaction in this family of compounds and possibly beyond [Science **352**, 958 (2016)].

In addition, we identify appropriate transverse fields to tune an Ising nematic quantum critical transition, and predict appropriate materials to realize such an effect. This is motivated by the growing evidence that nematic quantum criticality might be an important organizing principle affecting several families of high temperature superconductors. Specifically we identify 4f ferroquadrupole order as a realization of Ising nematic order, providing new avenues to study nematic quantum phase transitions in metallic systems. Finally we introduce the notion of using shear strain as a powerful new tuning parameter, providing a new means to access a metallic QCP in the absence of a magnetic field. (arXiv:1704.07841).

FUTURE PLANS

For FY18-20, we plan to add a critical study of metallic transport beyond the standard momentum-relaxation Boltzmann transport, in addition to the focus on broken symmetry phases and quantum phase transitions in strongly correlated materials.

The design and implementation of new types of experiment that probe the (often subtle) types of emergent order in complex materials will continue to be a major emphasis of our program. We previously highlighted the ability to exert anisotropic strain (which acts as an “ordering field” on electronic nematic fluctuations) in our transport, optical and scanning SQUID measurements, and the use of polar Kerr effect for time-reversal symmetry breaking tests. We recently added two new optic-based instruments, a photogalvanic instrument, where light with specific polarization induce directional current which in turn help determine the symmetry of the underlying electronic system. A new photothermal microscope is used in thermal diffusivity measurements, which are performed on micrometer-scale spots, hence allow for precise determination of transport anisotropy.

Selection of publications resulting from DOE sponsored research between 8/15 and 8/17

1. *Macroscopic character of composite high-temperature superconducting wires*, S.A.Kivelson and B. Spivak, Phys. Rev. B **92**, 184502 (2015) – Published 3 November 2015
2. *Symmetry constraints on the elastoresistivity tensor*, M. C. Shapiro, Patrik Hlobil, A. T. Hristov, Akash V. Maharaj, and I. R. Fisher, Phys. Rev. B **92**, 235147 (2015) – Published 28 December 2015
3. *Self-duality and a Hall-insulator phase near the superconductor-to-insulator transition in indium-oxide films*, N. P. Breznay, M. A. Steiner, S. A. Kivelson, and A. Kapitulnik, PNAS **113**, 280-285 (2016) – Published January 12, 2016
4. *Vestigial chiral and charge orders from bidirectional spin-density waves: Application to the iron-based superconductors*, R. M. Fernandez, S. A. Kivelson, and E. Berg, Phys. Rev. B **93**, 014511 (2016) – Published 19 January 2016
5. *Paired Insulators and High Temperature Superconductors*, T H Geballe and S A Kivelson, in “PWA90: A Lifetime of Emergence” (World Scientific, pg 127-132) – published Feb 2016
6. *Quantum oscillations in a bilayer with broken mirror symmetry: A minimal model for $YBa_2Cu_3O_{6+d}$* , A.V.Maharaj, Y. Zhang, B.J. Ramshaw, and S. A. Kivelson, Phys. Rev. B **93**, 94503 (2016) – Published 1 March 2016
7. *Ubiquitous signatures of nematic quantum criticality in optimally doped Fe-based superconductors*, Hsueh-Hui Kuo, J. Palmstrom, Jiun-Haw Chu, Steven A. Kivelson, and Ian R. Fisher, Science **352**, 958 (2016) – Published May 19th 2016
8. *Depth resolved domain mapping in tetragonal SrTiO₃ by micro-Laue diffraction*, Tyler A. Merz, Hilary Noad, R. Xu, H. Inoue, W. Liu, Y. Hikita, A. Vailionis, Kathryn A. Moler and Harold Y. Hwang Applied Physics Letters **108** 182901 (2016) – Published online 2 May 2016
9. *Measurement of the B_{1g} and B_{2g} components of the elastoresistivity tensor for tetragonal materials via transverse resistivity configurations*, M. C. Shapiro, A. T. Hristov, J. C. Palmstrom, Jiun-Haw Chu, and I. R. Fisher, Rev. Sci. Instrum. **87**, 063902 (2016) – Published online 10 June 2016
10. *Variation in superconducting transition temperature due to tetragonal domains in two-dimensionally doped SrTiO₃*, Hilary Noad, Eric M. Spanton, Katja C. Nowack, Hisashi Inoue, Minu Kim, Tyler A. Merz, Christopher Bell, Yasuyuki Hikita, Ruqing Xu, Wenjun Liu, Arturas Vailionis, Harold Y. Hwang, Kathryn A. Moler, Phys. Rev. B **94**, 174516 (2016) – Published 28 November 2016
11. *Disorder enabled band structure engineering of a topological insulator*, Yishuai Xu, Janet Chiu, Lin Miao, Haowei He, Zhanybek Alpichshev, A. Kapitulnik, Rudro R. Biswas, L. Andrew Wray, Nature Communications **8**, 14081 (2017) – Published online 03 February 2017
12. *Determination of the resistivity anisotropy of orthorhombic materials via transverse resistivity measurements*, P. Walmsley and I. R. Fisher, Rev. Sci. Instrum. **88**, 043901 (2017) – Published online 5 April 2017
13. *Intertwined order in a frustrated four-leg t-J cylinder*, J. F. Dodaro, H-C. Jiang, and S. A. Kivelson, Phys. Rev. B **95**, 155116 (2017) – Published 12 April 2017
14. *Polar Kerr effect studies of time reversal symmetry breaking states in heavy fermion superconductors*, E. R. Schemma, b, l, E. M. Levenson-Falk, A. Kapitulnik, PHYSICA C-Superconductivity and its Applications **535**, 13-19 (2017) - Published April 15 2017
15. *Particle-hole Symmetry Reveals Failed Superconductivity in the Metallic Phase of Two-Dimensional Superconducting Films*, Nicholas P. Breznay and Aharon Kapitulnik, Accepted for publication in Science Advances, 2017. (currently under journal embargo - therefore no archive publication)
16. *Time Reversal Symmetry Breaking in the B Phase of the Heavy Fermion Superconductor PrOs₄Sb₁₂*, E. M. Levenson-Falk, E. R. Schemm, M. B. Maple, Aharon Kapitulnik, arXiv:1609.07535.
17. *Current-phase relations of few-mode InAs nanowire Josephson junctions*, Eric M. Spanton, Mingtang Deng, Saulius Vaitiekėnas, Peter Krogstrup, Jesper Nygård, Charles M. Marcus, Kathryn A. Moler, – Published online 14 August 2017
18. *Holon Wigner Crystal in a Lightly Doped Kagome Quantum Spin Liquid*, H-C.Jiang, T. Devereaux, and S. A. Kivelson, Phys. Rev. Lett. **119**, 067002 (2017) – Published 7 August 2017
19. *Vestigial nematicity from spin and/or charge order in the cuprates*, L. Nie, A. V. Maharaj, E. Fradkin, and S. A. Kivelson, Phys. Rev. B accepted July 2017; arXiv:1701.02751
20. *Transverse fields to tune an Ising-nematic quantum critical transition*, A. V. Maharaj, E. W. Rosenberg, A. T. Hristov, E. Berg, R. M. Fernandes, Ian R. Fisher, Steven A. Kivelson, arXiv:1704.07841 (Submitted to PNAS)
21. *Superconductor to weak-insulator transitions in disordered Tantalum Nitride films*, N.P. Breznay, M. Tendulkar, Li Zhang, S-C Lee, A. Kapitulnik, arXiv:1705.01732, under review at Phys. Rev. B.

Novel and unconventional superconductors: quantum criticality and possible field-induced superconducting states

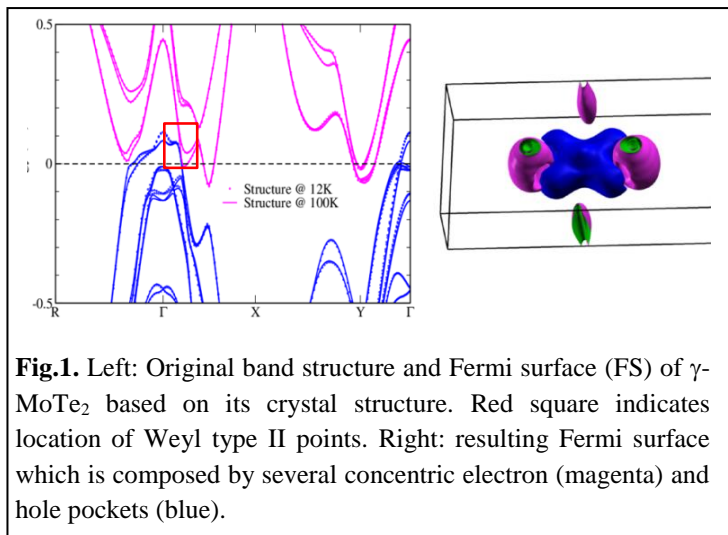
Luis Balicas – Physics Department and National High Magnetic Laboratory, FSU

Program Scope

In this program, we proposed a comprehensive effort to unveil the physical properties of a series of unconventional superconductors. For some of these compounds such as the Fe based or the heavy fermion superconductors, e.g. CeCu_2Ge_2 , the concept of quantum criticality or the existence of quantum fluctuations associated with the suppression of an order parameter, is believed to be relevant for the superconducting pairing mechanism. Other compounds such as URu_2Si_2 were claimed to display an exotic superconducting gap wave-function with possible point nodes, around which the nodal quasiparticles's Berry phase would seem to display topological properties leading to a “Weyl superconductor”. New Pd and chalcogenide based superconductors such as $\text{Nb}_2\text{Pd}_x\text{S}_5$, which are characterized by a complex electronic structure at the Fermi level, are found to display, depending on their electronic anisotropy, incredibly high superconducting upper critical fields suggesting the possibility an unconventional pairing symmetry. Finally, in the Fe based superconductors, such as in $\text{BaFe}_2(\text{As}_{1-x}\text{P}_x)_2$ and for some values of x , superconductivity coexists with a magnetic state raising the possibility of a time reversal symmetry broken superconducting state. The goal of our program is to unveil, and to characterize novel and unconventional (in the sense of unconventional electronic topology) superconductors, its relation to quantum criticality, and explore possible field-induced superconducting states.

Recent Progress - Bulk Fermi surfaces of the Weyl-type-II semi-metallic candidates γ - MoTe_2 and WP_2 (abstract title)

The electronic structure of semi-metallic transition-metal dichalcogenides, such as WTe_2 , orthorhombic γ - MoTe_2 [1], and WP_2 [2], are claimed to contain pairs of Weyl points or linearly touching electron and hole pockets associated with a non-trivial Chern number [1-3]. For this reason, these compounds were recently claimed to conform to a new class, deemed type-II, of Weyl semi-metallic systems. A series of angle resolved photoemission experiments (ARPES) claim a broad agreement with these predictions detecting, for example, topological Fermi arcs at the surface of the dichalcogenides crystals. We synthesized single-crystals of semi-



metallic MoTe₂, through a Te flux method, and of WP₂, via chemical vapor transport, to validate these predictions through measurements of their bulk Fermi surface (FS) *via* quantum oscillatory phenomena. For γ -MoTe₂ we find that the superconducting transition temperature depends on disorder as quantified by the ratio between the room- and low-temperature resistivities, suggesting the possibility of an unconventional superconducting pairing symmetry. Similarly to WTe₂, the magnetoresistivity of γ -MoTe₂ does not saturate at high magnetic fields and can easily surpass 10⁶ %. WP₂ exhibits a very low residual resistivity, i.e. $\rho_0 \cong 10$ n Ω cm, which leads to perhaps the largest non-saturating magneto-resistivity reported for any compound, i.e. 2.5 x 10⁷ % at 35 T. For γ -MoTe₂, the analysis of the de Haas-van Alphen (dHvA) signal superimposed onto the magnetic torque, indicates that the geometry of its FS is markedly distinct from the calculated one. A direct comparison between the previous ARPES studies and density-functional-theory (DFT) calculations reveals a disagreement in the position of the valence bands relative to the Fermi level ε_F . Here, we show that a shift of the DFT valence bands relative to ε_F , in

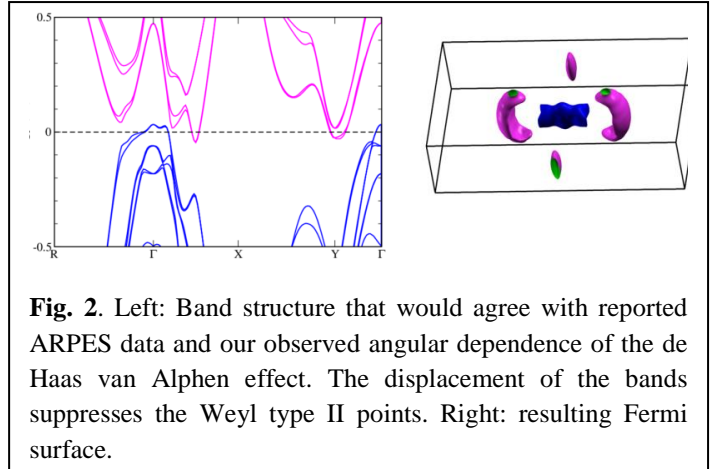


Fig. 2. Left: Band structure that would agree with reported ARPES data and our observed angular dependence of the de Haas van Alphen effect. The displacement of the bands suppresses the Weyl type II points. Right: resulting Fermi surface.

order to match the ARPES observations, and of the DFT electron bands to explain some of the observed dHvA frequencies, leads to a good agreement between the calculations and the angular dependence of the FS cross-sectional areas observed experimentally [4]. However, this relative displacement between electron- and hole-bands eliminates their crossings and, therefore, the Weyl type-II points predicted for γ -MoTe₂. For WP₂ we find that the angular dependence of the SdH frequencies is in excellent agreement with the first-principle calculations when the electron- and hole-bands are shifted by 30 meV with respect to the Fermi level [5]. This relative shift between bands could also suppress the predicted Weyl type II points in this compound. Here, we will not have time to discuss our recent results on Dirac type II and Dirac nodal line systems.

Future Plans

Currently, we are working to improve the sample quality of our URu₂Si₂ samples with goal of exploring its anomalous transport properties, such as Hall, thermal Hall and Nernst effects, in the mixed state, in an attempt to unveil its possible superconducting Weyl character. The same can be said about the hidden order, preliminary results, in samples of good but not of excellent quality, reveal anomalous effects such as a negative longitudinal magnetoresistivity, akin to the one observed in Weyl semi-metallic systems and ascribed to the Axial anomaly among Weyl points of opposite chirality. Disorder seems to weaken its possible topological properties, like the magnitude of the Nernst effect which is intrinsically associated to the Berry phase of the charge carriers. We are also exploring the electronic properties of the proposed

Dirac type II semimetal PdTe₂ which displays superconductivity and whose structure is related to the Nb_xPd_y(S,Se)_z superconducting compounds previously studied by us. Our preliminary studies indicate a good agreement between the geometry of its experimental Fermi surface, as determined via de Haas van Alphen effect, and the calculated one. This indicates that its overall calculated band structure is correct and that these compounds indeed are Dirac type II semimetals. It remains to be clarified if the Dirac point affects carriers at the Fermi level providing, for example, topological protection. Our preliminary study suggests the possibility of non-trivial Berry phases for the (Pd,Pt)Te₂ system, which could affect the aforementioned superconducting state. Concerning its superconducting properties, it does not display very high upper critical fields which point to an unconventional state. Currently, we are exploring a number of systems displaying non-trivial topology, via doping or intercalation, with the intent of stabilizing superconductivity

References

- [1] Y. Sun, S.C. Wu, M. N. Ali, C. Felser, and B. Yan, Phys. Rev. B 92, 161107 (2015); Z. Wang, D. Gresch, A. A. Soluyanov, W. Xie, S. Kushwaha, X. Dai, M. Troyer, R. J. Cava, and B. A. Bernevig, Phys. Rev. Lett. 117, 056805 (2016).
- [2] G. Autés, D. Gresch, M. Troyer, A. A. Soluyanov, and O. V. Yazyev, Phys. Rev. Lett. 117, 066402 (2016).
- [3] A. A. Soluyanov, D. Gresch, Z. Wang, Q. Wu, M. Troyer, X. Dai and B. A. Bernevig, Nature 527, 495-498 (2015).
- [4] D. Rhodes, R. Schönemann, N. Aryal, Q. Zhou, Q. R. Zhang, E. Kampert, Y.-C. Chiu, Y. Lai, Y. Shimura, G. T. McCandless, J. Y. Chan, D. W. Paley, J. Lee, A. D. Finke, J. P. C. Ruff, S. Das, E. Manousakis, and L. Balicas, arXiv:1605.09065 (under review)
- [5] R. Schönemann, N. Aryal, Q. Zhou, Y. -C. Chiu, K. -W. Chen, T. J. Martin, G. T. McCandless, J. Y. Chan, E. Manousakis, L. Balicas, arXiv:1706.10135 and Phys. Rev. B (RC), (in press).

Publications

1. *Origin of the butterfly magnetoresistance in a Dirac nodal-line system*, Y. -C. Chiu, K. -W. Chen, R. Schönemann, Q. Zhou, D. Graf, E. Kampert, T. Förster, G. T. McCandless, J. Y. Chan, R. E. Baumbach, M. D. Johannes, and L. Balicas, (under review).
2. *Bulk Fermi-surface of the Weyl type-II semi-metal candidate γ -MoTe₂*, D. Rhodes, R. Schönemann, N. Aryal, Q. Zhou, Q. R. Zhang, E. Kampert, Y.-C. Chiu, Y. Lai, Y. Shimura, G. T. McCandless, J. Y. Chan, D. W. Paley, J. Lee, A. D. Finke, J. P. C. Ruff, S. Das, E. Manousakis, and L. Balicas, arXiv:1605.09065 (under review).
3. *Magnetic anisotropy of the alkali iridate Na₂IrO₃ at high magnetic fields: evidence for strong ferromagnetic Kitaev correlations*, S. D. Das, S. Kundu, Z. Zhu, E. Mun, R. D. McDonald, G. Li, L. Balicas, A. McCollam, G. Cao, J. G. Rau, H.-Y. Kee, V. Tripathi, and S. E. Sebastian, arXiv:1708.03235 (under review).
4. *Fermi surface associated with neutral low energy excitations in a Kondo Insulator*, M. Hartstein, W. H. Toews, Y.-T. Hsu, B. Zeng, X. Chen, M. Ciomaga Hatnean, Q. R. Zhang, S. Nakamura, A. S. Padgett, G. Rodway-Gant, J. Berk, M. K. Kingston, G. H. Zhang, M. K. Chan, S. Yamashita, T. Sakakibara, Y. Takano, J. -H. Park, L. Balicas, N. Harrison, N. Shitsevalova, G.

Balakrishnan, G. G. Lonzarich, R. W. Hill, M. Sutherland, and S. E. Sebastian, *Nature Phys.* (in press).

5. *Fermi surface of the Weyl type-II metallic candidate WP₂*, R. Schönemann, N. Aryal, Q. Zhou, Y. -C. Chiu, K. -W. Chen, T. J. Martin, G. T. McCandless, J. Y. Chan, E. Manousakis, L. Balicas, arXiv:1706.10135; *Phys. Rev. B (RC)* (in press).

6. *Thermodynamic anomaly above the superconducting critical temperature in the quasi-one-dimensional superconductor Ta₄Pd₃Te₁₆* T. Helm, F. Flicker, R. Kealhofer, P. J. W. Moll, I. M. Hayes, N. P. Breznay, Z. Li, S. G. Louie, Q. R. Zhang, L. Balicas, J. E. Moore, and J. G. Analytis, *Phys. Rev. B* **95**, 075121 (2017).

7. *Possible devil's staircase in the Kondo lattice CeSbSe*, K.-W. Chen, Y. Lai, Y.-C. Chiu, S. Steven, T. Besara, D. Graf, T. Siegrist, T. E. Albrecht-Schmitt, L. Balicas, and R. E. Baumbach, *Phys. Rev. B* **96**, 014421 (2017).

8. *Spin excitations and the Fermi surface of superconducting FeS*, H. Man, J. Guo, R. Zhang, R. U. Schoenemann, Z. Yin, M. Fu, M. B. Stone, Q. Huang, Y. Song, W. Wang, D. Singh, F. Lochner, T. Hickel, I. Eremin, L. Harriger, J. W. Lynn, C. Broholm, L. Balicas, Q. Si, and P. Dai. *NPJ Quant. Mater.* **2**, 14 (2017).

9. *Temperature - Pressure phase diagram of the cubic Laves phase Au₂Pb*, K. W. Chen, D. Graf, T. Besara, A. Gallagher, N. Kikugawa, L. Balicas, T. Siegrist, A. Shekhter, R. E. Baumbach *Phys. Rev. B* **93**, 245152 (2016).

10. *Uncovering the behavior of Hf₂Te₂P and the candidate Dirac metal Zr₂Te₂P*, K.- W. Chen, S. Das, D. Rhodes, S. Memaran, T. Besara, T. Siegrist, E. Manousakis, L. Balicas, R. E. Baumbach, *J. Phys.-Condens. Mat.* **28**, 14LT01 (2016).

11. *Non-Ising-like two-dimensional superconductivity in a bulk single crystal*, Q. R. Zhang, D. Rhodes, B. Zeng, M. D. Johannes, and L. Balicas, *Phys. Rev. B* **94**, 094511 (2016).

12. *Hall-effect within the colossal magnetoresistive semimetallic state of MoTe₂*, Qiong Zhou, D. Rhodes, Q. R. Zhang, S. Tang, R. Schönemann, and L. Balicas, *Phys. Rev. B* **94**, 121101(R) (2016).

13. *Inter-planar coupling dependent magnetoresistivity in high purity layered metals*, N. Kikugawa, P. Goswami, A. Kiswandhi, E. S. Choi, D. Graf, R. E. Baumbach, J. S. Brooks, K. Sugii, Y. Iida, M. Nishio, S. Uji, T. Terashima, P. M. C. Rourke, N. E. Hussey, H. Takatsu, S. Yonezawa, Y. Maeno, L. Balicas, *Nature Comm.* **7**, 10903 (2016).

14. *Unconventional Fermi surface in an insulating state*, B. S. Tan, Y. -T. Hsu, B. Zeng, M. C. Hatnean, N. Harrison, Z. Zhu, M. Hartstein, M. Kiourlappou, A. Srivastava, M. D. Johannes, T. P. Murphy, J. H. Park, L. Balicas, G. G. Lonzarich, G. Balakrishnan, S. E. Sebastian, *Science* **349**, 287 (2015).

15. *Field-induced density wave in the heavy-fermion compound CeRhIn₅*, P.J.W. Moll, B. Zeng, L. Balicas, S. Galeski, F. F. Balakirev, E. D. Bauer and F. Ronning, *Nature Comm.* **6**, 6663 (2015).

16. *Spin-orbital liquid and quantum critical point in Y_{1-x}La_xTiO₃*, Z.Y. Zhao, O. Khosravani, M. Lee, L. Balicas, X. F. Sun, J. G. Cheng, J. S. Brooks, H. D. Zhou, E. S. Choi, *Phys. Rev. B* **91**, 161106(R) (2015).

17. *Field-induced quadrupolar quantum criticality in PrV₂Al₂₀*, Y. Shimura, M. Tsujimoto, B. Zeng, L. Balicas, A. Sakai, and S. Nakatsuji, *Phys. Rev. B* **91**, 241102(R) (2015).

18. *Role of spin-orbit coupling and evolution of the electronic structure of WTe₂ under an external magnetic field*, D. Rhodes, S. Das, Q. R. Zhang, B. Zeng, N. R. Pradhan, N. Kikugawa, E. Manousakis, and L. Balicas, *Phys. Rev. B* **92**, 125152 (2015).

Emerging Materials

Principal Investigator: John F. Mitchell (ANL); Co-PIs: D. Phelan (ANL), H. Zheng (ANL)

Program Scope

How do the remarkable properties of matter emerge from complex correlations of the atomic or electronic constituents, and how can we control these properties? How do we understand the critical roles of heterogeneity and disorder in materials that lie beyond the ideal? Emerging Materials pursues answers to these two questions by exploring the structure and behavior of quantum matter systems, those materials for which quantum mechanical effects lead to unexpected, remarkable properties. Currently, we focus on three exemplar areas of quantum materials science: topological quantum matter, electron correlation and spin-orbit coupling in oxides (including iridates), and random electric fields in disordered matter. *Emerging Materials* is well-positioned to lead the way in these focus topics. In particular, we are at the forefront of high-pressure floating zone crystal growth, which is opening new possibilities in oxide physics. Likewise, our recent advances in interpreting 3D mapping of diffuse scattering (collaborating with Argonne's *Neutron and X-ray Scattering* program) promise to give us a prominent role in the study of disorder and random fields. In these focus areas, our program deliverables are knowledge of the basic phenomenology of complex quantum states, understanding of how to manipulate these states or how to create new ones, and the novel, pedigreed samples that allow not only us, but also members of the broader condensed matter community to build on our work to create new frameworks for understanding quantum matter.

Recent Progress

Charge and Spin Stripes in Trilayer Nickelates Many mixed-valent TMOs adopt insulating 'charge-ordered' states, frequently with some variety of charge stripe,¹ found in cobaltites, cuprates, nickelates, and manganites. The case of nickelates plays a prominent role in charge-stripe physics, since mixed-valent $\text{Ni}^{2+}/\text{Ni}^{3+}$ compounds such as $\text{La}_{2-x}\text{Sr}_x\text{NiO}_4$ (formally $\text{Ni}^{2.33+}$) are structurally and electronically related to high- T_c cuprates. In this vein, Greenblatt and others synthesized powders of anion-deficient $\text{Ni}^{1+}/\text{Ni}^{2+}$ Ruddlesden-Popper (R-P) phases $R_{n+1}\text{Ni}_n\text{O}_{2n+2}$ ($R=\text{La}$, $n=2$; $R=\text{La}$, Pr , Nd , $n=3$) with a rigorously square planar Ni-O environment, Fig 1a.²

$\text{La}_4\text{Ni}_3\text{O}_8$ (La-438) undergoes a metal-insulator (MIT) phase transition on cooling through 105 K that has been attributed to a spin-density wave (SDW)³ or to a spin-state driven MIT transition.⁴ Unfortunately, a lack of single crystals to date has hampered definitive experimental understanding of this system. Using our high pressure floating-zone furnace, we successfully prepared crystals of the formally $\text{Ni}^{1.33+}$ La and Pr members of the 438 family. Using single crystal synchrotron and neutron diffraction, we found previously unidentified, weak superlattice reflections indicative of a three-fold periodic charge and spin stripe ground state in this 1/3-hole doped nickelate (Fig. 1c,d), agreeing exactly with

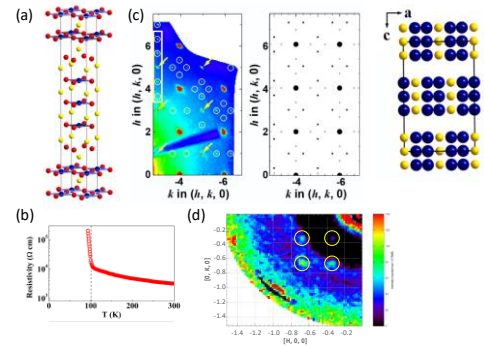


Fig. 1 (a) T' crystal structure of $\text{La}_4\text{Ni}_3\text{O}_8$ showing square planar coordination of Ni. (b) Resistive transition at $T_s \sim 105$ K. (c) $hk0$ plane below T_s showing superlattice reflections (left); simulated diffraction pattern (middle) using stacked charge stripe model (right). (d) neutron scattering shows expected spin-derived superlattice.

that for 1/3-hole doped single-layer nickelates. Unlike these latter materials, however, charge stripes in La-438 stack in an eclipsed fashion within the trilayer, contradicting simple Coulomb repulsion arguments. With collaborator M. Norman we established that the stacked charge stripe pattern is the ground state of La-438 and has predicted the form of the lattice distortion that opens a gap at the fermi level.⁵ We have also shown that the holes in the La-438 system are highly x^2-y^2 polarized, comparable to that found in cuprate superconductors. Even more intriguing, the Pr-438 system shows similar levels of orbital polarization, but remains metallic to below 2 K.⁹ These findings suggest that Pr-438, which in cuprate parlance would be overdoped, is perhaps the most faithful representative among the many high- T_c superconductor analogs.

Topological Matter ‘Extreme magnetoresistance’ (XMR), has been reported in a number of structurally simple binary semimetals, including tetragonal Weyl typified by semimetals NbP.⁶ XMR is characterized by a tremendous ($\sim 10^5$ %) increase in resistance in relatively modest (few T) magnetic fields. Two prevailing explanations have been posited for XMR: (a) topological protection that is lifted by magnetic field and (b) nearly perfect compensation of electron and hole volumes. We observed XMR in specimens of YSb grown in our laboratories and

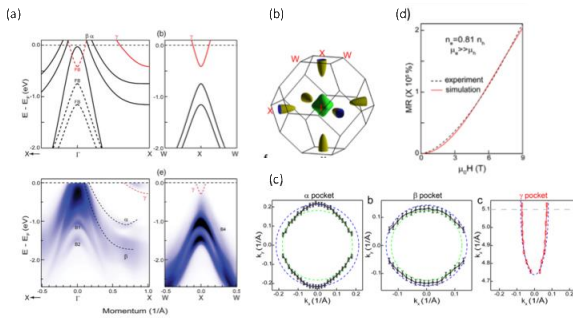


Fig. 2 XMR in YSb. (a) Calculated (top) and measured (bottom) band structure of YSb. (b) Calculated fermi surface showing hole pockets at X and electron pocket at Γ . (c) Estimates of electron and hole volumes from measured fermi surface (d) Two-band fit (solid line) to MR data (points).

collaborated with the Shen group at Stanford to probe the band structure via ARPES for signs of a nontrivial topological electronic band structure. As shown in Fig 2, YSb has a straightforward ARPES spectrum that agrees well with DFT calculations but shows no features expected of topologically protected states. Using the measured fermi surface, we estimated the electron and hole volumes, yielding an $e/h = 0.8$, significantly deviating from the near-perfect compensation required by the second model. By incorporating this e/h ratio as a fitting parameter into a standard two-band model for the MR, we showed excellent agreement both to the absolute magnitude and to the field dependence of our magnetoresistance data (Fig. 2d). The key

outcome of this fitting, however, is the need for a considerable imbalance between electron and hole mobility ($\mu_e/\mu_h \sim 300$), implicating a third interpretation for the origin of XMR in these semimetals in the case of moderate but incomplete carrier compensation.

Local ordering in relaxor ferroelectrics Together with the ANL *Neutron and X-ray Scattering* program, we have made use of recent advances in instrumentation that allow for efficient measurement of large volumes of diffuse x-ray (via continuous rotation) and neutron scattering (using the new instrument Corelli at the SNS) to survey the different forms of local order that occur in a collection of crystals that span the entire phase diagram of the model relaxor system $(1-x)\text{PbMg}_{1/3}\text{Nb}_{2/3}\text{O}_3-x\text{PbTiO}_3$ (PMN- x PT). We have identified four distinct forms, and by studying their compositional dependence, we have unambiguously resolved the coupling of each of the diffuse scattering signatures to the dielectric and electromechanical properties (Fig. 3). In particular, we uncovered a distinct correlation between ferroic diffuse scattering and piezoelectricity, which has important implications for the design of advanced piezoelectrics.

Moreover, our observations strongly connect ‘relaxor’ behavior to a competition between antiferrodistortive and ferroic order and inform the nature of the ground-state in relaxors which has long been controversial.

Future Plans

The influence of topology on itinerant electrons and spins: we will probe how real- and momentum-space Berry phases in semi-metals are connected and how this reciprocity can influence transport in spin textures and vice-versa. This would offer a novel approach for studying the mechanism of controlling mesoscale phenomena by atomic level effects and vice versa.

The interplay of electron correlation and spin-orbit coupling: we will take a fresh look at the electronic structure of iridates with the objective of isolating putative Jahn-Teller modes as a function of SOC, and we will study low-dimensional correlated nickelates, exploring dimensionality, doping, and disorder in single crystals we will grow via high-pO₂ zone methods.

The impact of random fields on long-range structure: we will develop an empirical foundation for random field models that extend beyond the RFIM, exploring static aspects of chemically-driven quenched disorder.

References

1. Ulbrich, H.; Braden, M. *Physica C* **2012**, *481*, 31–45.
2. Poltavets, V. V. et al. *Phys Rev B* **2011**, *83*, 014402.
3. Poltavets, V. V. et al. *Phys Rev Lett* **2010**, *104*, 206403.
4. Pardo, V. et al. *Phys Rev Lett* **2010**, *105*, 266402.
5. Botana, A. S. et al., *Phys Rev B* **2016**, *94*, 081105
6. Zhang, J. et al. *Nature Physics* **2017**, *518*, 179.
7. Guo, Y. et al. *J. Phys. Condens. Matter* **2003**, *15*, L77.
8. Grinberg, I. et al. *Phys. Rev. Lett.* **2007**, *99*, 267603.

Publications

1. “Magnetic Domain Tuning and the Emergence of Bubble Domains in the Bilayer Manganite La_{2-2x}Sr_{1+2x}Mn₂O₇ (x=0.32)” Jeong, J.; Yang, I.; Yang, J.; Ayala-Valenzuela, O. E.; Wulferding, D.; Zhou, J. S.; Goodenough, J. B.; de Lozanne, A.; Mitchell, J. F.; Leon, N.; Movshovich, R.; Jeong, Y.H.; Yeom, H.W.; Kim, J. *Phys. Rev. B* **2015**, *92*, 054426.
2. “New Insulating Antiferromagnetic Quaternary Iridates MLa₁₀Ir₄O₂₄ (M = Sr, Ba)” Zhao, Q.; Han, F.; Stoumpos, C. C.; Han, T.-H.; Li, H.; Mitchell, J. F. *Sci. Rep.* **2015**, *5*, 11705.
3. “Evidence of Photo-Induced Dynamic Competition of Metallic and Insulating Phase in a Layered Manganite” Li, Y.; Walko, D. A.; Li, Q.; Liu, Y.; Rosenkranz, S.; Zheng, H.; Mitchell, J. F. *J. Phys.: Condens. Matter* **2015**, *27* (49), 495602.
4. “Ferromagnetic Domain Behavior and Phase Transition in Bilayer Manganites Investigated at the Nanoscale” Phatak, C.; Petford-Long, A.K.; Zheng, H.; Mitchell, J.F.; Rosenkranz, S.;

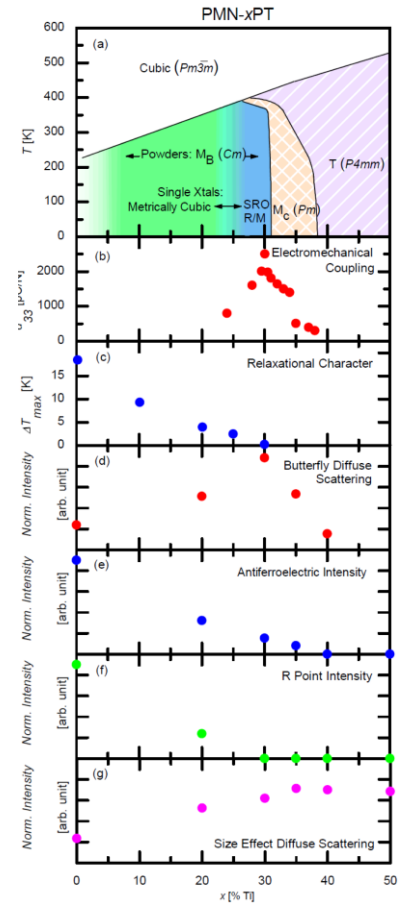


Fig. 3: (a) Phase diagram of PMN-xPT. Compositional dependence of (b) piezoelectric coupling after [7], (c) relaxational character after [8], and (d-g) different forms of diffuse scattering.

- Norman, M.R. *Phys. Rev. B* **2015**, 92, 224418.
5. “Antiferromagnetic Kondo lattice in the layered compound CePd_{1-x}Bi₂ and comparison to the superconductor LaPd_{1-x}Bi₂” F. Han, X. Wan, D. Phelan, C. C. Stoumpos, M. Sturza, C. D. Malliakas, Q. Li, T.-H. Han, Q. Zhao, D. Y. Chung, and M. G. Kanatzidis, *Phys. Rev. B* **2015**, 92, 045112.
 6. “Structure and Magnetism in LaCoO₃” Belanger, D.P.; Keiber, T.; Bridges, F.; Durand, A.M.; Mehta, A.; Zheng, H.; Mitchell, J.F.; Borzenets, V. *J. Phys. Condens. Matter* **2015**, 28, 025602.
 7. “Photo-modulated dynamic competition between metallic and insulating phases in a layered manganite” Li, Y.; Walko, D; Li, Q; Liu, Y.; Rosenkranz, S; Zheng, H.; Mitchell, J.F.; Wen, H.; Dufresne, E.; Adams, B. MRS Proceedings, 1636, mrsf13-1636-u6.09.
 8. “Isotropic and Anisotropic Regimes of the Field-Dependent Spin Dynamics in Sr₂IrO₄: Raman Scattering Studies” Gim, Y.; Sethi, A.; Zhao, Q.; Mitchell, J.F.; Cao, G.; Cooper, S.L. *Phys. Rev B* **2016**, 93, 024405.
 9. “Changes in the Electronic Structure and Spin Dynamics Across the Metal-Insulator Transition in La_{1-x}Sr_xCoO₃” Smith, R.X.; Hoch, M.J.R.; Moulton, W.G.; Kuhns, P.L.; Reyes, A.P.; Boebinger, G.S.; Zheng, H.; Mitchell, J.F. *Phys. Rev. B* **2016**, 93, 024204
 10. “Nonpercolative nature of the metal-insulator transition and persistence of local Jahn-Teller distortions in the rhombohedral regime of La_{1-x}Ca_xMnO₃” Shatnawi, M.; Bozin, E.S.; Mitchell, J.F.; Billinge, S.J.L. *Phys. Rev. B* **2016**, 93, 165138.
 11. “Simultaneous first-order valence and oxygen vacancy order/disorder transitions in (Pr_{0.85}Y_{0.15})_{0.7}Ca_{0.3}CoO_{3-x} via analytical transmission electron microscopy” Gulec, A.; Phelan, D. Leighton, C. Klie, R. *ACS Nano* **2016**, 10, 938.
 12. “Magnetotransport of single crystalline YSb” Ghimire, N.; Botana, A.; Phelan, D.; Zheng, H.; Mitchell, J.F. *J. Phys. Cond. Matt.* **2016**, 28, 235601.
 13. “Toward ‘Synthesis by Design:’ Controlling atomic correlations during inorganic materials synthesis” Soderholm, L.S.; Mitchell, J.F. *APL: Materials* **2016**, 4, 053212.
 14. “Stacked charge stripes in the trilayer nickelate La₄Ni₃O₈” Zhang, J.; Shen, Y.-S.; Zheng, H. Norman, M.R.; Mitchell, J.F. *Proc. Natl. Acad. Sci.*, **2016**, 113(32) 8945-8950.
 15. “Distinct Electronic Structure for the Extreme Magnetoresistance in YSb” He, J.F.; Zhang, C.F.; Ghimire, N.J.; Liang, T.; Jian, C.J.; Jiang, J.; Tang, S.J.; Chen, S.S.; He, Y.; Mo, S.K.; Hwang, C.C.; Hashimoto, M.; Lu, D.H.; Moritz, B.; Devereaux, T.P.; Chen, Y.L.; Mitchell, J.F.; Shen, Z.X. *Phys. Rev. Lett.* **2016**, 117(26), 267201.
 16. “Domain Behavior in Functional Materials Studied Using Lorentz Microscopy” Phatak, C.; Zhang, S.; Jiang, W; te Velthuis, S.G.E.; Hoffmann, A., Mitchell, J.F.; Zheng, H.; Norman, M.R.; Petford-Long, A.; *Microsc. and Microanalysis* **2016**, 22, 1660.
 17. “Etching of Cr Tips for Scanning Tunneling Microscopy of Cleavable Oxides” Huang, D.; Liu, S.; Zeljkovic, I.; Mitchell, J.F.; Hoffman, J.E. *Rev. Sci. Inst.* **2017**, 88(2), 023705.
 18. “High Pressure Floating-Zone Growth of Perovskite Nickelate LaNiO₃ Single Crystals” Zhang, J.; Zheng, H.; Ren, Y.; Mitchell, J.F. *Cryst. Growth Design* **2017**, 17(5), 2730.
 19. “Mimicking Cuprates: Large Orbital Polarization in a Metallic Square-Planar Nickelate” Zhang, J.; Botana, A.S.; Freeland, J.W.; Phelan, D.; Zheng, H.; Pardo, V.; Norman, M.; Mitchell, J.F. *Nature Physics* **2017**, 518, 179.
 20. “Single crystal growth and structural evolution across the 1st order valence transition in (Pr_{1-y}Y_y)_{1-x}Ca_xCoO_{3-δ}” Schreiber, N.J.; Zhang, J.; Zheng, H.; Freeland, J.W.; Cheng, Y.-S.; Mitchell, J.F.; Phelan, D. *J. Solid State Chem.* **2017**, 254, 69-74.

Dynamics of electronic interactions in superconductors and related materials

Dan Dessau, University of Colorado Boulder

Program Scope

We perform experimental studies of the dynamics of electronic interactions in high temperature superconductors (cuprates and pnictides), related transition metal oxides (nickelates, iridates, and ruthenates), and topological phases of matter. We primarily utilize high-resolution angle-resolved photoemission (ARPES). We have a large number of collaborators to supply us with unique bulk and thin-film single crystal materials of these samples, theoretical collaborators using both density functional and field-theoretical tools, and excellent access to both synchrotron radiation facilities as well as our own unique in-house laser-based ARPES setup.

Recent Progress

Here we focus on our recent ARPES experiments on trilayer Nickelates [1]. Layered nickelates have the potential for exotic physics similar to high T_C superconducting cuprates as they have similar crystal structures and these transition metals are neighbors in the periodic table. Previous studies on these materials were limited because of the lack of single crystalline materials, though the Mitchell group from Argonne has recently overcome this limitation via the use of a novel high-pressure floating-zone growth furnace.

Utilizing these newly available crystals, we have performed the first ARPES measurements on trilayer nickelates, initially studying the so-called 4-3-10 compound $\text{La}_4\text{Ni}_3\text{O}_{10}$. We have revealed its electronic structure and correlations, finding strong resemblances to the cuprates as well as a few key differences.

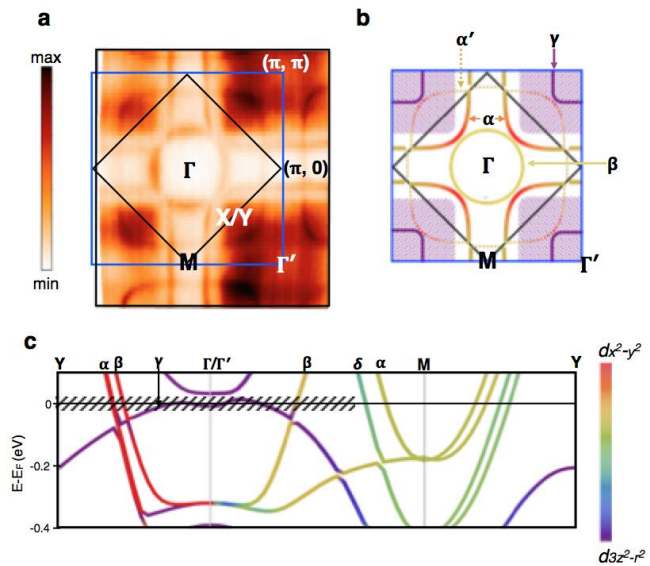


Fig 1 a) ARPES Fermi map of $\text{La}_4\text{Ni}_3\text{O}_{10}$. b) Schematic of the data of panel a, including a labeling of the three key bands (α, β, γ). c) Our calculation of the electronic structure of the same compound, including a color-coding of the orbital weight of the key bands according to whether they are principally $d_{x^2-y^2}$ symmetry or $d_{3z^2-r^2}$ symmetry. The α band with predominant $d_{x^2-y^2}$ symmetry is very similar to the band in cuprates that dominates cuprate physics.

We find a large hole-like Fermi surface that closely resembles the Fermi surface of optimally hole-doped cuprates (α band, see figure 1b, redrawn from the raw data of figure 1a)), including its dx^2-y^2 orbital character (figure 1c for theory, but also including polarization ARPES data not shown here), hole filling level, and strength of electronic correlations (mass enhancement, that we directly extract from the data). However, in contrast to cuprates, $\text{La}_4\text{Ni}_3\text{O}_{10}$ has some extra bands, most noticeably one of principally $d3z^2-r^2$ orbital character (γ band of figure 1a) that is massive and is extremely near the Fermi energy (see the hatched regions of figure 1b and 1c).

Figure 2 shows some details of the low energy (near- E_F) spectral features, which are most important for the physical properties such as transport and possible superconductivity. Panel a shows the data from the cuprate-like α band measured at low temperature and at 4

different places on the Fermi surface. No gapping or pseudogapping is observed, in contrast to this band in the cuprates which does gap. In contrast, panel c shows the γ band of the nickelate does gap at low temperatures, with this gap going away above $\sim 140\text{K}$. This temperature regime matches a change in the electrical resistivity (figure 1c), indicating a likely connection to this physics, though many more measurements should be carried out to better elucidate these connections and the underlying physics.

It is not yet understood why the α -band supports gaps, pseudogaps, and superconductivity in the cuprates but not in this family of the nickelates. The single-layer nickelates have been shown to support pseudogaps [2], but this is achieved by a large amount of doping that brings in disorder that is presumably damaging to any potential superconductivity. Other, related members of the nickelates may be better candidates.

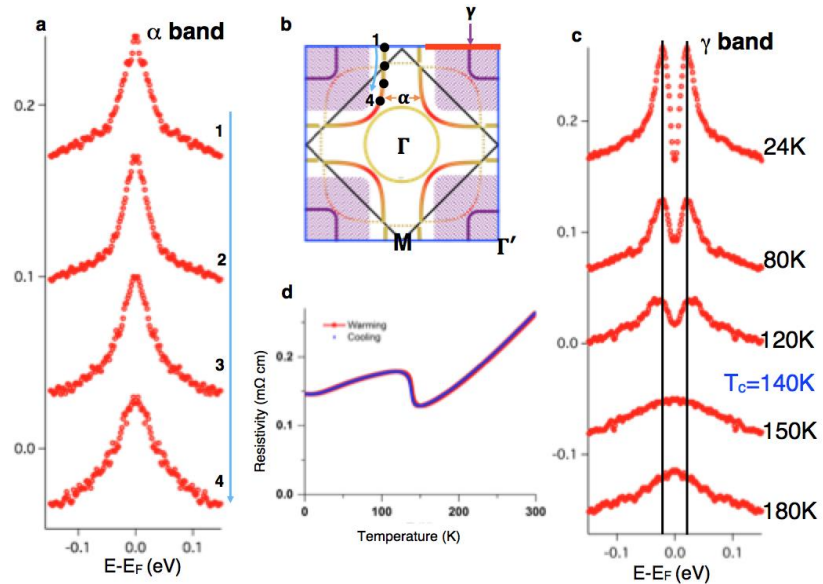


Fig 2. a) Near- E_F ARPES spectra at $T=30\text{K}$ from 4 locations along the α Fermi surface (see panel b). No gapping or pseudogapping is observed anywhere along this Fermi surface. c) Near- E_F ARPES spectra from the γ band (panel c), which shows a clear gapping at low temperatures (below $T \sim 140\text{K}$) but not above 140K . d) Resistivity as a function of temperature, showing a transition near 140K .

Future Plans

The nickelates represent many new opportunities for research in correlated electron systems, and we plan to continue working with the Mitchell group from Argonne to study these materials. High among these plans is to study the so-called 4-3-8 compounds, which are similar to the 4-3-10 samples discussed above but with two fewer oxygen atoms per unit cell. Compared to the 4-3-10 compounds that have close to a d^8 average electron count, the 4-3-8 compounds have an average electron count close to d^9 and so are expected to be more similar to the cuprates (especially the electron-doped ones). On the other hand, the 4-3-8 compounds are more brittle and more challenging to cleave and get excellent quality ARPES data from. We also hope to study bilayer nickelates if they become available as high quality crystals. One direction we will explore for obtain high quality ARPES on small or more-difficult-to-cleave crystals is to use the new microARPES and nanoARPES capabilities that are coming on-line at the ALS, Berkeley.

In addition to continued work on nickelates, we are continuing to make excellent progress on cuprate superconductors, using our recently developed tools for obtaining the electronic structure in the presence of strong self-energy /interaction effects and heterogeneity effects. Here we are focusing on understanding the transition from the non-superconducting pre-pairing and pseudogap states into the superconducting state, considering especially the impact of the rapidly evolving self-energy effects with temperature.

Other ongoing projects include studies of strong spin-orbit coupled systems, including some doped ruthenates and iridates and some topological materials, including those that show “XMR” or extreme magnetoresistance.

References

- [1] Haoxiang Li, Xiaoqing Zhou, Thomas Nummy, Junjie Zhang, Victor Pardo, Warren E. Pickett, J. F. Mitchell, D. S. Dessau, ^[1]Fermiology and Electron Dynamics of Trilayer Nickelate ($\text{La}_4\text{Ni}_3\text{O}_{10}$)” Nature Comm (2017)
- [2] M. Uchida, *et al.* Pseudogap of metallic layered nickelate $R_{2-x}\text{Sr}_x\text{NiO}_4$ ($R=\text{Nd}, \text{Eu}$) crystals measured using angle-resolved photoemission spectroscopy. *Phys. Rev. Lett.* **106**, 027001 (2011).

DOE Supported Publications in 2016 and 2017

Haoxiang Li, Xiaoqing Zhou, Thomas Nummy, Junjie Zhang, Victor Pardo, Warren E. Pickett, J. F. Mitchell, D. S. Dessau^[LSEP] "Fermiology and Electron Dynamics of Trilayer Nickelate ($\text{La}_4\text{Ni}_3\text{O}_{10}$)" *Nature Comm* (2017)

Matthew Brahlek, Nikesh Koirala, Maryam Salehi, Jisoo Moon, Wenhan Zhang, Haoxiang Li, Xiaoqing Zhou, Myung-Geun Han, Liang Wu, Thomas Emge, Hang-Dong Lee, Can Xu, Seuk Joo Rhee, Torgny Gustafsson, N. Peter Armitage, Yimei Zhu, Daniel S. Dessau, Weida Wu, and Seongshik Oh. "Disorder-driven topological phase transition in Bi_2Se_3 films" *PRB* 94, 165104 (2016)

Xiaoqing Zhou, Haoxiang Li, Justin Waugh, Stephen Parham, Heung-Sik Kim, Jennifer Sears, Andrew Gomes, Hae-Young Kee, Young-June Kim, Daniel Dessau "ARPES study of the Kitaev Candidate $\alpha\text{-RuCl}_3$ " *PRB* 94, 161106 (2016)

Yue Cao, Qiang Wang, Justin A. Waugh, Theodore J. Reber, Haoxiang Li, Xiaoqing Zhou, Stephen Parham, Nicholas C. Plumb, Eli Rotenberg, Aaron Bostwick, Jonathan D. Denlinger, Tongfei Qi, Michael A. Hermele, Gang Cao, Daniel S. Dessau "Hallmarks of the Mott-Metal Crossover in the Hole Doped $J=1/2$ Mott insulator Sr_2IrO_4 " (*Nature Communications* 7,11367 (2016)

Electron Spectroscopy

Peter D. Johnson, Chris Homes, Tonica Valla

Condensed Matter Physics and Materials Science Department, Brookhaven National Lab.

Program Scope

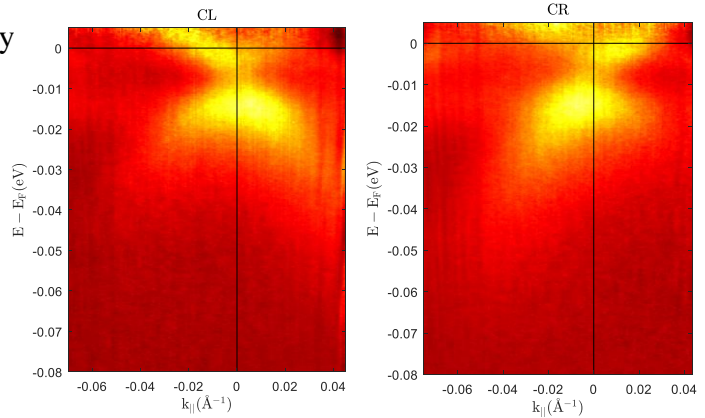
The focus of the electron spectroscopy program at BNL is the exploration of the electronic structure and electrodynamics of topological insulators (TI) and strongly correlated electron systems, with particular attention to emergent phenomena, using the complementary techniques of angle-resolved photoemission (ARPES) and optical spectroscopy. ARPES provides direct access to the electronic structure and to the self-energy effects reflecting the many-body interactions in a system. Optical conductivity measurements provide access to free-carrier and superfluid densities, relaxation rates, and infrared-active lattice modes. Both techniques are sensitive to the emergence of gaps in the spectral function including for instance charge density wave (CDW) and superconducting gaps.

A central goal of this program is to understand how the competing degrees of freedom lead to the complex phase diagrams and how the latter define the macroscopic properties. Studies of the TI and strongly correlated systems are extended to other low-dimensional materials and heavier transition-metal oxides (TMO) in which both the correlation and spin-orbit coupling energies are comparable to band energies. In these materials, the effects of strong spin-orbit coupling and correlations can lead to a myriad of different phases and phenomena. In addition, interaction of topological materials with materials displaying other ground states, in particular with magnetism and superconductivity, will be studied, as the proximity effect is predicted to produce exotic new phenomena, such as Majorana Fermions.[1] The latter could potentially see application in devices associated with quantum computing. In order to carry out these studies, instrumentation has been developed for both ARPES and optical reflectance studies featuring lab-based light sources as well as instrumentation for future beamlines at NSLS II.

Recent Progress

The two key research areas of high T_c superconductivity and topological insulators have recently converged in studies of $\text{FeTe}_{0.5}\text{Se}_{0.5}$ (FTS) where it has been reported that this Fe-based high T_c superconductor supports a topological surface state at the center of the Brillouin zone.[2-4] Such an observation generates considerable interest because it suggests that as the system enters the superconducting state, topological superconductivity in the surface region provides an environment for hosting zero energy bound states or Majorana Fermions (MF).[1] The latter particles, long sought-after in high energy particle physics, represent Fermions that are their own anti-particles. Aside from the fundamental interest in such exotic particles, they may have application as especially robust components for quantum computing. In our own previous studies of the FTS system we pointed to the role of spin-orbit coupling in lifting the degeneracy of the bands at the center of the zone and its potential role in the observed nematicity in these systems.[5] Those studies carried out at higher photon energies and lower energy and momentum resolution confirmed the role of spin-orbit interactions in lifting the degeneracy but

did not provide clear evidence of any topological state. More recently we have studied the system again using high-resolution laser based ARPES with variable light polarization, including both linear and circularly polarized incident light. As indicated in the figure we confirm the presence of a Dirac cone with helical spin structure as expected for a



topological surface state. These experimental studies are compared with theoretical studies that, unlike the previous studies, take account of the disordered local magnetic effects related to the paramagnetism observed in this system. Including magnetic contributions in the theoretical description of the normal state removes the necessity of arbitrarily adjusting the chemical potential as the calculated electronic band structure moves naturally into alignment with the experimental observations. However with the realignment of the band structure, the discussion of the nature of the band gap supporting the topological surface state changes.

The Dirac cone at the center of the Brillouin zone of FTS as seen using circularly polarized light. The Dirac point is located at approximately 5.0 meV below the chemical potential. In a) the incident light is left circularly polarized; and in b) right circularly polarized.

Future Plans

The Lab based activities in the Interdisciplinary Science Building (ISB) at BNL include new capabilities in the use of laser sources, which are proving particularly important for very high resolution studies at the center of the Brillouin zone. We are also developing new capabilities in pump-probe techniques. Lab based facilities also include spectrometers allowing a variety of optical conductivity studies. These lab based capabilities will be complimented in the very near future through the use of new capabilities at NSLS II. The new photoemission facility at the Electron-spectro Microscopy beamline will have focusing capabilities in the one micron range. New infra-red capabilities at NSLS II will allow optical conductivity studies in high magnetic fields and under high pressure.

A major new addition to the program will be the operation of the new OASIS instrument. This new capability brings together Molecular Beam Epitaxy (MBE FWP) with the spectroscopic probes, ARPES and Spectroscopic Imaging Scanning Tunneling Spectroscopy (SISTM FWP). OASIS, which is anticipated to come on line in the very near future, is an essential capability that will expand the studies of strongly correlated materials including the high Tc superconductors beyond the easily cleavable materials currently studied. It will also be critical in expanding the group's program into the studies of interaction of topological matter with superconductivity and magnetism in artificial hetero-structures. It is intended that all of the ARPES instrumentation, including that associated with OASIS, the laser based activities and the beamlines at NSLS II will be made compatible through the use of a Universal Sample Holder (USH). The optical conductivity systems will also be adapted to use this same USH. This will open up each MBE grown sample to a range of different experimental studies.

References

1. L. Fu and C. L. Kane, Phys. Rev. Lett. 100, 096407 (2008)
2. Z. Wang, P. Zhang, G. Xu, L. K. Zeng, H. Miao, X. Xu, T. Qian, H. Weng, P. Richard, A. V. Fedorov et al., Phys. Rev. B 92, 115119 (2015).
3. G. Xu, B. Lian, P. Tang, X-L. Qi and S-C. Zhang, Phys. Rev. Lett. 117, 047001 (2016)
4. P. Zhang et al., [arXiv:1706.05163](https://arxiv.org/abs/1706.05163) (2017)
5. P.D. Johnson, H.B. Yang, J.D. Rameau, G.D. Gu, Z. –H. Pan, T. Valla, M. Weinert, Phys Rev. Lett. 114, 167001 (2015)

Publications

P. D. Johnson, “Angle Resolved Photoemission”, Chapter in Synchrotron Light Sources and Free Electron Lasers, Springer International Publishing Switzerland 2015 , eds. Eberhard Jaeschke, Shaikat Khan, Jochen R. Schneider and Jerome B. Hastings, Springer International Publishing, Switzerland 2015.

Y. M. Dai, H. Miao, L. Y. Xing, X. C. Wang, P. S. Wang, H. Xiao, T. Qian, P. Richard, X. G. Qiu, W. Yu, C. Q. Jin, Z. Wang, P. D. Johnson, C. C. Homes, and H. Ding, Spin-Fluctuation-Induced Non-Fermi-Liquid Behavior with Suppressed Superconductivity in $\text{LiFe}_{1-x}\text{Co}_x\text{As}$, Phys. Rev. X 5, 31035 (2015).

D. E. McNally, S. Zellman, Z. P. Yin, K. W. Post, Hua He, K. Hao, G. Kotliar, D. Basov, C.C. Homes, and M. C. Aronson, From Hund’s insulator to Fermi liquid: Optical spectroscopy study of K doping in BaMn_2As_2 , Phys Rev B 92, 115142 (2015).

Christopher C. Homes, “Optical and Transport Properties” in Iron-Based Superconductivity, eds. P. D. Johnson, G. Xu, and W.-G. Yin, Springer Series in Material Science, Volume 211, pp. 187-219 (Springer, Heidelberg, 2015).

C. C. Homes, M. N. Ali, and R. J. Cava, Optical properties of the perfectly compensated semimetal WTe_2 , Phys. Rev. B 92, 161109(R) (Oct 2015).

P. Pervan, P. Lazic, M. Petrovic, I. rut Rakic, I. Pletikosic, M. Kralj, M. Milun, and T. Valla, Li adsorption versus graphene intercalation on $\text{Ir}(111)$: From quenching to restoration of the Ir surface state, Phys. Rev. B 92, 245415 (Dec 2015).

A. Kogar, et al., Surface Collective Modes in the Topological Insulators Bi_2Se_3 and $\text{Bi}_{0.5}\text{Sb}_{1.5}\text{Te}_3-x\text{Sex}$, Phys. Rev. Lett. 115, 257402 (Dec 2015).

H. W. Ji, I. Pletikosic, Q. D. Gibson, G. Sahasrabudhe, T. Valla, R. J. Cava, Strong topological metal material with multiple Dirac cones, Phys. Rev. B 93, 045315 (2016).

Y. M. Dai, H. Miao, L. Y. Xing, X. C. Wang, C. Q. Jin, H. Ding, and C. C. Homes, Coexistence of clean- and dirty-limit superconductivity in LiFeAs, *Phys. Rev. B* 93, 054508 (2016).

C. C. Homes, Y. M. Dai, J. Schneeloch, R. D. Zhong, G. D. Gu, Phonon anomalies in some iron telluride materials, *Phys. Rev. B* 93 125135 (2016).

H. X. Luo, W. W. Xie, J. Tao, I. Pletikosic, T. Valla, G. S. Sahasrabudhe, G. Osterhoudt, E. Sutton, K. S. Burch, E. M. Seibel, J. W. Krizan, Y. M. Zhu, R. J. Cava, Differences in Chemical Doping Matter: Superconductivity in $Ti_{1-x}Ta_xSe_2$ but Not in $Ti_{1-x}Nb_xSe_2$, *Chem. Mater.* 28 1927-1935 (2016).

S. K. Kushwaha, et al., Sn-doped $Bi_{1.1}Sb_{0.9}Te_2S$ bulk crystal topological insulator with excellent properties, *Nat. Commun.* 7, 11456 (2016).

Q. Li, D. E. Kharzeev, C. Zhang, Y. Huang, I. Pletikosic, A. V. Fedorov, R. D. Zhong, J. A. Schneeloch, G. D. Gu, T. Valla, Chiral magnetic effect in $ZrTe_5$, *Nature Physics* 12, 550 (2016).

H. X. Luo, K. Yan, I. Pletikosic, W. W. Xie, B. F. Phelan, T. Valla, R. J. Cava, Superconductivity in a Misfit Phase That Combines the Topological Crystalline Insulator $Pb_{1-x}Sn_xSe$ with the CDW-Bearing Transition Metal Dichalcogenide $TiSe_2$, *J. Phys. Soc. Jpn.* 85, 064705 (2016).

Z. R. Robinson, G. G. Jernigan, V. D. Wheeler, S. C. Hernández, C. R. Eddy, T. R. Mowll, E. W. Ong, C. A. Ventrice, H. Geisler, I. Pletikosic, H.B. Yang, and T. Valla, Growth and characterization of Al_2O_3 films on fluorine functionalized epitaxial graphene, *J. Appl. Phys.* **120**, 075302 (2016)

A. Akrap, et al., Magneto-Optical Signature of Massless Kane Electrons in Cd_3As_2 , *Phys. Rev. Lett.* 117, 136401, (2016).

Y. M. Dai, Ana Akrap, S. L. Bud'ko, P. C. Canfield, and C. C. Homes, Optical properties of AFe_2As_2 ($A = Ca, Sr, \text{ and } Ba$) single crystals, *Phys. Rev. B* 94, 195142, 2016.

R. Yang, Y.M. Dai, B. Xu, W. Zhang, Z. Qiu, Qiangtao Sui, C. C. Homes, and X. Qiu, Anomalous phonon behavior in superconducting $CaKFe_4As_4$: An optical study, *Phys. Rev. B* 95, 064506 (2017)

T. Yilmaz, W. Hines, Fu-Chang Sun, I. Pletikosić, J. Budnick, T. Valla, B. Sinkovic: Distinct effects of Cr bulk doping and surface deposition on the chemical environment and electronic structure of the topological insulator Bi_2Se_3 , *Appl. Surf. Sci.* 407, 371 (2017)

A.J. Frenzel, C. C. Homes, Q. D. Gibson, Y. M. Shao, K. W. Post, A. Charnukha, R. J. Cava, and D. N. Basov, Anisotropic electrodynamics of type-II Weyl semimetal candidate WTe_2 , *Phys. Rev. B* 95, 245140 (2017)

Session 5

**Interface-Driven Chiral Magnetism in Ultrathin Metallic Ferromagnets:
Towards Skyrmion Spintronics**

Geoffrey Beach

Magnetic Thin Films

**Principle Investigator: A. Hoffmann; Co-PIs: J. S. Jiang, V. Novosad, and J. E. Pearson
Materials Science Division, Argonne National Laboratory, Lemont, IL 60439**

Program Scope

The Magnetic Films Group creates, explores and derives new insights into novel fundamental physics and new materials related to magnetic phenomena. Towards this end we synthesize a variety of thin film heterostructures and more complex lithographically patterned device concepts with the goal to understand and control their physical properties. We focus especially on emerging new phenomena associated with the competition between spatial and magnetic length scales, as well as proximity effects. Our vision is to understand the ultimate limits of miniaturization and prepare magnetic materials with designed functionalities. Thus we tailor properties via systematic control of preparation conditions and manipulate dimensionalities and geometric confinement by thin film deposition via sputtering and electron-beam evaporation combined with advanced patterning and templating techniques. Additional complexity comes from coupled heterostructures, which integrate ferromagnets, antiferromagnets, superconductors, and insulators. Cutting-edge characterizations include the use of neutron-, synchrotron-, and electron-scattering and microscopy at DOE user facilities, as well as sophisticated in-house magnetotransport measurements, low-temperature high-magnetic-field magnetic force microscopy, broadband ferromagnetic resonance, and spatially resolved Brillouin light scattering microscopy. This infrastructure enables us to comprehensively investigate magnetization dynamics, magneto-transport phenomena, and interfacial coupling effects. These new phenomena push the boundaries of fundamental understanding of nanostructured magnetic materials and underlie novel applications ranging from information technologies to energy conversion.

Recent Progress

For this presentation we will focus on our recent work on investigating high-frequency dynamics in magnetic metamaterials. Magnetic metamaterials have tailored magnetic properties due to their artificial structure or geometric constraints. Examples are magnonic crystals or artificial spin ice systems. Artificial spin-ice systems are lithographically defined nanomagnets that mimic effects of frustration, which are characterized by competing interactions that cannot all be simultaneously minimized. This gives rise to highly degenerate magnetic configuration, which in turn result in magnonic crystals with reprogrammable energy-landscapes for magnon propagation. Thus these systems offer unique possibilities in magnon spintronics, since they enable to tailor the magnonic properties by design.

We recently succeeded in measuring the high-frequency response of a metallic artificial square spin-ice lattice made of $\text{Ni}_{80}\text{Fe}_{20}$ [27]. The nano-scaled bar magnets were patterned using electron beam lithography and measured using broadband ferromagnetic resonance spectroscopy. We observed a rich mode spectrum over the full frequency/field range and find an excellent qualitative agreement to a semianalytical model. We furthermore find indications that it might be possible to determine the spin-ice state by resonance experiments. These results are a first step towards the understanding of artificial geometrically frustrated magnetic systems in the GHz-regime.

We also explored the possibility to detect and drive spin dynamics in rectangular $\text{Ni}_{80}\text{Fe}_{20}/\text{Pt}$ antidote lattices, by spin pumping and inverse spin Hall effect [30], as well as spin torque ferromagnetic resonance. We find that the dynamics is determined by the design of the lattice. The results, confirmed by micromagnetic simulations, have direct implications on the development of engineered magnonics applications and devices.

Future Plans

Our previous experiments provide a good starting point to extend the investigation of artificial spin-ice systems beyond the past focus on the statistics of topological defects and the quasi-static evolution of magnetization states, and towards the connection between high-frequency dynamics and distribution of topological defects. Micromagnetic simulations already indicated that certain dynamic modes will only propagate along defect Dirac strings, which opens up exciting possibilities for guided energy and information flow in these magnonic systems. This means that a controlled manipulation of the topological defects in spin ice systems may enable fundamentally new ways of information processing with magnetization dynamics. For this purpose we will use artificial spin ice systems integrated with co-planar waveguides, which will allow direct optical access to the sample. Using Brillouin light scattering microscopy, it is then possible to acquire the local dynamic spectra and directly correlate them with existing topological defects. Indeed, preliminary measurements show significant inhomogeneities of the magnetization dynamics in these systems. We also will expand our studies to other materials with low magnetic damping, such as $\text{Co}_{25}\text{Fe}_{75}$ or yttrium iron garnet. The later will present challenges for creating sufficient dipolar coupling due to its low magnetization, which we will overcome with our new lithographic technique.[11,34] Furthermore, we will prepare artificial spin ice systems from bilayers of magnetic materials with different damping and magnetization, which enables new ways of tailoring frustration and thereby magnetization switching and dynamics. Lastly, we will locally manipulate magnetization either via integrated small-scale microwave antennas or through spin transfer torques by adding Pt to selective elements of the artificial spin ice. This allows defining arbitrary defect structures and enables a detailed test of the theoretical predictions of their dynamic behavior. Furthermore, it will be interesting to study the switching of an individual element and the onset of avalanches and spin-wave excitations.

Publications

1. J. Železný, P. Wadley, K. Olejník, A. Hoffmann, and H. Ohno, *Nature Phys.* (in press).
2. P. N. Lapa, J. Ding, C. Phatak, J. E. Pearson, J. S. Jiang, A. Hoffmann, and V. Novosad, *J. Appl. Phys.* (in press).
3. W. Jiang, G. Chen, K. Liu, J. Zang, S. G. E. te Velthuis, and A. Hoffmann, *Phys. Rep.* (in press).
4. M. B. Jungfleisch, W. Zhang, R. Winkler, and A. Hoffmann, in: *Spin Physics in Semiconductors, 2nd edition*, edited by Michael I. Dyakonov (Springer, New York, 2017), in press.
5. P. N. Lapa, J. Ding, J. E. Pearson, V. Novosad, J. S. Jiang, and A. Hoffmann, *Phys. Rev. B* **96**, 024418 (2017).
6. J. Sklenar, W. Zhang, M. B. Jungfleisch, H. Saglam, S. Grudichak, W. Jiang, J. E. Pearson, J. B. Ketterson, and A. Hoffmann, *Phys. Rev. B* **95**, 224431 (2017).

7. F. Hellman, A. Hoffmann, Y. Tserkovnyak, G. S. D. Beach, E. E. Fullerton, C. Leighton, A. H. MacDonald, D. C. Ralph, D. A. Arena, H. A. Dürr, P. Fischer, J. Grollier, J. P. Heremans, T. Jungwirth, A. V. Kimel, B. Koopmans, I. N. Krivorotov, S. J. May, A. K. Petford-Long, J. M. Rondinelli, N. Samarth, I. K. Schuller, A. N. Slavin, M. D. Stiles, O. Tchernyshyov, A. Thiaville, and B. L. Zink, *Rev. Mod. Phys.* **89**, 025006 (2017).
8. M. E. Stebliy, S. Jain, A. G. Kolesnikov, A. V. Ognev, A. S. Samardak, A. V. Davydebko, E. V. Sukovatitcina, L. A. Chebotkevich, J. Ding, J. Pearson, V. Khovaylo, and V. Novosad, *Sci. Rep.* **7**, 1127 (2017).
9. W. Jiang, X. Zhang, G. Yu, W. Zhang, X. Wang, M. B. Jungfleisch, J. E. Pearson, X. Cheng, O. Heinonen, K. L. Wang, Y. Zhou, A. Hoffmann, and S. G.E. te Velthuis, *Nature Phys.* **13**, 162 (2017).
10. P. N. Lapa, I. V. Roshchin, J. Ding, J. E. Pearson, V. Novosad, J. S. Jiang, and A. Hoffmann, *Phys. Rev. B* **95**, 020409(R) (2017).
11. M. B. Jungfleisch, J. Ding, W. Zhang, W. Jiang, J. E. Pearson, V. Novosad, and A. Hoffmann, *Nano Lett.* **17**, 8 (2017).
12. C. Di Giorgio, F. Bobba, A. M. Cuvolo, A. Scarfato, S. A. Moore, G. Karapetrov, D. D'Agostino, V. Novosad, V. Yefremenko, and M. Iavarone, *Sci. Rep.* **6**, 38557 (2016).
13. . Choi, X. Jiang, W. Bi, P. Lapa, R. K. Chouhan, D. Paudyal, T. Varga, D. Popov, J. Cui, D. Haskel, and J. S. Jiang, *Phys. Rev B* **94**, 184433 (2016).
14. J. Sklenar, W. Zhang, M. B. Jungfleisch, W. Jiang, H. Saglam, J. E. Pearson, J. B. Ketterson, and A. Hoffmann, *J. Appl. Phys.* **120**, 180901 (2016).
15. H. Saglam, W. Zhang, M. B. Jungfleisch, J. Sklenar, W. Jiang, J. E. Pearson, J. B. Ketterson, and A. Hoffmann, *Phys. Rev. B* **94**, 140412(R) (2016).
16. P. Li, T. Liu, H. Chang, A. Kalitsov, W. Zhang, G. Csaba, W. Li, D. Richardson, A. DeMann, G. Rimal, H. Dey, J. S. Jiang, W. Porod, S. B. Field, J. Tang, M. C. Marconi, A. Hoffmann, O. Mryasov, and M. Wu, *Nature Comm.* **7**, 12688 (2016).
17. V. Vlaminck, W. Yáñez, J. Hoffman, A. Hoffmann, and D. Niebieskikwiat, *Phys. Rev. B* **94**, 064404 (2016).
18. Y.-L. Wang, Z.-L. Xiao, A. Snezhko, J. Xu, L. E. Ocola, R. Divan, J. E. Pearson, G. W. Crabtree, and W.-K. Kwok, *Science* **352**, 962 (2016).
19. C. Phatak, S. Zhang, W. Jiang, S. G. E. te Velthuis, A. Hoffmann, J. F. Mitchell, H. Zheng, M. R. Norman, and A. Petford-Long, *Microsc. Microanal.* **22** (Suppl. 3), 1680 (2016).
20. M. B. Jungfleisch, W. Zhang, J. Sklenar, W. Jiang, J. E. Pearson, J. B. Ketterson, and A. Hoffmann, *Phys. Rev. B* **93**, 224419 (2016).
21. J. Ding, P. Lapa, S. Jain, T. Khaire, S. Lendinez, W. Zhang, M. B. Jungfleisch, C. M. Posada, V. G. Yefremenko, J. E. Pearson, A. Hoffmann, and V. Novosad, *Sci. Rep.* **6**, 25196 (2016).

22. W. Jiang, W. Zhang, G. Yu, M. B. Jungfleisch, P. Upadhyaya, H. Somaily, J. E. Pearson, Y. Tserkovnyak, K. L. Wang, O. Heinonen, S. G. E. te Velthuis, and A. Hoffmann, *AIP Adv.* **6**, 055602 (2016).
23. J. Sklenar, W. Zhang, M. B. Jungfleisch, W. Jiang, H. Saglam, J. E. Pearson, J. B. Ketterson, and A. Hoffmann, *AIP Adv.* **6**, 055603 (2016).
24. O. Heinonen, W. Jiang, H. Somaily, S. G. E. te Velthuis, and A. Hoffmann, *Phys. Rev. B* **93**, 094407 (2016).
25. W. Zhang, J. N. Sklenar, B. Hsu, W. Jiang, M. B. Jungfleisch, J. Xiao, F.Y. Fradin, Y. Liu, J. E. Pearson, J. B. Ketterson, Z. Yang, and A. Hoffmann, *APL Mater.* **4**, 032302 (2016).
26. S. M. Wu, W. Zhang, A. KC, P. Borisov, J. E. Pearson, J. S. Jiang, D. Lederman, A. Hoffmann, and A. Bhattacharya, *Phys. Rev. Lett.* **116**, 097204 (2016).
27. M. B. Jungfleisch, W. Zhang, E. Iacocca, J. Sklenar, J. Ding, W. Jiang, S. Zhang, J. E. Pearson, V. Novosad, J. B. Ketterson, O. Heinonen, and A. Hoffmann, *Phys Rev. B* **93**, 100401(R) (2016).
28. P. N. Lapa, T. Kaire, J. Ding, J. E. Pearson, V. Novosad, A. Hoffmann, and J. S. Jiang; *AIP Adv.* **6**, 056107 (2016).
29. J. Ding, S. Jain, P. N. Lapa, T. Kaire, S. Lendinez, C. M. Posada, W. Zhang, J. E. Pearson, A. Hoffmann, and V. Novosad, *AIP Adv.* **6**, 056102 (2016).
30. M. B. Jungfleisch, W. Zhang, J. Ding, W. Jiang, J. Sklenar, J. E. Pearson, J. B. Ketterson, and A. Hoffmann, *Appl. Phys. Lett.* **108**, 052403 (2016).
31. M. B. Jungfleisch, W. Zhang, J. Sklenar, J. Ding, W. Jiang, H. Chang, F. Y. Fradin, J. E. Pearson, J. B. Ketterson, V. Novosad, M. Wu, and A. Hoffmann, *Phys. Rev. Lett.* **116**, 057601 (2016).
32. S. A. Moore, G. Plummer, J. Fedor, J. E. Pearson, V. Novosad, G. Karapetrov, and M. Iavarone, *Appl. Phys. Lett.* **108**, 042601 (2016).
33. Y. L. Wang, L. R. Thoutam, Z. L. Xiao, B. Shen, J. E. Pearson, R. Divan, L. E. Ocola, G. W. Crabtree, and W. K. Kwok, *Phys. Rev. B* **93**, 045111 (2016).
34. S. Li, W. Zhang, J. Ding, J. E. Pearson, V. Novosad, and A. Hoffmann, *Nanoscale* **8**, 388 (2016).
35. M. B. Jungfleisch, W. Zhang, W. Jiang, and A. Hoffmann, *SPIN* **5**, 1530005 (2015).
36. A. C. Basaran, J. E. Villegas, J. S. Jiang, A. Hoffmann, and I. K. Schuller, *MRS Bulletin* **40**, 925 (2015).
37. J. Sklenar, W. Zhang, M. B. Jungfleisch, W. Jiang, H. Chang, J. E. Pearson, M. Wu, J. B. Ketterson, and A. Hoffmann, *Phys. Rev. B* **92**, 174406 (2015).
38. W. Zhang, M. B. Jungfleisch, F. Freimuth, W. Jiang, J. Sklenar, J. E. Pearson, J. B. Ketterson, Y. Mokrousov, and A. Hoffmann, *Phys. Rev. B* **92**, 144405 (2015).
39. A. Hoffmann and S. D. Bader, *Phys. Rev. Appl.* **4**, 047001 (2015).

Program Title: Quantum Order and Disorder in Magnetic Materials**Principal Investigator: Thomas F. Rosenbaum, California Institute of Technology****Program Scope**

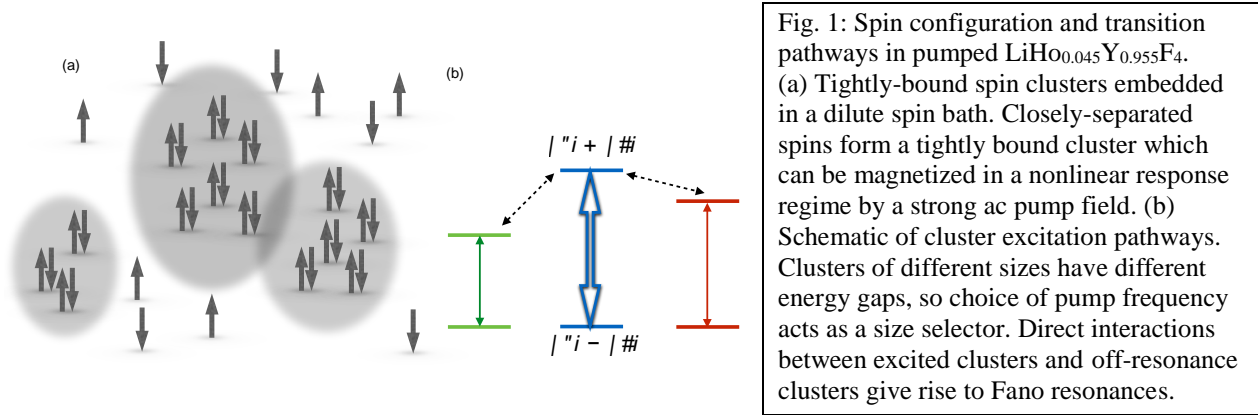
Disorder, competing interactions, and geometrical frustration on the mesoscopic scale can have profound macroscopic consequences, leading to materials with novel electronic, optical, and magnetic properties. Inhomogeneous quantum systems are particularly appealing in this context because they have a proclivity for stable self-organization on scales from nanometers to microns, and can exhibit pronounced fluctuations away from equilibrium. With the right choice of materials, there are manifest opportunities for tailoring the macroscopic response and for garnering insights into fundamental quantum properties such as coherence and entanglement. We seek here to explore and exploit model, disordered and geometrically frustrated magnets where coherent spin clusters stably detach themselves from their surroundings, leading to extreme sensitivity to finite frequency excitations and the ability to encode information. We take advantage of the ability to tune quantum tunneling with a “knob” in the laboratory, a field applied transverse to the ordering axis of magnetic dipoles. We propose to drive the systems into the nonlinear regime to parse tunneling pathways, decoherence from the thermodynamic spin bath, and the underlying structure of the complex free energy landscape. Moreover, by tuning the spin concentration along with the tunneling probability, it should be possible to study the competition between quantum entanglement and random field effects. As one passes from the quantum to the classical limit, clear implications develop for magnetic storage architectures. Finally, extensions from quantum ferromagnets to quantum antiferromagnets promise new physics as well as tests of universality. A combination of ac susceptometry, dc magnetometry, Barkhausen noise measurements, non-linear Fano experiments, optical spectroscopy, and neutron diffraction as functions of temperature, magnetic field, frequency, excitation amplitude, dipole concentration, and disorder should address issues of stability, overlap, coherence, and control.

Recent Progress

(A) Tunable Quantum Dynamics in a Disordered Magnet: Localization in quantum systems remains both fundamental to science as well as to technology. It is a venerable subject, starting with the work of Anderson – whose name is associated with disorder-induced localization – and Mott, whose Mott localization transition is due to repulsion between electrons. The combined problem of many-body localization persists to this day, and recently has acquired practical relevance for systems of quantum devices. A notable example is the “D-wave” processor, which attempts to implement adiabatic quantum computation, but may be limited as a matter of principle by localization effects.

To control these long-lived and independent states, it is necessary to know how they interact with each other and with the outside world. Minimizing the interactions between coherent localized states and a continuum of states in the broader environment is an important goal for realizing an effective quantum computer. However, these environmental couplings are by definition weak compared to the transitions among the states contributing to the spectrum for a particular localizing environment, making it difficult to study them directly. Recently, it has been posited that many weak couplings of this sort can be probed by pumping the system into a nonlinear response regime, saturating the discrete transition associated with the coherent state, and using the emergence of a Fano resonance to characterize the interactions with the continuum states. In

this work and as illustrated in Fig. 1, we use a magnetic adaptation of the Fano resonance technique to examine the coupling between coherent spin clusters quantum-mechanically isolated from the spin bath generated by other clusters of varying sizes.



Our work differs from the experiments in quantum optics in that we are examining emergent degrees of freedom in a (magnetic) many-body system rather than single-particle states in atoms and semiconductor quantum dots. At the same time, it represents a major advance over our own previous DOE-supported activity on hole-burning in the same magnetic system in that we uncover a remarkably simple phenomenology, including the discovery of a zero-crossing for the Fano effect, as a function of non-linear drive amplitude and quantum mixing via a transverse field (Fig. 2).

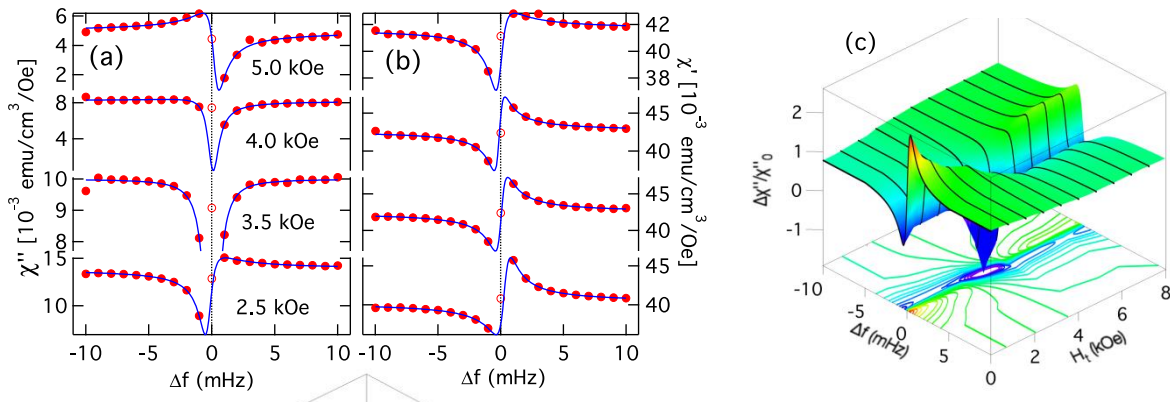


Fig. 2: Linear absorption as a function of transverse field at $T = 0.11$ K for a 202 Hz pump (a,b) Measured imaginary and real susceptibilities (points) and fits to a Fano resonance as a function of transverse field for a fixed 0.3 Oe pump. Transverse field-induced quantum tunneling tunes the resonant behavior without a corresponding increase in decoherence. (c) Normalized absorption as a function of frequency and transverse field. The zero-crossing at $H_t \sim 3.5$ kOe corresponds to a local minimum in the dissipation and a decoupling from the spin bath.

(B) Crackling Noise in the Quantum Limit: Domain motion creates Barkhausen noise in the magnetization of a ferromagnet. This type of crackling noise, which emerges as a varying longitudinal field traces out a ferromagnet's hysteresis loop, provides a statistical measure of the size and energy distribution of magnetic avalanches. In principle, Barkhausen noise can arise

from both thermal excitation of magnetic domains as well as quantum tunneling of the domains at sufficiently low temperatures. As illustrated in Fig. 3, we have been able to measure Barkhausen noise down to $T = 0.080$ K in the disordered, dipolar-coupled, Ising ferromagnet, $\text{LiHo}_{0.65}\text{Y}_{0.35}\text{F}_4$, with a Curie temperature of 0.98 K.

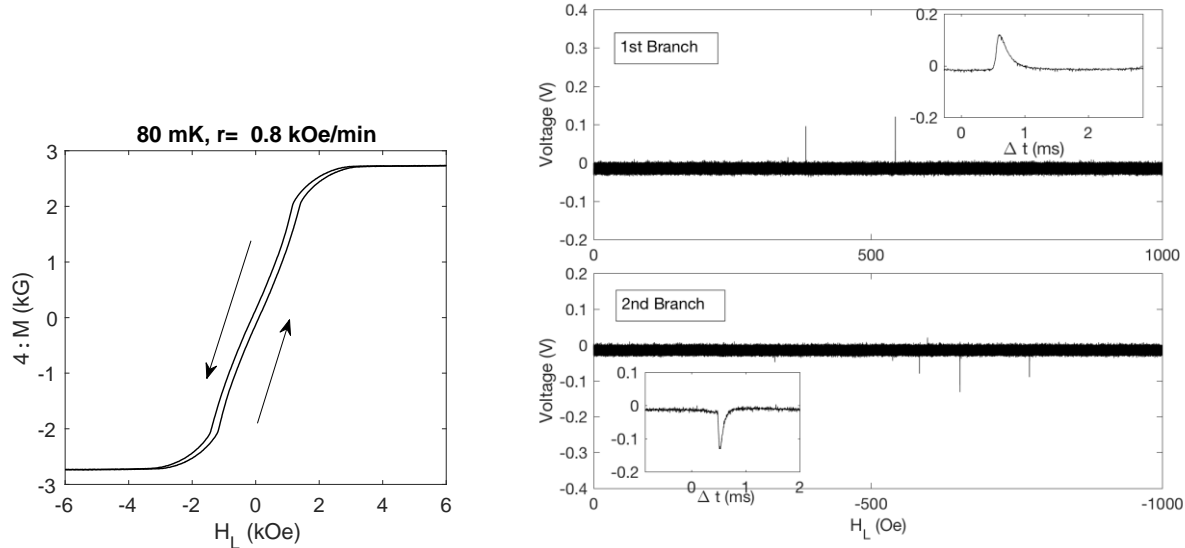


Fig. 3: Hysteresis loop (up and down branches) and Barkhausen noise in $\text{LiHo}_{0.65}\text{Y}_{0.35}\text{F}_4$ at $T = 0.080$ K.

It is not possible yet to definitively ascribe a quantum origin to the lowest temperature noise features, but we should be able to distinguish classical and quantum effects through the application of a transverse magnetic field. At small magnitudes, a transverse magnetic field primarily creates a site-random magnetic field that pins the domain walls, creating barriers to motion that increase with random field amplitude. The rising barrier height decreases the probability of reversal at a given applied field, and the pinning potential effectively can be increased or decreased on demand and, importantly, in a temperature-independent manner. As the magnitude of the transverse field is increased, one crosses into a quantum speedup regime, where the primary effect of the transverse field is to increase the tunneling probability of the domain walls by creating an admixture of “up” and “down” Ising spins. This effect is most pronounced at the lowest temperatures.

Future Plans

Quantum Coherence and Quenches: Via hole burning, we have demonstrated localization of excitations among interacting magnetic dipoles. For strong coupling to the heat bath, previous work has shown a trend towards spin freezing at low temperatures, and the current work shows no spectral hole burning in this strong coupling limit, corresponding to delocalized excitations. Reducing the coupling to the bath induces a transition to a spin liquid state where the excitations are localized to a very high degree, with a $Q \sim 10^5$ for the spectral hole. The small mixing between excited states of different spin clusters leads to a Fano effect, whose phenomenology for this complex system is remarkably simple, with a vanishing Fano parameter q coinciding with an inflection point in the ac magnetization induced by the drive field responsible for the hole-

burning. The ability to tune the interactions between the spin clusters and the background spin bath, and in particular the appearance of a dissipation-free state at the point where q vanishes, suggests a new avenue for creating long-lived quantum states with minimal decoherence and environmental coupling. We will map out the full phase space of transverse field, longitudinal pump field, frequency, and temperature to elucidate the conditions for maximal coherence. Of special interest are the transverse fields, such as 3.5 kOe (see Fig. 2), corresponding to level crossings in the electro-nuclear hyperfine levels of the Ho dipoles. The experiments will harness hole-burning for characterizing many-body localization, and also reveal how nonlinear quantum dynamics can lead to emergent two-level systems.

Finally, we plan preliminary experiments on quantum quenches. A quantum quench is the rapid tuning of a quantum parameter, such as magnetic field, that drives a material out of equilibrium and creates excitations, e.g., quasiparticles, vortices, and magnetic domain walls. Over the past decade, intense interest has converged on how the quench rate and material parameters, such as inter-particle interactions, determine the density and character of excitations created during the quench, and how equilibrium is eventually established. Understanding quantum quench dynamics is of practical and fundamental importance. For example, future quantum annealers used to solve combinatorial optimization problems will rely on a quantum material maintaining equilibrium during a slow quantum quench. In other cases, enhancing disequilibrium during and after a quench may improve device performance. An area of particular focus and potential impact involves measuring quenches across a phase transition, which is believed to give rise to universal behavior irrespective of microscopic material details. The Kibble-Zurek effect predicts that the density of excitations created during a quench scales as a power-law that depends on the critical exponents associated with the phase transition and the dimensionality. We will test these predictions in the model quantum ferromagnet, $\text{Li}(\text{Ho},\text{Y})\text{F}_4$, with varying amounts of disorder.

Recent Publications (Supported by BES)

1. “Sub-Kelvin Magnetic and Electrical Measurements in a Diamond Anvil Cell with *in situ* Tunability,” A. Palmer, D.M. Silevitch, Y. Feng, Y. Wang, R. Jaramillo, A. Banerjee, Y. Ren, and T.F. Rosenbaum, *Rev. Sci. Instrum.* **86**, 093901 (2015) [Editor’s Pick].
2. “Spiral Magnetic Order and Pressure-Induced Superconductivity in Transition Metal Compounds,” Y. Wang, Y. Feng, J.-G. Cheng, W. Wu, J.L. Luo, and T.F. Rosenbaum, *Nature Commun.* DOI:10.1038/ncomms13037 (2016).
3. “Optical Response from Terahertz to Visible Light of Electronuclear Transitions in $\text{LiYF}_4:\text{Ho}^{3+}$,” G. Matmon, S.A. Lynch, T.F. Rosenbaum, A.J. Fisher, and G. Aeppli, *Phys. Rev. B* **94**, 205132 (2016).
4. “Multiple Superconducting States Induced by Pressure in Mo_3Sb_7 ,” Y. Feng, Y. Wang, A. Palmer, L. Li, D.M. Silevitch, S. Calder, and T.F. Rosenbaum, *Phys. Rev. B* **95**, 125102 (2017).
5. “Probing Many-Body Localization in a Disordered Quantum Magnet,” D.M. Silevitch, G. Aeppli, and T.F. Rosenbaum, arXiv:1707.04952 (2017).
6. A. Dutta, G. Aeppli, B.K. Chakrabarti, U. Divakaran, T.F. Rosenbaum, and D. Sen, *Quantum Phase Transitions in Transverse Field Models: From Statistical Physics to Quantum Information* (Cambridge University Press, New Delhi, 2015), ISBN 978-1-107-06879-7.

Topological materials with complex long-range order.

Principle Investigator: James Analytis

Department of Physics, University of California, Berkeley, California 94720, USA

Program Scope

This program is focused on the study of strongly frustrated magnetic systems, particularly materials where Coulomb, kinetic and spin orbit energy scales conspire to give exotic exchange interactions. The current scope of the program can be summarized as follows.

- ***Using pressure and magnetic field to tune the ground state of Kitaev materials.*** Frustrated magnets have a rich array of possible ground states to choose from. A key question is whether we can couple to the appropriate energy scale to tune between these ground states. Magnetic field can be used to couple to the Zeeman response of local moments and take advantage of large g -factor anisotropies. Pressure can be used to tune the bond angles and distances between magnetic ions, with dramatic effects on the exchange energy.
- ***Using ultra-sensitive magnetic measurements to understand the nature of intertwined ground states.*** Many of the state in frustrated systems are extremely subtle, forming hidden orders that are intertwined with the known ones. By focusing on ultra-low noise magnetic measurements, we reveal the magnetic signatures of these hidden states.
- ***Using Resonant Inelastic X-ray Scattering techniques to understand magnon band structure.*** Resonant Inelastic X-ray techniques have come to the fore as the preeminent tools for the determination of excitations in correlated systems. We utilize these tools to determine the magnon dispersion of Kitaev candidate materials.
- ***Understanding the symmetry and thermodynamic response of states borne from magnetic frustration.*** By developing symmetry-sensitive thermodynamic techniques, we determine the existence and symmetry of hidden ordered states, as well as their thermal conductivity properties.

Recent Progress

Background. In the honeycomb iridates $A_2\text{IrO}_3$ (A is the alkali), an exotic kind of anisotropic exchange emerges which maps these structures onto a remarkable theoretical model pioneered by Kitaev [1]. The layered honeycomb structure is composed of octahedrally coordinated Ir^{4+} , bonded together along O_2 edges. The exchange pathway between spin-1/2 Ir, across these bonds is predicted to be highly anisotropic due to the spin-orbit coupling [2]. This material has three known polytypes, identified for the first time in our recent work [3].

(1) Field induced intertwined states. In our early work we discovered a thermodynamic transition at low temperatures as a function of field, and speculated that this may be an indication

of a possible Kitaev quantum phase transition [3]. In our current work, we have performed extensive investigation using detailed thermodynamic and scattering measurements.

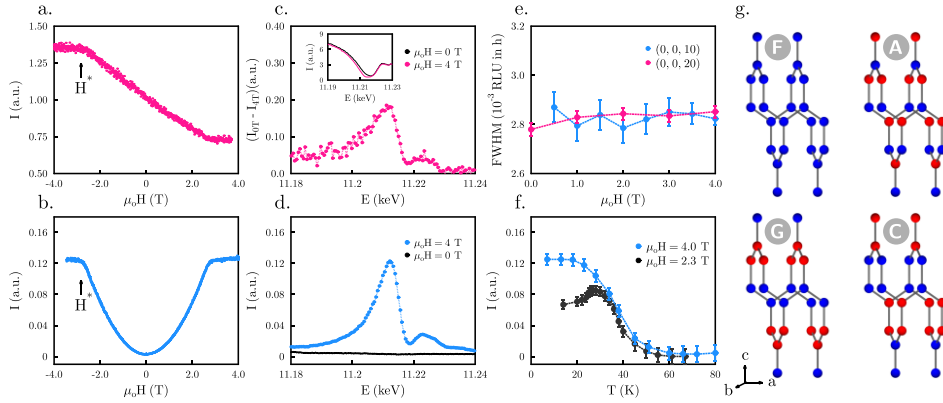


Figure 1: Field, energy and temperature dependence of the commensurate order $q = (0, 0, 0)$. Field dependence of the scattering intensity taken at $T = 5$ K and $E = 11.215$ keV around: (a) the structurally allowed $(2m, 0, 14n + 2m)$ peaks (e.g. $(0, 0, 20)$) which show a linear dependence and, (b) the symmetry disallowed peaks $(2m, 0, 12n \pm 2 + 6m)$ (e.g. $(0, 0, 10)$) which show a quadratic dependence to the applied field. A kink was again observed at $\mu_0 H^* = 2.8$ T. The energy dependence for the allowed peaks is shown in the inset (c) with a dip at the absorption edge $E = 11.215$ keV. The main panel (c) shows the difference between the intensity at $\mu_0 H = 0, 4$ T which can be attributed to a magnetic contribution. (d) Energy dependence of the magnetic peak $(2m, 0, 12n \pm 2 + 6m)$ taken at $\mu_0 H = 0.4$ T. (e) $(0, 0, 10)$ and $(0, 0, 20)$ peaks widths (a lower bound on the correlation length) remain constant under the applied field, suggesting there is no macroscopic phase separation. (f) Temperature dependence of the integrated intensities for the $(0, 0, 10)$ at applied fields above and below H^* . Above H^* the onset of the FIZZ state is continuous, while below H^* this onset is cut off by the incommensurate order. The Gaussian fit to the integrated RMXS intensity gives the χ^2 uncertainty shown by the error bars in (e) and (f). (g) Possible basis vectors describing the magnetic order of β -Li₂IrO₃, where F corresponds to ferromagnetic order, A to Néel order, C to stripy order and G to zig-zag order.

In this project we reveal evidence for nearly degenerate broken symmetry states in β -Li₂IrO₃, a signature of the underlying magnetic frustration. This compound is the simplest of the 3D harmonic honeycomb structures, composed of interwoven networks of hexagonal chains propagating in the $a \pm b$ directions. Importantly, Kitaev exchange along the c -axis bonds should couple spins pointing in the b -axis, making the b -axis magnetically special, and thus we focus on the response of the system to an applied field in this direction. We find that in this configuration, a relatively small field can induce a strongly correlated state with ‘zig-zag’ broken symmetry at the expense of the incommensurate order, providing evidence for strong correlations and a possible familial connection between different Mott-Kitaev systems.

In Fig. 1a,b we plot the field response of the scattering intensity at two kinds of reciprocal space points as a function of applied field, one belonging to structurally allowed $(2m, 0, 4n+2m)$ peaks and the other to structurally forbidden $(2m, 0, 12n \pm 2 + 6m)$ peaks, where n, m are two arbitrary integers. The appearance of structurally forbidden peaks immediately suggests that there is an additional $q = 0$ broken symmetry induced by the field. Fig. 1g we show the $q = 0$ broken symmetry states that could describe Ψ_V , denoted using the conventional nomenclature [4]. The symmetries of the state consistent with the primary features of the data above H^* are two-fold: G-type (zig-zag) broken symmetry and F-type order. Our observations are completely consistent with the Landau theory of second order phase transitions - the combined effect of magnetic field

and crystal symmetry is to act as a ‘field’ on Ψ_V , so that the observed zig-zag pattern is linearly coupled to magnetic field (leading to an intensity I_V that is quadratic in field, as seen in Fig. 1b).

(2) Pressure-induced quantum spin liquid state.

Honeycomb iridates such as γ - Li_2IrO_3 are argued to realize Kitaev spin-anisotropic magnetic exchange, along with Heisenberg and possibly other couplings. While systems with pure Kitaev interactions are candidates to realize a quantum spin-liquid ground state, in γ - Li_2IrO_3 it has been shown that the presence of competing magnetic interactions leads to an incommensurate spiral spin order at ambient pressure below 38 K. We study the pressure sensitivity of this magnetically ordered state in single crystals of γ - Li_2IrO_3 using resonant x-ray scattering (RXS) under applied hydrostatic pressures of up to 3.0 GPa. RXS is a direct probe of electronic order, and we observe the abrupt disappearance of the $q = (0.57, 0, 0)$ spiral order at a critical pressure $P_c = 1.4$ GPa with no accompanying change in the symmetry of the lattice.

In this work we use RXS to track the evolution of the γ - Li_2IrO_3 incommensurate spiral order with applied hydrostatic pressure, and observe the suppression of this magnetic phase. While we find no discontinuity in the lattice structure or an associated change in symmetry to the highest pressures measured, we observe an abrupt disappearance of the spiral Bragg peak at a critical pressure $P_c = 1.4$ GPa. This disappearance signals the transition to a distinct electronic ground state.

Figure 2A shows the pressure evolution of the spiral order peak amplitude, tracking its position along the $(H\ 0\ 0)$ axis as the pressure increases. We present a schematic pressure-temperature phase diagram for γ - Li_2IrO_3 in Fig. 2B; the dark region indicates the observed extent of the spiral magnetic order, and the shaded region represents the simplest associated phase boundary. Ongoing studies of this material indicate paramagnetic behavior with rapidly emerging magnetic anisotropy favoring the b (easy) axis direction at ambient pressure. As T approaches 0 K, P_c likely continues to represent a sharp phase boundary between the spiral magnetic order and the as-yet undetermined high- pressure electronic phase; the sharp disappearance could signal a first-order quantum phase transition.

Future Plans

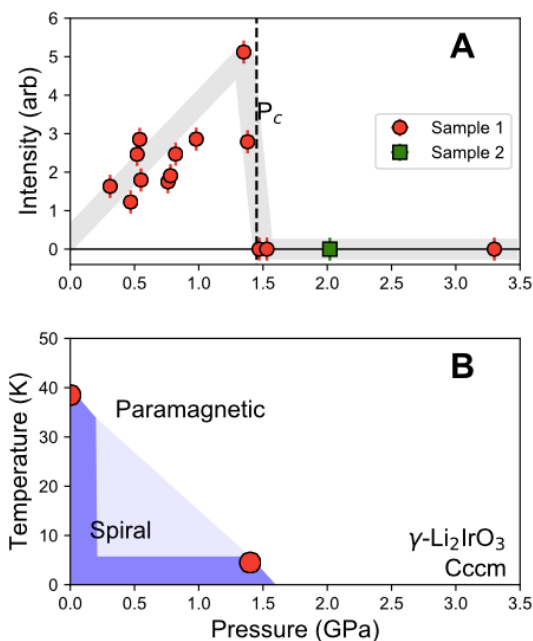


Figure 2: (a) Magnetic Bragg peak intensity versus applied pressure for two samples. The intensity for sample 1 disappears abruptly at $P_c = 1.4$ GPa; no magnetic is observed at 2.0 GPa for sample 2. (b) Schematic pressure-temperature magnetic phase diagram for γ - Li_2IrO_3 ; the dark region indicates the extent of direct studies of the spiral-order phase to date. No discontinuous change in the lattice (space group Cccm) is observed to 3.0 GPa.

- (1) **Low-noise magnetic measurements of hidden ordered states.** Preliminary studies has show evidence for new high temperature phase that have hitherto been undetected. Our observations strongly suggest that the phase structure of Kitaev iridates is much richer than previously supposed. Consequently, the low energy Hamiltonian of these materials will have to be reconsidered, with broad implications to our understanding of these systems.
- (2) **Resonant Inelastic X-ray Scattering studies.** Our recent measurement using state-of-the-art RIXS tools at the Advanced Photon Source have been able to resolve features in the magnon dispersion down to a few milli-electron Volts. In these tour de force experiments, we have shown that the incommensurate magnetic phases have extraordinarily large magnon group velocities.
- (3) **Doping studies.** While carriers are difficult to dope into these systems in general, we have had recent success in hole doping these systems, leading to a dramatic suppression of the incommensurate magnetic transition. However, a new transition arises in its wake, whose properties are highly unusual.

References

- [1] A. Kitaev, Ann. Phys. (NY) 321, 2 (2006).
- [2] Jackeli, G. & Khaliullin, G. Mott insulators in the strong spin-orbit coupling limit: from Heisenberg to a quantum compass and Kitaev models. Phys. Rev. Lett. 102, 017205 (2009)
- [3] Kimberly A Modic, James G Analytis, *et al.* Nature Communications 5, 4203 (2014)
- [4] A. Biffin, R. D. Johnson, Sungkyun Choi, F. Freund, S. Manni, A. Bombardi, P. Manuel, P. Gegenwart, and R. Coldea

Publications

- I.** Alejandro Ruiz, Alex Frano, Nicholas P. Breznay, Itamar Kimchi, Toni Helm, Iain Oswald, Julia Y. Chan, R. J. Birgeneau, Z. Islam, James G. Analytis, “Field-induced intertwined orders in 3D Mott-Kitaev honeycomb β -Li₂IrO₃”, Nature Communications (in press) arXiv:1703.02531
- II.** K.A. Modic, B.J. Ramshaw, Nicholas P. Breznay, James G. Analytis, Ross D. McDonald, Arkady Shekhter, “Robust spin correlations at high magnetic fields in the honeycomb iridates”, Nature Communications 8, Article number: 180 (2017)
- III.** Nicholas P. Breznay, Alejandro Ruiz, Alex Frano, Wenli Bi, Robert J. Birgeneau, Daniel Haskel, James G. Analytis, “Resonant x-ray scattering reveals possible disappearance of magnetic order under hydrostatic pressure in the Kitaev candidate γ -Li₂IrO₃”, Phys. Rev. B 96, 020402 (2017)
- IV.** A. Biffin, R. D. Johnson, I. Kimchi, R. Morris, A. Bombardi, J. G. Analytis, A. Vishwanath, and R. Coldea, “Noncoplanar and Counterrotating Incommensurate Magnetic Order Stabilized by Kitaev Interactions in γ -Li₂IrO₃”, Phys. Rev. Lett. 113, 197201 (2014)

- V. J. P. Hinton, S. Patankar, E. Thewalt, J. D. Koralek, A. Ruiz, G. Lopez, N. Breznay, I. Kimchi, A. Vishwanath, J. G. Analytis, J. Orenstein, “Photoexcited states of the harmonic honeycomb iridate γ -Li₂IrO₃”, Phys. Rev. B 92, 115154 (2015).

Emergent collective phenomena in artificial spin ice

Principal Investigator: Peter Schiffer, University of Illinois at Urbana-Champaign, Urbana, IL (pschiffe@illinois.edu)

Co-Investigator: Nitin Samarth, Pennsylvania State University, University Park, PA

Program Scope

This program encompasses studies of lithographically fabricated “artificial spin ice” arrays of nanometer-scale single-domain ferromagnetic islands in which the array geometry results in frustration of the magnetostatic interactions between the islands. These systems are analogs to a class of magnetic materials in which the lattice geometry frustrates interactions between individual atomic moments, and in which a wide range of novel physical phenomena have been observed. The advantage to studying lithographically fabricated samples is that they are both designable and resolvable: i.e., we can control all aspects of the array geometry, and we can also observe how individual elements of the arrays behave. In previous work, we have designed frustrated lattices, controlled the strength of interactions by changing the spacing of the islands, demonstrated that the island magnetic moment orientation is controlled by the inter-island interactions, and studied how these systems behave when they are thermalized by either raising the temperature to near the Curie temperature of the constituent material, or by inducing fluctuations at much lower temperatures by selection of moment size. Current work is focusing on exploiting these thermalization techniques and also understanding the nature of electrical transport in connected artificial spin ice structures.

Recent Progress

The past two years of this program have focused on several projects within the scope described above. All work has been done in close collaboration with the groups of Chris Leighton at the University of Minnesota, Cristiano Nisoli at Los Alamos National Laboratory, and Gia-Wei Chern at the University of Virginia. We also have published two short summary articles for broad readership, covering aspects of recent progress in the field [1,2]

Thermal annealing of artificial spin ice: Because of the large magnetic energy scales of the ferromagnetic islands in artificial spin ice, workers in the field were originally unable to find a technique to thermally anneal artificial spin ice into desired thermodynamic ensembles. We have now demonstrated a method for thermalizing artificial spin ice arrays by heating them to near the Curie temperature of the constituent material. This effectively allows us to reach the ground state of square ice and see charge ordering in kagome ice. We also have used this technique to make the first study of a vertex-frustrated system, the so-called “shakti lattice”, a structure that does

not directly correspond to any known natural magnetic material. We are now taking this method in two new directions. First we are studying the annealing process in detail with the goal of optimizing it, i.e., making sure that the process leads to the lowest energy state for the permalloy systems we are studying. Second, we have devised a system in which the annealing can be performed in the presence of a magnetic field. This allows us to explore the field-dependent phase diagram of a novel lattice that has emerged as a good model for different sorts of collective behavior.

Thermal fluctuations in artificial spin ice: To explore thermal behavior in these systems, we

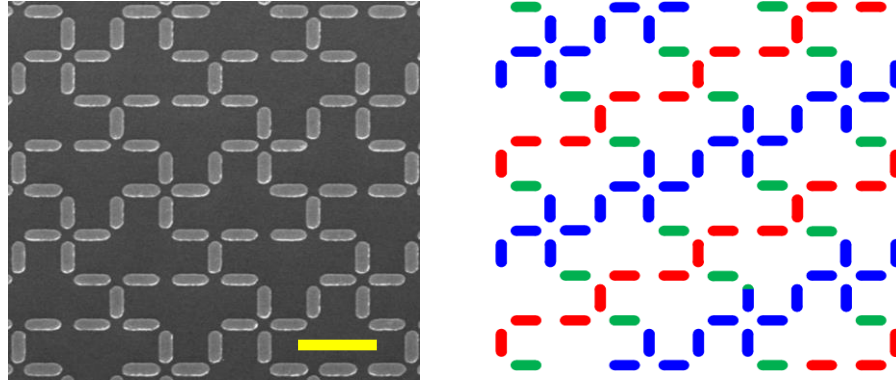


Figure 1 The tetris lattice. Right: SEM image of artificial spin ice in the tetris lattice (scale bar is 1 micron). Left: color-coded image showing the different quasi one-dimensional structures within the lattice.

have used photoemission electron microscopy with x-ray magnetic circular dichroism contrast (XMCD-PEEM). This imaging technique shows black/white contrast on the islands (which indicates whether the island magnetization has a positive or negative projection on the polarization of the incident x-rays) allowing the experiments to unambiguously identify the exact microstate of an array. The advantage of PEEM is that it can be employed with very thin islands whose moments are extremely soft and would be unmeasurable with a magnetic force microscope (MFM). Such thin islands can be grown such that their moments fluctuate thermally at room temperature but then freeze into a static configuration upon cooling. While these studies require access to a synchrotron facility, they allow the examination of moment fluctuations in artificial spin ice by comparing successive images. In collaboration with Andreas Scholl at LBNL, we have employed this technique to study another vertex-frustrated lattice unavailable in nature, the “tetris” lattice (figure 1). This lattice shows quasi-one dimensional behavior that maps onto a one-dimensional Ising model, and through a temperature-dependent study, we can see the development of thermal fluctuations associated with the vertex frustration [3]. We are now applying this technique to other lattice systems, including the shakti lattice, where we find that excitations are topologically protected by the vertex frustration.

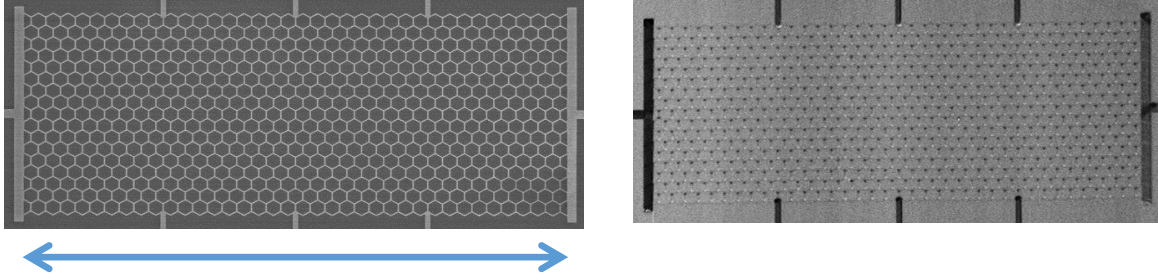


Figure 2. SEM and MFM images of hexagonal connected artificial spin ice network for electrical magnetotransport studies. The black and white dots on the MFM image correspond to effective magnetic charges at the lattice vertices, and the scale bar corresponds to 50 microns.

Transport studies of connected artificial spin ice structures: We are examining the electrical transport properties of connected artificial spin ice networks (figure 2), and we have completed studies of both the hexagonal and brickwork geometries [4,5]. Our data showed clear evidence of magnetic switching among the wires, both in the longitudinal and transverse magnetoresistance that we attribute largely to planar hall effects and anisotropic magnetoresistance. Working with our theorist collaborators, we then developed novel methods of modeling that reproduces and can explain virtually all of the features of the system (figure 3) and can be broadly applied to other ferromagnetic nanostructures [4]. One of our findings is that the vertices of these structures, although a small fraction of the system, play a critical role in their overall transport properties.

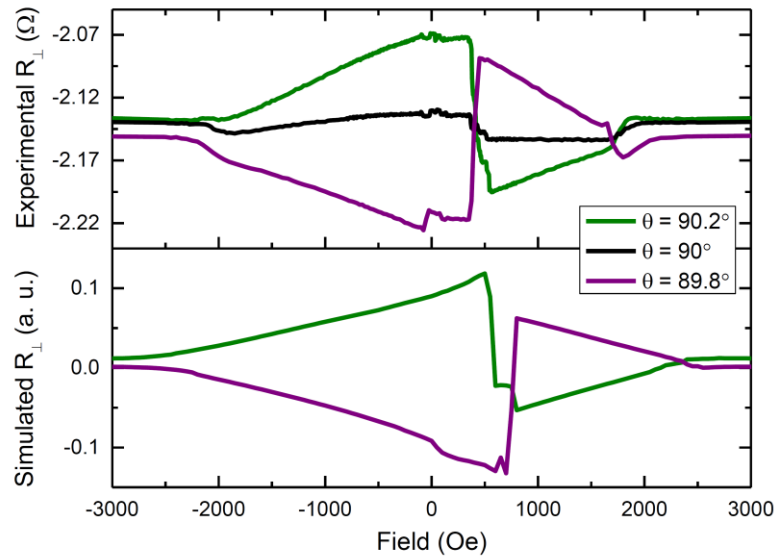


Figure 3. Experimental transverse magnetoresistance data (top) and simulations (bottom) for hexagonal connected artificial spin ice for a small range of the field angle θ near a symmetry direction. Note the close agreement, which can be attributed to including the influence of the vertex regions of the structure.

MOKE studies of perpendicular anisotropy arrays: Using submicron, spatially resolved Kerr imaging in an external magnetic field for islands with perpendicular magnetic anisotropy, we map out the evolution of island arrays during hysteresis loops. Resolving and tracking individual islands across four different lattice types and a range of interisland spacings, we can extract the individual switching fields of every island. This allows us to calculate global array parameters throughout the switching process, such as magnetization, nearest neighbor moment correlation, and switching field distributions. The switching field distribution is of particular interest, as it incorporates both island-island interactions and quenched disorder in island geometry. Our results indicate that disorder in these arrays is primarily a single-island property and provides a methodology by which to quantify such disorder [6]. We are also able to observe run-to-run deviations in the microstates that occur as the entire array magnetization evolves through a hysteresis loop. This affords us a unique perspective on how changes in the switching field of each island determine how these arrays undergo switching processes.

Future Plans

Future plans for this research program include the completion of the studies we have initiated that are discussed above. We are particularly interested in looking at thermal effects in transport studies and in examining new and exotic lattices with our thermalization techniques.

References and Publications

- [1] “Deliberate exotic magnetism via frustration and topology”, Cristiano Nisoli, Vassilios Kapaklis, and Peter Schiffer, *Nature Physics* **13**, 200-203 (2017).
- [2] “Frustration by design”, Ian Gilbert, Cristiano Nisoli and Peter Schiffer, *Physics Today* **69**, 54-59 (2016).
- [3] “Emergent reduced dimensionality by vertex frustration in artificial spin ice”, Ian Gilbert, Yuyang Lao, Isaac Carrasquillo, Liam O’Brien, Justin D. Watts, Michael Manno, Chris Leighton, Andreas Scholl, Cristiano Nisoli, and Peter Schiffer, *Nature Physics* **12**, 162–165 (2016).
- [4] “Understanding magnetotransport signatures in networks of connected permalloy nanowires”, B. L. Le, J.-S. Park, J. Sklenar, G.-W. Chern, C. Nisoli, J. Watts, M. Manno, D. W. Rench, N. Samarth, C. Leighton, P. Schiffer, *Physical Review B* **95**, 060405(R) – 1-5 (2017).
- [5] “Magnetic response of brickwork artificial spin ice”, Jungsik Park, Brian L. Le, Joseph Sklenar, Gia-Wei Chern, Justin D., Watts, and Peter Schiffer, *Physical Review B* **96**, 024436 (2017).
- [6] “Characterization of switching field distributions in Ising-like magnetic arrays”, Robert D. Fraleigh, Susan Kempinger, Paul E. Lammert, Sheng Zhang, Vincent H. Crespi, Peter Schiffer, and Nitin Samarth *Physical Review B* **95**, 144416 (2017).

Spintronics based on topological insulators

John Q. Xiao¹, Branislav Nikolic¹, Matt Doty², and Stephanie Law²

¹Department of Physics and Astronomy

²Department of Materials Science

University of Delaware

Newark, DE 19716

Program Scope

The major goals of the project are: (1) fabrication of topological insulator/ferromagnetic (TI/FM) heterostructures and investigation of current driven spin-orbital torques (SOT) in TI/FM to distinguish the contributions from TI surface state, spin Hall effect, and Rashba effect; (2) computational search and design of optimal TI/FM heterostructures; (3) SOT induced spin dynamic in TI/FM heterostructures; and (4) develop TI/FM with perpendicular magnetic anisotropy (PMA).

Recent Progress

Fabrication of TI/FM with clean interface is a challenging task since the TI layer is grown in MBE and FM layer is grown in magnetron sputtering. Typically, a cap Se layer is grown on TI layer and the Se layer is subsequently removed at high temperature and high vacuum in a sputtering system. By coordinating the TI film growth to be immediately before the FM deposition, we are able to fabricate TI/FM structures with extremely clean interfaces without the need for Se capping layers. This is only possible because our Bi₂Se₃ films are exceptionally stable under exposure to air and because the MBE growth and FM deposition tools are both available at UD.

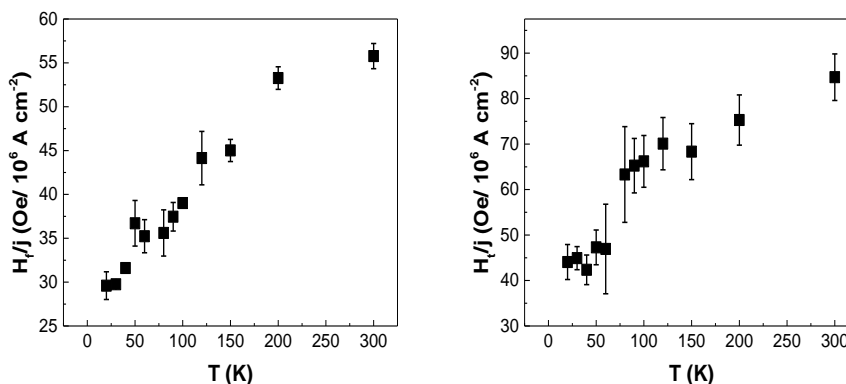


Figure 1, the temperature dependence of (a) the effective field of SOF (H_f) and (b) the effective field of SOT (H_t) for Bi₂Se₃(10nm)/NiFe(4nm) bilayer structures. The results are normalized to the current density J through the sample.

We first investigated the current induced damping-like torque, named as spin orbit torque (SOT), and field-like torque, named as spin orbit field (SOF) in Bi₂Se₃/NiFe bilayer structures. One of the representative results is shown in Figure 1, the temperature dependence of (a) the

effective field of SOF (H_f) and (b) the effective field of SOT (H_t) for $\text{Bi}_2\text{Se}_3(10\text{nm})/\text{NiFe}(4\text{nm})$ bilayer structures. The results are normalized to the current density J through the sample. . From Figure 1, the temperature dependence of (a) the effective field of SOF (H_f) and (b) the effective field of SOT (H_t) for $\text{Bi}_2\text{Se}_3(10\text{nm})/\text{NiFe}(4\text{nm})$ bilayer structures. The results are normalized to the current density J through the sample. , one finds that (1) the SOT effect is larger than SOF and (2) both effects decrease with decreasing temperatures. There are three potentials contributions to SOF and SOT: (1) TI surface state (TSS) which in generally gives rise to $H_f > H_t$. The effect weakly depends on the temperature; (2) Rashba effect which also leads to $H_f > H_t$ but the effect is decreasing with decreasing temperature; (3) spin Hall effect (SHE) which usually has $H_f < H_t$ and decrease with decreasing temperature since the bulk conductivity in TI is decreasing. By analyzing the results Figure 1, the temperature dependence of (a) the effective field of SOF (H_f) and (b) the effective field of SOT (H_t) for $\text{Bi}_2\text{Se}_3(10\text{nm})/\text{NiFe}(4\text{nm})$ bilayer structures. The results are normalized to the current density J through the sample. , we have observed significantly contributions from SHE, although we cannot completely rule out the contributions from TSS.

As we are puzzled by the results why we were not observing the strong effect from TSS, our theoretical effort has made a *major breakthrough* and shed light to this issue. Through unique theoretical and computational first-principles tools we developed, we revealed strong proximity band structure and spin textures on both sides of TI/FM interface. This novel topological matter is generated by quantum-mechanical hybridization of wave functions within nanometer thickness layers of (ferromagnetic or normal) metals in contact with topological insulators and, therefore, it cannot be replicated by searching for bulk material or their doping by impurities. *We unveiled for the first time striking new physical insight into real physical systems. Our findings dramatically change the interpretation of a surprisingly large number of experiments* conducted in spin-orbitronics and topological spintronics where a ferromagnetic metallic layer is brought into direct contact with a normal layer made of heavy metals (such as Pt, W and Ta), topological insulator, Weyl semimetal (such as WTe_2) or transition metal dichalcogenide (such as MoS_2). In all of these systems, strongly spin-orbit-coupled wave functions “leak out” from the normal layer side into the ferromagnetic layer side, to substantially modify energy-momentum dispersion of electrons within the ferromagnet and introduce complex spin-textures (giving rise to nonequilibrium spin density when current is passed) that *otherwise do not exist in isolated ferromagnetic layer*.

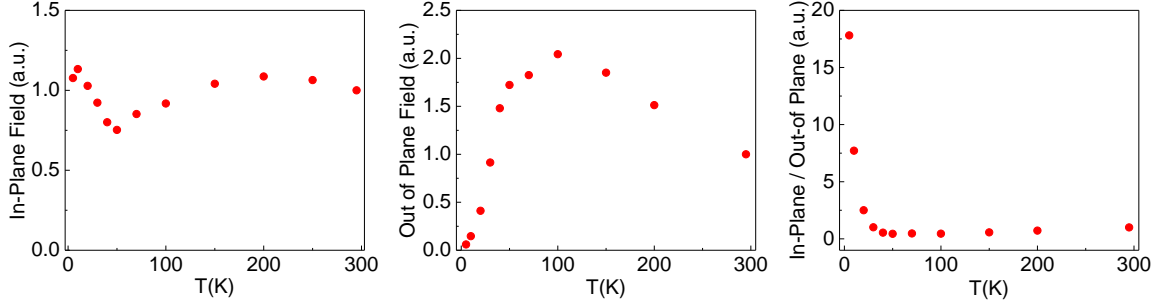


Figure 2, The temperature dependence of (a) in-plane effective field, i.e. H_f , (b) out-of-plane effective field (H_t) and the ratio of H_f/H_t .

This theoretical study immediately points out that Co would be a better FM for TI. In addition, according to our striking new insight, “applied current shunted through the metallic magnet” is actually favorable effect, as long as nanoscale thickness ferromagnet deposited on the top of topological insulator is permeated by spin textures. Guided by the theoretical predictions, we started to investigate $\text{Bi}_2\text{Se}_3/\text{Co}$ bilyaers. The preliminary results are shown in Figure 2, The temperature dependence of (a) in-plane effective field, i.e. H_f , (b) out-of-plane effective field (H_t) and the ratio of H_f/H_t .. Several features immediately point to the strong contributions from TI surface state (TSS): (1) the value of H_t (out of plane field) decrease dramatically at low temperature. This is because the bulk of Bi_2Se_3 is becoming insulating which effectively minimize SHE. (2) H_f weakly depends on the temperature. Above about 50K, the trend is due to the possible Rashba effect and TSS. Below 50K, the increasing of H_f with decreasing temperature clearly indicates the strong TSS contribution.

Finally, we are making progress towards the fabrication of electrical pump- optical probe time-resolved Magneto-Optical Kerr Effect (TRMOKE) to investigate SOF and SOT. The schematic of system is shown in Figure 3 The schematic of the TRMOKE system., the 81134A pulse pattern generator is synchronized with the mode-locked Mira laser pulse in 76 MHz and apply ultrafast pulse current (with ~ 50 ps rising edge) through the sample along Y axis (perpendicular to the table, parallel to the sample surface).

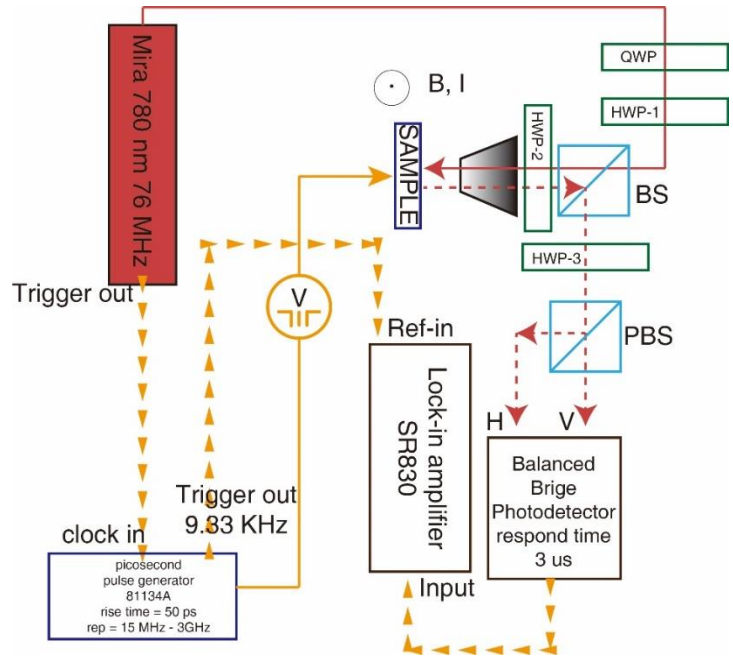


Figure 3 The schematic of the TRMOKE system.

By scanning the delay time in between the laser pulse and current pulse, the oscillation of the TR-MOKE signal can be observed. **Error! Reference source not found.** shows a preliminary result of the time-scan MOKE signal from a Pt(3nm)/FeNi(3nm) and Ta(3)/CoFeB/(2)/Ti(2) bilayers. The electrical pulse introduces SOT which tilts the magnetization out of the film plane, resulting in polar MOKE signal. We are currently developing algorithms to extract dynamic and static spin Hall angle as well as other important parameters. The successful development of TR-MOKE is critical to investigate switching behaviors.

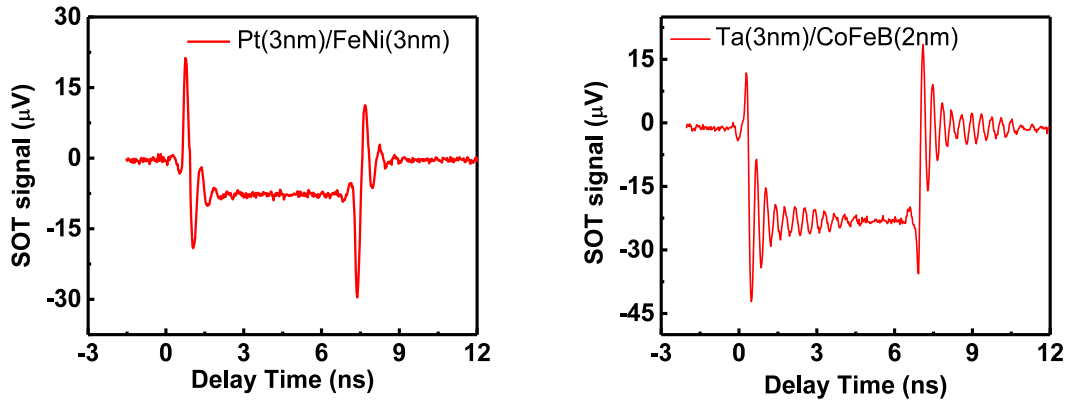


Figure 4 The time resolved MOKE signal from (a) Pt(3nm)/Py(3nm) and (b) Ta(3nm)/CoFeB(2nm) samples under an electrical pulse with pulse width of 6 ns.

Future Plans

- (1) We will perform quantitative analysis of the contributions from the SHE, Rashba effect and TI surface state using the temperature dependence of spin-orbit torques.
- (2) We will try to understand the band structure and spin textures in hybridized TI/FM interface at nanometer scale. Our theoretical calculation indicates the Dirac cone at the Bi₂Se₃/Co interface is hybridized with evanescent wave functions injected by three monolayers of Co, which is very different from the bulk metal. The tunneling anisotropic magnetoresistance (TAMR) measurement can serve as a sensitive probe of spin texture at the TI/Co interface.
- (3) We will develop TI/FM with perpendicular anisotropy. FM layers include Tm₃Fe₅O₁₂ (TmIG) or TbFeCo. While we already had some success in growing TmIG and TbFeCo with PMA, integration with TIs will be challenging.

Publications

1. T. Ginley, Y. Wang, S. Law, Topological Insulator Film Growth by Molecular Beam Epitaxy: A Review, Crystals. 6, 154 (2016). doi:10.3390/cryst6110154.
2. Y. Wang, T.P. Ginley, C. Zhang, S. Law, Transport properties of Bi₂(Se_{1-x}Te_x)₃ thin films grown by molecular beam epitaxy, J. Vac. Sci. Technol. B, 35, 02B106 (2017). doi:10.1116/1.4976622.

3. J. M. Marmolejo-Tejada, K. Dolui, P. Lazic, P.-H. Chang, S. Smidstrup, D. Stradi, K. Stokbro, and B. K. Nikolic, "Proximity band structure and spin textures on both sides of topological-insulator/ferromagnetic-metal interface and their transport probes," *Nano Lett.*, 10.1021/acs.nanolett.7b02511 (2017).

Session 6

Search for 3D Topological Superconductors using Laser-Based Spectroscopy

Principal Investigator: David Hsieh

Mailing Address: 1200 E. California Blvd., MC 149-33, California Institute of Technology,
Pasadena, CA 91125

E-mail: dhsieh@caltech.edu

(i) Program Scope

The goal of this research program is to experimentally identify three-dimensional topological superconductors (3D TSCs) and possible precursor phases of 3D TSCs in bulk crystals using laser-based spectroscopic techniques. It has been theoretically proposed that 3D TSCs may emerge upon suppressing certain odd-parity electronically ordered phases^{1,2}, in analogy to the situation in copper- and iron-based superconductors where even-parity superconductivity is proposed to emerge upon suppressing an even-parity electronic nematic liquid crystalline order^{3,4}. This suggests that rather than searching exclusively among known superconductors for a 3D TSC, one can search among materials that exhibit the requisite odd-parity “parent” electronic orders and attempt to suppress them via some external tuning parameter to induce a 3D TSC phase. Recently a new class of parity-breaking electronic liquid crystals (PB-ELC) has been predicted to exist in correlated metals with strong spin-orbit coupling⁵, which are candidates for such 3D TSC parent phases. A major component of this program is to develop techniques to identify these PB-ELCs and to devise strategies to drive them into 3D TSC phases.

(ii) Recent Progress

Development of a high speed RA-SHG technique

Unlike all previously reported examples of electronic liquid crystals⁶, PB-ELCs are characterized by a spontaneously spin-split 3D Fermi surface that breaks the inversion symmetry of the underlying lattice. Rotational anisotropy second harmonic generation (RA-SHG) experiments are particularly well-suited to detecting PB-ELC order for several reasons: (a) the leading-order electric-dipole contribution to SHG, which is described by a third-rank susceptibility tensor relating the incident electric field to the nonlinear polarization induced at twice the incident frequency via the equation $P_i(2\omega) = \chi_{ijk}E_j(\omega)E_k(\omega)$, is only allowed if inversion symmetry is broken; (b) RA measurements allow the full structure of χ_{ijk} to be resolved, which can in turn be used to determine the PB-ELC point group; (c) they can be performed in a spatially-resolved manner that removes the need for externally applied domain alignment fields. We developed a technique to perform high precision RA-SHG measurements⁷, which uses an array of fast mechanically spinning optical components to generate a rotating scattering plane (Fig. 1). The SHG light reflected at different scattering plane angles φ are then projected onto a circular locus of points on a 2D CCD camera. In this way, full RA-SHG patterns can be collected much faster than characteristic laser power fluctuation timescales, which allows for high symmetry refinement precision and also accommodates many types of sample environment.

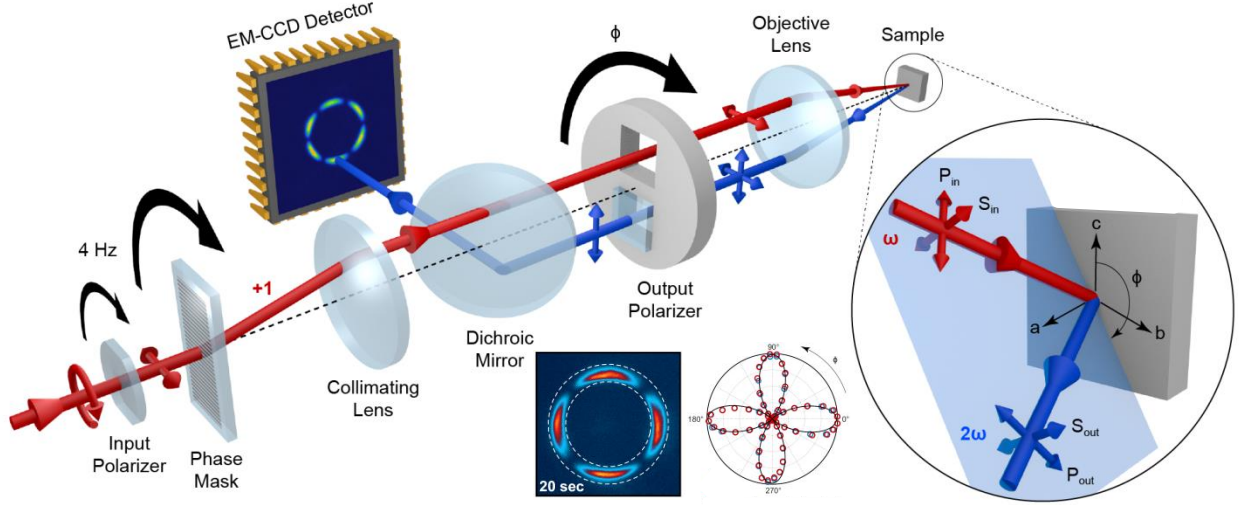


Fig. 1 Schematic of the RA-SHG apparatus (see Ref.[7] for details). The incoming and outgoing polarizations can be selected to be either S or P polarized to access different elements of the χ_{ijk} tensor. An example of raw data collected from an (001) oriented GaAs film in 20 seconds is shown below, together with a polar plot of SHG intensity versus ϕ extracted by radially integrating the raw data over the region bounded by the white dashed lines. The 4-fold rotational symmetry of the GaAs structure is clearly resolved.

Signatures of a PB-ELC phase identified using RA-SHG

It has recently been proposed that the strongly spin-orbit coupled metallic pyrochlore $\text{Cd}_2\text{Re}_2\text{O}_7$ hosts a PB-ELC phase at low temperature⁵. The order parameter of this phase could have the symmetries of either the odd-parity E_u or T_{2u} irreducible representation of the high temperature octahedral point group of $\text{Cd}_2\text{Re}_2\text{O}_7$. Previous work has shown that $\text{Cd}_2\text{Re}_2\text{O}_7$ undergoes an inversion breaking structural phase transition with E_u symmetry below a temperature $T_s \sim 200$ K that breaks three-fold rotational symmetry about the cubic $\langle 111 \rangle$ axis while preserving mirror symmetry about the $(1\bar{1}0)$ plane. However, no detection of any accompanying electronic order has been reported. To investigate this possibility, we performed spatially-resolved single domain RA-SHG measurements on the (111) surface of a $\text{Cd}_2\text{Re}_2\text{O}_7$ single crystal⁸. At temperatures $T > T_s$ we observed an RA-SHG pattern with six-fold rotational symmetry consistent with a (111) surface dominated SHG response (Fig. 2a), which is expected because the bulk is inversion symmetric at high temperatures. At $T < T_s$ we observed a dramatic increase in the SHG intensity consistent with bulk inversion symmetry breaking. However, the RA patterns revealed that in addition to a dominant bulk χ_{ijk} tensor with E_u symmetry, there is also a weaker bulk χ_{ijk} tensor of ostensible electronic origin with T_{2u} symmetry (Fig. 2b). By measuring the temperature dependence of the two χ_{ijk} tensors, which couple linearly to the E_u and T_{2u} order parameters, we found a critical exponent $\beta = 1/2$ for the T_{2u} order parameter and $\beta = 1$ for the E_u order parameter, consistent with a mean field prediction for a primary and secondary order parameter respectively. This suggests that a PB-ELC order with T_{2u} symmetry drives the transition at T_s .

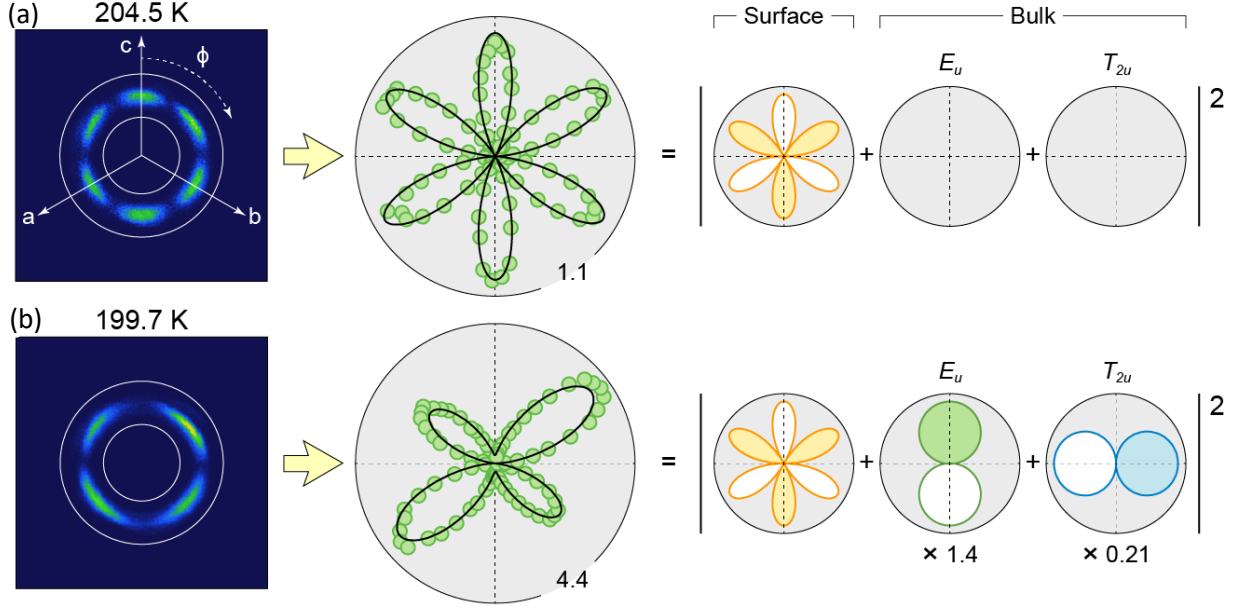


Fig. 2 (left column) Raw RA-SHG images acquired at temperatures (a) above and (b) below T_s . Concentric white circles show the radial integration region used to generate the RA patterns (middle column). The RA patterns are fit to the squared magnitude of a sum of surface, bulk E_u and bulk T_{2u} polarization $P(2\omega)$ terms (black curve). The magnitude of each component of the fit is illustrated in the right column, where filled (unfilled) petals denote a positive (negative) sign for the polarization (see Ref.[8] for details). Note the vertical $(1\bar{1}0)$ mirror plane is broken by the T_{2u} term.

An improper displacive transition established using coherent phonon spectroscopy

Based on our RA-SHG data on $\text{Cd}_2\text{Re}_2\text{O}_7$, it was deduced that the electronic T_{2u} order induces the E_u structural distortion as a secondary order parameter⁸. This mechanism does not require the E_u phonon to soften near T_s . However for many years, the leading hypothesis was that the transition is driven by the freezing of a soft zone-centered phonon mode with E_u symmetry⁹, which requires the natural frequency of the E_u phonon to monotonically approach zero near T_s . To resolve this debate, we carried out time-resolved coherent phonon spectroscopy measurements. Our experiments establish that the E_u phonon does not soften, but exhibits an anomalous lifetime broadening near T_s that explains the previous spurious signatures of phonon softening. Using a combination of time-resolved thermometry and time-dependent Landau theory, we show that this phenomenon is generic for materials with a linear coupling between primary and secondary order parameters of different symmetry, and should be found in many other electronic systems beyond PB-ELCs.

(iii) Future Plans

The electronic phase discovered in $\text{Cd}_2\text{Re}_2\text{O}_7$ is known as a “multipolar nematic” and is only one of several proposed forms of PB-ELC ordering⁵. We plan to apply our RA-SHG technique to search for these forms in other spin-orbit coupled correlated metals in the $5d$ transition metal

oxide family such as LiOsO_3 . We will also track the evolution of the PB-ELC order parameter as a function of externally applied hydrostatic pressure in effort to suppress the PB-ELC order and search for new emergent phases (e.g. 3D TSC) near the quantum critical point.

In addition to our work on PB-ELC phases, we are developing an ultra-low temperature and ultra-high energy resolution laser-based angle-resolved photoemission spectroscopy instrument, which will be used to directly search for the presence or absence of Majorana surface states in candidate 3D TSCs such as $\text{Cu}_x\text{Bi}_2\text{Se}_3$.

(iv) References

1. Kozii, V. & Fu, L. Odd-parity superconductivity in the vicinity of inversion symmetry breaking in spin-orbit-coupled systems. *Phys. Rev. Lett.* **115**, 207002 (2015).
2. Wang, Y., Cho, G. Y., Hughes, T. L. & Fradkin, E. Topological superconducting phases from inversion symmetry breaking order in spin-orbit-coupled systems. *Phys. Rev. B* **93**, 134512 (2016).
3. Keimer, B., Kivelson, S. A., Norman, M. R., Uchida, S. & Zaanen, J. From quantum matter to high-temperature superconductivity in copper oxides. *Nature* **518**, 179–186 (2015).
4. Fernandes, R. M., Chubukov, A. V. & Schmalian, J. What drives nematic order in iron-based superconductors? *Nat. Phys.* **10**, 97–104 (2014).
5. Fu, L. Parity-breaking phases of spin-orbit-coupled metals with gyrotropic, ferroelectric, and multipolar orders. *Phys. Rev. Lett.* **115**, 026401 (2015).
6. Fradkin, E., Kivelson, S. A., Lawler, M. J., Eisenstein, J. P. & Mackenzie, A. P. Nematic Fermi fluids in condensed matter physics. *Annu. Rev. Condens. Matter Phys.* **1**, 153–178 (2010).
7. See Ref.[4] of section (v).
8. See Ref.[2] of section (v).
9. A. Sergienko, I. & H. Curnoe, S. Structural order parameter in the pyrochlore superconductor $\text{Cd}_2\text{Re}_2\text{O}_7$. *J. Phys. Soc. Jpn.* **72**, 1607–1610 (2003).

(v) Publications Acknowledging DOE Support

1. J. W. Harter, D. M. Kennes, H. Chu, A. de la Torre, Z. Y. Zhao, J.-Q. Yan, D. G. Mandrus, A. J. Millis & D. Hsieh. Evidence of an improper displacive phase transition in $\text{Cd}_2\text{Re}_2\text{O}_7$ via time-resolved coherent phonon spectroscopy. *Submitted* (2017).
2. J. W. Harter, Z. Y. Zhao, J.-Q. Yan, D. G. Mandrus & D. Hsieh. A parity-breaking electronic nematic phase transition in the spin-orbit coupled metal $\text{Cd}_2\text{Re}_2\text{O}_7$. *Science* **356**, 295 (2017).
3. J. W. Harter, H. Chu, S. Jiang, N. Ni & D. Hsieh. Nonlinear and time-resolved optical study of the 112-type iron-based superconductor parent $\text{Ca}_{1-x}\text{La}_x\text{FeAs}_2$ across its structural phase transition. *Phys. Rev. B* **93**, 104506 (2016).
4. J. W. Harter, L. Niu, A. J. Woss & D. Hsieh. High-speed measurement of rotational anisotropy nonlinear optical harmonic generation using position-sensitive detection. *Optics Letters* **40**, 4671 (2015).

Study of Topological Superconductivity in Nanoscale Structures

Qi Li

Department of Physics, Pennsylvania State University, University Park, PA 16802

Project scope

The goal of the program is to synthesize and characterize topological superconductivity in topological insulator thin films and nanotubes using proximity effect with relatively high T_c s-wave superconductors. Topological insulators are a new type of state of matter which are insulating in bulk, but conducting on surfaces with many exotic physical properties. Topological surface states are chiral states following Dirac dispersion and display unique phenomena, such as spin-momentum locking and the suppression of non-magnetic backscattering. Topological states can also occur in superconductors, making them topological superconductors (TSCs). TSCs may be achieved in TIs either through doping or through coupling with an s-wave superconductor. Since the topological surface states are gapless with spin-momentum locking, the TSC surface states will have helical-Cooper pairs. This unique feature gives rise to a wide range of exotic physics, including the possibility of hosting Majorana Fermions.

This project aims to induce topological superconductivity using both thin films and nanotubes. We have studied epitaxial Bi_2Se_3 on NbSe_2 single crystals using Point Contact Spectroscopy (PCS) and combined with Angle Resolved Photoemission Spectroscopy (ARPES) through collaborations. Although there were anomalies reported in the electron tunneling spectra before, all were observed at very low temperatures and undistinguishable between the conventional proximity induced superconductivity through the bulk, gaped surface states (trivial) due to top and bottom surface hybridization, and the gapless (nontrivial) surface states. We conducted transport measurements using samples already characterized by ARPES to demonstrate the 2D chiral superconducting gap. We also synthesized Bi_2Se_3 nanotubes to maximize the surface to volume ratio with a goal to reduce the bulk contribution to the conduction. There are also other unique exotic properties in nanoscale structures due to the confinement effect of the topological phase. For example, quasi-one dimensional nanotubes are possible systems to host Majorana fermions. The main measurement approaches are using low temperature transport, electron tunneling and Josephson effects [1-6].

Recent Progress

Robustness of topological surface states against strong disorder in Bi_2Te_3 nanotubes. We have successfully synthesized and studied for the first time Bi_2Te_3 TI nanotubes grown using a solution phase method with a goal of increasing the surface to bulk volume ratio of TIs. Transport measurement results in TIs are often controversial and hindered by the bulk conduction. We were

able to fabricate the nanotubes with extremely insulating bulk at low temperatures due to disorder so that the bulk conduction was suppressed.⁶⁰ The bulk conductance follows Mott's variable range hopping and the surface states dominates the conduction at low temperatures below about 50 K. The conductance value is very close to e^2/h , one channel of quantum conductance. We have observed the magnetoresistance quantum oscillations as a function of the magnetic field along the axis of the nanotubes with a period of h/e , determined by the cross-sectional area of the outer surface. When a TI is confined in quasi 1D, a gap will be induced due to quantum confinement. When a magnetic field is applied along the 1D direction, the surface encloses odd multiples of half flux quanta, the surface states will become gapless due to a surface curvature induced Berry phase. Therefore, the conductance oscillate between the trivial and non-trivial states with increasing field, resulted in conductance oscillation. Even though the bulk has extremely short localization length, the surface states show long phase coherence length as demonstrated by the quantum oscillations. Numerical simulations conducted by Prof. C.X. Liu and Prof. Jainendra Jain at Penn State showed that the topological surface states will have substantially longer localization length than that of other non-topological states in nanowire geometries. This observation addressed a particular fundamental aspect of the topological surface states, i.e. their robustness to time-reversal invariant disorder and thus providing a direct confirmation of the inherently topological character of surface states. The results also demonstrated a viable route for revealing the properties of topological states by suppressing the bulk conduction using disorder.

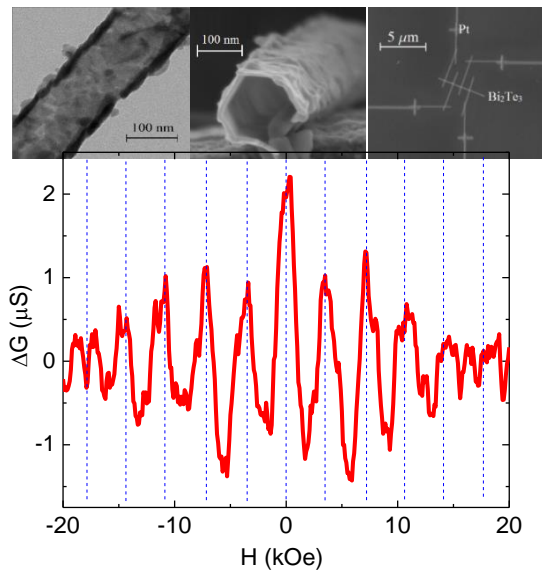


Fig. 1 shows the TEM and SEM images of a Bi_2Te_3 nanotube and conductance oscillations with magnetic field. The nanotube diameter is about 125 nm and the width ~ 10 nm and length $\sim 10 \mu\text{m}$.

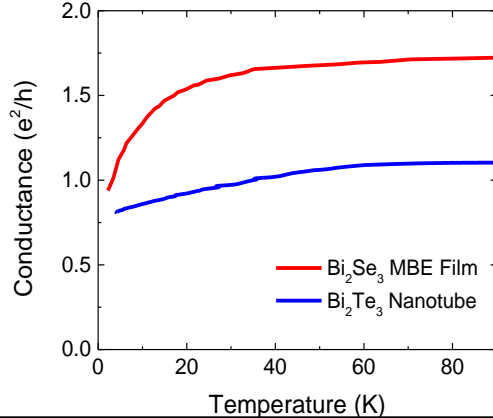


Fig. 2. The surface channel conductance obtained by subtracting the bulk conductance (VRH). Surface conductance of Bi_2Se_3 MBE films (Phys. Rev. B **84**, 073109 (2011)) is shown for comparison.

Anomalous resistance increase in Bi_2Te_3 nanotube when in contact with Nb we have tried to induce superconductivity into Bi_2Te_3 nanotubes with Nb contacts or combination of Nb and Au contacts (patterned by e-beam lithography). To our biggest surprise, we observed a sudden increase of the nanotube resistance when the Nb became superconducting. The anomalous resistance

increase disappears when the applied magnetic field reaches the H_{c2} of Nb, indicating that the effect is solely related to the superconducting transition of Nb.

Point contact spectroscopy in NbSe₂/Bi₂Se₃ bi-layers. We studied the proximity-effect induced superconductivity in epitaxial Bi₂Se₃ films on NbSe₂ using a point contact spectroscopy (PCS) method at low temperatures down to 40 mK. Our previous ARPES measurements revealed a 2D chiral superconducting energy gap. We conducted PCS measurement and extended the measurement to larger thickness than the ARPES measurements for samples without hybridization down to 40 mK to study the transport response of the TSC gap. For a 16 QL Bi₂Se₃, the bulk gap near the surface is $\sim 159 \mu\text{eV}$, while the surface states gap (induced by the proximity induced bulk superconductivity) is $\sim 120 \mu\text{eV}$ at 40 mK. The gap ratio is about the same for different thickness, suggesting the same superconducting coupling strength between the surface state and the bulk.

SD electron gases on (111) orientation transition metal oxide Recent theories have predicted possible topological insulator states and other intriguing phenomena in (111)-oriented perovskites where bilayers of transition metal ions form honeycomb lattices. We have created electron gases at the surfaces of insulating (111)-, (110)-, and (001) oriented SrTiO₃ single crystals or using amorphous cover layer. We obtained fully metallic behavior and high mobility. Anisotropic magnetoresistance measurement showed that it gave a nearly 6-fold, 2-fold and 4-fold symmetry for the (111), (110), and (001) surfaces.

Future Plans

This project will end by Dec. 20 2017. We will study the induced superconductivity in Bi₂Te₃ nanotubes for different nanotube diameter size using Nb and other superconducting contact leads. We will try to synthesize samples with different diameter and wall width so that a study the size effect will allow us to understand the quasi 1D to 2D behavior in TI and TSC so that the origin of the effect can be revealed.

Publications (acknowledge DOE support)

1. Yue-Wei Yin, Wei-Chuan Huang, Yu-Kuai Liu, Sheng-Wei Yang, Si-Ning Dong, Jing Tao, Yi-Mei Zhu, Qi Li¹ and Xiao-Guang Li “Octonary Resistance States in La_{0.7}Sr_{0.3}MnO₃/BaTiO₃/La_{0.7}Sr_{0.3}MnO₃ Multiferroic Tunnel Junctions”, *Advanced Electronic Materials* **1**, 11, (2015) (DOI: 10.1002/aelm.201500183)
2. W. C. Huang, Y. Lin, Y. W. Yin, L. Feng, D. L. Zhang, W. B. Zhao, Q. Li, and X. G. Li, Interfacial Ion Intermixing effect on four-resistance switching state in La_{0.7}Sr_{0.3}MnO₃/BaTiO₃/La_{0.7}Sr_{0.3}MnO₃ Multiferroic Tunnel Junctions, *ACS applied materials & interfaces* **8**, 10422-10429, (2016).
3. Renzhong Du, Hsiu-Chuan Hsu, Ajit C. Balam, Yuewei Yin, Sining Dong, Wenqing Dai, Weiwei Zhao, DukSoo Kim, Shih-Ying Yu, Jian Wang, Xiaoguang Li, Suzanne E. Mohny, Srinivas Tadigadapa, Nitin Samarth, Moses H.W. Chan, Jainendra. K. Jain,

Chao-Xing Liu, and Qi Li “Robustness of Topological Surface States Against Strong Disorder Observed in Bi₂Te₃ Nanotubes, *Phys. Rev. B* **93**, 195402 (2016).

4. Steve Carabello, Joseph G. Lambert, Jerome Mlack, Wenqing Dai, Qi Li, Ke Chen, Daniel Cunnane, X. X. Xi, and Roberto C. Ramos “Microwave resonant activation in hybrid single-gap/two-gap Josephson tunnel junctions” *J. Appl. Phys.* **120**, 123904 (2016)
5. F. Fang, H. Zhai, X. Ma, Y. W. Yin, Qi Li, and G. Lüpke, “Interface magnetization transition via minority spin injection” *Appl. Phys. Lett.* **109**, 232903 (2016) (doi: [10.1063/1.4972035](https://doi.org/10.1063/1.4972035))
6. Ludi Miao, Renzhong Du, Yuewei Yin and Qi Li “Anisotropic magneto-transport properties of electron gases at SrTiO₃ (111) and (110) surfaces”, *Appl. Phys. Lett.* **109**, 261604 (2016) (doi.org/10.1063/1.4972985)
7. F. Fang, Y. W. Yin, Qi Li, and G. Lüpke “Spin-polarized current injection induced magnetic reconstruction at oxide interface” *Scientific Reports* **7**, 40048 (2017) doi:10.1038/srep40048
8. F. Fang, H. Zhai, X. Ma, Y. W. Yin, Qi Li, and G. Lüpke, “Current-driven interface magnetic transition in complex oxide heterostructure” *J. Vac. Sci. Technol. B*; **35**, 04F101 (2017) (doi: [10.1116/1.4976587](https://doi.org/10.1116/1.4976587))
9. Wenqing Dai, Anthony Richardella, Renzhong Du, Weiwei Zhao, Xin Liu, C.X. Liu, Song-Hsun Huang, Raman Sankar, Fangcheng Chou, Nitin Samarth, and Qi Li. Proximity-effect-induced Superconducting Gap in Topological Surface States – A Point Contact Spectroscopy Study of NbSe₂/Bi₂Se₃ Superconductor-Topological Insulator Heterostructures. *Scientific Report* **7**, 7631 (2017)
10. Yuewei Yin and Qi Li, “A Review on All-perovskite Multiferroic Tunnel Junctions”, *Materiomics*. (2017) accepted.

Manuscript submitted

1. L. Miao, J. Wang, R. Du, Y. Yin, W. Zhao, M.H. Chan, and Qi Li “Band filling and electric field effects on anisotropic magnetoresistance of two-dimensional electron gases at SrTiO₃ (111)-, (110)-, and (001)-oriented surfaces” submitted to *Nat. Commun.* (2017)
2. Weichuan Huang, Yue-Wen Fang, Yuewei Yin, Bobo Tian, Wenbo Zhao, Chuangming Hou, Chao Ma, Qi Li, Evgeny Y. Tsymbal, Chun-Gang Duan, Xiaoguang, “Synapse Based on Magnetoelectrically Coupling Memristor”, submitted to *Nat. Nanotech.* (2017)
3. Renzhong Du, Ludi Miao, Yuewei Yin, Qi Li “Anomalous Resistance Increase on Bi₂Te₃ Nanotubes under the Proximity to Superconductors” unpublished.
4. DukSoo Kim, Renzhong Du, Shih-Ying Yu, Yuewei Yin, Sining Dong, Qi Li, Suzanne E. Mohney, Xiaoguang Li, Srinivas Tadigadapa, “Enhanced Thermoelectric Efficiency in Nanocrystalline Bismuth Telluride Nanotubes” submitted to *IEEE*

Superconducting In-doped SnTe Topological Crystalline Insulator Nanowires

Judy J. Cha, Mechanical Engineering and Materials Science, Yale University

Program Scope

The scope of the project is to synthesize In-doped SnTe nanowires that superconduct and exhibit transport signatures that can verify the predicted topological superconductivity. Tin telluride, SnTe, is a topological crystalline insulator that possesses Dirac-dispersive, spin-polarized surface states on {100}, {110}, and {111} surfaces of the crystal^[1, 2]. The surface states are protected by the crystal symmetry. Making SnTe superconducting is predicted to induce topological superconductivity. Superconductivity in In-doped SnTe bulk crystals has been studied in detail^[3-5]. Unconventional superconductivity signatures have been observed in In-doped SnTe bulk crystals^[6]. In one-dimensional nanowire geometry, Majorana modes are predicted at the ends of the nanowires^[7]. The project thus aims to synthesize In-doped SnTe nanowires and probe its superconductivity.

Recent Progress

We grew In-doped SnTe nanoplates, nanoribbons, and nanowires via chemical vapor deposition (CVD) where the distinction between different morphologies is loosely determined by the width of the nanostructures (Figure 1)^[8]. Structures with widths up to 300 nm are classified as nanowires. The indium doping concentration ranges between 4% and 6%, measured by energy dispersive X-ray (EDX) spectroscopy.

Superconducting behaviors of all three structures (nanoplates, nanoribbons, and nanowires) were measured to show subtle differences between structures (Figure 2). For nanoplates, a robust superconductivity with sharp superconducting transition is observed with the T_c of ~ 2.1 K. For nanoribbons, multiple T_c 's are observed with a gradual transition to the superconducting phase. For nanowires, the resistance saturates at a finite value, instead of reaching zero. The current-

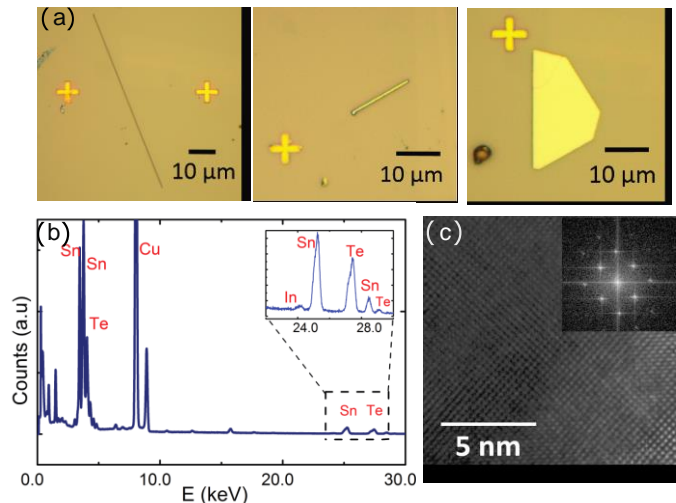


Figure 1. (a) In-doped SnTe nanowire, nanoribbon, and nanoplate. (b) Concentrations of In were measured by energy dispersive X-ray spectroscopy (EDX). (c) The cubic crystal structure is preserved after In doping.

voltage (I - V) curves and the differential resistances of the three devices were measured at $T = 0.35$ K (Figure 3). For the nanowire device, the I - V curve is nonlinear, but there is no supercurrent. Temperature and magnetic field dependence of the nanowire I - V characteristics confirms that the non-linearity is due to the onset of superconducting-like correlations.

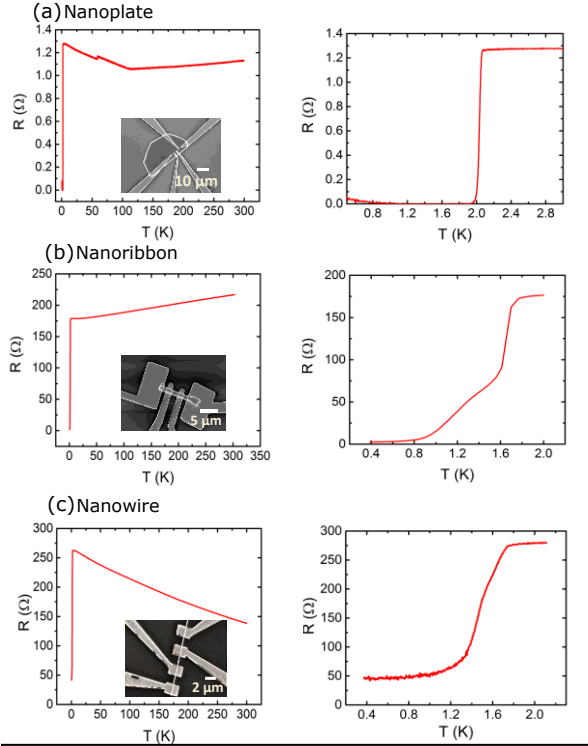


Figure 2. Superconducting transitions of In-doped SnTe nanoplate (a), nanoribbon (b), and nanowire (c). Unlike the sharp transition observed for the nanoplate, superconducting transitions of the nanoribbon and nanowire are gradual. For the nanowire, the resistance saturates to $R \sim 55 \Omega$.

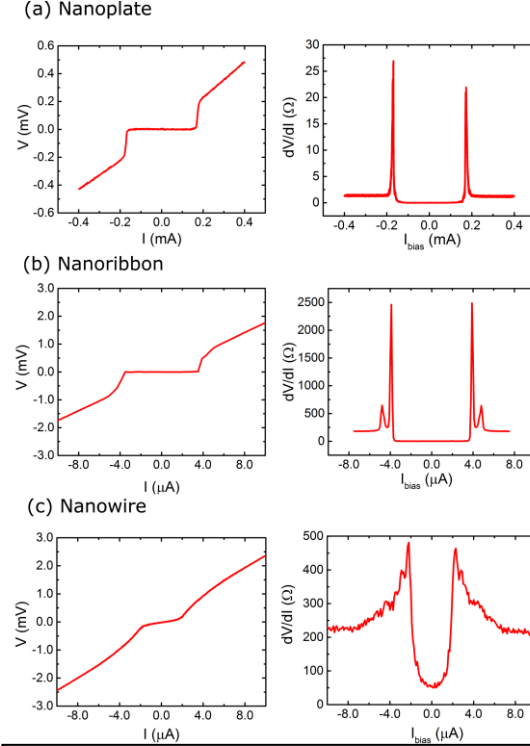


Figure 3. I - V characteristics of the nanostructures: (left) I - V curves and (right) differential resistances as a function of I_{bias} . (a) nanoplate, (b) nanoribbon, and (c) nanowire. For the nanoribbon and nanowire, the differential resistances show an extra spike or a broad peak.

The suppressed superconducting behavior of the nanowire device is attributed to the crystal quality of the nanowire. Other factors, such as quantum phase slips^[9], effects of the contacts, thermal fluctuations in nanowires, have been ruled out based on the rather large size and low resistance value of the nanowires, four terminal device geometry, and the absence of hysteresis in the I - V characteristics with forward and reverse current sweeps^[10]. For the crystal quality of the nanowires, two factors are identified to degrade the superconducting characteristics: spatial inhomogeneity of indium dopants and possible incorporation of gold impurities. Gold impurities are possible because gold nanoparticles are used as metal catalysts to promote growth of nanowires during the CVD growth. For silicon nanowires using gold metal catalysts, gold impurities have been observed inside the nanowires^[11]. Indium doping inhomogeneity was directly observed by using low voltage surface sensitive scanning electron microscopy (SEM) imaging operated at the acceleration voltage of 1 keV. On the surface of a

microcrystal, bright regions are observed, which contain high concentrations of indium, confirmed by EDX (Figure 4).

For nanoplates and nanoribbons, similar indium doping inhomogeneity can be expected, as growth conditions are identical for all three structures. We hypothesize that the reduced dimension of the nanowires compared to the other two morphologies enhances the relative effects of defects, such as indium dopant inhomogeneity, more in transport measurements of the nanowires.

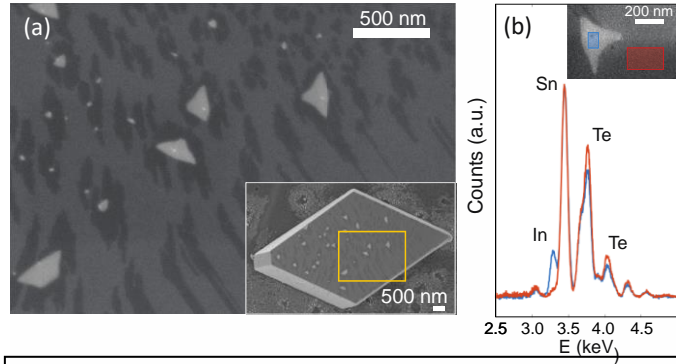


Figure 4. (a) SEM image of an In-doped SnTe microcrystal shows bright regions on the surface. (b) SEM-EDX spectra of a bright region show a higher concentration of indium, indicating indium inhomogeneity.

Future Plans

Our results highlight the importance of crystal quality for the superconducting behaviors of In-doped SnTe nanowires. Our future plans are to improve the indium dopant inhomogeneity and to understand how defects arise during synthesis.

To improve the inhomogeneity of indium dopants, we will use In-doped SnTe bulk crystals as source material instead of mixing InTe and SnTe powders together. Due to the dissimilar vapor pressures and sublimation temperatures, a mixture of InTe and SnTe powders may not create conditions that can promote uniform doping of indium into SnTe nanowires. The use of In-doped SnTe bulk crystals, which we will check the uniformity of indium dopants before nanowire growth, is expected to result in more uniform distribution of indium dopants in the nanowires.

We have observed dislocation-driven surface defects in SnTe microcrystals and nanostructures (Figure 5). These surface defects have not been carefully reported, although quite common in CVD grown samples. Fast cooling of the CVD growth

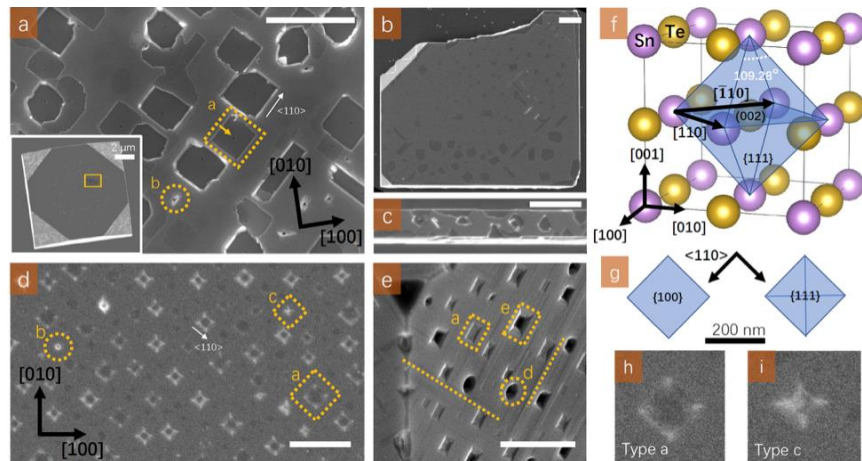


Figure 5. Square surface pits observed in SnTe microcrystal (a), nanoplate (b), and nanowire (c). (d, e) Surface pits observed in In-doped SnTe. (f) Crystal structure of SnTe. (g) Plan view illustrations of pit "a" and "c," with corresponding SEM images in (h) and (i). Scale bar = 500 nm.

eliminates surface defects. However, open cores stemming from dislocations persist. CVD growth conditions will be varied to find out how the growth kinetics induces formation of dislocations.

References

- [1] Fu, L., *Topological Crystalline Insulators*. Phys. Rev. Lett., 2011. **106**(10): p. 106802.
- [2] Hsieh, T.H., H. Lin, J. Liu, W. Duan, A. Bansil, and L. Fu, *Topological crystalline insulators in the SnTe material class*. Nat. Commun., 2012. **3**: p. 982.
- [3] Allen, P.B. and M.L. Cohen, *Carrier-concentration-dependent superconductivity in SnTe and GeTe*. Phys. Rev., 1969. **177**: p. 704 - 706.
- [4] Bushmarina, G.S., I.A. Drabkin, V.V. Kompaniets, R.V. Parfen'ev, D.V. Shamshur, and M.A. Shakhov, *Superconducting transition in SnTe doped with In*. Sov. Phys. Solid State, 1986. **28**: p. 612.
- [5] Erickson, A.S., J.H. Chu, M.F. Toney, T.H. Geballe, and I.R. Fisher, *Enhanced superconducting pairing interaction in indium-doped tin telluride*. Physical Review B, 2009. **79**(2): p. 024520.
- [6] Sasaki, S., Z. Ren, A.A. Taskin, K. Segawa, L. Fu, and Y. Ando, *Odd-Parity Pairing and Topological Superconductivity in a Strongly Spin-Orbit Coupled Semiconductor*. Phys. Rev. Lett., 2012. **109**(21): p. 217004.
- [7] Alicea, J., Y. Oreg, G. Refael, F. von Oppen, and M.P.A. Fisher, *Non-Abelian statistics and topological quantum information processing in 1D wire networks*. Nat Phys, 2011. **7**(5): p. 412-417.
- [8] Kumaravadivel, P., G.A. Pan, Y. Zhou, Y. Xie, P. Liu, and J.J. Cha, *Synthesis and superconductivity of In-doped SnTe nanostructures*. APL Materials, 2017. **5**(7): p. 076110.
- [9] Bezryadin, A., C.N. Lau, and M. Tinkham, *Quantum suppression of superconductivity in ultrathin nanowires*. Nature, 2000. **404**(6781): p. 971-974.
- [10] Tinkham, M., J.U. Free, C.N. Lau, and N. Markovic, *Hysteretic I - V curves of superconducting nanowires*. Phys. Rev. B, 2003. **68**(13): p. 134515.
- [11] Allen, J.E., E.R. Hemesath, D.E. Perea, J.L. Lensch-Falk, LiZ.Y, F. Yin, M.H. Gass, P. Wang, A.L. Bleloch, R.E. Palmer, and L.J. Lauhon, *High-resolution detection of Au catalyst atoms in Si nanowires*. Nat. Nanotechnol., 2008. **3**: p. 168-173.

Publications

- P. Liu, Y. Xie, E. Miller, Y. Ebine, P. Kumaravadivel, S. Sohn, J. J. Cha, "Dislocation-driven SnTe surface defects during chemical vapor deposition growth," under review (2017).
- P. Kumaravadivel, G. A. Pan, Y. Zhou, Y. Xie, P. Liu, J. J. Cha, "Synthesis and superconductivity of In-doped SnTe nanostructures," APL Materials **5**, 076110 (2017).
- J. M. Woods, J. Shen, P. Kumaravadivel, Y. Pang, Y. Xie, G. A. Pan, M. Li, E. I. Altman, L. Lu, J. J. Cha, "Suppression of magnetoresistance in thin WTe₂ flakes by surface oxidation," ACS Appl. Mater. & Interfaces **9**, p.23175 – 23180 (2017).
- J. Shen, J. M. Woods, Y. Xie, M. D. Morales-Acosta, J. J. Cha, "Structural phase transition and carrier density tuning in SnSe_xTe_{1-x} nanoplates," Adv. Elec. Mater. **2**, 1600144 (2016).

Project Title: Non-Centrosymmetric Topological Superconductivity
Principal Investigator: Johnpierre Paglione
Institution: University of Maryland
Email address: paglione@umd.edu

Project Scope

Topological insulator (TI) materials are distinguished from ordinary insulators by the so-called Z_2 topological invariants associated with the bulk band structure [1]. Several intriguing and potentially technologically useful properties make the TI states of particular interest beyond fundamental curiosities. In particular, TIs possess a surface state with a Dirac electronic dispersion similar to graphene, topologically protected against localization by time-reversal-invariant (i.e. non-magnetic) disorder. Spin and momentum are perfectly coupled in the chiral TI surface state, leading to novel magnetoelectric effects and much potential for advanced applications [2,3]. Furthermore, the realization of a condensed-matter version of Majorana quasiparticles, fermions that are their own anti-particle [4], has driven an entire field of interest in coupling TI states with superconductivity. First shown by Kitaev in the context of spinless $p_x + ip_y$ superconducting quantum wire [5], the possibility of localizing Majorana fermions at the boundaries of a topological superconductor – for instance at the edges of a wire or inside a vortex core – has great potential in realizing the next generation of fault-tolerant quantum computation [6]. Large families of new topological materials are waiting to be discovered in small-gap semiconductor systems and semimetals with high-Z elements [7], and true materials exploration is the only route to finding them. We have identified a new family of superconducting topological insulator compounds in the ternary half-Heusler system that not only show promise to realize TI states in stable, stoichiometric materials, but also to combine non-trivial topologies of both electron band structure and odd-parity superconducting states to produce a truly new realm of topological materials.

A non-trivial band structure that exhibits band ordering analogous to that of the known 2D and 3D TI materials was predicted in a variety of 18-electron half-Heusler compounds using first principles calculations [8,9]. The band structures of these compounds are very sensitive to the electronegativity difference of the constituents, resulting in semiconducting band gaps that can vary from zero (LaPtBi) to 4 eV (LiMgN) [8]. A subset of these compounds possess an inverted band structure, with the top of an s -type orbital-derived valence band lying below a p -type conduction band, with both centered at the high-symmetry Γ point and with no other bands crossing the Fermi level elsewhere in the Brillouin zone. Because such a band inversion changes the parity of the wavefunction, it provides the proper condition for the TI state, yielding a handy indicator of the potential for specific compounds to be TIs. This can be quantified by calculating the band structure and measuring the degree of band inversion; in the half-Heuslers, a sensitive tuning of band inversion is possible due to the tunable lattice constants [8,9]. With the ability to tune the energy gap and set the desired band inversion by appropriate choice of compound with appropriate hybridization strength (i.e., lattice constant) and magnitude of spin-orbit coupling (i.e., nuclear charge), the half Heusler family shows much promise for realizing the next generation of TI materials.

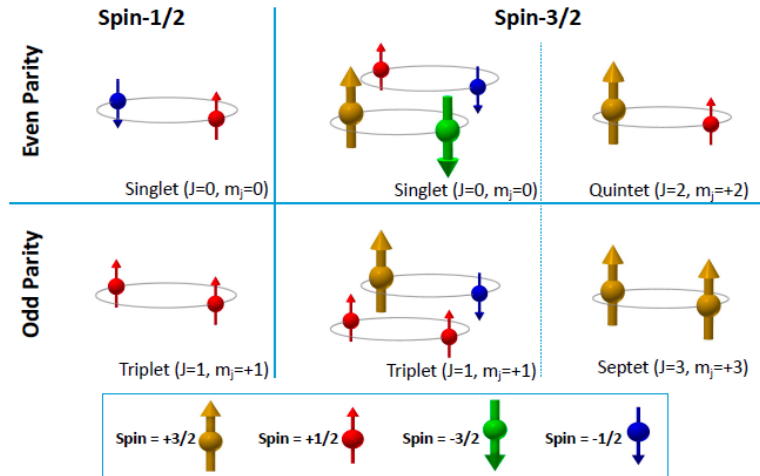


Figure 1: High-spin Cooper pairing in spin-3/2 systems.

Superconductors are among the most fascinating systems for realizing topological states, either via a proximity effect, or intrinsically via an odd-parity, time-reversal-invariant pairing state. Alongside the usual signature supercurrents arising from Cooper pair coherence, a direct analogy exists between superconductors and insulators: since the Bogoliubov-de Gennes (BdG) Hamiltonian for the quasiparticles of a superconductor is essentially analogous to that of a band insulator, one can consider the interesting possibility of TI surface states arising due to a superconducting “band gap”. Similar to TI systems, a topological superconductor (TSC) thus has a fully gapped bulk band structure and gapless surface Andreev bound states. Thus the search for TSCs in materials with strong band inversion is a promising direction. In the case of time-reversal-invariant (centrosymmetric) systems, a material is a TSC if it is an odd-parity, fully gapped superconductor and its Fermi surface encloses an odd number of time-reversal-invariant momenta in the Brillouin zone [10].

Superconductors without inversion symmetry, or non-centrosymmetric superconductors, promise a much more robust route to realizing TSC states. With inversion symmetry being one of two key symmetries for Cooper pairing (time reversal being the other), its absence has profound implications on the formation of Cooper pairs. With a non-trivial topology of the Bogoliubov quasiparticle wavefunction resulting in protected zero-energy boundary states analogous to those of TI systems, the promise of TSC in NC superconductors is very strong. With strong band inversion, the RPtBi and RPdBi ternary half-Heusler compounds are candidate TI systems as explained above. Furthermore, the situation in these compounds is further enriched by the $j=3/2$ total angular momentum index of the states in the Γ_8 electronic band near the chemical potential.

This arises from the strong atomic spin-orbit coupling of the $s=1/2$ spin and the $l=1$ orbital angular momenta in the p atomic states of Bi. The high crystal symmetry and the relatively simple band structure conspire to preserve the $j=3/2$ character of the low-energy electronic states, permitting Cooper pairs with angular momentum beyond the usual spin-singlet or spin-triplet states. In particular, as demonstrated schematically in Figure 1, high angular momentum even- and odd-parity pairing components with quintet ($J=2$) and septet ($J=3$) states are possible through the pairing combinations of $j=1/2$ and $j=3/2$ quasiparticles, permitting a solid-state analogue of the high-spin superfluidity discussed in the context of fermionic cold atomic gases [11,12]. Such an unprecedented exotic pairing state arises from new $j=3/2$ interactions that do not appear for the spin- $1/2$ case, allowing new opportunities for topological superconducting states.

Recent Progress

After completing a thorough study of the palladium-based rare earth-bismuthide (RPdBi) half-Heusler family, synthesizing high-quality crystalline specimens and fully characterizing their normal, superconducting and magnetic states, we are continuing to explore the interplay of topology, superconductivity and magnetism that this system presents. We synthesized the series of heavy-R compounds, including Sm, Gd, Tb, Dy, Ho, Er, Tm magnetic rare earths as well as Y and Lu non-magnetic elements. Electrical resistivity and magnetic susceptibility measurements of the RPdBi series has been performed down to 20 mK temperatures, revealing an interesting progression of superconducting phase transitions that evolves with rare earth species. We have found that superconductivity exists in most of these compounds, with a maximum transition $T_c = 1.6$ K found in the non-magnetic Y- and Lu-based compounds, and is systematically suppressed with increasing strength of magnetism from the magnetic rare

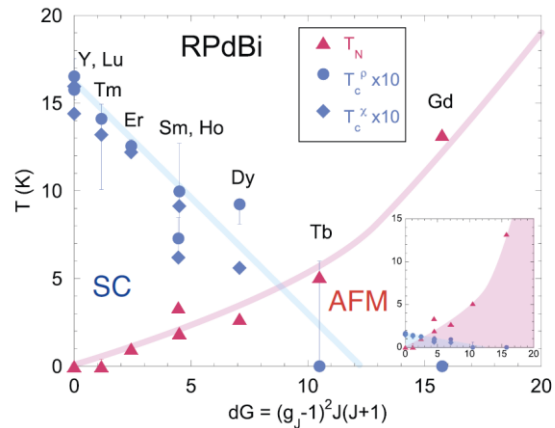


Figure 2: Phase diagram of RPdBi series, indicating evolution of superconducting (SC) and antiferromagnetic (AFM) ground states as a function of magnetic de Gennes factor. The plotted T_c is scaled by a factor of 10, and solid lines are guides to the eye. [Nakajima *et al*, Science Advances (2015)]

earth species. Neutron scattering experiments performed in collaboration with Dr. Jeff Lynn at NIST Gaithersburg have confirmed long-ranged antiferromagnetic order, which presents a representative scan of magnetic peaks in DyPdBi ($T_N=3.5$ K) and the AFM order parameter in TbPdBi ($T_N=4.9$ K). The R local moment sublattice leads to long-range antiferromagnetic (AFM) order in R=Sm, Gd, Tb, and Dy, as evidenced by abrupt drops in susceptibility. Low-temperature specific heat measurements confirm the thermodynamic AFM transitions, and reveal low-temperature ordering in HoPdBi and ErPdBi at 1.9 K and 1.0 K respectively. Furthermore, superconductivity coexists with long-range magnetic order as shown in Figure 2, as determined by neutron scattering experiments on TbPdBi, DyPdBi and HoPdBi, which all undergo antiferromagnetic ordering transitions before entering a superconducting state at a lower temperature. This presents two rather interesting aspects that warrant further investigation: coexistence of superconductivity with potential spin-triplet non-trivial topology along with a new type of proposed topological insulator system, the antiferromagnetic topological insulator. Besides the exotic collective modes, antiferromagnetism breaks time reversal and translational symmetries but preserves the combination of both symmetries, leading to a new, as yet unrealized type of topological system. *This work appeared in Science Advances in June 2015.*

We have pursued a joint experimental and theoretical effort to focus on understanding the topological superconducting state of the non-centrosymmetric material YPtBi [13], a clean limit superconductor with an extremely small electronic density of states at the Fermi level corresponding to a tiny carrier density $n = 2 \times 10^{18} \text{ cm}^{-3}$. The value of $T_c = 0.8$ K in YPtBi cannot be explained within the BCS theory framework due to the low carrier density [14]. Experimentally, a collaboration with Prof. Ruslan Prozorov at Ames National Lab continues to investigate the superconducting state of this material as well as related compounds such as the RPdBi (R=rare earth) and RPtSb-based compounds that contain superconducting ground states. The temperature variation of the London penetration depth was measured in single crystals of YPtBi by means of a tunnel diode resonator technique with temperatures down to 50 mK, yielding a very interesting linear temperature dependence that is indicative of the presence of line nodes in the superconducting energy gap of YPtBi with moderate impurity scattering. Theoretically, we have investigated the consequences of this result in collaboration with Prof. Daniel Agterberg at UM Wisconsin and Prof. Philip Brydon at Otago New Zealand. Their theoretical work, in collaboration with a postdoctoral fellow supported by this grant (Limin Wang) has led to a new understanding of the superconductivity in this system as arising from a spin-3/2 band structure, which is the first time such physics has been considered theoretically for a superconductor (previously only cold atomic gases and superfluid phases of helium) and also the first time it may be experimentally realized in any condensed matter state.

With a linear temperature dependence of the London penetration depth (Figure 3), we have inferred the existence of line nodes in the superconducting order parameter of YPtBi, implying the necessity of a mixed-parity Cooper pairing model with high total angular momentum, consistent with a high-spin fermionic superfluid state. Together with our collaborators, we have proposed a $k \cdot p$ model of the $j = 3=2$ fermions to

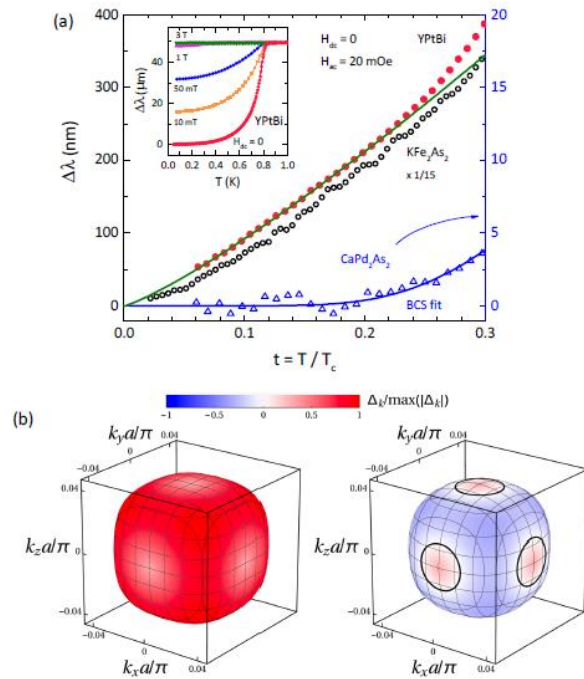


Figure 3: Evidence for line nodes and spin-3/2 singlet-septet mixed parity pairing model of YPtBi, with London penetration depth (top) and superconducting gap model (bottom) for the spin split Fermi surfaces. [H, Kim *et al.*, arXiv:1603.03375v4 (2017)]

explain how a dominant $J = 3$ septet pairing state is the simplest solution that naturally produces nodes in the mixed even-odd parity gap of this system. As shown in Figure 3, the gap structure resulting from this mixed singlet-septet state displays ring-shape line nodes on one of the spin-split Fermi surfaces, and is a natural generalization of the theory of $j=1/2$ noncentrosymmetric superconductors. *The theoretical model is now published in Phys. Rev. Lett. [15], and the experimental report is currently being reviewed for publication. Also, several theoretical works have been prompted by our experimental results [15-21].*

Future Plans

We continue to explore the exotic normal and superconducting state properties of this family of compounds to understand the nature of the normal and superconducting states, using our full arsenal of probes in combination with a systematic growth program aimed at comparing properties of the RPtBi and RPdBi series, including chemical doping in order to achieve the charge neutrality point, and disorder studies. Most interesting, tuning spin orbit coupling via elemental substitution may be a powerful method of both studying and controlling the parity of the superconducting state and the topology of the half-Heusler series.

References

1. C. L. Kane, E. J. Mele, Phys. Rev. Lett. 95, 146802 (2005); L. Fu, C. L. Kane, Phys. Rev. B 74, 195312 (2006).
2. J. E. Moore, Nature 464, 194 (2010).
3. M. Z. Hasan, C.L. Kane, Rev. Mod. Phys. 82, 3045 (2010); X.-L. Qi, S.-C. Zhang, *ibid* 83, 1057 (2011).
4. F. Wilczek, Nature Phys. 5, 614 (2009).
5. A. Y. Kitaev, , Phys.-Usp. 44, 131 (2001).
6. C. Nayak, S. H. Simon, A. Stern, M. Freedman, S. Das Sarma, Rev. Mod. Phys. 80, 1083 (2008).
7. B. Yan, S.-C. Zhang, Rep. Prog. Phys. 75, 096501 (2012).
8. S. Chadov *et al.*, Nature Mater. 9, 541 (2010).
9. H. Lin *et al.*, Nature Mater. 9, 546 (2010); D. Xiao *et al.*, Phys. Rev. Lett. 105, 096404 (2010); W. Feng *et al.*, Phys Rev B 82, 235121 (2010); W. Al-Sawai *et al.*, Phys Rev B 82, 125208 (2010).
10. L. Fu, E. Berg, Phys. Rev. Lett. 105, 097001 (2010).
11. T.-L. Ho and S. Yip, Phys. Rev. Lett. 82, 247 (1999).
12. W. Yang, Y. Li, and C. Wu, Phys. Rev. Lett. 117, 075301 (2016).
13. N. P. Butch, P. Syers, K. Kirshenbaum, A. P. Hope, and J. Paglione, Phys. Rev. B 84, 220504 (2011).
14. M. Meinert, Phys. Rev. Lett. 116, 137001 (2016).
15. P. M. R. Brydon, L. Wang, M. Weinert, and D. F. Agterberg, Phys. Rev. Lett. 116, 177001 (2016).
16. W. Yang, T. Xiang, C. Wu, arXiv:1707.07261.
17. L. Savary, J. Ruhman, J.W.F. Venderbos, L. Fu, P.A. Lee, arXiv:1707:03831.
18. I. Boettcher, I.F. Herbut, arXiv:1707.03444.
19. C. Timm, A.P. Schnyder, D.F. Agterberg, P.M.R. Brydon, arXiv:1707.02739.
20. V. Kozii, J.W.F. Venderbos, L. Fu, Sci. Adv. 2, e1601835 (2016).
21. T. Nomoto, H. Ikeda, Phys. Rev. Lett. 117, 217002 (2016).

Publications

Y. Nakajima, R. Hu, K. Kirshenbaum, A. Hughes, P. Syers, X. Wang, K. Wang, R. Wang, S.R. Saha, D. Pratt, J.W. Lynn, and J. Paglione, “*RPdBi half-Heusler semimetals: a new family of non-centrosymmetric magnetic superconductors*”, Science Advances 1, e1500242 (2015).

H. Baek, J. Ha, D. Zhang, B. Natarajan, J. P. Winterstein, R. Sharma, R. Hu, K. Wang, S. Ziemak, J. Paglione, Y. Kuk, N. B. Zhitenev, and J. A. Stroscio, “*Creating Nanostructured Superconductors by Local Current Annealing of the Half-Heusler Alloy YPtBi*”, Phys. Rev. B 92(9), 094510 (2015).

H. Kim, K. Wang, Y. Nakajima, R. Hu, S. Ziemak, P. Syers, L. Wang, H. Hodovanets, J.D. Denlinger, P.M.R. Brydon, D.F. Agterberg, M.A. Tanatar, R. Prozorov, J. Paglione, “*Beyond Spin-Triplet: Nodal Topological Superconductivity in a Noncentrosymmetric Semimetal*”, submitted to Science Advances (arXiv:1603.03375).

Nanostructure Studies of Strongly Correlated Materials

Douglas Natelson, Dept. of Physics and Astronomy, Rice University

Program Scope

Strongly correlated materials exhibit rich phenomenology due to competing ordered states, including superconductivity, metal-insulator transitions, and magnetic ordering. This program employs nanostructure techniques, traditionally applied to conventional metal and semiconductor systems, to examine open questions in correlated materials. The program is presently focused on systems in which Fermi liquid (FL) theory, with low energy excitations well described as long-lived, weakly interacting quasiparticles, is suspected to be violated. In *bad metals*, the electronic mean free path inferred from simple transport is unphysically small, comparable to the lattice spacing. In *strange metals* such as the normal state of the optimally doped cuprate superconductors, the resistivity scales unconventionally with T , implying unusual scattering mechanisms or poor definition of quasiparticles. In both bad and strange metals, the nature and degree of collectiveness of the low energy electronic excitations remains unclear.

Electronic transport on the mesoscopic scale has proven to be an excellent tool for understanding the low energy properties of metals and semiconductors. In the conventional FL picture, as T approaches zero, quasiparticles remain well-defined and their quantum coherence persists for longer time (and spatial) scales, predicted to diverge at $T = 0$. This results in quantum interference corrections to semiclassical conduction[1, 2], such as weak localization magnetoresistance, magnetic field-dependent and time-dependent universal conductance fluctuations (UCF), and Aharonov-Bohm magnetoconductance oscillations in mesoscopic rings. The theories for quantitative analysis of these effects assume “good” metallicity $-k_F l \gg 1$, where k_F is the Fermi wavevector and l is the electronic mean free path. We are examining transport on similar scales in bad metals and strange metals on similar scales at low temperatures. Even if the lowest energy charge-carrying excitations are not well modeled as simple quasiparticles, as T decreases there should be some quantum coherence effects that manifest.

The second set of experiments uses tunneling shot noise spectroscopy to examine charge-carrying excitations in strange metals. Shot noise is a consequence of the quantization of charge, and is frequency independent out to a high frequency cutoff set by the electronic transit time and energy scale of transmission variation (hundreds of GHz for tunnel junctions). For independent electrons at $T = 0$, the spectral density of current fluctuations is $S_I = 2eI A^2/\text{Hz}$, where e is the charge and I is the average current. In situations where the electrons are not independent, $S_I = F 2eI$, where F is the Fano factor[3]. Pairing or bunching of electrons can enhance F above 1, while inelastic processes or charge renormalization can suppress F . Present experiments are looking at shot noise in tunneling between normal metals and strange metals, as well as shot noise in tunneling between strange metals. Specifically, we are attempting to examine tunneling between cuprate superconductors in the normal state, and between normal metals and YRh_2Si_2 , a heavy fermion compound that exhibits strange metallicity in the quantum critical regime[4].

Recent Progress

In addition to some nice work on nanostructures exhibiting quantum magnetism, in the last two years, we have made progress in both looking for mesoscopic effects in non-Fermi liquids and in initial shot noise spectroscopy measurements of correlated materials. In previous periods we had demonstrated that atomic hydrogen intercalative doping of VO_2 suppresses the

low temperature insulating state, and stabilize a correlated metallic state down to cryogenic temperatures[5-7]. This stabilization results from the alteration of the occupancy of the V 3d orbitals due to H-O charge transfer, as well as strain of the lattice[8]. The resulting bad metal state has a resistivity typically $\sim 1 \text{ m}\Omega\text{-cm}$, exceeding the Mott-Ioffe-Regel limit, with a very flat temperature dependence and without any clear signs of impending strong localization.

We have examined electronic transport in three forms of this material: Single-crystal nanowires, plate-like single crystals, and in (rutile) *c*-directed epitaxial films on rutile TiO_2 , with intercalative doping performed via timed exposure to atomic hydrogen produced via hot filament. Hydrogen doping leads to a strong decrease in the Hall coefficient, consistent with electronic doping as expected; however, interpreting the Hall coefficient in terms of single-band transport gives an unphysically large carrier density even in the undoped high temperature metallic state. Multiband transport is clearly at work in this material.

In all three platforms, we observed a positive magnetoresistance (MR) that grew with decreasing temperature below about 20 K. The doped epi films showed an emergent negative MR peak at 4 K and below. In functional form and magnitude, these phenomena are reminiscent of weak (anti)localization (WL/WAL), the quantum correction that involves interference of quasiparticles traversing loop-like trajectories. The MR is approximately isotropic in magnetic field direction, suggesting that the samples are quasi-3d with respect to these localization processes. In WL/WAL this would imply a coherence length $\sim 10\text{-}20 \text{ nm}$, also roughly consistent with the MR field scale. However, the theoretical expressions for WL/WAL assume $k_{\text{Fl}} \gg 1$; while it is possible to fit the data with those functional forms, any parameters extracted from such fits must then be viewed skeptically. These results have been published in *J. Phys. Condens. Matt.*, and we hope that this work spurs greater interest in the theoretical community about the issue of quantum corrections to conduction in non-Fermi liquids.

Through collaboration with Prof. Susanne Stemmer at UCSB, we also performed experiments designed to compare transport down to the sub-micron scale in oxide quantum wells. At the interface between SrTiO_3 (STO) and other insulating perovskite oxides, interfacial charge transfer can lead to the formation of a high-density two-dimensional electron gas. When a STO layer is embedded between layers of SmTiO_3 (SmTO), the resulting conductive quantum well is conductive, and depending on STO layer thickness, has a temperature-dependent resistance that can be FL (thicker layers) or non-FL-like (thinner layers). In magnetotransport measurements on Hall bar-style devices etched from such quantum wells, we did not observe systematic differences between nominally FL and NFL structures. However, we did find a

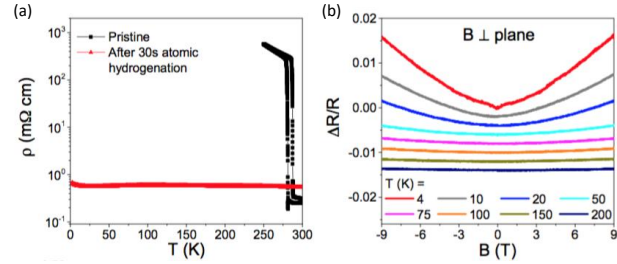


Fig. 1. (a) H doping stabilizes a bad metal H_xVO_2 down to cryogenic temperatures. (b) Weak localization-like magnetoresistance in H_xVO_2 film.

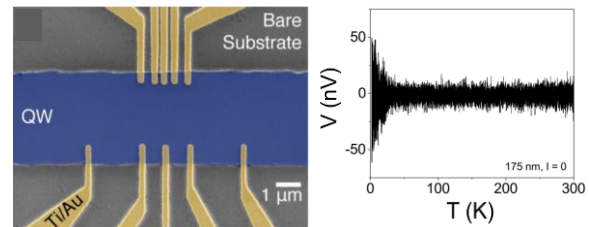


Fig. 2. Etched $\text{SmTiO}_3/\text{SrTiO}_3/\text{SmTiO}_3$ quantum wells show voltage fluctuations that grow at low T even with no applied current.

striking effect, time-dependent low-frequency ($1/f$ -like) voltage fluctuations that grew as $T \rightarrow 0$. These fluctuations had no clear dependence on magnetic field, and were suppressed in larger-area contacts. While superficially resembling mesoscopic time-dependent UCF, and correlating with observations of magnetic field-dependent UCF in both device sets, these voltage fluctuations persisted even in the *absence* of an external driving current. The growth of fluctuations as T is lowered rules out Johnson-Nyquist noise as a mechanism.

Fluctuating voltages in the absence of a current could also originate from time-varying fluctuations of the thermopower of the electron gas. The idea is that time-varying two-level defects produced by the etching process used to define the Hall bar structure can alter the local thermopower by an amount that grows with decreasing temperature; ensemble averaging over different regions then explains suppressed fluctuations in larger area contacts. Control experiments in related structures fabricated without the etching step show no such fluctuations. These results have been published in *ACS Nano*, and we hope they spur further theoretical and experimental investigations of mesoscopic effects in such oxide materials.

We have also been measuring shot noise in preparation for examining such effects in strange metals as described above. We have constructed a rf noise measurement probe for insertion into our Quantum Design PPMS cryostat, and used this probe and our broadband rf lock-in technique to examine, as proof of concept, the shot noise in conventional tunnel junctions based on Au/monolayer hBN/Au. This work has been published in *Appl. Phys. Lett.*, and shows conventional noise response in these junctions as a function of bias from room temperature down to cryogenic temperatures.

At the same time, we have made measurements in two types of devices incorporating strange or bad metals. In collaboration with Prof. Shane Cybart and Prof. Robert Dynes, we performed transport and shot noise measurements on planar tunnel junctions in YBCO films, with the junctions fabricated by them using helium ion beam processing. While we had some early encouraging data, subsequent iterations using device fabrication runs found very little noise. We are moving away from this approach because of concerns that etching-induced disorder[9] may make it difficult to measure intrinsic tunneling response in these planar structures. Our new approach is described below. Using hBN as a tunneling barrier, we have also made preliminary measurements of tunneling shot noise between a normal metal (Au) and a bad metal, H_xVO_2 . As shown in the figure, those first measurements show rather unusual features, with a definite asymmetry depending on whether electrons are injected into or withdrawn from the bad metal.

Future Plans

In the coming period our primary focus will be the shot noise measurements described above, in three platforms. First and foremost, we have begun collaborating with Dr. Ivan Bozovic at Brookhaven National Laboratory, with Mr. Panpan Zhou the now-senior student on the project, spending two months at BNL working to grow and pattern vertical tunneling structures based on $La_xSr_{1-x}CuO_2$ (LSCO). These structures are based on tunneling junctions previously employed[10] to examine the relationship between cuprate superconductivity and

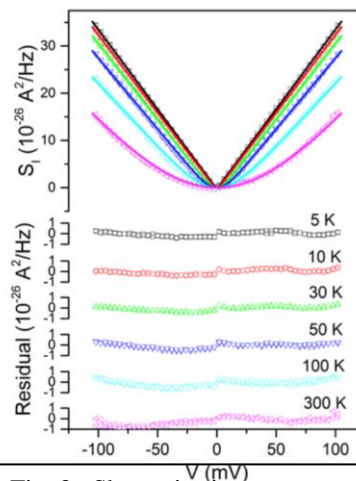


Fig. 3. Shot noise in Au/hBN/Au tunnel junction at various temperatures.

antiferromagnetism. The insulating layer in these structures is one unit cell thick undoped La_2CuO_4 . We will examine the tunneling response and the tunneling shot noise in three sets of these junctions prepared with different doping levels, ranging from optimally doped ($x = 0.15$) to underdoped ($x = 0.08$). The measurements will take place from well into the normal state (room temperature) down through the onset of the pseudogap phase in the underdoped material, to the superconducting state. We will also look for any variation as a function of external magnetic field, though this is unlikely to be a relevant perturbation at this temperature range. The data will be analyzed and compared with normal metal tunneling structures.

Second, we will continue applying our capability of using monolayer hBN as a tunnel barrier to perform shot noise spectroscopy measurements on junctions between a gold top contact and an epitaxial thin film of YbRh_2Si_2 grown by our collaborator, Prof. Silke Bühler-Paschen. We have films available, and have developed a means of depositing monolayer hBN with an integrated Au top electrode. These studies offer a chance to observe shot noise in tunneling in and out of a quantum critical heavy fermion metal, providing a window on how the incoherence of charge dynamics in the quantum critical regime affects charge injection or removal. An advantage of this system is its tunability with temperature – well above 20 K the expectation is that the system will likely have conventional metal properties – and magnetic field – with the quantum critical regime[11] “centered” on a field of about 0.7 T. The ability to compare noise data in different electronic regimes in a single device is appealing.

Third, we will follow up on the intriguing tunneling noise experiments in the H_xVO_2 system. In addition to doped nanowire-based devices, we will continue our collaboration with Prof. Darrell Schlom at Cornell to examine tunneling shot noise in the high temperature, correlated metallic phase of undoped VO_2 films.

References

1. S. Datta, *Electronic Transport in Mesoscopic Systems* 1997: Cambridge University Press.
2. Y. Imry, *Introduction to Mesoscopic Physics* 2008: Oxford University Press.
3. Y.M. Blanter and M. Buttiker, *Physics Reports* **336**(1-2), 1-166 (2000).
4. S. Friedemann *et al.*, *Proc. Nat. Acad. Sci.* **107**(33), 14547-14551 (2010).
5. J. Wei *et al.*, *Nat. Nano.* **7**(6), 357-362 (2012).
6. H. Ji, J. Wei, and D. Natelson, *Nano Lett.* **12**(6), 2988-2992 (2012).
7. J. Lin *et al.*, *Nano Lett.* **14**(9), 5445-5451 (2014).
8. Y. Filinchuk *et al.* *Amer. Chem. Soc.* **136**(22), 8100-8109 (2014).
9. A. Gozar, N.E. Litombe, J.E. Hoffman, and I. Božović, *Nano Letters* **17**(3), 1582-1586 (2017).
10. I. Bozovic, G. Logvenov, M. Verhoeven, P. Caputo, and E. Goldobin, *Nature* **422**(6934), 873 (2003).
11. P. Gegenwart, Q. Si, and F. Steglich, *Nat Phys* **4**(3), 186-197 (2008).

Publications

1. Jiangtan Yuan *et al.*, *Adv. Mater.* **27**, 5605-5609 (2015).
2. Will J Hardy *et al.*, *ACS Nano* **10**, 5941-5946 (2016).
3. Will J. Hardy *et al.*, *J. Phys. Condens. Matt.* **29**, 185601 (2017).
4. Panpan Zhou *et al.*, *Appl. Phys. Lett.*, **110**, 133106 (2017).
5. Will J. Hardy *et al.*, *ACS Nano* **11**, 3760-3766 (2017).

Session 7

Project Title: Epitaxial Complex Oxides

PIs: Ho Nyung Lee (hnlee@ornl.gov), G. Eres, T. Z. Ward, C. M. Rouleau, and H. M. Christen

Oak Ridge National Laboratory, Oak Ridge, TN 37831

Program Scope

The overarching goal of this project is on understanding, controlling, and ultimately designing epitaxial complex oxide thin films and heterostructures to obtain novel functionalities. Our specific objectives are to create such functionalities in complex oxides by epitaxial stabilization, to control order parameters, e.g. spin, electron, charge, and lattice, in interfacial oxides to achieve novel functionalities, and to probe the growth and functionality dynamically to provide foundational insight required for the design of new functional materials. A variety of *in situ* and *ex situ* characterization techniques are employed to unveil detailed information on crystallographic orientation and structure, electronic and ionic transport, and various functionalities, such as magnetism, ferroelectricity, and superconductivity. In addition, a combination of microstructural imaging and local spectroscopy, neutron scattering, optical and soft x-ray spectroscopy, and theory play key roles in all aspects of this work. Thus, the outcome of this work will result in enhanced understanding of interfacial behaviors and properties of complex oxides, providing unprecedented guidance in the design of technologically relevant materials for energy conversion and storage.

Recent Progress

The research has been focused on the discovery of new materials and phenomena arising from well-controlled, functionally cross-coupled interfaces. In particular, we have focused on the development of *5d* based heterostructures to explore strong spin-orbit coupling (SOC) and interfacial charge transfer. Understanding interfacial magnetic coupling in ferroic heterostructures using neutron scattering has been also one of the main focus areas. Selected research highlights are listed as follows:

Anomalous Hall effect discovered in a quantum oxide heterostructure: The anomalous Hall effect was discovered in heterostructures composed of alternating layers of *3d* antiferromagnetic insulator and *5d* paramagnetic metal, which exhibit no such behavior in the bulk. [Nichols 2016] Artificial quantum oxide heterostructures composed of the antiferromagnetic insulator SrMnO₃ and the paramagnetic metal SrIrO₃ were grown by pulsed laser epitaxy on SrTiO₃ substrates. Polarized neutron reflectometry (Fig. 1) and soft x-ray absorption spectroscopy have uncovered that there exists interfacial charge transfer, creating ferromagnetically ordered spins at the interface of the *3d-5d* oxide quantum heterostructure [Okamoto 2017]. As

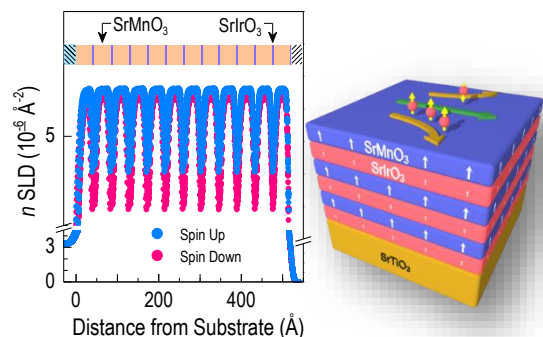


Figure 1. (Left) Graph shows neutron spin up and spin down scattering length density from a SrMnO₃/SrIrO₃ *3d/5d* superlattice on a SrTiO₃ substrate, indicating ferromagnetically ordered spins. (Right) Schematic of the quantum heterostructure with the induced magnetization represented by white arrows, while the anomalous Hall effect is illustrated on the top layer.

ferromagnetism and the anomalous Hall effect, which produces an extraordinary large Hall coefficient, are absent from either parent compound, their emergence in the superlattices provides the first experimental evidence of strong coupling at the interface of $3d$ and $5d$ oxides. This work demonstrates that strong SOC is instrumental in defining novel properties arising from atomically precise $3d$ – $5d$ interfaces, and that the low-dimensional effect together with the precise controllability of interfacial magnetism is an important factor to be considered in developing novel quantum materials.

Neurons unveil interfacial magnetism tuned dynamically by ionic-liquid assisted ferroelectric switching: Electrostatic control of magnetism with ferroelectricity at the interface between ferromagnetic $\text{La}_{0.8}\text{Sr}_{0.2}\text{MnO}_3$ and ferroelectric $\text{PbZr}_{0.2}\text{Ti}_{0.8}\text{O}_3$ has been discovered by polarized neutron reflectometry. [Meyer 2016, Herklotz 2017] This finding not only proves the ferroelectric field effect control of magnetism, but also emphasizes the necessity of separating bulk properties from interfacial phenomena in magnetoelectric materials. Here, we used polarized neutron reflectometry (PNR) to probe the interfacial magnetization in a ferroelectric–correlated oxide ($\text{PbZr}_{0.2}\text{Ti}_{0.8}\text{O}_3/\text{La}_{0.8}\text{Sr}_{0.2}\text{MnO}_3$) heterostructure. The difficulty in large area switching of the ferroelectric polarization with conventional methods was overcome by gating using ionic liquids, which allowed the charged ions to segregate at the interface. From this novel approach, we were able to dynamically probe the reversible modulation of the interfacial magnetism, which occurs in a few nanometers of the interface, by ferroelectric field effects.

Stretching a metal into an insulator: Combining experiment and theory, stretching a crystalline thin film of a transition metal oxide, strontium cobaltite ($\text{SrCoO}_{3-\delta}$), was shown to decrease the energetic stability of oxygen in the material. [Petrie 2016] The oxygen atoms were able to move more freely through channels in the thin film crystal (Fig. 2), increasing the number of missing oxygen atoms in the material (defects called vacancies). Impressively, these strain-induced oxygen vacancies were created at temperatures as low as 300°C , which is lower than previously possible, and in environments that usually decrease oxygen vacancies. Furthermore, this higher vacancy concentration converted a metal into an insulator. While of immediate benefit for low temperature energy production and storage devices and sensors, the ability to artificially control oxygen vacancy content in any environment is crucial for variety of functional materials, such as high-temperature superconductors, colossal magnetoresistors, memristors, and spintronic devices.

Time-resolved measurements of island size evolution confirm universal rules for oxide film growth: We demonstrated dynamic scaling of the island size distributions during film growth of a prototype oxide, validating a universal rule for oxide film growth that a single length scale describes the growth kinetics independent of growth conditions. This finding simplifies the acquisition of critical information about the interplay of nucleation, growth, and coalescence of islands on oxide surfaces that is the key to discovering

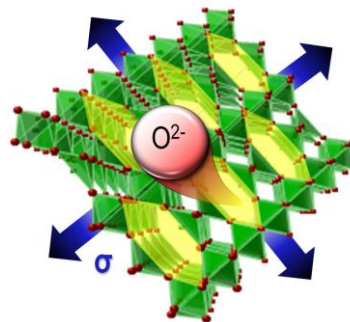


Figure 2. Stretching or compressing a material allows tailoring the concentration of missing oxygen atoms that directly affects the physical properties. The stretching of a thin film decreases the stability of oxygen in the crystalline structure, allowing oxygen atoms to move more freely through channels (yellow). This creates more missing oxygen atoms in the crystalline structure. In contrast, compression stabilizes the oxygen atoms and prevents the formation of these vacancies.

novel structures and compositions of complex oxides for advanced information and energy technologies. The correlation length, the single length scale for describing the island spacings, was determined by time-resolved measurements of the surface x-ray diffraction diffuse scattering intensity during pulsed laser deposition of SrTiO₃. [Eres 2016]

Future Plans

Understanding the interplay among strong correlations, quantum confinement, and spin-orbit coupling in 3d–5d quantum oxide heterostructures: The strong correlation among the spin, charge, orbital, and lattice degrees of freedom in complex oxides is at the heart of what makes these materials so promising for technological upheavals in applications. Therefore, by taking advantage of the inherent sensitivity of correlated electron oxides to external stimuli, including strain, chemical pressure, defects, etc., we will investigate various heterostructures designed to control the order parameters to disentangle the underlying complexity toward realization of better control over the quantum mechanical behaviors and physical properties. Particular focus will be on understanding the interplay among strong electron correlations, quantum confinement, and SOC in creating topological states of electrons in 3d–5d transition metal oxide thin films and heterostructures. Our recent work discovered a possibility of inducing the anomalous Hall effect by interfacial charge transfer. Moreover, compositional inversion symmetry breaking in SrIrO₃ based heterostructures with strong SOC resulted in the topological Hall effect, indicating the formation of skyrmions. Therefore, we will focus on studying details on the underlying mechanism on their formation and control in short-period oxide heterostructures and superlattices. Synthesis of ferromagnetic double perovskites composed of 3d and 5d transition metals will be also performed. The 3d element with strong electron correlations that drive local magnetism and the 5d element with itinerant electrons with strong SOC offer the essential ingredient for creating topological phases and materials, such as quantum anomalous Hall insulators or Chern insulators. Double perovskites, including Sr₂FeReO₆ and Ba₂FeReO₆, will be studied by growing epitaxial films on (111)-oriented perovskite substrates.

Controlling physical properties through hybrid interface synthesis: Advanced heterostructure synthesis has brought us exquisite capabilities to manipulate complex oxide film and interfacial properties. Using an integrated synthesis and characterization system combining pulsed laser deposition, molecular beam epitaxy, x-ray and ultraviolet photoelectron spectroscopy, and scanning tunneling microscopy, we aim to explore the physical properties of quantum heterostructures via the synthesis of hybrid interfaces, i.e. interfaces between different classes of complex materials or between materials that require different synthesis methods. As an example, interfaces between topologically non-trivial materials and complex oxides potentially allow for a significantly more robust interfacial functionality. Using detailed *in situ* electron spectroscopy in conjunction with *ex situ* magnetometry and quantum transport measurements, we aim to study interfacial structures and properties of hybrid interfaces between topologically non-trivial materials and complex oxides to understand interfacial charge transfer, magnetic exchange coupling across the interface, and the resulting interfacial spin structures and spin-polarized quantum transport properties. Neutron scattering will be used to understand interfacial magnetic coupling of the hybrid interfaces.

Selected Publications (selected from a total of 67 publications)

1. W. S. Choi and H. N. Lee, "Strain tuning of electronic structure in Bi₄Ti₃O₁₂-LaCoO₃ epitaxial thin films", *Phys. Rev. B* **91**, 174101 (2015).
2. A. Herklotz, K. Dörr, T. Z. Ward, G. Eres, H. M. Christen, M. D. Biegalski, "Stoichiometry control of complex oxides by sequential pulsed-laser deposition from binary-oxide targets", *Appl. Phys. Lett.* **106**, 131601 (2015).
3. S. Lee, T. L. Meyer, C. Sohn, D. Lee, J. Nichols, D. Lee, S. S. A. Seo, J. W. Freeland, T. W. Noh, and H. N. Lee, "Electronic structure and insulating gap in epitaxial VO₂ polymorphs," *APL Mater.* **3**, 126109 (2015).
4. T. L. Meyer, L. Jiang, S. Park, T. Egami, and H. N. Lee, "Strain-relaxation and critical thickness of epitaxial La_{1.85}Sr_{0.15}CuO₄ films," *APL Mater.* **3**, 126102 (2015).
5. H. Jeon and H. N. Lee, "Structural evolution of epitaxial SrCoO_x films during topotactic phase transition," *AIP Advances* **5**, 127123 (2015).
6. H. N. Lee, S. S. A. Seo, W. S. Choi, and C. M. Rouleau, "Growth control of oxygen stoichiometry in homoepitaxial SrTiO₃ films by pulsed laser epitaxy in high vacuum," *Sci. Rep.* **6**, 19941 (2016).
7. A. Herklotz, S. R. Rus, and T. Z. Ward, "Continuously Controlled Optical Band Gap in Oxide Semiconductor Thin Films," *Nano Lett.* **16**, 1782 (2016).
8. S. Lee, I. N. Ivanov, J. K. Keum, and H. N. Lee, "Epitaxial stabilization and phase instability of VO₂ polymorphs," *Sci. Rep.* **6**, 19621 (2016).
9. J. Petrie, C. Mitra, H. Jeon, W. S. Choi, T. Meyer, F. A. Reboredo, J. W. Freeland, G. Eres, and H. N. Lee, "Strain control of oxygen vacancies in epitaxial strontium cobaltite films," *Adv. Funct. Mater.* **26**, 1564 (2016).
10. T. L. Meyer, H. Jeon, X. Gao, J. R. Petrie, M. F. Chisholm, and H. N. Lee, "Symmetry-driven atomic rearrangement at a brownmillerite-perovskite interface," *Adv. Electron. Mater.* **2**, 1500201 (2016).
11. A. Herklotz, A. T. Wong, T. Meyer, M. D. Biegalski, H. N. Lee, and T. Z. Ward, "Controlling octahedral rotations in a perovskite via strain doping," *Sci. Rep.* **6**, 26491 (2016).
12. J. Nichols, X. Gao, S. Lee, T. L. Meyer, J. W. Freeland, V. Lauter, D. Yi, J. Liu, D. Haskel, J. R. Petrie, E. Guo, A. Herklotz, D. Lee, T. Z. Ward, G. Eres, M. R. Fitzsimmons, and H. N. Lee, "Emerging magnetism and anomalous Hall effect in iridate-manganite heterostructures," *Nature Comm.* **7**, 12721 (2016).
13. A. Herklotz, H. W. Guo, A. T. Wong, H. N. Lee, P. D. Rack, and T. Z. Ward, "Multimodal responses of self-organized circuitry in electronically phase separated materials," *Adv. Electro. Mater.* **2**, 1600189 (2016).
14. G. Eres, J. Z. Tischler, C. M. Rouleau, H. N. Lee, H. M. Christen, P. Zschack, and B. C. Larson, "Dynamic scaling and island growth kinetics in pulsed laser deposition of SrTiO₃," *Phys. Rev. Lett.* **117**, 206102 (2016).
15. T. L. Meyer, A. Herklotz, V. Lauter, J. W. Freeland, J. Nichols, E.-J. Guo, S. Lee, T. Z. Ward, N. Balke, S. V. Kalinin, M. R. Fitzsimmons, and H. N. Lee, "Enhancing interfacial magnetization with a ferroelectric," *Phys. Rev. B* **94**, 174432 (2016).
16. X. Gao, S. Lee, J. Nichols, T. L. Meyer, T. Z. Ward, M. F. Chisholm, and H. N. Lee, "Nanoscale self-templating for oxide epitaxy with large symmetry mismatch," *Sci. Rep.* **6**, 38168 (2016).
17. D. Lee, X. Gao, L. Fan, E.-J. Guo, T. O. Farmer, W. T. Heller, T. Z. Ward, G. Eres, M. R. Fitzsimmons, M. F. Chisholm, and H. N. Lee, Nonequilibrium synthesis of highly porous single-crystalline oxide nanostructures, *Adv. Mater. Interfaces*, **4**, 1601034 (2017).
18. D. Lee and H. N. Lee, Controlling oxygen mobility in Ruddlesden-Popper Oxides, *Materials* **10**, 368 (2017).
19. L. Fan, X. Gao, D. Lee, E. J. Guo, S. Lee, P. C. Snijders, T. Z. Ward, G. Eres, M. F. Chisholm, H. N. Lee, Kinetically controlled fabrication of single-crystalline TiO₂ nanobrush architectures with high energy {001} facets, *Adv. Sci.* 1700045 (2017).
20. A. Herklotz, E. Guo, T. L. Meyer, S. Dai, T. Z. Ward, H. N. Lee, and M. R. Fitzsimmons, Reversible control of interfacial magnetism through ionic-liquid-assisted polarization switching, *Nano Lett.* **17**, 1665 (2017).
21. S. Lee, X.-G. Sun, A. A. Lubimtsev, X. Gao, G. Panchapakesan, T. Z. Ward, G. Eres, M. F. Chisholm, S. Dai, and H. N. Lee, Persistent electrochemical performance in epitaxial VO₂(B), *Nano Lett.* **17**, 2229 (2017).
22. J. Nichols, S. Yuk, C. Sohn, H. Jeon, J. W. Freeland, V. R. Cooper, and H. N. Lee, Electronic and magnetic properties of epitaxial SrRhO₃ films, *Phys. Rev. B* **95**, 245121 (2017).
23. E. Guo, T. Charlton, H. Ambaye, R. Desautels, H. N. Lee, and M. R. Fitzsimmons, Orientation control of interfacial magnetism at La_{0.67}Sr_{0.33}MnO₃/SrTiO₃ interfaces, *ACS Appl. Mater. Interfaces* **9**, 19307 (2017).
24. S. Okamoto, J. Nichols, C. Sohn, S. Kim, T. W. Noh, and H. N. Lee, Charge transfer in iridate-manganite superlattices, *Nano Lett.* **17**, 2126 (2017).
25. E. J. Guo, J. R. Petrie, M. A. Roldan, Q. Li, R. D. Desautels, T. Charlton, A. Herklotz, J. Nichols, J. W. Freeland, S. V. Kalinin, H. N. Lee, and M. R. Fitzsimmons, Spatially resolved large magnetization in ultrathin BiFeO₃, *Adv. Mater.* 1700790 (2017).

Program Title: Atomic Engineering Oxide Heterostructures: Materials by Design

Principle Investigator: H. Y. Hwang^{1,2*}; Co-PIs: Y. Hikita¹, J.-S. Lee³, and S. Raghu^{1,4}

¹Stanford Institute for Materials & Energy Sciences, SLAC National Accelerator Laboratory, Menlo Park, CA 94025

²Department of Applied Physics, Stanford University, Stanford, CA 94305

³Stanford Synchrotron Radiation Lightsource, SLAC National Accelerator Laboratory, Menlo Park, CA 94025

⁴Department of Physics, Stanford University, Stanford, CA 94305

**hyhwang@slac.stanford.edu*

Program Scope

A central aim of modern materials research is the control of materials and their interfaces to atomic dimensions. In the search for emergent phenomena and ever-greater functionality in devices, transition metal oxides have enormous potential. They host a vast array of properties, such as orbital ordering, unconventional superconductivity, magnetism, and ferroelectricity, as well as quantum phase transitions and couplings between these states. Our broad objective is to develop the science and technology arising in heterostructures of these novel materials. Using atomic scale growth techniques we explore the synthesis and properties of novel interface phases. Magnetotransport, x-ray, and optical probes are used to determine the static and dynamic electronic and magnetic structure. The experimental efforts are guided and analyzed theoretically, particularly with respect to superconductivity and new states of emergent order. A wide set of tools, ranging from analytic field theory methods to exact computational treatments, are applied towards the understanding and design of heterostructures.

Recent Progress

The Density and Disorder Tuned Superconductor-Metal Transition in Two Dimensions [1]: Quantum ground states which arise at atomically controlled oxide interfaces provide an opportunity to address key questions in condensed matter physics, including the nature of two-dimensional (2D) metallic behavior often observed adjacent to superconductivity. In the 2D superconductor at the LaAlO₃/SrTiO₃ interface, a metallic ground state emerges upon the collapse of superconductivity with field-effect back gating. Strikingly, such metallicity is accompanied with a pseudogap, in analogy to the cuprates. Here, we utilize independent control of carrier density and disorder of the interfacial superconductor using dual electrostatic gates, which enables the comprehensive examination of the electronic phase diagram approaching zero temperature. We find that the pseudogap corresponds to precursor pairing, and the onset of long-range phase coherence forms the superconducting dome. The gate-tuned superconductor-metal transition approaching zero temperature is driven by macroscopic phase fluctuations of Josephson coupled superconducting puddles.

2D Limit of Crystalline Order in Perovskite Membrane Films [2]: Long-range order and phase transitions in 2D systems – such as magnetism, superconductivity (as above), and crystallinity – have been important research topics for decades. The issue of 2D crystalline order has reemerged recently, with the development of exfoliated atomic crystals. Understanding the dimensional limit of crystalline phases, with different types of bonding and synthetic techniques, is at the foundation of low-dimensional materials design. Here we study ultrathin membranes of freestanding perovskite oxides with isotropic (3D) bonding. Atomically controlled membranes

are released after synthesis by dissolving an underlying epitaxial layer. Although all unreleased films are initially single-crystalline, the freestanding membrane lattice collapses below a critical thickness (~ 5 unit cells). This crossover from algebraic to exponential decay of the crystalline coherence length is analogous to the 2D topological Berezinskii-Kosterlitz-Thouless (BKT) transition. The transition is likely driven by chemical bond breaking at the 2D layer - 3D bulk interface, defining an effective dimensional phase boundary for coherent crystalline lattices.

Strong Polaronic Behavior in a Weak Coupling Superconductor [3]: The nature of superconductivity in the dilute semiconductor SrTiO₃ has remained an open question for more than 50 years. The extremely low carrier densities (10^{17} - 10^{20} cm⁻³) at which superconductivity occurs suggests an unconventional origin outside of the adiabatic limit in which the Bardeen-Cooper-Schrieffer (BCS) and Migdal-Eliashberg (ME) theories are based. Using our newly developed method for engineering band alignments at oxide interfaces, we have measured the doping evolution of the dimensionless electron-phonon interaction strength (λ) and superconducting gap in Nb-doped SrTiO₃ by high resolution tunneling spectroscopy. In the normal state, we observe evidence for strong electron-phonon coupling to the highest energy longitudinal optical (LO) phonon mode ($\lambda \sim 1$). Yet when cooled below the superconducting transition temperature (T_c), we observe a single superconducting gap corresponding to the weak-coupling limit of BCS theory, indicating an order of magnitude smaller coupling ($\lambda \sim 0.1$). This surprising result suggests the relevance of BCS beyond the Migdal limit in which it was derived, and that SrTiO₃ is an ideal system to probe superconductivity over a wide range of carrier density, adiabatic parameter, and electron-phonon coupling strength.

Future Plans

- Investigation of materials and order parameters in one dimension, by integrating soluble buffer layers with e-beam lithography of oxide heterostructures.
- Using static/dynamic strain in oxide heterostructures to manipulate and control domain structure in distorted perovskites, and their coupling to electronic/magnetic properties.
- Development of hot-electron spectroscopy in correlated electron systems using perpendicular transport in oxide heterostructures.

References

1. Z. Y. Chen, A. G. Swartz, H. Yoon, H. Inoue, T. A. Merz, D. Lu, Y. W. Xie, H. T. Yuan, Y. Hikita, S. Raghu, and H. Y. Hwang, "The Density and Disorder Tuned Superconductor-Metal Transition in Two Dimensions," submitted.
2. S. S. Hong, J. H. Yu, D. Lu, A. F. Marshall, Y. Hikita, Y. Cui, and H. Y. Hwang, "Two-Dimensional Limit of Crystalline Order in Perovskite Membrane Films," *Science Advances*, in review.
3. A. G. Swartz, H. Inoue, T. A. Merz, Y. Hikita, S. Raghu, T. P. Devereaux, S. Johnston, and H. Y. Hwang, "Strong Polaronic Behavior in a Weak Coupling Superconductor," *Proceedings of the National Academy of Sciences*, in review.

Publications

1. A. L. Fitzpatrick, S. Kachru, J. Kaplan, S. Raghu, G. Torroba, and H. Wang, "Enhanced pairing of quantum critical metals near $d=3+1$," *Physical Review B* **92**, 045118 (2015).
2. Y. Ren, H. T. Yuan, X. Y. Wu, Z. Y. Chen, Y. Iwasa, Y. Cui, H. Y. Hwang, and K. Lai,

- “Direct Imaging of Nanoscale Conductance Evolution in Ion-Gel-Gated Oxide Transistors,” *Nano Letters* **15**, 4730 (2015).
3. P. Hlobil, A. Maharaj, P. Hosur, M.C. Shapiro, I.R. Fisher, and S. Raghu, “Elastoconductivity as a probe of broken mirror symmetries,” *Physical Review B* **92**, 035148 (2015).
 4. K. O. Ruotsalainen, C. J. Sahle, T. Ritschel, J. Geck, M. Hosoda, C. Bell, Y. Hikita, H. Y. Hwang, T. T. Fister, R. A. Gordon, K. Hamalainen, M. Hakala, and S. Huotari, “Inelastic X-ray Scattering in Heterostructures: Electronic Excitations in $\text{LaAlO}_3/\text{SrTiO}_3$,” *Journal of Physics: Condensed Matter* **27**, 335501 (2015).
 5. W. Cho, C. Platt, R. H. McKenzie and S. Raghu, “Spin-triplet superconductivity in a weak-coupling Hubbard model for the quasi-one-dimensional compound $\text{Li}_{0.9}\text{Mo}_6\text{O}_{17}$,” *Physical Review B* **92**, 134514 (2015).
 6. T. Tachikawa, M. Minohara, Y. Hikita, C. Bell, and H. Y. Hwang, “Tuning Band Alignment Using Interface Dipoles at the Pt/Anatase TiO_2 Interface,” *Advanced Materials* **27**, 7458 (2015).
 7. S. Raghu, G. Torroba, and H. Wang, “Metallic quantum critical points with finite BCS couplings,” *Physical Review B* **92**, 205104 (2015) [Editor’s suggestion].
 8. H. Inoue, A. G. Swartz, N. J. Harmon, T. Tachikawa, Y. Hikita, M. E. Flatte, and H. Y. Hwang, “Origin of the Magnetoresistance in Oxide Tunnel Junctions Determined Through Electric Polarization Control of the Interface,” *Physical Review X* **5**, 041023 (2015).
 9. A. Cheung and S. Raghu, “Topological properties of ferromagnetic superconductors,” *Physical Review B* **93**, 134516 (2016).
 10. Y. Hikita, K. Nishio, L. C. Seitz, P. Chakthranont, T. Tachikawa, T. F. Jaramillo, and H. Y. Hwang, “Band Edge Engineering of Oxide Photoanodes for Photoelectrochemical Water Splitting: Integration of Subsurface Dipoles with Atomic-Scale Control,” *Advanced Energy Materials* **6**, 1502154 (2016).
 11. K. Kazunori, H. Y. Hwang, and Y. Hikita, “Thermodynamic Guiding Principles in Selective Synthesis of Strontium Iridate Ruddlesden-Popper Epitaxial Films,” *APL Materials* **4**, 036102 (2016).
 12. T. Merz, H. Noad, R. Q. Xu, H. Inoue, W. J. Liu, Y. Hikita, A. Vailionis, K. A. Moler, and H. Y. Hwang, “Depth Resolved Domain Mapping in Tetragonal SrTiO_3 by Micro-Laue Diffraction,” *Applied Physics Letters* **108**, 182901 (2016) [Editor’s Pick].
 13. F. Gunkel, C. Bell, H. Inoue, B. J. Kim, A. G. Swartz, T. A. Merz, Y. Hikita, S. Harashima, H. Sato, M. Minohara, S. Hoffmann-Eifert, R. Dittmann, and H. Y. Hwang, “Defect Control of Conventional and Anomalous Electron Transport at Complex Oxide Interfaces,” *Physical Review X* **6**, 031035 (2016).
 14. H. K. Lee, I. Barsukov, A. G. Swartz, B. Kim, L. Yang, H. Y. Hwang, and I. N. Krivorotov, “Magnetic Anisotropy, Damping, and Interfacial Spin Transport in Pt/LSMO Bilayers,” *AIP Advances* **6**, 055212 (2016).
 15. M. Mulligan and S. Raghu, “Composite fermions and the field-tuned superconductor-insulator transition,” *Physical Review B* **93**, 205116 (2016).
 16. Y. Frenkel, N. Hacham, Y. Shperber, C. Bell, Y. W. Xie, Z. Y. Chen, Y. Hikita, H. Y. Hwang, and B. Kalisky, “Anisotropic Transport at the $\text{LaAlO}_3/\text{SrTiO}_3$ Interface Explained by Microscopic Imaging of Channel-Flow over SrTiO_3 Domains,” *ACS Applied Materials & Interfaces* **8**, 12514 (2016).
 17. Z. Y. Chen, H. T. Yuan, Y. W. Xie, D. Lu, H. Inoue, Y. Hikita, C. Bell, and H. Y. Hwang, “Dual-Gate Modulation of Carrier Density and Disorder in an Oxide Two-Dimensional Electron System,” *Nano Letters* **16**, 6130 (2016).
 18. C. Platt, W. Cho, R. H. McKenzie, R. Thomale, and S. Raghu, “Spin-orbit coupling and odd-parity superconductivity in the quasi-one-dimensional compound $\text{Li}_{0.9}\text{Mo}_6\text{O}_{17}$,” *Physical*

- Review B* **93**, 214515 (2016).
19. T. Tsuyama, S. Chakraverty, S. Macke, N. Pontius, C. Schuessler-Langeheine, H. Y. Hwang, Y. Tokura, and H. Wadati, "Photoinduced Demagnetization and Insulator-to-Metal Transition in Ferromagnetic Insulating BaFeO₃ Thin Films," *Physical Review Letters* **116**, 256402 (2016).
 20. H. T. Yuan, Z. K. Liu, G. Xu, B. Zhou, S. F. Wu, D. Dumcenco, K. Yan, Y. Zhang, S.-K. Mo, P. Dudin, V. Kandyba, M. Yablonskikh, A. Barinov, Z. X. Shen, S. C. Zhang, Y. S. Huang, X. D. Xu, Z. Hussain, H. Y. Hwang, Y. Cui, and Y. L. Chen, "Evolution of the Valley Position in Bulk Transition-Metal Chalcogenides and their Mono-Layer Limit," *Nano Letters* **16**, 4738 (2016).
 21. M. Mulligan, S. Raghu, and M. P. A. Fisher, "Emergent particle-hole symmetry in the half-filled Landau level," *Physical Review B* **94**, 075101 (2016).
 22. L. C. Seitz, C. F. Dickens, K. Nishio, Y. Hikita, J. Montoya, A. Doyle, C. Kirk, A. Vojvodic, H. Y. Hwang, J. K. Nørskov, and T. F. Jaramillo, "A Highly Active and Stable IrO_x/SrIrO₃ Catalyst for the Oxygen Evolution Reaction," *Science* **353**, 1011 (2016).
 23. D. Lu, D. J. Baek, S. S. Hong, L. F. Kourkoutis, Y. Hikita, and H. Y. Hwang, "A New Synthetic Route to Freestanding Single Crystal Perovskite Films and Heterostructures," *Nature Materials* **15**, 1255 (2016).
 24. A. G. Swartz, H. Inoue, and H. Y. Hwang, "Electric Polarization Control of Magnetoresistance in Complex Oxide Heterojunctions," *Proceedings of the Society of Photo-Optical Instrumentation Engineers* **9931**, Spintronics IX, 99310G:1-14 doi:10.1117/12.2239022 (2016).
 25. D. J. Gray, T. A. Merz, Y. Hikita, H. Y. Hwang, and H. Mabuchi, "Orientation-Resolved Domain Mapping in Tetragonal SrTiO₃ Using Polarized Raman Spectroscopy," *Physical Review B* **94**, 214107 (2016).
 26. H. Noad, E. M. Spanton, K. C. Nowack, H. Inoue, M. Kim, T. A. Merz, C. Bell, Y. Hikita, R. Q. Xu, W. J. Liu, A. Vailionis, H. Y. Hwang, and K. A. Moler, "Variation in Superconducting Transition Temperature Due to Tetragonal Domains in Two-Dimensionally Doped SrTiO₃," *Physical Review B* **94**, 174516 (2016).
 27. D. J. Baek, D. Lu, Y. Hikita, H. Y. Hwang, and L. F. Kourkoutis, "Ultrathin Epitaxial Barrier Layer to Avoid Thermally Induced Phase Transformation in Oxide Heterostructures," *ACS Applied Materials & Interfaces* **9**, 54 (2017).
 28. C.-F. Zhang, Z.-K. Liu, Z.-Y. Chen, Y. W. Xie, R.-H. He, S.-J. Tang, J.-F. He, W. Li, T. Jia, S. N. Rebec, E. Y. Ma, H. Yan, M. Hashimoto, D.-H. Lu, S.-K. Mo, Y. Hikita, R. G. Moore, H. Y. Hwang, D.-H. Lee, and Z.-X. Shen, "Ubiquitous Strong Electron Phonon Coupling at the Interface of FeSe/SrTiO₃," *Nature Communications* **8**, 14468 (2017).
 29. H. Wang, S. Raghu, and G. Torroba, "Non-Fermi Liquid Superconductivity: Eliashberg versus the Renormalization Group," *Physical Review B* **95**, 165137 (2017).
 30. X. Liu, J.-H. Kang, H. T. Yuan, J.-H. Park, S. J. Kim, Y. Cui, H. Y. Hwang, and M. L. Brongersma, "Electrical Tuning of a Quantum Plasmonic Resonance," *Nature Nanotechnology* DOI:10.1038/nano.2017.103 (2017).
 31. Y. Frenkel, N. Haham, Y. Shperber, C. Bell, Y. W. Xie, Z. Y. Chen, Y. Hikita, H. Y. Hwang, E. K. H. Salje, and B. Kalisky, "Imaging and Tuning Polarity at SrTiO₃ Domain Walls," *Nature Materials*, in press.
 32. M. Minohara, Y. Hikita, C. Bell, H. Inoue, M. Hosoda, H. K. Sato, H. Kumigashira, M. Oshima, E. Ikenaga, and H. Y. Hwang, "Dielectric Collapse at the LaAlO₃/SrTiO₃ (001) Heterointerface Under Applied Electric Field," *Scientific Reports*, in press.
 33. T. Tachikawa, H. Y. Hwang, and Y. Hikita, "Enhancing the Barrier Height in Oxide Schottky Junctions Using Polar AgTaO₃," *Applied Physics Letters*, in press.

Program Title: Novel Synthesis of Quantum Epitaxial Heterostructures by Design

Principle Investigator: Chang-Beom Eom

Mailing Address: Room 2166 ECB, 1550 Engineering Drive, University of Wisconsin-Madison, Madison, WI 53706

E-mail: eom@engr.wisc.edu

Program Scope

Quantum materials such as topological insulators, interfacial 2D electron gas (2DEG), novel superconductors and multiferroics have been fertile ground for new discoveries, due particularly to the delicate balance between charge, spin, orbital, and lattice ordered states tuned by external parameters. Such materials can exhibit exciting emergent phenomena whose description requires new quantum mechanical models to be developed and experimentally validated. Atomic level controlled synthesis is critical for all experimental studies.

Epitaxial thin films of quantum materials are advantageous both for study of fundamental science and for development of new applications. These films can be of comparable or higher quality than available bulk single crystals, but more importantly deposition conditions can be maintained far from equilibrium, so that metastable phases (nonexistent in nature) can be obtained by epitaxial stabilization. Furthermore, growth of artificially layered superlattices, and control of film crystallographic orientation probe fundamental intrinsic properties of quantum materials such as dimensionality, anisotropy, and electronic correlations.

This program focuses on the novel synthesis of epitaxial heterostructures by controlling point defects, strain, and interfaces at the atomic level to understand the relationship between structure and emergent quantum phenomena, and to design and create unique quantum materials tuned to take advantage of the properties only possible in this unique epitaxial heterostructures. The **thrusters** of our proposed work are:

(1) *Development of Novel Synthesis Route for Epitaxial Thin Film Heterostructures with Controlled Point Defects.*

Modern quantum materials are very sensitive to defects, and require a new synthesis route to produce high-quality epitaxial oxide thin films and interfaces. We are developing a chemical pulsed laser deposition (CPLD) growth process that promises dramatically lower concentration of *point defects*. The higher quality epitaxial films and heterostructures remove several roadblocks that have limited the development of new science using quantum materials.

(2) *Coupled bilayers of oxide interfacial electron and hole gases*

The 2DEG at oxide heterointerfaces has resulted in several important discoveries, however the equivalent *hole* gas has been elusive, primarily due to the presence of point defects and other impurities. Coexistence of both 2DEG and 2D hole gas (2DHG) in a single heterostructure allows a new quantum material based on interaction of the hole and electron gas over only a few unit cells, leading to new functionalities and emergent phenomena.

(3) *Strain- and Interface engineered Superconducting Heterostructures*

Quantum materials supporting interfacial superconductivity are delicately sensitive to point defects. Our new synthesis routes now allow exploration of strain- interface- and electric-field dependent superconducting properties, such as the interaction of monolayer FeSe with strain- and interface engineered SrTiO₃ films, the control of T_c by lattice distortion in strain-engineered pnictides thin films.

Recent Progress

1. Two-Dimensional Hole Gas at Oxide Interfaces

The discovery of two-dimensional electron gas (2DEG) at the $\text{LaAlO}_3/\text{SrTiO}_3$ interface has revealed a plethora of new properties not present in conventional semiconductor heterostructures, becoming a focal point of novel device applications. Its counterpart, two-dimensional hole gas (2DHG), has long been expected to complement 2DEG and provide versatile functionalities. However, while 2DEG has been widely observed, the 2DHG has been elusive. We demonstrate a highly-mobile 2DHG in epitaxially-grown $\text{SrTiO}_3/\text{LaAlO}_3/\text{SrTiO}_3$ heterostructures. Using electrical transport measurements and in-line electron holography charge density mapping, we provide direct evidence of 2DHG coexisting with 2DEG at complementary heterointerfaces in the same structure. First-principles calculations, coherent Bragg rod analysis, and depth-resolved cathodoluminescence spectroscopy consistently support our finding that eliminating ionic point-defects is key to realize 2DHG. The coexistence of 2DEG and 2DHG in a single oxide heterostructure provides a platform for exciting new physics of confined electron-hole systems and for developing novel applications.

We choose (001) $\text{SrTiO}_3/\text{LaAlO}_3/\text{SrTiO}_3$ (STO/LAO/STO) heterostructures to realize the 2DHG. If the STO substrate is TiO_2 -terminated, *p*-type and *n*-type interfaces are expected to form at the top and the bottom of the STO/LAO/STO heterostructure, respectively, to avoid the polar catastrophe. The polar discontinuity may, however, be also resolved by the accumulation of positively-charged oxygen vacancies at the top interface. This is evident from our first-principles calculations indicating the absence of 2DHG when oxygen vacancies are formed in STO or LAO close to the top interface. This implies that, even though one can fabricate a high-quality *p*-type interface, the interface may still be electrically insulating due to the ionized oxygen vacancies. Therefore, we focus on (1) building an atomically-sharp *p*-type interface consisting of SrO/AlO_2 layers, and (2) minimizing oxygen vacancies near the *p*-type interface.

We synthesized STO/LAO thin films by pulsed laser deposition with *in-situ* RHEED on TiO_2 -terminated (001) STO substrates, with the substrate interface designed to host the 2DEG, and the top STO/LAO interface to host the 2DHG. To minimize the oxygen vacancy formation, oxygen partial pressure in the chamber was kept high during the growth. The samples were also *in-situ* post annealed in oxygen ambient. The magnified atomic structure (Fig. 1a) indicates that a high-quality SrO/AlO_2 interface has been built between the top STO and LAO thin films. The Atomic-scale energy dispersive X-ray spectroscopy (EDS) elemental maps show the chemically-abrupt top interface (Fig. 1b). The electron density map determined by synchrotron X-ray surface diffraction-based coherent Bragg rod analysis (COBRA) across the interface shows that the top interface consists of SrO and AlO_2 layers as we designed (Fig. 1c).

We examined the electrical transport properties of the top and the bottom interfaces in the STO/LAO/STO heterostructure. The magnetic field-dependent Hall resistance R_{xy} (H) measured

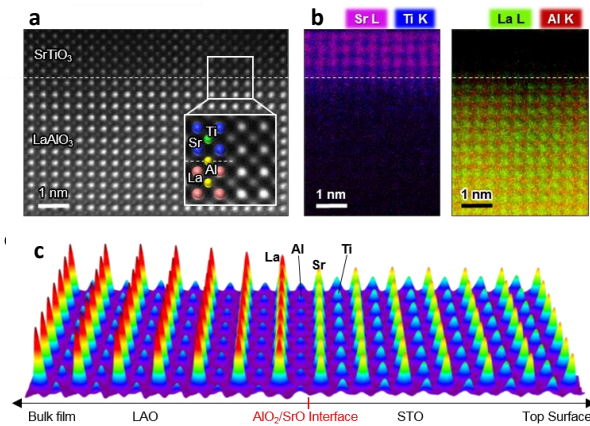


Figure 1. **a**, STEM images obtained at the top STO/LAO interface. **b**, EDS elemental mapping. **c**, COBRA-derived cation electron density map across the interface.

at the top interface clearly shows a positive Hall coefficient, while the bottom interface shows negative. It is notable that the mobility of 2DHG is comparable and even slightly higher than the mobility of 2DEG at low temperature. The electrons are known to be strongly coupled to phonons in the LAO/STO system forming large polarons. As the result, the effective electron mass renormalizes to a larger value of $2.5 m_0$. On the contrary, holes are weakly coupled to phonons, which is evident from the calculated electron-phonon coupling matrix element for the valence band maximum being seven times smaller than that at the conduction band minimum. Hence, considering the electron-phonon coupling, it is likely that the effective mass of holes is comparable or even smaller than the effective mass of electrons. This qualitatively explains the relatively large hole mobility being comparable to the electron mobility.

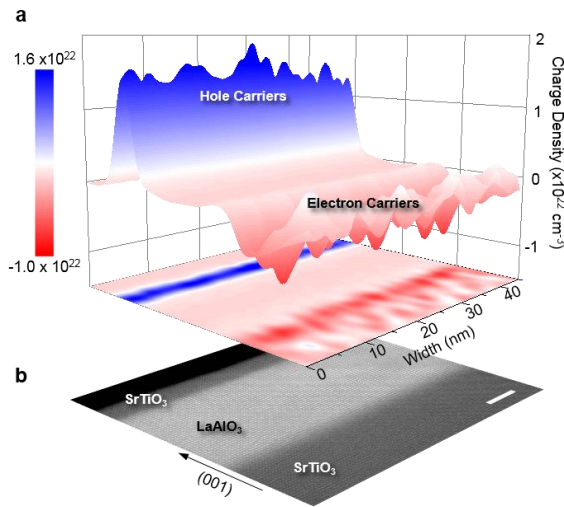


Figure 2. a, The charge density map obtained by the in-line electron holography technique. b, The STEM-ADF image of the entire STO/LAO/STO heterostructure.

Using in-line electron holography, we directly demonstrate that the 2DHG is formed at the STO/LAO interface. The in-line electron holography, using a field-emission TEM, can map the internal charge distribution by retrieving phase shift information of the transmitted electron beam. A high density of positive charges is clearly observed at the top interface, while the bottom interface showed negative charges.

The presence of holes at the top interface can be more strongly supported by verifying the lack of oxygen vacancy near the interface. To obtain more detailed information about the oxygen vacancy distribution, we performed depth-resolved cathodoluminescence spectroscopy analyses. The top STO exhibited a considerably small sign of oxygen vacancy,

which is even smaller than that of bulk STO substrate. All these structural studies unambiguously show that the 2DHG was realized in oxide heterostructures containing minimal oxygen vacancy.

The coexistence of 2DEG and 2DHG in a single oxide heterostructure enables exploration of the exciting new physics of confined electron-hole systems, including long-lifetime bilayer excitons, Coulomb drag with spin-orbit coupling, bilayer electron-hole superconductivity, and Bose-Einstein condensation of excitons.

Future Plans

(1) Strain control of superconductivity in BaFe₂As₂ Pnictide thin film heterostructures

Control of the detailed atomic configurations in Fe-based superconductors is crucial for understanding the fundamental mechanisms of its unconventional superconductivity. For instance, structural distortion from an ideal Fe-As tetrahedron is believed to be related to the superconducting transition temperature, and can play a role in explaining the high- T_c superconductivity in Fe-based materials. Biaxial strain is a much more natural way to tune the tetrahedral geometry, accomplished in a thin-film geometry by different lattice constant substrates rather than by hydrostatic pressure in bulk system. In-plane strain in thin films can be controlled by substrates, which provide the excellent platform for tuning the wide range of thermal and lattice mismatch between thin films and the substrates. We plan to modify superconductivity in high quality epitaxial doped and undoped BaFe₂As₂ pnictide thin films heterostructures by in-plane

strain induced by substrates, tuning the As-Fe-As bond angle for understanding the macroscopic quantum phenomena of pnictide superconductors. This approach enables tuning the bond angle in a single material platform. Our approach is based on biaxial strain of single crystal films controlled by various substrates with different lattice and thermal expansion mismatch.

(2) *Suppression of the charge density wave in BaBiO₃/BaPbO₃ bilayers and superlattices*

We will grow BaBiO₃ and BaPbO₃ bilayers and heterostructures to investigate the possibility of engineering high T_c superconducting structures. Bulk BaBiO₃ has a charge density wave that opens a semiconducting bandgap and exists for Bi concentrations of ~35% and higher. By growing ~4 nm BaBiO₃ the charge density wave is suppressed in single layers. We hope to utilize thin BaBiO₃ layers to suppress the charge density wave, separated by BaPbO₃ conducting layers, engineering a new quantum material through superlattice heteroepitaxy. In order to limit chemical intermixing, smooth surfaces are required, which we can achieve on LaLuO₃. If the charge density wave is a competing phase that limits T_c in bulk BPBO, this artificial suppression may enable doping to higher levels. The first superlattices have been grown and preliminary results show a cubic-like structure and superconductivity. Raman spectroscopy, terahertz spectroscopy, and synchrotron diffraction will be used to characterize the charge density wave and octahedral tilting of these superlattices as a function of temperature to explore structure-property relationships in artificial bismuthates.

Publications (which acknowledge DOE support)

1. “Polar Metals by Geometric Design”, T. H. Kim, D. Puggioni, Y. Yuan, L. Xie, H. Zhou, N. Campbell, P. J. Ryan, Y. Choi, J.-W. Kim, J. R. Patzner, S. Ryu, J. P. Podkaminer, J. Irwin, Y. Ma, C. J. Fennie, M. S. Rzchowski, X. Q. Pan, V. Gopalan, J. M. Rondinelli, and C. B. Eom, *Nature*, **533**, 68 (2016)
2. “Imprint Control of BaTiO₃ Thin films *via* Chemically-induced Surface Polarization Pinning”, H. Lee, T. H. Kim, J. J. Patzner, H. Lu, J. W. Lee, H. Zhou, W. Chang, M. K. Mahanthappa, E. Y. Tsymbal, A. Gruverman, and C. B. Eom, *Nano Letters*, **16**, 2400 (2016)
3. “Tailoring LaAlO₃/SrTiO₃ interface metallicity by oxygen surface adsorbates”, Weitao Dai, Sanjay Adhikari, Andrés Camilo Garcia-Castro, Aldo H. Romero, Hyungwoo Lee, Sangwoo Ryu, Chang Beom Eom, Cheng Cen, *Nano Letters* **16**, 2739 (2016)
4. “Tunable electron-electron interactions in LaAlO₃/SrTiO₃ nanostructures” Guanglei Cheng, Michelle Tomczyk, Alexandre B. Tacla, Hyungwoo Lee, Shicheng Lu, Josh P. Veazey, Mengchen Huang, Patrick Irvin, Sangwoo Ryu, Chang-Beom Eom, Andrew Daley, David Pekker, Jeremy Levy, *Phys. Rev. X* **6**, 041042 (2016)
5. “Localized GHz frequency electrodynamic behavior of an optimally-doped Ba(Fe_{1-x}Co_x)₂As₂ epitaxial film” Tamin Tai, Behnood G. Ghamsari, J.H. Kang, S. Lee, C.B. Eom, Steven M. Anlage, *Physica C: Superconductivity and its Applications*, **532**, 44, (2017)
6. “Origin of the emergence of higher T_c than bulk in iron chalcogenide thin films” Sehun Seo, Jong-Hoon Kang, Myeong Jun Oh, Il-Seok Jeong, Jianyi Jiang, Genda Gu, Jung-Woo Lee, Jongmin Lee, Heesung Noh, Eric Hellstrom, Joo-Hyoung Lee, Y. J. Jo, Chang-Beom Eom, and Sanghan Lee, *submitted to Scientific Reports* (2017) (under revision)
7. “Two-Dimensional Hole Gas at Oxide Interfaces”, H. Lee, N. Campbell, J. Lee, T. J. Asel, T. R. Paudel, H. Zhou, J. W. Lee, B. Noesges, L. J. Brillson, S. H. Oh, E. Y. Tsymbal, M. S. Rzchowski, and C. B. Eom, *submitted to Nature Materials*, (2017) (under revision)
8. “Shubnikov-de Haas-Like Quantum Oscillations in Artificial One-Dimensional LaAlO₃/SrTiO₃ Electron Channels”, Guanglei Cheng, Anil Annadi, Shicheng Lu, Hyungwoo Lee, Jung-Woo Lee, Mengchen Huang, Chang-Beom Eom, Patrick Irvin, Jeremy Levy, *submitted to Phys. Rev. Letts.* (2017)

The Investigation of Oxygen Vacancies in Magnetic-Ferroelectric Heterostructures

Mikel Holcomb, Department of Physics & Astronomy, West Virginia University

Co-PI: Aldo Romero, Department of Physics & Astronomy, West Virginia University

Program Scope

Oxygen vacancies play a significant, yet not always well understood, role in many complex oxide systems.^{1,2} The research goal of this work is to understand how oxygen vacancies affect magnetization and magnetoelectric coupling in $\text{La}_x\text{Sr}_{1-x}\text{MnO}_3$ and $\text{La}_x\text{Sr}_{1-x}\text{MnO}_3/\text{BaTiO}_3$ model heterostructures with a collaborative experimental and theoretical approach. Electrical control of this magnetic material is actually not surprising if we also observe that pure SrMnO_3 was theoretically predicted,³ and later experimentally corroborated,⁴ to be, by itself, one of the few single-phase multiferroic materials when a small strain is applied. Similar systems, including those Holcomb has studied, are well known to produce magnetoelectric coupling.^{5,6} Even though, experimentally, it has been found that oxygen content can have a significant effect on LSMO properties,^{7,8} there is not a great deal of experimental comparison between the theoretically obtained electronic properties of LSMO and the oxygen concentration. The proposed objectives of the project are to: 1) develop and characterize high-quality heterostructures for controlling oxygen vacancies and study the effects on epitaxial bulk and interface properties, 2) analyze depth-dependent measurement of oxygen vacancies, atomic valence, magnetization, structure, and stoichiometry and their relation to magnetization and magnetoelectric coupling, and 3) develop electronic, magnetic and structural calculations to help interpret the experimental findings.

Recent Progress

High quality thin films have been grown by pulsed laser deposition, and optimized through in-situ reflection high energy electron diffraction, as well as x-ray diffraction and atomic force microscopy (objective 1). Many bulk and depth dependent properties (magnetization, valence, lattice parameters, etc.) of the LSMO thin films and their relation to magnetization have been explored both experimentally and theoretically for a variety of sample thicknesses (objectives 2 & 3). For

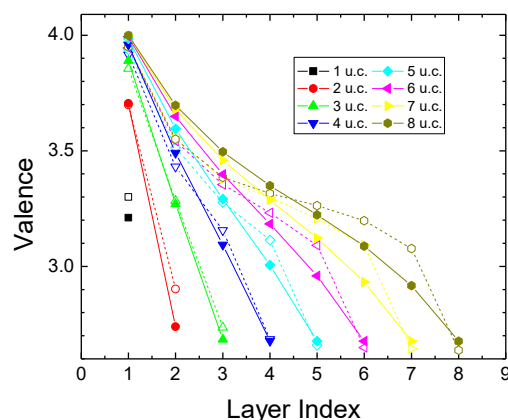


Fig 1. Comparison of plane-resolved Mn valence for the best fit (solid points) and theory (open points). The surface is at layer 1.

example, polarized neutron reflectivity measurements at NIST have allowed depth-dependent magnetization on a few optimized and oxygen deficient films in order to identify signatures from oxygen vacancies. The theoretical models are currently limited to the LSMO/substrate layers, but accuracy on these models is important before the ferroelectric layer is added.

Even without a ferroelectric layer, we see a significant change in the Mn atomic valence (Figure 1) across the depth of our thin films. Some of this can be explained by the fact that LSMO/STO is a polar interface. We believe this polar interface is attracting the oxygen vacancies, which has been supported by theoretical calculations that only match our depth dependent valence when oxygen vacancies are present at the interface.

We began our computational efforts by defining the methods and approximations. Since one of the most important characteristics of the LSMO system is that it is an alloy, we cannot rely on a supercell approach to describe its properties. The physics due to the ordering of a supercell may be very different than that of an alloy, where the A-site cation placement is random. Due to this potential difference from the A-site placement, we have decided to use the Virtual Crystal approximation (VCA), where an alloyed atom is replaced by a pseudo atom which is a relative alloy combination of the atomic information of the alloying (lanthanum and strontium). We have tested this approximation by predicting the ground state geometry, the octahedral tilting value, the Mn

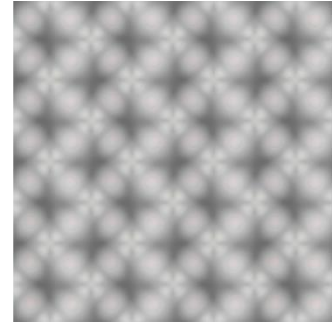


Fig 2. Theoretical simulation of STM microscopy of STO/LSMO when there is no oxidation at the surface. The theoretical thin-film contains four layers of LSMO on top of 6 STO layers.

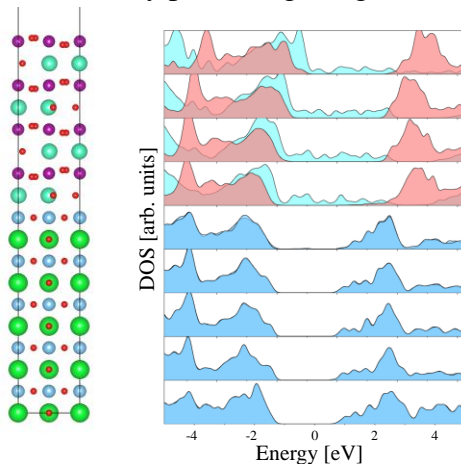


Fig 3. Spin dependent layer-by-layer electronic density of states for four layers of LSMO on top of STO. Each panel corresponds to a layer of either STO (five bottom panels) or LSMO (top four panels). We have found that in LSMO one of the spins have metallic behavior while the other have insulator behavior.

magnetic moment and the electron band gap. In general, we get good agreement with existing results. Our next goal was to describe the actual experiment, where a LSMO thin film is deposited on top of an SrTiO₃ (STO) substrate. Here we have decided to use three different approaches: (i) we have assumed that the LSMO will grow following exactly the STO structure (ii) the LSMO will follow the STO structure for few layers and then it will relax to the PNMA ground state (iii) the LSMO will remain in its own ground state by tries to match the STO cell parameters. We have concluded our analysis of (iii) and we are in the process of finishing (i) and (ii). For every one of those cases we have studied the thickness dependence of the electronic and magnetic properties of

STO/(LSMO) $_m$ with values of m equal to 2, 4 and 8 unit cells. We have found that LSMO's lowest energy configuration is Pnma when it is under the STO strain. However, we have also found that the energy difference between the cubic structure and the Pnma is only 0.8meV/atom for 2 layers of LSMO, which raises the possibility that the LSMO is cubic ferromagnetic, at least during the first growth layers, as it has been claimed experimentally. We have also found that the monotonic decay dependence of the valence charge of manganese will follow the experimental measurements only when we consider that the LSMO surface is fully oxidized and all oxygen octahedrals are well terminated. Additionally, the theoretical values get closer to experiment when vacancies are introduced in LSMO. Energetics also indicate that the energy difference between a vacancy at the interface and in the following LSMO layer is smaller than room temperature, which indicates that there is not an energetic preference in having the vacancy in any of these layers.

Future Plans

As proposed, in Year 2 our experimental plan is to focus on the ferroelectric poling of these samples and the effect of this poling on the bulk and depth-dependent sample properties (valence, magnetization, structure, oxygen vacancy concentration, ME coupling).

The theoretical effort in Year 2 will continue optimizing the model for better consistency with our depth dependent structure, valence and magnetization measurements. Our current models vary given the crystal structure. For example, the experimental out of plane lattice parameter varies across the thickness of the film; thus the model needs to be adjusted to account for this change as well if accurate results are to be expected.

Ab-initio calculations will continue with the aim to support experimental measures. At this moment, we have learned the process for the appropriate use of the theoretical tools implemented in the QE package with VCA as well as the way to extract the necessary information to feedback with the experimental part of this project. We will also use the Green's function method (KKR method) to find the alloy magnetic exchange couplings. We will explore a bit more the possibility that LSMO remain cubic after more than 2-layers. This will allow us to relate the role of octahedral rotations in the charge transfer that has been observed experimentally. We will also continue our calculations with oxygen vacancies by varying its location and vacancy density. We will calculate specific electronic properties as the Bader charges, band structure, electronic density of states to identify where changes are manifested. In addition to the papers listed below, we plan to submit a paper on the depth-dependent magnetization and oxygen vacancy concentration measured by polarized neutron reflectivity and supported by bulk vibrating sample magnetometry on other samples. Additionally, we will measure and develop depth-dependent models based on x-ray dichroism, which can measure these samples more quickly and potentially with better resolution than current neutron measurements allow.

References

1. Pacchioni G, "Oxygen Vacancy: The Invisible Agent on Oxide Surfaces," *Chem Phys Chem* **4**, 1041 (2003).
2. Jeen H, Choi WS, Biegalski MD, Folkman CM, Tung IC, Fong DD, Freeland JW, Shin D, Ohta H, Chisholm MF, and Lee HN, "Reversible Redox Reactions in an Epitaxially Stabilized SrCoO_x Oxygen Sponge," *Nature Materials* **12**, 1057 (2013).
3. Lee JH and Rabe KM, "Epitaxial-Strain-Induced Multiferroicity in SrMnO₃ from First Principles," *Phys. Rev. Lett.* **104**, 207204 (2010).
4. Becher C, Maurel L, Aschauer U, Lilienblum M, Magén C, Meier D, Langenberg E, Trassin M, Blasco J, Krug IP, Algarabel PA, Spaldin NA, Pardo JA and Fiebig M, "Strain-induced Coupling of Electrical Polarization and Structural Defects in SrMnO₃ Films," *Nature Nanotechnology* **10**, 661–665 (2015).
5. Zhou J, Tra VT, Dong S, Trappen R, Marcus MA, Jenkins CA, Wolfe E, Frye C, Polisetty S, Lin J-L, Chu Y-H and Holcomb MB, "Thickness Dependence of La_{0.7}Sr_{0.3}MnO₃/PbZr_{0.2}Ti_{0.8}O₃ Magnetoelectric Interfaces," *Applied Physics Letters* **107**, 141603 (2015).
6. Huang C-Y, Zhou J, Tra VT, White R, Trappen R, N'Diaye AT, Spencer M, Frye C, Cabrera GB, Nguyen V, LeBeau JM, Chu Y-H, Holcomb MB, "Imaging Magnetic and Ferroelectric Domains and Interfacial Spin in Magnetoelectric La_{0.7}Sr_{0.3}MnO₃/PbZr_{0.2}Ti_{0.8}O₃ Heterostructures," *J. Phys.: Condens. Matt.* **27**, 504003 (2015).
7. De León-Guevara AM, Berthet P, Berthon J, Millot F, Revcolevschi A, Anane A, Dupas C, Le Dang K, Renard JP and Veillet P, "Influence of Controlled Oxygen Vacancies on the Magnetotransport and Magnetostructural Phenomena in La_{0.85}Sr_{0.15}MnO_{3-δ} Single Crystals," *Phys. Rev. B* **56**, 6031 (1997).
8. Wilson ML, Byers JM, Dorsey PC, Horwitz JS, Chrisley DB and Osofsky MS, "Effects of Defects on Magnetoresistivity in La_{0.7}Sr_{0.3}MnO₃," *J. Appl. Phys.* **81**, 4971 (1997).

Publications

Robbyn Trappen, Wilfredo Ibarra-Hernandez, Vu Thanh Tra, Chih-Yeh Huang, Sobhit Sing, Jinling Zhou, Guerau Cabrera, Andrés Camilo, Garcia-Castro, Ying-Hao Chu, Shuai Dong, Aldo Romero and Mikel B. Holcomb, Thickness dependent Mn valence in La_{0.7}Sr_{0.3}MnO₃ thin films, (in draft) Planned submission to *NanoLetters*, ~September

Navid Mottaghi, Shalini Kumari, Robbyn Trappen, Saeed Yousefi Sarrah, Chih-Yeh Huang, Guerau Cabrera, Mohindar Seehra, Mikel Holcomb, Insights into magnetic dead layer in La_{0.7}Sr_{0.3}MnO₃ thin films from temperature, magnetic field and thickness dependence of their magnetization, (in draft) Planned submission to MMM Proceedings, September

Robbyn Trappen, Jinling Zhou, Vu Thanh Tra, Chih-Yeh Huang, Matthew A. Marcus, Shalini Kumari, Shuai Dong, Ying-Hao Chu and Mikel B. Holcomb, Depth dependent atomic valence determination by synchrotron techniques, (in draft) Planned submission to *Journal of Synchrotron Radiation*, ~November

Project Title: Novel Regimes of Spin Transport: Pure Spin Currents in Antiferromagnets and Time-Resolved Studies of Spin Dynamics

Principle Investigator: Fengyuan Yang; **Co-PI:** Ezekiel Johnston-Halperin

Mailing Address: Department of Physics, The Ohio State University, Columbus, OH 43210

Email: fyyang@physics.osu.edu

Project Scope:

The goal of this DOE project is to investigate the dynamic spin transport behavior in magnetic heterostructures including ferro-/ferri-magnetic (FM) and antiferromagnetic (AF) insulators and understand the magnetic excitations responsible for spin conduction. The generation, manipulation, and detection of spin currents have been the central focus of spintronics for over two decades. In recent years, pure spin currents driven by ferromagnetic resonance (FMR) spin pumping or a thermal gradient have attracted intense interest and become one of the most active frontiers in condensed matter physics. In both of these regimes a dynamic excitation of the magnetization results in the transfer of spin angular momentum in the absence of net charge flow, a long-sought goal for the field. Extensive research efforts over the last few years have demonstrated pure spin currents in a broad range of materials, including nonmagnetic (NM) metals and semiconductors, FM and AF metals and insulators. These developments have significantly advanced our understanding of dynamically-driven spin transport in heterostructures, offering new paradigms for energy-efficient, spin-based information processing, data storage and sensing applications.

Pure spin currents can be carried by either the spin degree of freedom of charge carriers or magnetic excitations in both FMs and AFs, opening entirely new classes of materials for exploration. Most interestingly, AF insulators, which have been largely absent in charge-based spin transport, become a desirable choice of materials for pure spin transport due to their intrinsically high resonance frequencies (THz), low magnetic damping, and high efficiency of spin conversion at interfaces. In addition, the inherently dynamic nature of this process drives the need for a comprehensive understanding of the dynamic interplay between spin, charge and magnetic excitations in FM, AF, and NM heterostructures. Ultrafast optical pump-probe techniques provide an ideal platform for pursuing these investigations. We have demonstrated highly efficient and long-preserving spin transport in AF insulators excited by spin pumping using high quality $\text{Y}_3\text{Fe}_5\text{O}_{12}$ (YIG) films. Building on our expertise in microwave to terahertz spin dynamics, we are carrying out collaborative research project to: (1) investigate dynamically generated pure spin currents in AF insulators excited by FMR and thermally driven spin pumping in YIG/AF/Pt trilayers to reveal mechanisms of spin transfer in AF insulators and across interfaces, and (2) study the dynamics and coupling of non-equilibrium spin excitations in heterostructures of FMs, AFs, semiconductors, and NM metals using ultra-fast optical excitation to probe the magnetic dynamics and pure spin currents in the time domain. Below, we describe the recent progress of this project.

Recent Progress

1. FMR and thermally driven spin transport through an antiferromagnetic NiO layer

We studied thermally driven longitudinal spin Seebeck effect (LSSE) through an AF layer using our Pt(6 nm)/NiO(t_{NiO})/YIG(250 nm) trilayers, where the NiO thickness was varied between 0 and 10 nm (in collaboration with Prof. Joseph Heremans at Ohio State). A thermal gradient generates ferromagnetic magnons in the YIG layer. At the YIG/NiO interface, the YIG magnons excite antiferromagnetic magnons in the NiO spacer. Then at the NiO/Pt interface, the AF magnons produce spin-polarized electrons and a spin current in Pt, which was converted to

an inverse spin Hall effect (ISHE) voltage in Pt for detection. Figure 1(a) shows the temperature dependence of the spin Seebeck coefficient S_y (V_{ISHE} normalized by temperature gradient) between 50 and 420 K for five samples with NiO thicknesses of 0, 1, 2, 5, and 10 nm. The temperature dependence of LSSE shows a maximum at a temperature T_M that decreases monotonically with the NiO thickness. Using the data in Fig. 1(a), we determine that the LSSE signal decays exponentially with increasing NiO thickness at all temperatures, from which we extract the attenuation length between 2.0 and 5.5 nm within the temperature range of 180 and 420 K with the maximum attenuation length observed at 360 K. This implies that NiO is most

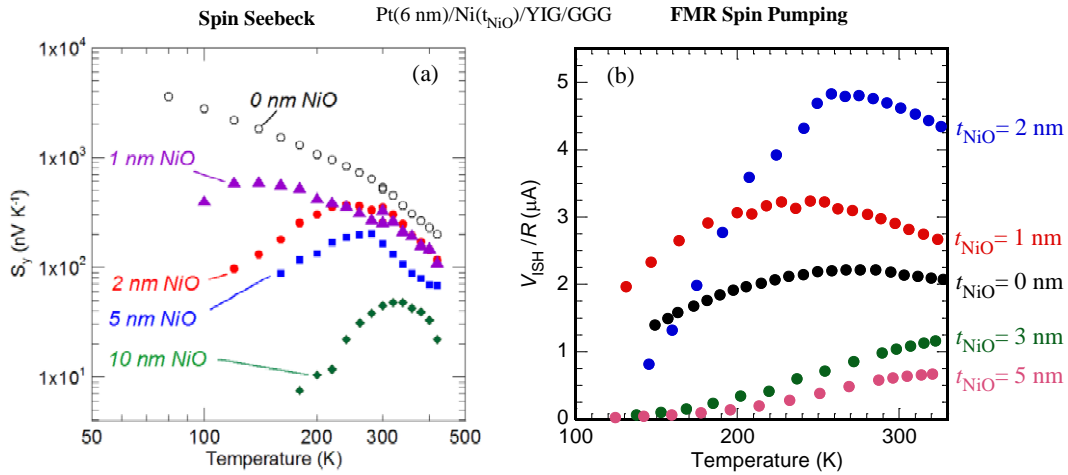


Fig. 1. (a) Temperature dependence of (a) the LSSE and (b) normalized FMR-driven spin pumping signals on the Pt(6 nm)/Ni(t_{NiO})/YIG trilayers. A maximum at a temperature T_M is observed for the YIG/NiO/Pt trilayers, which increases with increasing NiO thickness. (For the spin pumping data of the 3 and 5 nm NiO samples, the peak temperatures are above the upper limit of the instrument).

transparent to magnon propagation near the paramagnet-antiferromagnet transition. This work was published in Physical Review B in July 2016 [1].

We also carried out FMR driven spin pumping measurements using a variable-temperature cavity on Pt(6 nm)/NiO(t_{NiO})/YIG(20 nm) trilayers with t_{NiO} between 1 and 5 nm. Figure 1(b) shows the temperature dependence of ISHE voltage normalized by sample resistance for this series between 120 and 330 K. We observe enhancement of the spin pumping signals for the samples with $t_{\text{NiO}} = 1$ and 2 nm in comparison to the Pt/YIG bilayer ($t_{\text{NiO}} = 0$ nm). For the $t_{\text{NiO}} = 1$ and 2 nm samples, a peak in V_{ISHE}/R at 230 and 260 K, respectively is seen, corresponding to the paramagnet-antiferromagnet transition, similar to the LSSE results in Fig. 1(a). The difference in the transition temperatures between LSSE and spin pumping results may be due to the difference in the frequencies of magnon excitations responsible for the spin currents. The shifting of the peak to higher temperatures for thicker NiO layers agrees with a decrease in the expected suppression of the AF transition temperature in thinner AF films. We did not observe the peak for the 3 and 5 nm samples, which we suspect is due to that their peaks are above the instrument's available temperature regime.

2. Picosecond spin Seebeck effect in normal-metal/YIG bilayers

Through collaboration with Prof. David Cahill at the University of Illinois at Urbana Champaign, we studied the longitudinal spin Seebeck effect in Au/YIG and Cu/YIG bilayer systems using the time-resolved magneto-optic Kerr effect (TR-MOKE) technique which provides sub-picosecond (ps) time resolution. The ps time resolution is orders of magnitude faster than previous ISHE detection of LSSE in NM/FM systems. In addition, the ultrafast

optical pump-probe measurement is a clean technique that is not susceptible to some spurious effects associated with electrical detection of LSSE. The ps time scale of the excitation laser

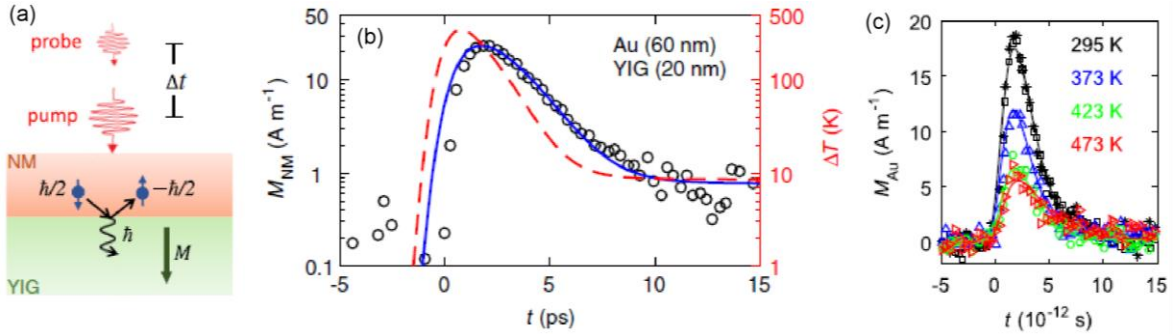


Fig. 2. (a) Schematic diagram of absorption of a picosecond pump laser pulse generates a temperature difference between NM electrons and YIG magnons. Interfacial coupling between electrons and magnons induces spin accumulation in NM, which is probed by time-delayed probe laser pulses. (b) TR-MOKE data for Au/YIG/GGG sample, probing thermally induced spin accumulation in Au. Solid lines show fit curves obtained using the spin diffusion model, and dashed lines show temperature excursion of electrons. (c) TR-MOKE measurement measured on a Au/YIG sample at different temperatures. Solid lines show fit curves obtained using the spin

pulses generate sizable temperature differences of the order of 10 to 100 K across the Au/YIG and Cu/YIG interfaces, which allow us to selectively probe the interfacial LSSE.

Figure 2(a) schematically shows the experimental setup of the TR-MOKE measurements on NM/YIG bilayers. During the pump-probe measurements, a magnetic field of ~ 0.4 T is applied perpendicular to the film plane, which rotates the YIG magnetization out of plane. If a significant amount of spin accumulation is generated in the Au or Cu layer due to the spin Seebeck effect, the resulting non-equilibrium magnetization rotates the polarization of probe light upon reflection. We detect this polar Kerr effect with a train of sub-ps optical pulses at the same repetition rate of 80 MHz as the pump light with variable time delay. Figure 2(b) shows the TR-MOKE results for an Au(60 nm)/YIG(20 nm) sample, which measure thermally-induced spin accumulation in the Au layer. The measured time evolution of spin accumulation induced by laser excitation indicates transfer of angular momentum across the normal metal/YIG interfaces on a ps time scale, too short for contributions from a bulk temperature gradient in YIG. By fitting the TR-MOKE data to the spin diffusion model, we obtain the spin relaxation time (τ_s) of 0.8 to 1.7 ps for Au on YIG and 3.7 ps for Cu on YIG. The fitting also gives a parameter α , which is a product of spin mixing conductance and spin Seebeck coefficient, between $3 \times 10^7 \text{ Am}^{-2} \text{ K}^{-1}$ and $3 \times 10^8 \text{ Am}^{-2} \text{ K}^{-1}$ for Au/YIG and Cu/YIG interfaces. Using temperature-dependent measurements, we find that the fit parameter α decreases monotonically with temperature and vanishes approximately at the Curie temperature of YIG. Our measurements indicate that the LSSE is active at the picosecond time scale. This work was published in Physical Review Letters in January 2017 [2].

Future Plans

We are currently working on variable temperature (10 – 300 K) FMR spin pumping studies of YIG/AF/NM systems with various AF materials of both polycrystalline and epitaxial films in a microwave cavity at ~ 9.65 GHz in collaboration with Prof. P. Chris Hammel at Ohio State. The AF insulators under investigation include NiO, CoO, and MnO. This will reveal the interesting phenomena and underlying mechanisms responsible for spin transport in Pt/AF/YIG trilayers with different AF materials and at various AF layer thicknesses, allowing for systematic understanding of magnonic spin transport in AF insulators. Given by our results in longitudinal

spin Seebeck measurements of spin transport in Pt/NiO/YIG trilayers as shown above, we will investigate thermally driven spin transport in Pt/AF/YIG trilayers within a broad range of temperatures and sample structures.

Following our published work on picosecond spin Seebeck effect in NM/YIG bilayers, we will continue our study of ultrafast spin transport and magnetization dynamics in oxide and metallic systems, including heterostructures with AF insulator layers and other nonmagnetic metals. All of these research activities are fully supported by DOE.

References:

- [1]. A. Prakash, J. Brangham, F. Y. Yang, and J. P. Heremans, “Spin Seebeck effect through antiferromagnetic NiO,” *Phys. Rev. B* **94**, 014427 (2016).
- [2]. J. Kimling, G.-M. Choi, J. T. Brangham, T. Matalla-Wagner, T. Huebner, T. Kuschel, F. Y. Yang, and D. G. Cahill, “Picosecond spin Seebeck effect,” *Phys. Rev. Lett.* **118**, 057201 (2017).

Publications which acknowledge DOE support (05/15/2015 – 5/14/2017)

1. S. Singh, J. Katoch, T. C. Zhu, K. Y. Meng, T. Y. Liu, J. T. Brangham, F. Y. Yang, M. Flatté, R. Kawakami. “Strong modulation of spin currents in bilayer graphene by static and fluctuating proximity exchange fields,” *Phys. Rev. Lett.* **118**, 187201 (2017). [Editor’s Suggestion]
2. H. L. Wang, C. H. Du, P. C. Hammel and F. Y. Yang, “Comparative determination of $Y_3Fe_5O_{12}/Pt$ interfacial spin mixing conductance by spin-Hall magnetoresistance and spin pumping,” *Appl. Phys. Lett.* **110**, 062402 (2017).
3. J. Kimling, G.-M. Choi, J. T. Brangham, T. Matalla-Wagner, T. Huebner, T. Kuschel, F. Y. Yang, and D. G. Cahill, “Picosecond spin Seebeck effect,” *Phys. Rev. Lett.* **118**, 057201 (2017). —“Spin Caloritronics: Bulk isn’t everything,” Research Highlight by *Nature Nanotech.* 12, 186 (2017).
4. J.C. Gallagher, K.Y. Meng, J. Brangham, H.L. Wang, B.D. Esser, D.W. McComb, and F.Y. Yang, “Robust Zero-Field Skyrmion Formation in FeGe Epitaxial Thin Films,” *Phys. Rev. Lett.* **118**, 027201 (2017).
5. A. Prakash, J. Brangham, F. Y. Yang, and J. P. Heremans, “Spin Seebeck effect through antiferromagnetic NiO,” *Phys. Rev. B* **94**, 014427 (2016).
6. R. Morrow, J. R. Soliz, A. J. Hauser, J. C. Gallagher, M. A. Susner, M. D. Sumption, A. A. Aczel, J. Q. Yan, F. Y. Yang, P. M. Woodward, “The effect of chemical pressure on the structure and properties of A_2CrOsO_6 ($A = Sr, Ca$) ferrimagnetic double perovskite,” *J. Solid State Chem.* **238**, 46 (2016).
7. A. O. Mandru, J. P. Corbett, J. M. Lucy, A. L. Richard, F. Y. Yang, D. C. Ingram, A. R. Smith, “Structure and magnetism in Ga-rich MnGa/GaN thin films and unexpected giant perpendicular anisotropy in the ultra-thin film limit,” *Appl. Surf. Sci.* **367**, 312 (2016).
8. Y. Pu, P. M. Odenthal, R. Adur, J. Beardsley, A. G. Swartz, D. V. Pelekhov, M. E. Flatté, R. K. Kawakami, J. Pelz, P. C. Hammel and E. Johnston-Halperin, “FMR driven spin pumping and electrical spin injection in silicon-based metal-oxide-semiconductor heterostructures,” *Phys. Rev. Lett.* **115**, 246602 (2015).
9. S.A. Manuilov, C.H. Du, R. Adur, H.L. Wang, V.P. Bhallamudi, F.Y. Yang, and P.C. Hammel, “Spin pumping from spinwaves in thin film YIG,” *Appl. Phys. Lett.* **107**, 042405 (2015).

10. H. L. Wang, C. H. Du, P. C. Hammel, and F. Y. Yang, "Spin transport in antiferromagnetic insulators mediated by magnetic correlations," *Phys. Rev. B* **91**, 220410(R) (2015).
11. Y.-H. Chiu, N. G. Minutillo, R. E. A. Williams, G. J. Smith, D. W. McComb, J. A. Carlin, E. Johnston-Halperin, F. Y. Yang, "Photoluminescence Evolution in GaAs/AlGaAs Core/Shell Nanowires Grown by MOCVD: Effects of Core Growth Temperature and Substrate Orientation," *J. Cryst. Growth* **429**, 1 (2015).

Session 8

Electrical generation of valley magnetization in 2D transition metal dichalcogenides

Kin Fai Mak

Department of Physics, Penn State University

Electrons in two-dimensional (2D) Dirac materials such as gapped graphene and single-layer transition metal dichalcogenides possess a new two-fold valley degree of freedom corresponding to the K and K' valleys of the Brillouin zone. The valley degree of freedom carries orbital magnetic moment. A net valley magnetization forms the basis for valley-based applications. Although the control of valley magnetization by circularly polarized light and by a vertical magnetic field has now become routine, the development of practical valleytronic devices requires the pure electrical control of valley magnetization. In this talk, I will discuss our recent experimental results on the generation of valley magnetization on the channel edges of monolayer and bilayer MoS₂ transistors by the valley Hall effect [1], and in the bulk of strained monolayer MoS₂ by the valley magnetoelectric effect [2].

References:

- [1] J. Lee, K. F. Mak, & J. Shan "Electrical control of the valley Hall effect in bilayer MoS₂ transistors," *Nature Nanotech.* **11**, 421-425 (2016).
- [2] J. Lee, Z. Wang, H. Xie, K. F. Mak, & J. Shan, "Valley magnetoelectricity in single-layer MoS₂," *Nature Mater.* **16**, 887-891 (2017).

Quantum Transport in 2D Semiconductors

James Hone, Columbia University, Dept. of Mechanical Engineering

Cory Dean, Columbia University, Dept. of Physics

Program Scope

This project focuses on fundamental studies of quantum transport in two-dimensional transition metal dichalcogenides and their related heterostructures. Areas of study include: understand fundamental limits of quantum device characteristics, including scattering mechanisms, material and interfacial impurities, and electrical contacts; determining intrinsic properties of the 2D semiconductor TMDs such as the effective band mass, spin orbit coupling, and electron-phonon coupling; and measurement of novel quantum transport properties unique to the TMDs including the hierarchy of quantum Hall states and valley Hall effects.

Recent Progress

Direct measurement of quantum transport in 2D semiconductors has proven difficult due to low material quality and difficulties in making Ohmic contacts at low temperature. Toward the first challenge, we have utilized WSe₂ grown by techniques developed in the lab of Luis Balicas (Nat. High Magnetic Field Lab / FSU), which has defect density below 10¹¹/cm². Toward the second challenge, we have partially circumvented the contact issue by using a single electron transistor (SET) fabricated directly on top of a hBN / WSe₂ / hBN heterostructure to measure the electronic compressibility of the WSe₂. In this measurement, the electrical contact to the WSe₂ only has to be sufficient to allow slow charging in response to an applied gate voltage. Such SET-based techniques have previously been employed with GaAs-based systems but not with 2D semiconductors. We performed measurements of monolayer WSe₂ at the National High Magnetic Field Laboratory, at fields up to 35 T.

Together, these improvements allow us to provide a near-complete map of the Landau Level spectrum of monolayer WSe₂, as shown in Figure 1, which shows the inverse compressibility ($d\mu/dn$) as a function of gate voltage and applied field. Well-developed Landau ‘fans’ are seen for both the valence (VB) and conduction (CB) bands, which are well fit by the general relation $B = nh/\nu e$, with the filling factor ν shown. By extrapolating the slopes of the LL gaps to $B = 0$, we find a separation in gate voltage of 2.7 V between the two bands, arising from the band gap of the material. Because the higher spin-split bands in WSe₂ are expected to be ~ 500 meV and ~ 30 meV removed from the lowest-energy VB and CB, respectively, this data reflects only the lowest spin-split bands.

A striking aspect of these LL maps is a clear alternation between large and small gaps, for all observed states in the CB and beginning at $\nu=-6$ for the VB. In the CB, gaps at odd-valued ν are more pronounced than those at even-valued ν throughout the accessible range of electron density. In contrast, the VB the dominant parity in ν changes from odd to even as the hole

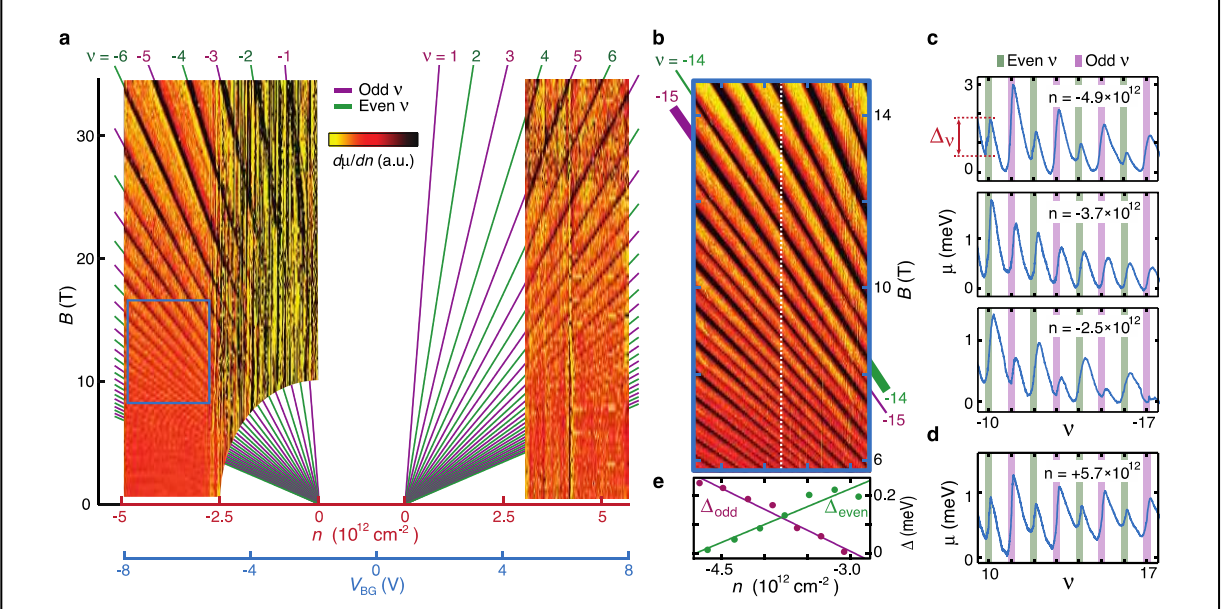


Figure 1. Ambipolar Landau level dispersion. **a**, The inverse compressibility $d\mu/dn$ of the WSe_2 produces a characteristic Landau fan as a function of carrier density n and magnetic field B . **b**, Zooming in on the valence band (blue outline in **a**) reveals that the gap magnitude alternates, and that the dominant gaps occur at odd ν for high hole density and for even ν at low density. The crossover occurs at $n \approx -3.8 \times 10^{12} \text{ cm}^{-2}$ (dashed white line), and has no discernible dependence on B . **c**, The chemical potential μ acquired along three vertical cuts in the VB fan confirms the density-dependence of the LL gap sequence. At high hole density (top), gaps at odd filling dominate, whereas the ones as even filling dominate at low density (bottom). At the cross-over density (middle), consecutive gaps are equal.

density is reduced (Fig. 1c), with a cross-over point at $n \approx -3.8 \times 10^{12} \text{ cm}^{-2}$, independent of B (white dotted line in Fig. 1b).

Figure 2d shows the proposed structure of the Landau levels derived from the data shown in Figure 1. The alternating pattern of gaps arises from breaking of the degeneracy between the K and K' valleys, which are spin-polarized. Within a given valley, the LL spacing is given by the cyclotron energy, whereas the Zeeman splitting between valleys is given by an effective Lande g^* -factor g^* . Since both are proportional to applied field, the number of valley-polarized bands is independent of field, and provides a measure of the ratio between the Zeeman and cyclotron energies. In the CB, g^* is below 2, the Zeeman energy is smaller than the cyclotron energy, and the pattern of alternating gaps appears for all LLs. In contrast, for the VB we find that g^* is above 10, and there are 6 ‘valley-polarized’ LLs before the alternating sequence begins. In addition, the reduction in g^* with increased carrier density causes the shift in gap pattern from even-odd to odd-even. The values of m^* and g^* derived from the data are shown in Fig. 2a,b. The large value of g^* indicates strong electron-electron interactions

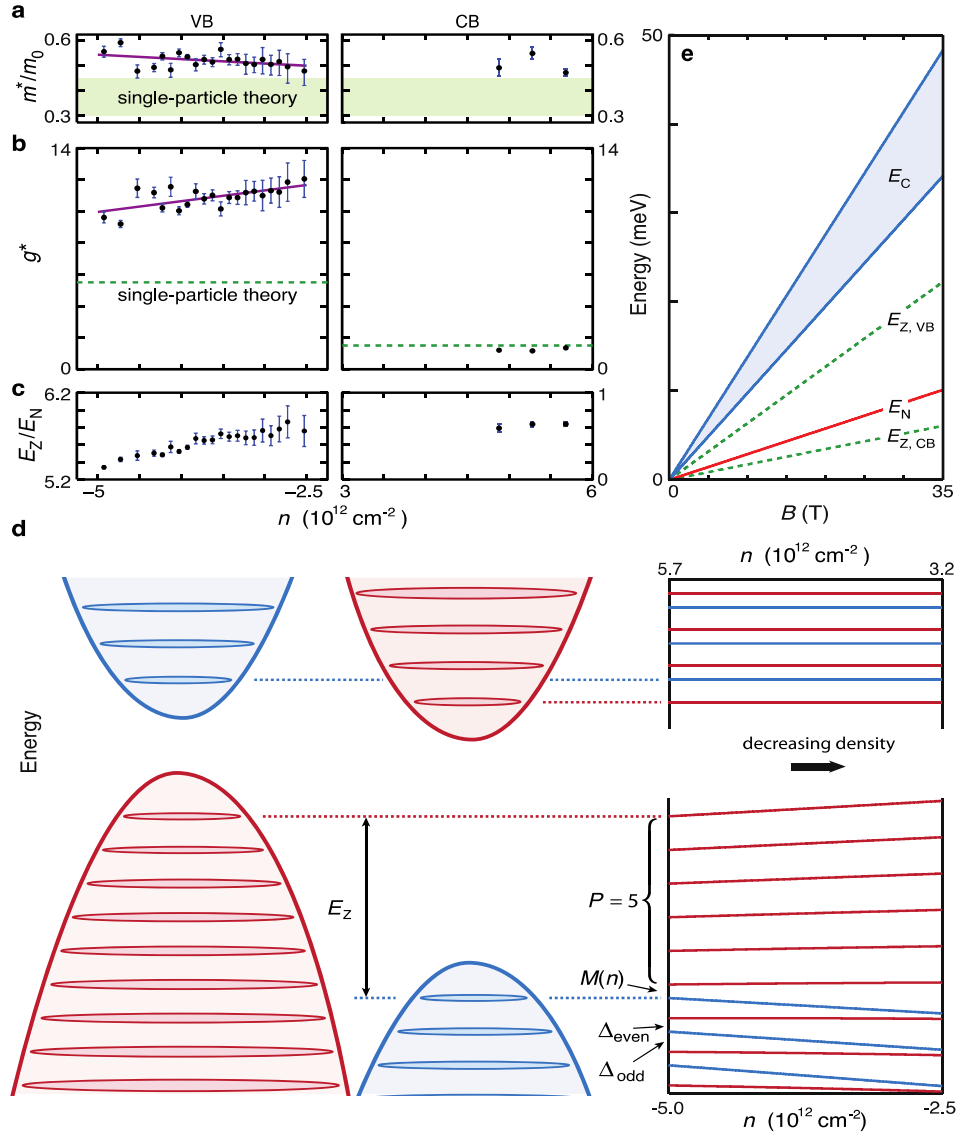


Figure 2. Extracted parameters and effects of interactions. **a**, Effective carrier mass and **b**, Landé g -factor for each accessible density for the VB and CB (black dots), and best-fit lines (purple). The green area/dotted line represent typical theoretical predictions from a single-particle model. Both m^* and g^* are enhanced in the VB compared to such predictions. The extraction of g^* in the CB assumes $P = 0$ (see text and Supplementary Information). **c**, The ratio of Zeeman to cyclotron energy ($E_Z/E_N = m^*g^*/m_0$) is less than 1 in the CB but between 5-6 in the VB. **d**, Schematic of LL structure versus carrier density, assuming the m^* and g^* shown by solid purple lines in **a** and **b** for the VB, and average values of the three points in the CB. The offset between the spin-locked valleys in the VB is given by the fixed integral polarization $P = 5$ and the residual density-dependent contribution $M(n)$. In the CB, we observe an odd-dominant sequence of gaps at all accessible electron densities, but our experiment cannot distinguish between the plotted sequence and one with the opposite shift between valleys. **e**, Energy scales in WSe₂ in the absence of carrier interactions. The cyclotron energy (red line) and total Zeeman energies in the VB and CB (green dotted lines) all scale linearly with B . The Coulomb energy (blue shaded region) is the largest energy in the system even at high density (plotted here for $2.5 \times 10^{12} \text{ cm}^{-2} \leq n \leq 5 \times 10^{12} \text{ cm}^{-2}$). As a result, many-body interactions are expected to significantly enhance the Zeeman effect.

The combination of a large single-particle Zeeman scale and high effective mass leads to a large Zeeman-to-cyclotron ratio, which is further enhanced by interactions even at high carrier densities. Our observed E_Z/E_N goes up to 5.8 in the VB (Fig. 2c), which is a factor of 2.6 higher than expected from a single-particle model, a factor of 2 higher than measured in multi-layer WSe₂ [1], and a factor of ~ 6 higher than in ZnO, which has the largest intrinsic E_Z/E_N reported in an engineered quantum well [2].

Future Plans

In the upcoming year, we will extend these measurements to other 2D semiconductors and improve contact techniques to improve the data near the band edges. In addition, the large measured value of E_Z/E_N , in conjunction with the high density of states, suggests the possibility that exchange interactions are strong enough to satisfy the Stoner criterion, implying potential itinerant ferromagnetism at zero magnetic field. This property, which has only recently been observed in a select few 2D materials [3, 4], would additionally be field effect tunable in the case of ML WSe₂. We will search for magnetism in these materials by fabricating SQUID loops directly onto the heterostructures.

References

1. S. Xu, J. Shen, G. Long, Z. Wu, Z.-q. Bao, C.-C. Liu, X. Xiao, T. Han, J. Lin, Y. Wu, H. Lu, J. Hou, L. An, Y. Wang, Y. Cai, K. M. Ho, Y. He, R. Lortz, F. Zhang, and N. Wang, *Physical Review Letters* 118, 067702 (2017).
2. A. Tsukazaki, A. Ohtomo, M. Kawasaki, S. Akasaka, H. Yuji, K. Tamura, K. Nakahara, T. Tanabe, A. Kamisawa, T. Gokmen, J. Shabani, and M. Shayegan, *Physical Review B* 78, 233308 (2008).
3. C. Cong, L. Li, Z. Li, H. Ji, A. Stern, Y. Xia, T. Cao, W. Bao, C. Wang, Y. Wang, Z. Q. Qui, R. J. Cava, S. G. Louie, J. Xia, and X. Zhang, *Nature* 546, 265 (2017).
4. B. Huang, G. Clark, E. Navarro-Moratalla, D. R. Klein, R. Cheng, K. L. Seyler, D. Zhong, E. Schmidgall, M. A. McGuire, D. H. Cobden, W. Yao, D. Xiao, P. Jarillo-Herrero, and X. Xu, *Nature* 546, 270 (2017).

Publications

Martin V. Gustafsson, Matthew Yankowitz, Carlos Forsythe, Daniel Rhodes, Kenji Watanabe, Takashi Taniguchi, James Hone, Xiaoyang Zhu, and Cory R. Dean, “Ambipolar Landau levels and strong band-selective carrier interactions in monolayer WSe₂”, submitted.

Van der Waals Heterostructures: Novel Materials and Emerging Phenomena

Feng Wang

Materials Sciences Division, Lawrence Berkeley National Laboratory

Program Scope

This program aims to exploit extraordinary new scientific opportunities enabled by designing van der Waals (vdW) heterostructures that allow creation of novel functional materials with unprecedented flexibility and control. The key innovation here is that atomically-thin 2D layers with wide-ranging properties can be grown separately and then stacked together to form a new class of materials – van der Waals-bonded heterostructures - in which each layer can be engineered separately. This offers an unlimited design space for new materials exhibiting a wide range of quantum phenomena, such as field-tunable charge density waves, magnetism, quantum spin Hall effect, and superconductivity. Additional unique control of few-layer systems may be achieved through tunable electrostatic gating, mechanical strain, and inter-layer coupling. We propose to explore new quantum phenomena in these systems, ranging from field-induced 2D magnetism and 2D superconductivity to semiconductor heterojunctions and exciton Bose-Einstein condensates. This will enable tunable 2D magnetic order, novel topological phases, and quasi-2D engineered condensates that have so far only been theorized but not experimentally observed.

Recent Progress

(1) Ultralong valley lifetime in WSe₂/MoS₂ heterostructures.

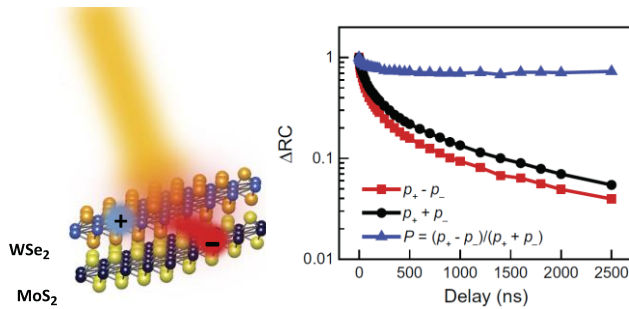


Fig. 1: Left: Illustration of ultrafast electron transfer process in WSe₂/MoS₂ heterostructure. Right: Decay dynamics of the total hole population (black dots), valley-polarized hole population (red squares), and degree of valley polarization P (blue triangles). The decay of the valley-polarized hole population of $\sim 1 \mu\text{s}$ is mainly due to the total population decay. The valley polarization, however, does not show any apparent decay in $2.5 \mu\text{s}$, corresponding to an ultralong valley depolarization lifetime exceeding $40 \mu\text{s}$.

A pair of degenerate direct bands are present at the K and K' points in the momentum space of hexagonal TMD monolayers, giving rise to a new valley degree of freedom known as the valley pseudospin. Tremendous progresses have been made in exploring the valley pseudospin of 2D TMDs. Many challenges, however, still exist for potential valleytronics applications. Chief among them is the relatively short valley lifetime. It was recently shown both theoretically and experimentally that the valley lifetime of excitons in TMD monolayers is severely constrained by the electron-hole exchange

interaction through the Maialle-Silva-Sham mechanism, which can annihilate an exciton in one valley and create another exciton in the other valley, i.e. depolarize the valley pseudospin, within picoseconds. The valley pseudospin of individual electrons or holes, however, is not affected by this mechanism and can have much longer lifetime. Recently **Wang** and **Crommie** in our program collaborated to demonstrate efficient generation of ultralong lived valley polarization in $\text{WSe}_2/\text{MoS}_2$ heterostructures [1]. Using ultrafast pump-probe spectroscopy that covers time scale from femtoseconds to microseconds, we show that perfectly valley-polarized holes can be generated in the WSe_2 layer within 50 fs owing to the ultrafast charge transfer processes in the $\text{WSe}_2/\text{MoS}_2$ heterostructure. These valley-polarized holes exhibit a population decay lifetime of over 1 μs , and a depolarization lifetime (i.e. inter-valley scattering lifetime) over 40 μs at 10 Kelvin. The ultralong valley lifetime observed here, orders of magnitude longer than previously reported values, will enable new ways to probe and manipulate valley and spin degrees of freedom in TMDs.

(2) Interlayer electron-phonon interactions in WSe_2/hBN heterostructures

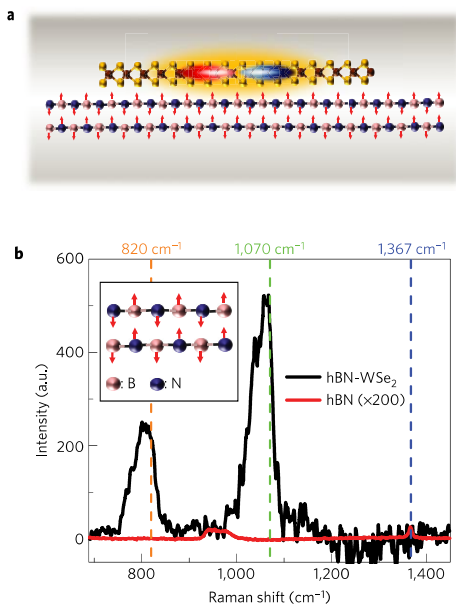


Fig. 2: (a) Illustration of interlayer electron-phonon coupling, where the phonon vibration in hBN couples to the exciton states in WSe_2 . (b) Raman spectrum of the heterostructure shows prominent hBN phonon Raman peaks strongly enhanced by resonant excitation of WSe_2 .

Electron-electron interactions between adjacent 2D layers in van der Waals heterostructures can give rise to a variety of fascinating physical behavior such as mini-Dirac cones and the Hofstadter's butterfly pattern in graphene/hBN heterostructures. Similarly, exploiting interactions between electrons in one layered material and phonons in an adjacent material could enable new ways to control electron-phonon coupling and realize novel quantum behavior that is not possible before. **Wang** and **Zettl** in the program collaborated to demonstrate, for the first time, an extraordinary interlayer electron-phonon coupling in WSe_2/hBN heterostructures, as illustrated in Fig. 2a.[2] Vibration modes of hBN lattice (labeled with red arrows) can significantly modulate the behavior of electrons and holes in WSe_2 (red and blue clouds), thus enabling efficient interlayer electron-phonon coupling. Experimentally, such interaction manifests as emerging resonant Raman scattering processes that involve both hBN phonon vibrations and WSe_2 electronic resonances: Two prominent new Raman peaks appear in the heterostructure composed of WSe_2 encapsulated in hBN flakes, with the Raman

shifts corresponding to the hBN ZO phonon mode and the hBN ZO + WSe_2 A_{1g} combinatorial mode, respectively (Fig. 2b). These Raman modes are remarkably strong, with intensities three orders of magnitude higher than the Raman signal of phonons in pure hBN. Excitation spectroscopy reveals that the new Raman peaks of hBN ZO phonons are enhanced by WSe_2

electronic transitions in a double-resonance process. In addition, we show that the new Raman peaks from the interlayer electron-phonon couplings in the heterostructure can be controlled efficiently through electrostatic gating of the monolayer WSe₂. Our study demonstrates for the first time the presence of remarkable interlayer electron-phonon interactions in van der Waals heterostructures, which will be important for understanding electron behavior from carrier mobility to energy relaxation dynamics in 2D materials.

(3) Intrinsic ferromagnetism in two-dimensional van der Waals crystals

The realization of long-range ferromagnetic order in two-dimensional van der Waals crystals, combined with their rich electronic and optical properties, could lead to new magnetic, magnetoelectric and magneto-optic applications. In two-dimensional systems, the long-range magnetic order is strongly suppressed by thermal fluctuations; according to the Mermin–Wagner theorem, however, these thermal fluctuations can be counteracted by magnetic anisotropy. Previous efforts, based on defect and composition engineering, or the proximity effect, introduced magnetic responses only locally or extrinsically. Recently *Zhang, Louie* and *Qiu* in our program collaborated to discover intrinsic long-range ferromagnetic order in pristine Cr₂Ge₂Te₆ atomic layers, as revealed by scanning magneto-optic Kerr microscopy. In this magnetically soft, two-dimensional van der Waals ferromagnet, we achieved unprecedented control of the transition temperature (between ferromagnetic and paramagnetic states) using very small fields (smaller than 0.3 tesla). This result is in contrast to the insensitivity of the transition temperature to magnetic fields in the three-dimensional regime. We found that the small applied field leads to an effective anisotropy that is much greater than the near-zero magnetocrystalline anisotropy [3], opening up a large spin-wave excitation gap. We explain the observed phenomenon using renormalized spin-wave theory and conclude that the unusual field dependence of the transition temperature is a hallmark of soft, two-dimensional ferromagnetic van der Waals crystals. Cr₂Ge₂Te₆ is a nearly ideal two-dimensional Heisenberg ferromagnet and so will be useful for studying fundamental spin behaviours, opening the door to exploring new applications such as ultra-compact spintronics.

Future Plans

(1) Investigate the dynamic transport of valley current in TMD heterostructures. We will build on our observation of the ultralong lived valley-polarized holes in WSe₂/MoS₂ heterostructures to explore the dynamic transport of photo-excited valley polarization in the heterostructures, which can lead to a pure spin and valley current.

(2) Investigate the coupling of the spin-valley excitation in TMD and 2D ferromagnetism in WSe₂/Cr₂Ge₂Te₆ heterostructures. We will build on our discovery of 2D ferromagnetism in Cr₂Ge₂Te₆ to explore its coupling to the unique spin and valley degree of freedom in TMDs in their heterostructure.

(3) Investigate 2D quantum spin Hall insulator in monolayer 1T'-WTe₂. We will investigate further the topological edge state present in the atomically thin 1T'-WTe₂ and the effect of magnetic dopants on such edge states using scanning tunneling spectroscopy.

References

- [1] J. Kim, C. Jin, B. Chen, et al, *Science Advances*, 3(7), (2017) doi:10.1126/sciadv.1700518
- [2] C. Jin, J. Kim, J. Suh, et al, *Nature Physics*, 13(2), 127-131, (2017)
- [3] C. Gong, L. Li, Z. Li, et al, *Nature* 546, 265–269 (2017)

Publications

1. C. Jin, J. Kim, J. Suh, et al, *Nature Physics*, 13(2), 127-131, (2017)
2. J. Kim, C. Jin, B. Chen, et al, *Science Advances*, 3(7), (2017) doi:10.1126/sciadv.1700518
3. S. G. Drapcho, J. Kim, X. Hong, et al, *Physical Review B*, 95(16), 165417, (2017)
4. C. Gong, L. Li, Z. Li, et al, *Nature* 546, 265–269 (2017)
5. A.-Y. Lu, H. Zhu, J. Xiao, et al, *Nature Nanotechnology*, 12, 744–749 (2017),
6. S. Tang, C. Zhang, D. Wong, et al, *Nature Physics* (2017) (doi:10.1038/nphys4174).
7. J. Li, L. R. Shelford, P. Shafer, et al, *Phys. Rev. Lett.* 117, 076602 (2016).
8. Zhiyong Qiu, Jia Li, Dazhi Hou, et al, *Nature Communications* 7, 12670 (2016).
9. Ying Sun, You Ba, Aitian Chen, et al, *ACS Appl. Mater. Interfaces* 9, 10855–10864 (2017).
10. Q. Li, T. P. Ma, M. Yang, et al, *Phys. Rev. B* 96, 024420 (2017).
11. Q. Li, A. Tan, A. Scholl, et al, *Appl. Phys. Lett.* 110, 262405 (2017).

Program title: Spectroscopic investigations of novel electronic and magnetic materials

Principle Investigator: Janice L. Musfeldt

Affiliation: Departments of Chemistry and Physics, University of Tennessee, Knoxville TN 37996

Contact: (865) 974-3392 or musfeldt@utk.edu

Program scope

The goal of our research program is to develop a fundamental understanding of the mechanisms underlying the interplay between charge, structure, and magnetism in complex materials. This insight facilitates the development of tunable multifunctional solids and nanomaterials, which are scientifically and technologically important. Our main strategy involves investigating the spectroscopic response of functional materials like multiferroics, quantum magnets, frustrated systems, and compounds containing domain walls or 4- and 5d centers, and we perform these measurements under external stimuli (like high magnetic fields and pressures) and at very small sizes where quantum confinement becomes apparent. By so doing, we learn about the relationships between different ordered and emergent states, explore the dynamic aspects of coupling, and gain insight into the generality of these phenomena and their underlying mechanisms. In addition to broadening the understanding of novel solids under extreme conditions, multifunctional materials and their assemblies are of interest for light harvesting, spintronics, and solid state lubrication applications.

Recent progress

Several exciting discoveries were made under the auspices of our Department of Energy-supported program during the past year. Briefly, they include (i) revealing the spectroscopic signatures of chirality in the metallic ferromagnet $\text{Fe}_{1/3}\text{TaS}_2$, (ii) testing the breakdown mechanism and tendency toward a high pressure metallic state in multiwall WS_2 nanotubes, and (iii) exploring the size-dependence of spin-charge coupling in $\alpha\text{-Fe}_2\text{O}_3$. What brings these findings together is the interplay between charge, structure, and magnetism and the spectroscopic techniques with which we investigate these phenomena. A broad range of educational, outreach, and service activities also takes place under the auspices of this Department of Energy grant. The majority were in the area of conference organization (for instance, the 2015 Telluride workshop on spin-orbit coupling in 4- and 5d materials, the 2016 Gordon Research Conference on single sheet materials, and the developing 2018 Telluride meeting) and service to the National High Magnetic Field Laboratory and National Synchrotron Light Source.

Hidden chirality in the metallic ferromagnet $\text{Fe}_{1/3}\text{TaS}_2$: Research on engineered superlattice materials has blossomed in recent years due to the discovery of unexpected properties deriving from interface effects. Naturally occurring superlattices like intercalated oxides and chalcogenides are of contemporary interest as well. Examples include the chiral helimagnets $\text{Cr}_{1/3}\text{NbS}_2$ and $[\text{Pb}_2\text{BiS}_3][\text{AuTe}_2]$, superconducting Pd-intercalated IrTe_2 , and interlayer I-doped BiOIO_3 nanoplates. The chiral ferromagnet $\text{Fe}_{1/3}\text{TaS}_2$ attracted our attention in this context. This system is part of a larger family of materials based upon 2H-TaS_2 that have a set of stable, well-ordered intercalation plateaus at $x=1/4$ and $1/3$ [Fig. 1]. In order to explore intercalation effects on the fundamental excitations of a chiral ferromagnet, we measured the spectroscopic response

of $\text{Fe}_{1/3}\text{TaS}_2$ and compared our findings with the $x=0$ and $1/4$ compounds as well as complementary first principles calculations. Strikingly, separation of chalcogenide slabs by atomically thin layers of iron introduces a second free carrier response due to a peak in the density of states at the Fermi level along with a set of localized bands that are intimately connected to the density and pattern of the Fe centers. Symmetry breaking in $\text{Fe}_{1/3}\text{TaS}_2$ is evident in the charge density pattern at the Fermi surface, the hole \rightarrow electron pocket crossover near the K-point, and the characteristic set of low energy electronic excitations between spin split bands that cross the Fermi surface. Signatures of chirality are firmly embedded in the bound carrier excitations as well, which we analyze by tracking trends in the hybridized Fe- and Ta-containing bands. Importantly, these effects are exposed in a metallic system, so in addition to providing opportunities to compare correlation vs. spin-orbit effects in Fe-containing chalcogenides, they reveal ideas that may be useful in the hunt for metallic ferroelectrics.

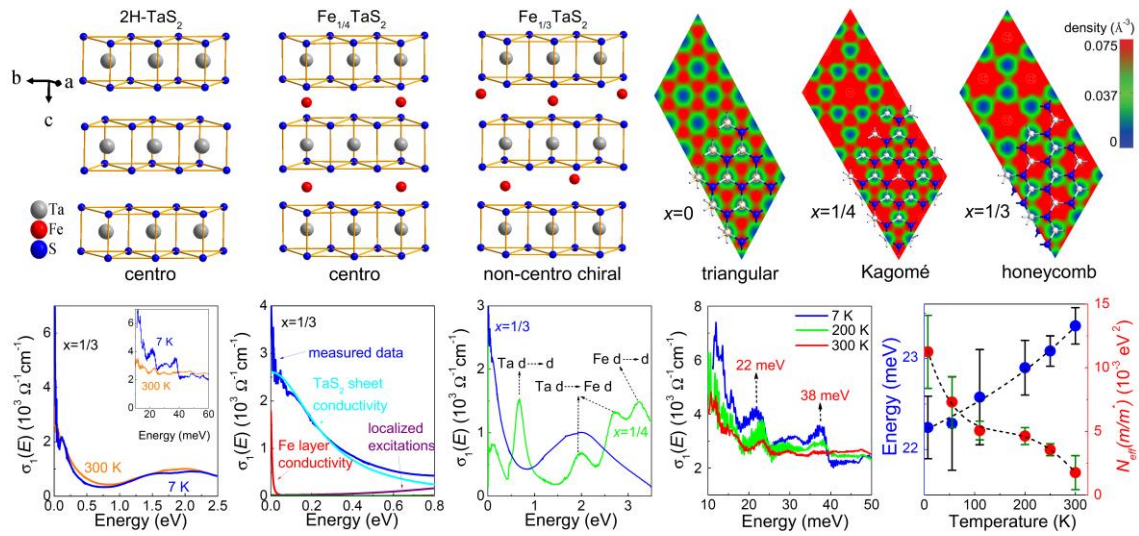


Fig. 1: Crystal structures of 2H-TaS_2 and the $x=1/4$ and $1/3$ compounds, charge density, and optical properties of the $x=1/3$ material which reveal several unique signatures of chirality.

Uncovering the pressure-induced breakdown mechanism and low energy electronic structure in WS_2 nanotubes: The dynamics of transition metal dichalcogenide particles and tubes have interested our team for some time because they are superior platforms for fundamental studies of confinement, control of electronic properties with substitutional doping, and novel mechanical and tribological properties. The recent development of reliable, large scale synthetic methods is, for the first time, allowing work on WS_2 nanotubes. One puzzle of fundamental and practical importance relates to how the transition metal dichalcogenide tubes break down under extremely high strain. At the same time, little is known about the electronic properties of nanoscale chalcogenides under pressure. In order to evaluate theoretically-proposed mechanisms of tube breakdown and search for evidence of pressure-induced metalization, we brought together synchrotron-based infrared and Raman spectroscopies, diamond anvil cell techniques, and an analysis of frequency shifts and lattice dynamics to unveil the vibrational properties of multiwall WS_2 nanotubes under compression [Fig. 2]. While most of the vibrational modes display similar hardening trends, the Raman-active A_{1g} breathing mode is almost twice as responsive, suggesting that the nanotube breakdown pathway under strain proceeds through this displacement. At the same time, the previously unexplored high pressure infrared response provides unexpected insight into the electronic properties of the multiwall WS_2 tubes. The

development of a localized absorption is fit to the percolation model, indicating that the nanotubes display a modest macroscopic conductivity due to hopping from tube to tube. These findings extend the understanding of chalcogenides under extreme conditions.

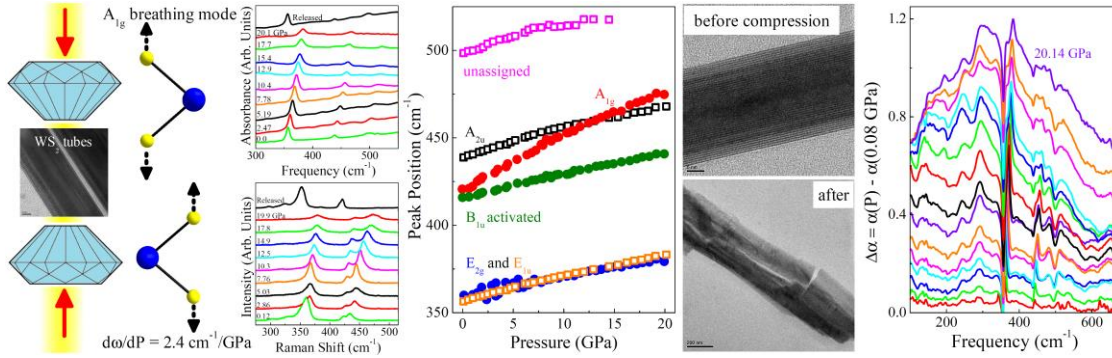


Fig. 2: Schematic of the diamond anvil cell, breathing mode displacement pattern, infrared and Raman response of the WS₂ nanotubes under pressure, TEM images supporting this mechanism, and development of a low-energy bound carrier excitation under pressure.

Magneto-chromic sensing and size-dependent collective excitations in iron oxide nanoparticles: Charge-lattice coupling is one of the most celebrated interactions in functional materials. It underlies a variety of scientifically and technologically important processes including superconductivity, charge density wave formation, vibronic coupling, and photochemical reactions. Less is known, however, about how size can be used to control spin-charge interactions. We identified $\alpha\text{-Fe}_2\text{O}_3$, commonly known as hematite, as a model antiferromagnet with which to test these ideas. Here, we combine optical and magneto-optical spectroscopies with complementary vibrational and magnetic property measurements to reveal finite length scale effects in nanoscale $\alpha\text{-Fe}_2\text{O}_3$ [Fig. 3]. Analysis of the vibronically-activated d -to- d on-site excitations uncovers enhanced color contrast at particle sizes below approximately 75 nm due to size-induced enhancement of spin-charge coupling that is suppressed again below the superparamagnetic limit. Various mechanistic tests demonstrate the importance of a robust spin-flop transition; when the spin-flop is incomplete or absent, the color contrast is reduced or suppressed, respectively. The spin-charge coupling mechanism also accounts for systematic shifts in the magnon sideband frequency, from which we extract precisely how the fundamental exciton softens with decreasing size. These findings provide a general strategy for generating large field-induced color contrast for emerging magneto-chromic sensor applications reveal a size dependence to the collective excitations that may advance the development of magnonics.

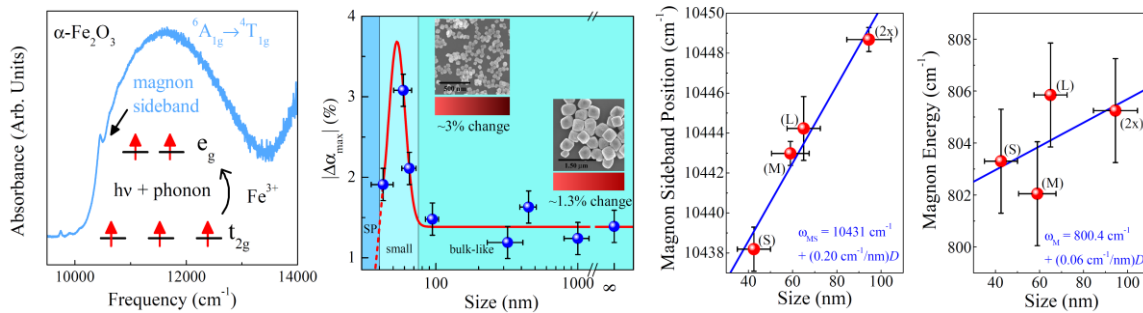
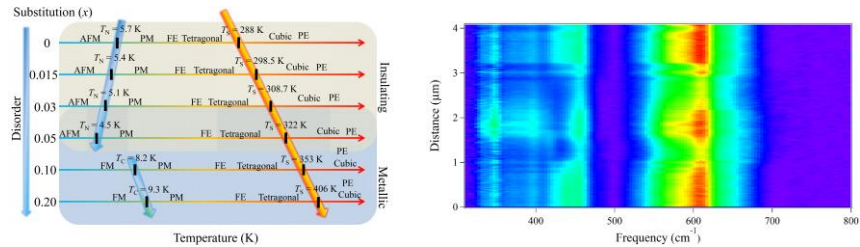


Fig. 3: Close-up view of the ${}^6A_{1g} \rightarrow {}^4T_{1g}$ on-site excitation of Fe³⁺ and the magnon sideband, field-induced optical contrast as a function of size, and trends in the magnon side band and magnon energies from which the size dependence of the fundamental exciton can be revealed.

Future plans

Several exciting efforts are planned for the coming year. Briefly, they include (i) employing dichroic probes of charge, structure, and magnetism to develop magnetic field-temperature phase diagrams of room temperature multiferroic $\text{LuFe}_2\text{O}_4\text{:LuFeO}_3$ superlattices, (ii) revealing the competition between metallicity, disorder, and ferroelectricity in Nb-substituted EuTiO_3 [left, Fig. 4], (iii) probing the spectroscopic signatures of ferroelastic domain walls in $\text{Ca}_3\text{Ti}_2\text{O}_7$ [right, Fig. 4], (iv) exploring finite length scale effects on vibronic coupling in nanoscale CuGeO_3 , and (v) investigating the properties of atomically-thin MnPS_3 and MnPSe_3 to reveal the thickness-dependent vibrational properties. Outreach includes service to the several different national laboratories as well as organization of the 2018 Telluride workshop on spin-orbit coupling and the GMAG session on complex bulk oxides at the 2018 American Physical Society meeting.

Fig. 4: Development of ferroelectricity and ferromagnetism in EuTiO_3 with Nb substitution and tip-enhanced infrared spectrum across two ferroelastic domain walls in $\text{Ca}_3\text{Ti}_2\text{O}_7$.



Publications emanating from this grant (2016 – 2017)

1. *Revealing the pressure-induced breakdown pathway in WS_2 nanotubes*, K. R. O’Neal, J. G. Cherian, A. Zak, R. Tenne, Z. Liu, and J. L. Musfeldt, *Nano Lett.* **16**, 993 (2016).
2. *Tuning g-factors of core-shell nanoparticles by controlled positioning of magnetic impurities*, G. D. Sanders, J. L. Musfeldt, and C. J. Stanton, *Phys. Rev. B.* **93**, 075431 (2016).
3. *Optical spectroscopy and band gap analysis of hybrid improper ferroelectric $\text{Ca}_3\text{Ti}_2\text{O}_7$* , J. G. Cherian, T. Birol, N. C. Harms, B. Gao, S. -W. Cheong, D. Vanderbilt, and J. L. Musfeldt, *Appl. Phys. Lett.* **108**, 262901 (2016).
4. *Magneto-chromic sensing and size-dependent collective excitations in iron oxide nanoparticles*, K. R. O’Neal, J. M. Patete, P. Chen, B. S. Holinsworth, J. M. Smith, C. Marques, J. W. Simonson, M. C. Aronson, S. A. McGill, S. S. Wong, and J. L. Musfeldt, *Phys. Rev. B.* **95**, 125416 (2017).
5. *Magnetic field tunability of spin polarized excitations in a high temperature magnet*, B. S. Holinsworth, J. G. Cherian, D. Mazumdar, N. C. Harms, H. Sims, A. Gupta, S. A. McGill, and J. L. Musfeldt, submitted, *Phys. Rev. B.*
6. *Frustration and glassy character in multiferroic $\text{RIn}_{1-x}\text{Mn}_x\text{O}_3$ ($R = \text{Tb}, \text{Dy}, \text{Gd}$)*, P. Chen, B. S. Holinsworth, K. R. O’Neal, X. Luo, C. V. Topping, S. -W. Cheong, J. Singleton, E. S. Choi, and J. L. Musfeldt, submitted, *Phys. Rev. B.*
7. *Size-dependent spectroscopic properties of the spin-Peierls compound CuGeO_3* , K. R. O’Neal, A. al-Wahish, Z. Li, G. Dhalenne, A. Revcolevschi, X. -T. Chen, and J. L. Musfeldt, submitted, *Phys. Rev. B.*
8. *Hidden chirality in the metallic ferromagnet $\text{Fe}_{1/3}\text{TaS}_2$* , S. Fan, I. Manuel, A. al-Wahish, K. A. Smith, K. R. O’Neal, C. J. Won, J. W. Kim, S. -W. Cheong, J. T. Heraldsen, and J. L. Musfeldt, submitted, *Phys. Rev. Lett.*

Probing Linewidths and Biexciton Quantum Yields of Single Cesium Lead Halide Nanocrystals in Solution

Moungi G. Bawendi, Massachusetts Institute of Technology – Department of Chemistry

Program Scope

The extraordinary optical properties of lead-based halide perovskites have recently been translated into colloidal cesium lead halide (CsPbX_3 X=Cl, Br, I) perovskite nanocrystals (PNCs). PNCs (**figure 1**) exhibit high emission quantum yields even in the absence of surface

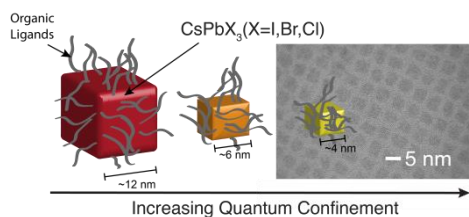


Figure 1: Cesium lead halide perovskite nanocrystals exhibiting quantum confinement.

passivating shells, can be obtained via remarkably robust syntheses, and exhibit band-gap tunability via both composition tuning and size-dependent quantum confinement.¹ Their compelling characteristics render PNCs a promising alternative to II-IV nanocrystals like CdSe. As such, they have been demonstrated in a plethora of applications like LEDs, light down-shifting, and low-threshold lasing.^{2,3} The targeted advancement of these applications requires an in-depth

understanding of the excited state dynamics in PNCs. For instance, identifying the origin of the emission linewidth may allow improvements in the color purity of PNC-based light-emitting devices. Determining which physical parameters control the Auger rate would facilitate the realization of PNC-based single photon sources or lasers by either directed maximization or minimization of multiexciton quantum yields.

Conventionally, the multiexciton quantum yield and the emission linewidth of single nanocrystals are measured with single molecule spectroscopy, where the single nanocrystal properties are surveyed one particle at a time. However, the still limited photo-stability of PNCs has hampered the interrogation of confined PNCs with these fairly perturbative single nanocrystal techniques.⁴

We overcome the limitations of conventional single nanocrystal spectroscopy imposed by the instability of PNCs by utilizing solution-based photon-correlation methods pioneered in our group.^{5,6} With our techniques, millions of single PNCs are probed for only a few excitation cycles each rendering our experiments highly statistically robust and minimally perturbative. With solution-phase photon-correlation Fourier spectroscopy (s-

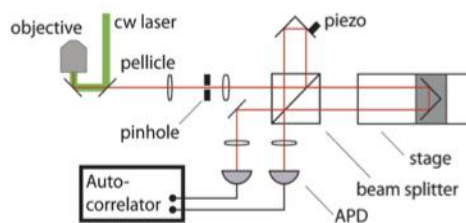


Figure 2: s-PCFS combines photon-correlation and Fourier spectroscopy to extract single NC and ensemble spectral linewidth.

PCFS), we measure the ensemble averaged single PNC linewidth with high temporal resolution, in the absence of photo-bleaching, and with high statistical robustness (**figure 2**).^{7,8} We assess the biexciton to the single exciton quantum yield ratio (BX/X QY ratio) by low flux, pulsed excitation anti-bunching measurements in solution (s-g⁽²⁾), where we histogram two-photon events detected after the same (biexciton emission) and different (exciton emission) excitation pulses.⁶

In this project, we use s-PCFS and s-g⁽²⁾ to elucidate the effects of quantum confinement and the halide composition on the single PNC emission linewidth and the BX/X QY ratio. Our goal is to formulate guidelines for the synthetic improvement of PNCs and to elucidate the fundamentals of confined excitons in lead-based perovskites.

Recent Progress

In our paper in revision at *Nano Letters*, we report the first comprehensive study of the BX/X QY ratio and the single PNC emission linewidth in PNCs. We include highly confined

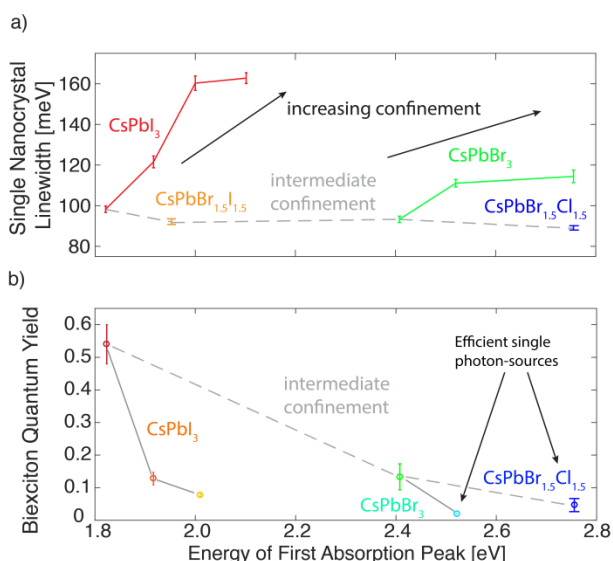


Figure 3: We have surveyed the single NC linewidth (a) and biexciton quantum yield (b) as a function of halide composition and degree of confinement.

PNCs previously inaccessible to single nanocrystal spectroscopy due to their instability. Using s-PCFS, we have undertaken a systematic survey of the single PNC linewidth as a function of the degree of confinement and halide composition. We find that sample inhomogeneity plays only a minor role in determining the ensemble emission linewidth and that the single NC linewidth increases strongly with the degree of confinement (**figure 3a**). These results are consistent with strong coupling of the excited state to surface bath modes in PNCs with high surface-to-volume ratios. We suggest that nanocrystal surface rigidification, for instance with suitable ligand chemistry, could significantly narrow the emission linewidth of PNCs.

Moreover, we find that the BX/X QY ratio depends both on the PNC size and halide composition, likely due to transitory charge carrier separation in PNCs with relaxed confinement (**figure 3b**). Our results have important implications for the technological application of PNCs. Highly confined bromide PNCs and mixed bromide/chloride PNCs exhibit BX/X QY ratios as low as ~2% rendering them potential single photon sources. Intermediately confined iodide PNCs display BX/X QY ratios of ~50%, possibly improving their performance in high flux LED applications.

Future Plans

In this project, we will continue to unravel the fundamental excitonic properties of lead-based perovskite nanomaterials. We will follow a synergistic approach combining the power of our photon-correlation based spectroscopies with targeted chemical synthesis. Specifically, we will investigate the effect of different chemical surface modifications of PNCs on the single PNC emission properties to identify ways to tailor the multiexciton emission quantum yield and the linewidth of single PNCs. Performing photon-correlation measurements on single PNCs at low temperatures, we will investigate the exciton fine-structure, exciton dephasing, and spectral diffusion in PNCs as a new quantum confined material.

References

- (1) Protesescu, L.; Yakunin, S.; Bodnarchuk, M. I.; Krieg, F.; Caputo, R.; Hendon, C. H.; Yang, R. X.; Walsh, A.; Kovalenko, M. V. Nanocrystals of Cesium Lead Halide Perovskites (CsPbX_3 , $X = \text{Cl, Br, and I}$): Novel Optoelectronic Materials Showing Bright Emission with Wide Color Gamut. *Nano Lett.* **2015**, *15*, 3692–3696.
- (2) Yakunin, S.; Protesescu, L.; Krieg, F.; Bodnarchuk, M. I.; Nedelcu, G.; Humer, M.; De Luca, G.; Fiebig, M.; Heiss, W.; Kovalenko, M. V. Low-Threshold Amplified Spontaneous Emission and Lasing from Colloidal Nanocrystals of Caesium Lead Halide Perovskites. *Nat. Commun.* **2015**, *6*, 8056.
- (3) Li, G.; Tan, Z. K.; Di, D.; Lai, M. L.; Jiang, L.; Lim, J. H. W.; Friend, R. H.; Greenham, N. C. Efficient Light-Emitting Diodes Based on Nanocrystalline Perovskite in a Dielectric Polymer Matrix. *Nano Lett.* **2015**, *15*, 2640–2644.
- (4) Park, Y. S.; Guo, S.; Makarov, N. S.; Klimov, V. I. Room Temperature Single-Photon Emission from Individual Perovskite Quantum Dots. *ACS Nano* **2015**, *9*, 10386–10393.
- (5) Cui, J.; Beyler, A. P.; Marshall, L. F.; Chen, O.; Harris, D. K.; Wanger, D. D.; Brokmann, X.; Bawendi, M. G. Direct Probe of Spectral Inhomogeneity Reveals Synthetic Tunability of Single-Nanocrystal Spectral Linewidths. *Nat. Chem.* **2013**, *5*, 602–606.
- (6) Beyler, A. P.; Bischof, T. S.; Cui, J.; Coropceanu, I.; Harris, D. K.; Bawendi, M. G. Sample-Averaged Biexciton Quantum Yield Measured by Solution-Phase Photon Correlation. *Nano Lett.* **2014**, *14*, 6792–6798.
- (7) Cui, J.; Beyler, A. P.; Marshall, L. F.; Chen, O.; Harris, D. K.; Wanger, D. D.; Brokmann, X.; Bawendi, M. G. Direct Probe of Spectral Inhomogeneity Reveals Synthetic Tunability of Single-Nanocrystal Spectral Linewidths. *Nat. Chem.* **2013**, *5*, 602–606.
- (8) Marshall, L. F.; Cui, J.; Brokmann, X.; Bawendi, M. G. Extracting Spectral Dynamics from Single Chromophores in Solution. *Phys. Rev. Lett.* **2010**, *105*, 1–4.

Publications

1. Caram JR, Bertram SN, Utzat H, Hess WR, Carr JA, Bischof TS, Beyler AP, Wilson MWB, Bawendi MG. PbS Nanocrystal Emission is Governed by Multiple Emissive States. *Nano Letters*. **2016**, 16 (10), 6070–6077.
2. Caram JR, Doria S, Eisele DM, Freyja FS, Sinclair TS, Rebentrost P, Lloyd S, Bawendi MG. Room Temperature Micron-Scale Exciton Migration in Stabilized Emissive Molecular-Aggregates. *Nano Letters*. **2016**, 16 (11), 6808-6815.
3. Bischof TS, Caram JR, Beyler AP, Bawendi MG. Extracting the average single molecule biexciton photoluminescence lifetime from a solution of chromophores. *Optics Letters*. **2016**, 270464.
4. Coropceanu I, Rossinelli A, Caram JR, Freyja FS, Bawendi MG. Slow-Injection Growth of Seeded CdSe/CdS Nanorods with Unity Fluorescence Quantum Yield and Complete Shell to Core Energy Transfer. *ACS Nano*. **2016**, 10(3), 3295-3301.
5. Han H-S, Niemeyer E, Huang Y, Kamoun WS, Martin JD, Bhaumik J, Chen Y, Roberge S, Cui J, Martin MR, Fukumura D, Jain RK, Bawendi MG, Duda DG. Quantum dot/antibody conjugates for in vivo cytometric imaging in mice. *Proceedings of the National Academy of Sciences of the United States of America*. **2015**, 112, 1350-1355.
6. Cui J, Beyler AP, Coropceanu I, Cleary L, Avila TR, Chen Y, Cordero JM, Heathcote SL, Harris DK, Chen O, Cao J, Bawendi MG. The Evolution of the Single-Nanocrystal Fluorescence Linewidth with Size and Shell: Implications for Exciton-Phonon Coupling and the Optimization of Spectral Linewidths. *Nano Letters*. **2015**, 16,289-296.
7. Bruns OT, Bischof TS, Harris DK, Shi Y, Riedemann L, Reiberger T, Barlelt A., Jaworski FB, Franke D, Wilson MWB, Chen O, Wei H, Hwang GW, Montana D, Coropceanu I, Kloepper J, Heeren J, Fukumura D, Jensen KF, Jain RK, Bawendi MG. Next generation in vivo optical imaging with short-wave infrared quantum dots. *Nature Biomedical Engineering*. **2017**,1.
8. Carr JA, Franke D, Caram JR, Perkinson CF, Askoxylakis V, Datta M, Fukumura D, Jain RK, Bawendi MG, Bruns OT, Shortwave Infrared Fluorescence Imaging with the Clinically Approved Near-Infrared Dye Indocyanine Green, *bioRxiv*. **2017**, doi: 10.1101/100768.

Submitted:

1. Utzat H, Shulenberger KE, Achorn OA, Nasilowski N, Sinclair TS, and Bawendi MG, Probing Linewidths and Biexciton Quantum Yields of Single Perovskite Nanocrystals in Solution, (*under revision, Nano Letters*).
2. Chen Y, Montana DM, Wei H, Cordero JM, Schneider M, Guével XL, Chen O, Bruns OT, Bawendi MG, Short-wave Infrared in vivo Imaging with Gold Nanoclusters, (*under revision, Nano Letters*).

Session 9

Program Title: Experimental studies of magnetism, correlations, and quantum criticality in a 2D electron system with point defects.

Principal Investigator: Eva Y. Andrei

**Mailing Address: Department of Physics, Rutgers University, 136 Frelinghuysen Rd,
Piscataway, NJ 08904**

I. Program Scope

The emergence of novel phases in the presence of electronic correlations, is one of the central problems in condensed matter physics. An example of this phenomenon is the so called Kondo effect in metals containing magnetic impurities, whereby coupling to the conduction electrons leads to screening of the magnetic moment, so that an initially magnetic material becomes non-magnetic as the temperature is lowered below a critical “Kondo temperature”. While the Kondo effect in conventional metals, where the density of states is flat and the conduction electrons are described by a Fermi liquid, has been studied extensively and is by now well understood, much less is known about Kondo screening in unconventional materials where the density of states exhibits pseudo-gap behavior.

This program aims to explore the emergence of physical phenomena and possible device applications associated with magnetism and its screening in low dimensional electron systems. We focus on graphene and other 2D materials with local magnetic moments induced by point defects, primarily vacancies. The pseudo-gap dispersion of electrons in graphene is expected to lead to unusual screening of magnetic moments that is characterized by a zero temperature quantum critical transition which separates magnetic from non-magnetic behavior. One particularly interesting consequence of this transition, that is unique to gateable 2D materials, is the possibility of tuning the presence and strength of Kondo screening by shifting the chemical potential away from charge neutrality with a gate voltage. Consequently it should be possible to switch the magnetic moments in graphene, on or off, with an electric field. This is important not only as a realization of a new class of quantum critical transitions, but also as a potential building block in spintronics applications.

Our strategy for achieving the program objectives is to start out by developing a fundamental understanding of the undisturbed 2D material of interest in its pristine form. 2D materials, being only one or few atoms thick, are extremely susceptible to external disturbances. As a result, the uncontrolled exposure to the environment such as substrates adsorbents or electrical leads can obscure their intrinsic properties. It is therefore critical to develop strategies to ensure minimally invasive experimental conditions. For example in our earlier DOE funded work we have demonstrated that it is possible to effectively isolate graphene from the environment by using a perfectly matched pristine substrate or by eliminating the substrate altogether in a suspended sample geometry. The former resulted in the first observation of Landau levels [1, 2] while the latter led to the discovery of ballistic transport on micrometer length scales in graphene [3]. For magneto-transport measurements we developed a technique to isolate these suspended samples from lead-induced perturbations resulting in the first observation of the fractional quantum Hall effect in graphene [4]. For accessing the intrinsic local electronic properties in STM measurements, where suspending the sample is not practical, we focused our efforts on finding ways to render the substrate minimally invasive. This resulted in stacking two layers of graphene one on top of the other which resulted in the first observation of twist-induced Van-Hove singularities, and in the demonstration of single layer behavior and decoupling from substrate in double graphene layers with large twist angle [5]. Armed with techniques to ensure access to the intrinsic electronic properties of 2D materials we are now in the process of exploring the consequences of controllably introducing local defects, various substrates and geometric constraints.

The research in this project utilizes a wide range of expertise and experimental techniques developed in our group. These include sample preparation and fabrication techniques and characterization tools [6] that allow us to access and probe the electronic properties of 2D systems and to follow their evolution with parameters such as distance from a point defect, with magnetic field, doping and local screening.

The characterization techniques deployed in this program cover a range of local probes such as low temperature scanning tunneling microscopy, scanning tunneling spectroscopy, Landau level spectroscopy, atomic force microscopy, intermediate range probes such as Raman spectroscopy, and global probes such transport and magneto-transport and Seebeck coefficient.

II. Recent Progress

Gate Controlled Kondo Screening of a Local Magnetic Moment in Graphene

Summary. Graphene in its pristine form has provided unprecedented access to novel electronic properties that emerge from its ultrarelativistic charge carriers. While the electronic properties have been the focal point of intense investigations, little attention was devoted to the magnetic properties of graphene. This is because graphene, similar to other Carbon allotropes, is non-magnetic. In fact it is one of the most diamagnetic non-superconducting materials. Our recent work has centered on the emergence of magnetism in graphene when its perfect honeycomb lattice is disrupted by single atom vacancies. Using scanning tunneling microscopy (STM) and spectroscopy (STS), and numerical renormalization group calculations (NRG), we have shown that vacancies enable to host, control and manipulate the spin degree of freedom in graphene. Moreover they provide direct access to the physics of Kondo screening in a pseudogap system. Highlights of our findings include:

1) Using the spectroscopic signature of Kondo screening we showed that the local magnetic moment hosted by a vacancy in graphene is screened below a certain temperature allowing to extract the Kondo temperature for each vacancy.

2) Demonstrated that Kondo screening can be controlled by a gate voltage.

3) Discovered that Kondo screening in this system strongly depends on the local curvature.

4) Mapped the hitherto elusive quantum phase transition separating magnetically screened from non-screened states in a pseudogap system.

5) The ability to control the magnetic moment by a gate voltage and by the local curvature demonstrated in this work paves the way to electrostatic and mechanical control of magnetism.

This work is summarized in a manuscript which is currently under review.

Recent progress on other aspects of this project, was reported in the publications listed at the end of this document.

Background. In normal metals, the magnetic moment of impurity spins disappears below a characteristic “Kondo temperature”, T_K , that marks the formation of an entangled state of polarized conduction-band electrons which screen the local moment. In contrast, moments embedded in insulators remain unscreened at all temperatures. This raises the question about the fate of magnetic moments in intermediate pseudogap systems, such graphene and high T_c superconductors, which are gapless but have a vanishing density of states (DOS) at the Fermi energy, E_F . In these systems theory predicts a quantum phase-transition at a critical coupling strength which separates a magnetic phase from a Kondo-screened phase, as depicted in Fig.1D. However, attempts to experimentally confirm the existence of this phase transition and the intriguing physical phenomena it entails, such as the very large values of T_K and the possibility to electrostatically control the magnetic moment, have thus far been elusive.

Graphene, with its linear DOS and tunable chemical potential, provides a playground for exploring the physics of this magnetic quantum phase-transition. We focused on the magnetic moments induced at the site of single-atom vacancies in graphene. The removal of a carbon atom from the honeycomb lattice induces a magnetic moment stemming from the unpaired electrons at the vacancy site. This moment has two contributions, one due to the removal of an electron from the π band and the other from the unpaired electrons in the broken σ -orbitals. The former couples ferromagnetically to the conduction electrons, which precludes it from contributing to the Kondo effect. In perfectly flat graphene the contribution from the broken σ -bonds is similarly unscreened because the σ orbital is orthogonal to the π -orbital conduction band. However, this constraint is removed in the presence of a local curvature which projects the σ orbital out of the plane and removes the orthogonality with the π -band. The highly flexible nature of the graphene membrane thus makes it possible to tune the hybridization strength and to generate Kondo screening of

the σ orbital moment by introducing a local curvature. This allowed us to control the magnetic moment at the atomic scale and to study the gate tunable pseudogap Kondo physics over coupling strengths ranging from subcritical to supercritical.

The question of whether or not Kondo screening occurs in graphene has been under debate for quite some time, owing to contradictory conclusions drawn from magnetometry and resistivity measurements. On the one hand, magnetometry measurements on irradiated graphene embedded in graphite laminates showed vacancy induced magnetism with Curie behavior and no evidence of Kondo screening down to the lowest experimental temperatures, consistent with the early theoretical predictions. In contrast, resistivity measurements on irradiated single layer exfoliated graphene, did reveal a resistivity minimum and logarithmic scaling indicative of Kondo screening with unusually large values of $T_K \sim 90\text{K}$.

Our work, owing to its local nature and the wide range of the local coupling-strengths, addressed the contradiction between the earlier measurements and helped resolve it. Both earlier measurements were global in nature and each was sensitive to a different aspect of the problem. Magnetometry probes the magnetic moment and therefore only sees vacancies that are not screened, while transport, which is sensitive to the enhanced scattering from the Kondo cloud, is only sensitive to vacancies whose moment is Kondo screened. Therefore, in the presence of variations in the local coupling-strengths these techniques, being sensitive to complementary properties, have led to opposite conclusions. The local nature of our spectroscopy measurements resolved this ambiguity. It made it possible to correlate Kondo screening with the local curvature and with the chemical potential and to identify the quantum phase transition between a screened and an unscreened spin.

Experimental techniques and findings. We employed a local spectroscopic technique, STS, to identify Kondo screening of the vacancy magnetic moment by the distinctive zero-bias resonance it produces in the DOS. Our study covering several hundred vacancies on different substrates over a wide range of coupling strengths revealed the characteristic signatures of pseudogap Kondo screening, including the existence of a critical coupling strength and the strong dependence of screening on the carrier density. The ability to tune the Kondo screening by means of a gate voltage provides a mechanism for electrostatic switching between magnetic and non-magnetic states.

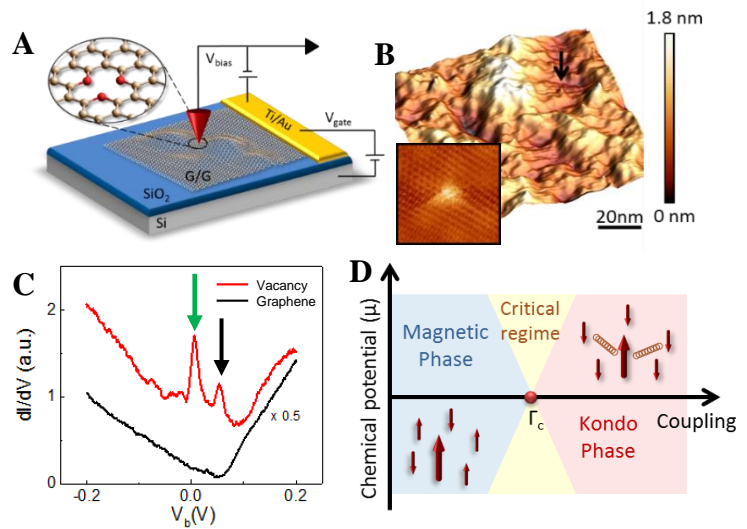


Figure 1. Kondo-peak at a vacancy in graphene. (A) Schematics of the experimental set up. Sample consists of a twisted double layer graphene supported on an SiO_2 substrate. (B) STM topography of the G/G/ SiO_2 surface. The arrow indicates an isolated vacancy. Inset: atomic resolution topography of a single atom vacancy shows the triangular interference pattern characteristic of single atom vacancies in graphene. (C) dI/dV spectra at the vacancy center (top curve) and far from it (bottom curve). Green arrow shows the position of the Kondo resonance and black arrow marks the zero-mode peak (D) Schematic phase diagram of the pseudo-gap Kondo effect. The critical regime (yellow) separates the magnetic phase (unscreened moment) from the Kondo phase (screened moment). Arrows represent the ground state of the system with the large arrow corresponding to the vacancy spin and the smaller ones belonging to the conduction band electrons.

III. Future Plans

Our recent results have shown that it is possible to tune the Kondo transition in graphene with a gate voltage. This is important not only as a realization of a new class of quantum critical transitions, but also

as a potential building block in spintronics applications. In view of these findings we will continue to explore physical phenomena and possible device applications associated with magnetism and Kondo screening in low dimensional electron systems. One of the offshoots of the present work is to explore the effect of magnetic moments and their Kondo screening on the thermal properties of the material. We will measure the Seebeck and Nernst coefficients in irradiated graphene to investigate the possibility of thermal switching by electrostatic gating across the Kondo transition. In addition to our graphene work we will explore the emergence of local magnetic moments induced by point defects, in various 2D layers including MoS₂ and other transition metal dichalcogenides.

The experimental probes will include thermal transport, scanning tunneling microscopy and spectroscopy, Landau level spectroscopy, atomic force microscopy and magneto transport. Substrates will include atomically flat hBN as well as exfoliated thin layers of small gap transition metal dichalcogenide crystals.

IV. References

- [1] G. Li, E.Y. Andrei, Observation of Landau levels of Dirac fermions in graphite, *Nature Physics*, 3 (2007) 623-.
- [2] G. Li, A. Luican, E.Y. Andrei, Scanning Tunneling Spectroscopy of Graphene on Graphite, *Physical Review Letters*, 102 (2009) 176804.
- [3] X. Du, I. Skachko, A. Barker, E.Y. Andrei, Approaching ballistic transport in suspended graphene, *Nature Nanotechnology*, 3 (2008) 491-495.
- [4] X. Du, I. Skachko, F. Duerr, A. Luican, E.Y. Andrei, Fractional quantum Hall effect and insulating phase of Dirac electrons in graphene, *Nature*, 462 (2009) 192.
- [5] A. Luican, G. Li, A. Reina, J. Kong, R.R. Nair, K.S. Novoselov, A.K. Geim, E.Y. Andrei, Single-Layer Behavior and Its Breakdown in Twisted Graphene Layers, *Physical Review Letters*, 106 (2011) 126802.
- [6] G. Li, A. Luican, E.Y. Andrei, Self-navigation of an STM tip toward a micron sized sample, *Rev. Sci. Instrum.*, 82 (2011).

V. Recent Publications acknowledging DOE support

- Gate Controlled Kondo Screening of a Local Magnetic Moment in Graphene, J. Mao, Y. Jiang, PW Lo, D. May, G. Li, GY Guo, F. Anders and E. Y. Andrei, *Science* under review.
- Tuning a Circular p-n Junction in Graphene from Quantum Confinement to Optical Guiding, Y. Jiang, J. Mao, D. Moldovan, M. Ramezani Masir, G. Li, K. Watanabe, T. Taniguchi, F. M. Peeters and E. Y. Andrei, *Nature Nanotechnology* (2017) in press.
- Observing a Scale Anomaly in Graphene: A Universal Quantum Phase Transition, O. Ovdad, J. Mao, Y. Jiang, E. Y. Andrei, and E. Akkermans, *Nature Communications* (2017) in press.
- Visualizing Strain-Induced Pseudo Magnetic Fields in Graphene through an hBN Magnifying Glass, Y. Jiang, J. Mao, J. Duan, X. Lai, K. Watanabe, T. Taniguchi, F. M. Peeters and E. Y. Andrei, *Nano Lett.*, 17, 2839 (2017)
- Realization of a Tunable Artificial Atom at a Charged Vacancy in Graphene, J. Mao, Y. Jiang, D. Moldovan, G. Li, K. Watanabe, T. Taniguchi, M.R. Masir, F. M. Peeters, E.Y. Andrei, *Nature Physics* 12, 545–549 (2016)
- High Thermoelectric Power Factor in Graphene/hBN Devices, J. Duan, X. Wang, X. Lai, G. Li, T. Taniguchi, K. Watanabe, M. Zebarjadi, E. Y. Andrei, *PNAS* 113 (50) 14272 (2016)
- Local and Global Screening Properties of Graphene Revealed through Landau Level Spectroscopy, C.P. Lu, M. Rodriguez-Vega, G. Li, A. Luican, K. Watanabe, T. Taniguchi, E. Rossi, E.Y. Andrei *PNAS* 113, 6623, (2016)
- Localized electronic states at grain boundaries on the surface of graphene and graphite, A. Luican-Mayer *et al* *2D Materials* 3, 031005, (2016)
- Fold-assisted transport in graphene systems, R. Carrillo-Bastos, C. Leon, D. Faria, A. Latge, E.Y. Andrei, and N. Sandler, *Phys. Rev. B* 94, 125422 (2016)
- Nanoscale Internal Fields in a Biased Graphene–Insulator–Semiconductor Structure, Sylvie Rangan *et al*, *The Journal of Physical Chemistry Letters* 7 (17), 3434 (2016)

Symmetries, Interactions and Correlation Effects in Carbon Nanotubes

Gleb Finkelstein, Physics Department, Duke University, Durham, NC 27708

Program Scope

1) The PI's group has developed a unique platform for studying the effects of dissipation and interactions in "quantum impurity" systems, which is based on carbon nanotube quantum dots with dissipative leads. Here, the quantum dot plays the role of the quantum impurity, while the leads provide interactive environment in which it is embedded. Our earlier works identifier a quantum critical point (QCP) in this system, which is enabled by dissipation / interactions in the leads [1,2]. We are now particularly interested in probing non-equilibrium physics at the QCP. Non-equilibrium phenomena in interacting quantum systems are notoriously difficult, and we are exploring them in collaboration with Harold Baranger (supported by DOE CMT program).

2) The second major research direction is the study of the graphene-based Josephson junctions [technically, "superconductor-normal metal-superconductor" (SNS) junctions.] These junctions have attracted intense interest of the condensed matter community with the development of ballistic encapsulated graphene. In the past year, we have investigated all the known SNS regimes, namely: diffusive, short and long ballistic.

Recent Progress

1) The non-linear I-V curves at an interacting quantum critical point (QCP) are hard to measure and typically out of reach theoretically. We have measured the I-V curves at the QCP that we have previously identified [1,2] for different strength of dissipation and confirmed the empirical scaling relation that we have proposed earlier. The availability of the data allowed our theory colleagues to calculate these curves, both numerically and analytically. We find that the measurement and the calculation match without fitting parameters. To our knowledge, this is the only example in which a full understanding of the non-equilibrium regime at the QCP has been achieved. The manuscript is under review at PRX (<https://arxiv.org/abs/1609.04765>).

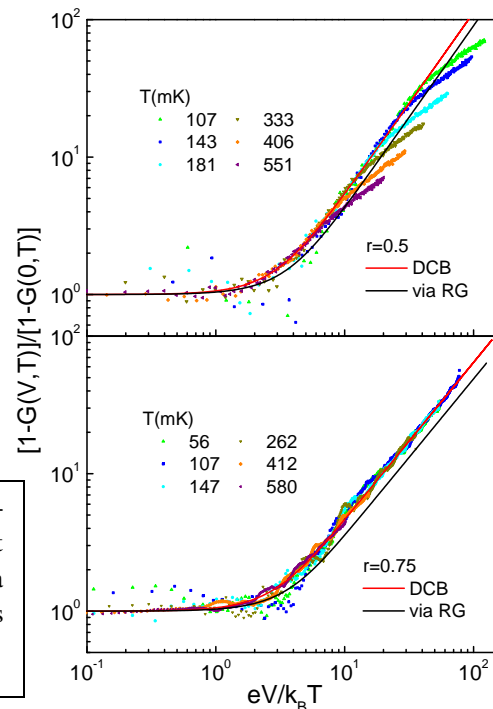


Figure 1. Universal scaling of differential conductance in the non-equilibrium regime (bias comparable or larger than temperature) at the QCP. The DCB line is the analytical theory, while RG is a numerical approximation. The data are measured on two samples with a different dissipation strength ($r=0.5$ and 0.75).

2) We recently studied SNS (superconductor-normal-superconductor) junctions made of graphene encapsulated in hexagonal boron nitride, h-BN (Figure 2a). The junctions are ballistic, as could be judged from Figure 2b, which demonstrates that the normal state conductance G_N divided by the junction width W does not change with the lengths of the junctions. Furthermore, for N-doping (positive V_G), the conductance is very close to the quantum limit $G_0 = Ne^2/h$ (yellow dashed line; here N is the number of transverse electron modes.) For P-doping, the conductance is suppressed due to the PN junctions formed at each contact interface.

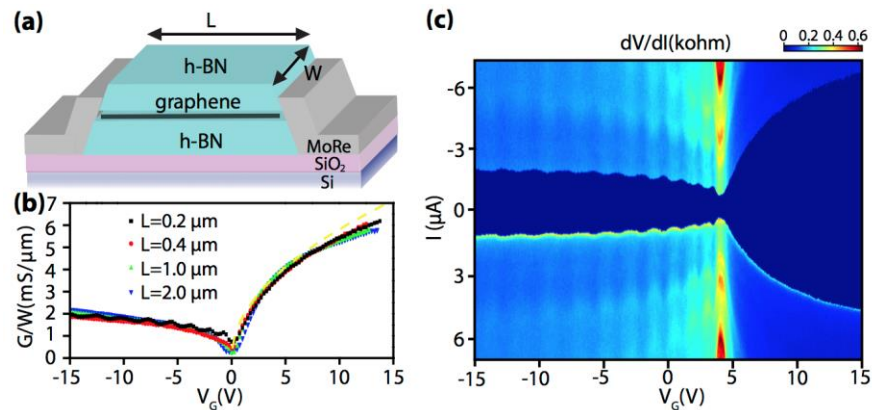


Figure 2. a) Schematic of a Josephson junction made of graphene encapsulated in h-BN, contacted by superconducting molybdenum-rhenium leads. (b) Gate dependence of the normal state conductance G for several channel lengths, demonstrating the length independent (ballistic) sample conductance. (c) Differential resistance dV/dI (plotted vs. gate and bias) vanishes in the superconducting regime (dark region).

Figure 2c shows the differential resistance dV/dI of the 200-nm long junction measured vs. I and V_G . The dark region around zero bias corresponds to the supercurrent, I_C . At negative voltages, the Fabry-Perot oscillations are visible due to the partial reflections from the PN interfaces in both the magnitude of the supercurrent (extent of the dark region) and the normal resistance (vertical blue stripes).

In Figure 3, we extract the values of the critical current for the same set of junctions and plot them vs. temperature. $I_C(T)$ shows exponential scaling which has been predicted for ballistic junctions in the '70s, but to our knowledge had not been observed before.

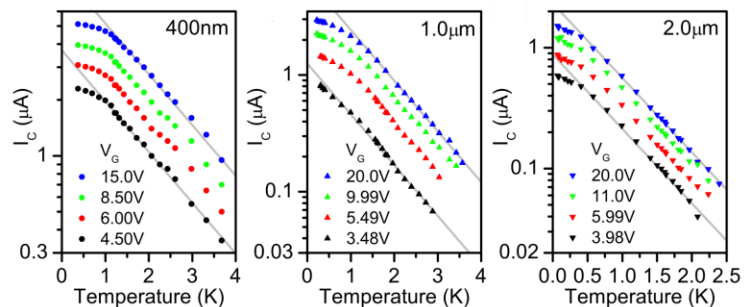


Figure 3. Critical current for 3 junctions of length $L = 0.4, 1,$ and 2 microns (see labels), plotted on a semi-log scale vs. T . Several gate voltages are presented for each junction. At higher temperatures the critical current is found to scale as $\exp(-k_B T / \delta E)$, as predicted for the ballistic junctions. The slope of $\log(I_C)$ vs. T is found to be independent of V_G . Indeed, in graphene junctions, $\delta E \approx \hbar v_F / 2\pi L$ is expected to be independent of the carrier density and inversely proportional to L .

Finally, in the same type of samples, we demonstrated that superconducting current could flow in the quantum Hall regime. To observe Landau quantization in a small ballistic sample, the magnetic field B should be large enough for the cyclotron orbits to fit within the sample boundaries: $B > \hbar k_F / \pi e L$. At these high fields (typically $B \sim 1$ T), we found that a very small superconducting current (~ 1 nA) may still flow through the sample (Figure 4). The superconducting branch is clearly visible at the lowest temperature (40 mK) but gets washed away by phase diffusion at $T \sim 0.5$ K.

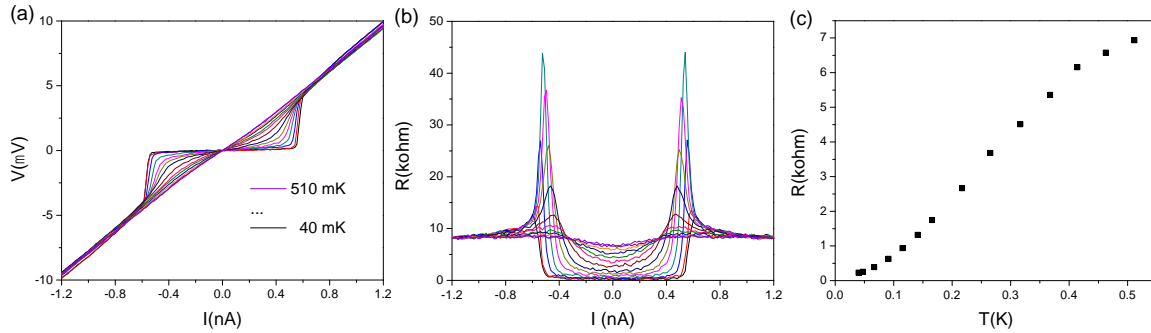


Figure 4. a) V-I curves measured at $B = 1$ T and $\nu = 2$ in the temperature range 40-500 mK. The supercurrent branch is clearly visible at the lowest temperature (40 mK) for $I < 0.5$ nA. b) The temperature dependence of the dV/dI curves. The differential resistance is suppressed at zero bias and peaks at ~ 0.5 nA where the junction switches from the superconducting to the normal branch. c) The suppressed zero-bias resistance is gradually washed away by $T \sim 0.5$ K due to the phase diffusion mechanism.

The supercurrent shows extreme sensitivity to magnetic field, exhibiting a robust interference pattern with a period of $\delta B \sim 0.5$ mT, corresponding to the flux quantum threaded through the sample circumference. The periodicity implies that the supercurrent is carried by the edge states. Our result demonstrates that the QH edge states in graphene can be reliably coupled to a superconductor.

Future Plans

1. a) We plan to further explore the non-equilibrium regime achieved by biasing the nanotube quantum dot at the QCP [1-2]. We will create tunnel probe (separate from the two contacts creating the non-equilibrium) by covering the nanotube with a narrow h-BN (2-4 monolayers) using the techniques developed for graphene. On top of the h-BN, we will place a tunnel electrode, which could be either metallic or made from graphene to match the nanotube work function. The measurement will provide information analogous to the density of states but in a highly correlated and non-equilibrium regime. b) We will create double quantum dots by using the same type of nanotube samples with a h-BN top layer as discussed in (a). However, using a thicker h-BN layer will allow us to create a top gate instead of the tunneling electrode. We will explore the double dot in dissipative environment, searching for the new type of a quantum phase transition (QPT) between the singlet and the “Kondo molecule” predicted recently by Harold Baranger and his group. c) In addition to the more ambitious projects (a-b),

we are continuing to work on a topic outlined in the original proposal: spinful resonant level with dissipation, including the Kondo effect with dissipation.

2) We are particularly interested in using graphene to explore systems with tunable dissipation. Many predictions exist for quantum phase transitions that should occur as a function of dissipation, both in Josephson junctions and in non-superconducting systems. Bilayer graphene, whose resistance could be changed in a wide range, is particularly promising. In the simplest case, a Josephson junction and its dissipative leads could be made from the same graphene crystal. The resistance of the leads could be then tuned by dedicated gates, allowing one to explore the dissipation-driven superconducting-insulator transition in a *single* junction, previously accessible only by fabricating a series of samples with different dissipation. We will also explore using graphene as a tunable dissipative element in the nanotube quantum dots.

References

1. H.T. Mebrahtu, I.V. Borzenets, D.E. Liu, H. Zheng, Y.V. Bomze, A.I. Smirnov, H.U. Baranger and G. Finkelstein, *Quantum phase transition in a resonant level coupled to interacting leads*. **Nature** **488**, p. 61-64 (2012).
2. H.T. Mebrahtu, I.V. Borzenets, H. Zheng, Y.V. Bomze, A.I. Smirnov, S. Florens, H.U. Baranger and G. Finkelstein, *Observation of Majorana quantum critical behavior in a resonant level coupled to a dissipative environment*. **Nature Physics** **9**, p. 732 (2013).

Publications in 2016-2017

1. F. Amet, C.T. Ke, I.V. Borzenets, Y.-M. Wang, K. Watanabe, T. Taniguchi, R.S. Deacon, M. Yamamoto, Y. Bomze, S. Tarucha, G. Finkelstein, *Supercurrent in the quantum Hall regime*, **Science** **352**, p. 966-969 (2016). <http://science.sciencemag.org/content/352/6288/966>
2. I.V. Borzenets, F. Amet, C.T. Ke, A.W. Draelos, M.T. Wei, A. Seredinski, K. Watanabe, T. Taniguchi, M. Yamamoto, S. Tarucha, G. Finkelstein, *Ballistic graphene Josephson junctions from the short to the long junction regime*, **Physical Review Letters** **117**, 237002 (2016). <http://dx.doi.org/10.1103/PhysRevLett.117.237002>
3. Chung-Ting Ke, Anne W. Draelos, Ivan V. Borzenets, Gareth Jones, Monica Craciun, Francois Amet, Michihisa Yamamoto, Yuriy Bomze, Saverio Russo, Seigo Tarucha, and Gleb Finkelstein, *Critical current and Thouless energy in long diffusive graphene-based Josephson junctions*, **Nano Letters** **16**, p. 4788 (2016). <http://dx.doi.org/10.1021/acs.nanolett.6b00738>
4. G. Zhang, C.-H. Chung, C.T. Ke, C.-Y. Lin, H. Mebrahtu, A.I. Smirnov, G. Finkelstein, H.U. Baranger, *Universal Nonequilibrium I-V Curve at an Interacting Impurity Quantum Critical Point*, Submitted to **Physical Review X** (2017). <https://arxiv.org/abs/1609.04765>

August, 2017

Novel SP²-bonded Materials and Related Nanostructures

PI: Alex Zettl, Lawrence Berkeley National Laboratory and UC Berkeley. Co PI's: Marvin Cohen, Lawrence Berkeley National Laboratory and UC Berkeley; Michael Crommie, Lawrence Berkeley National Laboratory and UC Berkeley; Alessandra Lanzara, Lawrence Berkeley National Laboratory and UC Berkeley; Steven Louie, Lawrence Berkeley National Laboratory and UC Berkeley

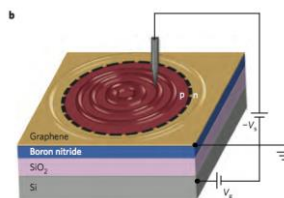
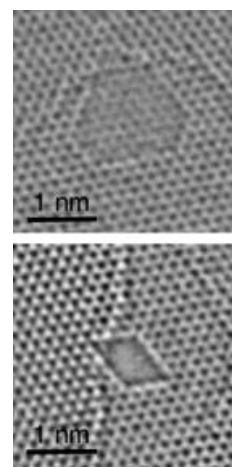
Program Scope

Experimental and theoretical investigation of nanostructures based on sp²-bonded carbon and boron nitride, and related layered or low-D materials. Experimental approaches encompass synthesis, and characterization utilizing STM, AFM, ARPES, TEM, transport, and mechanical properties. Theory includes ab-initio approaches.

Recent Progress

Electrostatic confinement of charge carriers in graphene is governed by Klein tunnelling, a relativistic quantum process in which particle-hole transmutation leads to unusual anisotropic transmission at p-n junction boundaries. Reflection and transmission at these boundaries affect the quantum interference of electronic waves, enabling the formation of novel quasi-bound states. We have used scanning tunnelling microscopy to map the electronic structure of Dirac fermions confined in quantum dots defined by circular graphene p-n junctions. The quantum dots were fabricated using a technique involving local manipulation of defect charge within the insulating substrate beneath a graphene monolayer. Inside such graphene quantum dots we observe resonances due to quasi-bound states and directly visualize the quantum interference patterns arising from these states. Outside the quantum dots Dirac fermions exhibit Friedel oscillation-like behaviour. Bolstered by a theoretical model describing relativistic particles in a harmonic oscillator potential, our findings yield insights into the spatial behavior of electrostatically confined Dirac fermions.

The atomic structure, stability, and dynamics of defects in hexagonal boron nitride (h-BN) has been investigated using an aberration-corrected transmission electron microscope operated at 80 kV between room temperature and 1000 °C. At temperatures above 700 °C, parallelogram- and hexagon-shaped defects with zigzag edges become prominent, in contrast to the triangular defects typically observed at lower temperatures. The appearance of 120° corners at defect vertices indicates the coexistence of both N- and B-terminated zigzag edges in the same defect. In situ dynamics studies show that the hexagonal holes grow by electron-induced sputtering of B-N chains, and that at high temperatures these chains can migrate from one defect corner to another. We complement the experiments with first-principles calculations which consider the thermal equilibrium formation



TEM images of tailored holes in hBN (top) and schematic for STM-induced quantum wells in graphene over hBN (bottom)

energy of different defect configurations. It is shown that, below a critical defect size, hexagonal defects have the lowest formation energy and therefore are the more-stable configuration, and triangular defects are energetically metastable but can be “frozen in” under experimental conditions. We have also explored the possible contributions of several dynamic processes to the temperature-dependent defect formation.

We have performed a combined scanning tunneling microscopy/spectroscopy and GW theoretical study of the electronic structure of high quality single- and few-layer MoSe₂ grown on bilayer graphene. We find that the electronic (quasiparticle) bandgap, a fundamental parameter for transport and optical phenomena, decreases by nearly one electron volt when going from one layer to three due to interlayer coupling and screening effects. Our results show a clear picture of the evolution of the electronic wavefunction hybridization in the valleys of both the valence and conduction bands as the number of layers is changed. This demonstrates the importance of layer number and electron-electron interactions on van der Waals heterostructures, and helps to clarify how their electronic properties might be tuned in future 2D nanodevices.

Future Plans

We shall explore the local electronic properties of new nanoscale quantum structures built on single-layer and bilayer graphene using novel fabrication techniques that are compatible with TEM and scanned probe microscopy. For example, arrays of tailored holes in BN will be mated to graphene monolayers or bilayers, thereby inducing random or periodic potentials. Tests will be performed for unusual plasmonic effects and supercollimation. Multi-quantum-dot systems will be fabricated on single-layer graphene by injecting space charge directly into the insulating BN substrate using the STM tip in order to create local gates beneath the graphene. This will allow the exploration of inter-dot hybridization in a completely new quantum regime where interactions are driven by Dirac fermions undergoing relativistic Klein tunneling rather than conventional nonrelativistic tunneling. Our new local gating technique will allow fabrication of graphene quantum dots of arbitrary shape, enabling wavefunction imaging of quantum-chaotic systems in the unexplored ultra-relativistic regime. Quantum dots fabricated in bilayer graphene are expected to behave very differently from monolayer graphene quantum dots since electrons incident on bilayer pn boundaries are predicted to undergo anti-Klein tunneling. We will explore the local electronic properties of bilayer quantum dots in this new physical regime at the surface of BN-supported field-effect transistors. In addition to local gating through space-charge patterning of insulating substrates (as described above) we will also use atomic and molecular patterning directly at the surface of graphene layers in order to create and image quantum-confined structures that have more well-defined edges at the atomic scale and that exhibit new engineered topologies.

Using the ab initio GW and GW-BSE approach, we shall explore theoretically the electric field induced bandgap and optical spectrum of biased bilayer graphene. In particular, we investigate the importance of electron-hole interaction (excitonic) effects and band topology on the optical response of this system.

We shall also investigate theoretically the structure and properties of Ir atoms, dimers and clusters on graphene through first-principles calculations. The work seeks to understand the

scanning tunneling microscopy results and the influence of strong spin-orbit interactions of Ir on the combined system.

Publications

- 1) A. J. Bradley, M. M. Ugeda, F. H. da Jornada, D.Y. Qiu, W. Ruan, Y. Zhang, S. Wickenburg, A. Riss, J. Lu, S. K. Mo, Z. Hussain, Z.X. Shen, S. G. Louie, and M. F. Crommie, "Probing the Role of Interlayer Coupling and Coulomb Interactions on Electronic Structure in Few-Layer MoSe₂ Nanostructures" *Nano Lett.* **15**, 2594 (2015).
- 2) A. Yan, W. Chen, C. Ophus, J. Ciston, Y. Lin, K. Persson, and A. Zettl. "Identifying different stacking sequences in few-layer CVD-grown MoS₂ by low-energy atomic-resolution scanning transmission electron microscopy," *Phys. Rev. B*, **93**, 041420(R) doi: 10.1103/PhysRevB.93.041420 (2016).
- 3) J. Velasco, Jr., L. Ju, D. Wong, S. Kahn, J. Lee, H.-Z. Tsai, C. Germany, S. Wickenburg, J. Lu, T. Taniguchi, K. Watanabe, A. Zettl, F. Wang, and M.F. Crommie. "Nanoscale control of rewriteable doping patterns in pristine graphene/boron nitride heterostructures," *Nano Letters*, 2016, **16** (3) 1620–1625, doi: 10.1021/acs.nanolett.5b04441 (2016).
- 4) H. Long, A. Harley-Trochimczyk, T. He, T. Pham, Z. Tang, T. Shi, A. Zettl, W. Mickelson, C. Carraro, and R. Maboudian. "In-situ localized growth of porous tin oxide films on low power microheater platform for low temperature CO detection," *ACS Sensors* (2016) **1** (4) 339–343 doi: 10.1021/acssensors.5b00302.
- 5) Y. Sasaki, R. Kitaura, J.M. Yuk, A. Zettl, and H. Shinohara. Efficient preparation of graphene liquid cell utilizing direct transfer with large-area well-stitched graphene." *Chem Phys Lett.* **650**, pp107-112, doi: 10.1016/j.cplett.2016-02-066 (2016)
- 6) H. Long, A. Harley-Trochimczyk, T. Pham, Z. Tang, T. Shi, A. Zettl, C. Carraro, M.A. Worsley, and R. Maboudian. "High Surface Area MoS₂/Graphene Hybrid Aerogel for Ultrasensitive NO₂ Detection Advanced Functional Materials" DOI: 10.1002/adfm.201601562
- 7) J. Lee, D. Wong, J. Velasco, Jr., J.F. Rodriguez-Nieva, S. Kahn, H.-Z. Tsai, T. Taniguchi, K. Watanabe, A. Zettl, F. Wang, L.S. Levitov, and M.F. Crommie. "Imaging Electrostatically Confined Dirac Fermions in Graphene Quantum Dots." *Nat Phys.* doi: 10.1038/nphys3805 (2016).
- 8) S. Onishi, M. Moreno Ugeda, Y. Zhang, Y. Chen, C. Ojeda-Aristizabal, H. Ryu, S.-K. Mo, Z. Hussain, Z.-X. Shen, M. Crommie, and A. Zettl. "Selenium capped monolayer NbSe₂ for two-dimensional superconductivity studies." *Physica Status Solidi B*, doi: 10.1002/pssb.201600235 (2016).
- 9) H. Rasool, G. Dunn, A. Fathalizadeh, and A. Zettl. "Graphene-sealed Si/SiN cavities for high-resolution in-situ EM of nanoconfined solutions." *Physica Status Solidi B: Basic Solid State Physics* DOI: 10.1002/pssb.201600232 (2016)
- 10) H. Reza Barzegar, T. Pham, A.V. Talyzin, and A. Zettl. "Synthesis of graphene nanoribbons inside boron nitride nanotubes." *Physica Status Solidi B: Basic Solid State Physics*, doi: 10.1002/pssb.201600294 (2016)
- 11) O. Ergen, S.M. Gilbert, S.J. Turner, and A. Zettl. "Hexagonal boron nitride as a cationic diffusion barrier to form a graded band gap perovskite heterostructure." *Physica Status Solidi B*, advance online publication, doi: 10.1002/pssb.201600234 (2016)

- 12) T. Pham, A.L. Gibb, S.M. Gilbert, C. Song, and A. Zettl. "Formation and dynamics of electron-irradiation-induced defects in hexagonal boron nitride at elevated temperatures." Nano Letters DOI: 10.1021/acs.nanolett.6b03442
- 13) T. Sun, J. Kim, J.M. Yuk, A. Zettl, F. Wang, and C. Chang-Hasnain. "Surface-normal electro-optic spatial light modulator using graphene integrated on a high-contrast grating resonator." Optics Express <https://doi.org/10.1364/OE.24.026035>
- 14) O. Ergen, S.M. Gilbert, T. Pham, S.J. Turner, M.T.Z. Tan, M.A. Worsley, and A. Zettl. "Graded band gap perovskite solar cells. Nature Materials doi:10.1038/nmat4795
- 15) 14) X. Ye, M.R. Jones, L.B. Frechette, Q. Chen, A.S. Powers, P. Ercius, G. Dunn, G.M. Rotskoff, S.C. Nguyen, V.P. Adiga, A. Zettl, E. Rabani, P.L. Geissler, and A.P. Alivisatos. "Single-particle mapping of nonequilibrium nanocrystal transformations." Science, 354, 6314, p. 874, doi: 10.1126/science.aah4434 (2016).
- 16) A. Rao, H. Long, A. Harley-Trochimczyk, T. Pham, A. Zettl, C. Carraro, and R. Maboudian. "In Situ Localized Growth of Ordered Metal Oxide Hollow Sphere Array on Microheater Platform for Sensitive, Ultra-Fast Gas Sensing." ACS Applied Materials and interfaces. Volume 9, issue 3, pg 2634-2641. DOI: 10.1021/acsami.6b12677
- 17) S. Onishi, M. Jamei, and A. Zettl. "Narrowband noise study of sliding charge density waves in NbSe₃ nanoribbons." New Journal of Physics. Vol 19, article number 023001 DOI: 10.1088/1367-2630/aa5912
- 18) Claudia Ojeda-Aristizabal, Elton J. G. Santos, Seita Onishi, Aiming Yan, Haider I. Rasool, Salman Kahn, Yinchuan Lv, Drew W. Latzke, Jairo Velasco Jr, Michael F. Crommie, Matthew Sorensen, Kenneth Gotlieb, Chiu-Yun Lin, Kenji Watanabe, Takashi Taniguchi, Alessandra Lanzara, and Alex Zettl "Molecular Arrangement and Charge Transfer in C60/Graphene Heterostructures." ACS Nano DOI: 10.1021/acsnano.7b00551
- 19) Dillon Wong, Fabiano Corsetti, Yang Wang, Victor W. Brar, Hsin-Zon Tsai, Qiong Wu, Roland K. Kawakami, Alex Zettl, Arash A. Mostofi, Johannes Lischner, and Michael F. Crommie "Spatially resolving density-dependent screening around a single charged atom in graphene." Phys Review B <https://doi.org/10.1103/PhysRevB.95.205419>
- 20) Hu Long, Leslie Chan, Anna Harley-Trochimczyk, Lunet E. Luna, Zirong Tang, Tielin Shi, Alex Zettl, Carlo Carraro, Marcus A. Worsley, Roya Maboudian. "3D MoS₂ Aerogel for Ultrasensitive NO₂ Detection and Its Tunable Sensing Behavior." Advanced Materials Interfaces doi.org/10.1002/admi.201700217

Program Title: Charge and Energy Transfer in Molecular Superconductors and Molecular Machines

Principal Investigator: Saw Wai Hla

Mailing Address: 251B Clippinger Lab, Physics & Astronomy Department, Ohio University, Athens, OH 45701.

Email: hla@ohio.edu

Program Scope

This proposal seeks to advance our understanding and control over charge and energy transfer processes as well as spintronic behaviors of exotic molecular materials including individual molecular machines and molecular superconductors on materials surfaces. For the molecular machine research, we investigate individual molecular motors, and molecular transport devices operating at the quantum regime on surfaces using advanced scanning probe techniques at low temperature in ultrahigh environment. For molecular superconductivity research, we study atomic level interactions between the molecular superconducting clusters and two dimensional electron gas as well as manipulation of molecular charge density waves. As a part of the project, we also develop novel instrumentation techniques such as synchrotron X-ray tunneling microscopy and spectroscopy to advance our fundamental understanding of materials properties in quantum regimes. Our project includes both conventional and innovative components, and the achievements of these projects will impact on fundamental understanding of charge and energy transfer processes in exotic molecular materials for potential applications in energy sciences.

Recent Progress

We have made progress in a number of research fronts. We have completed our research on finding how charge and energy transfer in molecular motors couple to spintronic and mechanical properties. Here, molecular legs act as a pseudo insulating system to maintain the charge but the whole motor exhibits a Kondo resonance indicating coupling of spin to the substrate. We have also explored similar system that exhibits a Kondo resonance by isolating magnetic molecules with semiconducting nanoribbons on Au(111) surface [1]. For the synchrotron based scanning probe microscope development, we are able to distinguish X-ray excited tunneling and photo-ejected current process [2], which is an important step to determine to measure charge and energy transfer processes in molecular systems. In the following, we describe completed research projects under this grant.

I. Transient Kondo resonance in molecular motors

A nanomotor consumes energy and converts it into mechanical motion or work. In the previous DOE supported grant period, we have demonstrated controlled clockwise and counterclockwise rotation of a molecular motor by injecting tunneling electrons into specific parts of a molecular motor [Perera et al., Nature Nanotechnol. 8, 46-51 (2013)]. Our goal in the current project is to understand how the charge and energy are transfer processes couple to mechanical motion and spin interactions within a molecular motor.

Molecular motors used here are designed to exhibit machine functions, and are composed of three parts (Fig. 1a): The top part is a five-arm rotor where four of the arms have a ferrocene group attached at their ends while the fifth arm is truncated beyond the phenyl ring. The bottom part is a molecular *tripod* designed to stand upright and to remain stationary on the surface. Each

leg of the *tripod* is tethered to the surface by a thioether group (SEt), a sulfur atom bearing an ethyl substituent. On metallic surfaces such as Au(111), the sulfur atom at each leg of the tripod binds to the surface thereby acting as an atomic glue. In macroscopic machines, rotating and stationary parts can be connected with ball bearings. Similarly, the *rotor* and *tripod* here are connected by a ruthenium (Ru) atom through coordinated bonding, which acts as an *atomic ball bearing*. The Fe atoms in ferrocene units at the arms of the motor and the central Ru atomic ball bearing do not exhibit magnetism, and therefore this motor in its ground state is not spin active. However, a magnetic moment can be artificially introduced in the motor by means of inelastic electron tunneling (IET). By attaching an additional electron to an unoccupied state, the molecular motor becomes spin active, and exhibits a Kondo effect (Fig. 1b). Surprisingly, we have detected Kondo effect in the entire motor, both at the four ferrocene arms as well as the central Ru atom locations. To understand the observed spintronic behavior, we have collaborated

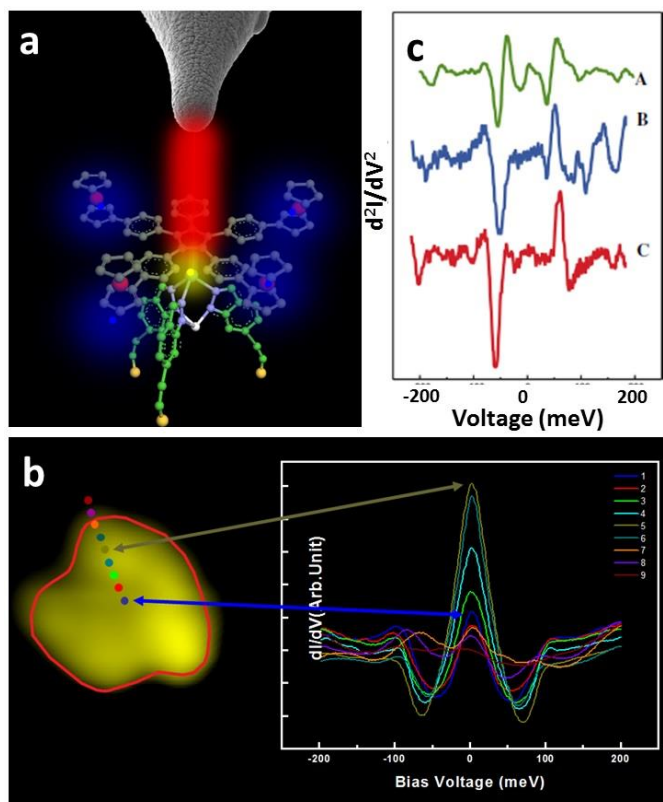


Fig. 1. (a) When an inelastic tunneling electron is captured by the motor, a new charge redistribution occurs at the ferrocene arms (blue) and Ru atom ball bearing (yellow). (b) STM image (left) shows the locations of measured dI/dV spectra revealing Kondo resonances (right). (c) Vibrational (d^2I/dV^2) spectra measured on top of ferrocene units of the molecular motor.

properties of individual molecular motors and will enable designing complex multiple functional molecular machines to operate on materials surfaces in future.

Larry Curtiss group from Argonne National Lab and Sergio Ulloa group from Ohio University to carry out spin DFT calculations. The calculations reveal that upon charge injection, charge redistribution occurs inside the motor due to Coulomb interaction. As a result, the entire motor becomes magnetic. The trapped electron is then transfer to the metal substrate and the motor dissipates the excess energy via a mechanical motion by means of vibration relaxation. For the current study, we have used electrons having up to 100 meV energy to attach the motor. This energy is sufficient to excite the ferrocene vibration of the motor arms, which occurs ~ 60 meV energy range. This vibration relaxation generates additional side bands in the Kondo signature (Fig. 1b, dI/dV curves), which is further confirmed by means of vibrational spectroscopy analyses (d^2I/dV^2) (Fig. 1c). The peak at +60 meV and a dip at -60 meV in d^2I/dV^2 signal corresponds to the ferrocene group vibrational mode of the metal atom (Fe) and cyclopentadienyl rings. This work impacts fundamental understanding of how charge and energy transfer processes couple to the spintronic and mechanical

II. A superconducting raft in the Fermi sea

How a molecular superconductor interacts with two dimensional electron gas at the interface with a metal is an intriguing question. In previous DOE supported work, we have studied charge

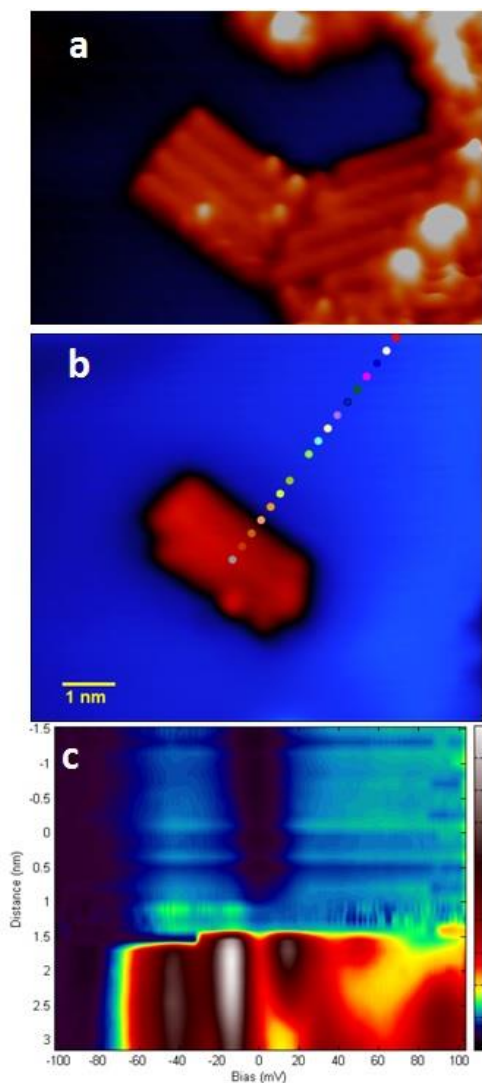


Fig. 2. (a) Charge transfer molecular chains form a raft shape structure. (b) A molecular raft at a bare surface area. (c) dI/dV map measured across superconductor-metal boundary shows evolution of gap state.

transfer based molecular superconducting system formed by a *Bechgaard salt*, $(\text{BETS})_2\text{-GaCl}_4$, on a $\text{Ag}(111)$ surface [Clark et al., *Nature Nanotechnol.* 5, 261-265 (2010)] and found superconducting gap at the nanoscale even for small molecular chains composed of just four molecule pairs. In this part of the project, we investigate how nanoscale superconducting molecular clusters interact with the free surface state electrons at the atomic level by combining tunneling spectroscopy and STM manipulation. We find that $(\text{BETS})_2\text{-GaCl}_4$ can assemble one dimensional molecular chains on $\text{Ag}(111)$ surface (Fig. 2a and 2b) and exhibit superconductivity below 6.8 K. By using STM lateral manipulation scheme, molecular chains with different sizes, which we label as molecular rafts due to their appearances, (Fig. 2a) are relocated on bare $\text{Ag}(111)$ surface area to expose them to interact with the free surface state electrons (Fig. 2b). Tunneling spectroscopic data acquired across the superconductor-metal boundary reveal how superconducting gap evolve to the Fermi sea as a function of the size of the molecular rafts (Fig. 2c). This work impacts fundamental understanding of unconventional superconductivity in a molecular charge transfer system

enabling manipulation and control of electronic interactions at the atomic scale.

Future Plans

Following our previous work of self-assembled dipolar rotors that exhibit coupled rotation of up to 500 motors when electric field energy is provided [3], we are investigating how charge and energy is transferred between the neighboring motors. We are also investigating Kondo effect of molecular transport devices (molecular cars) on $\text{Au}(111)$ surface by combining tunneling spectroscopy and molecular manipulation. Recently, we have made significant advances in synchrotron X-ray scanning tunneling microscopy (SX-STM) instrumentation development [4,7] and measurements that now enable to probe buried interfacial magnetism as well. We are currently preparing a beam time request to Advanced Photon Source for investigation of our molecular motors with SX-STM technique. Here, we wish to develop 3-dimensional elemental

and magnetic mapping on single molecular motors. Results from all of these planned experiments are expected to make significant impact on our understanding of charge and energy transfer processes occurring in quantum regimes as well as control over these process to design novel materials and systems.

List of Publications Acknowledging Current DOE Grant (from 09/2015 to date)

Published or in press:

1. Y. Li, A. Ngo, A. DiLullo, K.Z. Latt, H. Kersell, B. Fisher, P. Zapol, S.E. Ulloa & S.-W. Hla. Anomalous Kondo resonance mediated by semiconducting graphene nanoribbons in a molecular heterostructure. *Nature Communications* (2017) (in press).
2. H. Kersell, N. Shirato, M. Cummings, H. Chang, D. Miller, D. Rosenmann, S.-W. Hla, V. Rose. Detecting element specific electrons from a single cobalt nanocluster with synchrotron X-ray scanning tunneling microscopy. *Appl. Phys. Lett.* (2017) (in press).
3. Y. Zhang, H. Kersell, R. Stefak, J. Echeverria, V. Iancu, U. G. E. Perera, Y. Li, A. Deshpande, K.-F. Braun, C. Joachim, G. Rapenne, & S.-W. Hla. Simultaneous and coordinated rotational switching of all molecular rotors in a network. *Nature Nanotechnology* **11**, 706-711 (2016).
4. A. Dilullo, N. SHirato, M. Cummings, H. Kersell, H. Chang, D. Rosenmann, D. Miller, J.W. Freeland, S.-W. Hla, & V. Rose. Local X-ray magnetic circular dichroism study of Fe/Cu(111) using a tunneling smart tip. *J. Synchrotron. Rad.* **23**, 574-578 (2016).
5. J. Niederhausen, H.R. Kersell, C. Christodoulo, G. Heimel, H. Wonneberger, K. Müllen, J.P. Rabe, S.-W. Hla, & N. Koch. Monolayer phases of a dipolar perylene derivative on Au(111) and surface potential built-up in multilayers. *Langmuir* **32**, 3587-3600 (2016).

Submitted:

6. K. Kotturi, M. Raeisi, K. Z. Latt, Y. Zhang, K. Perumal, R. Rabbani, S. Sarkar, Y. Li, S.-W. Hla, and E. Masson. Anatomy of a Supramolecular Nanocar.
7. N. Shirato, H. Chang, H. Kersell, M. Cummings, C. Preissner, D. Rosenman, S.-W. Hla, V. Rose Highly versatile low temperature ultrahigh vacuum synchrotron X-ray scanning tunneling microscope for photon-enhanced spectroscopy with chemical and magnetic contrast.

Session 10

Project Title: Quantum Materials

Principal Investigator: Joseph Orenstein; Co-PI's: R.J. Birgeneau, E. Bourret, A. Lanzara, DH Lee, JE Moore, R. Ramesh, Lawrence Berkeley National Laboratory

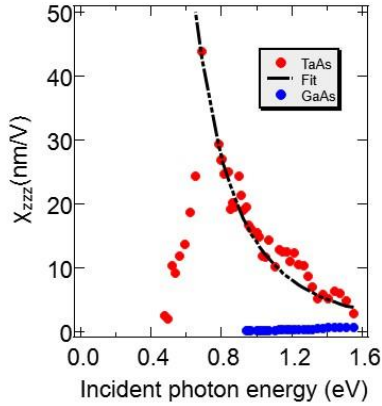
Program Scope

The LBNL Quantum Materials program focuses on condensed matter systems in which quantum mechanics plays an essential role in determining the nature of phases and the transitions that take place between them. The goal of the program is to understand, manipulate, and control these phases. To achieve this goal, the Quantum Materials program brings together theorists and experimentalists with expertise in (i) thin film and bulk crystal fabrication, (ii) advanced characterization tools including ARPES, ultrafast optical pump/probe, neutron and X-ray scattering, (iii) fundamental and phenomenological theory. Currently the program is focused on three overlapping themes – high-temperature superconductivity, topological phases of matter, and systems in which strong-spin orbit coupling generates exotic magnetism. Specific material systems under investigation are the mononictide family of Weyl semimetals, transition metal oxides, such as cuprates and iridates, and iron-chalcogenide and iron-pnictide superconductors.

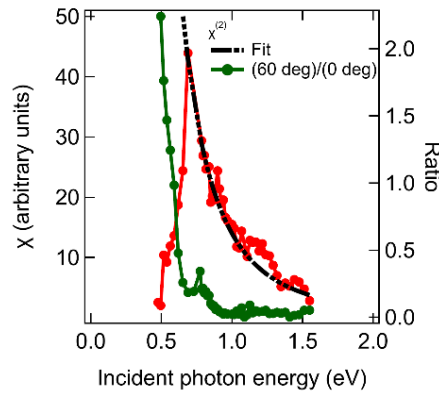
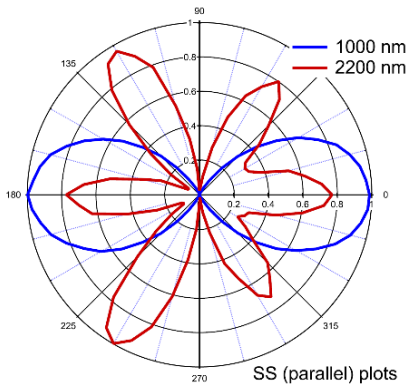
Recent Progress

Although Weyl fermions have proven elusive in high-energy physics, their existence as emergent quasiparticles has been predicted in certain crystalline solids in which either inversion or time-reversal symmetry is broken [1]. Recently they have been observed in transition metal mononictides (TMMPs) such as TaAs, a class of noncentrosymmetric materials that heretofore received only limited attention [2]. The question that arises is whether the emergent Weyl quasiparticles will generate novel, enhanced, and/or technologically applicable electronic properties. The TMMPs are polar metals, a rare subset of inversion-breaking crystals that would allow spontaneous polarization, were it not screened by conduction electrons. Despite the absence of spontaneous polarization, polar metals manifest other signatures of inversion-symmetry breaking, most notably a nonlinear optical polarizability, $\chi^{(2)}(\omega_1, \omega_2; \omega_1 \pm \omega_2)$, which gives rise to sum and difference frequency generation.

In recent progress we have made the first observation of second harmonic generation (SHG) in the TMMPs TaAs, NbAs, and TaP [3]. In SHG light of fundamental frequency ω_0 generates radiation at twice the fundamental, or $2\omega_0$. In our initial work [2] we measured SHG in response to ultrashort laser pulses centered at 800 nm, corresponding to $\hbar\omega_0 \cong 1.55$ eV. These measurements revealed a giant, highly-anisotropic second-harmonic response in the TMMPs TaAs, TaP, and NbAs which not anticipated by theoretical prediction. With the fundamental and second harmonic fields oriented parallel to the polar axis, the value of $\chi^{(2)}(\omega_0, \omega_0; 2\omega_0)$ at 800 nm is larger by almost one order of magnitude than its value in the archetypal electro-optic materials GaAs and ZnTe, and in fact larger than reported in any crystal to date.



The spectrum of the SHG response, together with a comparison to the response of GaAs is shown in Fig. 1. The value of $\chi^{(2)}(\omega_0, \omega_0; 2\omega_0)$ at 0.65 eV is ≈ 400 times for TaAs than for



GaAs. Fig. 2 shows that the relative value of the different components of the $\chi^{(2)}$ tensor changes rapidly at the same frequency at which the SHG response function peaks, as indicated by the change from a polar pattern with two lobes to one with six as the pump energy is lowered. The abrupt nature of this change is illustrated in Fig. 2a, where we plot the ratio of amplitude at 0 and 60 degrees as a function of $\hbar\omega_0$.

Future research:

The goal of future research is to understand the role of bandstructure geometry, specifically the Berry curvature, in generating anomalously large nonlinear optical response functions. Working towards this goal requires progress in both experiment and theory. In terms of theory, ab initio calculations of nonlinear response, particularly for crystals with lower symmetry than GaAs are still in an early stage. Experimentally, we wish to pursue measurements of nonlinear response to energies much closer to the Fermi energy and the position of the Weyl nodes. To accomplish this we are developing a THz interferometer based on electro-optic generation of high intensity electric field pulses.

References

- [1] Wan, X., Turner, A. M., Vishwanath, A. & Savrasov, S. Phys. Rev. B **83**, 205101 (2011).
- [2] Xu, S.-Y. et al. Science **349**, 613_617 (2015).

[3] L. Wu, S. Patankar, T. Morimoto, N. Nair, E. Thewalt, A. Little, J. Analytis, J. Moore, and J. Orenstein, *Nature Physics* 13, 350 (2016).

Publications

1. J. P. Hinton, S. Patankar, E. Thewalt, A. Ruiz, G. Lopez, N. Breznay, A. Vishwanath, J. Analytis, and J. Orenstein, J. D. Koralek, I. Kimchi, "Photoexcited states of the harmonic honeycomb iridate γ - Li_2IrO_3 ," *Phys. Rev. B* 92, 115154 (2015).
2. Z. Yan, D. Meier, J. Schaab, R. Ramesh, E. Samulon and E. Bourret, "Growth of high-quality hexagonal ErMnO_3 single-crystals by the pressurized floating-zone method," *Journal of Crystal Growth* 409, 75 (2015).
3. Shudan Zhong, J. Orenstein, and Joel E. Moore, "Optical gyrotropy from axion electrodynamics in momentum space," *Phys. Rev. Lett.* 115, 117403 (2015).
4. Meng Wang, Ming Yi, Huibo Cao, C. de la Cruz, S.K. Mo, Q.Z. Huang, E. Bourret-Courchesne, Pengcheng Dai, D. H. Lee, Z.X. Shen and R. J. Birgeneau, "Mott localization in a pure stripe antiferromagnet $\text{Rb}_{1-x}\text{Fe}_{1.5-y}\text{S}_2$," *Phys. Rev. B*, 92, 121101(R) (2015).
5. Meng Wang, P. Valdavia, Ming Yi, J.X. Chen, W.L. Zhang, R.A. Ewings, T.G. Perring, Yang Zhao, L.W. Harriger, J.W. Lynn, Pengcheng Dai, D. H. Lee, D.X. Yao, and R. J. Birgeneau, "Spin waves and spatially anisotropic exchange interactions in the $S=2$ stripe antiferromagnet $\text{Rb}_{0.8}\text{Fe}_{1.5}\text{S}_2$," *Phys. Rev. B*, 92, 041109(R) (2015).
6. P. N. Valdavia, MG Kim, TR Forrest, ZJ Xu, M Wang, H Wu, LW Harriger, E. D. Bourret-Courchesne, and R. J. Birgeneau, "Copper-substituted iron telluride: A phase diagram," *Phys. Rev. B* 91, 224424 (2015).
7. Itamar Kimchi, Radu Coldea, and A. Vishwanath, "Unified theory of spiral magnetism in the harmonic-honeycomb iridates α , β , and γ Li_2IrO_3 ," *Phys. Rev. B* 91, 245134 (2015).
8. Romain Vasseur and Joel E. Moore, "Multifractal orthogonality catastrophe in one-dimensional random quantum critical points," *Phys. Rev. B* 92, 054203 (2015).
9. R. Vasseur, C. Karrasch, and J. E. Moore, "Expansion potentials for exact far-from-equilibrium spreading of particles and energy," *Phys. Rev. Lett.* 115, 267201 (2015).
10. C.R. Rotundu, T.R. Forrest, N.E. Phillips and R.J. Birgeneau, "Specific Heat of $\text{Ba}_{0.59}\text{K}_{0.41}\text{Fe}_2\text{As}_2$, an Fe-Pnictide Superconductor with $T_c=36.9\text{K}$, and a New Method for Identifying the Electron Contribution," *J. Phys. Soc. Jpn.* 84, 114701 (2015).
11. M.G. Kim, M. Wang, G.S. Tucker, P.N. Valdavia, D.L. Abernathy, S.Chi, A.D. Christianson, A.A. Axcel, T. Hong, T.W. Heitmann, S. Ran, P.C. Canfield, E.D. Bourret-Courchesne, A. Kreyssig, D.H. Lee, A.I. Goldman, R.J. McQueeney, and R.J. Birgeneau, "Spin Dynamics near a putative quantum critical point in Cu-substituted BaFe_2As_2 and its relation to high temperature superconductivity", *Phys. Rev. B* 92, 214404 (2015).
12. M. Yi, M. Wang, A.F. Kemper, S.-K. Mo, Z. Hussain, E. Bourret-Courchesne, A. Lanzara, M. Hashimoto, D.H. Lu, Z.-X. Shen, and R.J. Birgeneau, "Bandwidth and Electron Correlation-Tuned Superconductivity in $\text{Rb}_{0.8}\text{Fe}_2(\text{Se}_{1-z}\text{S}_z)_2$," *Physical Review Letters* 115, 6403 (2015).

13. Jian Liu, D. Kriegner, L. Horak, D. Puggioni, C. Rayan Serrao, R. Chen, D. Yi, C. Frontera, V. Holy, A. Vishwanath, J. M. Rondinelli, X. Marti, and R. Ramesh, "Strain-induced nonsymmorphic symmetry breaking and removal of Dirac semimetallic nodal line in an orthoperovskite iridate," *Phys. Rev. B* 93, 005100 (2016).
14. A.K. Yadav, C.T. Nelson, S.L. Hsu, Z. Hong, J. D. Clarkson, C. M. Schlepüetz, A. R. Damodaran, P. Shafer, E. Arenholz, L.R. Dedon, D. Chen, A. Vishwanath, A. M. Minor, L.Q. Chen, J.F. Scott, L. W. Martin, and R. Ramesh, "Observation of polar vortices in oxide superlattices," *Nature* 530, 198 (2016).
15. Daniel Varjas, Adolfo G. Grushin, Roni Ilan, Joel E. Moore, "Dynamical piezoelectric and magnetopiezoelectric effects in polar metals from Berry phases and orbital moments," *Phys. Rev. Lett.* 117, 257601 (2016).
16. Andrew C. Potter, Romain Vasseur, "Symmetry constraints on many-body localization", *Phys. Rev. B* 94, 224206 (2016).
17. Romain Vasseur, Aaron J. Friedman, S. A. Parameswaran, Andrew C. Potter, "Particle-hole symmetry, many-body localization, and topological edge modes", *Phys. Rev. B* 93, 134207 (2016).
18. L. Wu, S. Patankar, T. Morimoto, N. Nair, E. Thewalt, A. Little, J. Analytis, J. Moore, and J. Orenstein, "Giant anisotropic nonlinear response in transition metal monopnictide Weyl semimetals," *Nature Physics* 13, 350 (2016).
19. Romain Vasseur, Hubert Saleur, "Universal Entanglement Dynamics following a Local Quench", *SciPost Phys.* 3, 001 (2017).

Science of 100 Tesla

Neil Harrison, Los Alamos National Laboratory

Program Scope

In unconventional superconductors, there is an essential need to understand the pairing mechanism with the eventual aim of tailor making superconductors with significantly higher transition temperatures. To reach this point, we must first understand the normal (i.e. non-superconducting) state from which unconventional pairing originates. Owing to the very high superconducting transition temperatures in the high temperature superconductors, or very slow Fermi velocities in strongly correlated f -electron superconductors, the coherence lengths tend to be shorter than those in conventional BCS superconductors [1], thus requiring magnetic fields of order 100 T to access the normal state. Unconventional pairing in many cases appears to be associated with the competition between different phases, and the superconducting transition temperature is often found to be highest at a quantum critical point, where a phase transition is tuned to zero temperature by chemical doping [2,3] or pressure [4,5]. Identifying whether quantum criticality truly occurs in the high- T_c cuprates, however, has proven to be extremely challenging from the experimental perspective [6]. There is still no consensus on which of the various proposed phases may actually become quantum critical. Very strong magnetic fields can resolve this problem by providing direct access to phase transitions tuned towards zero temperature [7], and by enabling changes in electronic structure to be seen in a low temperature regime that is free from thermal fluctuations. Magnetotransport, cyclotron quantization and Fermi surface (e.g. by way of magnetic quantum oscillations) measurements in magnetic fields of order 100 T all provide critical information relating to changes in the underlying normal state electronic structure.

Recent Progress

It is in the cuprate family of high- T_c superconductors in which routine access to 90 T plus magnetic fields has proven to be especially crucial for making significant breakthroughs towards their understanding [7,8,9]. Turning first to the phase diagram of transition temperature T_c versus hole doping p (see Fig. 1), one of the long standing questions has been whether direct evidence for a quantum critical point can be found to lie hidden beneath the superconducting dome. By use of the 100TMSM we were able to detect magnetic quantum oscillations to dopings as high as $p = 0.152$ (much higher than previously possible), just shy of optimal doping at $p \sim 0.16$ (see Figs. 1b and c). The effective mass extracted from the temperature-dependence of the oscillations is found to climb steeply towards optimal doping, providing the first direct thermodynamic evidence for quantum critical behavior. The inverse effective mass extrapolates to zero near $p_c = 0.18$ (inverted triangle), indicating this to be the likely location of a quantum critical point. Another quantum critical point near $p_c = 0.08$ had previously been reported in an earlier study (also done as part of our 100 T science program).

The two dopings at which quantum critical behavior is found are also the same dopings at which superconductivity is most robust under the application of a magnetic field. The effect of a magnetic field is to initially split the superconducting dome into two, centered on $p = 0.08$ and $p = 0.18$. Once the magnetic fields exceeds ~ 50 T, only the higher of these is found to survive, and is expected to persist to magnetic fields as high as 130 T [10]. The higher of the two quantum critical points lies close to the point in which various earlier measurements had indicated the pseudogap to vanish (on extrapolation). It also lies close to the doping in which the Kerr effect (possibly indicative of broken time-reversal symmetry) is found to extrapolate to zero [11] and the highest hole doping at which short range charge order is reported in $\text{YBa}_2\text{Cu}_3\text{O}_{6+x}$ [12].

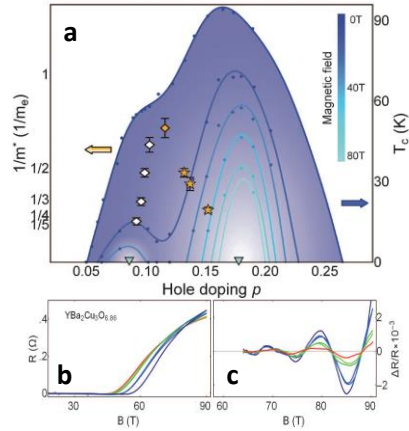


Fig. 1. **a.** T_c (right-hand-axis) versus p phase diagram of $\text{YBa}_2\text{Cu}_3\text{O}_{6+x}$ in which p is tuned by varying the oxygen concentration x . The contours indicate suppressed values of T_c in the presence of a magnetic field, plotted in different colors according to the scale shown in the inset. Also plotted is the inverse effective mass $1/m^*$ (left-hand-axis), showing that it extrapolates to zero at two different hole dopings near $p = 0.08$ and $p = 0.18$. Inverted triangles indicate putative quantum critical points. **b.** Magnetoresistance of a sample in which $x = 0.86$ (i.e. $p = 0.152$) at different temperatures. **c.** Magnetic quantum oscillations in the resistance, after having subtracted the background.

Turning to the Fermi surface geometry, angle resolved magnetic quantum oscillation experiments have enabled us to settle the question as to the origin of the multiple observed frequencies in $\text{YBa}_2\text{Cu}_3\text{O}_{6+x}$. We have now performed angle-resolved magnetic quantum oscillation measurements on both $\text{YBa}_2\text{Cu}_3\text{O}_{6+x}$ [8] and $\text{YBa}_2\text{Cu}_4\text{O}_8$ [9] (the latter shown in Fig. 4a), yielding nearly identical results in the two systems. In the case of $\text{YBa}_2\text{Cu}_4\text{O}_8$, the high resistive transition of ~ 40 T requires the angle-resolved measurements to be made in magnetic fields of 90 T [9]. A wide range in field is needed to access a sufficiently large number of oscillations over a sufficiently broad range of angles. The data in both materials can be simulated using a bilayer-split magnetic breakdown scenario [13,14,15], using similar values of the bilayer splitting and effective g -factor. The prominent central quantum oscillation frequency 532 T in $\text{YBa}_2\text{Cu}_3\text{O}_{6+x}$ and 640 T in $\text{YBa}_2\text{Cu}_4\text{O}_8$ is produced by quasiparticles tunneling across the bilayer gap in the nodal region (k_g) where the tunneling probability approaches unity at high magnetic fields. The beat pattern originates from magnetic breakdown combination frequencies of weaker amplitude.

Spin-orbit interactions are found to play a surprisingly important role in $\text{YBa}_2\text{Cu}_3\text{O}_{6+x}$ [14,16]. The overall Zeeman splitting of the dominant amplitude orbit is found to be consistent with an electron g -factor of $g \approx 2$ in both $\text{YBa}_2\text{Cu}_3\text{O}_{6+x}$ and $\text{YBa}_2\text{Cu}_4\text{O}_8$. The side frequencies, however, have an effective g -factor < 1 that is significantly suppressed, which can be understood if local asymmetry of each of the CuO_2 planes composing the bilayers is taken into consideration. Here, Rashba spin-orbit coupling within each of the planes gives rise to mixing between the spin-up and spin-down Landau levels. The emergence of prominent spin-orbit effects is only expected to be possible if the observed magnetic quantum oscillations originate from a section of Fermi surface that is located close to the nodal locations in the Brillouin zone in momentum-space.

Future Plans

The crucial connection between the observed quantum critical behavior [8], the pseudogap and a specific form of broken symmetry is still missing [6]. It also remains unknown whether the observed increase in effective mass with doping originates purely from electron-electron correlations or whether an enhancement of the electron-phonon coupling might occur. Broken rotational symmetry (or nematicity) is one candidate for broken symmetry that appears to be common to different families of unconventional superconductors. While there is extensive evidence for broken rotational symmetry in the underdoped cuprates coming from different types of measurement, direct evidence for broken rotational symmetry affecting the Fermi surface has thus far remained elusive (both at zero and high magnetic fields [8]). Similarly elusive is direct experimental evidence for the in-plane shape of the reconstructed Fermi surface that is predicted to have a diamond shape resulting from biaxial charge-density wave ordering [13,14,15].

Observation of the latter would put the mechanism of Fermi surface reconstruction on a very solid footing. Finally, there is the question of the universality of the phase diagram. For example, it has yet to be determined whether the doping-dependent trends (i.e. Fermi surface topology, effective mass and phase transitions) seen in $\text{YBa}_2\text{Cu}_3\text{O}_{6+x}$ are universal to the cuprates, or whether they are unique to $\text{YBa}_2\text{Cu}_3\text{O}_{6+x}$.

References

[1] J. S. Brooks and J. R. Schrieffer, *Handbook of High -Temperature Superconductivity: Theory and Experiment* (Springer, 2007). [2] J. G. Analytis *et al.* *Nature Phys.* **10**, 194 (2014). [3] T. Shibauchi, A. Carrington, Y. Matsuda. *Annual Rev. Cond. Matt. Phys.* **5**, 113 (2014). [4] N. D. Mathur *et al.* *Nature* **394**, 39 (1998). [5] P. Gegenwart, Q. Si, F. Steglich. *Nature Phys.* **4**, 186 (2008). [6] B. Keimer, *et al.* *Nature* **518**, 179 (2015). [7] F. F. Balakirev, *et al.* *Nature* **424**, 912 (2003). [8] S.E. Sebastian, *et al.* *Nature* **511**, 61 (2014). [9] B. S. Tan, *et al.* *Proc. Nat. Acad. Sci. USA.* **112**, 9568 (2015). [10] G. Grissonnanche, *et al.* *Nature Commun.* **5**, 3280 (2014). [11] J. Xia *et al.* *Phys. Rev. Lett.* **100**, 127002 (2008). [12] S. Blanco-Canosa, *et al.* *Phys. Rev. B* **90**, 054513 (2014). [13] S. E. Sebastian *et al.* *Phys. Rev. Lett.* **108**, 1109403 (2012). [14] A. K. R. Briffa, *et al.* *Phys. Rev. B* **93**, 094502 (2016). [15] A. V. Maharaj *et al.* *Phys. Rev. B* **93**, 094503 (2016). [16] N. Harrison, B. J. Ramshaw, A. Shekhter, *Scientific Reports* **5**, 10914 (2015).

Publications

[1] Electronic in-plane symmetry breaking at field-tuned quantum criticality in CeRhIn_5 ; Ronning, F.; Helm, T.; Hirer, K. R. S.; *et al.* *NATURE* **548**, 313 (AUG 17 2017)

[2] Robust spin correlations at high magnetic fields in the harmonic honeycomb iridates; Modic, K. A.; Ramshaw, B. J.; Betts, J. B.; *et al.* *NATURE COMMUNICATIONS* **8**, 180 (AUG 1 2017).

[3] Tricritical point from high-field magnetoelastic and metamagnetic effects in UN; Shrestha, K.; Antonio, D.; Jaime, M.; *et al.* *SCIENTIFIC REPORTS* **7**, 6642 (JUL 26 2017).

[4] Hall number across a van Hove singularity; Maharaj, Akash V.; Esterlis, Ilya; Zhang, Yi; *et al.* *PHYSICAL REVIEW B* **96**, 045132 (JUL 24 2017).

[5] Piezomagnetism and magnetoelastic memory in uranium dioxide; Jaime, M.; Saul, A.; Salamon, M.; *et al.* *NATURE COMMUNICATIONS* **8**, 99 (JUL 24 2017).

[6] Reduction of the low-temperature bulk gap in samarium hexaboride under high magnetic fields; Wolgast, S.; Eo, Y. S.; Sun, K.; *et al.* *PHYSICAL REVIEW B* **95**, 245112 (JUN 13 2017).

[7] Combining microscopic and macroscopic probes to untangle the single-ion anisotropy and exchange energies in an S=1 quantum antiferromagnet; Brambleby, Jamie; Manson, Jamie L.; Goddard, Paul A.; *et al.* *PHYSICAL REVIEW B* **95**, 134435 (APR 20 2017).

[8] Magnetic phase diagram and electronic structure of UPt_2Si_2 at high magnetic fields: A possible field-induced Lifshitz transition, Grachtrup, D. Schulze; Steinki, N.; Suellow, S.; *et al.* *PHYSICAL REVIEW B* **95**, 134422 (APR 14 2017).

[9] Magnetic-field-induced vortex-lattice transition in $\text{HgBa}_2\text{CuO}_{4+\delta}$; Lee, Jeongseop A.; Xin, Yizhou; Stolt, I.; *et al.* *PHYSICAL REVIEW B* **95**, 024512 (JAN 23 2017)

[10] Tricritical point of the f-electron antiferromagnet USb_2 driven by high magnetic fields; Stillwell, R. L.; Liu, I.-L.; Harrison, N.; *et al.* *PHYSICAL REVIEW B* **95**, 014414 (JAN 12 2017)

[11] Adiabatic physics of an exchange-coupled spin-dimer system: Magnetocaloric effect, zero-point fluctuations, and possible two-dimensional universal behavior; Brambleby, J.; Goddard, P. A.; Singleton, J.; *et al.* *PHYSICAL REVIEW B* **95**, 024404 (JAN 5 2017)

[12] Hourglass Dispersion and Resonance of Magnetic Excitations in the Superconducting State of the Single-Layer Cuprate $\text{HgBa}_2\text{CuO}_{4+\delta}$ Near Optimal Doping; Chan, M. K.; Tang, Y.; Dorow, C. J.; *et al.*; *PHYSICAL REVIEW LETTERS* **117**, 277002 (DEC 29 2016)

[13] Magnetic properties of $\text{Sr}_3\text{NiIrO}_6$ and $\text{Sr}_3\text{CoIrO}_6$: Magnetic hysteresis with coercive fields of up to 55 T; Singleton, John; Kim, Jae Wook; Topping, Craig V.; *et al.* *PHYSICAL REVIEW B* **94**, 224408 (DEC 8 2016)

[14] Fermi-surface topologies and low-temperature phases of the filled skutterudite compounds $\text{CeOs}_4\text{Sb}_{12}$ and $\text{NdOs}_4\text{Sb}_{12}$; Ho, Pei Chun; Singleton, John; Goddard, Paul A.; *et al.* *PHYSICAL REVIEW B* **94**, 205140 (NOV 28 2016)

- [15] Shubnikov-de Haas quantum oscillations reveal a reconstructed Fermi surface near optimal doping in a thin film of the cuprate superconductor $\text{Pr}_{1.86}\text{Ce}_{0.14}\text{CuO}_4$ $\pm\delta$; Breznay, Nicholas P.; Hayes, Ian M.; Ramshaw, B. J.; *et al.* PHYSICAL REVIEW B **94**, 104514 (SEP 16 2016)
- [16] Number of holes contained within the Fermi surface volume in underdoped high-temperature superconductors; Harrison, N.; PHYSICAL REVIEW B **94**, 085129 (AUG 16 2016)
- [17] Single reconstructed Fermi surface pocket in an underdoped single-layer cuprate superconductor; Chan, M. K.; Harrison, N.; McDonald, R. D.; *et al.* NATURE COMMUNICATIONS **7**, 12244 (JUL 2016)
- [18] Anisotropy: Spin order and magnetization of single-crystalline $\text{Cu}_4(\text{OH})_6\text{FBr}$ barlowite, Han, Tian-Heng; Isaacs, Eric D.; Schlueter, John A.; *et al.* PHYSICAL REVIEW B **93**, 214416 (JUN 15 2016)
- [19] Antiferromagnetism in a Family of $S=1$ Square Lattice Coordination Polymers $\text{NiX}_2(\text{pyz})_2$ ($X = \text{Cl, Br, I, NCS}$; $\text{pyz} = \text{Pyrazine}$); Liu, Junjie; Goddard, Paul A.; Singleton, John; *et al.* INORGANIC CHEMISTRY **55**, 3515 (APR 4 2016)
- [20] Control of the third dimension in copper-based square-lattice antiferromagnets; Goddard, Paul A.; Singleton, John; Franke, Isabel; *et al.* PHYSICAL REVIEW B **93**, 094430 (MAR 25 2016)
- [21] Quantum oscillations in a bilayer with broken mirror symmetry: A minimal model for $\text{YBa}_2\text{Cu}_3\text{O}_{6+\delta}$; Maharaj, Akash V.; Zhang, Yi; Ramshaw, B. J.; *et al.* PHYSICAL REVIEW B **93**, 094503 (MAR 1 2016)
- [22] Experimental and Theoretical Electron Density Analysis of Copper Pyrazine Nitrate Quasi-Low-Dimensional Quantum Magnets; Dos Santos, Leonardo H. R.; Lanza, Arianna; Barton, Alyssa M.; *et al.* JOURNAL OF THE AMERICAN CHEMICAL SOCIETY **138**, 2280 (FEB 24 2016)
- [23] Pulsed field magnetization in rare-earth kagome systems; Hoch, M. J. R.; Zhou, H. D.; Mun, E.; *et al.* JOURNAL OF PHYSICS-CONDENSED MATTER **28**, 046001 (FEB 3 2016)
- [24] Bimetallic MOFs $(\text{H}_3\text{O})_x[\text{Cu}(\text{MF}_6)(\text{pyrazine})_2]\text{center dot}(4-x)\text{H}_2\text{O}$ ($M = \text{V}^{4+}$, $x=0$; $M = \text{Ga}^{3+}$, $x=1$): co-existence of ordered and disordered quantum spins in the V^{4+} system; Manson, Jamie L.; Schlueter, John A.; Garrett, Kerry E.; *et al.* CHEMICAL COMMUNICATIONS **52**, 12653 (2016)
- [25] Magnetic Structure and Exchange Interactions in Quasi-One-Dimensional $\text{MnCl}_2(\text{urea})_2$; Manson, Jamie L.; Huang, Qing-zhen; Brown, Craig M.; *et al.* INORGANIC CHEMISTRY **54**, 11897 (DEC 21 2015)
- [26] Monoclinic crystal structure of $\alpha\text{-RuCl}_3$ and the zigzag antiferromagnetic ground state; Johnson, R. D.; Williams, S. C.; Haghighirad, A. A.; *et al.* PHYSICAL REVIEW B **92**, 235119 (DEC 10 2015)
- [27] Magnetotransport signatures of a single nodal electron pocket constructed from Fermi arcs; Harrison, N.; Sebastian, S. E. PHYSICAL REVIEW B **92**, 224505 (DEC 7 2015)
- [28] Zeeman effect of the topological surface states revealed by quantum oscillations up to 91 Tesla; Zhang, Zuocheng; Wei, Wei; Yang, Fangyuan; *et al.* PHYSICAL REVIEW B **92**, 235402 (DEC 1 2015)
- [29] Magnetization of underdoped $\text{YBa}_2\text{Cu}_3\text{O}_y$ above the irreversibility field; Yu, Jing Fei; Ramshaw, B. J.; Kokanovic, I.; *et al.* PHYSICAL REVIEW B **92**, 180509 (NOV 23 2015)
- [30] Magnetic ground state of the two isostructural polymeric quantum magnets $[\text{Cu}(\text{HF}_2)(\text{pyrazine})_2]\text{SbF}_6$ and $[\text{Co}(\text{HF}_2)(\text{pyrazine})_2]\text{SbF}_6$ investigated with neutron powder diffraction; Brambleby, J.; Goddard, P. A.; Johnson, R. D.; *et al.* PHYSICAL REVIEW B **92**, 134406 (OCT 7 2015)
- [31] Successive Magnetic-Field-Induced Transitions and Colossal Magnetoelectric Effect in Ni_3TeO_6 ; Kim, Jae Wook; Artyukhin, S.; Mun, E. D.; *et al.* PHYSICAL REVIEW LETTERS **115**, 137201 (SEP 24 2015)
- [31] Fragile charge order in the nonsuperconducting ground state of the underdoped high-temperature superconductors; Tan, B. S.; Harrison, N.; Zhu, Z.; *et al.* PROCEEDINGS OF THE NATIONAL ACADEMY OF SCIENCES OF THE UNITED STATES OF AMERICA **112**, 9568 (AUG 4 2015)
- [32] Broken rotational symmetry on the Fermi surface of a high- T_c superconductor; B. J. Ramshaw, N. Harrison, S. E. Sebastian, S. Ghannadzadeh, K. A. Modic, D. A. Bonn, W. N. Hardy, Ruixing Liang & P. A. Goddard; QUANTUM MATERIALS **2**, 8 (2017).
- [33] Magnetic field tuning of an excitonic insulator between the weak and strong coupling regimes in quantum limit graphite; Z. Zhu, R. D. McDonald, A. Shekhter, B. J. Ramshaw, K. A. Modic, F. F. Balakirev & N. Harrison; SCIENTIFIC REPORTS **7**, 1733 (2017)

Probing competing chemical, electronic, and spin correlations for materials functionality

Athena S. Sefat, David Parker, & Zheng Gai
Oak Ridge National Laboratory

Program Scope

Recent, often serendipitous, discoveries of functional materials have demonstrated great potential for a wide variety of applications, including magnetic sensors, permanent magnets, magnetocaloric refrigerators, and superconducting wires. To understand the causes of superconducting and magnetic behavior, this project probes materials near their transition temperatures. The Overarching Goal is to understand how local chemical, electronic, and spin competitions lead to global changes in temperature-dependent behavior of antiferromagnetism and superconductivity. To achieve this goal, we will pursue three Specific Aims: (1) elucidate the role of *atomic-level chemistry* for causing antiferromagnetic or superconducting phase transitions; (2) clarify the impact of *local disorder* on magnetic and superconducting transitions; and (3) understand the effect of *structural dimensionality* on magnetic phase transitions. Through tightly-integrated feedback between synthesis, theory, and characterization of crystalline solids across a range of length scales (cm to pm), this project will allow tuning of improved materials with desired functionality at relevant temperatures.

Recent Progress

We have made substantial progress in the past two years, and briefly summarize a few of our research-led manuscripts below. We have primarily focused on materials related to iron-arsenide superconductors, and this work is an expanded extension of PI's Early Career Award that ended in April of 2015.

- Thallium-doping (5%) of BaFe_2As_2 (122) crystal causes a surprising rise of the antiferromagnetic transition temperature (T_N), related to magneto-elastic coupling and atomic-level chemistry. Here we find the surprising increase of T_N with chemical doping (x) in 122 (Fig. 1). [Publications: ref. 12]

- Chemical clustering accompanied by electronic uniformity increases critical transition temperatures (T_c) and current densities (J_c) in crystals of $\text{Ba}(\text{Fe}_{1-x}\text{Co}_x)_2\text{As}_2$. Also, combined scanning tunneling microscopy, spectroscopy and local barrier height were used to show that although the cleavage surface and hence morphologies are variable, the superconducting gap maps show the same gap widths and nanometer size variations irrelevant to the morphology. [ref. 26, 28]

- The 'lattice parameter' changes and trends with chemical doping in iron-arsenides were summarized in a review paper: we concluded that all high-temperature superconductors have nearly tetragonal structures with a -lattice parameter close to 4 Å, and that superconductivity can depend strongly on the c -lattice parameter changes with chemical substitution. For example, our analyses showed that a decrease in c -lattice parameter *is required* to induce 'in-plane' superconductivity in 122 structures (Figure 2). [ref. 27]

Figure 1: Heat capacity showing T_N peaks with x .

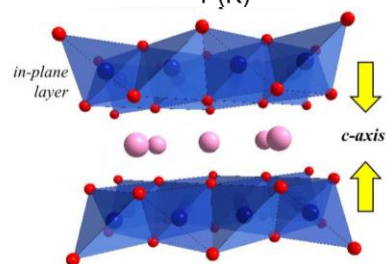
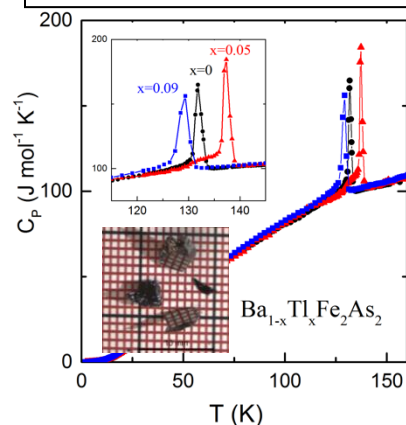


Figure 2: $B\text{Fe}_2\text{As}_2$ crystal structure (B : Ba, Ca, or Sr).

- Single- and double-layered compounds based on tetrahedrally-coordinated transition metals of T=Fe and Cu, with chemical compositions of CaT_2P_2 and CaT_6P_5 , show low density of states for Cu compounds and metallic behavior, while Fe compounds are the opposite. The details of structural dimensionality and chemical T-P layers dictate properties. [ref. 21]
- The property change of 122 was investigated by using the heaviest transition-metal element ($5d$, gold). We find that $5d$ is more effective in reducing magnetism in 122 than its counter $3d$ Cu; but at the same time, we find short-range magnetic fluctuations and local disorder that prevent superconductivity. [ref. 3]
- By investigating two high- T_c Tl-based cuprates, we find that addition of Li_2O enhances superconductivity of $\text{Tl}_2\text{Ba}_2\text{Ca}_2\text{Cu}_3\text{O}_{10}$, while thermal annealing increases T_c by ~ 25 K in $\text{Tl}_2\text{Ba}_2\text{Ca}_2\text{Cu}_3\text{O}_{10}$ related to small c -lattice parameter change and disorder of Ca/Tl positions. [ref. 4,6]
- The hexagonal FeS and FeSe, unlike their tetragonal counterparts, possess a robust magnetic character, arising from c -axis Fe-Fe chains that lead to a van Hove singularity [ref. 30]
- Silver-doping of 122 gives persistent magnetism not allowing superconductivity: DOS calculations show disruption of Ag dopants on electronic structure of 122, unlike that of cobalt dopants. [ref. 23]
- Tetragonal FeS can have coexistence of antiferromagnetism and superconductivity and show a variety of bulk behaviors depending on average stoichiometry and lattice parameters. [ref. 25]

Future Plans

We want to enable the prediction and tuning of antiferromagnetic ordering temperatures in materials and understand its relationship to local and average nuclear and spin structures, dopant concentration, chemical and electronic disorder, and structural dimensionality, for giving superconductivity. For example, a goal is to understand the reasons for the widely varying Néel temperatures (T_N) in the 122s of BFe_2As_2 with $B = \text{Ba, Sr, Ca, and Eu}$; theoretically we explore the energetics of competing states, such as the checkerboard nearest-neighbor antiferromagnetic state, that may be responsible for the differing ordering points. In fact, our preliminary theoretical work on BaFe_2As_2 suggests the possibility for enhancing T_N through uniaxial pressure along an in-plane direction. In addition, we want to understand how synthesis can affect structural bonding/crystal lattice details to tune T_N in a material such as CaFe_2As_2 (which can have varying T_N , and even no T_N with collapsed-tetragonal phase) [Saparov, B. et al. *Scientific Report* 4 (2014), 4120; Gofryk, K. et al. *Phys. Rev. Lett.* 112 (2014), 186401.] and EuFe_2As_2 (T_N can vary between 175 and 185 K in crystals) [unpublished]. Moreover, our recent neutron scattering result shows two-dimensional (2D) spin fluctuations in the 3D-structured FeAs binary that may be prone to high-temperature superconductivity if properly doped; we seek theoretical input and pressure measurements for decreasing T_N in hopes of achieving T_c . Also, we are planning to compare local electronic density-of-states of BaFe_2As_2 with lightly 4%-doped (hole) Cr-doped versus (electron) Ni-doped crystals, to understand the causes of superconductivity in Ni-122 in relation to such small chemical disorders (hard to theoretically calculate).

Publications

Note: This project was funded in August 2015, so the below is list of publications beyond this date; the PIs are underlined.

- 1) Mirmelstein, A.; Podlesnyak, A.; dos Santos, A.M.; Ehlers, G.; Kerbel, O.; Matvienko, V.; Sefat, A.S.; et al. “Pressure-induced structural phase transition in CeNi: X-ray and neutron scattering studies and first-principles calculations,” *Physical Review B* **92**, 54102 (2015).

- 2) Khasanov, R.; Guguchia, Z.; Eremin, I.; Luetkens, H.; Amato, A.; Biswas, P.K.; Rugg, C.; Susner, M.A.; Sefat, A.S.; et al. “Pressure-induced electronic phase separation of magnetism and superconductivity in CrAs,” *Scientific Reports* **5**, 13788 (2015).
- 3) Li, L.; Cao, H.; McGuire, M.A.; Kim, J.S.; Stewart, G.R.; Sefat, A.S., “Role of magnetism in superconductivity of BaFe₂As₂: Study of 5d Au-doped crystals,” *Physical Review B* **92**, 94504 (2015).
- 4) Shipra, R.; Sefat, A.S., “Effect of Li₂O on the microstructure, magnetic and transport properties of Tl-2223 superconductor,” *Physica C: Superconductivity and its applications* **519**, 108 (2015).
- 5) Moseley, D.; Yates, K.A.; Branford, W.R.; Sefat, A.S.; et al. “Signatures of filamentary superconductivity in antiferromagnetic BaFe₂As₂ single crystals,” *Europhysics Letters* **111**, 37005 (2015).
- 6) Shipra, R.; Idrobo, J.C.; Sefat, A.S., “Structural and superconducting features of Tl-1223 prepared at ambient pressure,” *Superconductor Science & Technology* **28**, 115006 (2015).
- 7) Liu, Z.; Biegalski, M.D.; Su, S.L.; Shang, S.; Marker, C.; Liu, J.; Li, L.; Fan, L.; Meyer, T.L.; Wong, A.T.; Nichols, J.A.; Chen, D.; You, L.; Chen, Z.; Wang, K.; Wang, K.; Ward, T.Z.; Gai, Z.; Lee, H.N.; Sefat, A.S.; et al. “Epitaxial growth of intermetallic MnPt films on oxides and large exchange bias,” *Advanced Materials* **28**, 118 (2015).
- 8) McGuire, M.A.; Parker, D.S. “Superconductivity at 9 K in Mo₅PB₂ with evidence for multiple gaps,” *Physical Review B* **93**, 064507 (2016).
- 9) Liu, Z.Q.; Li, L.; Gai, Z.; Clarkson, J.D.; Hsu, S.L.; Wong, A.T.; Fan, L.S.; Lin, M.-W.; Rouleau, C.M.; Ward, T.Z.; Lee, H.N.; Sefat, A.S.; et al. “Full electroresistance modulation in a mixed-phase metallic alloy,” *Physical Review Letter* **116**, 097203 (2016).
- 10) Liu, Z.; Biegalski, M.D.; Hsu, S.L.; Shang, S.; Marker, C.; Liu, J.; Li, L.; Fan, L.; Meyer, T.L.; Wong, A.T.; Nichols, J.A.; Chen, D.; You, L.; Chen, Z.; Wang, K.; Wang, K.; Ward, T.Z.; Gai, Z.; Lee, H.N.; Sefat, A.S.; et al. “Epitaxial growth of intermetallic MnPt films on oxides and large exchange bias,” *Advanced Materials* **28**, 118 (2016).
- 11) Oleaga, A.; Shvallya, V.; Sefat, A.S.; et al. “Transport thermal properties of LiTaO₃ pyroelectric sensor from 15 K to 400 K and its application to the study of critical behavior in EuCo₂As₂,” *International Journal of Thermophysics* **37**, 4 (2016).
- 12) Sefat, A.S.; Li, L.; Cao, H.B.; McGuire, M.A.; Sales, B.C.; Custelcean, R.; and Parker, D.S. “Anomalous magneto-elastic and charge doping effects in thallium-doped BaFe₂As₂,” *Scientific Reports* **6**, 21660 (2016).
- 13) Roekeghem, A.; Richard, P.; Shi, X.; Wu, S.; Zeng, L.; Saparov, B.; Ohtsubo, Y.; Qian, T.; Sefat, A.S.; et al. “Tetragonal and collapsed-tetragonal phases of CaFe₂As₂ – a view from angle-resolved photoemission and dynamical mean field theory,” *Physical Review B* **93**, 245139 (2016).
- 14) Mohanty, D.; Dahlberg, K.; King, D.M.; David, L.A.; Sefat, A.S.; et al. “Modification of Ni-rich FCG NMC and NCA cathodes by atomic layer deposition: Preventing surface phase transitions for high-voltage lithium-ion batteries,” *Scientific Reports* **6**, 26532 (2016).
- 15) Zhang, W.L.; Yin, Z.P.; Ignatov, A.; Bukowski, Z.; Karpinski, J.; Sefat, A.S.; et al. “Raman scattering study of spin-density-wave-induced anisotropic electronic properties in AFe₂As₂ (A = Ca, Eu),” *Physical Review B* **93**, 205106 (2016).
- 16) Chen, X.; Harriger, L.; Sefat, A.; et al. “Strain-activated structural anisotropy in BaFe₂As₂,” *Physical Review B* **93**, 144118 (2016).

- 17) Shanavas, K.V.; Lindsay, L.; Parker, D.S. “Electronic structure and electron-phonon coupling in TiH₂,” *Scientific Reports* **6**, 28102 (2016).
- 18) Zhang, W.L.; Sefat, A.S.; et al. “Stress-induced nematicity in EuFe₂As₂ studied by Raman spectroscopy,” *Physical Review B* **94**, 014513 (2016).
- 19) Zhang, W.L.; Richard, P.; Roekeghem, A.; Nie, S.M.; Xu, N.; Zhang, P.; Miao, H.; Su, S.F.; Yin, J.X.; Fu, B.B.; Kong, L.Y.; Qian, T.; Wang, Z.J.; Fang, Z.; Sefat, A.S.; et al. “Angle-resolved photoemission observation of Mn-pnictide hybridization and negligible band structure renormalization in BaMn₂As₂ and BaMn₂Sb₂,” *Physical Review B* **94**, 15515 (2016).
- 20) Vilmercati, P.; Mo, S.K.; Fedorov, A.; McGuire, M.; Sefat, A.; et al. “Nonrigid band shift and nonmonotonic electronic structure changes upon doping in the normal state of the pnictide high-temperature superconductor Ba(Fe_{1-x}Co_x)₂As₂,” *Physical Review B* **94**, 195147 (2016).
- 21) Li, L.; Parker, D.S.; dela Cruz, C.R.; Sefat, A.S. “Multi-layer chalcogenides with potential for magnetism and superconductivity,” *Physica C* **531**, 25 (2016).
- 22) Salem-Sugui, S.J.; Moseley, D.; Stuard, S.J.; Alvarenga, A.D.; Sefat, A.S.; et al. “Effects of proton irradiation on flux-pinning properties of underdoped Ba(Fe_{0.96}Co_{0.04})₂As₂ pnictide superconductor,” *Journal of Alloys and Compounds* **694**, 1371 (2017).
- 23) Li, L.; Cao, H.; Parker, D.S.; Kuhn S.J.; Sefat, A.S. “Persistent magnetism in silver-doped BaFe₂As₂ crystals,” *Physical Review B* **94**, 134510 (2016).
- 24) Ziatdinov, M.A.; Maksov, A.B.; Li, L.; Sefat, A.S.; et al. “Deep data mining in real space: Separation of intertwined electronic responses in a lightly-doped BaFe₂As₂,” *Nanotechnology* **27**, 475706 (2016).
- 25) Kuhn, S.; Kidder, M.; Chance, W.M.; Dela Cruz, C.R.; McGuire, M.A.; Parker, D.S.; Li, L.; Debeer-Schmitt, L.M.; Ermentrout, J.M.; Littrell, K.; Eskildsen, M.; Sefat, A.S. “FeS: Structure and composition relations to superconductivity and magnetism,” *Physica C: Superconductivity and its Applications* **534**, 29 (2017).
- 26) Zou, Q.; Wu, Z.M.; Fu, M.M. Zhang, C.M.; Rajput, S.; Wu, Y.P.; Li, L.; Parker, D.S.; Kang, J.; Sefat, A.S.; Gai, Z. “Effect of surface morphology and magnetic impurities on the electronic structure in cobalt-doped BaFe₂As₂ superconductors,” *Nano Letters* **17**, 1642 (2017).
- 27) Konzen, L.M.N.; Sefat, A.S. “Lattice parameters guide superconductivity in iron-arsenides,” *Journal of Physics: Condensed Matter* **29**, 083001 (2017).
- 28) Li, L.; Zheng, Q.; Zou, Q.; Rajput, S.; Ijaduola, A.O.; Wu, Z.; Wang, X.P.; Cao, H.B.; Somnath, S.; Jesse, S.; Chi, M.; Gai, Z.; Parker, D.; Sefat, A.S. “Improving superconductivity in BaFe₂As₂-based crystals by cobalt clustering and electronic uniformity,” *Scientific Reports* **7**, 949 (2017).
- 29) Mohanty, D.; Mazumder, B.; Devaraj, A.; Sefat, A.S.; et al. “Resolving the degradation pathways in high-voltage oxides for high-energy-density lithium-ion batteries; Alteration in chemistry, composition and crystal structures,” *Nano Energy* **36**, 76 (2017).
- 30) Parker, D.S. “Strong 3D and 1D magnetism in hexagonal Fe-chalcogenides FeS and FeSe vs. weak magnetism in hexagonal FeTe”, *Scientific Reports* **7**, 3388 (2017).
- 31) Richard, P.; Roekeghem, A. van; Lv, B.Q.; Qian, T.; Kim, T.K.; Hoesch, M.; Hu, J.-P.; Sefat, A.S.; et al. “Is BaCr₂As₂ symmetrical to BaFe₂As₂ with respect to half 3d shell filling?” *Physical Review B* **95**, 184516 (2017).

Magneto-optical Study of Correlated Electron Materials in High Magnetic Fields

Principal Investigator: Dmitry Smirnov; Co-PI: Zhigang Jiang

Address: National High Magnetic Field Laboratory, Tallahassee, FL 32312

Email: smirnov@magnet.fsu.edu

Program Scope

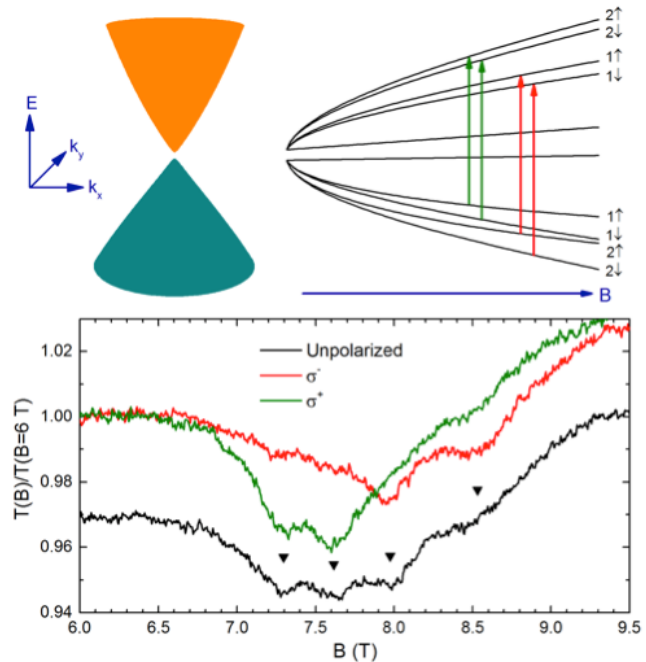
This program is focused on studying electronic structure, low-energy excitations, and many-body effects in novel electronic materials via magneto-optical spectroscopy. We extend our interest from graphene to topological insulators (TIs) and transition metal dichalcogenides (TMDs) and expand our technical approach to include linear/circular polarization resolved infrared (IR), Raman and photoluminescence (PL) magneto-spectroscopies. A focal point of our current research is the emerging behavior at or near a critical state when a narrow-gap semiconductor closes its gap and develops an inverted band structure that may host topologically protected states.

Recent Progress

Landau level spectroscopy of massive Dirac fermions in ZrTe₅

Finding a large band gap TI is crucial to future room-temperature (corresponding to ~25 meV) device applications. Zirconium pentatelluride (ZrTe₅) has attracted substantial interest lately in the wave of Dirac and topological material exploration due to the theoretical prediction of a large-gap quantum spin Hall insulator phase in its monolayer form [1]. Theory also predicts that the electronic structure of bulk ZrTe₅ resides near the phase boundary between weak and strong topological insulators (TIs) [1,2], providing an ideal platform for studying topological phase transitions.

The topological nature of bulk ZrTe₅ is currently under intense debate, with interpretations ranging from strong/weak TI to Dirac semimetal. To understand its electronic structure, we have carried out a thorough IR spectroscopy study of mechanically exfoliated ZrTe₅ thin crystals



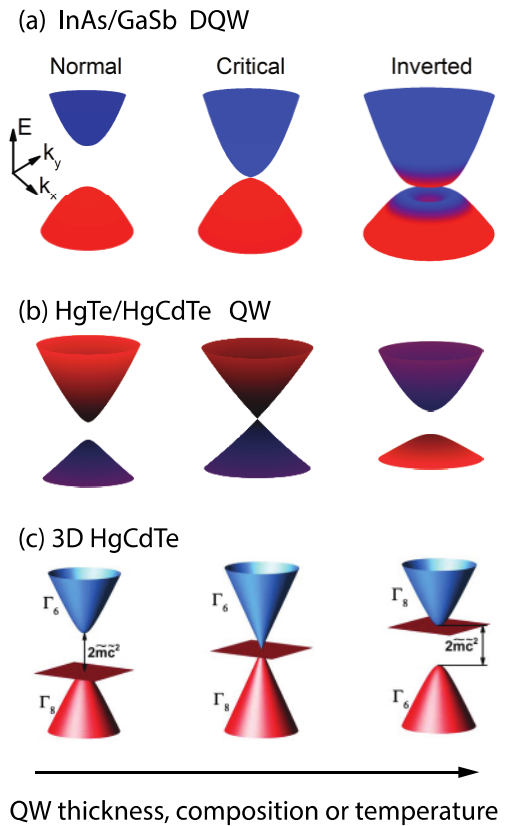
Top: Electronic structure of ZrTe₅ and the corresponding LLs in magnetic fields. Bottom: Circular polarization resolved measurements determine the nature of the observed optical transitions.

near the intrinsic limit. At zero magnetic field, our samples show graphene-like optical absorption, which signifies their two-dimensional (2D) nature. Because of the low carrier density, we are able to observe a series of interband Landau-level (LL) transitions that exhibit the characteristic dispersion of 2D massive Dirac fermions, similar to that in graphene but with a small relativistic mass corresponding to a 9.4 meV energy gap. Using the newly developed circular polarized magneto-IR capability, we separate the σ^+ and σ^- active transitions and resolve a fourfold splitting of low-lying LL transitions. These observations enable further exploration of the origin in the splitting: (i) the band asymmetry breaks the degeneracy of the dipole allowed interband LL transitions, and (ii) the breaking of the remaining two-fold degeneracy is due to a combined effect of large g -factor and a small energy gap in this system. Our results suggest that the electronic structure of ZrTe_5 is 2D-like and support a Dirac semimetal interpretation but with a small relativistic mass (or gap).

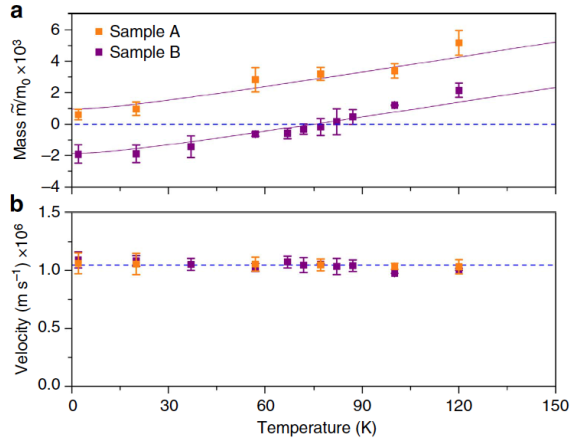
Semiconductor to semimetal transition in 2D and 3D topological materials

Semiconductor to semimetal transition describes the evolution of the electronic band structure from a normal to an inverted state, which can be driven by the effect of quantum confinement, temperature, strain, magnetic field, etc. Such transition has seen renewed interest in recent years, as it is identified as a “topological” phase transition in several material systems including $\text{HgTe}/\text{HgCdTe}$ and InAs/GaSb quantum wells (QWs), and 3D HgCdTe .

In collaboration with Drs. Wei Pan and John Klem at the Sandia Labs, we have systematically studied the LL structure of a series of InAs/GaSb double QWs from the normal to the inverted state. We show that owing to the low carrier density of our samples, the magneto-absorption spectra evolve from a single cyclotron resonance peak in the normal state to multiple absorption peaks in the inverted state with distinct magnetic field dependence. Using an eight-band Pidgeon-Brown model, we are able to explain all the major absorption peaks observed in our experiment. We demonstrate that the semiconductor to semimetal transition in InAs/GaSb double QWs can be realized by manipulating the quantum confinement, the strain, and the magnetic field.



Evolution of the band alignment in (a) InAs/GaSb double QWs, (b) $\text{HgTe}/\text{HgCdTe}$ QWs, and (c) 3D HgCdTe near the critical gapless state. Semiconductor to semimetal transition is controlled by the QW thickness, material composition, or temperature. Adopted after Refs. [3,4] and Publications [2,7].



Parameters of Kane fermions in 3D HgCdTe extracted from IR magneto-spectroscopy data: (a) Rest mass (or gap) and (b) band velocity. The blue dashed line represents the theoretical value.

where the low-energy electronic dispersion mimics the relativistic dynamics of Dirac particles. These 3D Dirac-like quasiparticles, so-called Kane fermions [5], feature Dirac cones crossed at the vertex by an additional flat band.

Future Plans

Probing energy, symmetry and dispersion of low-lying excitations and studying the (quantum) phase transitions in novel electronic materials via magneto-optical spectroscopy is a longstanding goal of this program. In the next funding period, we plan to investigate phase transitions in quantum spin Hall insulator (QSHI) systems in a broader parameter space by adding pressure/strain as a new tunability, while continuing to explore exotic, optically excited states in TIs and atomically thin materials with strong spin-orbit coupling (such as TMDs).

Phase transitions in InAs/GaSb and HgTe QWs. Quantum phase transitions in InAs/GaSb and HgTe QWs are of fundamental interest. A QSHI phase is expected to occur in the inverted state, leading to intriguing transport phenomena such as dissipationless helical edge modes. However, the experimental evidence of QSHI to date is largely from edge-mode transport measurements, which could be contaminated by artifacts due to the inevitable chemical etching process in device fabrication. We plan to investigate the strain/pressure- and temperature-driven semiconductor to semimetal transitions in these two QW systems using bulk-sensitive magneto-IR spectroscopy and compare experimental results with the $\mathbf{k} \cdot \mathbf{p}$ calculations.

Phase transitions in Dirac/Weyl semimetals. The objective here is to investigate the phase transitions, including 3D to 2D transition and weak/strong TI to Dirac/Weyl semimetal transition, in topological semimetals such as or similar to ZrTe₅ (Dirac), HfTe₅ (Dirac), TaIrTe₄ (Weyl), and NbP (Weyl). In Dirac/Weyl semimetals with layered structures, we plan to study the effects of quantum confinement (or layer thickness) or interlayer coupling (tuned by external

In 3D systems, electronic bands with linear (conical) dispersion are found in Weyl and Dirac semimetals, or in a conventional gapless semiconductor such as Cd_xHg_{1-x}Te near the critical concentration, $x_c \sim 0.17$, separating the regions with trivial and inverted band alignments. Variation of the QW thickness or Cd content does not allow continuous tuning of the system across the gapless state. However, it can be achieved by changing the temperature (or pressure). In collaboration with Dr. Frederic Tepe (University of Montpellier, France), we have explored the continuous evolution of band structure of bulk HgCdTe using magneto-IR spectroscopy as temperature is tuned across the phase transition,

high pressure). Implementation of high-field high-pressure magneto-spectroscopy techniques represents a major experimental development task.

References

- [1] H. M. Weng, X. Dai, and Z. Fang, *Phys. Rev. X* **4**, 011002 (2014).
- [2] Z. Fan, Q.-F. Liang, Y. B. Chen, S.-H. Yao, and J. Zhou, *Scientific Reports* **7**, 45667 (2017).
- [3] B. A. Bernevig, T. L Hughes, and S. C. Zhang, *Science* **314**, 1757 (2006).
- [4] J. Ludwig, Yu. B. Vasilyev, N. N. Mikhailov, J. M. Poumirol, Z. Jiang, O. Vafek, and D. Smirnov, *Phys. Rev. B* **89**, 241406(R) (2014).
- [5] M. Orlita et al. *Nature Physics* **10**, 233 (2014).

Publications

1. “*Landau-level spectroscopy of massive Dirac fermions in single-crystalline ZrTe₅ thin flakes*”, Y. Jiang, Z. L. Dun, H. D. Zhou, Z. Lu, K.-W. Chen, S. Moon, T. Besara, T. M. Siegrist, R. E. Baumbach, D. Smirnov, and Z. Jiang, *Phys. Rev. B* **96**, 041101(R) (2017).
2. “*Probing the semiconductor to semimetal transition in InAs/GaSb double quantum wells by magneto-infrared spectroscopy*,” Y. Jiang, S. Thapa, G. D. Sanders, C. J. Stanton, Q. Zhang, J. Kono, W. Lou, K. Chang, S. D. Hawkins, J. F. Klem, W. Pan, D. Smirnov, and Z. Jiang, *Phys. Rev. B* **95**, 045116 (2017).
3. “*Magnetic brightening and control of dark excitons in monolayer WSe₂*”, X. Zhang, T. Cao, Z. Lu, Y. C. Lin, F. Zhang, Y. Wang, Z. Li, J. C. Hone, J. A. Robinson, D. Smirnov, S. G. Louie, T. F. Heinz, *Nature Nanotechnology* (2017), doi:10.1038/nnano.2017.105.
4. “*Quantum Oscillations at Integer and Fractional Landau Level Indices in Single-Crystalline ZrTe₅*,” W. Yu, Y. Jiang, J. Yang, Z. L. Dun, H. D. Zhou, Z. Jiang, P. Lu, and W. Pan, *Scientific Reports* **6**, 35357 (2016).
5. “*Magnetoinfrared spectroscopic study of thin Bi₂Te₃ single crystals*,” L.-C. Tung, W. Yu, P. Cadden-Zimansky, I. Miotkowski, Y. P. Chen, D. Smirnov, and Z. Jiang, *Phys. Rev. B* **93**, 085140 (2016).
6. “*Unraveling Photoinduced Spin Dynamics in the Topological Insulator Bi₂Se₃*,” M. C. Wang, S. Qiao, Z. Jiang, S. N. Luo, and J. Qi, *Phys. Rev. Lett.* **116**, 036601 (2016).
7. “*Temperature-driven massless Kane fermions in HgCdTe crystals*,” F. Tepe, M. Marcinkiewicz, S. S. Krishtopenko, S. Ruffenach, C. Consejo, A. M. Kadykov, W. Desrat, D. But, W. Knap, J. Ludwig, S. Moon, D. Smirnov, M. Orlita, Z. Jiang, S. V. Morozov, V. I. Gavrilenko, N. N. Mikhailov, and S. A. Dvoretiskii, *Nature Communications* **7**, 12576 (2016).
8. “*Electronic properties of unstrained unrelaxed narrow gap InAs_xSb_{1-x} alloys*,” S. Suchalkin, J. Ludwig, G. Belenky, B. Laikhtman, G. Kipshidze, Y. Lin, L. Shterengas, D. Smirnov, S. Luryi, W. L. Sarney, and S. P. Svensson, *Journal of Physics D: Applied Physics* **49**, 105101 (2016).

Vortex Lattice and Vortex Core Structure in $\text{HgBa}_2\text{CuO}_{4+\delta}$ Single Crystals

William P. Halperin, Northwestern University

Program Scope

My program, entitled Antiferromagnetism and Superconductivity, was supported from grant DE-FG02-05ER46248 during the past three years to investigate the role of competing interactions on superconducting behavior, including electronic ordering and antiferromagnetism. There are three classes of superconductors studied here: i) cuprates ii) pnictides and iii) the topological superconductor UPT_3 . The project has concentrated on nuclear magnetic resonance (NMR) studies over a wide range of magnetic fields of the vortex state of cuprates and pnictides. NMR is uniquely suited to unveil magnetic order and dynamics respectively through site-specific NMR spectra and relaxation as well as its possible coexistence with superconductivity. In this

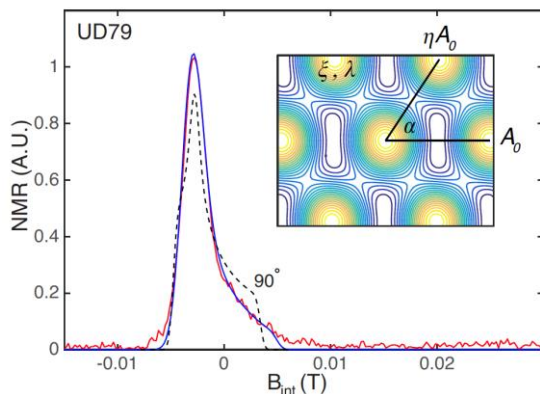


Figure 1. Vortex lattice NMR (Redfield) lineshape of the first high-frequency satellite for the apical site of Hg1201, which would correspond to 168.6 MHz in Fig. 2, ($T_c = 79$ K, ΔT_c of 1.5 K) at $T = 35$ K, $H = 16.5$ T, below the vortex freezing temperature ~ 40 K. Inset, the corresponding vortex lattice from a fit to the theory given by the blue curve. Comparison is made with a constraint for a VL with a square lattice.

abstract I focus on one aspect, the work at high field performed at Northwestern University (up to 14 T) extended to higher fields (up to 30 T) at the National High Magnetic Field Laboratory (NHMFL).

Additionally, our past work on the unconventional superconductor UPT_3 has demonstrated that this unique compound is a topological superconductor with odd-parity. Its chiral symmetry appears to be manifest in an unusual vortex lattice structure that has been investigated using small angle neutron scattering (SANS). Notably, the single crystals grown by my research group are the highest quality ever produced and are of such significant size and quality that they are ideal for neutron scattering up to magnetic fields that extend into the elusive C vortex phase above 1.6 T.

Recent Progress

We have investigated vortex structures in the single layer cuprate Hg1201 using ^{17}O nuclear magnetic resonance (NMR) methods up to very high magnetic fields using facilities at the National High Magnetic Field Laboratory to complement capability in my laboratory up to 14 T. This will include investigation of the vortex structures, from which penetration depth, coherence length, and vortex lattice symmetry will be determined. Characterization of bound states in the vortex cores will be performed using NMR spatially selective techniques we have pioneered in prior work. A fundamental question of the nature of electronic ordering will be directed toward answering the question is there broken time reversal symmetry, which is of central importance to the understanding of high temperature superconductivity in cuprates. In the figure above I show the magnetic field probability distribution, $P(H)$, which is given by the NMR spectrum and lineshape. This is the first measurement of $P(H)$ using a quadrupolar satellite that is made possible by an exceptionally intrinsically narrow NMR line (in the normal state). This approach is

immune from complications from overlap in the spectra from various oxygen sites as is the case in YBCO for example.

Future Plans

The main project on vortex structure and vortex core physics looking forward requires two advances in experimental technique combining capabilities developed in my laboratory and supported by the DOE/BES program. The first of these is the application of spin-spin relaxation rate ($1/T_2$) using ^{17}O NMR which is sensitive to magnetic fluctuations[1]. There is evidence in YBCO from earlier work in my laboratory that the vortex core breaks time reversal symmetry[2] and we seek to determine the slow dynamics of such behavior in a simpler high temperature superconducting cuprate, Hg1201 in the range of doping that we can prepare spanning underdoped to overdoped thereby determining the relationship of this putative symmetry to pseudogap physics. The second requirement is critically important and builds upon our earlier work with ^{17}O NMR YBCO aligned powders[3]. This is the use of spatially resolved NMR to isolate the probe nucleus in the vortex core. These works require the use of high magnetic fields with which my group has extensive experience up to 42 T in the hybrid magnet at NHMFL[4]. The proposed work takes advantage of single crystals of Hg1201 grown at Los Alamos by Mun Chan on which we perform oxygen isotope exchange and correspondingly the tuning of doping to achieve the results we have reported previously. This work will be performed by Ingrid Stolt a graduate student in my group and who has participated in the initial research on vortex structure in Hg1201 published this year, that was part of the PhD thesis of Peter Lee who graduated this past year[5].

References

1. High Field Vortex Phase Diagram of $\text{YBa}_2\text{Cu}_3\text{O}_7$ from ^{17}O NMR, H.N. Bachman, A.P. Reyes, V.F. Mitrovic, W.P. Halperin, A. Kleinhammes, P. Kuhns, and W.G. Moulton, *Phys. Rev. Lett.* **80**, 1726 (1998).; A.M. Mounce, Sangwon Oh, Jeongseop A. Lee, W.P. Halperin, A.P. Reyes, P.L. Kuhns, M.K. Chan, C. Dorow, L. Ji, D. Xia, X. Zhao, M. Greven, Absence of Static Current-Loop Magnetism at the Apical Oxygen Site in $\text{HgBa}_2\text{CuO}_{4+\delta}$ from NMR, *Phys. Rev. Lett.* **111**, 187003 (2013).
2. Coherent Charge and Spin Density Waves in Underdoped $\text{HgBa}_2\text{CuO}_{4+\delta}$, Jeongseop A. Lee, Yizhou Xin, W. P. Halperin, A. P. Reyes, P. L. Kuhns, M. K. Chan, *New J. Phys.* **19**, 033024 (2017).
3. Spatially Resolved Electronic Structure Inside and Outside the Vortex Core of a High Temperature Superconductor, V. F. Mitrovic, E. E. Sigmund, M. Eschrig, H. N. Bachman, W.P. Halperin, A.P. Reyes, P. Kuhns, and W.G. Moulton, *Nature* **413**, 501 (2001).
4. Antiferromagnetism in the Vortex Cores of $\text{YBa}_2\text{Cu}_3\text{O}_{7-d}$, V. F. Mitrovic, E. E. Sigmund, W.P. Halperin, A.P. Reyes, P. Kuhns, W.G. Moulton, *Phys. Rev B. Rapid* **67**, 220503 (2003).
5. Magnetic Field Induced Vortex Lattice Transition in $\text{HgBa}_2\text{CuO}_{4+\delta}$, Jeongseop A. Lee, Yizhou Xin, I. Stolt, W. P. Halperin, A. P. Reyes P. L. Kuhns, M. K. Chan, *Phys. Rev.B* **95**, 024512 (2017).

Publications

1. Observation of broken time-reversal symmetry in the B phase of the heavy fermion superconductor UPt₃, E. R. Schemm, W. J. Gannon, C. Wisne, W. P. Halperin, A. Kapitulnik, *Science* **345**, 190 (2014).
2. Enhanced self-diffusion of adsorbed methanol in silica aerogel, J.A. Lee, A.M. Mounce, S. Oh, A.M. Zimmerman, W.P. Halperin, *Phys. Rev. B* **90**, 174501 (2014).
3. Nodal gap structure and order parameter symmetry of the unconventional superconductor UPt₃, W. J. Gannon, W. P. Halperin, C. Rastovski, K. J. Schlesinger, J. Hlevyack, C. Steiner, M. R. Eskildsen, A. B. Vorontsov, J. Gavilano, U. Gasser, G. Nagy, *New J. Phys.* **17**, 023041 (2015).
4. Nuclear Magnetic Resonance Measurements and Electronic Structure of Pu(IV) in [(Me)₄N]₂ PuCl₆, Andrew M. Mounce, Hiroshi Yasuoka, Georgios Koutroulakis, Jeongseop A. Lee, Herman Cho, Frédéric Gendron, Eva Zurek, Brian L. Scott, Julie A. Trujillo, Alice K. Slemmons, Justin N. Cross, Joe D. Thompson, Stosh A. Kozimor, Eric D. Bauer, Jochen Autschbach, and David L. Clark, *Inorg. Chem.* **55**, 8371 (2016).
5. Persistence of slow fluctuations in the overdoped regime of Ba(Fe_{1-x}Rh_x)₂As₂ superconductors, L. Bossoni, M. Moroni, P. C. Canfield, W. P. Halperin, M. H. Julien, H. Mayaffre, A. Reyes and P. Carretta, *Phys. Rev. B* **93**, 224517 (2016).
6. Coherent Charge and Spin Density Waves in Underdoped HgBa₂CuO_{4+δ}, Jeongseop A. Lee, Yizhou Xin, W. P. Halperin, A. P. Reyes, P. L. Kuhns, M. K. Chan, *New J. Phys.* **19**, 033024 (2017).
7. Magnetic Field Induced Vortex Lattice Transition in HgBa₂CuO_{4+δ}, Jeongseop A. Lee, Yizhou Xin, I. Stolt, W. P. Halperin, A. P. Reyes P. L. Kuhns, M. K. Chan, *Phys. Rev. B* **95**, 024512 (2017).

Poster Sessions

Experimental Condensed Matter Physics Principal Investigators' Meeting

POSTER SESSION I Monday, September 11, 2017

1. *Towards a universal description of vortex matter in superconductors*
Leonardo Civale, Los Alamos National Laboratory
2. *APS conference for undergraduate women in physics*
Ted Hodapp, American Physical Society
3. *Designing metastability: coercing materials to phase boundaries*
T. Zac Ward, Oak Ridge National Laboratory
4. *Fermi gases in bichromatic superlattices*
John Thomas, North Carolina State University
5. *Experimental study of novel relativistic Mott insulators in the two dimensional limit*
Claudia Ojeda-Aristizabal, California State University, Long Beach
6. *Complex states, emergent phenomena, and superconductivity in intermetallic and metal-like compounds*
Sergey Bud'ko, Ames Laboratory
7. *High magnetic field microwave spectroscopy of two-dimensional electron systems in GaAs and graphene*
Lloyd Engel, Florida State University
8. *Nanostructured materials: from superlattices to quantum dots*
Ivan Schuller, University of California, San Diego
9. *Probing electron correlations in 1D electronic materials using single quantum channels*
Jeremy Levy, University of Pittsburgh
10. *Infrared Hall effect in correlated electronic materials*
Dennis Drew, University of Maryland
11. *Nanoscale electrical transfer and coherent transport between atomically-thin materials*
Douglas Strachan, University of Kentucky
12. *Proximity effects and topological spin currents in van der Waals heterostructures*
Ben Hunt, Carnegie Mellon University
13. *Spin dependent transport in metallic nanoparticles*
Dragomir Davidovic, Georgia Tech
14. *Fundamental studies of high-anisotropy nanomagnets*
George Hadjipanayis, University of Delaware
15. *Time-resolved spectroscopy of insulator-metal transitions: exploring low-energy dynamics in strongly correlated systems*
Gunter Luepke, College of William and Mary

16. *Superconductivity and magnetism in d- and f-electron materials*
Brian Maple, University of California, San Diego
17. *Correlated and complex materials*
Brian Sales, Oak Ridge National Laboratory
18. *Establishing the consequences of intertwined order parameters in spatially modulated superconductors*
Greg MacDougall, University of Illinois, Champaign
19. *Quantum Hall systems in and out of equilibrium*
Michael Zudov, University of Minnesota
20. *Effects of lateral broken crystal symmetries on spin-orbit torques and magnetic anisotropy*
Daniel Ralph, Cornell University
21. *Charge inhomogeneity in correlated electronic systems*
Barry Wells, University of Connecticut
22. *Imaging electrons in atomically layered materials*
Bob Westervelt, Harvard University

Experimental Condensed Matter Physics Principal Investigators' Meeting

POSTER SESSION II Tuesday, September 12, 2017

1. *Non-equilibrium magnetism: materials and phenomena*
Frances Hellman, Lawrence Berkeley National Laboratory
2. *Spin effects in magnetic and non-magnetic 2d correlated insulators*
Phil Adams, Louisiana State University
3. *Exploring photon-coupled fundamental interactions in colloidal semiconductor based hybrid nanostructures*
Min Ouyang, University of Maryland
4. *Exploring superconductivity at the edge of magnetic or structural instabilities*
Ni Ni, University of California, Los Angeles
5. *Spectroscopy of degenerate one-dimensional electrons in carbon nanotubes*
Jun Kono, Rice University
6. *Spin-coherent transport under strong spin-orbit interaction*
Jean Heremans, Virginia Polytechnic Institute and State University
7. *Controlling superconductivity via tunable nanostructure arrays*
Nadya Mason, University of Illinois, Champaign
8. *Dynamics of emergent crystallinity in photonic quantum materials*
Jon Simon, University of Chicago
9. *Experiments on nonsymmorphic topological and Weyl semimetals*
N. Phuan Ong, Princeton University
10. *Cold exciton gases in semiconductor heterostructures*
Leonid Butov, University of California, San Diego
11. *Tuning quantum fluctuations in low-dimensional and frustrated magnets*
Arthur Ramirez, University of California, Santa Cruz
12. Raman spectroscopy of pnictide and other unconventional superconductors
Girsh Blumberg, Rutgers University
13. *Synthesis and observation of emergent phenomena in Heusler compound heterostructures*
Chris Palmström, University of California, Santa Barbara
14. *Understanding iron superconductors/focus on nodal behavior*
Gregory Stewart, University of Florida
15. *Digital synthesis - a pathway to create and control novel states of condensed matter*
Anand Bhattacharya, Argonne National Laboratory
16. *Bose-Einstein condensation of magnons and potential device applications*
John Ketterson, Northwestern University

17. *Understanding and controlling conductivity transitions in correlated solids: spectroscopic studies of electronic structure in vanadates*
Kevin Smith, Boston University
18. *Spin-polarized scanning tunneling microscopy studies of nanoscale magnetic and spintronic nitride systems*
Arthur Smith, Ohio University
19. *Nanoscale magnetic Josephson junctions and superconductor/ferromagnet proximity effects for low-power spintronics*
Ilya Krivorotov, University of California, Irvine
20. *LaCNS: Building neutron scattering infrastructure in Louisiana for advanced materials*
John DiTusa, Louisiana State University
21. *Superconductivity and magnetism*
Wai-Kwong Kwok, Argonne National Laboratory

Poster Abstracts

Program Title: **Spin Effects in Low Dimensional Correlated Systems**

Principle Investigator: **Philip W. Adams**

Mailing Address: **Department of Physics and Astronomy, Louisiana State University, Baton Rouge, LA 70803**

Email: **adams@phys.lsu.edu**

Program Scope

This program focuses on the magneto-transport, non-equilibrium relaxation, and spin-resolved density-of-states properties of disordered two-dimensional paramagnetic, ferromagnetic, and superconducting systems. Specifically, we are currently investigating Zeeman-limited superconductivity in crystalline Al films, and in hybrid structures containing spin-orbit generating Pb islands. We are also investigating the critical current and critical field behavior of 2D Pb structures having non-trivial multiply connected geometries. In addition, we provide heat capacity measurements for Prof. Shane Stadler's studies of NiMnSi-based and Ni₂MnGa-based magnetocalorics.

Recently we have been investigating the Zeeman-limited phase diagram (PD) of epitaxially-grown crystalline Al films. This was the first such study made on a relatively low disorder system (see Pub. 6). Indeed, all previous studies of the Zeeman-mediated (spin-paramagnetic) superconducting transition have been made on highly disordered quenched condensed films. In addition to lower disorder, epitaxial layer-by-layer growth gives one unprecedented control of sample thickness.

A second line of investigation focuses on lateral proximity structures comprised several monolayer-thick Al films with imbedded Pb islands, see Fig 1. Via precise control of the UHV Pb deposition and annealing process (on Si-111), Ken Shih's group at UT Austin are able to form nanoscale Pb islands having a tunable average separation. Our interest is in how the Pb islands induce spin orbit coupling into the superconducting Al matrix. Specifically, we are measuring the average spin-orbit coupling parameter of the films as a function of the Pb island separation.

We are also studying the perpendicular critical field behavior of 7 ML- thick Pb nano-mesh films having a complex multiply connected structure, as can be seen in Fig. 2. The mesh wires are 7 ML high and about 50 nm wide. These structures are similar to the more widely studied geometric superconducting networks [1], which exhibit interesting flux quantization effects such as complex frustration-driven magnetoresistance. In contrast, our samples offer the opportunity to study these Little-Parks-like effects [2] in a

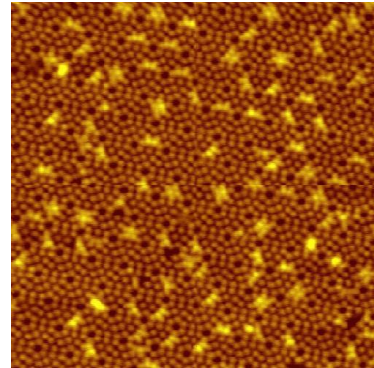


Fig 1. STM image of Pb clusters that were subsequently capped with a 15 ML Al film. (30nm x 30nm)

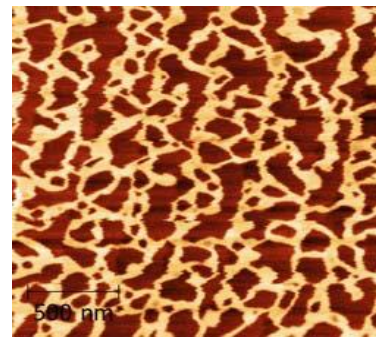


Fig 2. STM image of a 7 ML-thick Pb nano-mesh. (2 μ m x 2 μ m)

disordered network. Furthermore STM analysis of the specific geometrical characteristics of the meshes will allow us to correlate the critical field properties of the mesh network with its physical structure.

Recent Progress

Spin-imbalanced superconductivity is a historically important problem that remains at the forefront of condensed matter physics [3,4]. By the late 1960's it was known that a Zeeman field could induce a spatially modulated order parameter in a spin singlet superconductor, i.e. the Ferrel-Fulde-Larkin-Ovchinnikov (FFLO) state [3,4], near the critical field phase boundary. To date, however, no definitive signature of an FFLO phase has been identified, although extensive circumstantial evidence for the phase has emerged in recent years [5,6,7,8,9]. We recently completed a project in which we mapped out the Zeeman-limited phase diagram of crystalline Al films as a function of film thickness in the range of 7 ML to 30 ML.

These phase diagrams were compared to those expected of a homogeneous BCS ground state. The Zeeman critical field transition is first-order at low temperature but the observed hysteresis is substantially smaller than the expected BCS limits of stability. In particular the supercooling phase boundary (normal to superconducting boundary) resides at substantially larger fields than predicted by homogeneous theory. This suggests that an intermediate high-field inhomogeneous phase preempts the transition to the BCS phase. This intermediate superconducting phase may be a disordered remnant of FFLO.

Shown in Fig. 3 are the parallel critical field transitions of a selection of Al/Pb-cluster films. The green vertical line represents the Clogston-Chandrasekhar (Zeeman) critical field of an infinitely thin film having no spin-orbit scattering [3,4]. The legend indicates the average separation between Pb clusters, where $d = \infty$ corresponds to a 15 ML Al film with no clusters, and $d = 0$ corresponds to a 15 ML Al film deposited over a complete ML of Pb. Note that the critical field increases rapidly with decreasing d . From these data our collaborator Gianluigi Catelani can extract the spin-orbit coupling parameter. Clearly there is a halo of spin-orbit coupling induced around each cluster. Our goal is to establish the lateral length scale of these halos.

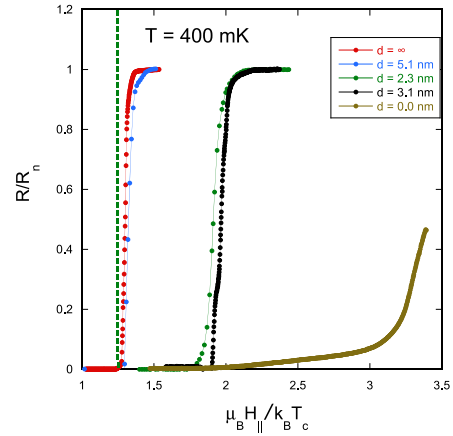


Fig 3. Parallel (Zeeman) critical field transition in Al/Pb-cluster film as a function of the cluster separation d .

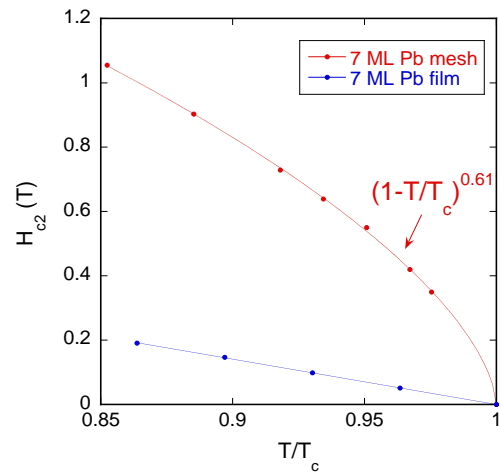


Fig 4. Scaling behavior of the perpendicular critical field of a Pb mesh film, such as the one shown in Fig. 2.

Finally, we have just completed measurements of the perpendicular critical field H_{c2} and the critical current behavior of Pb mesh samples such as shown in Fig. 2. The multiply connected topology naturally lends itself to frustration effects as the superconductor attempts to quantize the magnetic flux thru the quasi-random distribution of voids. Interestingly, this purely topological effect gives rise to an anomalous scaling behavior of the critical field. Shown in Fig. 4 is the temperature dependence of H_{c2} near T_c for a 7 ML mesh sample and a corresponding uniform coverage 7 ML-thick sample. Note that the uniform film exhibits the expected linear temperature dependence. In contrast the mesh exhibits a power law behavior with a critical exponent near $2/3$. The analysis of this data is ongoing but we should begin working on a manuscript soon.

Future Plans

In the near future we will begin a series of experiments aimed at exploring the Zeeman critical field transition and its associated dynamics in a multiply connected geometry. We have established the characteristics of the Zeeman-limited phase diagram in continuous, epitaxial films and we not would like to extend these studies to the more complex case of a multiply connected geometry. This is a “high risk – high reward” project that is motivated by Jim Valles’ pioneering studies of the S-I transition on nano-honeycombed substrates [40,41]. Specifically, the Valles group observed field-induced oscillations in the normal state resistance of critically disordered films that were deposited on the honeycombed substrates (see Fig. 17). The oscillations are attributed to quantized flux through the substrate holes. Indeed, the oscillations are reminiscent of Little-Parks oscillations [42], but they occur in the insulating phase of the films. This surprising result indicates that, near the critical field, the insulating phase of the films is populated by incoherent Cooper pairs.

We have obtained honeycombed substrates from Valles’ group, and plan to deposit a thin Al film on them, along with a tunneling counter-electrode. We can carefully align the film to parallel orientation, in which case the magnetic flux through the honeycomb pores is near zero. By tilting the film slightly out of parallel orientation, we will induce a perpendicular component of the magnetic field and a corresponding magnetic flux through the pores. The average unit cell area for the pores is $A \sim 8 \times 10^3 \text{ nm}^2$, thus one flux quanta per unit cell can be obtained with a perpendicular field of $\sim 0.25 \text{ T}$. Since the parallel critical field in our Al films is near 6 T, we can introduce a flux quantum into the honeycomb pores by rotating out of parallel by only 2.5 degrees. Our goal is to look for oscillations in the film resistance and/or tunneling conductance as a function of tilt angle at various points in the hysteretic critical field region.

References

1. Y. Xiao, D.A. Huse, P.M. Chaikin, M. Higgins, S. Bhattacharya, and D. Spencer, Phys. Rev. B **65**, 214503 (2002); O. Sato and M. Kato, Phys. Rev B **68**, 094509 (2003).
2. W.A. Little and R.D. Parks, Phys. Rev. Lett. **9**, 9 (1962).
3. P. Fulde and R. A. Ferrell, Phys. Rev. **135**, A550 (1964).

4. A. I. Larkin and Y. N. Ovchinnikov, *Zh. Eksp. Teor. Fiz.* **47** (1964).
5. H. A. Radovan, N. A. Fortune, T. P. Murphy, S. T. Hannahs, E. C. Palm, S. W. Tozer, and D. Hall, *Nature* **425**, 51 (2003).
6. G. Koutroulakis, M. D. Stewart, V. F. Mitrovi, M. Horvati, C. Berthier, G. Lapertot, and J. Flouquet, *Phys. Rev. Lett.* **104**, 087001 (2010).
7. H. Mayaffre, S. Kramer, M. Horvatic, C. Berthier, K. Miyagawa, K. Kanoda, and V. F. Mitrovic, *Nature Physics* **10**, 928 (2014).
8. R. Leo and E. S. Daniel, *Rep. Prog. Phys.* **73**, 076501 (2010).
9. Y.-a. Liao, A. S. C. Rittner, T. Paprotta, W. Li, G. B. Partridge, R. G. Hulet, S. K. Baur, and E. J. Mueller, *Nature* **467**, 567 (2010).
10. H. Q. Nguyen, S. M. Hollen, M. D. Stewart, Jr., J. Shainline, A. J. Yin, J. M. Xu, and J. M. Valles, Jr., *Phys. Rev. Lett.* **103**, 157001 (2009).

Publications (2015 - 2017)

1. “Non-equilibrium Dynamics in Zeeman-Limited Superconducting Al Films”, J.C. Prestigiacomo and P.W. Adams, *J. Low Temp. Phys.* 183, 238 (2016).
2. “An Exploration of Some Magnetic Fundamentals in EuSe Using mu SR”, I. Terry, **P.W. Adams**, N. Bykovetz, S.R. Giblin, Z. Guguchi, R. Khasanov, J. Klein, C.L. Lin and T.J. Liu, *AIP Adv.* **6**, 055705 (2016).
3. “Ultra-thin Two-Dimensional Superconductivity with Strong Spin-orbit Coupling”, H. Nam, H. Chen, T.J. Liu, J. Kim, C. Zhang, J. Yong, T.R. Lemberger, P.A. Katz, J.R. Kirtley, K.A. Moler, **P.W. Adams**, A.H. Macdonald, C-K Shih, *PNAS* **113**, 10513 (2016).
4. “Complex Superconductivity in the Non-centrosymmetric Compound Re_6Zr ”. M.A. Kahn, A.B. Karki, T. Samanta, D. Browne, S. Stadler, I. Vekhter, A. Pandey, **P.W. Adams**, D.P. Young, S. Teknowijoyo, K. Cho, R. Prozorov, and D.E. Graf, *Phys. Rev. B* **94**, 144515 (2016).
5. “The influence of Hydrostatic Pressure on the Magnetic and Magnetocaloric Properties of DyRu_2Si_2 ”, A.U. Saleheen, T. Samanta, M. Khan, **P.W. Adams**, D.P. Young, I. Dubenko, N. Ali, and S. Stadler, *J. App. Phys.* **121**, 045101 (2017).
6. “Zeeman-limited Superconductivity in Crystalline Al Films”, **P.W. Adams**, H. Nam, C.K. Shih, and G. Catelani, *Phys. Rev. B* **95**, 094520 (2017).
7. “Origin of Multicaloric Phenomena: Combined Magnetocrystalline and Magnetostrictive Coupling”, T. Samanta, P. Lloveras, A.U. Saleheen, D.L. Lepkowski, E. Kramer, I. Dubenko, **P.W. Adams**, D.P. Young, M. Barrio, J.L. Tamarit, N. Ali, and S. Stadler, *Phys. Rev B* (under review)
8. “The Effects of Hydrostatic Pressure on the Martensitic Transition, Magnetic, and Magnetocaloric Effects of $\text{Ni}_{45}\text{Mn}_{43}\text{CoSn}_{11}$ ”, S. Pandey, A. Saleheen, A. Quetz, J.-H. Chen, A. Aryal, I. Dubenko, **P. W. Adams**, S. Stadler, and N. Ali, *MRS Comm.* (under review)

Program Title: Digital Synthesis: A Pathway to New Materials at Interfaces of Complex Oxides

Principle Investigator : Anand Bhattacharya

Address: Materials Science Division, Bldg. 223, 9700 S. Cass Ave., Argonne National Laboratory, Argonne, IL 60657.

email: anand@anl.gov

Program Scope:

In our program, we seek to create superlattices and heterostructures incorporating complex oxides, and in the near future topological semi-metals, where novel electronic and magnetic properties emerge. We synthesize these materials using molecular beam epitaxy (MBE) based techniques. This allows us to tailor chemically precise interfaces with roughness comparable to or less than the length scales for interfacial charge transfer and exchange interactions. The complex oxides host diverse collective states of condensed matter. The richness of observed phenomena in these materials, which have also presented some of the greatest challenges to our understanding, are due to their strongly interacting degrees of freedom. Surfaces and interfaces between complex oxides provide an environment where these degrees of freedom may ‘reconstruct’, leading to properties that are qualitatively different from those of their bulk constituents. We seek to discover and explore states with novel responses to external electric and magnetic fields, thermal gradients and pulsed ‘ultra-fast’ excitations, and to understand why these occur based on probes of electronic, magnetic and chemical structure. The properties that we explore include non-collinear and geometrically frustrated magnetism, novel spin Seebeck and Nernst effects, proximity induced superconductivity, reversible motion of O through crystal lattices driven by electric fields, and transient non-equilibrium behavior of correlated states in response to ‘ultra-fast’ excitations. In several projects, our work is carried out in close collaboration with colleagues whose expertise is complementary to our own. The recent addition of Dillon Fong to our program will substantially enhance our efforts towards understanding the role of structural distortions and defects in determining the electronic and magnetic properties of oxide interfaces, and in controlling these during synthesis. We have also begun a new direction in the area of topological semi-metals where we seek to create epitaxial thin films and heterostructures which will serve as model systems to realize the many novel effects that have been predicted for this class of materials.

The properties that we explore include non-collinear and geometrically frustrated magnetism, novel spin Seebeck and Nernst effects, proximity induced superconductivity, reversible motion of O through crystal lattices driven by electric fields, and transient non-equilibrium behavior of correlated states in response to ‘ultra-fast’ excitations. In several projects, our work is carried out in close collaboration with colleagues whose expertise is complementary to our own. The recent addition of Dillon Fong to our program will substantially enhance our efforts towards understanding the role of structural distortions and defects in determining the electronic and magnetic properties of oxide interfaces, and in controlling these during synthesis. We have also begun a new direction in the area of topological semi-metals where we seek to create epitaxial thin films and heterostructures which will serve as model systems to realize the many novel effects that have been predicted for this class of materials.

Recent Progress (since 2015):

1. *Non-collinear magnetism via charge transfer at interfaces between correlated metals:* In conventional semiconductors and metals, a mismatch between electronic energy levels at an interface leads to charge transfer that equilibrates the chemical potential, resulting in interfacial

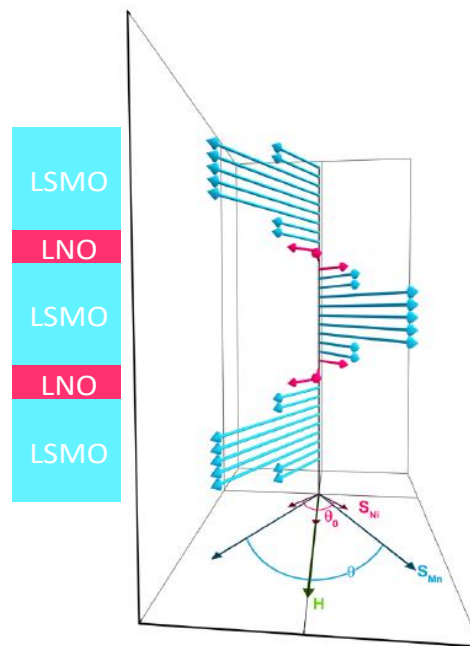


Fig. 1. A non-collinear helical magnetic structure develops in superlattices comprising of two correlated metals $\text{La}_{2/3}\text{Sr}_{1/3}\text{MnO}_3$ and LaNiO_3 as a result of interfacial charge transfer and exchange interactions. (J. Hoffman et al., PRX 2016)

electric fields and band bending. In narrow band *correlated metals*, often derived from doping a parent Mott insulator, interfacial charge transfer can have profound consequences leading to changes in the electronic and magnetic ground state of the interfacial region. Due to the relatively large screening length in metallic 3d perovskite oxides, this interfacial region can extend a substantial distance away from the interface. In superlattices of $(\text{La}_{2/3}\text{Sr}_{1/3}\text{MnO}_3)_9/(\text{LaNiO}_3)_n$ where both constituent materials are metals, we used neutron scattering and x-ray absorption spectroscopy to show that interfacial transfer of electrons from $\text{La}_{2/3}\text{Sr}_{1/3}\text{MnO}_3$ into LaNiO_3 and interfacial exchange interactions leads to a *non-collinear* magnetic structure (Fig. 1). Our data are consistent with the development of a *spin-helix* within the LaNiO_3 layers. (J. Hoffman et al., *Phys. Rev X* (2016)). Measurements of the angular dependence of Nernst effect combined with anisotropic magnetoresistance data, as well as resonant x-ray scattering at the Ni L-edge confirm the non-collinear helimagnetic structure measured using neutron scattering on the same samples (*unpublished*). We also have ongoing collaboration with Prof. Jian-Min Zuo's group (UIUC) and with Dr. Albina Borisevich (ORNL) to understand how charge transfer might affect local electronic properties near these interfaces using transmission electron microscopy (STEM EELS). In the near future, we plan to explore proximity induced superconductivity in the helimagnetic LNO layers.

2. *Spin Seebeck Effect in Correlated Paramagnets and Antiferromagnets*: We have developed a new approach for generating spin currents in *patterned* magnetic heterostructures via the Spin Seebeck effect (SSE). By using a microscale on-chip local heater, we are able to generate a large thermal gradient confined to the chip surface *without* a large increase in the total sample temperature (S. Wu et al., *Appl. Phys. Lett.* 2014; *J. Appl. Phys.* 2015). This approach allows the study of the Spin Seebeck effect at very low temperatures (even less than 1K), as the total heat load from the patterned heater wire can be readily handled by standard cryostats. Using this approach, we discovered a large spin Seebeck effect in paramagnetic correlated insulators $\text{Gd}_3\text{Ga}_5\text{O}_{12}$ (GGG) and DyScO_3 (DSO), where the signal grows strongly in magnitude below $\sim 20\text{K}$. (S. Wu et al., *Phys. Rev. Lett.* 2015). We also observed a very substantial SSE signal from antiferromagnetic insulator MnF_2 (S. Wu et al., *Phys. Rev. Lett.* (2016)). The magnitude of the observed signal is larger than that seen from the prototypical ferromagnetic insulator $\text{Y}_3\text{Fe}_5\text{O}_{12}$ (YIG). This work opens up the class of materials where a large SSE signal can be obtained.

3. *Dilutely doped SrTiO_3 in the Extreme Quantum Limit*: We doped high quality single crystals of SrTiO_3 by annealing in ultra-high vacuum conditions. This led to the formation of a homogeneous three dimensional electron gas (3DEG), whose carrier density could be tuned all the way down to $\sim 5 \times 10^{15}/\text{cm}^3$. The 3DEG shows no sign of carrier freeze-out down to 20 mK. We observed Shubnikov – de Haas (SdH) oscillations in resistivity at dilution fridge temperatures and high magnetic fields (measurements carried out at the National High Magnetic Field laboratory in Tallahassee, FL). The carrier density inferred from the SdH measurements agree with Hall data. At sufficiently high fields, we were able to drive the 3DEG into the quantum limit where all carriers occupy the lowest Landau level – a first (A. Bhattacharya et al., *Nature Communications* (2016)). In this limit, the kinetic energy is partially quenched and we expect correlations between electrons to become more important. We found that the I-V characteristic becomes non-linear. Furthermore, the increased degeneracy with increasing magnetic field causes the Fermi level E_F to drop in the lowest Landau level, which leads to puddle formation when E_F becomes comparable to the disorder potential.

Future Plans: a) *Thermo galvanic effects as a probe of magnetic correlations in the absence of static long range order*: There are several known materials systems, including candidate

quantum spin liquids, where geometric frustration or low dimensionality leads to the absence of long range order even in the presence of strong exchange/dipolar interactions between spins. As our previous work has shown, such materials may also give rise to spin currents when subjected to thermal gradients (SSE). We will use the SSE to probe magnetic correlations and fluctuations within these materials as a function of applied magnetic field and temperature with the goal of teasing out the nature of their magnetic excitations. For quantum spin liquids, and low dimensional magnets, these excitations can be qualitatively different.¹ A similar approach using the Nernst effect is being used by us to probe magnetic correlations in conducting correlated materials, particularly in regions where long-range order is absent or too weak to be detected via conventional scattering probes.

b) *Oxide MBE growth of 4d and 5d transition metal oxides:* We have set up a new oxide MBE system that will enable us to synthesize thin films and heterostructures of oxides incorporating 4d and 5d transition metals. The materials of interest include perovskite iridates, that have been the focus of much recent activity due to the interplay of spin-orbit coupling and Mott physics.² Metallic 4d and 5d transition metal oxides may also be effective detectors of spin currents via the inverse spin Hall effect. Our synthesis approach will enable novel doping techniques such as interfacial charge transfer and delta-doping.

c) *Topological semi-metals:* We are planning to grow thin films of 3-dimensional topological semi-metals³ using MBE based approaches. The class of materials includes the Weyl and Dirac semi-metals. Several target compounds have been identified and an effort is now underway. We seek to create large area high quality epitaxial thin films that will enable us to explore a wide variety of novel phenomena involving transport in magnetic and gate electric fields, strain and proximity effects.

d) *Electric field induced motion of O atoms across oxide interfaces:* A new direction in our program will be in understanding and controlling O vacancies at interfaces using electric fields. O vacancies are known to affect electronic and magnetic phase transitions in correlated oxides.⁴ The motion of O atoms can be controlled with electric fields. We have identified several compounds where interfacial O motion may lead to new phenomena. We will carry out studies of electronic/magnetic properties as well as structural chemical changes using synchrotron based techniques to better understand the mechanisms linking O ion motion to magnetic/electronic properties.

References:

¹ "Quantum spin liquids: a review." Savary, Lucile, and Leon Balents, *Rep. Prog. Phys.* **80**, 016502 (2016).

² "Novel $J_{\text{eff}} = 1/2$ Mott state induced by relativistic spin-orbit coupling in Sr_2IrO_4 ." B. J. Kim et al. *Phys. Rev. Lett.* **101**, 076402 (2008).

³ "Dirac fermions in solids: from high- T_c cuprates and graphene to topological insulators and Weyl semimetals." Oskar Vafeek and Ashvin Vishwanath, *Annu. Rev. Condens. Matter Phys.* **5**, 83-112 (2014).

⁴ "Reversible redox reactions in an epitaxially stabilized SrCoO_x oxygen sponge." Hyoungjeen Jeon, Woo Seok Choi, Michael D. Biegalski, Chad M. Folkman, I-Cheng Tung, Dillon D. Fong, John W. Freeland et al. *Nature Materials* **12**, 1057-1063 (2013).

Publications (supported by Department of Energy, Basic Energy Sciences, since 2015):

- P1. "Effect of defects on reaction of NiO surface with Pb-contained solution" J. Kim, B. Hou, C. Park, C. B. Bahn, J. Hoffman, J. Black, A. Bhattacharya, N. Balke, H. Hong, J. H. Kim, and S. Hong, S., 2017. *Scientific Reports*, 7 (2017)
- P2. "Elemental and lattice-parameter mapping of binary oxide superlattices of $(\text{LaNiO}_3)_4/(\text{LaMnO}_3)_2$ at atomic resolution." Ji-Hwan Kwon, Ping Lu, Jason Hoffman, Renliang Yuan, Aram Yoon, Anand Bhattacharya, and Jian-Min Zuo. *Semiconductor Science and Technology* **32**, 014002 (2016).
- P3. "Oscillatory Non-collinear Magnetism Induced by Interfacial Charge Transfer in Metallic Oxide Superlattices." Jason Hoffman, B. J. Kirby, J. Kwon, J. W. Freeland, I. Martin, O. G. Heinonen, P. Steadman, Hua Zhou, Christian M. Schlepütz, Suzanne G. E. te Velthuis, Jian-Min Zuo, Anand Bhattacharya, *Phys. Rev. X* **6**, 041038 (2016).
- P4. "Spatially inhomogeneous electron gas deep in the extreme quantum limit of strontium titanate", Anand Bhattacharya, Brian Skinner, Guru Khalsa, Alexey V. Suslov, *Nature Communications* **7**, 12974 (2016). doi:10.1038/ncomms12974
- P5. "Towards spin-polarized two-dimensional electron gas at a surface of an antiferromagnetic insulating oxide", R. Mishra, Y.-M. Kim, Q. he, X. Huang, S.-K. Kim, M. A. Susner, A Bhattacharya, D. D. Fong, S. T. Pantelidis, A. Y. Borisevich, *Phys. Rev. B* **94**, 045123 (2016).
- P6. "In situ surface/interface x-ray diffractometer for oxide molecular beam epitaxy." J. H. Lee, I. C. Tung, S-H. Chang, A. Bhattacharya, D. D. Fong, J. W. Freeland, and Hawoong Hong. *Review of Scientific Instruments* **87**, no. 1 (2016): 013901.
- P7. "Antiferromagnetic spin Seebeck Effect." Stephen M. Wu, Wei Zhang, Amit KC, Pavel Borisov, John E. Pearson, J. Samuel Jiang, David Lederman, Axel Hoffmann, and Anand Bhattacharya. *Phys. Rev. Lett.* **116**, 097204 (2016).
- P8. "Near-nanoscale-resolved energy band structure of $\text{LaNiO}_3/\text{La}_{2/3}\text{Sr}_{1/3}\text{MnO}_3/\text{SrTiO}_3$ heterostructures and their interfaces." Thaddeus J. Asel, Hantian Gao, Tyler J. Heintz, Drew Adkins, Patrick M. Woodward, Jason Hoffman, Anand Bhattacharya, and Leonard J. Brillson. *J. Vac. Sci. Tech. B* **33**, 04E103 (2015).
- P9. "Spin Seebeck devices using local on-chip heating", S. M. Wu, F. Y. Fradin, J. Hoffman, A. Hoffmann, A. Bhattacharya, *J. Appl. Phys.* **117**, 17C509 (2015).
- P10. "Paramagnetic Spin Seebeck Effect", S. M. Wu, JE Pearson, A Bhattacharya, *Phys. Rev. Lett.* **114**, 186602 (2015).
- P11. "Spectral Weight Redistribution in $(\text{LaNiO}_3)_n/(\text{LaMnO}_3)_2$ superlattices from Optical Spectroscopy", P. Di Pietro, J. Hoffman, A. Bhattacharya, S. Lupi, A. Perucchi, *Phys. Rev. Lett.* **114**, 156801 (2015).
- P12. "Spin waves in micro-structured yttrium iron garnet nanometer-thick films", M. B. Jungfleisch, Wei Zhang, Wanjun Jiang, Houchen Chang, J. Sklenar, S.M. Wu, J. E. Pearson, A. Bhattacharya, J. B. Ketterson, Mingzhong Wu, A. Hoffmann, *J. Appl. Phys.* **117**, 17D128 (2015).

Project Title: Raman spectroscopy of pnictide and other unconventional superconductors

Principle Investigator: Girsh Blumberg

Mailing Address: Department of Physics & Astronomy, Rutgers University,
136 Frelinghuysen Road, Piscataway NJ 08854-8019

E-mail: girsh@physics.rutgers.edu

Program Scope

The objectives of this project are to investigate the manner in which charge, spin, orbital and lattice interactions and dynamics evolve through various low temperature phases of “strongly correlated materials” by employing polarization resolved electronic Raman scattering spectroscopy, and to clarify the microscopic origin of collective behavior like charge, spin, or orbital density waves and unconventional superconductivity is induced in these materials by electron correlations. Among the anticipated outcomes of this project are (i) the elucidation of the microscopic origin of superconductivity in the iron-pnictide family of materials, including the evaluation of the role of electronic correlations in both normal and superconducting states, the role of proximity to nematic and/or magnetically ordered states, the mechanisms of formation of the superconducting order parameter and its symmetry; (ii) insights into how to design new materials with enhanced superconducting properties; and (iii) determination of a spectrum of collective excitation in superconductors and in heavy fermion materials with “hidden orders”.

Recent Progress and Future Plans

Heavy Fermions. Many novel electronic ground states have been found to emerge from the hybridization between localized *d*- or *f*-electron states and conduction electron states in correlated electron materials. The HF compound URu₂Si₂ hosts two competing staggered phases: a non-magnetic *Hidden Order* (HO) phase and a *Large Moment Antiferromagnetic* (LMAF) phase. Both phases are principally due to special ordering of the uranium *5f* orbitals. The PI and his collaborators used polarization resolved Raman spectroscopy to identify the symmetry of low energy excitations above and below the HO transition, to uncover the hidden order parameter, and to study the interrelation between the HO phase and the LMAF phase. From the symmetry analysis of the discovered collective mode, the PI and collaborators determined that the HO parameter breaks local vertical and diagonal reflection symmetries at the uranium sites, resulting in states with distinct chiral properties:

- (1) The HO phase is the *Chirality Density Wave* which breaks local chiral symmetry [9]; and
- (2) The LMAF phase is the *Orbital Moment Density Wave* which breaks local time reversal symmetry [3].

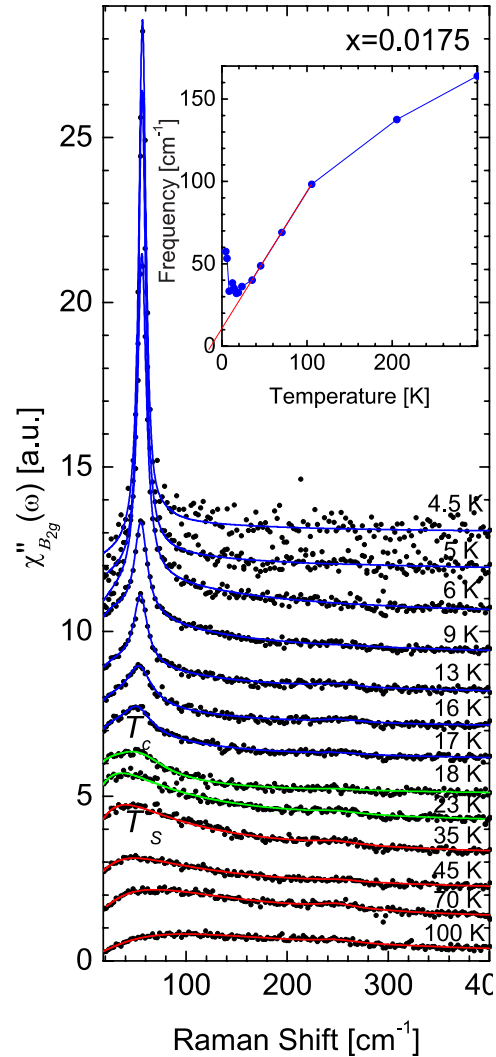
The nature of these almost degenerate HO and LMAF phases has been theorized before, but the experimental signature of the direct interrelation between them was lacking. The PI and his

collaborators drive and detect dynamic oscillations between HO and LMAF states by using polarized light, and as such provide direct experimental evidence for a unified order parameter describing the competing phases [3]. The experiment is a realization of a similar 1961 proposal by A. Bardasis and J. R. Schrieffer to study unconventional sub-dominant pairing in the superconductors.

As a continuation of this work, the PI and collaborators will study the symmetry and properties of the superconducting state emerging only from the *Chirality Density Wave* below $T_c = 1.5$ K.

Multiband pnictide superconductors. Iron-pnictides present a new paradigm of multi-band superconductivity in proximity to nematic transition and spin density wave (SDW) order. Most FeAs compounds share a common phase diagram which in the underdoped region is marked by a structural transition at temperature T_S from tetragonal to orthorhombic phase followed by an SDW transition at T_{SDW} , slightly below T_S . The orthorhombic distortion at T_S breaks C_4 rotational symmetry while the translational symmetry is broken due to doubling of the unit cell either at or above T_{SDW} . The system provides exceptional setting to study coexistence or competition between quadrupole fluctuations, superconductivity, and density-wave phases.

We performed multiple series of polarized low-temperature Raman scattering studies of phononic, electronic, inter-band and magnetic excitations on many following families of compounds: CaFe_2As_2 , $(\text{Sr}_2\text{VO}_3)_2\text{Fe}_2\text{As}_2$, $\text{Fe}_{1+x}(\text{TeSe})$, $\text{K}_{0.75}\text{Fe}_{1.75}\text{Se}_2$, $\text{BaFe}_{1.9}\text{Pt}_{0.1}\text{As}_2$, $\text{Ca}(\text{Co}_x\text{Fe}_{1-x})_2\text{As}_2$, $\text{NaFe}_{1-x}\text{Co}_x\text{As}$, $\text{Ba}_{1-x}\text{K}_x\text{Fe}_2\text{As}_2$, $\text{FeSe}_{1-x}\text{S}_x$ and others. The Raman susceptibility shows critical non-symmetric charge fluctuations across the entire phase diagram. The charge fluctuations are interpreted in terms of waves of quadrupole intra-orbital excitations. We demonstrate that above the structural phase transition the quadrupolar fluctuations with long correlation times are precursor to the discrete four-fold symmetry breaking transition. This is manifested in the critical slowing down of XY-symmetry collective fluctuations observed in dynamical Raman susceptibility and strong enhancement of the static Raman susceptibility. Below superconducting

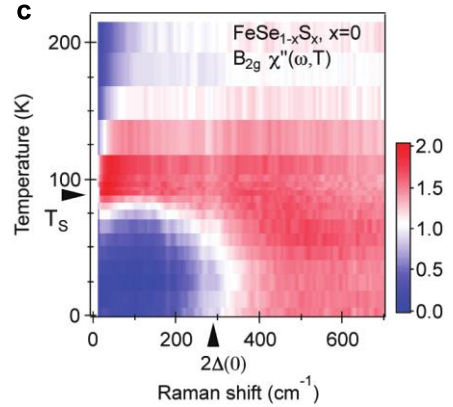


$\text{NaFe}_{1-x}\text{Co}_x\text{As}$: Evolution of XY Raman susceptibility showing the development of the critical mode and emergency of the sharp collective response in the SC phase [7].

transition, these collective excitations undergo a metamorphosis into a coherent in-gap collective mode of extraordinary strength and at the same time serve as glue for non-conventional superconducting pairing [2, 4-8, 10].

In the most recent studies of $\text{FeSe}_{1-x}\text{S}_x$, the system which does not show long range magnetic order, we have discovered that a gap reminiscent to a mean-field order parameter opens up in the spectra of XY symmetry below T_s . The data is interpreted as formation of the stripe-type quadrupole wave order which is competing with ferro-quadrupole fluctuations. The interpretation provides explanation for the recently reported anisotropic electronic properties in the nematic phase as well as for the puzzling orbital selective superconductivity.

We will continue spectroscopic study of the oxypnictide compounds across the phase diagram as a function of carrier concentration, temperature, strain, and magnetic field.



FeSe: T-dependence of Raman response of the nematic fluctuations and the development of nematic gap below T_s . [Work in progress]

ACKNOWLEDGMENTS The work is done in collaboration with P. Dai, B.S. Dennis, K. Haule, A. Ignatov, H.-H. Kung, M.B. Maple, Y. Matsuda, J.A. Mydosh, J. Paglione, A. Sefat, T. Shibauchi, V.K. Thorsmolle, N.L. Wang, S.F. Wu, Z. Yin, W.-L. Zhang, C. Zhang. Research was supported by U.S. DOE, Office of BES, Award DE-SC0005463.

Publications

1. H.-H. Kung, M. Salehi, I. Boulares, A.F. Kemper, N. Koirala, M. Brahlek, P. Lostak, C. Uher, R. Merlin, X. Wang, S.-W. Cheong, S. Oh, G. Blumberg. Surface vibrational modes of the topological insulator Bi_2Se_3 observed by Raman spectroscopy. [Phys. Rev. B **95**, 245406 \(2017\)](#).
2. S.-F. Wu, P. Richard, H. Ding, H.-H. Wen, Guotai Tan, Meng Wang, Chenglin Zhang, Pengcheng Dai, G. Blumberg. Superconductivity and electronic fluctuations in $\text{Ba}_{1-x}\text{K}_x\text{Fe}_2\text{As}_2$ studied by Raman scattering. [Phys. Rev. B **95**, 085125 \(2017\)](#).
3. H.-H. Kung, S. Ran, N. Kanchanavatee, V. Krapivin, A. Lee, J.A. Mydosh, K. Haule, M.B. Maple, and G. Blumberg. The analogy between the 'hidden order' and the orbital antiferromagnetism in URu_2Si_2 . [Phys. Rev. Lett. **117**, 227601 \(2016\)](#).
4. W.-L. Zhang, Athena S. Sefat, H. Ding, P. Richard, and G. Blumberg. Stress-induced nematicity in EuFe_2As_2 studied by phononic Raman spectroscopy. [Phys. Rev. B **94** 014513 \(2016\)](#). Featured in [Kaleidoscope](#).
5. W.-L. Zhang, Z. P. Yin, A. Ignatov, Z. Bukowski, Janusz Karpinski, Athena S. Sefat, H. Ding, P. Richard, and G. Blumberg. Raman scattering study of spin-density-wave-induced anisotropic electronic properties in AFe_2As_2 ($\text{A}=\text{Ca}, \text{Eu}$). [Phys. Rev. B **93** 205106 \(2016\)](#).

6. Daixiang Mou, Aashish Sapkota, H.-H. Kung, Viktor Krapivin, Yun Wu, A. Kreyssig, Xingjiang Zhou, A. I. Goldman, G. Blumberg, Rebecca Flint, and Adam Kaminski, Discovery of unconventional charge density wave at the surface of $K_{0.9}Mo_6O_{17}$. [Physics Review Letters **116** 196401 \(2016\)](#).
7. V. K. Thorsmølle, M. Khodas, Z. P. Yin, Chenglin Zhang, S. V. Carr, Pengcheng Dai, and G. Blumberg. Critical Charge Fluctuations in Iron Pnictide Superconductors. [Phys. Rev. B **93** 054515 \(2016\)](#). (Cited 22 times. Web of Science featured this publication as **highly cited paper**: received enough citations to place it in the top 1% of the academic field of Physics based on a highly cited threshold for the field and publication year.)
8. S. Ziemak, K. Kirshenbaum, S. R. Saha, R. Hu, J.-P. Reid, R. Gordon, L. Taillefer, D. Evtushinsky, S. Thirupathaiah, S. V. Borisenko, A. Ignatov, D. Kolchmeyer, G. Blumberg, and J. Paglione. Isotropic multi-gap superconductivity in $BaFe_{1.9}Pt_{0.1}As_2$ from thermal transport and spectroscopic measurements. [Superconductor Science and Technology. Invited submission for focus issue on Multicomponent Superconductivity 28\(1\):014004 \(2015\)](#).
9. H.-H. Kung, R. E. Baumbach, E. D. Bauer, V. K. Thorsmølle, W.-L. Zhang, K. Haule, J. A. Mydosh, and G. Blumberg. Chirality density wave of the 'hidden order' phase in URu_2Si_2 . [Science **347** 1339 \(2015\)](#). (Cited 22 times)
10. S.-F. Wu, W.-L. Zhang, D. Hu, H.-H. Kung, A. Lee, H.-C. Mao, P.-C. Dai, H. Ding, P. Richard and G. Blumberg. Collective excitations of dynamic Fermi surface deformations in $BaFe_2(As_{0.5}P_{0.5})_2$. [arXiv e-print](#).

37 invited and contributed conference presentations acknowledging this DOE grant support are listed at <http://girsh.rutgers.edu/index.php/talks/>

Program Title: Complex States, Emergent Phenomena, and Superconductivity in Intermetallic and Metal-Like Compounds

Principle Investigators: Paul Canfield (FWP leader), Sergey Bud'ko, Yuji Furukawa, David Johnston, Adam Kaminski, Vladimir Kogan, Makariy Tanatar, Ruslan Prozorov. Division of Materials Science and Engineering, Ames Laboratory, Iowa State University, Ames, IA 50011

Program Scope: Our FWP focuses on discovering, understanding and ultimately controlling new and extreme examples of complex states, emergent phenomena, and superconductivity. Materials manifesting specifically clear or compelling examples (or combinations) of superconductivity, strongly correlated electrons, quantum criticality, and exotic, bulk magnetism are of particular interest given their potential to lead to revolutionary steps forward in our understanding of their complex, and potentially energy relevant, properties. The experimental work consists of new materials development and crystal growth, combined with detailed and advanced measurements of microscopic, thermodynamic, transport and electronic properties, at extremes of pressure, temperature, magnetic field, and resolution. The theoretical work focuses on understanding and modeling transport, thermodynamic and spectroscopic properties using world-leading, phenomenological approaches to superconductors and modern, quantum many-body theory.

The priority of this FWP is the development and understanding of model systems combined with agile and flexible response to, and leadership in, a rapidly-changing materials landscape. To accomplish this goal, our combined synthetic, characterization and theory efforts operate both in series and in parallel. This work supports the DOE mission by directly addressing the Grand Challenge of understanding the Emergence of Collective Phenomena: Strongly Correlated Multiparticle Systems and is a key contributor to fulfilling the Ames Laboratory Scientific Strategic Plan for preeminence in solid-state materials discovery, synthesis, and design; this FWP designs, discovers, characterizes and understands systems that shed light on how remarkable properties of matter emerge from complex correlations of the atomic or electronic constituents and, as a result, provides better control of these properties. These efforts directly address research priorities identified in the Basic Research Needs Workshops on *Quantum Materials for Energy Relevant Technology* and *Synthesis Science for Energy Relevant Technology*.

Recent Progress: Fe-based superconductivity: The effects of pressure, strain and substitution on Fe-based superconductors continues to reveal the delicate interplay between electronic, magnetic, and structural interactions and states in these high- T_c compounds. By careful and systematic growth [1], optimization, and characterization we have been able determine the details of the T-P phase diagram of FeSe [2,3], as well as Fe(Se_{1-x}S_x). By a combination of pressure dependent transport, scattering and Mossbauer spectroscopy we have been able to identify and understand the cascade of pressure induced phases and relate them to the commonly understood T-P and T-x

phase diagrams for the BaFe_2As_2 based materials. We also undertook a large effort to grow, characterize and understand the newly discovered $\text{CaKFe}_4\text{As}_4$ system [4,5]. Whereas some of the superconducting properties of $\text{CaKFe}_4\text{As}_4$ are similar to near optimally doped $(\text{Ba}_{0.5}\text{K}_{0.5})\text{Fe}_2\text{As}_2$, it is highly ordered, has a new, half-collapsed-tetragonal phase under pressure, and unique Ca and K sites as well as two As sites, and a changed point symmetry for the Fe site. In addition, we have been able to substitute Co and Ni onto the Fe site and stabilize a new form, spin-vortex-crystal, of antiferromagnetic order that does not entail nematic / orthorhombic ordering [6].

Progression from local moment magnetism to fragile magnetism: The progression from local moment magnetism to fragile / tunable magnetism has been another focus of our efforts. We have studied a variety of rare earth based phosphides and arsenides such as RPd_2P_2 , as well as EuT_2X_2 for $T = \text{Mn, Co}$ and $X = \text{As, P}$. As a step toward more fragile moments, similar to those found in the Fe-based superconductors, we have studied AET_2As_2 for $\text{AE} = \text{Ba, Sr, Ca}$ and $T = \text{Cr, Mn, Co}$ and Pd [7]. Finally we have found exceptionally fragile magnetism that can be driven to quantum phase transitions by modest pressure in LaCrGe_3 [8].

Future Plans: We plan to better understand the new, fragile magnetic state we have discovered in the Ni- and Co-substituted $\text{CaKFe}_4\text{As}_4$. The spin-vortex-crystal antiferromagnetic ordering is a new form of order for Fe-based superconductors and does not, formally, have any orthorhombic state associated with it. Further substitution, pressure and strain studies, using our full suite of thermodynamic, transport and spectroscopic measurements, will allow us to understand, master and integrate this system into our broader sense of Fe-based superconductivity. We will also search for other examples of transition metal based fragile magnetism such as we have found in LaCrGe_3 . Our intent is to determine what features are necessary and/or sufficient for the emergence of superconductivity.

Another objective of the FWP is to continue to expand its abilities to measure thermodynamic, transport, spectroscopic properties as a function of applied pressure, stress and strain. We intend to increase the pressure range of our resistivity and magnetization measurements to above 10 GPa. We plan to implement elasto-resistivity measurements in applied magnetic fields up to 14 T and establish London penetration measurements (via tunnel diode oscillator technique) for pressures up to 2 GPa. The FWP will also provide the pressure expertise to help other Ames Lab FWPs to implement pressure as part of their routine characterization repertoires.

Finally, having invested significant effort in building a laboratory-based, tunable, high resolution, laser ARPES system over the past several years, we will further enhance its capabilities to low temperatures ($<5\text{K}$) and use this system to address a number of key questions about superconductivity. For example, the order parameter is the most important characteristic of a SC because it contains key information about the pairing mechanism. ARPES is the only technique that can directly measure the momentum dependence of the SC gap. There are several areas where the unique capabilities of the tunable, high resolution laser ARPES system can lead to significant breakthroughs. We propose to study the order parameter of iron arsenic superconductors in 3-

dimensional momentum space with higher precision than previously possible. Surprisingly, after 8 years of intensive research, this issue still remains elusive, with a number of seemingly contradictory results. The problem with direct measurements of the SC gap in the pnictides is that most of the synchrotron facilities do not have sufficient energy resolution in order to make accurate measurements along k_z . Measurements of the superconducting gap with traditional laser ARPES systems are performed at fixed photon energy and thus lack critical k_z information. We will use our tunable laser ARPES spectrometer to address this key issue using single crystals of pure and substituted $\text{CaKFe}_4\text{As}_4$. Our measurements will focus on the 3-dimensional momentum dependence of the SC gap across the phase diagram. Such information is absolutely critical in order to firmly establish the symmetry of the order parameter across the phase diagram in iron arsenic high temperature SC and identify the correct pairing mechanism.

References

1. A. E. Böhmer, V. Taufour, W. E. Straszheim, T. Wolf, P. C. Canfield, Variation of transition temperatures and residual resistivity ratio in vapor-grown FeSe. *Physical Review B* **94**, 024526 (2016).
2. U. S. Kaluarachchi, V. Taufour, A. E. Böhmer, M. A. Tanatar, S. L. Bud'ko, V. G. Kogan, R. Prozorov, P. C. Canfield, Nonmonotonic pressure evolution of the upper critical field in superconducting FeSe. *Physical Review B* **93**, 064503 (2016).
3. K. Kothapalli, A. E. Bohmer, W. T. Jayasekara, B. G. Ueland, P. Das, A. Sapkota, V. Taufour, Y. Xiao, E. Alp, S. L. Bud'ko, P. C. Canfield, A. Kreyssig, A. I. Goldman, Strong cooperative coupling of pressure-induced magnetic order and nematicity in FeSe. *Nature Communications* **7**, 12728 (2016).
4. W. R. Meier, T. Kong, U. S. Kaluarachchi, V. Taufour, N. H. Jo, G. Drachuck, A. E. Böhmer, S. M. Saunders, A. Sapkota, A. Kreyssig, M. A. Tanatar, R. Prozorov, A. I. Goldman, F. F. Balakirev, A. Gurevich, S. L. Bud'ko, P. C. Canfield, Anisotropic thermodynamic and transport properties of single-crystalline $\text{CaKFe}_4\text{As}_4$. *Physical Review B* **94**, 064501 (2016).
5. D. X. Mou, T. Kong, W. R. Meier, F. Lochner, L. L. Wang, Q. S. Lin, Y. Wu, S. L. Bud'ko, I. Eremin, D. D. Johnson, P. C. Canfield, A. Kaminski, Enhancement of the Superconducting Gap by Nesting in $\text{CaKFe}_4\text{As}_4$: A New High Temperature Superconductor. *Physical Review Letters* **117**, 277001 (2016).
6. W. R. Meier, Q.-P. Ding, A. Kreyssig, S. L. Bud'ko, A. Sapkota, K. Kothapalli, V. Borisov, R. Valentí, C. D. Batista, P. P. Orth, R. M. Fernandes, A. I. Goldman, Y. Furukawa, A. E. Böhmer, P. C. Canfield, Hedgehog spin-vortex crystal stabilized in a hole-doped iron-based superconductor. arXiv:1706.01067
7. N. S. Sangeetha, A. Pandey, Z. A. Benson, D. C. Johnston, Strong magnetic correlations to 900 K in single crystals of the trigonal antiferromagnetic insulators SrMn_2As_2 and CaMn_2As_2 . *Physical Review B* **94**, 094417 (2016).
8. V. Taufour, U. S. Kaluarachchi, R. Khasanov, M. C. Nguyen, Z. Guguchia, P. K. Biswas, P. Bonfa, R. De Renzi, X. Lin, S. K. Kim, E. D. Mun, H. Kim, Y. Furukawa, C. Z. Wang, K. M. Ho, S. L. Bud'ko, P. C. Canfield, Ferromagnetic Quantum Critical Point Avoided by the

Appearance of Another Magnetic Phase in LaCrGe_3 under Pressure. *Physical Review Letters* **117**, 037207 (2016).

Publications

The FWP published over 100 papers in FY 2016 and 2017 (to date) and their list will not fit within allocated space. This includes 10 papers published in *Physical Review Letters* and *Physical Review X*, 65 in *Physical Review B*, 3 papers in Nature family of Journals and 3 papers in Science family of journals. Below we list few selected papers published in this period both above in references as well as below.

9. P. C. Canfield, S. L. Bud'ko, Preserved entropy and fragile magnetism. *Reports on Progress in Physics* **79**, 084506 (2016).
10. A. Kaminski, S. Rosenkranz, M. R. Norman, M. Randeria, Z. Z. Li, H. Raffy, J. C. Campuzano, Destroying Coherence in High-Temperature Superconductors with Current Flow. *Physical Review X* **6**, 031040 (2016).
11. D. X. Mou, A. Sapkota, H. H. Kung, V. Krapivin, Y. Wu, A. Kreyssig, X. J. Zhou, A. I. Goldman, G. Blumberg, R. Flint, A. Kaminski, Discovery of an Unconventional Charge Density Wave at the Surface of $\text{K}_{0.9}\text{Mo}_6\text{O}_{17}$. *Physical Review Letters* **116**, 196401 (2016).
12. Anand, V. K., Dhaka, R. S., Lee, Y., Harmon, B. N., Kaminski, A., Johnston, D. C., Physical properties of metallic antiferromagnetic $\text{CaCo}_{1.86}\text{As}_2$ single crystals, *Physical Review B* **89**, 214409 (2014)
13. M. A. Tanatar, A. E. Bohmer, E. I. Timmons, M. Schutt, G. Drachuck, V. Taufour, K. Kothapalli, A. Kreyssig, S. L. Bud'ko, P. C. Canfield, R. M. Fernandes, R. Prozorov, Origin of the Resistivity Anisotropy in the Nematic Phase of FeSe. *Physical Review Letters* **117**, 127001 (2016).
14. V. Taufour, U. S. Kaluarachchi, V. G. Kogan, Constraints on the merging of the transition lines at the tricritical point in a wing-structure phase diagram. *Physical Review B* **94**, 060410 (2016).
15. Y. Tokiwa, B. Piening, H. S. Jeevan, S. L. Bud'ko, P. C. Canfield, P. Gegenwart, Super-heavy electron material as metallic refrigerant for adiabatic demagnetization cooling. *Science Advances* **2**, e1600835 (2016).
16. K. Cho, M. Konczykowski, S. Teknowijoyo, M. A. Tanatar, Y. Liu, T. A. Lograsso, W. E. Straszheim, V. Mishra, S. Maiti, P. J. Hirschfeld, R. Prozorov, Energy gap evolution across the superconductivity dome in single crystals of $(\text{Ba}_{1-x}\text{K}_x)\text{Fe}_2\text{As}_2$. *Science Advances* **2**, e1600807 (2016).
17. A. E. Böhmer, A. Sapkota, A. Kreyssig, S. L. Bud'ko, G. Drachuck, S. M. Saunders, A. I. Goldman, P. C. Canfield, Effect of Biaxial Strain on the Phase Transitions of $\text{Ca}(\text{Fe}_{1-x}\text{Co}_x)_2\text{As}_2$. *Physical Review Letters* **118**, 107002 (2017).
18. Y. Wu, L. L. Wang, E. Mun, D. D. Johnson, D. X. Mou, L. N. Huang, Y. Lee, S. L. Bud'ko, P. C. Canfield, A. Kaminski, Dirac node arcs in PtSn_4 . *Nature Physics* **12**, 667-671 (2016).

Project Title: Cold Exciton Gases in Semiconductor Heterostructures

PI: Leonid Butov, University of California San Diego

Program Scope

An indirect exciton, IX, is a bound pair of an electron and a hole confined in spatially separated quantum well layers. IXs form a platform for studying a system of cold bosons:

- Long lifetimes of IXs allow them to cool down to low temperatures below the temperature of quantum degeneracy. This gives an opportunity to realize and study cold excitons.
- IXs have built-in dipole moments and, as a result, interact repulsively. This leads to strong correlations in IXs.
- Due to built-in IX dipole moments, IX energy can be controlled by voltage. This gives an opportunity to create tailored potential landscapes for IXs by voltage.
- The long lifetimes allow IXs to travel over large distances before recombination. This gives an opportunity to study exciton transport by imaging spectroscopy.
- The spatial separation between an electron and a hole in IX and the suppression of exciton scattering in a coherent IX gas result to the suppression of spin relaxation. This allows the realization of long-range spin currents.

The goal of this project is to explore IXs in GaAs coupled quantum well heterostructures and in new heterostructures based on single-atomic-layers of transition-metal dichalcogenides (TMD).

Recent Progress

1. Pancharatnam-Berry phase in condensate of IXs [1] (Fig. 1). We will present the observation of the Pancharatnam-Berry phase in a condensate of IXs in a GaAs coupled quantum well structure. The Pancharatnam-Berry phase leads to phase shifts of interference fringes in IX interference patterns. Correlations are found between the phase shifts, polarization pattern of IX emission, and onset of IX spontaneous coherence. The Pancharatnam-Berry phase is acquired due to coherent spin precession in IX condensate.

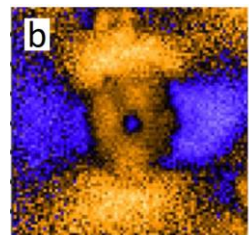
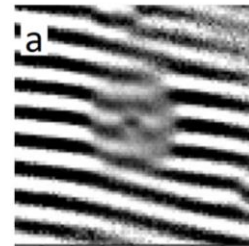


Fig. 1. (a) Interference fringes in IX interferometry pattern. (b) Linear polarization of IX emission.

2. IXs at room temperature in TMD heterostructures [2] (Fig. 2). We will present the observation of IXs at room temperature in TMD van der Waals heterostructure. The room-temperature data include long IX lifetimes, orders of magnitude longer than lifetimes of direct excitons in single-layer TMD, and control of IX energy by voltage. The IXs in TMD heterostructure are characterized by the high binding energy making them stable at room temperature and giving the opportunity both for exploring fundamental phenomena in excitonic systems and developing excitonic devices at high temperatures.

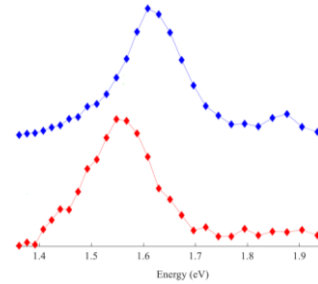


Fig. 2. Emission of IXs in TMD heterostructure for different voltages at room temperature.

3. Other recent results, which will not be presented at the meeting:

3a. Excitons in multi-layer van der Waals heterostructures [3]. We studied excitons in a double quantum well van der Waals heterostructure made of atomically thin layers of MoS₂ and hexagonal boron nitride. The emission of neutral and charged excitons was controlled by gate voltage, temperature, and both the helicity and the power of optical excitation.

3b. Overview of excitonic devices [4]. The IX properties form the basis for the development of excitonic devices. In [4], we overviewed our studies of excitonic devices. We presented traps, lattices, conveyers, and ramps for studying basic properties of cold IXs – cold bosons in semiconductor materials. We also present proof-of-principle demonstration for excitonic signal processing devices.

3c. Overview of fundamental phenomena in IXs [5]. The IX properties give an opportunity to experimentally study cold composite bosons. In [5], we overviewed our studies of cold IXs over the past decade, presenting spontaneous coherence and condensation of excitons, spatially modulated exciton state, long-range spin currents and spin textures, and exciton localization–delocalization transitions.

3d. Spin lifetime of excitons [6]. We studied spin lifetime of excitons in coupled semiconductor quantum wells in the presence of in-plane magnetic field. An increase of the spin relaxation time at low magnetic fields followed by decrease at higher fields was observed.

3e. IX correlations [7]. We developed a method for determining correlations in IXs. It involves subjecting the IXs to a periodic electrostatic potential and measuring amplitudes of IX energy and intensity modulations. We demonstrated a proof-of-principle of the method and found strong correlations in a dipolar matter of IXs. This method of determining correlations is general and can be applied for a variety of other systems, e.g. electron layers and cold atoms.

Future Plans

We plan to study spin currents in IXs by polarization-resolved imaging experiments both in GaAs and TMD heterostructures following recent findings described above in 1 and 2 in section “Recent Progress”. We also plan to study spin currents and spin polarization textures in optically generated IXs. The long range spin currents appear in a coherent IX gas and we plan to analyze the relation between coherence and spin currents. We plan to work on the development of control of the spin currents. We also plan to study IXs in lattices using shift-interferometry imaging and study the effect of the lattice potential on IX coherence.

Publications

1. J.R. Leonard, A.A. High, A.T. Hammack, M.M Fogler L.V. Butov, K.L Campman, A.C. Gossard, Pancharatnam-Berry phase in condensate of indirect excitons, in preparation.
2. E.V. Calman, C.J. Dorow, M.M. Fogler, L.V. Butov, S. Hu, A. Mishchenko, A.K. Geim, Indirect excitons at room temperature in van der Waals heterostructures, in preparation.
3. E.V. Calman, C.J. Dorow, M.M. Fogler, L.V. Butov, S. Hu, A. Mishchenko, A.K. Geim, Control of excitons in multi-layer van der Waals heterostructures, *Appl. Phys. Lett.* 108, 101901 (2016).
4. L.V. Butov, Excitonic devices, *Superlattices and Microstructures* 108, 2 (2017).
5. L.V. Butov, Collective Phenomena in Cold Indirect Excitons, *J. Exp. Theor. Phys.* 122, 434 (2016).
6. P. Andreakou, A.V. Mikhailov, S. Cronenberger, D. Scalbert, A. Nalitov, A.V. Kavokin, M. Nawrocki, L.V. Butov, K.L. Campman, A.C. Gossard, M. Vladimirova, Influence of magnetic quantum confined Stark effect on the spin lifetime of indirect excitons, *Phys. Rev. B* 93, 115410 (2016).
7. M. Remeika, J.R. Leonard, C.J. Dorow, M.M. Fogler, L.V. Butov, M. Hanson, A.C. Gossard, Measurement of exciton correlations using electrostatic lattices, *Phys. Rev. B* 92, 115311 (2015).

Towards a Universal Description of Vortex Matter in Superconductors

PI Leonardo Civale, Co-PI Boris Maiorov

MPA Division, Condensed Matter and Magnet Science,

Los Alamos National Laboratory, Los Alamos, NM 87545

e-mail: lcivale@lanl.gov

Program Scope

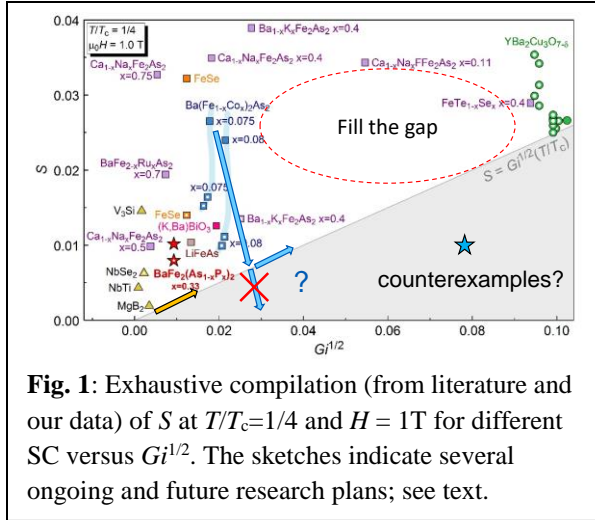
Our overall goal is to improve the understanding of superconducting vortex matter by developing a general description valid for all superconductors (SC), including those still undiscovered. Our approach is to compare and contrast systems with vastly different properties under a broad spectrum of conditions, and to manipulate and control the pinning landscapes at the nanoscale.

Vortex physics has been a topic of continuous interest since the discovery of the oxide high temperature superconductors (HTS).^(1,2) The rich and complex vortex phenomena in these materials, with proliferation of solid and liquid phases and fast non-equilibrium dynamics, arise from the strong thermal fluctuations, which are a consequence of the small coherence length (ξ) and large anisotropy (γ).⁽²⁾ On the other hand, fluctuations effects are an intrinsic obstacle for applications; moreover the problem is general and will also occur in any new-discovered HTS.

The modern picture of vortex matter has been developed to describe the oxide HTS,⁽²⁾ thus it is important to test it in other systems if we intend to develop a universal description. The Fe-based SC, a large new family of HTS with broad ranges of parameters, provided this opportunity. We have found that the pinning mechanisms in oxide and Fe-based HTS have many commonalities, that the models developed for the former are valid for the later, and that we can manipulate the pinning landscapes in both families of HTS using similar methods, such as chemical introduction of non-superconducting phases.⁽⁴⁾ This understanding allowed us to obtain record high J_c and H_{irr} both in YBCO and Ba122 films.^(4,5,8,13) We also obtain useful comparative information from other SC such as MgB_2 ,^(7,9) borocarbides, anisotropic low T_c materials such as $NbSe_2$, and even Nb.⁽³⁾

Recent Progress

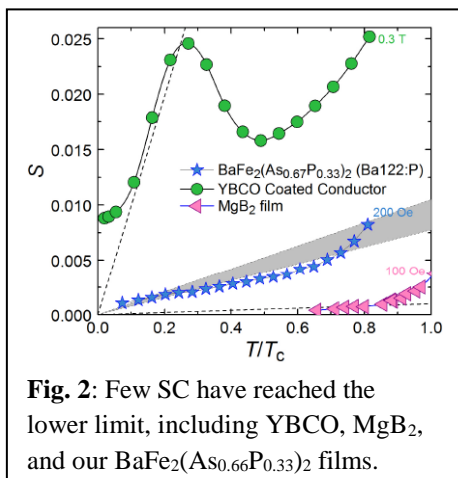
Vortex creep is the decay of the persistent current in a superconductor because of thermal fluctuations,⁽²⁾ which allow vortices to jump out of the pinning centers even for $J < J_c$. The decay is logarithmic in time and is quantified by the normalized creep rate $S = -d\ln(J)/d\ln(t)$. Creep was known in conventional low T_c superconductors (LTS), but in most cases S was very small. In contrast, the much stronger thermal fluctuations in the oxide HTS such as YBCO results in orders of magnitude larger S .^(2,13) These large creep rates significantly reduce the effective J_c (by a factor of 2 or even more), with obvious negative impact for applications. Thus, finding methods to reduce creep must be considered an integral part of enhancing J_c .



The scale of thermal fluctuations is given by the Ginzburg number (Gi), which measures the ratio of the thermal to the condensation energy in a minimum SC volume.⁽²⁾ Typical Gi values are $\sim 10^{-8}$ for NbTi; $\sim 10^{-7}$ - 10^{-4} for MgB_2 ; $\sim 10^{-5}$ - 10^{-4} for AFe_2As_2 and $\sim 10^{-2}$ for YBCO. It has been universally accepted that larger Gi produces faster creep, and this qualitative understanding was enough to explain, for instance, the much higher S in YBCO than in NbTi. However, until now a general quantitative correlation had not been established.

Our interest in this topic was initially motivated by the experimental observation that, although according to their Gi numbers Fe-based SC should have creep rates in between those of LTS and HTS, in fact they usually exhibit S values as high as or even higher than YBCO. We set the solution of this puzzle as one of our main priorities at the beginning of the last period of our proposal, and we found the answer: Gi only sets the minimum S , achieving it requires pinning landscape optimization.⁽⁴⁾ We learned this mostly from irradiation studies (by ourselves and other groups) of AFe_2As_2 clean single crystals, which show that S can be significantly reduced by adding pinning centers, in contrast to the cases of YBCO and MgB_2 where it remains unchanged.

This led us to our main recent result.⁽¹³⁾ We showed that there is a universal minimum achievable creep rate in the Anderson-Kim (AK) regime ($J \sim J_c$) in all superconductors, $S_{\min} \sim A \cdot Gi^{1/2}(T/T_c)$, set by physics laws and material parameters. Here A is a pinning-landscape dependent factor, with $A \sim 1$ for samples with the highest J_c achieved to date (0.2-0.3 of the depairing limit). Fig. 1 shows a compilation of S vs. $Gi^{1/2}$ for many SC. The gray triangle in the lower right indicates the region of unobtainable low S values according to our model, and indeed we found not a single exception in the literature. Only a few SC have reached the lower limit, including YBCO, MgB_2 , Co-doped Ba122 crystals and our $\text{BaFe}_2(\text{As}_{0.66}\text{P}_{0.33})_2$ films (Fig. 2).



Our discovery has a broad impact with fundamental and technological relevance: we claim that there is a lower limit for the creep of any superconductor, even those not yet discovered. Moreover, for any new discovered SC the lowest possible S can be predicted by simply calculating Gi . This involves measuring T_c , ξ , penetration depth (λ) and γ , a process that can be achieved in weeks, as opposed to years of trial and error landscape manipulation.

Future Plans

1) We will manipulate and tune pinning landscapes to further explore $S(Gi)$ in the AK regime: Fig. 1 contains data collected independently by different groups, without any unifying picture in mind. We will populate this plot by selecting samples and controllably modifying their properties. We will search for counterexamples, i.e., samples in the supposedly inaccessible region. There is a clear gap in the data for $10^{-3} < Gi < 10^{-2}$. We will obtain samples in that region, or produce them through tuning of properties. Irradiations will give us the possibility to start with a clean SC and move the $S(Gi)$ data point for the same sample across the figure. We will start with two systems: **(a)** Co-doped Ba122 crystals: We already know that they can reach the lower S limit. What happens if we keep adding disorder? *Hypothesis:* S will not decrease below the $S_{\min}(Gi)$ line and it will start to increase because Gi increases. **(b)** Undoped MgB_2 is a clean SC. Carbon doping reduces the electronic mean free path and decreases ξ (dirty limit), increasing Gi . We found that in both cases

S is near S_{\min} , but interestingly C-doping increases J_c and also S because Gi increases. We will irradiate clean MgB_2 films or crystals; we expect $S(Gi)$ to follow the $S_{\min}(Gi)$ line as Gi increases.

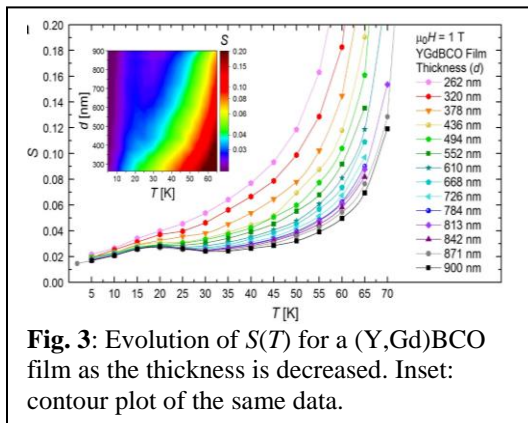


Fig. 3: Evolution of $S(T)$ for a (Y,Gd)BCO film as the thickness is decreased. Inset: contour plot of the same data.

2) Thermal creep beyond the AK limit: We will search for universal lower limits for S in regimes where creep is collective and glassy. We are currently studying (Y,Gd)Ba₂Cu₃O₇ films with strong-pinning landscape composed of random point defects and sparse nanoparticles, which exhibit particularly low S at low H and intermediate T . As we reduce the film thickness

(d) by ion milling, S remains almost unchanged in the AK regime, but increases dramatically at higher T when d becomes smaller than the size of the vortex bundle (Fig. 3). We use this method to extract the collective pinning length for this mixed landscape, $L_c^{mp}(T, H)$, which had been neither theoretically nor experimentally explored until now.

3) Beyond thermal fluctuations: We will search for a universal lower limit for the **quantum creep** rate, analogous to $S_{\min}(Gi)$. We will start by studying very clean LTS crystals that exhibit unexpectedly high S . We will use model systems (nanopatterned devices) to explore quantum creep and the quantum to thermal transition, a topic of broad present interest (e.g., for SC qubits).

Our long term goal is to determine the lower limit for vortex creep for all pinning regimes.

References

1. BES report “Basic Research Needs for Superconductivity”, 2006.
2. For a comprehensive theoretical review of vortex physics, see “Vortices in high-temperature superconductors”, G. Blatter *et al.*, *Rev. Mod. Phys.* **66**, 1125 (1994).

3. “Characterizing collective behavior of vortices in disordered superconductors”, S. Eley, R. Willa, M. Miura, M. David Henry, and L. Civale, in preparation, to be submitted to *Nature Physics*.
4. See our last BES FWP renewal document, August 2016.

Publications (since September 2015)

5. “Upward shift of the vortex solid phase in high-temperature-superconducting wires through high density nanoparticle addition”, M. Miura, B. Maiorov, F. Balakirev, T. Kato, Y. Takagi, T. Izumi and L. Civale, *Scientific Reports* **6**, 20436 (2015).
6. “Increase in vortex penetration field on Nb ellipsoid coated with a MgB_2 thin film”, Teng Tan, M.A. Wolak, X.X. Xi, T. Tajima and L. Civale, *Proceedings of the 17th International Conference on RF Superconductivity (SRF 2015)*, Whistler, BC, Canada (Invited presentation), p. 512.
7. “Vortex matter in the two-band superconductor MgB_2 ”, L. Civale and A. Serquis, in *Intermediate superconductors for applications: MgB_2* , ed. R. Flukiger, World Scientific, (2016).
8. “Viewpoint: A new scaling approach and quantitative J_c angular measurement using magnetization”, B. Maiorov, *Supercond. Sci. Technol.* **29**, 030501 (2016).
9. “Magnesium diboride coated bulk niobium: a new approach to higher acceleration gradient”, Teng Tan, M.A. Wolak, X.X. Xi, T. Tajima and L. Civale, *Scientific Reports* **6**, 35879 (2016).
10. “Investigation of the physical properties of the $Ce_2MAI_7Ge_4$ ($M = Co, Ir, Ni, Pd$) heavy fermion compounds”, N.J. Ghimire, S.K. Cary, S. Eley, N.A. Wakeham, P.F.S. Rosa, T. Albrecht-Schmitt, M. Janoschek, C.M. Brown, L. Civale, J.D. Thompson, F. Ronning and E.D. Bauer, *Phys. Rev. B*, **93**, 205141 (2016).
11. “Quantum critical scaling in the disordered itinerant ferromagnet $UCo_{1-x}Fe_xGe$ ”, K. Huang, S. Eley, L. Civale, E.D. Bauer, R.E. Baumbach, M.B. Maple and M. Janoschek, *Phys. Rev. Lett.* **117**, 237202 (2016).
12. “Domain engineering in the highly anisotropic ferromagnet $CeRu_2Ga_2B$ via vector magnetic fields”, D. Wulferding, Hoon Kim, J. Jeong, O.E. Ayala-Valenzuela, M. Lee, H.C. Choi, F. Ronning, L. Civale, R.E. Baumbach, E.D. Bauer, J.D. Thompson, R. Movshovich and Jeehoon Kim, *Scientific Reports* **7**, 46296 (2017).
13. “Universal Lower Limit on Vortex Creep in Superconductors”, S. Eley, M. Miura, B. Maiorov and L. Civale, *Nature Materials* **16**, 409 (2017).
14. “Missing magnetism in $Sr_4Ru_3O_{10}$: Indication for Antisymmetric Exchange Interaction”, F. Weickert, L. Civale, B. Maiorov, M. Jaime, M.B. Salamon, E. Carleschi, A.M. Strydom, R. Fittipaldi, V. Granata and A. Vecchione, *Scientific Reports* **7**, 3867 (2017).
15. “Selective mass enhancement close to the quantum critical point in $BaFe_2(As_{1-x}P_x)_2$ ”, V. Grinenko, K. Iida, F. Kurth, D.V. Efremov, S.-L. Drechsler, I. Cherniavskii, I. Morozov, J. Hänisch, T. Förster, C. Tarantini, J. Jaroszynski, B. Maiorov, M. Jaime, A. Yamamoto, I. Nakamura, R. Fujimoto, T. Hatano, H. Ikuta and R. Hühne, *Scientific Reports* **7**, 4589 (2017).
16. “Tuning nanoparticle size in perovskite thin films for efficient energy applications”, M. Miura, B. Maiorov, M. Sato, M. Kanai, T. Kato, T. Kato, T. Izumi, S. Awaji, P. Mele, M. Kiuchi and T. Matsushita, submitted to *Nature Energy* (2017).

17. “Nuclear magnetic resonance investigation of the novel heavy fermion system $\text{Ce}_2\text{CoAl}_7\text{Ge}_4$ ”, A.P. Dioguardi, P. Guzman, P.F.S. Rosa, N.J. Ghimire, S. Eley, S.E. Brown, J.D. Thompson, E.D. Bauer, and F. Ronning, submitted to *Phys. Rev. B* (2017).

Spin Polarized Tunneling in Aluminum Nanoparticles

Dragomir Davidovic, Georgia Institute of Technology

Program Scope

In quantum magnetism and quantum computing, weak electronic signals at millikelvin temperatures need amplification. One problem faced is that the quantum information we are trying to extract from the solid state or from a Qubit is fragile, which means that a lot of that information is usually lost in the classical measurement process. For example, we would like to study the motion of spins in a quantum material like spin-ice or in a ferromagnetic nanoparticle, to observe quantum effects in that motion. However, measurements of such motion is nowadays very inefficient, even using the highest sensitivity detectors such as SQUIDS (superconducting quantum interference devices). Ideally the measurements should be done in a properly matched amplifier operating in the quantum limit of noise, in which case the noise imparted by the measurement process is determined by the Heisenberg uncertainty principle, as opposed to classical noise (which transforms information that we do not gather into entropy). We envision a new era in condensed matter physics where the fundamental electronic properties of solids are studied with that limit of sensitivity. In case of a magnetic nanoparticle, for example, we would measure magnetic precession directly in real time, in such a way that the measurement process is the only source of noise as demanded by the Heisenberg uncertainty principle.

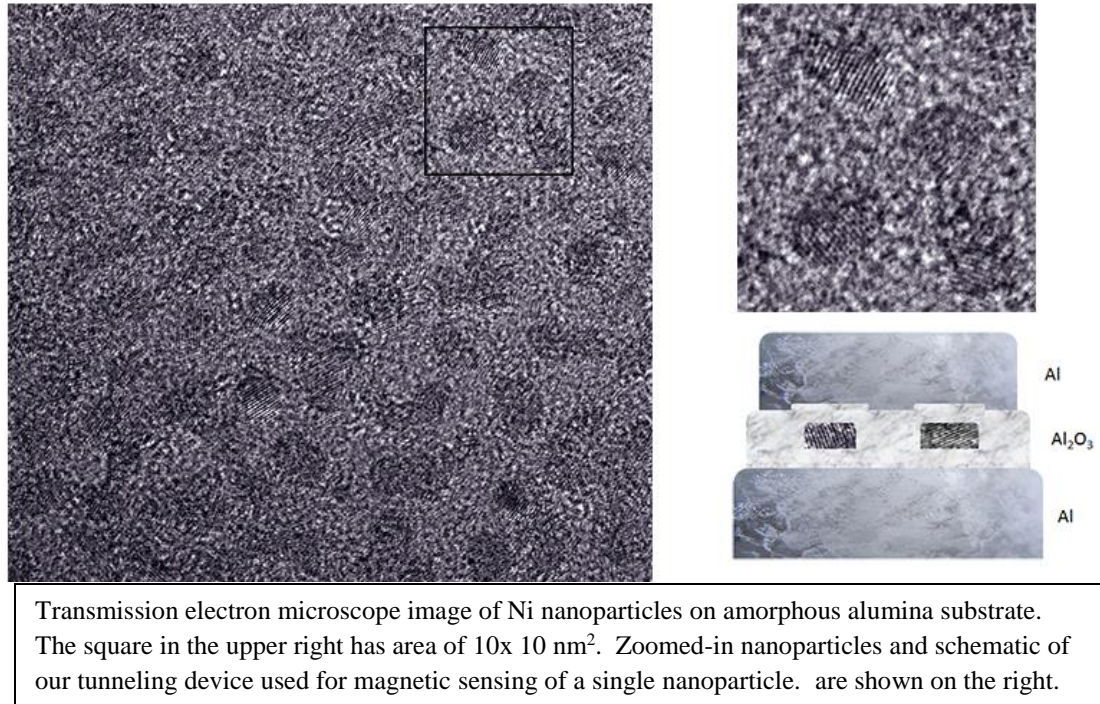
To this end, in this program we build and study silicon-germanium heterojunction bipolar transistors, for interfacing classical electronics apparatus and quantum electronic behavior of solid state devices, directly at millikelvin temperature, and ideally on the same microchip. Gone will be the inefficient coaxial cables and interconnects between room temperature electronics and the physics samples. Particular emphasis is given on interfacing and readout of magnetic signals in nanomagnets like ferromagnetic nanoparticles and quantum magnets such as quantum spin liquids.

Recent Progress

Real-Time Detection of Spin Diffusion and Damping in Individual Metallic Ferromagnetic Nanoparticles. (Submitted to Physical Review Letters)

It has been widely believed, until recently, that the damping time in ferromagnets cannot be arbitrarily long. However, spins in semiconducting quantum dots prove otherwise: exceptionally long relaxation times of single electron spins have been observed, of up to 170 ms in GaAs and 6 on P-donors in Si. Since magnetic nanoparticles are a bridge between bulk ferromagnets and single electron spins, they may also have unusually long damping time. However, the damping time in nanoparticles has not been measured yet.

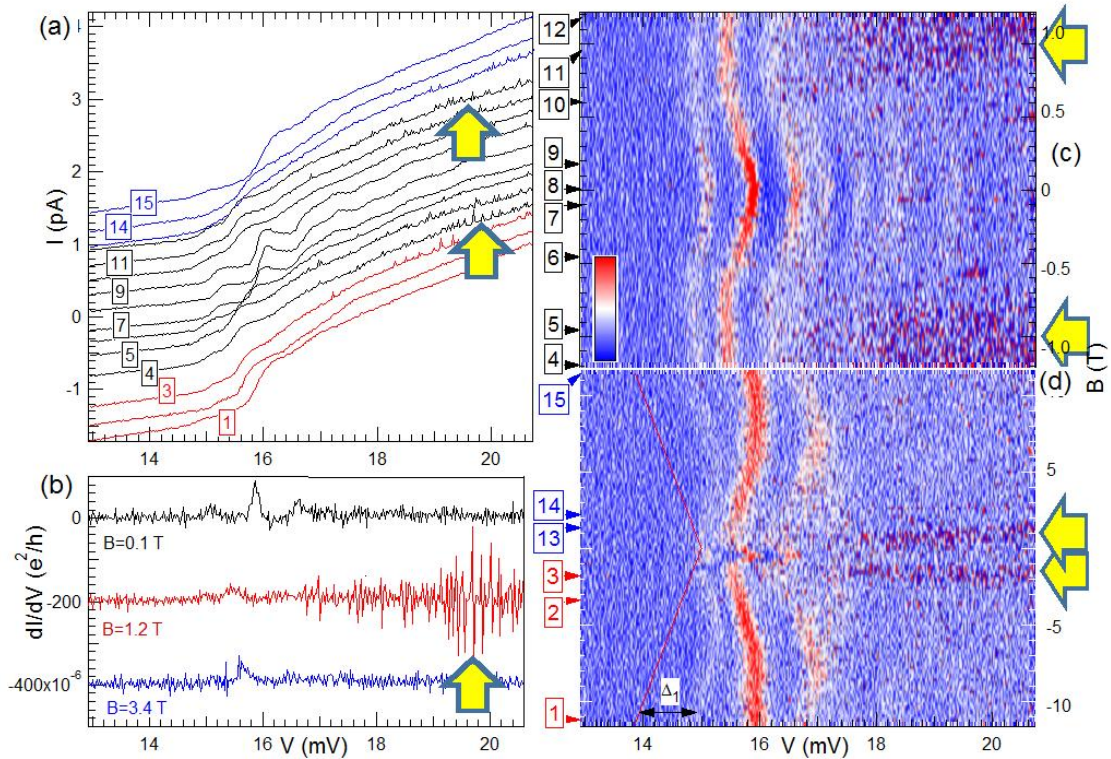
In this activity, we introduce a highly sensitive technique to observe magnetization



motion in single Ni nanoparticles in real-time, based on charge sensing by electron tunneling at millikelvin temperature. This technique mimics single-shot spin readout in semiconducting quantum dots, which we adapted to spin-1000 particle. The technique is much more sensitive than SQUIDs, for detecting small changes in magnetic moment. The figures above display the device we use to study the magnetic properties, while the figure on the following page shows how we detect magnetic motion in the particle.

The magnetic signal is the effective charge noise indicated by the boxed yellow arrows. As the magnetization is displaced because of the coupling to the electrons, it produces an internal charge displacement of the particle that we measure as the shift in chemical potential (e.g., shift in current). Since noise and damping in detailed balance are fundamentally related (fluctuation dissipation theorem), we obtain the magnetic damping directly from this data in the time domain. The technique is self-calibrating, by measuring the shifts of discrete level energies with magnetic field [indicated by Δ_1 for the lowest level in (d)], which establish the conversion between magnetization orientation and chemical potential shift.

The magnetic damping time is 10ms, which is record long in a ferromagnet and a new benchmark for damping. The impact of observing such a long damping time is in demonstrating how magnetic dynamics needs to be studied in nanoparticles or other nanometer scale magnets, e.g., by real time detection, not by ferromagnetic resonance and other traditional techniques. Thus we believe that our advance will impact the field of nanomagnetism by opening new regimes of magnetodynamics for exploration in individual nanoparticles and other nano-objects, with a possibility to measure macroscopic quantum effects.

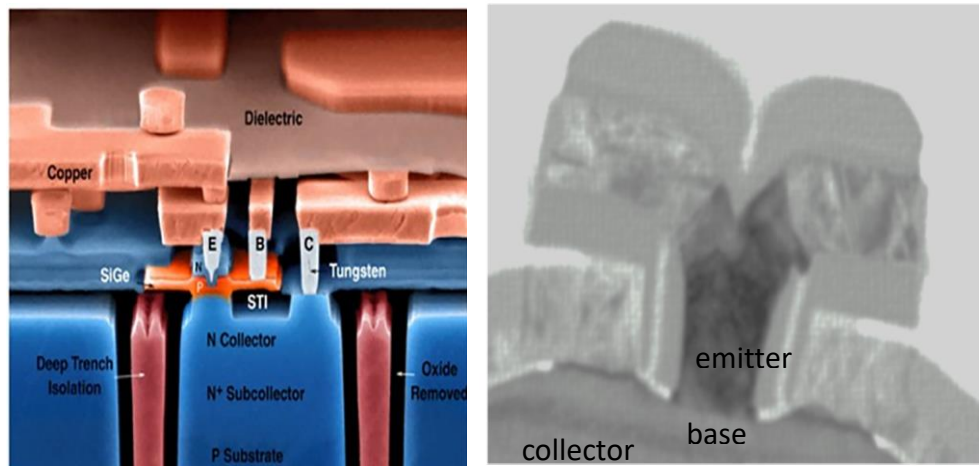


Sample 1 at 70mK: (a) Current versus voltage at fixed magnetic fields. (b) Differential conductance versus voltage, at $B=0.1, 1.2,$ and 3.4 T, respectively. In (a,b) the curves are offset vertically for clarity. The boxed yellow arrow indicates the **spin signal**, which is particularly striking for the red line at $B=1.2$ T. (c) and (d) Differential conductance, showing discrete level shifts with magnetic field and enhanced noise in the magnetic field intervals (0.7,1.5)T. Color bar indicates the conductance interval $-1e-4, 5e-4$ in units of e^2/h .

Interfacing classical measurement apparatus and solid state quantum object.

In this activity, we are developing a technique to embed the device under test into the integrated SiGe-circuit operating down to millikelvin temperature (but much can be done at 1.5 and 4.2 K). We have selected SiGe technology, which presently embodies four distinct generations in production worldwide, at more than two dozen companies, and is commercially accessible via multiple foundries. Available SiGe heterojunction bipolar transistor (HBT) performance goes to over 400 GHz (at 130 nm emitter length). The figure below displays SiGe transistor with a 90 nm width emitter length and 10 nm base width.

Left: large scale view of the 90 nm SiGe HBT. Right: SEM image of the 90 nm bipolar transistor (SiGe-HBT), with a ~15nm base width.



Until now our goals were to understand the physics of transistor operation at mK temperature. SiGe-HBT are bipolar transistors (e.g., NOT field effect transistors), and the mechanism of amplification at deep cryogenic temperature has not been known. We demonstrated that the collector current in these advanced HBTs is mostly due to ideal quantum mechanical tunneling of electrons under the potential barrier extending through the entire base. Due to exponential dependence of tunneling probability on barrier height, a large tunneling current is switched on by a moderate amount of current required to increase the base voltage. This remarkable simplicity of amplification in advanced SiGe-HBTs at deep cryogenic temperatures stands in contrast with more complex amplification in a field effect transistor. Realization of such an amplifier in a robust and manufacturable silicon-germanium transistor is a critical step toward manufacturing complex but useful circuits operating on basic principles of quantum mechanics.

Future Plans

We are testing magnetic tunnel junctions at room temperature using the SiGe electronics. We are currently building a broadband SiGe amplifier operating in 20-40GHz regime. Our goals are to cool down these junctions interfaced with the integrated circuit (which will have the amplifier, and eventually a mixer and an rf-amplifier), to create a generic shot noise spectrometer operating near the quantum limit. The spectrometer will be a microchip, and we make hundreds of them, one for each sample. We will attach samples to the circuit input, by lithography on the SiGe die at Georgia Tech (magnetic junctions and particles, as well as superconductors and other quantum solid state materials.) while the chips will be custom ordered from Global Foundries. In terms of physics, in simple words we are interested in first listening to what these magnets and superconductors do at this frequency range, close to quantum limit of sensitivity. We are also measuring spin transfer torque in magnetic nanoparticles.

Publications

“Voltage-Driven Spin-Transfer Torque in a Magnetic Particle”, P. Gartland and D. Davidovic, Applied Physics Letters, 107, 172401 (2015)

"Evidence of Magnetic Inversion in Single Ni Nanoparticles", W. Jiang, P. Gartland, and D. Davidovic, Scientific Reports **6**, 36156 (2016).

"Operation of SiGe HBTs Down to 70mK", H. Ying, B. R. Wier, J. Dark, N. E. Lourenco, L. Ge, A. P. Omprakash, M. Mourigal, D. Davidovic, and J. D. Cressler, IEEE Electron Device Letters, **38**, No. 1, 12 (2017).

"Tunneling, Current Gain, and Transconductance in Silicon-Germanium Heterojunction Bipolar Transistors Operating at Millikelvin Temperatures" D. Davidović, H. Ying, J. Dark, B. R. Wier, L. Ge, N. E. Lourenco, A. P. Omprakash, M. Mourigal, and J. D. Cressler, Phys. Rev. Applied **8**, 024015 (2017) – Published 18 August 2017

LaCNS: Building Neutron Scattering Infrastructure in Louisiana for Advanced Materials

J. F. DiTusa¹ (ditusa@phys.lsu.edu), D. Zhang², J. Zhang¹, W. A. Shelton³, R. Jin¹, V. T. John⁴, R. Kumar², Z. Mao⁵, E. Nesterov², E. W. Plummer¹, S. W. Rick⁶, G. J. Schneider², D. P. Young¹, P. T. Sprunger¹, M. Khonsari⁷

¹*Department of Physics and Astronomy, Louisiana State University, Baton Rouge, LA 70803*

²*Department of Chemistry, Louisiana State University, Baton Rouge, LA 70803*

³*Department of Chemical Engineering, Louisiana State University, Baton Rouge, LA 70803*

⁴*Dept. of Chem. and Biomolecular Engineering, Tulane University, New Orleans, LA 70118*

⁵*Department of Physics and Engineering Physics, Tulane University, New Orleans, LA 70118*

⁶*Department of Chemistry, University of New Orleans, New Orleans, LA 70148*

⁷*Louisiana Board of Regents, Baton Rouge, LA 70821*

Program Scope: This DOE EPSCoR / LA Board of Regents program aims to build neutron scattering infrastructure capable of treating both soft and hard materials. Our objectives include: discovery of the coupling of degrees of freedom that determine the emergent properties of complex materials, training of talented students in synthesis and neutron scattering techniques who will become the next generation of neutron users, and building a base of users of SNS and HFIR.

The scientific focus of this program is to understand the role of coupling in emergent complex materials and its impact on structure/property relationships, and to explore how this information can be applied in the guided-design of materials. Our goal is to tune dominant couplings to enhance critical properties in order to derive new functionality. In the hard materials, we focus on transition metal oxides where electronic, magnetic, phononic, and orbital degrees of freedom along with their couplings, are all important in creating novel behaviors, non-centrosymmetric (NCS) structured materials where the Dzyaloshinskii-Moriya, DM, interaction leads to interesting magnetic structures and spin textures, and Dirac systems where magnetic ordering likely leads to the formation of Weyl semimetal states. In the soft materials, we explore the role of secondary interactions in determining the structural and dynamic properties of polymeric systems.

Recent Progress

Here we review some of the work performed on the NCS magnets that represents a small subset of the work performed within the LaCNS program. In 2009, small angle neutron scattering in a small pocket of the (H,T) -phase diagram (so-called *A* phase) of the prototypical non-centrosymmetric itinerant magnet MnSi resulted in the discovery of a bulk skyrmion lattice (SkL) phase [1]. Since then, control of the size and helicity of magnetic Skyrmions is at the heart of an intense research activity worldwide. These countable magnetic defects, carrying a quantum of electromagnetic flux, are envisioned as potential building blocks for next-generation electronics [2].

Previously, it has been shown that the magnetic properties of MnSi can be tuned by chemical substitution of Mn [3], or by application of hydrostatic [4] or uniaxial [5] pressure. Quite generally, doping and hydrostatic pressure lead to a suppression of magnetic order and hence the

disappearance of the SkL. On the other hand, uniaxial pressure was found to stabilize these over a larger portion of the (H,T) -space. The uniaxial pressure, which emulates lateral strains inherent to thin films, implies a contraction in one direction with an expansion in the orthogonal direction. It thus remains unclear which is the driving force leading to the extension of the SkL.

Here, instead of the traditional substitution of the magnetic Mn ions, Si is replaced by a small amount of Al or Ga. As shown in [6], slight substitution of Si by Al (3.8 %) appears to dramatically increase the critical temperature, T_c (+30%) and ordered magnetic moment (+20%). It is remarkable that such a small change in the material structure, a small increase of the unit cell volume by $\approx 0.5\%$, induces such drastic improvements of its magnetic properties despite enhanced chemical disorder. In turn, the lattice expansion is homogeneous and its effect can be studied in a transparent way. Most importantly, we have shown that such a negative pressure leads to an extension of the so-called A phase as well as a T -induced reversal of the sign of anomalous Hall effect (AHE, Fig. 1c,d)[6]. These features imply (i) a drastically enhanced stability of the SkL and (ii) the unique possibility to choose the chirality of the magnetic structure – hence of the SkL- by a simple T change. This would open a completely new and unexpected avenue in the field of Skyrmionics. Our small-angle neutron scattering (SANS) experiments, Fig. 2, have confirmed the increased stability of the SkL while indicating no strong dependence of the helical wavelength with Al or Ga substitutions.

In contrast, Ir substitution for Mn, $Mn_{1-x}Ir_xSi$ has much the same effect as Co or Fe substitutions [7]. By using magnetization and SANS measurements, we have investigated the magnetic behavior of $Mn_{1-x}Ir_xSi$ system to explore the effect of increased carrier density and spin-orbit interaction on the magnetic properties of MnSi. We have determined estimates of the spin wave stiffness and the DM, interaction strength and compare with $Mn_{1-x}Co_xSi$ and $Mn_{1-x}Fe_xSi$ [3]. Despite the large differences in atomic mass and size of the

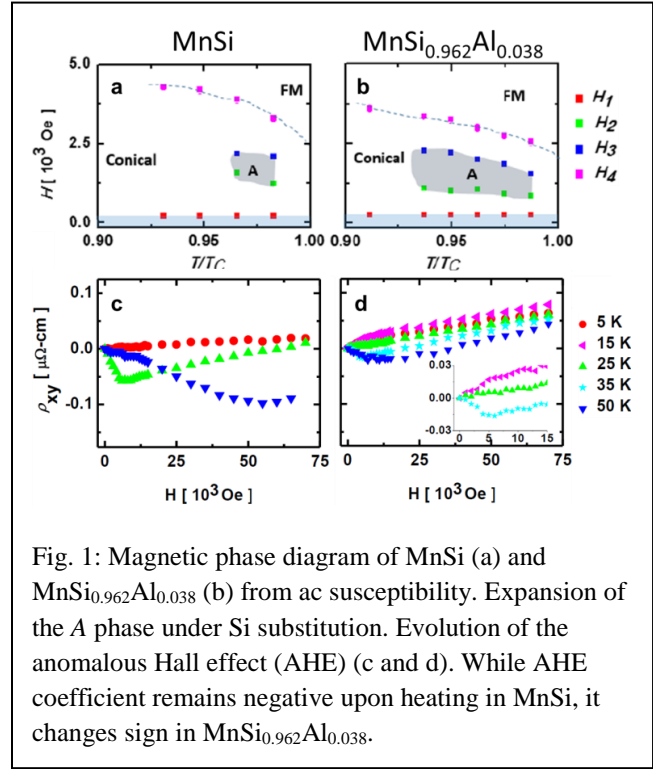


Fig. 1: Magnetic phase diagram of MnSi (a) and MnSi_{0.962}Al_{0.038} (b) from ac susceptibility. Expansion of the A phase under Si substitution. Evolution of the anomalous Hall effect (AHE) (c and d). While AHE coefficient remains negative upon heating in MnSi, it changes sign in MnSi_{0.962}Al_{0.038}.

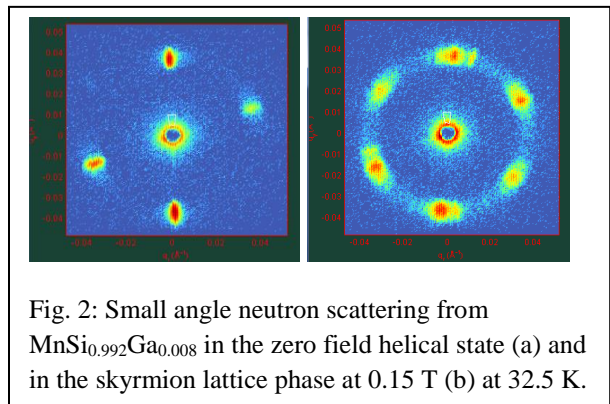


Fig. 2: Small angle neutron scattering from MnSi_{0.992}Ga_{0.008} in the zero field helical state (a) and in the skyrmion lattice phase at 0.15 T (b) at 32.5 K.

substituted elements, $\text{Mn}_{1-x}\text{Co}_x\text{Si}$ and $\text{Mn}_{1-x}\text{Ir}_x\text{Si}$ surprisingly show nearly identical variations in their magnetic properties with substitution. We find a systematic dependence of the transition T , the ordered moment, the helix period and the DM interaction strength with electron count for $\text{Mn}_{1-x}\text{Ir}_x\text{Si}$, $\text{Mn}_{1-x}\text{Co}_x\text{Si}$, and $\text{Mn}_{1-x}\text{Fe}_x\text{Si}$ [3, 8] indicating that the magnetic behavior is primarily dependent upon the additional carrier density rather than on the mass or size of the substituting species. This indicates that the variation in magnetic properties, including the DM interaction strength, are primarily controlled by the electronic structure as Co and Ir are isovalent. Our work suggests that although the rigid band model of electronic structure along with Moria's model of weak itinerant magnetism describe this system surprisingly well, phenomenological models for the DM interaction strength are not adequate to describe this system.

Future Plans

Future work in this area extends these investigations to materials beyond the well-known $B20$ structured materials in order to explore the consequences of the DM interaction and search for spin textures in other NCS structured magnets. This includes materials having the ZrAlNi crystal structure (space group $P-62m$) such as ScFeGe shown in Fig. 3a [9]. Here, we have determined that ScFeGe has a transition to a magnetic state at 39 K with a moderate hexagonal anisotropy (Fig. 3b). In addition, there is a sharp metamagnetic transition near 6.6 T for fields along the ab plane (Fig. 3c). Our single crystal neutron diffraction taken on instruments HB-3A and HB-1A at HFIR (ORNL) revealed an incommensurate ordering wave vector of $(0\ 0\ 0.193)$, see Fig. 3d.

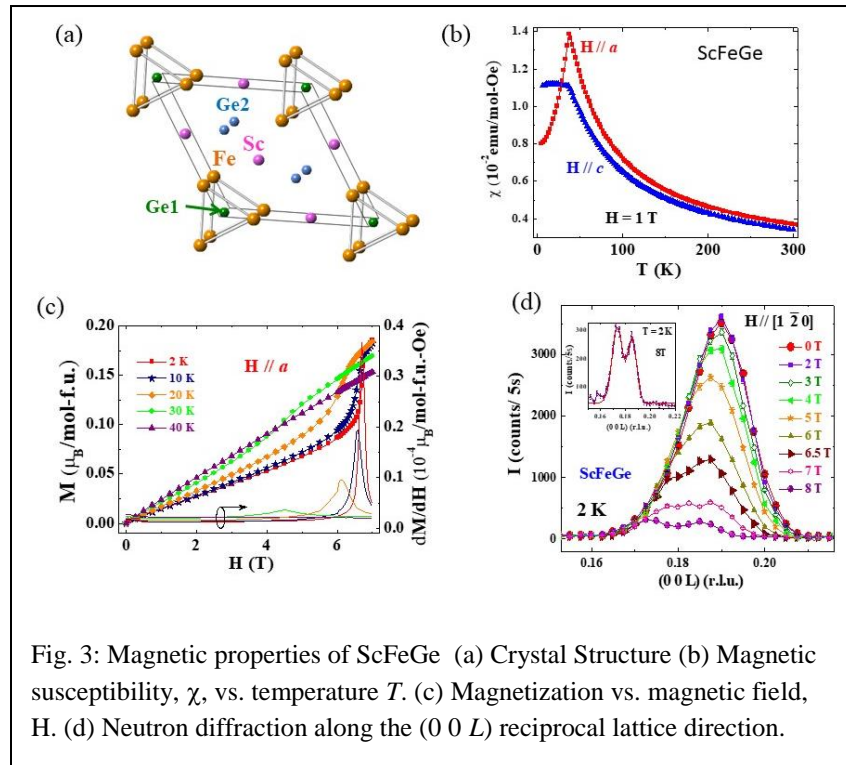


Fig. 3: Magnetic properties of ScFeGe (a) Crystal Structure (b) Magnetic susceptibility, χ , vs. temperature T . (c) Magnetization vs. magnetic field, H . (d) Neutron diffraction along the $(0\ 0\ L)$ reciprocal lattice direction.

A full refinement of a data set that included 105 magnetic reflections indicated that the ground state was helimagnetic with an ordered magnetic moment of only $0.53\ \mu_B$. Thus, we have discovered a highly itinerant and incommensurate helimagnetic metal in a NCS structured material where the helimagnetism is likely to be caused by the DM interaction. Furthermore, our neutron diffraction measurements performed in a magnetic field of up to 8 T revealed that the

metamagnetic transition shown in Fig. 3c is accompanied by a splitting of the incommensurate

magnetic scattering into two components as shown the main frame and inset of Fig. 3d. Thus, the magnet state has developed a long period modulation (~39 nm) or phase segregates into regions with two distinct magnetic wavevectors. We are continuing to explore this unusual magnetic material as experiments indicate a change to the crystal structure within a unit cell as a magnetic field is applied. In addition, there are a large number of compounds that form in this crystal structure, including several that are likely to be magnetic making this an excellent platform to explore the consequences of the DM interaction in NCS systems.

References

- [1] S. Mühlbauer, B. Binz, F. Jonietz, C. Pfleiderer, A. Rosch, A. Neubauer, R. Georgii, and P. Böni, *Science* **323**, 915 (2009).
- [2] A. Fert, V. Cros, and J. Sampaio, *Nature Nanotechnology* **8**, 152 (2013).
- [3] A. Bauer, A. Neubauer, C. Franz, W. Munzer, M. Garst, and C. Pfleiderer, *Phys. Rev. B* **82**, 064404 (2010).
- [4] C. Pfleiderer, D. Reznik, L. Pintschovious, H. v. Lohneysen, M. Garst, and A. Rosch, *Nature* **427**, 227 (2004) and references therein.
- [5] Y. Nii, T. Nakajima, A. Kikkawa, Y. Yamasaki, K. Ohishi, J. Suzuki, Y. Taguchi, T. Arima, Y. Tokura, and Y. Iwasa, *Nature Communications* **6**, 8539 (2015).
- [6] C. Dhital, M. A. Khan, M. Saghayezhian, W. A. Phelan, D. P. Young, R. Y. Jin, and J. F. DiTusa, *Phys Rev B* **95**, 024407 (2017).
- [7] C. Dhital, L. DeBeer-Schmitt, Q. Zhang, W. Xie, D. P. Young, and J. F. DiTusa, <http://arxiv.org/abs/1707.05673>.
- [8] J. Teyssier, E. Giannini, V. Guritanu, R. Viennois, D. Van Der Marel, A. Amato, and S. N. Gvasaliya, *Phys. Rev. B*, **82**, 064417 (2010).
- [9] B. Y. Kotur and R. I. Andrusyak, *Dopovidi Akademii Nauk Ukrainskoi RSR Seriya B-Geologichini Khimichni Ta Biologichni Nauki* **12**, 40-43 (1984).

Publications

- 1) Brooks AJ, Ge J, Kirka MM, Dehoff RR, Bilheux HZ, Kardjilov N, Manke I, Butler LG, Porosity detection in electron beam melted Ti-6Al-4V using high-resolution neutron imaging and grating-based interferometry. *Progress in Additive Manufacturing* (2017). <https://link.springer.com/article/10.1007/s40964-017-0025-z/fulltext.html>
- 2) Cao G, Xie W, Phelan WA, DiTusa JF, Jin R. 2017. Electrical anisotropy and coexistence of structural transitions and superconductivity in IrTe₂. *Phys Rev B* **95**, 035148 (2017). <http://journals.aps.org/prb/abstract/10.1103/PhysRevB.95.035148>
- 3) Dhital C, Khan MA, Saghayezhian M, Phelan WA, Young DP, Jin RY, DiTusa JF. Effect of negative chemical pressure on the prototypical itinerant magnet MnSi. *Phys Rev B* **95**, 024407 (2017). <https://journals.aps.org/prb/abstract/10.1103/PhysRevB.95.024407>

- 4) Diao Z, Lee HN, Chisholm MF, Jin R. Thermoelectric properties of $\text{Bi}_2\text{Sr}_2\text{Co}_2\text{O}_y$ thin films and single crystals. *Physica B: Cond Matt* **511**, 42-46 (2017).
<http://www.sciencedirect.com/science/article/pii/S0921452617300479>
- 5) Du P, Li A, Li X, Zhang Y, Do C, He L, Rick SW, John V, Kumar R, Zhang D. Aggregation of cyclic polypeptoids bearing zwitterionic end-groups with attractive dipole-dipole and solvophobic interactions: A study by small-angle neutron scattering and molecular dynamics simulation. *Phys Chem Chem Phys* **19**, 14388-14400 (2017).
<http://pubs.rsc.org/en/content/articlelanding/2017/cp/c7cp01602f#!divAbstract>
- 6) Liu JY, Hu J, Zhang Q, Graf D, Cao HB, Radmanesh SMA, Adams DJ, Zhu YL, Cheng GF, Liu X, Phelan WA, Wei J, Jaime M, Balakirev F, Tennant DA, DiTusa JF, Chiorescu I, Spinu L, Mao ZQ. A magnetic topological semimetal $\text{Sr}_{1-y}\text{Mn}_{1-z}\text{Sb}_2$ ($y, z < 0.1$). *Nature Materials* (published online) (2017).
<http://www.nature.com/nmat/journal/vaop/ncurrent/full/nmat4953.html?foxtrotcallback=true>
- 7) Patterson MC, DiTusa MF, McFerrin CA, Kurtz RL, Hall RW, Poliakoff ED, Sprunger PT. Formation of environmentally persistent free radicals (EPFRs) on ZnO at room temperature: Implications for the fundamental model of EPFR generation. *Chem Phys Lett* **670**, 5-10 (2017).
<http://www.sciencedirect.com/science/article/pii/S0009261416310260?np=y>
- 8) Rivero P, Meunier V, Shelton WA. Half-metallic ferromagnetism in $\text{Sr}_3\text{Ru}_2\text{O}_7$. *Phys Rev B* **95**, 195106 (2017). <https://journals.aps.org/prb/abstract/10.1103/PhysRevB.95.195106>
- 9) Vinokurov V, Stavitskaya A, Ivanov E, Shrestha L, Ariga K, Darrat Y, Lvov Y. Formation of metal clusters in halloysite clay nanotubes. *Sci Tech Adv Mat* **18**, 147-151 (2017).
<http://www.tandfonline.com/doi/abs/10.1080/14686996.2016.1278352>
- 10) Wang H, Luo J, Lou W, Ortmann JE, Mao ZQ, Liu Y, Wei J. Probing chiral superconductivity in Sr_2RuO_4 underneath the surface by point contact measurements. *New J Phys* **19**, 053001 (2017). <http://iopscience.iop.org/article/10.1088/1367-2630/aa65c5/meta>
- 11) Xuan S, Gupta S, Li X, Bleuel M, Schneider GJ, Zhang D. Synthesis and Characterization of Well-defined PEGylated Polypeptoids as Protein-resistant Polymers. *Biomacromolecules* **18**, 951-964 (2017). <http://pubs.acs.org/doi/abs/10.1021/acs.biomac.6b01824>
- 12) Zhang Q, Ye F, Tian W, Cao H, Chi S, Hu B, Diao Z, Tennant DA, Jin R, Zhang J, Plummer W. Manganese-induced magnetic symmetry breaking and its correlation with the metal-insulator transition in bilayered $\text{Sr}_3(\text{Ru}_{1-x}\text{Mn}_x)_2\text{O}_7$. *Phys Rev B* **95**, 220403(R) (2017).
<https://journals.aps.org/prb/abstract/10.1103/PhysRevB.95.220403#sthash.EuKL14FV.dpuf>
- 13) Zhang Y, Xuan S, Owoseni O, Omarova M, Li X, Saito M, He J, McPherson G, Raghavan S, Zhang D, John V. Amphiphilic Polypeptoids Serve as the Connective Glue to Transform

Liposomes into Multilamellar Structures with Closely Spaced Bilayers. *Langmuir* **33**, 2780-2789 (2017). <http://pubs.acs.org/doi/abs/10.1021/acs.langmuir.6b04190>

14) Zhu M, Peng J, Hong T, Prokes K, Zou T, Mao ZQ, Ke XL. Field-induced metastability of the modulation wave vector in a magnetic soliton lattice. *Phys Rev B* **95**, 134429 (2017). <https://journals.aps.org/prb/abstract/10.1103/PhysRevB.95.134429>

15) Zhu M, Peng J, Tian W, Hong T, Mao ZQ, Ke X. Tuning the competing phases of bilayer ruthenate $\text{Ca}_3\text{Ru}_2\text{O}_7$ via dilute Mn impurities and magnetic field. *Phys Rev B* **95**, 144426 (2017). <https://journals.aps.org/prb/abstract/10.1103/PhysRevB.95.144426>

17) Zhu M, Shanavas KV, Wang Y, Zou T, Sun WF, Tian W, Garlea VO, Podlesnyak A, Matsuda M, Stone MB, Keavney D, Mao ZQ, Singh DJ, and Ke X. Non-Fermi surface nesting driven commensurate magnetic ordering in Fe-doped Sr_2RuO_4 . *Phys Rev B* **95**, 054413 (2017) <https://journals.aps.org/prb/abstract/10.1103/PhysRevB.95.054413>

18) Zou T, Lee CC, Tian W, Cao HB, Zhu M, Qian B, dela Cruz CR, Ku W, Mao ZQ, Ke X. G-type magnetic order in ferropnictide $\text{Cu}_x\text{Fe}_{1-y}\text{As}$ induced by hole doping on As sites. *Phys Rev B* **95**, 054414 (2017). <https://journals.aps.org/prb/abstract/10.1103/PhysRevB.95.054414>

19) Arai K, Sagawa N, Shikata T, Sternhagen, GL, Li X, Guo L, Do C, and Zhang D. Pronounced dielectric and hydration/dehydration behaviors of monopolar poly(n-alkyl glycine)s in aqueous solution. *J Phys Chem B* **120**, 9978-9986 (2016). <http://pubs.acs.org/doi/abs/10.1021/acs.jpcc.6b05379>

20) Feng J, Tan A, Wagner S, Liu J, Mao Z, Ke X, and Zhang P. Charge modulation and structural transformation in TaTe_2 studied by scanning tunneling microscopy/spectroscopy. *Appl Phys Lett* **109**, 021901 (2016). <http://scitation.aip.org/content/aip/journal/apl/109/2/10.1063/1.4958616>

21) Liu J, Hu J, Cao H, Zhu Y, Chuang A, Graf D, Adams DJ, Radmanesh SMA, Spinu L, Chiorescu I, and Mao Z. Nearly massless Dirac fermions hosted by Sb square net in BaMnSb_2 . *Scien Rep (Nature Publ)* **6**, 30525 (2016). www.nature.com/articles/srep30525

22) Zou T, Cao H, Liu GQ, Peng J, Gottschalk M, Zhu M, Zhao Y, Leao JB, Tian W, Mao ZQ, and Ke X. Pressure-induced electronic and magnetic phase transitions in a Mott insulator: Ti-doped $\text{Ca}_3\text{Ru}_2\text{O}_7$ bilayer ruthenate. *Phys Rev B* **94**, 041115 (R) (2016). <http://journals.aps.org/prb/abstract/10.1103/PhysRevB.94.041115>

23) Bhaskaran-Nair K, Kowalski K, and Shelton, WA. Coupled cluster Green function: Model involving single and double excitations. *J Chem Phys* **144**, 144101 (2016). <http://scitation.aip.org/content/aip/journal/jcp/144/14/10.1063/1.494496>

- 24) Carrillo J-MY, Siebers Z, Kumar R, Matheson MA, Ankner JF, Goswami M, Bhaskaran-Nair K, Shelton WA, Sumpter BG, and Kilbey SM. Petascale simulations of the morphology and the molecular interface of bulk heterojunctions. *ACS Nano* **10**, 7008-7022 (2016).
<http://pubs.acs.org/doi/full/10.1021/acsnano.6b03009>
- 25) Dionisi C, Hanafy N, Nobile C, De Giorgi ML, Rinaldi R, Casciaro S, Lvov Y, and Leporatti S. Halloysite clay nanotubes as carriers for curcumin: Characterization and application. *IEEE Transactions on Nanotechnology* **15**, 720-724 (2016).
https://www.researchgate.net/publication/293010472_Halloysite_Clay_Nanotubes_as_Carriers_for_Curcumin_Characterization_and_Application
- 26) Hu J, Liu JY, Graf D, Radmanesh SMA, Adams DJ, Chuang A, Wang Y, Chiorescu I, Wei J, Spinu L, and Mao ZQ. π Berry phase and Zeeman splitting of Weyl semimetal TaP. *Scien Rep* (Nature Publ) **6**, 18674 (2016). <http://www.nature.com/articles/srep18674>
- 27) Li A, Lu L, Li X, He LL, Do C, Garno JC, and Zhang D. Amidine-mediated Zwitterionic ring-opening polymerization of n-alkyl n-carboxyanhydride: Mechanism, kinetics, and architecture elucidation. *Macromolecules* **49**, 1163-1171 (2016).
<http://pubs.acs.org/doi/full/10.1021/acs.macromol.5b02611>
- 28) Lvov Y, DeVilliers M, and Fakhrullin R. The application of halloysite tubule nanoclay in drug delivery. *Expert Opinion Drug Delivery* **13**, 977-986 (2016).
<https://www.ncbi.nlm.nih.gov/pubmed/27027933>
- 29) Lvov Y, Wang WC, Zhang LQ, and Fakhrullin RF. Halloysite clay nanotubes for loading and sustained release of functional compounds. *Adv Mater* **28**(6), 1227-1250 (2016).
<http://onlinelibrary.wiley.com/doi/10.1002/adma.201502341/full>
- 30) Peng J, Hu J, Gu XM, Zhou GT, Liu JY, Zhang FM, Wu XS, and Mao ZQ. Normal and inverse bulk spin valve effects in single-crystal ruthenates. *Appl Phys Lett* **108**, 162402 (2016).
<http://scitation.aip.org/content/aip/journal/apl/108/16/10.1063/1.4947489>
- 31) Rivero P, Meunier V, and Shelton WA. Electronic, structural, and magnetic properties of LaMnO₃ phase transition at high temperature. *Phys Rev B* **93**, 024111 (2016).
<http://journals.aps.org/prb/abstract/10.1103/PhysRevB.93.024111#fulltext>
- 32) Rivero P, Meunier V, and Shelton WA. Uniaxial pressure-induced half-metallic ferromagnetic phase transition in LaMnO₃. *Phys Rev B* **93**, 094409 (2016).
<http://journals.aps.org/prb/abstract/10.1103/PhysRevB.93.094409#fulltext>
- 33) Rivero P, Meunier V, and Shelton WA. Surface properties of hydrogenated diamond in the presence of adsorbates: a hybrid functional DFT study. *Carbon* **110**, 469-479 (2016).
<http://www.sciencedirect.com/science/article/pii/S0008622316308107>

- 34) Tully J, Yendluri R, and Lvov Y. Halloysite clay nanotubes for enzyme immobilization. *Biomacromolecules* **17**, 615-621 (2016).
<http://pubs.acs.org/doi/full/10.1021/acs.biomac.5b01542>
- 35) Xuan ST, Lee CU, Chen C, Doyle AB, Zhang YH, Guo L, John VT, Hayes D, and Zhang D. Thermoreversible and injectable ABC polypeptoid hydrogels: Controlling the hydrogel properties through molecular design. *Chem Mat* **28**, 727-737 (2016).
<http://pubs.acs.org/doi/full/10.1021/acs.chemmater.5b03528>
- 36) Youm SG, Hwang E, Chavez CA, Li X, Chatterjee S, Lusker KL, Lu L, Strzalka J, Ankner JF, Losovyj Y, Garno JC, and Nesterov EE. Polythiophene thin films by surface-initiated polymerization: Mechanistic and structural studies. *Chem Mat* **28**, 4787-4805 (2016).
<http://pubs.acs.org/doi/full/10.1021/acs.chemmater.6b01957>
- 37) Bhaskaran-Nair K, Kowalski K, Jarrell M, Moreno J, and Shelton WA. Equation of motion coupled cluster methods for electron attachment and ionization potential in polyacenes. *Chem Phys Lett* **641**, 146-152 (2015).
<http://www.sciencedirect.com/science/article/pii/S0009261415008349>
- 38) Bhaskaran-Nair K, Valiev M, Deng SHM, Shelton WA, Kowalski K, and Wang XB. Probing microhydration effect on the electronic structure of the GFP chromophore anion: Photoelectron spectroscopy and theoretical investigations. *J Chem Phys* **143**, 224301 (2015).
<http://scitation.aip.org/content/aip/journal/jcp/143/22/10.1063/1.4936252>
- 39) Dzamukova MR, Naumenko EA, Lvov YM, and Fakhrullin RF. Enzyme-activated intracellular drug delivery with tubule clay nanoformulation. *Scien Rep* (Nature Publ) **5**, 10560 (2015). <https://www.ncbi.nlm.nih.gov/pmc/articles/PMC4432568/>
- 40) Qian B, Hu J, Liu J, Han Z, Zhang P, Guo L, Jiang X, Zou T, Zhu M, Dela Cruz CR, Ke X and Mao ZQ. Weak ferromagnetism of $Cu_xFe_{1+y}As$ and its evolution with Co doping. *Phys Rev B* **91**, 014504 (2015). <http://journals.aps.org/prb/pdf/10.1103/PhysRevB.91.014504>
- 41) Wang H, Lou W, Luo J, Wei J, Liu Y, Ortmann JE, and Mao ZQ. Enhanced superconductivity at the interface of W/Sr_2RuO_4 point contacts. *Phys Rev B* **91**, 184514 (2015).
<http://journals.aps.org/prb/pdf/10.1103/PhysRevB.91.184514>

Papers Recently Submitted:

- 1) Brooks AJ, Ge J, Dutrow B, Cao G, Jin R, Kirka MM, Dehoff RR, Bilheux HZ, Kardjilov N, Hussey DS, Butler LG. Neutron grating-based interferometry of crystals and additive manufacturing samples. *Physics Procedia* (submitted).

- 2) Cai X, Ying YA, Ortmann JE, Sun WF, Mao ZQ, and Liu Y. Magnetoresistance oscillations and the half-flux-quantum state in spin triplet superconductor Sr_2RuO_4 (submitted).
- 3) Chatterjee S, Karam TE, Rosu C, Li X, Youm SG, Do C, Haber LH, Russo PS, Nesterov EE. Silica-Conjugated Polymer Hybrid Nanoparticles Prepared by Surface-Initiated Polymerization. *Chem Mater* (submitted).
- 4) Dhital C, DeBeer-Schmitt L, Zhang Q, Xie W, Young DP, DiTusa JF. Exploring the origins of the Dzyaloshinski-Moria interaction in MnSi . *Physical Review B* (submitted).
- 5) Gyawali G, Sternfield S, Kumar R, and Rick S.W. Coarse grained models of aqueous and pure liquid alkanes. *J Chem Theory Comput* (submitted).
- 6) Liu JY, Hu J, Graf D, Zou T, Zhu M, Shi Y, Che S, Radmanesh SMA, Lau CN, Spinu L, Chiorescu I, Cao H, Ke X, and Mao ZQ. Unusual interlayer quantum transport behavior caused by the zeoth Landau level in YbMnBi_2 . *Nat Comm* (accepted).
- 7) Owoseni O, Zhang Y, He J, Li X, Lal J, Raghavan S, Bose A, and John V. Nanostructured amphiphile mesophases as buoyant gel dispersants (submitted).
- 8) Peng J, Gu MQ, Gu XM, Zhou GT, Gao XY, Liu JY, Xu WF, Liu GQ, Ke X, Zhang L, Han H, Qu Z, Fu DW, Cai HL, Zhang FM, Mao ZQ and Wu XS, Mott transition controlled by lattice-orbital coupling in double layer ruthenates. *Phys Rev X* (submitted).
- 9) Tam Y-T, Zhang T, Zou T, dos Santos AM, Hu J, Yao D-X, Mao ZQ, Ke X, Ku W. Unusually stronger quantum fluctuation with larger spins: Novel phenomena revealed by emergent magnetism in pressurized high-temperature superconductor FeSe . *Phys Rev X* (submitted).
- 10) Wu Y, Ning Z, Cao H, Cao G, Shelton WA, Benavides KA, McCandless GT, Jin R, Chan JY, DiTusa JF. Spin density wave instability in a ferromagnet. *Phys Rev Lett* (submitted).
<http://arxiv.org/abs/1704.06727>
- 11) Ying YA, Zakrzewski BM, Cai X, Mills S, Yan X, Staley NE, Wang Z, Sun WF, Mao ZQ, and Liu Y. Sensitive Josephson junction detection of chiral edge currents in Sr_2RuO_4 . *Appl Phys Lett* (submitted).
- 12) Zwijnenburg M, Berardo E, Kaplan F, Bhaskaran-Nair K, Shelton WA, Vansetten M, Kowalski K. Benchmarking the fundamental electronic properties of small TiO_2 nanoclusters by GW and Coupled Cluster Theory calculations. *J Chem Theory Comp* (submitted).

THz plasmonics and topological optics of Weyl semimetals

H. Dennis Drew and Andrei Sushkov, University of Maryland, College Park, MD 20742

Program Scope

THz magneto-optical properties of 3D topological Dirac and Weyl semimetals are under investigation. These include the study of the predicted novel magneto-electric effects arising from the underlying Berry curvature and magneto plasmonic effects in the absence of an applied magnetic field. Surface plasmon polaritons in Weyl semimetals are predicted to strongly deviate from the usual metallic response. Cyclotron resonance in the extreme quantum limit is being studied on Dirac semimetals to directly probe the chiral $N=0$ Landau level. The electronic band structure is being spectroscopically characterized through FTIR zero-field reflectance and/or cyclotron resonance measurements. The unique THz effects predicted in these materials may have important applications in THz technology.

Recent Progress

The first year of the project has consisted primarily of a buildup of the facilities for THz measurements on Dirac and Weyl semimetals and the characterization of several Dirac and Weyl semimetals for the proposed measurements. These measurements are necessary for characterization of the band structure for the design of the magneto-plasmon experiments and the analysis of the future experimental results. Reflectance measurements were made on Na_3Bi , Cd_2As_3 and TaAs.^{1,2,3,4,5,6,7,8} Similar measurements on other materials are in progress. THz pump-probe measurements have also been made on TaAs. These measurements are in order to characterize the carrier and plasmonic dynamics in Dirac and Weyl semimetals.

Single crystals of TaAs have been characterized by THz reflectance and magneto-reflection in Faraday geometry and Voigt geometry. Figure 1 shows a reflectivity spectrum measured at 10 K (blue) and fitted Drude-Lorentz model spectra (magenta). Plasmon frequency is determined by $\epsilon_1(\omega_p)=0$ condition and we find $\omega_p=167 \text{ cm}^{-1}$. Drude-Lorentz model gives Drude strength $1.5 \times 10^7 \text{ cm}^{-2}$ and scattering rate 5 cm^{-1} at 10 K.

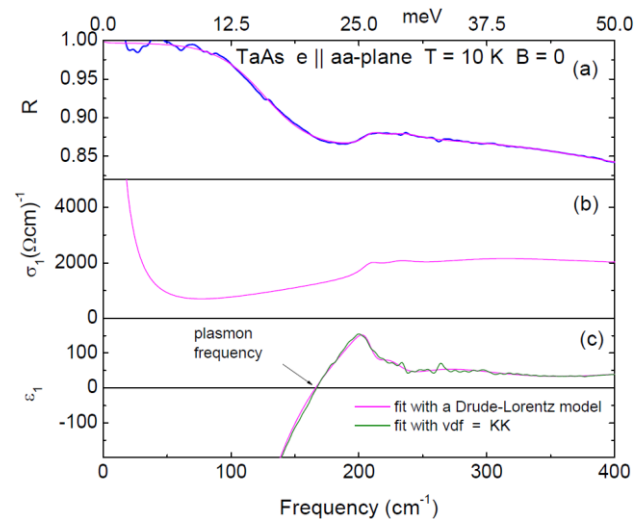


Fig. 1. The reflectivity, the optical conductivity, and the dielectric constant of TaAs.

The magneto-reflectance spectra for the Faraday geometry are shown in Fig. 2. These spectra were obtained following the method suggested in Refs. 10 and 11. The optical conductivities shown in Fig. 2 are obtained by simultaneous fit of experimentally measured reflectivity ratios $R(B,\omega)/R(0,\omega)$ and the Faraday angle $\Theta(B,\omega)$ using a variational dielectric function of Reffit program. In the derived conductivity plots there is evidence for the extreme quantum limit of cyclotron resonance in the W1 pocket.^{6,7} This observation permits the determination of the band parameters and the Fermi energy for W1 pocket. This is information critical for design of the magneto-plasma experiments and the analysis of the resulting data.

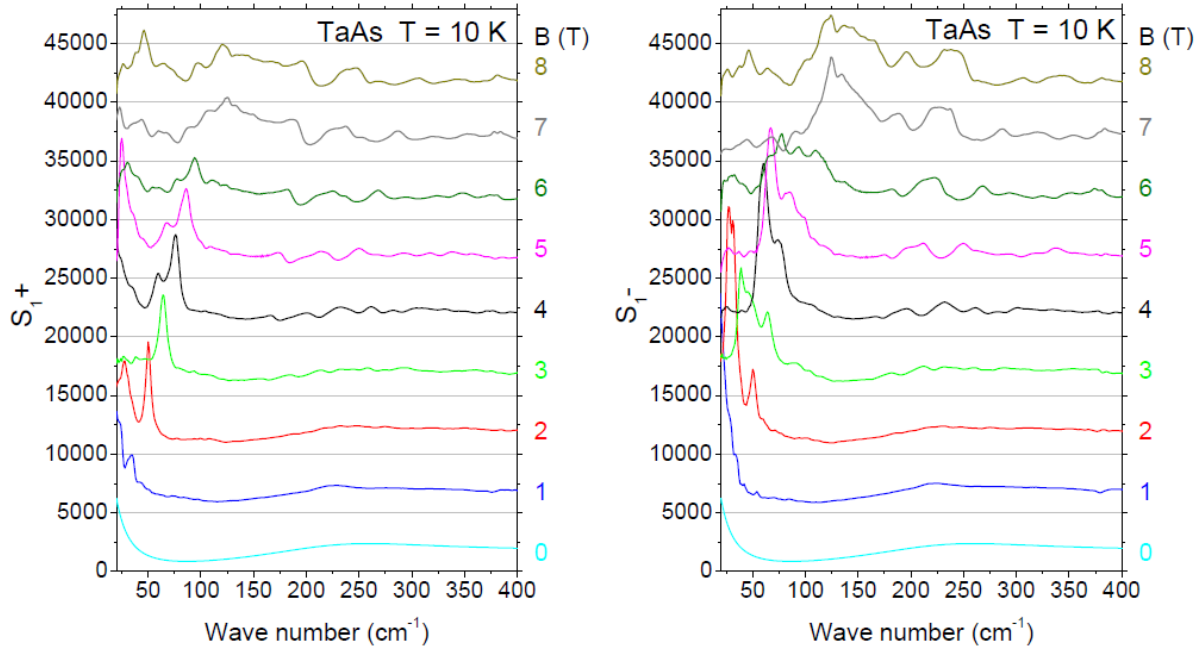


Fig. 2. The optical conductivity of a Weyl semimetal TaAs in two circular polarizations measured in Faraday geometry: $B \parallel k \parallel c$ -axis.

Figure 3 shows so-called fan diagram where peak positions found in the conductivity spectra are plotted vs. magnetic field B . All peaks observed above 150 cm^{-1} follow nearly linear dependence on B -field and extrapolate to around 150 cm^{-1} frequency at $B = 0$ and show up in both circular polarizations at the same frequencies but stronger in σ_1 -spectra. We interpret these peaks as transitions between Landau levels in the trivial hole band and the conduction band above it. Because of non-parabolicity of the bands 150 cm^{-1} (19 meV) therefore represents an upper limit of the energy gap which is much smaller than found in band theory.⁷

Future Plan

We also plan to characterize other Weyl and Dirac systems that are coming on line. The community is looking for the “hydrogen atom” of the Weyl semimetal. GdPtBi is one new

system that becomes Weyl only in an applied magnetic field. Metallic gratings are being fabricated on the most interesting and well characterized Dirac and Weyl samples in order to measure the dispersion of the magneto-plasmons with wavevector. In another experiment gates will be applied to the samples in order to study the Fermi arc surface states by modulation reflectance spectroscopy at THz frequencies.

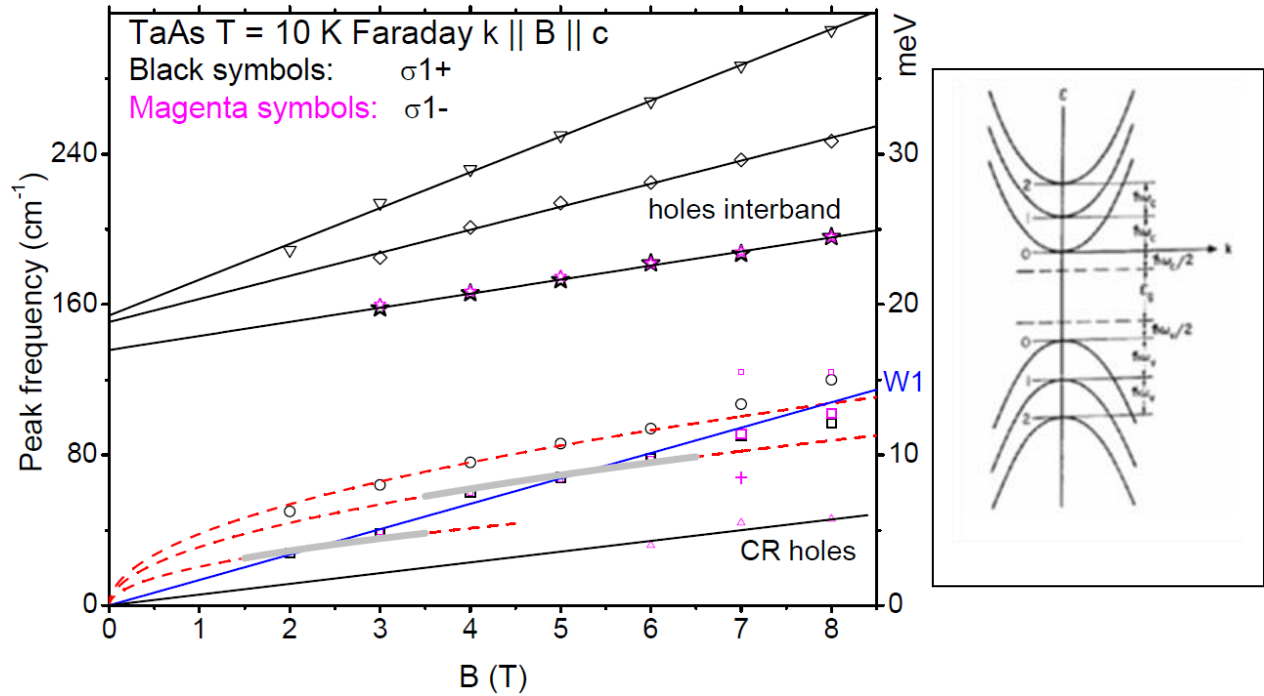


Fig. 3. Fan diagram for magneto-optical transitions observed in TaAs in Faraday geometry. Red curves are $y \sim \sqrt{B}$ functions and they are simply a guide to the eye. Low frequency peaks extrapolated to the origin are cyclotron resonances of free carriers including Weyl electrons. The grey lines correspond to the Landau level transitions allowed in W1. Inset illustrates explanation of the straight lines as interband Landau transitions for trivial holes.

References

1. J. Hofmann and S. D. Sarma, "Surface plasmon polaritons in topological Weyl semimetals," *Phys. Rev. B* **93**, 241402 (2016).
2. E. D. Palik and J. K. Furdyna, "Infrared and microwave magnetoplasma effects in semiconductors," *Rep. Prog. Phys.* **33**, 1193 (1970).
3. F. M. D. Pellegrino, et al., "Helicons in Weyl semimetals", *Phys. Rev. B* **92**, 201407(R), (2015).
4. G. S. Jenkins, A. B. Sushkov, H. D. Drew, J. W. Krizan, S. Kushwaha, Q. Gibson, R. J. Cava, A. Bansil, R. Carey, B. Barbiellini, and C. Lee, "Temperature dependent 3D

- Dirac cone and carrier dynamics in Na₃Bi and Cd₃As₂*”, Phys. Rev. B 94, 085121 (2016).
5. M. Neupane, S. Xu, R. Sankar, N. Alidoust, G. Bian, C. Liu, I. Belopolski, T.-R. Chang, H.-T. Jeng, H. Lin, A. Bansil, F. Chou, and M. Z. Hasan, “*Observation of a topological 3D Dirac semimetal phase in high-mobility Cd₃As₂*” Nature Commun. 05, 3786 (2014).
 6. P. E. C. Ashby and J. P. Carbotte, “*Magneto-optical conductivity of Weyl semimetals*”, Phys. Rev. B **87**, 245131 (2013).
 7. Chi-Cheng Lee, et al., “*Fermi surface interconnectivity and topology in Weyl fermion semimetals TaAs, TaP, NbAs, and NbP*”, Phys. Rev. B 92, 235104 (2015).
 8. Andrei Sushkov, Gregory Jenkins, Dennis Drew, Mohammad Jadidi, Bing Shen and Ni Ni, “THz magneto-optical study of Weyl semimetal TaAs”, Bulletin of the American Physical Society, 62, No. 4 (2017).
 9. M. Mehdi Jadidi, Yigit Aytac, Ryan J. Suess, Andrei B. Sushkov, Gregory S. Jenkins, James G. Analytis, H. Dennis Drew, and Thomas E. Murphy, “Time-resolved Optical Study of Carrier Dynamics in the Weyl Semimetal TaAs”, Bulletin of the American Physical Society, 62, No. 4 (2017).
 10. Levallois, J., Nedoliuk, I. O., Crassee, I. and Kuzmenko, A. B. “*Magneto-optical Kramers-Kronig analysis*”, Review of Scientific Instruments 86, 033906 (2015).
 11. de Visser, P. J. *et al.* “*Suppressed Magnetic Circular Dichroism and Valley-Selective Magnetoabsorption due to the Effective Mass Anisotropy in Bismuth*”, Phys. Rev. Lett. 117, 017402 (2016).

Publications

“*Three-dimensional Dirac cone carrier dynamics in Na₃Bi and Cd₃As₂*” G. S. Jenkins, C. Lane, B. Barbiellini, A. B. Sushkov, R. L. Carey, Fengguang Liu, J. W. Krizan, S. K. Kushwaha, Q. Gibson, Tay-Rong Chang, Horng-Tay Jeng, Hsin Lin, R. J. Cava, A. Bansil, and H. D. Drew, Phys. Rev. B 94, 085121 (2016).

“*THz magneto-optical study of Weyl semimetal TaAs*”, Andrei Sushkov, Gregory Jenkins, Dennis Drew, Mohammad Jadidi, Bing Shen and Ni Ni, Bulletin of the American Physical Society, 62, No. 4 (2017).

“*Time-resolved Optical Study of Carrier Dynamics in the Weyl Semimetal TaAs*”, M. Mehdi Jadidi, Yigit Aytac, Ryan J. Suess, Andrei B. Sushkov, Gregory S. Jenkins, James G. Analytis, H. Dennis Drew, and Thomas E. Murphy, Bulletin of the American Physical Society, 62, No. 4 (2017).

High magnetic field microwave spectroscopy of two-dimensional electron systems in GaAs and graphene

Lloyd W. Engel, National High Magnetic Field Laboratory, Florida State University, engel@magnet.fsu.edu

Current Scope of project

The project is to perform microwave spectroscopy on two-dimensional electron systems (2DES) exhibiting the quantum Hall effects in GaAs/Al_xGa_{1-x}As quantum well samples, and also in graphene. The focus of the work is on electron solids in high magnetic field. The simplest such solid is the Wigner solid (WS) [1-9] a triangular lattice of individual carriers. Microwave spectroscopy is of value in studying electron solids because they exhibit a striking resonance, which is understood as a pinning mode [5-7,10-12], in which pieces of the solid oscillate within the confining potential of the residual disorder of the sample. Fig. 1 illustrates the transmission-line-based set-up.

The pinning mode resonance is an experimental signature of an electron solid state, and has been used to find many different types of electron solid, most recently of quasiholes of the fractional quantum Hall effect (FQHE) near Landau filling $\nu = 1/2$ [10].

Pinning modes can also be used to characterize these states, to detect solid-solid phase transitions [11,12] or to distinguish components of a mixture [10]. Our work continues on the many transitions between solids seen in lower ν bilayer states in wide quantum wells (WQWs). We have also studied double quantum wells with one layer containing composite fermion liquid and the other layer a WS with a clear pinning mode.

Work is continuing as well on graphene samples, in which now easily observe FQHEs [13-19] at microwave frequencies.

Recent Progress

In collaboration with M. Shayegan, we continue studies of electron solid in wide quantum wells (WQWs), and observing transitions between these different solids.

1. Low Landau filling bilayer solid phases of GaAs wide quantum Wells: tilted field (paper in preparation)

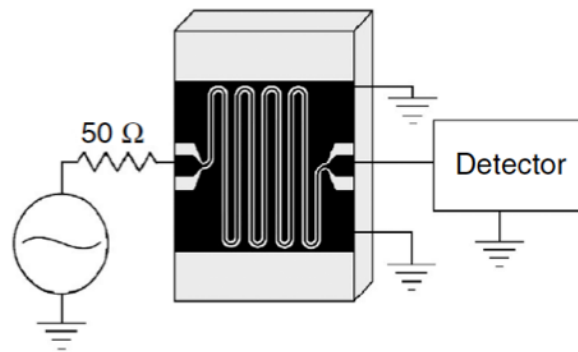


Figure 1: Schematic of sample with coplanar waveguide transmission line pattern, metal film shown as black. The transmission line couples capacitively to the 2D electron system beneath it.

We have extended the studies of our paper [11] which identified phase transitions in an 80 nm wide quantum well (WQW), at low Landau fillings (ν) under conditions for which the electrons in the WQW form a bilayer, by examining these transitions in the presence of in-plane magnetic fields, by tilting the samples in the magnetic field. This gives a clue as to the origins of the phase transitions

In sufficient in-plane field the tunneling between layers is suppressed and the transitions occur at fixed ν , independent of further increase in in-plane field or in the density, n (as long as the perpendicular field is changed to keep ν fixed). This same condition of ν -determined transitions occurs at large enough n . Such behavior is consistent with the transitions being driven by composite-fermion vortex number changes, as was considered theoretically in the single-layer case [20].

2 Solid of quasiholes of possibly non Abelian $\frac{1}{2}$ FQHE in WQW (Hatke *et al.*, PRB 2017. [10])

Recently, some half-integer FQHEs have been thought to exhibit non-Abelian statistics, which besides their fundamental importance are of possible application in quantum computing schemes. The reported solid is a new state of matter: a Wigner solid of quasihole excitations of the $\frac{1}{2}$ FQHE. According to recent theory [21], in a WQW like the one we study, the $\frac{1}{2}$ FQHE excitations of which the solid is formed, can have non-Abelian statistics.

The microwave spectra of a WQW for ν just below $1/2$, under conditions for which the $1/2$ FQHE [19] is present, show two resonances, as shown in Fig. 2a. The lower-peak frequency (f_{pk}) resonance has the same f_{pk} resonance as is found in the insulator at lower ν . The higher- f_{pk} resonance exhibits intensity variations in striking agreement with that expected for a pinning mode of WS of the quasiholes of this FQHE state. This resonance is also quite sensitive to asymmetrization of the growth-direction charge distribution in the quantum well by gate bias, as the $\frac{1}{2}$ FQHE is in dc [22]. The presence of the two resonances shows the sample forms states with multiple components. The lower- f_{pk} resonance in the spectra is due to an admixture (small near $\nu=1/2$) of a WS that is unrelated to the $\frac{1}{2}$ FQHE, and is the low- ν limiting state in these samples.

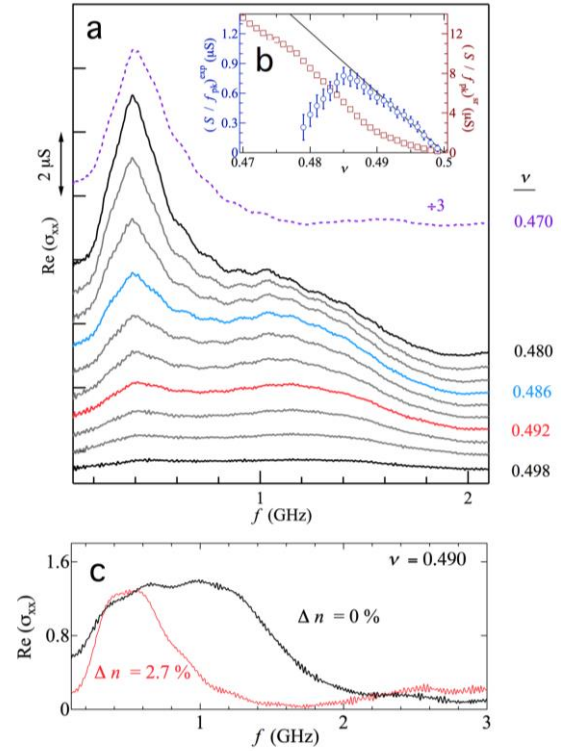


Figure 2: a) Spectra near $\nu=1/2$, ν marked at right. Two resonances are present. b) S/f_{pk} is integrated $\text{Re } \sigma_{xx}(f)$ divided by peak frequency for the two resonances and is proportional to participating charge by sum rule. Blue for higher f_{pk} resonance, red for lower f_{pk} . Solid gray line is calculated without parameters for quasiholes of $\frac{1}{2}$ FQHE. c) Effect of top-bottom charge imbalance Δn on spectra. Higher- f_{pk} resonance disappears on imbalance. Data in c) taken in different cooldown, at slightly different density.

3. Wigner solid affected by nearby composite fermion liquid

A recent paper [23] showed that in double quantum well samples whose carrier density is much larger in one layer than it is in the other, it is possible to have a composite fermion (CF) metal with filling $\nu \sim 1/2$ in the majority layer, but a Wigner solid state in the minority layer. We have studied the pinning resonance of the minority layer in detail for double wells set up in this way. The minority layer f_{pk} , dips when there are FQHE states in the majority layer, as shown in Fig. 2a. We analyze the resonance to calculate the charge density, n_{osc} that produces it in two ways, one from f_{pk} alone, and one from the integrated absorption of the resonance line. We find n_{osc} is reduced from the known density, n_L , of the minority layer, and agrees between the two calculations over a wide range of majority-layer ν , ν_H .

The interpretation is that at each lattice site there is some positive local charge density in the majority layer, essentially an image lattice of charge density $n_I = n_L - n_{osc}$, which is shown vs ν_H , in Fig. 3b. Hence the measurement of the pinning resonance gives an estimate of local compressibility of the CF metal, and shows the incompressibility of FQHE states, at which n_I is vanishing or reduced.

4. Microwave measurements of graphene

In close collaboration with the group of Cory Dean at Columbia, we are measuring low-disorder graphene confined in hexagonal BN (hBN) stacks, using graphite as a back gate. We measure using a coplanar waveguide transmission line patterned onto the top of the stack, and coupled capacitively to the graphene. As shown in Fig.4, we can easily resolve

FQHE's [13,14] in bilayer graphene [15-19] We are working to reduce the excitation power and hence the temperature of the graphene, and also to remove reflections that can modulate the conductivity sensitivity of the measurement with frequency.

Future Plans

We plan to measure pinning modes of GaAs holes in in-plane field, and of AIAs under uniaxial strain, both of which may form anisotropic WS. Without symmetry breaking fields we will study well-developed WS in GaAs quantum wells with charge distributions pushed up against an interface, to

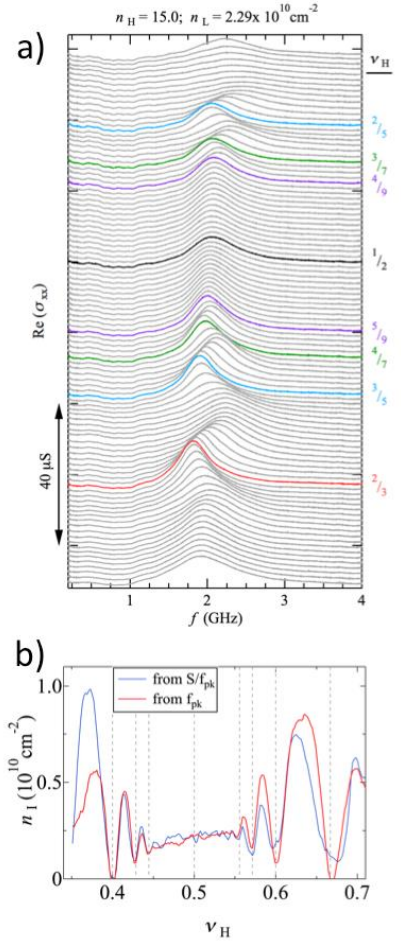


Figure 3: a) Many spectra, $Re(\sigma_{xx})$ vs f , offset vertically proportional to majority layer filling ν_H . b) Image charge density, n_I vs ν_H , calculated from f_{pk} alone (red) and from sum rule (blue), proportional to S/f_{pk} , where S is the integrated $Re(\sigma_{xx})$ vs f for the resonance.

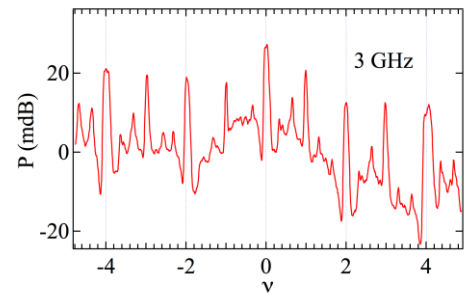


Figure 4: power transmitted through a coplanar waveguide on bilayer graphene, vs filling factor, ν , which was varied by sweeping gate bias at 18 T fixed magnetic field.

compare with the situation when the charge distribution centered in the well.

We will continue to improve the measuring technique and sample quality for graphene to look for frequency dependence due to pinning modes or (in bilayer) intra-Landau level cyclotron modes [24].

References Cited

1. Y. E. Lozovik and V. I. Yudson, JETP Letters 22, 11 (1975).
2. P. K. Lam and S. M. Girvin Phys. Rev. B **30** 473 (1984).
3. D. Levesque, J. J. Weis, and A. H. MacDonald, Phys. Rev. B **30** 1056 (1984).
4. H. Fukuyama and P. A. Lee, Phys. Rev. B, **18** 6245 (1978).
5. E. Y. Andrei et al., Phys. Rev. Lett. **60**, 2765 (1988).
6. F. I. B. Williams et al., Phys. Rev. Lett. **66**, 3285 (1991).
7. P. D. Ye et al., Phys. Rev. Lett. **89**, 176802 (2002)
8. J. Jang, et al. Nature Physics **13**, 3470 (2016).
9. L. Tiemann, T. D. Rhone, N. Shibata, and K. Muraki, Nature Physics **10**, 648 (2014).
10. A. T. Hatke, et al., Phys. Rev. B **95**, 045417 (2017).
11. A. T. Hatke et al. Nature Communications **6**, 7071 (2015).
12. A. T. Hatke et al. Nature Communications **5**, 4154 (2014).
13. X. Du et al., Nature **462**, 192 (2009) .
14. K. I. Bolotin et al., Nature **462**, 196 (2009).
15. C. R. Dean et al., Nature Physics **7**, 693 (2011).
16. P. Maher et al., Science 345,61 (2014).
17. Y. Kim et al., Nano Lett. **15**, 7445 (2015)
18. F. Amet et al., Nature Communications 5838 (2015)
19. G. Diankov et al., Nature Communications **7** 13908 2016
20. Jun-Won Rhim, J. K. Jain, and Kwon Park, Phys. Rev. B 92, 121103(R) (2015).
21. W. Zhu, Zhao Liu, F. D. M. Haldane, and D. N. Sheng, Phys. Rev. B **94**, 245147 (2016).
22. Y. W. Suen et al., Phys. Rev. Lett. **68**, 1379 (1992).
23. H. Deng et al., Phys Rev Lett 117 096601 (2016).
24. Y. Barlas, R. Cote, K. Nomura, and A. H. MacDonald, Phys. Rev. Lett. **101** 097601 (2008).

Publications resulting from DOE sponsored research

A. T. Hatke, Y. Liu, L. W. Engel, M. Shayegan, L. N. Pfeiffer, K. W. West and K. W. Baldwin, “Microwave spectroscopic observation of a Wigner solid of the $\nu=1/2$ fractional quantum Hall effect”, Phys. Rev. B **95**, 045417 (2017).

A. T. Hatke, Y. Liu, L. W. Engel, M. Shayegan, L. N. Pfeiffer, K. W. West and K. W. Baldwin, “Microwave spectroscopy of the low- filling-factor bilayer electron solid in a wide quantum well”, Nature Communications **6**, 7071 (2015).

B.-H. Moon, L. W. Engel, D. C. Tsui, L. N. Pfeiffer, and K. W. West, “Microwave pinning modes near Landau filling $\nu = 1$ in two-dimensional electron systems with alloy disorder”, Phys. Rev. B **92**, 035121 (2015).

Program Title: Electronic Structure and Spin Correlations in Novel Magnetic Structures

Principal Investigators: George Hadjipanayis (University of Delaware) in collaboration with PI David J. Sellmyer; Co-PI: Ralph Skomski (University of Nebraska); Address: Dept. of Physics & Astronomy, University of Delaware, Newark, DE 19716; E-mail: hadji@udel.edu

Program Scope

This project is focused on advancing through fundamental research the discovery and understanding of new materials important in magnetism and nanoscience. The specific focus is on nanometer-length-scale and real structure control of new or metastable structures as a means of creating materials with high magnetization, high spin polarization, large magnetocrystalline anisotropy and high ordering temperatures. Innovative aspects of the research include synthesis of new magnetic nanostructures with special non-equilibrium fabrication techniques. The proposed research consists of two main parts. The first is aimed at preparation and properties of complex or metastable transition-metal compounds where anisotropic crystal structures and nanostructuring are expected to lead to novel magnetic properties. Several types of systems are being explored including (Fe,Co,Mn)-rich compounds with Sn and B, and variants of ThMn₁₂-type compounds based on Zr and Ce. Also we are investigating a new scheme for developing high coercivity in easy-plane systems through nanostructuring. These types of materials may have potential impact in ultra-strong permanent magnets and extremely high density magnetic recording media. The second part is focused on exploring new high-anisotropy structures expected to have relatively high Curie temperatures and controllable spin polarizations. This work aims at correlating electronic structure, judicious alloying, and the effects of disorder on compounds with properties potentially useful for future magnetoelectronic devices.

Our research is based on a continuing collaboration in experimental and theoretical work between groups at the Universities of Nebraska and Delaware. A broad set of experiments is performed over a wide temperature range. These include structural characterization by x-ray diffraction, analytical and high-resolution electron microscopy, Lorentz microscopy and transport measurements. Magnetic measurements include dc magnetization to fields of 7 T between 4.2 and 1000 K with SQUID and PPMS magnetometry. The results are correlated with theoretical work with first-principle density functional theory (DFT) and analytical simulations to study spin polarization, magnetic nanostructures, anisotropies, magnetic interactions, and magnetization reversal mechanisms

Recent Progress

Background: Our recent work has focused on the synthesis and properties of nanoclusters and nanostructures of magnetic compounds having new or metastable crystal structures as well as on bulk magnetic compounds with the ThMn₁₂ structure based on Zr and Ce the most abundant rare earth element. We have used a variety of growth routes including non-equilibrium processes such as cluster deposition, sputtering and rapid quenching from the melt. Additional methods have included wet-chemical, mechanochemical, and sonochemical processes. A few examples of our recent research are explained below to highlight the important physics and technological aspects of these nanoclusters and nanostructured magnetic materials.

1. Nanostructures with High-Anisotropy

Discussion: We have reported the fabrication of rare-earth-free **Co₃Si** nanoparticles which have properties that are attractive for permanent-magnet development. DFT calculations show that bulk Co₃Si has an easy-plane anisotropy with a high $K_1 \approx -64 \text{ Merg/cm}^3$ (-6.4 MJ/m^3) and magnetic polarization of 9.2 kG (0.92 T). In spite of having a negative anisotropy that generally leads to negligibly low coercivities in bulk crystals, Co₃Si nanoparticles exhibit high coercivities

(17.4 kOe at 10 K and 4.3 kOe at 300 K), Figure 1. This result is a consequence of the unique nanostructure made possible by an effective easy-axis alignment in the cluster-deposition method and explained using micromagnetic analysis as a nanoscale phenomenon involving quantum-mechanical exchange interactions. A similar behavior has been observed in Co_2Ce particles. This compound in bulk has been reported to have magnetic ordering temperatures in the cryogenic range. However, our recent studies in Co_2Ge nanoparticles showed that nanostructuring leads to highly anisotropic particles with the same crystal structure as in bulk but with much higher magnetic ordering temperatures (over 400 C) and with coercivity close to 1 kOe.

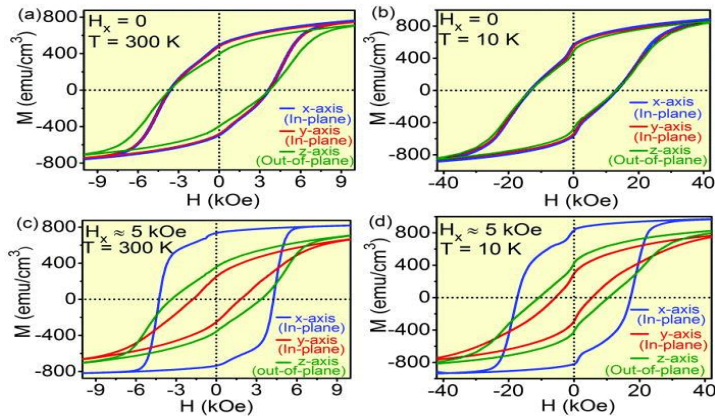


Figure 1. Hysteresis loops of Co_3Si nanoparticle films deposited in an alignment field; (a) and (b) $H_x = 0$ and (c) and (d) $H_x \approx 5$ kOe, where T is the measurement temperature. The measurement directions are x (blue), y (red), and z (green). The shoulders in (a)–(d) are caused by the hcp-Co minority phase and, probably, by some uncoupled easy-plane particles.

Significance: The understanding and control of exchange interactions, spin-orbit effects, spin coupling across interfaces, and spin correlations in new and metastable structures are fertile areas for new research to enable the design and discovery of new functional materials.

2. Rare Earth-Lean/Free Compounds with the Tetragonal ThMn_{12} Structure

Discussion: In the course of studying the stability of the 1:12 tetragonal structure in arc-melted $\text{Zr}_{1-x}\text{Ce}_x\text{Fe}_{10}\text{Si}_2$ alloys, we discovered a new metastable rare earth-free $\text{ZrFe}_{10}\text{Si}_2$ compound which possesses room-temperature saturation magnetization of 11.4 kG, Curie temperature of 325 °C and uniaxial magnetocrystalline anisotropy with an anisotropy field of 18.7 kOe. Figure 2 shows the structure, an x-ray diffraction pattern and the magnetic properties of this compound. These intrinsic magnetic characteristics as well as the absence of expensive rare-earths and Co make the compounds interesting for development of low-cost permanent magnets; a coercivity of 0.7 kOe has been obtained in melt-spun $\text{ZrFe}_{10}\text{Si}_2$ alloy. A limited, 30%, Sm substitution for Zr increases the anisotropy field to 40.7 kOe; with the magnetic hardness parameter of 1.31 and the theoretical energy product of almost 35 MGOe, the $\text{Zr}_{0.7}\text{Sm}_{0.2}\text{Fe}_{10}\text{Si}_2$ compound containing as little as 2.3 at.% rare earth is a good candidate for filling the “gap” existing between the very inexpensive ferrite magnets and the much costlier magnets based on Nd-Fe-B and Sm-Co.

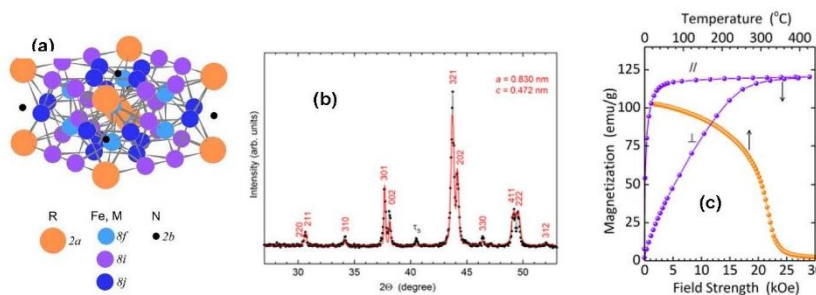


Figure 2. a) Unit cell of $\text{R}(\text{Fe},\text{M})_{12}\text{ThMn}_{12}$ -type structure, b) XRD spectrum and c) magnetic properties.

Significance: Our approach provides useful insights for developing next-generation materials for permanent magnets which are rare earth lean/free.

Future Plans

We will continue to produce new nanostructured Co(Fe)- and Mn-based magnetic compounds of fundamental and technological importance. A further investigation will be carried out to understand the effects of size confinement on the ground-state electronic structure and associated spin correlations in nanoclusters and nanostructured materials in which complex interactions including DM (Dzyaloshinsky-Moriya) effects may exist. We will also continue our studies on tetragonal R(Fe,Co)₁₂-based and 5:1:2-based compounds.

References Acknowledging DOE Support

1. P. Lukashev, P. Kharel, S. Gilbert, B. Staten, N. Hurley, R. Fuglsby, Y. Huh, S. Valloppilly, W. Zhang, K. Yang, R. Skomski, and D.J. Sellmyer, "Investigation of Spin-Gapless Semiconductivity and Half-Metallicity in Ti₂MnAl-Based Compounds," *Appl. Phys. Lett.* **108**, 141901 (1-5) (2016).
2. F.M. Abel, V. Tzitzios, D.J. Sellmyer, and G.C. Hadjipanayis, "Low-Temperature FCC to L1₀ Phase Transformation in CoPt(Bi) Nanoparticles," *AIP Advances* **6**, 056013 (1-5) (2016).
3. F.M. Abel, V. Tzitzios, G.C. Hadjipanayis, "New Approach for Direct Chemical Synthesis of Hexagonal Co Nanoparticles," *J. Magn. Magn. Mater.* **400**, 1 (2016).
4. A.A. El-Gendy, G.C. Hadjipanayis, "Room Temperature Magnetocaloric Effect in Mn_{1.25}Fe_{1.75}Ga Heusler Alloys," *J. Alloys. Compd.* **665**, 319-322 (2016).
5. P. Manchanda, A. Enders, D. J. Sellmyer, and R. Skomski, "Hydrogen-Induced Ferromagnetism in Two-Dimensional Pt Dichalcogenides," *Phys. Rev. B* **94**, 104426-1-5 (2016).
6. W.Y. Zhang, P. Kharel, I.A. Al-Omari, J.E. Shield, and D.J. Sellmyer, "Effect of Element Substitution on Nanostructure and Hard Magnetism of Rapidly Quenched Nd₂Fe₁₄B," *Philosophical Magazine* **96:26**, 2800-2807 (2016).
7. R. Skomski and D. J. Sellmyer, "Nonadiabatic Berry Phase in Nanocrystalline Magnets," *AIP Advances* **7**, 055802 (1-4) (2017).
8. M. Khan, O. Alshammari, B. Balasubramanian, B. Das, D.J. Sellmyer, A.U. Saleheen, and S. Stadler, "Controlling the Microstructure and Associated Magnetic Properties of Ni_{0.2}Mn_{3.2}Ga_{0.6} Melt-Spun Ribbons by Annealing," *AIP Advances* **7**, 056230 (1-7) (2017).
9. V. Tzitzios, G. Basina, N. Tzitzios, V. Alexandrakis, X. Hud, and G. Hadjipanayis, "Direct Liquid Phase Synthesis of Ordered L1₀ FePt Colloidal Particles with High Coercivity Using an Au Nanoparticle Seeding Approach," *New J. Chem.* **40**, 10294 (2016).
10. M. A. Koten, P. Manchanda, B. Balamurugan, R. Skomski, D. J. Sellmyer, J. E. Shield, "Ferromagnetism in Laves-phase WFe₂ Nanoparticles," *APL Mater.* **3**, 076101 (2015).
11. A.M. Gabay, G.C. Hadjipanayis, "Application of Mechanochemical Synthesis to Manufacturing of Permanent Magnets," *JOM* **67**, 1329-1335 (2015).
12. Bhaskar Das, Balamurugan Balasubramanian, Priyanka Manchanda, Pinaki Mukherjee, Ralph Skomski, George C. Hadjipanayis, and David J. Sellmyer, "Mn₅Si₃ Nanoparticles: Synthesis and Size-Induced Ferromagnetism," *Nano Lett.* **16**, 1132-1137 (2016).
13. T. Rana, P. Manchanda, B. Balasubramanian, A. Kashyap, T.R. Gao, I. Takeuchi, J. Cui, S. Biswas, R. Sabirianov, D.J. Sellmyer, R. Skomski, "Micro-magnetism of MnBi:FeCo Thin Films," *J. Phys. D: Appl. Phys.* **49**, 6 (1-6) (2016).
14. A.M. Gabay, G.C. Hadjipanayis, "ThMn₁₂-Type Structure and Uniaxial Magnetic Anisotropy in ZrFe₁₀Si₂ and Zr_{1-x}Ce_xFe₁₀Si₂ Alloys," *J. Alloys Compd.* **657**, 133-137 (2016).
15. A.M. Gabay, A. Martín-Cid, J.M. Barandiaran, D. Salazar, G.C. Hadjipanayis, "Low-Cost Ce_{1-x}Sm_x(Fe,Co,Ti)₁₂ Alloys for Permanent Magnets," *AIP Adv.* **6**, 056015 (2016).
16. B. Balasubramanian, P. Manchanda, R. Skomski, P. Mukherjee, S. Valloppilly, B. Das, G.C. Hadjipanayis, and D.J. Sellmyer, "High-Coercivity Magnetism in Nanostructures with Strong Easy-Plane Anisotropy," *Appl. Phys. Lett.* **108**, 152406 (pp. 1-4) (2016).

17. A.M. Gabay, R. Cabassi, S. Fabbri, F. Albertini, G.C. Hadjipanayis, "Structure and Permanent Magnet Properties of $Zr_{1-x}R_xFe_{10}Si_2$ Alloys with $R = Y, La, Ce, Pr$ and Sm ," *J. Alloys Compd.* **683**, 271-275 (2016).
18. R. Madugundo, G.C. Hadjipanayis, "Anisotropic Mn-Al-(C) Hot-Deformed Bulk Magnets," *J. Appl. Phys.* **119**, 013904 (2016).
19. Y. Jin, P. Kharel, P. Lukashev, S. Valloppilly, B. Staten, J. Herran, I. Tadic, M. Mitrakumar, B. Bhusal, A. O'Connell, R. Skomski, D.J. Sellmyer *et al.*, "Magnetism & Electronic Struct. CoFeCrX ($X=Si, Ge$) Heusler Alloys," *J. Appl. Phys.* **120**, 053903-1-5 (2016).
20. R. Skomski and J. M. D. Coey, "Magnetic Anisotropy — How Much is Enough for a Permanent Magnet?," *Scripta Mater.* **112**, 3-8 (2016).
21. P. Manchanda and R. Skomski, "2D Transition-Metal Diselenides: Phase Segregation, Electronic Structure, and Magnetism," *J. Phys.: Condens. Matter* **28**, 064002-1-6 (2016).
22. M. Madugundo, O. Koylu-Alkan, G.C. Hadjipanayis, "Bulk Mn-Al-C Permanent Magnets Prepared by Various Techniques," *AIP Adv.* **6**, 056009 (2016).
23. Y. Jin, P. Kharel, S. R. Valloppilly, X.-Z. Li, D. R. Kim, G. J. Zhao, T. Y. Chen, R. Choudhary, A. Kashyap, R. Skomski, and D. J. Sellmyer, "Half-Metallicity in Highly L_{21} -Ordered CoFeCrAl Thin Films," *Appl. Phys. Lett.* **109**, 142410-1-5 (2016).
24. K. Löwe, M. Duerrschnabel, L. Molina-Luna, R. Madugundo, B. Frincu, H.J. Kleebe, O. Gutfleisch, G.C. Hadjipanayis, "Microstructure and Magnetic Properties of Melt-Spun Alnico-5 Alloys," *J. Magn. Magn. Mater.* **407**, 230-234 (2016).
25. R. Choudhary, T. Komesu, P. Kumar, P. Manchanda, K. Taguchi, T. Okuda, K. Miyamoto, P. A. Dowben, R. Skomski, and A. Kashyap, "Exchange Coupling and Spin Structure in Cobalt-on-Chromia Thin Films," *Europhys. Lett.* **115**, 17003-1-4 (2016).
26. R. Choudhary, P. Kumar, P. Manchanda, D.J. Sellmyer, P.A. Dowben, A. Kashyap, and R. Skomski, "Interface-Induced Spin Polarization in Graphene on Chromia," *IEEE Magn. Lett.* **7**, 1-4 (2016).
27. A.M. Gabay, G.C. Hadjipanayis, "Mechanochemical Synthesis of Magnetically Hard Anisotropic $RFe_{10}Si_2$ Powders with R Representing Combinations of Sm, Ce and Zr ," *J. Magn. Magn. Mater.* **422**, 43-48 (2017).
28. A. Martín-Cid, A.M. Gabay, D. Salazar, J.M. Barandiaran, G.C. Hadjipanayis, "Tetragonal Ce-Based Ce-Sm(Fe, Co, Ti)₁₂ Alloys for Permanent Magnets," *Physica Status Solidi C: Current Topics in Solid State Physics* **13**, 962-964 (2016).
29. R. Skomski, B. Balamurugan, P. Manchanda, M. Chipara, and D.J. Sellmyer, "Size Dependence of Nanoparticle Magnetization," *IEEE Trans. Magn.* **53** (1), 2300307 (2017).
30. Y. Jin, J. Waybright, P. Kharel, I. Tadic, J. Herran, P. Lukashev, S. Valloppilly, and D.J. Sellmyer, "Effect of Fe Substitution on the Structural, Magnetic and Electron-Transport Properties of Half-Metallic Co_2TiSi ," *AIP Advances* **7**, 055812 (1-6) (2017).
31. R. Skomski, B. Balamurugan, D.J. Sellmyer, "Magnetism of Nanomaterials," in *Magnetic Nanomaterials: Fundamentals, Synthesis and Applications*, Y. Hou and D.J. Sellmyer, Eds., Wiley-VCH, Verlag (2017), pp. 29-80.
32. P. Manchanda, D. J. Sellmyer, and R. Skomski, "Huge Magnetic Anisotropies in Magnetic Nanostructures," *Magnetics Technology International* **2015**, 36-40 (2015).
33. R. Skomski, "Permanent Magnets: History, Current Research, and Outlook," in *Novel Functional Magnetic Materials*, Editor: A. Zhukov, Springer, Berlin 2016, p. 359-395.
34. B. Balasubramanian, D.J. Sellmyer, "Nanostructuring, Orientation, and Annealing," in *Gas Phase Synthesis of Nanoparticles*, Ed. Y. Huttel (Wiley-VCH, Weinheim, 2017), pp. 287-303.
35. Y. Hou and D.J. Sellmyer, Eds. *Magnetic Nanomaterials: Fundamentals, Synthesis and Applications*, Wiley-VCH, Weinheim (2017).

Program Title: Non-Equilibrium Magnetism: Materials and Phenomena

Principle Investigator: Frances Hellman; Co-PIs Jeff Bokor, Peter Fischer, Steve Kevan, Sayeef Salahuddin, Lin-Wang Wang; Materials Sciences Division, LBNL

Program Scope

This program focuses on the fundamental science of non-equilibrium magnetic materials and phenomena with emphasis on those enabled by interfaces and spin-orbit coupling. It encompasses design, fabrication, measuring, and modeling of static and dynamic magnetic properties of heterostructured thin films exhibiting strong spin-orbit interactions and inversion symmetry breaking due to interfaces. The research addresses three interrelated sub-projects:

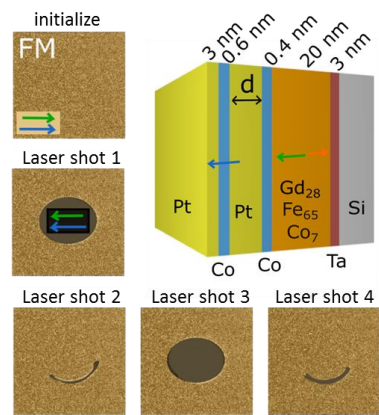
- i) Dynamics and thermodynamics of static and quasi-static novel thin film spin structures such as skyrmions and chiral magnetic textures and domain walls
- ii) Strong spin accumulation, spin transfer, and consequent control of magnetization created by interfaces between ferromagnet/non-magnet with strong spin-orbit coupling
- iii) Highly non-equilibrium magnetic states produced through electron or optical pumping at time scales ranging from nsec to fsec

Through strategic choice of materials and utilizing a collective expertise in growth, magnetic, electrical, optical, and thermodynamic characterization, spectromicroscopy, and theoretical modeling, the NEMM team aims to control the strength of the critical underlying, sometimes competing, interactions (spin-orbit, exchange, single ion anisotropy, Dzyaloshinskii-Moriya, Coulomb, disorder) within and between dissimilar materials in proximity to each other, enabling development of models for resulting magnetic states and their dynamics. Theoretical modeling provides a basis for understanding the structure (atomic, electronic, magnetic) and dynamics (electron and spin transport, magnetization response) of these states, and guides exploration of the multidimensional space of new material systems.

Recent Progress

1. Single shot ultrafast all optical magnetization switching of ferromagnetic Co/Pt multilayers using α -GdFeCo. A single femtosecond optical pulse has been used to fully reverse the magnetization of a ferromagnetic film within picoseconds. To date, this type of ultrafast switching has been restricted to ferrimagnetic GdFeCo films, while all optical switching of ferromagnetic films require multiple pulses, which is slower and less energy efficient. Here, we demonstrate magnetization switching induced by a single laser pulse in various ferromagnetic Co/Pt multilayers grown on GdFeCo, by exploiting the exchange coupling between these two magnetic films. The stack and typical magneto-optical (MO) images of a sequence of all-optical switching (single laser shot) events are presented in the figure. Table-top depth-sensitive time-resolved MO experiments show Co/Pt magnetization switches within 7 psec. [A17]

We also showed [A8] that for the helicity-independent all-optical switching (HI-AOS) of GdFeCo films, the incident laser pulse duration can be as long as 15 psec, much longer than in previous work. This result provided key insight into the role of the transient non-equilibrium electron and phonon temperatures in the HI-AOS process. This switching can be triggered by diffusion of high temperature electronic heat currents from



Magneto-optical images of a GdFeCo/[Co/Pt] stack, that illustrate the possibility of switching the magnetization in both layers, via single linearly polarized laser shots.

adjacent laser-heated layers. We also observed ultrafast demagnetization on psec time scales in Co/Pt ferromagnetic thin films, induced by psec pulses of pure electric current [A12]. These results provided scientific underpinning for the demonstration of psec switching of GdFeCo thin films using psec pulses of pure electric current [B16], a result significant for applications.

2. Spin-orbit torque switching of thick ferrimagnetic GdFeCo: Spin-orbit torque measurements in ferrimagnetic $\text{Gd}_{21}(\text{Fe}_{90}\text{Co}_{10})_{79}$ films with perpendicular magnetic anisotropy and thicknesses up to 30nm have been measured using second harmonic Hall voltage detection. Both damping-like and field-like torques show an inverse linear dependence on thickness that indicates their interfacial nature. The spin-Hall angle remains constant over the thickness range of 10 to 30nm $\text{Gd}_{21}(\text{Fe}_{90}\text{Co}_{10})_{79}$. Remarkably, this interfacial torque is able to switch a 30-nm-thick $\text{Gd}_{21}(\text{Fe}_{90}\text{Co}_{10})_{79}$ film with good thermal stability ($\approx 100\text{k}_B\text{T}$). [A18]

3. Effect of strain and film thickness on the transition temperature of FeRh. The effect of strain and (separately) film thickness was determined on the antiferromagnetic-to-ferromagnetic phase transition temperature of FeRh thin films by both experiment and density functional calculations. Strain was introduced by epitaxial growth on MgO , SrTiO_3 and KTaO_3 substrates. Film thicknesses below 15 nm substantially suppress the transition temperature T^* to below room temperature in unstrained films. For strained films, tensile/compressive strain decrease/increase T^* respectively. KTaO_3 substrates produce sufficient compressive strain to increase the transition temperature of 10 nm FeRh films above room temperature, useful for proposed applications limited by $T^* < 300\text{K}$ at small thicknesses. [A19]

4. Enhanced magnetization, anomalous Hall effect, and spin polarization in amorphous Fe-Si alloys: Spin polarization P of amorphous and crystalline $\text{Fe}_{0.65}\text{Si}_{0.35}$ films was determined by point contact Andreev reflection spectroscopy. P of the crystalline alloy is 40%, similar to that of common magnetic metals. P of the amorphous alloy is 70%, significantly higher than most ferromagnets, including numerous Heusler compounds theoretically predicted to be half-metals. The enhanced spin polarization and magnetization is attributed to modification of the local environments in the amorphous structure. In addition, the anomalous Hall effect, suitably normalized by magnetization and charge carrier concentration, is very large and independent of the longitudinal conductivity, suggesting an intrinsic AHE mechanism in a system that lacks periodicity. This is remarkable because it indicates a *local* atomic level Berry phase. Recent theoretical work on AHE in disordered amorphous ferromagnets using tight binding theory is consistent with this hypothesis. [A20]

5. Nanosecond X-ray Photon Correlation Spectroscopy on Magnetic Skyrmions: In collaboration with groups from SLAC and UCSD, we performed X-ray photon correlation spectroscopy method exploiting the recent development of the two-pulse mode at the Linac Coherent Light Source. By using coherent resonant X-ray magnetic scattering, we studied nanosecond spontaneous fluctuations in thin films of multilayered Fe/Gd that exhibit ordered stripe and skyrmion lattice phases. The correlation time of the fluctuations was found to differ between the skyrmion phase and the stripe-skyrmion boundary. This technique will enable a significant new area of research on the study of equilibrium fluctuations. [A11]

Future Plans

1. Understand the *fast time dependence* (7 psec) of the HI-AOS switching in the coupled Co/Pt-GdFeCo heterostructures, what parameters determine it (*which* exchange constant, effect of spin orbit coupling/orbital angular momentum).

- i. Vary T_c , M of the FM layer (by varying the Co/Pt layer thicknesses – see e.g. A2), compare to varying d , to determine effect of exchange constant
 - ii. Vary the strength of the magnetic anisotropy in each layer to gain further insight into the nature of the interlayer-couplings
 - iii. Understand the role of ultrafast spin currents in the switching process
 - iv. Investigate switching these layered structures using psec pure *electrical current pulses*
 - v. Investigate the combination of psec electrical heating of magnetic thin films together with spin current injection using spin-orbit torque to understand and expand the mechanisms for ultrafast control of magnetism
2. Are *non-collinear spin structures* (which are expected to exist in heavy metal-ferromagnet bilayers such as this) present or important in this Co/Pt-GdFeCo heterostructure? The broader goal is controlling stability and motion of *non-collinear spin structures*. We plan to perform XPCS studies on fluctuations taking advantage of the new COSMIC beamline at ALS:
 - i. Discovery of skyrmion and biskyrmions phases in heavy metal/ferromagnetic films
 - ii. Current control of skyrmion motion and biskyrmion orientation in FeGd films
 - iii. Skyrmion fluctuations measured with fast XPCS with free electron lasers
 - iv. Thermal- and field-driven intermittency in non-collinear spin phases
 3. Do the same parameters control *spin-orbit torque* switching as the ultrafast HI-AOS? (via electrical current passing *only* through the heavy metal layer). Separate the effects of interface-induced vs bulk-induced spin current generation and transfer by designing heterostructures with different ferromagnets and heavy metals.
 4. Theoretical modeling of the fast time reversal using *Time Dependent DFT (TDDFT)* calculations. Connecting the microscopic magnetic dynamics model with TDDFT
 5. Vary the ferromagnetic layer entirely e.g. *a*-Fe-Si alloys with tunable exchange, M , T_c

Publications: FY16 and FY17 to date (Oct 2015-Aug 2016):

A) Select Publications primarily supported and intellectually driven by this FWP (20 total)

1. X. Shi, P. Fischer, V. Neu, D. Elefant, J. C.T. Lee, D. A. Shapiro, M. Farmand, T. Tylliszczak, H.-W. Shiu, S. Marchesini, S. Roy, S. D. Kevan, *Soft x-ray ptychography studies of nanoscale magnetic and structural correlations in thin SmCo5 films*, [Appl Phys Lett **108**, 094103 \(2016\)](#)
2. M. Charilaou, C. Bordel, P.-E. Berche, B. B. Maranville, P. Fischer, F. Hellman, “Magnetic properties of ultrathin discontinuous Co/Pt multilayers: comparison with short-range ordered and isotropic CoPt3 films”, *Phys Rev B* 93 224408 (2016)
3. J. Gorchon, Y. Yang, and J. Bokor, "Model for multishot all-thermal all-optical switching in ferromagnets," *Phys Rev B* 94 020409(R) (2016)
4. N. Roschewsky, T. Matsumura, S. Cheema, F. Hellman, T. Kato, S. Iwata, S. Salahuddin, “Spin-orbit torques in ferrimagnetic GdFeCo alloys”, *Appl. Phys. Lett.* 109, 112403 (2016)
5. J. Karel, C. Bordel, D. S. Bouma, A. de Lorimier-Farmer, H.J. Lee, F. Hellman, “Scaling of the Anomalous Hall Effect in Lower Conductivity Regimes”, *Eur. Phys. Lett.* 114, 57004 (2016)
6. S. Wang, C. Antonakos, C. Bordel, D. Bouma, P. Fischer, F. Hellman, *Ultrathin IBAD MgO films for epitaxial growth on amorphous substrates and sub-50 nm membranes*, [Appl Phys Lett **109** 191603 \(2016\)](#)
7. J Gorchon, R.B. Wilson, Y. Yang, A. Pattabi, J. Chen, L. He, J. Wang, M. Li, J. Bokor, *Role of electron and phonon temperatures in the helicity-independent all-optical switching of GdFeCo* [Phys. Rev. B **94**, 184406 \(2016\)](#)

8. R.B. Wilson, J.Gorchon, Y.Yang, Ch.-H.Lambert, [S.Salahuddin, J. Bokor](#), *Ultrafast Magnetic Switching of GdFeCo with Electronic Heat Currents*, [Phys Rev B 95, 180409\(R\) \(2017\)](#)
9. Zhanghui Chen, Weile Jia and [Lin-Wang Wang](#), *SGO: An ultrafast engine for atomic structure global optimization by differential evolution*. Computer Physics Communications (<https://doi.org/10.1016/j.cpc.2017.05.005>) in press
10. [F. Hellman](#), A. Hoffmann, Y. Tserkovnyak, G.S.D. Beach, E.E. Fullerton, C. Leighton, A.H. MacDonald, D.C. Ralph, D.A. Arena, H.A. Durr, [P. Fischer](#), J. Grollier, J.P. Heremans, T. Jungwirth, A.V. Kimel, B. Koopmans, I.N. Krivorotov, S.J. May, A.K. Petford-Long, J.M. Rondinelli, N. Samarth, I.K. Schuller, A.N. Slavin, M.D. Stiles, O. Tchenyshyov, A. Thiaville, B.L. Zink, *Interface-Induced Phenomena in Magnetism*, [Rev Mod Phys 89, 025006 \(2017\)](#)
11. R. B. Wilson, Y. Yang, J. Gorchon, Ch-H. Lambert, [S. Salahuddin, J. Bokor](#) *Electric Current Induced Ultrafast Demagnetization*, [Phys Rev B 96, 045105 \(2017\)](#)
12. [P. Fischer](#), Magnetic imaging with polarized soft x-rays, [J Phys D 50 313002 \(2017\)](#)
13. J. C. T Lee, S. K. Mishra, V. S. Bhat, R. Streubel, B. Farmer, X. Shi, L. E. De Long, I. McNulty, [P. Fischer, S. D. Kevan, S. Roy](#), Magnetically charged superdomain walls in a square artificial spin ice lattice, PRL (2016) submitted
14. R.B Wilson, Ch.-H. Lambert, J. Gorchon, Y. Yang, [S. Salahuddin, J. Bokor](#), *Electron-phonon interaction during optically induced ultrafast magnetization dynamics of Au/GdFeCo bilayers* [arXiv:1609.00648v1](#)
15. J. Gorchon, Ch.-H. Lambert, Y. Yang, A. Pattabi, R.B. Wilson, [S. Salahuddin, J. Bokor](#), Single shot ultrafast all optical magnetization switching of ferromagnetic Co/Pt multilayers, [Appl. Phys. Lett. 111, 02401\(2017\)](#) (DOI:10.1063/1.4994802)
16. N Roschewsky, Ch.-H. Lambert and [S Salahuddin](#), *Spin-orbit torque switching of ultra large-thickness ferrimagnetic GdFeCo*, [Phys. Rev. B 96, 064406, 2017.](#)
17. Effect of Strain and Thickness on the Transition Temperature of Epitaxial FeRh Thin-Film, A. Ceballos, Zhanghui Chen, O. Schneider, C. Bordel, [Lin-Wang Wang, F. Hellman](#), submitted to Appl. Phys. Lett.
18. J. Karel, J. Martinez, Y. N. Zhang, J. A. Gifford, J. Zhang, G. J. Zhao, D. R. Kim, B. C. Li, R. Q. Wu, T. Y. Chen, [F. Hellman](#), "*Enhanced Spin Polarization of Amorphous Fe_{0.65}Si_{0.35} Thin Films Revealed by Andreev Reflection Spectroscopy*", submitted to Phys. Rev. Mater.

B) Select Collaborative Publications (16 total)

1. J. C. T Lee, J. Chess, S. A. Montoya, X. Shi, N. Tamura, S. K. Mishra, [P. Fischer](#), B. McMorran, S. K. Sinha, E. Fullerton, [S. D. Kevan](#), S. Roy, "Synthesizing Skyrmion Bound Pairs in Fe-Gd Thin Films", Appl Phys Lett 109 022402 (2016).
2. S. Montoya, S. Couture, J. J. Chess, J.C.T. Lee, N. Kent, D. Henze, S.K. Sinha, M.-Y. Im, [S.D. Kevan, P.Fischer](#), B.J.McMorran, V.Lomakin, S.Roy, E.E.Fullerton, Tailoring magnetic energies to form dipole skyrmions and skyrmion lattices, [Phys Rev B 95 024415 \(2017\)](#)
3. S.A.Montoya, S. Couture, J. J. Chess, J. C. T Lee, N. Kent, D. Henze, M.-Y. Im, [S.D. Kevan, P. Fischer](#), B. J. McMorran, S. Roy, V. Lomakin, E.E. Fullerton, *Resonant properties of dipole stabilized skyrmions in amorphous Fe/Gd multilayers* [Phys Rev B 95 224405 \(2017\)](#)
4. M. H. Seaberg, B. Holladay, J. C. T. Lee, M. Sikorski, A. H. Reid, S. A. Montoya, G. L. Dakovski, J. D. Koralek, G. Coslovich, S. Moeller, W. F. Schlotter, R. Streubel, [S. D. Kevan, P. Fischer](#), E. E. Fullerton, J. L. Turner, F.-J. Decker, S. K. Sinha, S. Roy, J. J. Turner, *Nanosecond X-ray Photon Correlation Spectroscopy on Magnetic Skyrmions*, Phys Rev Lett. 119 067403 (2017) featured APS Physics Synopsis: Two-Pulse X Rays Probe Skyrmions

Program Title: Spin-Coherent Transport under Strong Spin-Orbit Interaction
Principal Investigator: Jean J. Heremans
Mailing Address: Department of Physics, Virginia Tech, Blacksburg, VA 24061
Email: heremans@vt.edu

Program Scope

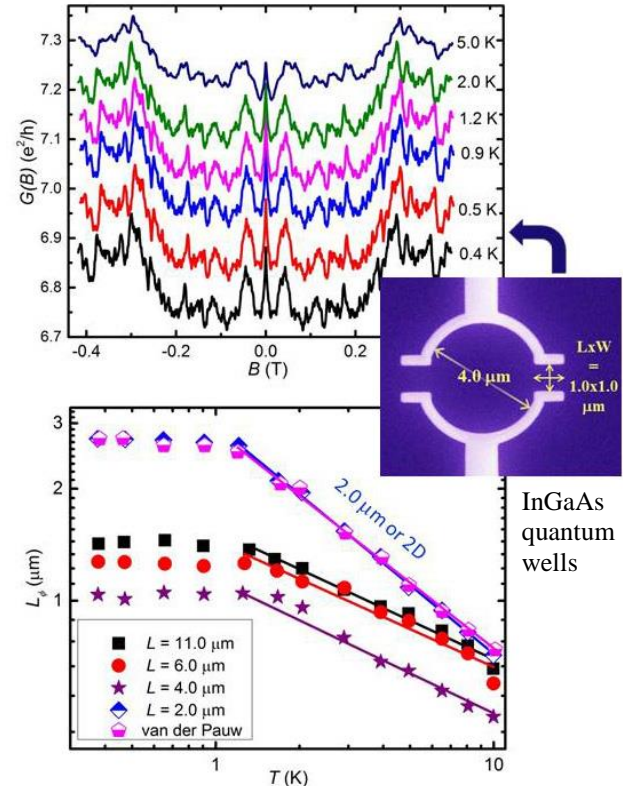
The project aims to gain fundamental insight in the physics driven by electron spins in solids, and particularly in spin coherence phenomena, quantum states, and phenomena arising from spin-orbit interaction. The project focuses on the spin physics arising when electrons are studied and interact over small length scales, lengths similar to the quantum phase coherence length and spin coherence length and the carrier mean-free-path in the materials used. By the emphasis on quantum and spin coherence, a unique understanding of coherent spin-dependent electronic processes is obtained. Materials studied in the project include the semimetal Bi in thin film form and narrow-gap semiconductor heterostructures of InSb, InAs and InGaAs, patterned by nanolithographic techniques into mesoscale and nanoscale geometries. The main experimental tools used to characterize the spin properties over the small length scales are low-temperature quantum electronic transport and magnetotransport, sensitive tools that rely on processes such as quantum interference and can access properties of quantum states. In Bi thin films, the objectives are to acquire insight in the electron spin polarization and electronic transport under strong spin-orbit interaction, in the interplay between spin-orbit interaction and the relatively unexplored hyperfine interaction, and in the hyperfine interaction itself, between electronic and nuclear spins. In InSb, InAs and InGaAs quantum wells, the objectives are to acquire insight in spin coherence under ballistic transport and in spin polarization in small structures, using nanofabricated spin interferometer structures relying on spin-orbit interaction. In InSb, InAs and InGaAs quantum wells, the objective also includes the characterization of quantum states arising from the Aharonov-Casher quantum-mechanical phase and its associated effective vector potential, which is an effective description of spin-orbit interaction. The Aharonov-Casher phase, which has deep implications, is the electromagnetic dual of the Aharonov-Bohm phase, obtained by exchanging the magnetic fields and electric charges in the Aharonov-Bohm phase by electric fields and magnetic moments (spin). The interactions studied (hyperfine, spin-orbit, electron-electron) modify electronic transport and quantum states and have ramifications for other semimetal, semiconductor and insulator materials of scientific and technological interest as hosts for new quantum states of matter.

Recent Progress

Quantum coherence: geometry and electron-electron interactions

Quantum-interference measurements of spin- and quantum phase coherence show geometrical dependences that once taken into account can be used to characterize properties of quantum states. Measurements show the influence of geometry on coherence in mesoscopic systems entering via geometrical restrictions on accumulation of geometrical phases, geometrical

dependence of electron-electron interactions, and coupling to classical environment [P2-P6]. The quantum geometrical phases (Aharonov-Casher, Aharonov-Bohm...) and kinematic Berry's phases characterize novel quantum states of matter for potential applications in future quantum technologies, and it is by their dependence on the geometry of the system that we were able to deduce several salient properties [P3,P5,P6] (prev. work, electromagnetic mapping). Yet, electron-electron interactions and interaction of the quantum system with the classical environment are both important decoherence channels requiring quantification. Using universal conductance fluctuations [P2,R1,R2] and antilocalization [P3,R3,R4] we hence studied the quantum phase coherence lengths in mesoscopic arenas, as function of the length and width of side-wires connecting the arenas to the wider environment [P2] and in narrow channels as function of channel length (Fig.). Both experiments were performed on InGaAs/InAlAs. In the arenas with side-wires (inset Fig.), decoherence by coupling to the classical environment [R5] and electron-electron interaction Nyquist decoherence in short (ergodic) wires [R6-R8] compete and result in a dependence of phase coherence length on device geometry. Nyquist scattering results from dephasing of a given electron by the fluctuating electromagnetic environment from the other electrons. How the mesoscopic device geometry is sampled by the electron trajectories results in a dependence on geometry of Nyquist scattering [R6-R8]. The findings show that geometry plays a role in interpretation of phase coherence, and that electron-electron interactions tend to dominate this aspect. The findings are important also for the proper design of devices relying on properties of new quantum states of matter.



Top: Magnetoconductances of the geometry in the middle inset, showing universal conductance fluctuations. Bottom: phase coherence lengths vs temperature in mesoscopic wires of various lengths.

Electromagnetic signatures of the chiral anomaly in Weyl semimetals

A magnetometry diagnostic procedure for the chiral magnetic effect in Weyl semimetals was introduced [P1] based on the fundamental equations of axion electrodynamics, as an alternative to negative magnetoresistance [see e.g. R9]. The procedure is based on the penetration of magnetic fields over characteristic length scales in Weyl semimetals, as inspired by the Meissner effect in superconductors. The physics leads to the Beltrami equation for the magnetic field \mathbf{B}

[R10], $\nabla \times \mathbf{B} = \zeta \mathbf{B}$, which can be solved for different sample geometries. Unlike the essentially one-dimensional Meissner problem leading to a decay of the magnetic field inside the material, axion electrodynamics in this case leads to a more intricate three-dimensional conformation. The work fits in the exploration of new quantum states of matter and contributes a new experimental approach for Weyl semimetals.

Future Plans

- Characterization of Bi hyperfine interaction via quantum transport. In previous work in semiconductor heterostructures and in Bi thin films and wires, we studied the spin coherence length limited by spin-orbit interaction using quantum transport experiments sensitive to decoherence. Prominent among other mechanisms limiting spin coherence lengths is the hyperfine interaction, coupling the carrier spins to the nuclear spins. The aim is to understand the role of hyperfine interactions in spin decoherence in Bi thin films and mesoscopic structures.
- Epitaxial thin films of pyrochlore bismuth iridates. The structural, compositional, and electrical transport properties of epitaxial thin films of pyrochlore bismuth iridates are fertile ground for discovery of novel topological electronic states arising from the interplay of electron-electron interactions and spin-orbit interaction. Particular emphasis will be placed on magnetotransport and quantum transport.

References

- R1) M. Rudolph and J. J. Heremans, "Spin-orbit interaction and phase coherence in lithographically defined bismuth wires", *Phys. Rev. B* **83**, 205410 (2011).
- R2) J. J. Lin and J. P. Bird, "Recent experimental studies of electron dephasing in metal and semiconductor mesoscopic structures", *J. Phys.: Condens. Matter* **14**, R501 (2002).
- R3) G. Bergmann, "Weak localization and its applications as an experimental tool", *Int. J. Mod. Phys. B* **24**, 2015 (2010).
- R4) R. L. Kallaher, J. J. Heremans, W. Van Roy and G. Borghs, "Spin and phase coherence lengths in InAs wires with diffusive boundary scattering", *Phys. Rev. B* **88**, 205407 (2013).
- R5) D. K. Ferry, A. M. Burke, R. Akis, R. Brunner, T. E. Day, R. Meisels, F. Kuchar, J. P. Bird and B. R. Bennett, "Open quantum dots-probing the quantum to classical transition", *Semicond. Sci. Technol.* **26**, 043001 (2011).
- R6) C. Texier, P. Delplace and G. Montambaux, "Quantum oscillations and decoherence due to the electron-electron interaction in metallic networks and hollow cylinders", *Phys. Rev. B* **80**, 205413 (2009).
- R7) M. Ferrier, A. C. H. Rowe, S. Guéron, H. Bouchiat, C. Texier and G. Montambaux, "Geometrical dependence of decoherence by electronic interactions in a GaAs/GaAlAs square network", *Phys. Rev. Lett.* **100**, 146802 (2008).

R8) T. Capron, C. Texier, G. Montambaux, D. Mailly, A. D. Wieck and L. Saminadayar, “Ergodic versus diffusive decoherence in mesoscopic devices”, *Phys. Rev. B* **87**, 041307(R) (2013).

R9) C.-L. Zhang, S.-Y. Xu, I. Belopolski, Z. Yuan, Z. Lin, B. Tong, G. Bian, N. Alidoust, C.-C. Lee, S.-M. Huang, T.-R. Chang, G. Chang, C.-H. Hsu, H.-T. Jeng, M. Neupane, D. S. Sanchez, H. Zheng, J. Wang, H. Lin, C. Zhang, H.-Z. Lu, S.-Q. Shen, T. Neupert, M. Z. Hassan and S. Jia, “Signatures of the Adler-Bell-Jackiw chiral anomaly in a Weyl fermion semimetal”, *Nat. Commun.* **7**, 10735 (2016).

R10) R. V. Buniy and T. W. Kephart, “Generalized helicity and Beltrami fields”, *Journal of Physics: Conference Series* **544**, 012008 (2014).

Publications (project’s last two years)

P1) E. Barnes, J. J. Heremans and D. Minic, “Electromagnetic signatures of the chiral anomaly in Weyl semimetals”, *Phys. Rev. Lett.* **117**, 217204 (2016).

P2) Yuantao Xie, Clément Le Priol and J. J. Heremans, “Geometrical dependence of quantum decoherence in circular arenas with side-wires”, *J. Phys.: Condens. Matter* **28**, 495003 (2016).

P3) J. J. Heremans, Yuantao Xie, S. L. Ren, C. Le Priol and M. B. Santos, “Mapping electromagnetic dualities via quantum decoherence measurements in 2D materials”, *Proc. SPIE 9932, Carbon Nanotubes, Graphene, and Emerging 2D Materials for Electronic and Photonic Devices IX*, 993207 (2016), doi:10.1117/12.2236967.

P4) Yuantao Xie, J. J. Heremans and M. B. Santos, “Effect of two-dimensional parity symmetry breaking in Aharonov-Bohm interference phenomena”, *Integr. Ferroelectr.* **174**, 8 (2016).

P5) S. L. Ren, J. J. Heremans, C. K. Gaspe, S. Vijayaragunathan, T. D. Mishima and M. B. Santos, “Determination of time-reversal symmetry breaking lengths in an InGaAs Sagnac interferometer array”, *J. Phys.: Condens. Matter* **27**, 185801 (2015).

P6) J. J. Heremans, R. L. Kallaher, M. Rudolph and M. B. Santos, “Magnetoelectric mapping as observed in quantum coherence phenomena under strong spin-orbit interaction”, *Integr. Ferroelectr.* **166**, 10 (2015).

P7) M. K. Hudait, M. Clavel, P. S. Goley, Yuantao Xie and J. J. Heremans, “Magnetotransport properties of epitaxial Ge/AlAs heterostructures integrated on GaAs and silicon”, *ACS Appl. Mater. Interfaces* **7**, 22315 (2015).

P8) V. Deo, Yao Zhang, V. Soghomonian and J. J. Heremans, “Quantum interference measurement of spin interactions in a bio-organic/semiconductor device structure”, *Scientific Reports (Nature Publ. Group)* **5**, 9487 (2015).

APS CONFERENCES FOR UNDERGRADUATE WOMEN IN PHYSICS

THEODORE HODAPP, APS

DOE Grant DE-SC0011076

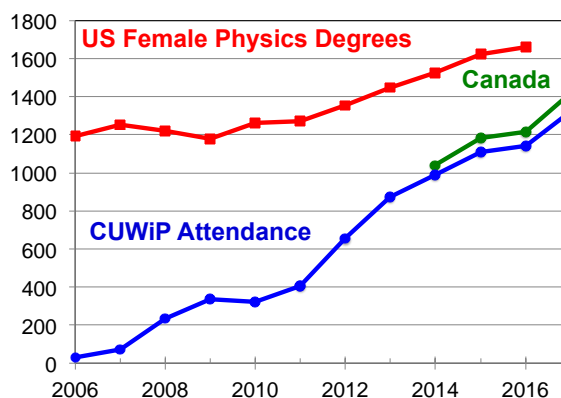
1) PROGRAM SCOPE

The APS Conferences for Undergraduate Women in Physics (CUWiP), held annually since 2006, provide female physics majors with information, resources, and motivation to support their pursuit of an undergraduate physics degree, graduate education, and a career in physics. These conferences offer (i) inspirational talks by female physicists; (ii) student presentation sessions; (iii) workshops and panel discussions on summer research, graduate school, physics careers, professional development, and issues facing underrepresented minority women and first-generation college students; and (iv) ample opportunities for networking and informal mentoring. The conferences have an amplification effect by producing student “ambassadors” for physics when the participants return to their home institutions.

The long-term vision of the CUWiP organizers is to increase the number of women who complete their undergraduate degree and pursue graduate school and/or a career in physics. To best carry out this vision, the project leadership makes a special effort to choose sites for the conferences in diverse areas of the country, to recruit participants from underrepresented groups, including at community colleges, and to design the conferences to meet these student’s needs as effectively as possible.

2) RECENT PROGRESS

The number of conferences has grown from six in 2013 to ten broadly geographically distributed conferences in 2017, and will be expanding to eleven in 2018. The number of participants has shown remarkable growth, increasing from 29 students in the first year to about 900 in 2013. During the time period of this award, the participation has increased to about 1300 in 2017. Conference attendance has more than tripled since APS first became involved following the 2011 conferences.



The conferences have also recently inspired replication of the events in Canada (hosting its 4th conference in 2017), and the UK (planning its third this coming year). Discussions with Canadian leaders are exploring the idea of unifying the events to allow Canadian events to become a part of these APS-sponsored meetings, with a likely first unified conference in 2019.

Major achievements in the project include developing infrastructure that makes the conferences more sustainable and efficient to organize -- by implementing a national student application and registration process with administrative support from APS, by developing a

repository of online materials to help future local organizing committees host effective conferences that satisfy the goals of APS CUWiP, and by introducing a host-site application process, also through APS.

The organizational details of each conference were handled by Local Organizing Committees (LOC). A National Organizing Committee (NOC) met by phone approximately monthly to guide the overall organization of the conferences, specification of the content of the application and registration forms, etc. Members of the NOC include a three-person chair line, current and past heads of LOCs, several APS staff members, and the assessment team.

This project included formal assessment by Professors Eric Brewe (Drexel) and Zahra Hazari (Florida International University), who have described their findings in a report based on pre- and post-conference surveys. The assessment team designed pre-conference and post-conference surveys that were implemented by APS and administered online. The assessment report made several recommendations that were implemented for the 2017 conferences, and assessment in 2017 revealed gains in several areas including student's sense of how to progress as a physicist, and their interest in pursuing various employment tracks.

To select future sites, APS and the NOC implemented a national host-site application process that was used for 2015 host-site proposals and was fine-tuned to improve the process for subsequent years. Details can be seen at: www.aps.org/programs/women/workshops/cuwip-host.cfm.

All conferences organized panel discussions or workshops on topics such as applying for summer research, graduate school or employment in industry, and on the breadth of physics-related career opportunities. Many of the conferences included tours of laboratories -- from small departmental labs to large national laboratories. Some participants had the opportunity to present their own research results in poster sessions or presentations. In addition to the conference activities for undergraduates, a couple of the conferences offered short parallel programs for local high school students, with some sessions overlapping with the undergraduate program.

As an aid to improving the quality of the conference experience, we have, for the past four years, held a leadership gathering at APS headquarters in College Park, MD in late May or early June. Here we bring together past and future site leaders, project leadership, and the project's assessment personnel. Site leaders indicate this meeting as extremely valuable in understanding resources available from APS and other sources, and for planning an effective timeline. Site leaders often leave having thrown out portions of their existing plans and having replaced them with a clearer sense of how to assemble the various pieces of a conference that will better achieve their goals.

3) FUTURE PLANS

We are currently organizing the 2018 APS CUWiP at eleven sites – Arizona State University, Cal Poly Pomona/Pomona College/Harvey Mudd College, Columbia University, George Washington University, Iowa State University, Rochester Institute of Technology,

University of Kansas, University of North Florida, University of Oregon, University of Toledo, and University of Virginia. We are also preparing for site selection for 2019 sites. We will continue to incorporate the recommendations from our assessment efforts. We are planning a repeat of the Leadership Gathering in June 2018, and are updating our assessment instruments to probe other questions including more detailed measures of sexual harassment witnessed or experienced by participants. We expect several publications to result from the data we are gathering at these conferences.

Project leadership (NOC leadership) meets regularly to consider strategic directions for the events, and to handle any issues that arise. One important role is to reach out to universities in geographic areas that are less well covered, and to universities that have fewer financial resources to encourage them to consider hosting a future event. They and APS staff also speak to various audiences to continue to improve the messages presented at conferences, professional development opportunities available, and to invite groups to consider bringing their message to these energetic young women.

Proximity Effects and Topological Spin Currents in van der Waals Heterostructures

Ben Hunt

Bose-Einstein Condensation of Magnons

J. B. Ketterson
Department of Physics and Astronomy
Northwestern University

Program Scope

The major goal of this project is to verify the reports by the groups of B. Hillebrands and S. O. Demokritov in Germany using Brillouin spectroscopy that a dynamic Bose-Einstein condensate (BEC) of magnons forms in yttrium iron garnet (YIG) under parametric two magnon pumping. We are working toward detecting the microwave emissions associated with a condensate using a close coupled antenna patterned on the YIG surface. The magnon minimum occurs at some imprecisely known wave vector while antennas must have a fixed wavevector. These can be made identical by tipping the magnetic field *out of plane*. Hence we are measuring the out of plane behavior of the YIG magnon spectrum.

Recent Progress

In pursuit of this goal we just completed a study of the long wavelength part of the magnon spectrum in the forward volume (FV) backward volume (BV) plane. Note the radical disagreement with available theory [1].

Future Plans

The next step is to pump our system, either resonantly or parametrically (as did the German group) and search for a condensate signal.

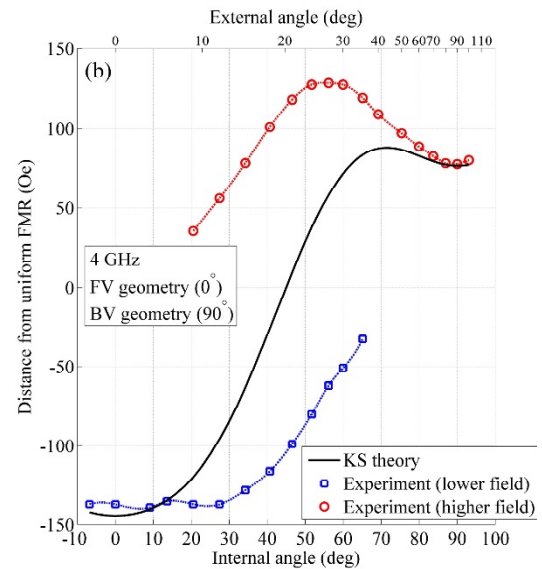
References

1. *Theory of Dipole-Exchange Spin-Wave Spectrum for Ferromagnetic-Films with Mixed Exchange Boundary-Conditions*, B. A. Kalinikos, and A. N. Slavin, *Journal of Physics C-Solid State Physics* **19**(35), 7013-7033 (1986).

Publications (citing DOE)

1. *Magnetostatic spin-waves in YIG films: Comparison between theory and experiment for arbitrary field directions*, J. Lim, W. Bang, J. Trossman, D. Amanov, C. C. Tsai, M. B. Jungfleisch, A. Hoffmann, and J. B. Ketterson (in preparation).

2. *Ferromagnetic resonance of a YIG film in the low frequency regime*, S. Lee, S. Grudichak, J. Sklenar, C. C. Tsai, M. Jang, Q. H. Yang, H. W. Zhang, J. B. Ketterson, *J. of Appl. Phys.* **120**(3), 033905 (2016).



Angular dependence of 50 μ 4GHz spin waves in the plane containing the BV (0°) and FV (90°) modes. The continuous curve is the Kalinikos-Slavin theory.

Project Title: Spectroscopy of Degenerate One-Dimensional Electrons in Carbon Nanotubes

Principal Investigator: Junichiro Kono

Mailing Address: Department of Electrical and Computer Engineering, Rice University, Houston, Texas 77005, U.S.A.

Email Address: kono@rice.edu

Program Scope

The goal of this research program is to understand the fundamental properties of degenerate one-dimensional (1-D) electrons in single-wall carbon nanotubes (SWCNTs). SWCNTs provide an ideal 1-D environment in which to study many-body physics. Semiconducting SWCNTs exhibit rich optical spectra dominated by extremely stable 1-D excitons, whereas metallic SWCNTs contain massless 1-D carriers with ultralong mean-free paths. Despite the large number of electrical, optical, and magnetic studies of SWCNTs during the last two decades, most of the predicted exotic properties of interacting 1-D electrons have yet to be observed, and some of the reported experimental results remain highly controversial.

Here, using an arsenal of spectroscopic methods from the terahertz to the visible spectral range, including ultrafast optical spectroscopy and ultrahigh magnetic fields, we aim to probe correlations and many-body effects in this prototypical 1-D nanostructure. These studies can provide a wealth of new insights into the nature of strongly correlated carriers in the ultimate 1-D limit that will lead to novel nanodevice concepts and implementations.

Specifically, the primary objective of this research program is to address the following key questions and issues, which are of critical importance in many-body physics:

- ‘Spinons’ and ‘holons’ in high magnetic fields: What will be the signatures of spin-charge separation in electron spin resonance? Will a magnetic field split spinon and holon peaks differently, as predicted?
- Optical conductivity of Tomonaga-Luttinger liquids: How will many-body effects modify the frequency, temperature, and magnetic field dependences of dynamic conductivity of metallic SWCNTs? Will there be any scaling laws indicative of quantum criticality?
- Light emission from high-density 1-D excitons: How will excitons in SWCNTs behave at quantum degenerate densities? How will the bosonic characters of 1-D excitons manifest themselves in emission spectra? Will they cooperate to emit superradiantly?

The overall theme of this research is based on one of the emergent concepts in condensed matter physics today. Namely, dynamical, non-equilibrium, and nonlinear aspects of many-body effects in quantum-confined systems have been poorly addressed to date despite the fact that one can expect a wide range of extraordinary phenomena that are not expected in bulk solids or atoms/molecules. In addition, they will undoubtedly become important when one wants to operate any electrical or photonic nanodevices. Particular emphasis is placed on the dynamic 1-D phenomena in the terahertz, infrared, and optical frequency ranges, which is a widely open research field that deserves more exploration both from basic and applied points of view. Because they are direct band gap materials, SWCNTs are one of the leading candidates to unify electronic and optical functions in nanoscale circuits and elucidate how electron correlations can affect and control finite-frequency phenomena in 1-D systems.

Recent Progress

Although the one-dimensional character of electrons, holes, and excitons in *individual* SWCNTs has stimulated much interest [1], its macroscopic manifestation has been difficult to observe. We have developed a simple but robust method for preparing large-area films of aligned SWCNTs by utilizing spontaneous alignment that occurs during vacuum filtration [2]. The produced films (see, e.g., Fig. 1) are globally aligned and are highly packed, and the film thickness is controllable in a wide range, from a few nm to ~100 nm. This method is applicable to any SWCNTs suspended in aqueous solution. By combining this method with recently developed chirality- and type-sorting techniques, we were able to fabricate aligned and chirality-enriched SWCNT films. Semiconductor films exhibited polarized photoluminescence, polarization-dependent photocurrent, and strong conductivity anisotropy.

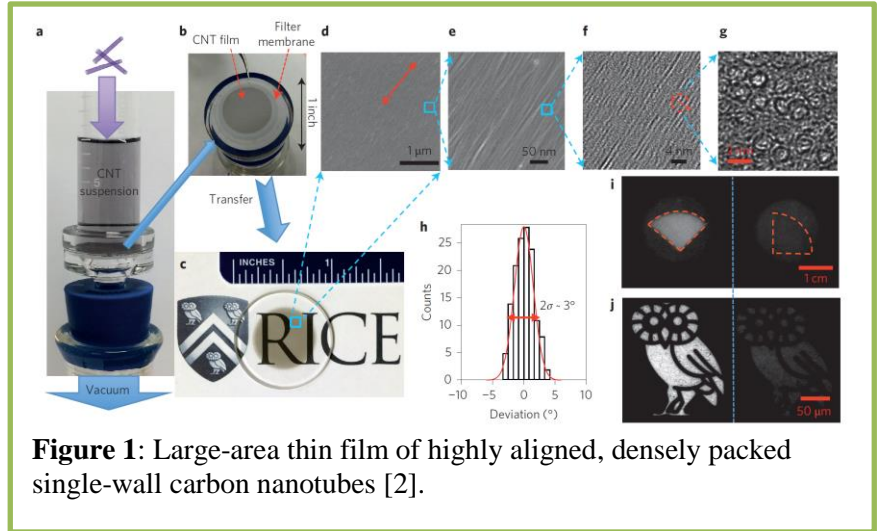


Figure 1: Large-area thin film of highly aligned, densely packed single-wall carbon nanotubes [2].

The development of these films allow for unique opportunities to systematically study the spectroscopic response at low temperatures and in high magnetic fields for either semiconducting or metallic carbon nanotube films in order to answer the primary research questions listed above.

We measured polarization-dependent Raman spectra for these aligned SWCNT films and analyzed the data using standard equations for the angular dependence of SWCNT Raman spectra to determine the value of the nematic order parameter, S , to be 0.96 for this particular film. We also measured polarization-dependent transmission spectra of this film in a wide spectral range, from the terahertz to the visible. There was essentially no detectable attenuation within experimental errors for the perpendicular polarization in the entire range whereas there was a prominent, broad peak at 0.02 eV in the parallel case due to the plasmon resonance, similar to our previous studies [1,3,4]. In the near-infrared and visible ranges, we clearly observed the first two interband transitions for semiconducting nanotubes and the first interband transition in metallic nanotubes in the parallel polarization case. These peaks were absent for the perpendicular polarization, for which we instead observed a broad absorption feature in an intermediate energy region, which we attributed to the cross-polarized E_{12}/E_{21} peak. Such a transition, theoretically predicted more than 20 years ago, has been previously observed in polarized photoluminescence excitation spectroscopy experiments in individualized SWCNTs. We observed this transition in our best-aligned films of large-diameter, arc-discharge

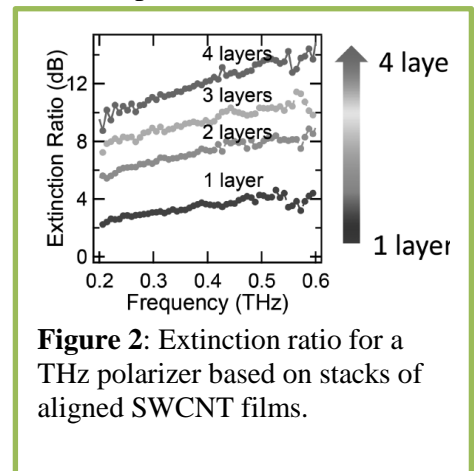


Figure 2: Extinction ratio for a THz polarizer based on stacks of aligned SWCNT films.

SWCNTs only when S is nearly 1 and only when the tube density and thickness are high enough. We further increased the diameter of our aligned SWCNT films from 1 inch to 2 inches [5] and used portions of the larger film to increase the extinction ratio for a THz polarizer based on stacks of aligned films (see, e.g., Fig. 2) greatly enhancing the performance of our previous carbon nanotube THz polarizer [6].

Future Plans

We will perform gigahertz, terahertz, and infrared spectroscopy experiments on these aligned large-scale carbon nanotubes films to understand their 1-D nature on a macroscopic scale. We will use modern nonlinear and ultrafast optical methods, combined with our unique capabilities of studying materials in ultrahigh magnetic fields using a 30 T table-top magnet [7,8]. Furthermore, using the developed method, we will be trying to fabricate single crystals of single-chirality single-wall carbon nanotubes (see Fig. 3). Such crystals are expected to exhibit new phenomena arising from the intrinsically one-dimensional nature of the interacting electrons in these systems in a chirality-specific manner.

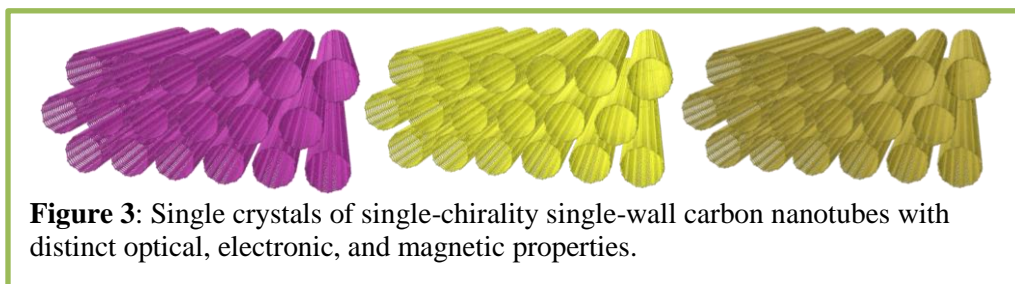


Figure 3: Single crystals of single-chirality single-wall carbon nanotubes with distinct optical, electronic, and magnetic properties.

References

1. S. Nanot, E. H. Háróz, J.-H. Kim, R. H. Hauge, and J. Kono, “Optoelectronic Properties of Single-Wall Carbon Nanotubes,” *Adv. Mater.* **24**, 4977 (2012).
2. X. He, W. Gao, L. Xie, B. Li, Q. Zhang, S. Lei, J. M. Robinson, E. H. Háróz, S. K. Doorn, R. Vajtai, P. M. Ajayan, W. W. Adams, R. H. Hauge, and J. Kono, “Wafer-Scale Monodomain Films of Spontaneously Aligned Single-Walled Carbon Nanotubes,” *Nature Nanotechnol.* **11**, 633 (2016).
3. Q. Zhang, E. H. Háróz, Z. Jin, L. Ren, X. Wang, R. Arvidson, A. Lüttge, and J. Kono, “Plasmonic Nature of the Terahertz Conductivity Peak in Single-Wall Carbon Nanotubes,” *Nano Lett.* **13**, 5991 (2013).
4. L. Ren, Q. Zhang, C. L. Pint, A. K. Wójcik, M. Bunney, T. Arikawa, I. Kawayama, M. Tonouchi, R. H. Hauge, A. A. Belyanin, and J. Kono, “Collective Antenna Effects in the Terahertz and Infrared Response of Highly Aligned Carbon Nanotube Arrays,” *Phys. Rev. B* **87**, 161401(R) (2013).
5. N. Komatsu, W. Gao, P. Chen, C. Guo, A. Babakhani, and J. Kono, “Modulation-Doped Multiple Quantum Wells of Aligned Single-Wall Carbon Nanotubes,” *Adv. Func. Mater.* **27**, 1606022 (2017).
6. L. Ren, C. L. Pint, L. G. Booshehri, W. D. Rice, X. Wang, D. J. Hilton, K. Takeya, I. Kawayama, M. Tonouchi, R. H. Hauge, and J. Kono, “Carbon Nanotube Terahertz Polarizer,” *Nano Lett.* **9**, 2610 (2009).

7. G. T. Noe, H. Nojiri, J. Lee, G. L. Woods, J. Léotin, and J. Kono, "A Table-Top, Repetitive Pulsed Magnet for Nonlinear and Ultrafast Spectroscopy in High Magnetic Fields Up to 30 T," *Rev. Sci. Instr.* **84**, 123906 (2013).
8. G. T. Noe, I. Katayama, F. Katsutani, J. J. Allred, J. A. Horowitz, D. M. Sullivan, Q. Zhang, F. Sekiguchi, G. L. Woods, M. C. Hoffmann, H. Nojiri, J. Takeda, and J. Kono, "Single-Shot Terahertz Time-Domain Spectroscopy in Pulsed High Magnetic Fields," *Optics Express* **24**, 30328 (2016).

Publications

1. N. Komatsu, W. Gao, P. Chen, C. Guo, A. Babakhani, and J. Kono, "Modulation-Doped Multiple Quantum Wells of Aligned Single-Wall Carbon Nanotubes," *Advanced Functional Materials* **27**, 1606022 (2017).
2. X. He, W. Gao, L. Xie, B. Li, Q. Zhang, S. Lei, J. M. Robinson, E. H. Hároz, S. K. Doorn, R. Vajtai, P. M. Ajayan, W. W. Adams, R. H. Hauge, and J. Kono, "Wafer-Scale Monodomain Films of Spontaneously Aligned Single-Walled Carbon Nanotubes," *Nature Nanotechnology* **11**, 633 (2016).
3. D. Tristant, A. Zubair, P. Puech, F. Neumayer, S. Moyano, R. J. Headrick, D. E. Tsentalovich, C. C. Young, I. C. Gerber, M. Pasquali, J. Kono, and J. Léotin, "Enlightening the Ultrahigh Electrical Conductivities of Doped Double-Wall Carbon Nanotube Fibers by Raman Spectroscopy and First-Principles Calculations," *Nanoscale* **18**, 19668 (2016).
4. M. Krottenmüller, W. Gao, B. Anis, J. Kono, and C. A. Kuntscher, "High-Pressure Optical Study of Small-Diameter Chirality-Enriched Single-Wall Carbon Nanotubes," *Physica Status Solidi B* **253**, 2446 (2016).
5. Zubair, D. E. Tsentalovich, C. C. Young, M. S. Heimbeck, H. O. Everitt, M. Pasquali, and J. Kono, "Carbon Nanotube Fiber Terahertz Polarizer," *Applied Physics Letters* **108**, 141107 (2016).
6. K. Erickson, X. He, A. A. Talin, B. Mills, R. H. Hauge, Y. Kawano, J. Kono, and F. Léonard, "Figure of Merit for Carbon Nanotube Photothermoelectric Detectors," *ACS Nano* **9**, 11618 (2015).
- 7.

Nanoscale magnetic Josephson junctions and superconductor/ferromagnet proximity effects for low-power spintronics

Ilya Krivorotov, Department of Physics and Astronomy, University of California at Irvine

Oriol T. Valls, School of Physics and Astronomy, University of Minnesota

Program Scope

The goal of this program is to investigate novel effects arising from coupling between proximity and spin-dependent transport in nanoscale multilayer systems made of ferromagnetic (F) and superconducting (S) materials. The first is the modification of the differential conductance $G(V)$, the giant magneto-resistance (GMR), and the spin transfer torque (STT), in metallic spin valves, induced by proximity to a superconducting layer. We expect the angular dependence of these quantities to develop large π -periodic, bias-dependent components that are induced by the proximate superconductor. This is in sharp contrast to the 2π -periodic, bias-independent behavior in conventional metallic spin valves. The second is tuning of the Josephson current in Josephson junctions with spin valve barriers via control of the magnetic state of the barrier. We expect giant variation of the critical current in response to a weak external magnetic field that rotates the spin valve magnetic moments from the anti-parallel to the parallel configuration. This effect originates from modulation of the long-range spin-triplet super-current by magnetic non-collinearity within the barrier. The third is enhancement of the critical current in Josephson junctions with ferromagnetic barriers by spin orbit interaction (SOI). Addition of an ultra-thin layer with strong spin orbit interaction to the barrier is expected to increase the critical current via SOI-induced generation of a long-range spin-triplet component of the supercurrent.

Recent Progress

a. Experiment

Bias dependence of angular magneto-resistance in superconductor/spin valve nanowires.

We developed a process for fabrication of nanowire devices from S/F/N/F/AF multilayers, and measured significant magneto-resistance (MR) in these nanowires. We found that a very gentle physical etching process is needed to make nanowires out of the Nb/Co/Cu/Co/CoO multilayer films while preserving the film-level magnitude of the magneto-resistance. The key to successful fabrication of nanowires with high MR is very slow etching of the multilayer by argon ion milling during the nanowire patterning stage and cooling of the substrate throughout the etching process.

We made measurements of the angular dependence of current-in-plane (CIP) MR in Nb/Co/Cu/Co/CoO nanowires as a function of the bias current near the superconducting transition temperature T_c of the multilayer. These measurements reveal an unexpectedly strong modification of the angular dependence of the MR by the bias current as illustrated in Fig. 1. The

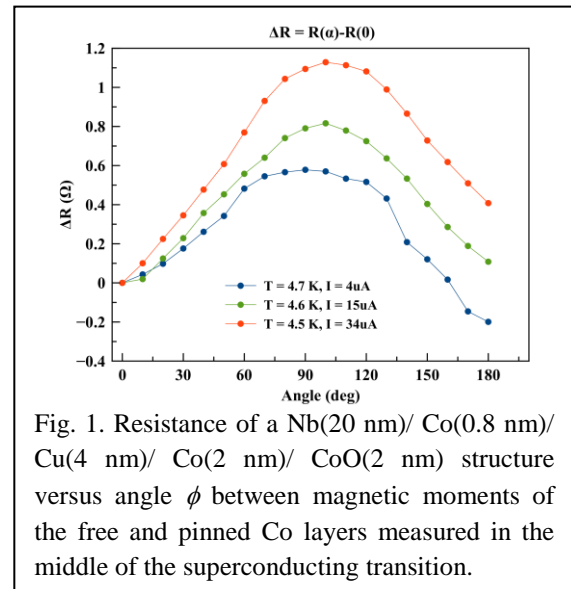


Fig. 1. Resistance of a Nb(20 nm)/ Co(0.8 nm)/ Cu(4 nm)/ Co(2 nm)/ CoO(2 nm) structure versus angle ϕ between magnetic moments of the free and pinned Co layers measured in the middle of the superconducting transition.

data in Fig. 1 shows the resistance difference between the parallel (0°) and antiparallel (180°) configurations of the free and fixed Co layers of the spin valve changes sign as a function of the bias current. This bias dependence of MR can be explained by spin current injection [1] from the Co/Cu/Co spin valve to the Nb layer driven by a combination of (i) a pure spin Hall current and (ii) a pure spin Seebeck current arising from a temperature gradient perpendicular to the multilayer plane that arises from Ohmic heating of the layers [2]. Such pure spin currents flowing perpendicular to the multilayer plane are analogous to the spin-polarized electrical current in the current-perpendicular-to-plane (CPP) geometry driven by voltage bias that is applied perpendicular to the plane of the layers.

CPP MR nano-contact devices. In order to understand the effects of pure spin currents and spin polarized electrical current on the MR in S/F/N/F multilayers, we designed and made a new type of MR nano-contact device shown in Fig. 2, which enables simultaneous measurements of the MR in the CIP and CPP geometries for the same sample. The device consists of a rectangular top nano-contact made at the intersection between a S/F/N/F nanowire and a top lead nanowire. These devices made at UCI show sub-Ohm 4-point CPP resistance indicative of clean interface between the S/F/N/F nanowire and the top lead nanowire making Ohmic contact to each other in the junction area.

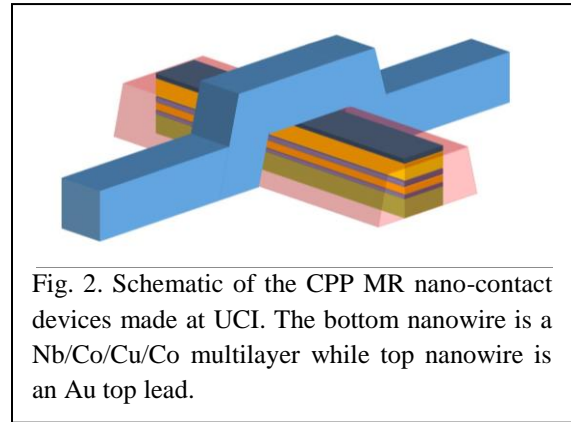


Fig. 2. Schematic of the CPP MR nano-contact devices made at UCI. The bottom nanowire is a Nb/Co/Cu/Co multilayer while top nanowire is an Au top lead.

Figure 3 shows CPP resistance of a $0.25 \times 0.15 \mu\text{m}^2$ nano-contact to a $0.15 \mu\text{m}$ -wide Nb(30 nm)/ Co(10 nm)/ Cu(10 nm)/ Co(5 nm) nanowire measured as a function of magnetic field applied parallel to the wire. The top panel shows the 4-point MR data above the superconducting transition temperature T_c of the Nb layer while the bottom panel shows the data below T_c . It is clear from the data that significant GMR is present both above and below T_c in this test device. Both the CPP resistance and the GMR increase upon transition of the Nb layer into the superconducting state. This is indicative of a relatively high resistance of the Co/Nb interface. We have determined that this effect is intrinsic to the Nb/Co interface. The observed variation of $\Delta R/R_0$ upon the normal metal/superconductor transition of the Nb layer is relatively small. This is expected and consistent with the theory described in the theory section below because relatively thick Co layers were employed in these initial test devices. Measurements of the devices with thin ($< 1 \text{ nm}$) Co free layers are in progress.

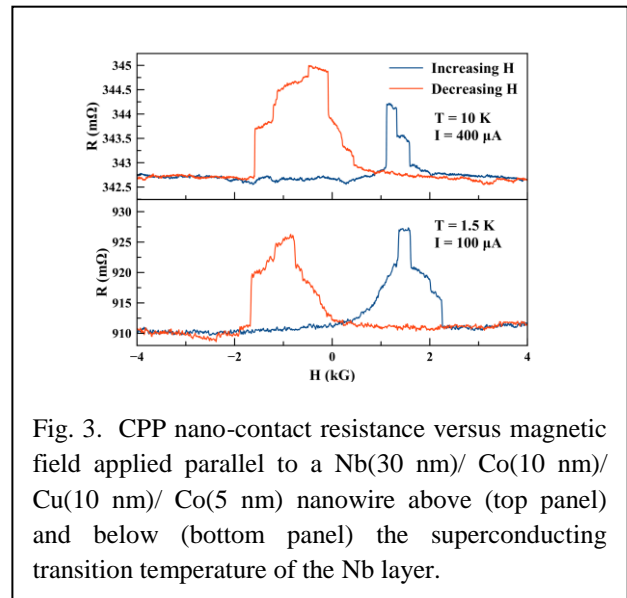


Fig. 3. CPP nano-contact resistance versus magnetic field applied parallel to a Nb(30 nm)/ Co(10 nm)/ Cu(10 nm)/ Co(5 nm) nanowire above (top panel) and below (bottom panel) the superconducting transition temperature of the Nb layer.

In these devices, theory predicts strong variation of the angular dependence of MR upon the normal metal/superconductor transition of the Nb layer [1].

b. Theory

Bias dependent conductance in S/F/N/F structures. We have performed extensive calculations of the bias-dependent conductance $G(V)$ for Nb/Co/Cu/Co samples, using actual material parameters and realistic thickness values for the different layers, and taking into account the unavoidable scattering at the interfaces.

The calculations have been performed using fully self-consistent methods, which are absolutely necessary to ensure that current is conserved. For each geometrical and material characteristics, results for $G(V)$ are obtained as a function of the angle ϕ between the magnetization of the Co layers, the objective being to determine the conditions that are optimal for obtaining the best valve effects. The temperature dependence of the transport (the relevant parameter being T/T_c) has also been calculated. An example is shown in Fig.

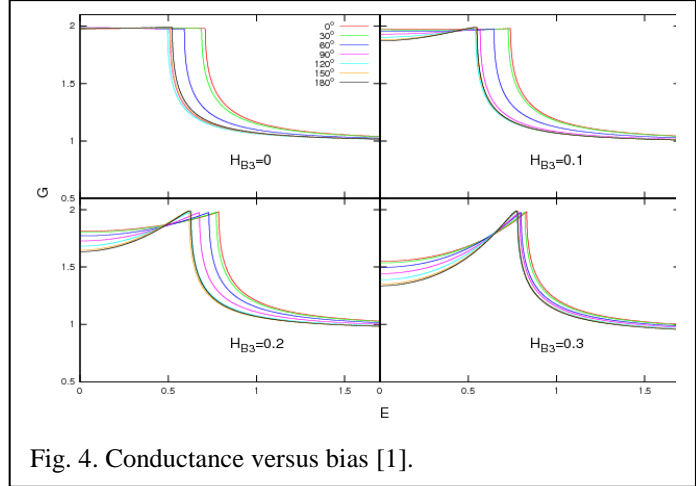


Fig. 4. Conductance versus bias [1].

4, where $G(V)$ in natural units is given as a function of E/Δ_0 for several values of the scattering barrier between Nb and the inner Co layer. These results for the conductance recently published in Ref. [1] are only an extremely small fraction of those calculated. We have obtained a very extensive database of results for different parameter values: for each set of geometrical and barrier parameters, a full set of $G(V)$ or I/V curves is obtained for many values of ϕ . These results are summarized in a data base with a user-friendly interface. This data base is used for optimization of the device parameters made at UCI.

Spin currents and Spin Transfer Torque (STT).

We have developed a method to calculate the spin current and the STT in S/F/F structures. The method and some preliminary results are included in Ref. [1]. A sample of the results published there for STT is shown in Fig. 5. The figure shows three components of the STT for in a F/F/S structure, plotted as a function of position.

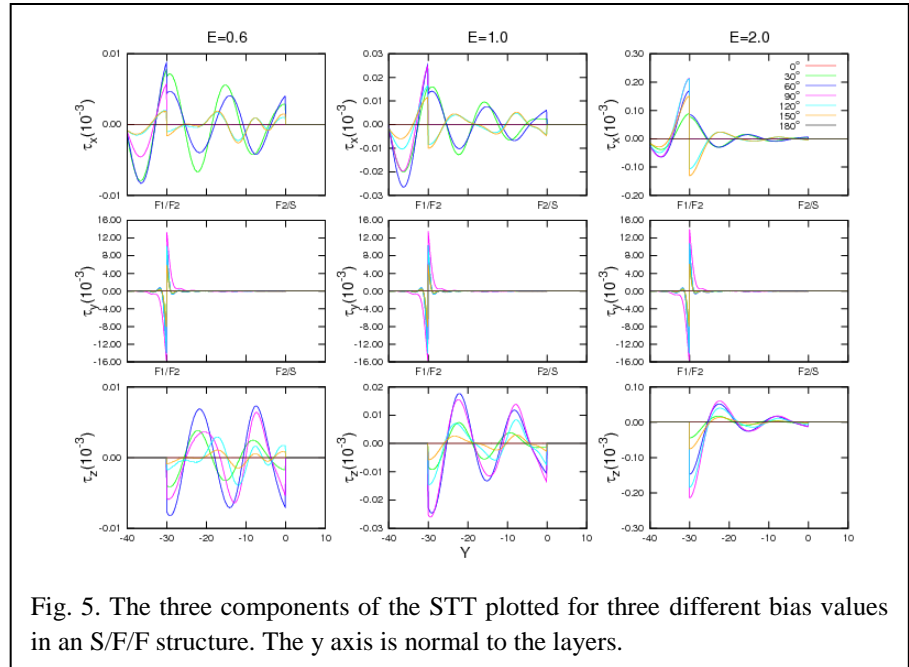


Fig. 5. The three components of the STT plotted for three different bias values in an S/F/F structure. The y axis is normal to the layers.

Only the important portion of the sample is included in the plot: the 0 in the horizontal axis is at the S interface and -30 is at the interface between the two F layers.

Future Plans

- We are performing a series of measurements on S/F/N/F nanowires where the temperature gradient is decoupled from the direct electrical bias current in order to unambiguously separate the spin Seebeck and spin Hall contributions to the observed bias dependence of MR.
- Measurements of the angular dependence of MR as a function of the Co layer thickness in the nano-contact devices are currently under way.
- The UNM group initiated theoretical work for a fully self-consistent calculation of the transport properties of Nb/Co/Cu/Co/Nb Josephson junctions. These Josephson junction devices are being fabricated at UCI.

References

1. Evan Moen and Oriol T. Valls, Transport in ferromagnet/superconductor spin valves, Phys. Rev. B 054503 (2017).
2. C. Safranski, I. Barsukov, H. K. Lee, T. Schneider, A. Jara, A. Smith, H. Chang, K. Lenz, J. Lindner, Y. Tserkovnyak, M. Wu, and I. N. Krivorotov, Spin caloritronic nano-oscillator, Nat. Commun. **8**, 117 (2017).

Publications

1. Evan Moen and Oriol T. Valls, Transport in ferromagnet/superconductor spin valves, Phys. Rev. B 054503 (2017).
2. Klaus Halterman, Oriol T. Valls, and Chien-Te Wu, Charge and spin currents in ferromagnetic Josephson junctions, Phys. Rev. B **92**, 174516 (2015).
3. Evan Moen and Oriol T. Valls, Transport in ferromagnet/superconductor spin valves, Phys. Rev. B 054503 (2017).
4. C. Safranski, I. Barsukov, H. K. Lee, T. Schneider, A. Jara, A. Smith, H. Chang, K. Lenz, J. Lindner, Y. Tserkovnyak, M. Wu, and I. N. Krivorotov, Spin caloritronic nano-oscillator, Nat. Commun. **8**, 117 (2017).
5. B. Ramaswamy, J. M. Algarin, I. N. Weinberg, Y.-J. Chen, I. N. Krivorotov, J. A. Katine, B. Shapiro, E. Waks, Wireless current detection by near field induction from a spin transfer torque nano-oscillator, Appl. Phys. Lett. **108**, 242403 (2016).
6. A. A. Jara, I. Barsukov, B. Youngblood, Yu-Jin Chen, J. Read, Hua Chen, P. Braganca, and I. N. Krivorotov, Highly textured IrMn₃(111) thin films grown by magnetron sputtering, IEEE Magn. Lett. **7**, 3104805 (2016).
7. H. K. Lee, I. Barsukov, A. G. Swartz, B. Kim, L. Yang, H. Y. Hwang, and I. N. Krivorotov, Magnetic anisotropy, damping and interfacial spin transport in Pt/LSMO/STO(001) thin films, AIP Advances **6**, 055212 (2016).
8. F. Hellman *et al.*, Interface-Induced Phenomena in Magnetism, Rev. Mod. Phys. **89**, 025006 (2017).

Superconductivity & Magnetism

W. –K. Kwok; Co-PIs: U. Welp, A. E. Koshelev, V. Vlasko-Vlasov, Z. L. Xiao, Y. L. Wang
Mailing Address: Materials Science Division, Argonne National Laboratory, 9700 S. Cass Ave., Argonne IL 60439

Program Scope

This program explores novel physical phenomena associated with superconductivity and its interplay with magnetism, determines the origins of these phenomena and explores innovative applications for superconductivity. Our current goal is to discover and control novel physical phenomena in superconductivity and vortex matter that can emerge through *tailored heterogeneity* induced by particle irradiation, magnetic texture and thermal hotspots. Presently, we are focused on investigating (i) modified nodal structures of candidate topological superconductors via irradiation (ii) vortex pinning behavior via heterogeneous magnetic textures in hybrid ferromagnetic/superconducting structures and (iii) enhancement of THz radiation output in high-temperature superconducting meso-crystals via controlled spatial thermal heterogeneity. We maintain leading programs in experiment and theory, with each deriving strong benefit from close mutual cooperation. Below, we highlight our recent work on creating a novel reconfigurable and rewritable artificial magnetic charge ice structure and its potential for manipulating superconducting flux quanta.

Recent Progress

Artificial spin ice systems are used to explore geometrically frustrated systems and have potential applications in data storage, memory, and logic devices [1]. Experimental realization and manipulation of *long-range order* for the various, almost degenerate spin ice configurations (i.e. ‘ice-rule’ of pairs of opposing spins pointing in and out at the vertex) are key challenges in current artificial spin ice research. Extensive experiments have been conducted using various thermal and magnetization approaches to obtain ordered states of the artificial *square* spin ice structure [2-4]. However, long-range ordering could only be realized for the diagonally polarized Type II (two neighboring spins pointing in and two out) magnetic state through magnetization [5, 6]. For the nominal Type I ground state (two pairs of opposing spins pointing in and out), sizable domains and crystallites were obtained only in samples heated above their Curie temperatures [2]. We solved the key issue of obtaining long-range order of the Type I

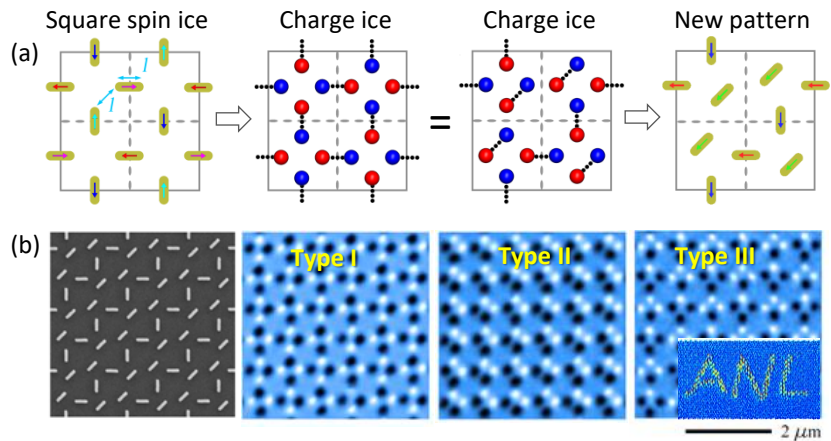


Fig. 1 (a) Square spin/charge ice structure consisting of magnetic nanobars (left) mapped to a new pattern which preserves the dumbbell magnetic charge ice structure – red (+) and blue (-) charges (right). (b) Scanning electron microscopy (SEM) image (left) of patterned nanomagnets (300 nm * 80 nm * 25 nm) and magnetic force microscopy (MFM) images (right) of Type I, II and III magnetic charge configurations obtained with an in-plane magnetic field at various orientations. Inset demonstrates the local write/read/erase multi-functionality with an MFM.

ground state through a novel approach by decoupling the magnetic charge pattern from the spin-ice pattern to produce an artificial *magnetic charge ice* with *reconfigurable long-range ordering* of eight different configurations including the Type III (three spins in/out and one out/in) state [7]. Figure 1a shows the mapping of a typical square spin ice structure consisting of magnetic nanobars onto a new configuration that preserves the *magnetic charge* structure of the square spin ice. The new configuration of nanobars and the corresponding magnetic force microscopy (MFM) images of the Type I, II and III states are shown in Fig. 1b. Applying an in-plane magnetic field along different directions converts the entire sample from one magnetic state to another. Furthermore, an MFM tip can manipulate the local charge states to achieve write/read/erase multi-functionality (inset Fig. 1b). This globally reconfigurable and locally rewritable magnetic charge ice provides a new platform to explore phase transitions and defect formation, as well as spin and magnetic charge dynamics.

In a follow-on study, we deposited our magnetic charge-ice structure onto a MoGe superconducting film to explore the mutual interaction between various spin-ice configurations and superconducting flux quanta as shown in Fig. 2a. The reconfigurable magnetic charge ice structures provide ice-like pinning potentials [8, 9] to create novel vortex lattices and to control their dynamics. Figure 2b highlights the critical current peaks/kinks associated with the each of the in-situ controlled magnetic charge ice configurations. The corresponding flux quanta pattern derived from molecular dynamics simulations is shown in Fig. 2c. Furthermore, the built-in asymmetric nature of the Type II and Type III magnetic charge ice configurations, could lead to vortex ratchet motion where an AC current induced driving force can rectify flux quanta movement along a fixed direction. By in-situ tuning of the magnetic charge configurations, we can expect a switchable and reversible rectification effect. Geometric frustration of flux quanta can also be designed into the magnetic charge configuration (Fig. 2c), thus providing an intriguing ferromagnetic/superconducting hybrid system to investigate the dynamic process of geometric frustration since flux quanta can be easily driven by externally applied currents. The dual ability to switch magnetic charge configurations and to control the flux quanta density may allow in-situ control of geometric frustration.

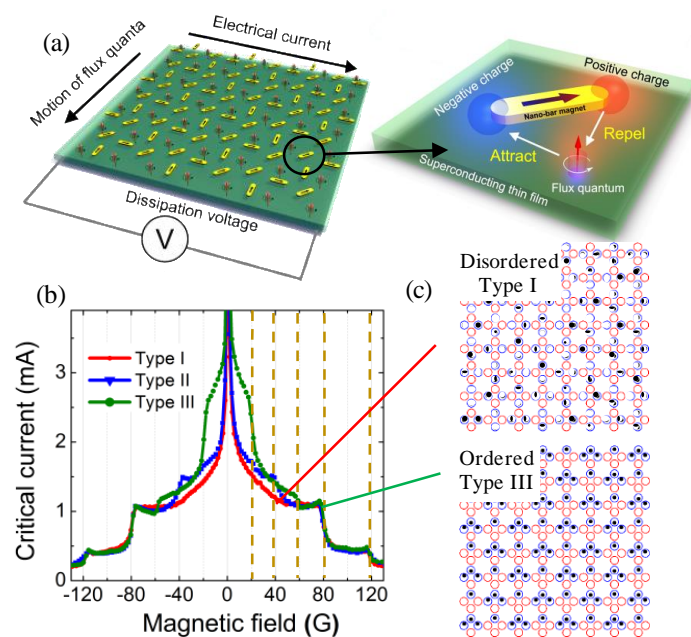


Fig. 2 (a) Hybrid structure of an array of nanoscale bar magnets of an artificial spin ice on top of a MoGe superconducting thin film. (b) Magnetic field dependent superconducting critical currents under three magnetic charge-ice configurations (Type I, II and III). Sharp features arise in the critical current at simple fractions and multiples of the matching field as indicated by the dashed lines. The matching field, 40 G, corresponds to one vortex per magnetic plaquette (c) Simulated flux quantum distributions under Type I and Type III magnetic charge ice configurations at 1 and 2 times the matching field, respectively.

Future Plans

We plan to extend the above studies to BSCCO and YBCO cuprate high-temperature superconductors to probe the ubiquitous vortex liquid state. We expect the creation of various ordered ‘vortex-structures’ in the liquid state with different viscosity that could arrest vortex flow in the liquid. These emergent vortex-liquid structures with tailored viscosities may lead to new functionalities such as mitigating vortex flow in the event of a magnet quench in high-temperature superconductors. Finally, such reconfigurable magnetic textured structures could be mapped to other electric/magnetic particle and quasiparticle systems, such as magnetic skyrmions, electrons in two-dimensional electron gas, as well as magnetic colloidal particles. This research could stimulate future investigation of reconfigurable properties in *smart, active materials*.

References

- [1] C. Nisoli, R. Moessner, P. Schiffer, *Artificial spin ice: Designing and imaging magnetic frustration*, Rev. Mod. Phys. **85**, 1473 (2013)
- [2] S. Zhang, I. Gilbert, C. Nisoli, G. W. Chern, M. J. Erickson, L. O’Brien, C. Leighton, P. E. Lammert, V. H. Crespi, P. Schiffer, *Crystallites of magnetic charges in artificial spin ice*, Nature **500**, 553 (2013)
- [3] A. Farhan, P. M. Derlet, A. Kleibert, A. Balan, R. V. Chopdekar, M. Wyss, J. Perron, A. Scholl, F. Nolting, L. J. Heyderman, *Direct observation of thermal relaxation in artificial spin ice*, Phys. Rev. Lett. **111**, 057204 (2013).
- [4] X. Ke, J. Li, C. Nisoli, P. E. Lammert, W. McConville, R. F. Wang, V. H. Crespi, P. Schiffer, *Energy minimization and ac demagnetization in a nanomagnet array*, Phys. Rev. Lett. **101**, 037205 (2008).
- [5] Z. Budrikis, J. P. Morgan, J. Akerman, A. Stein, P. Politi, S. Langridge, C. H. Marrows, R. L. Stamps, *Disorder strength and field-driven ground state domain formation in artificial spin ice: Experiment, simulation, and theory*, Phys. Rev. Lett. **109**, 037203 (2012).
- [6] A. Remhof, A. Schumann, A. Westphalen, H. Zabel, N. Mikuszeit, E. Y. Vedmedenko, T. Last, U. Kunze, *Magnetostatic interactions on a square lattice*, Phys. Rev. **B 77**, 134409 (2008).
- [7] Y. L. Wang, Z. L. Xiao, A. Snezhko, J. Xu, L. E. Ocola, R. Divan, J. E. Pearson, G. W. Crabtree, W. K. Kwok, *Rewritable artificial magnetic charge ice*, Science **352**, 962 (2016)
- [8] A. Libal, C. J. Olson Reichhardt, and C. Reichhardt, *Creating Artificial Ice States Using Vortices in Nanostructured Superconductors*, Phys. Rev. Lett. **102**, 237004 (2009); S. Zhang, I. Gilbert, C. Nisoli, Gia-Wei Chern, M. J. Erickson, L. O’Brien, C. Leighton, P. E. Lammert, V. H. Crespi, P. Schiffer, *Crystallites of magnetic charges in artificial spin ice*, Nature **500**, 553 (2013).
- [9] M. L. Latimer, G. R. Berdiyrov, Z. L. Xiao, F. M. Peeters, W. K. Kwok, *Realization of Artificial Ice Systems for Magnetic Vortices in a Superconducting MoGe Thin Film with Patterned Nanostructures*, Phys. Rev. Lett. **111**, 067001 (2013).

Publications (2016-2017)

1. *Enhancing superconducting critical current by randomness*, Y. L. Wang, L. R. Thoutam, Z. L. Xiao, B. Shen, J. E. Pearson, R. Divan, L. E. Ocola, G. W. Crabtree, W. –K. Kwok, Physical Review **B 93**(4), 045111 (2016)
2. *Microscopic parameters from high-resolution specific heat measurements on superoptimally*

- substituted BaFe₂(As_{1-x}P_x)₂ single crystals*, Z. Diao, D. Campanini, L. Fang, W. -K. Kwok, U. Welp, A. Rydh, *Physical Review* **B 93**(1), 014509 (2016)
3. *Charge-screening role of c-axis atomic displacements in YBa₂Cu₃O_{6+x} and related superconductors*, E. S. Bozin, A. Huq, B. Shen, H. Claus, W. -K. Kwok, J. M. Tranquada *Physical Review* **B 93**(5), 054523 (2016)
 4. *Effect of proton irradiation on superconductivity in optimally doped BaFe₂(As_{1-x}P_x)₂ single crystals*, M. P. Smylie, M. Leroux, V. Mishra, L. Fang, K. M. Taddei, O. Chmaissem, H. Claus, A. Kayani, A. Snezhko, U. Welp, W. -K. Kwok, *Physical Review* **B 93**(11), 115119 (2016)
 5. *Feasibility and electromagnetic analysis of a FEBCO superconducting undulator*, Ibrahim Kesgin, Matthew Kasa, Charles Doose, Yury Ivanyushenkov, Yifei Zhang, Alan Knoll, Paul Brownsey, Drew Hazelton and Ulrich Welp, *Superconductor Science & Technology* **29**(5), 055001 (2016)
 6. *Rewritable Artificial Magnetic Charge Ice*, Y. L. Wang, Z. L. Xiao, A. Snezhko, J. Xu, L. E. Ocola, R. Divan, J. E. Pearson, G. W. Crabtree and W. -K. Kwok, *Science* **352**, 962 (2016)
 7. *Pinning, Flux Diodes and Ratchets for Vortices Interacting with Conformal Pinning Arrays* C. J. Olson Reichhardt, Y. L. Wang, Z. L. Xiao, W. -K. Kwok, D. Ray, C. Reichhardt, B. Janko, *Physica C* **533**, 148 (2017)
 8. *Vortex cutting in superconductors*, A. Glatz, V.K. Vlasko-Vlasov, W.K. Kwok, G. W. Crabtree, *Physical Review* **B 94**, 064505 (2016)
 9. *Large spin-orbit coupling and helical spin textures in 2D heterostructure [Pb₂BiS₃][AuTe₂]* L. Fang, J. Im, W. DeGottardi, Y. Jia, A. Glatz, K. A. Matveev, W. K. Kwok, G. W. Crabtree and M. G. Kanatzidis, *Scientific Reports* **6**, 35313 (2016)
 10. *Crossing fields in thin films of isotropic superconductors*, V. K. Vlasko-Vlasov, F. Colauto, A. A. Buzdin, D. Carmo, A. M. H. Andrade, A. A. M. Oliveira, W. A. Ortiz, D. Rosenmann, and W. -K. Kwok, *Physical Review* **B 94**(18), 184502 (2016)
 11. *Triode for Magnetic Flux Quanta*, V. K. Vlasko-Vlasov, F. Colauto, T. Benseman, D. Rosenmann, W. -K. Kwok, *Scientific Reports* **6**, 36847 (2016)
 12. *Evidence of nodes in the order parameter of the superconducting doped topological insulator Nb_xBi₂Se₃ via penetration depth measurements*, M. P. Smylie, H. Claus, U. Welp, W.-K. Kwok, Y. Qiu, Y. S. Hor and A. Snezhko, *Physical Review* **B 94**(18), 180510 (2016)
 13. *Hybridization gap in the semiconducting compound SrIr₄In₂Ge₄*, Nicholas P. Calta, Jino Im, Lei Fang, Thomas C. Chasapis, Daniel E. Bugaris, Duck Young Chung, Wai-Kwong Kwok, Mercuri G. Kanatzidis, *Inorganic Chemistry* **55**, 12477 (2016)
 14. *Effect of hexagonal patterned arrays and defect geometry on the critical current of superconducting films*, A. Sadovskyy, Y. L. Wang, Z. -L. Xiao, W. -K. Kwok and A. Glatz *Physical Review* **B 95**, 075303 (2017)
 15. *Magnetic gates and guides for superconducting vortices*, V. K. Vlasko-Vlasov, F. Colauto, A. I. Buzdin, D. Rosenmann, T. Benseman, and W. -K. Kwok, *Phys. Rev.* **B 95**, 144504 (2017)
 16. *High-resolution Thermal Micro-imaging Using Europium Chelate Luminescent Coatings* Timothy M. Benseman, Yang Hao, Vitalii K. Vlasko-Vlasov, U. Welp, A. E. Koshelev, W. K. Kwok, R. Divan, C. Kiser, C. Watanabe, K. Kadowaki, JOVE-Journal of Visualized Experiments Issue: **122** Article Number: e53948 (2017)
 17. *Manipulating Abrikosov vortices with soft magnetic stripes*, V. Vlasko-Vlasov, F. Colauto, A. I. Buzdin, D. Rosenmann, T. Benseman, W.-K. Kwok, *Phys. Rev.* **B 95**, 174514 (2017)

Non-Coulombic frictional drag currents in coupled LaAlO₃/SrTiO₃ nanowires

Jeremy Levy^{1,2} and Patrick Irvin^{1,2}

**¹Department of Physics and Astronomy, University of Pittsburgh, Pittsburgh, Pennsylvania
15260, USA**

²Pittsburgh Quantum Institute, Pittsburgh, Pennsylvania 15260, USA

Program Scope

This research program focuses on the investigation of strong electron correlations in quasi-one-dimensional oxide nanostructures. The archetypical system consisting of heterostructures formed from an ultrathin layer of LaAlO₃ and TiO₂-terminated SrTiO₃ offers a unique laboratory for probing strong correlations due to intrinsic richness of the physical system and its ability to be modulated at extreme nanoscale dimensions. Under suitable conditions, SrTiO₃ is known to exhibit a variety of important properties associated with strong electronic correlations, especially superconductivity and magnetism. Understanding the nature of these electronic correlations at fundamental scales, and in reduced spatial dimensions, will provide the scientific basis for new energy technologies, information technologies, and materials.

The research is motivated by discoveries and technical advances in Levy's lab, specifically, (1) pioneering work to create conductive nanostructures to be created in LaAlO₃/SrTiO₃ heterointerfaces with 2 nm spatial resolution, (2) the discovery of a novel correlated electronic phases in which electrons pair without forming a superconductor, and (3) the demonstrated ability to form high-quality electron waveguides capable of achieving ballistic electron transport over micrometer-scales.

Central to the motivation of this work is the goal of developing a full microscopic understanding of electron pairing mechanism in LaAlO₃/SrTiO₃ nanostructures. Understanding the "glue" that leads to pairing and superconductivity in a doped semiconductor will help to form a scientific basis for the correlated oxide nanoelectronics platform being developed. We are also probing fundamentally new quasiparticle excitations using an unprecedented combination of experimental methodologies. Experiments already underway with artificially defined short-period superlattices (5 nm period) to demonstrate the feasibility of this approach. We are also utilizing a milli-Kelvin scanning probe microscope that can directly perturb and probe electron

nanostructures. Thematically, the proposed research falls under a grander vision to combine some of the most important and interesting challenges in the physics of semiconductor nanostructures and correlated electronic materials.

Recent Progress

Current progress has focused on observations of frictional drag between two conducting $\text{LaAlO}_3/\text{SrTiO}_3$ nanowires that are electrically isolated from one another but in close proximity. When a current is sourced through one system (the “drive” system), it may induce a voltage in the other (the “drag” system). This effect is most generally known as frictional drag or Coulomb drag and was first proposed by Pogrebinskii [1] as a method to probe correlations among the charge carriers of the system. Drag signals performed by other groups in semiconductor or graphene materials have been dominated by Coulomb interactions; at large separations, non-Coulombic interactions become apparent [2,3].

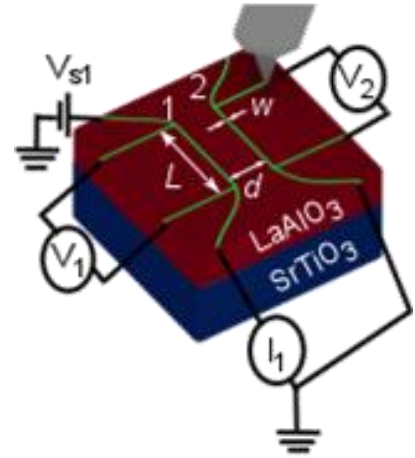


Figure 1. Frictional drag device and experimental setup.

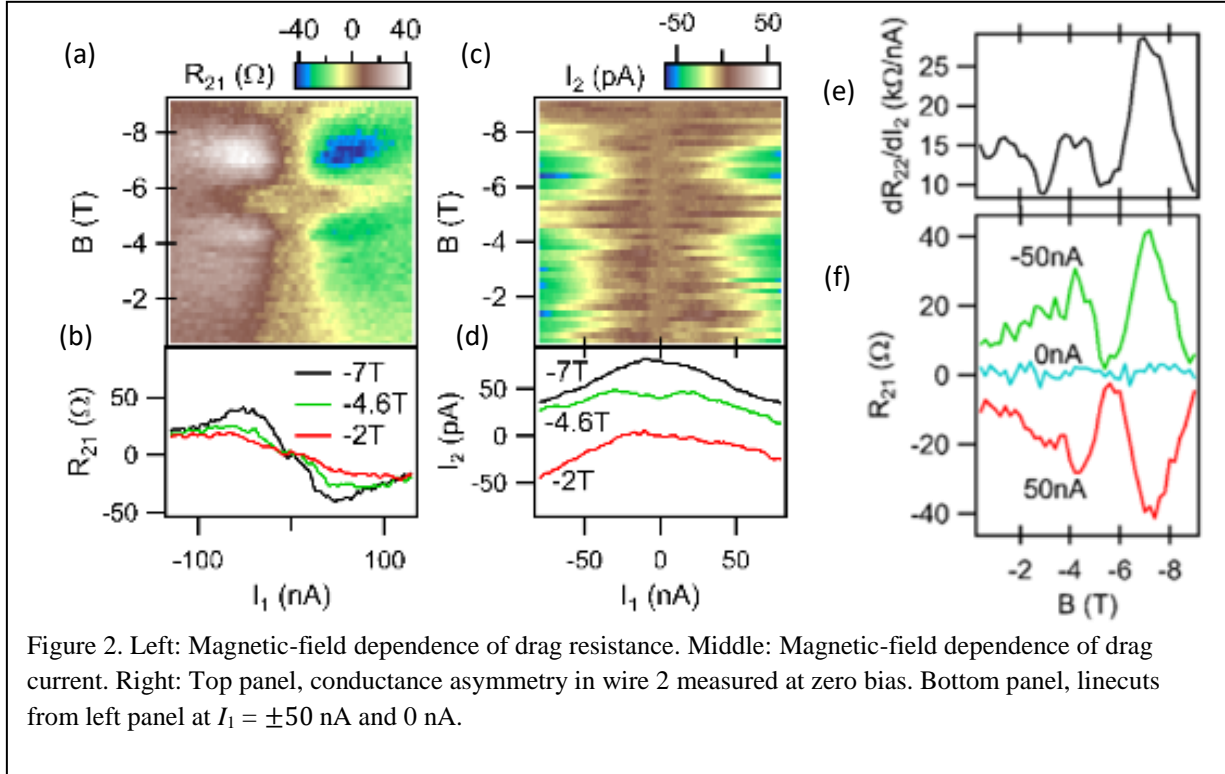
We have performed frictional drag measurements in coupled $\text{LaAlO}_3/\text{SrTiO}_3$ nanowires. Devices are fabricated by *c*-AFM lithography on $\text{LaAlO}_3/\text{SrTiO}_3$ heterointerfaces with 3.4 u.c. of LaAlO_3 deposited on a SrTiO_3 substrate by pulsed laser deposition. The general setup is shown in Figure 1. Key parameters are the nanowire length L , the nanowire separation d and the nanowire width w . Frictional drag phenomena are investigated in coupled $\text{LaAlO}_3/\text{SrTiO}_3$ nanowires by sourcing current in one wire and measured the induced voltage in the other wire. Alternatively, current can be sourced in one wire, while drag current is measured in the other wire. Most of the interesting behavior is observed at temperatures below $T \sim 500$ mK, where ballistic transport within conductive nanowires have been reported by us [4]. The frictional drag system (Fig. 1) consists of two parallel nanowires of width $w \sim 10$ nm, length $L = 400$ nm to 1.5 μm , and separation $d = 40$ nm to 1.5 μm . One nanowire has four terminals (wire 2), allowing for 4-terminal measurements, while the other has three terminals (wire 1).

Figure 2 shows typical behavior for such an experiment, which has been carried out on more than a dozen such structures. The drag resistance $R_{21} = dV_2/dI_1$ (Fig. 2(a,b)), measured as a function of magnetic field B and drive current I_1 , is antisymmetric with respect to the sourcing current. The antisymmetry in drag resistance implies a unidirectional (symmetric) drag current and is confirmed by the direct current drag measurement (Fig. 2(c,d)). The observed unidirectional current drag is ascribed to slight asymmetries within nanowires.

The four-terminal resistance $R_{22}(B)$ yields information that is strongly correlated with the observed asymmetry. Nonlinearities in nanowire resistance at zero-bias “trans-resistance”

dR_{22}/dI_2 (Fig. 2(e)) provide a useful quantitative measure of the observed asymmetry, which is highly correlated with the drag resistance. The strong antisymmetry of R_{drag} is highlighted by taking line cuts of R_{drag} at $I_{drive} = 0$ nA, ± 50 nA (Fig. 2(f)).

These results provide new insights into non-Coulombic electron-electron interaction effects that must be accounted for in any full description of electron transport at oxide interfaces.



By comparing the maximum R_{drag} for devices with various L and d (see Table I and also Figure 3), we see that the drag resistance does not decrease significantly for a large range of separations d . If R_{drag} arose primarily due to Coulomb interactions between the charge carriers, we would expect, due to the rapidly decreasing interaction between the nanowires, that the signal would decay quickly as the separation is increased. We therefore conclude that the dominant interactions between the nanowires are non-Coulombic in nature.

While the origin of this non-Coulombic interaction is not at all understood, its long-range nature may prove useful in energy harvesting applications [35, 36] in which noise in the drive wire is rectified in the drag wire [37]. The long-range nature of the interaction allows the noise source to be placed far from the energy harvesting wire. Apart from applications, this strong interaction is worth understanding as it may be related to the strong electron-electron attraction that leads to pairing and superconductivity in SrTiO₃-based heterointerfaces.

TABLE I. The length L , nanowire separation d , 2- and 4/3-terminal, and drag resistances for several devices. The device shown in Fig. 2 is marked in boldface.

Device	L	d	$R_{2T,1}$	$R_{2T,2}$	R_{11}	R_{22}	$R_{\text{Drag},1}$	$R_{\text{Drag},2}$
1A	400 nm	40 nm	58-72 k Ω	42-48 k Ω	32-43.5 k Ω	8.4-9.2 k Ω	20 Ω	60 Ω
1B	400 nm	40 nm	22-30.8 k Ω	25.5-33.5 k Ω	8.6-12.5 k Ω	14-18.3 k Ω	14.1 Ω	4 Ω
1D	1 μm	300 nm	36.5-46.5 k Ω	25-45.8 k Ω	NA	8.7-18 k Ω	50.6 Ω	23.2 Ω
1E	1 μm	450 nm	40-108 k Ω	29-34 k Ω	NA	6.4-7.5 k Ω	200 Ω	38.5 Ω
1F	1.5 μm	550 nm	27-35 k Ω	29-63.4 k Ω	NA	7.8-11.8 k Ω	15 Ω	52 Ω
2A	1.5 μm	550 nm	33-76.6 k Ω	22-29 k Ω	NA	NA	27 Ω	26 Ω
2B	1.5 μm	550 nm	23-36.2 kΩ	22-51 kΩ	11-16 kΩ	3.7-5.5 kΩ	19 Ω	41 Ω
2C	1.5 μm	1.5 μm	16.5-26.5 k Ω	22-37 k Ω	10.2-14.8 k Ω	2.7-4.1 k Ω	10 Ω	8.5 Ω
3A	400 nm	200 nm	50-127 k Ω	26.6-37 k Ω	29-98 k Ω	5.2-6.7 k Ω	136 Ω	86 Ω

Future Plans

In future investigations, frictional drag experiments can be repeated with nanowires that exhibit quantized ballistic transport [4]. We are also developing a phenomenological model (not discussed here), and investigating the superconducting regime, which is qualitatively distinct. In addition, the dimensionality of one or both conductors can be varied easily (e.g., 0D and 2D), to study electron correlations under different conditions.

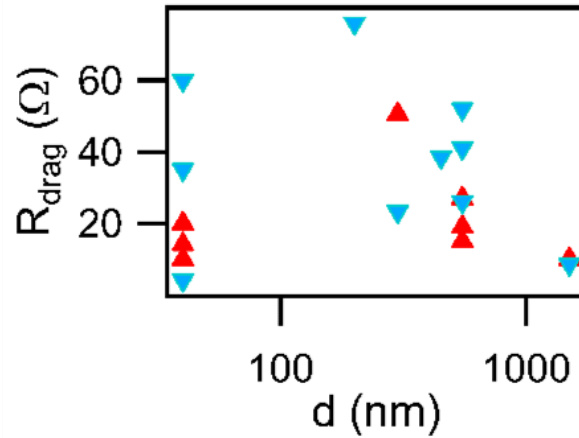


Figure 3. Separation dependence of drag resistance measured from wire 1 (red) and wire 2 (blue.) for devices listed in Table 1.

References

- [1] M. B. Pogrebinskii, Sov. Phys.-Semicond. 11, 372 (1977).
- [2] T. J. Gramila, J. P. Eisenstein, A. H. MacDonald, L. N. Pfeiffer, and K. W. West, Phys. Rev. B 47, 12957 (1993).
- [3] H. C. Tso, P. Vasilopoulos, and F. M. Peeters, Phys. Rev. Lett. 68, 2516 (1992).
- [4] A. Annadi et al., arXiv: 1611.05127

Publications

- [1] Y. Tang, A. Tylan-Tyler, H. Lee, J.-W. Lee, M. Tomczyk, M. Huang, C.-B. Eom, P. Irvin, J. Levy, arXiv: 1707.01171

Spin-Polarized Current Injection Induced Magnetic Reconstruction at Oxide Interface

F. Fang¹, Y. W. Yin², Qi Li² & G. Lüpke¹

¹Department of Applied Science, College of William & Mary, Williamsburg, Virginia 23187, USA.

²Department of Physics, Pennsylvania State University, University Park, Pennsylvania 16802, USA.

Program Scope

Electric-field control of magnetization has received intense investigations in the past decade for fast, low-power magnetic recording, sensors and spintronic device applications. This three-year research grant (DE-FG02-04ER46127) focuses on the study of a variety of magnetoelectric (ME) coupling effects and coherent spin dynamics in a broad range of complex multiferroic (MF) oxide heterostructures using interface-specific and time-resolved nonlinear-optical techniques. A major innovation in this program is the study of ME coupling effects in ferromagnetic (FM) manganite/ferroelectric (FE) oxide thin-film Schottky heterojunctions, including electron-doped BaTiO₃ and BiFeO₃. The coexistence of the FE phase and conductivity is interesting because such a conducting bistable material introduces new functionalities. Building on key advances of the previous award period, our program concentrates on two major themes: (i) to determine the interfacial ME coupling mechanism and its correlation with charge transfer, orbital states and strain states induced by the substrate or film thickness using the interface-specific magnetization-induced second-harmonic generation (MSHG) technique, and (ii) to investigate its effect on the coherent spin precession in these strongly correlated systems as a new path for fast magnetic switching utilizing the time-resolved magneto-optical Kerr effect (TRMOKE) technique. The goal of these studies is to elucidate the static and dynamic magnetic interactions and their correlations with the electronic structure and strain states at the valence and lattice mismatched interfaces, which can be artificially engineered. The science addresses issues of energy dissipation and the coupling between electronic and magnetic order in such advanced multifunctional materials, of fundamental importance to our understanding of solid-state properties and has numerous applications.

Recent Progress

Electrical manipulation of magnetism presents a promising way towards using the spin degree of freedom in very fast, low-power electronic devices. Though there has been tremendous

progress in electrical control of magnetic properties using ferromagnetic nanostructures, an opportunity of manipulating antiferromagnetic (AFM) states should offer another route for creating a broad range of new enabling technologies. Here we selectively probe the interface magnetization of $\text{SrTiO}_3/\text{La}_{0.5}\text{Ca}_{0.5}\text{MnO}_3/\text{La}_{0.7}\text{Sr}_{0.3}\text{MnO}_3$ (STO/LCMO/LSMO) heterojunctions and discover a new spin-polarized current injection induced interface magnetoelectric effect [1]. The accumulation of majority spins at the interface causes a sudden, reversible transition of the spin alignment of interfacial Mn ions from AFM to FM exchange-coupled, while the injection of minority electron spins alters the interface magnetization from C-type to A-type AFM state. In contrast, the bulk magnetization remains unchanged. We attribute the current-induced interface ME effect to modulations of the strong double-exchange interaction between conducting electron spins and local magnetic moments. The effect is robust and may serve as a viable route for electronic and spintronic applications.

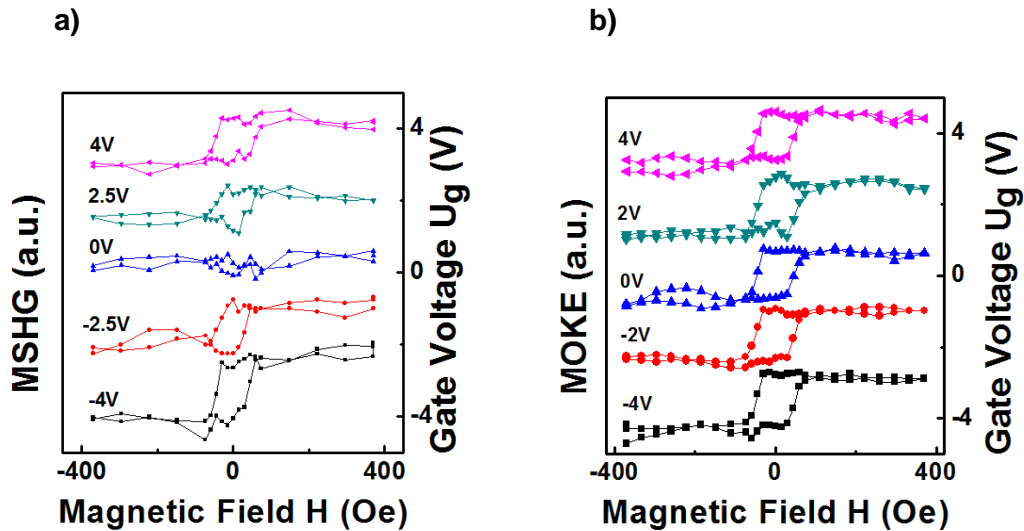


Figure 1: Magnetic hysteresis loops from STO/LCMO/LSMO heterostructure, (a) MSHG and (b) MOKE measurements as a function of gate voltage U_g . The interfacial LSMO layer exhibits magnetic transitions, while the bulk LSMO maintains the FM state. All of the experiments are performed at 78 K.

The MSHG technique is well suited for probing the interfacial magnetic state where the inversion symmetry is broken. The characteristic length scale for our MSHG data is the length of one unit cell, because second-harmonic generation is forbidden (in dipole approximation) in centrosymmetric media. For comparison, magneto-optical Kerr effect (MOKE) measurements are carried out to detect the LSMO bulk magnetic properties. All of the experiments are performed at 78 K, which is well below the Curie temperature of LSMO. Figure 1a displays voltage-dependent MSHG loops for the STO/LCMO/LSMO heterostructure varying from -4 V

to +4 V. MSHG loops are observed at negative voltage but disappear near zero voltage. The loops reappear at +2.5 V. In contrast, MOKE loops are always observed over the whole voltage range (Fig. 1b). Since coercive fields of MSHG and MOKE loops are very similar, we attribute this phenomenon to a new interfacial ME effect in the LSMO layer. The magnetic properties of the ultrathin (1 nm) LCMO interlayer are not observed or distinguished, as it initially is AFM at zero gate voltage and can be tuned to other states by different carrier injection (a special kind of doping). The results are important for the transport properties of magnetic tunneling junctions, because an interfacial magnetic transition may notably change the spin polarization of the tunneling current and thus be decisive for tunneling magnetoresistance.

Future Plans

Next, we are planning to investigate the manipulation of charge ordering in Fe_3O_4 by field cooling. The conductivity of magnetite drops by two orders of magnitude below the Verwey temperature, known as the Verwey transition, due to the formation of charge ordering. However, a thorough explanation of the driving mechanism of the Verwey transition in magnetite has not been provided yet. Hence, the detection and the associated manipulation of charge ordering in Fe_3O_4 are significant in clarifying the Verwey transition. The presence of ordered pattern leads to symmetry breaking of the crystalline structure in magnetite. Therefore, we will perform second-harmonic generation (SHG) measurement on single-crystalline Fe_3O_4 to directly reveal the effect correlated with charge ordering. The sample is field-cooled with the assistance of an ultrafast laser, which controls the fractional area of the two charge ordering patterns in single crystalline magnetite. The results of SHG measurements may help verify the existence of the charge ordering state with single orientation that is highly desirable for the exploration of the origin of the Verwey transition.

We will also investigate the magnetization dynamics in the exchange-coupled system $\text{Co}_2\text{FeAl}/(\text{Ga,Mn})\text{As}$. $(\text{Ga,Mn})\text{As}$ has been studied extensively in the past decades due to its excellent performance in semiconductor spintronic devices. Co_2FeAl is a desirable spintronic material because of its high spin polarization, low Gilbert damping constant, and high Curie temperature. In combination, $\text{Co}_2\text{FeAl}/(\text{Ga,Mn})\text{As}$ bilayers induce exchange-coupling modulation across the heterostructure interface which can drive the ferromagnetic magnetization. This idea might have great potential in magnetic recording and spintronic devices. We are now looking into magnetic dynamic properties of $\text{Co}_2\text{FeAl}/(\text{Ga,Mn})\text{As}$ bilayer heterostructure with time-resolved magneto-optic Kerr effect measurements. When photo-excited, the interface spins in $(\text{Ga,Mn})\text{As}$ are strongly modulated and thus produce the magnetic torque on the Co_2FeAl layer, driving its magnetization precession. By modeling the data with Landau-Lifshitz-Gilbert equation, the magnetic parameters such as anisotropy fields, exchange-coupling field, and the Gilbert damping constant will be obtained from the measured field dependence and

temperature dependence of the magnetization precession frequency. Our results will help promote the development of low-energy consumption magnetic device concepts.

References

1. F. Fang, Y. W. Yin, Qi Li, and G. Lüpke, Spin-polarized current injection induced magnetic reconstruction at oxide interface, *Scientific Reports* 6:40048, DOI: 10.1038/srep40048 (2017).

Publications

1. F. Fang, Y. W. Yin, Qi Li, and G. Lüpke, Spin-polarized current injection induced magnetic reconstruction at oxide interface, *Scientific Reports* 6:40048, DOI: 10.1038/srep40048 (2017).
2. F. Fang, H. Zhai, X. Ma, Y. W. Yin, Qi Li, and G. Lüpke, Current-driven interface magnetic transition in complex oxide heterostructure, *J. Vac. Sci. Technol. B* 35, 04F101 (2017); doi: 10.1116/1.4976587.
3. Wei Zheng, Xiao Liu, Gunter Lüpke, Aubrey T. Hanbicki, and Berend T. Jonker, The Road Towards Nonlinear Magneto-Plasmonics, *Proc. SPIE* 9931, Spintronics IX, 99312W (November 4, 2016); doi:10.1117/12.2238941.
4. F. Fang, H. Zhai, X. Ma, Y. W. Yin, Qi Li, and G. Lüpke, Interface magnetization transition via minority spin injection, *Appl. Phys. Lett.* 109, 232903 (2016), doi: 10.1063/1.4972035.
5. Wei Zheng, Xiao Liu, Aubrey T. Hanbicki, Berend T. Jonker, and Gunter Lüpke, Nonlinear Magneto-Plasmonics, *Optical Materials Express* 5(11), 2597 (2015).
6. X. Ma, F. Fang, Q. Li, J. Zhu, Y. Yang, Y. Z. Wu, H. B. Zhao, and G. Lüpke, Ultrafast spin exchange-coupling torque via photo-excited charge-transfer processes, *Nat. Commun.* 2015 Oct 28;6:8800. doi: 10.1038/ncomms9800.
7. X. Ma, L. Ma, P. He, H. B. Zhao, S. M. Zhou, and G. Lüpke, Role of Anti-Site Disorder on Intrinsic Gilbert Damping in $L1_0$ FePt films, *Phys. Rev. B*, 91, 014438 (2015).

Observation of spin and charge stripes in $\text{La}_{2-x-y}\text{Eu}_y\text{Sr}_x\text{CuO}_4$

G. J. MacDougall, P. Abbamonte, S. L. Cooper, E. Fradkin, and D. Van Harlingen

Department of Physics, University of Illinois at Urbana-Champaign

Program Scope

The research program at Illinois seeks to establish the generality and full implications of phase-sensitive coupling between charge and superconducting order parameters in materials exhibiting charge inhomogeneity. Specifically, we are seeking to first confirm experimentally a number of unique phenomena predicted by Berg *et al* [1,2] for the cuprate material $\text{La}_{2-x}\text{Ba}_x\text{CuO}_4$ (LBCO), commonly believed to contain such coupling [3,4], and then extend the work to include several other superconducting families. As a part of this goal, we are identifying material families with co-existing charge and superconducting orders, and attempting to understand the details of the coupling between the order parameters. In the long term, we hope these are the first steps in identifying symmetry-based unifying principles, which might provide the foundation for a universal phenomenological theory, appropriate to describe to multiple families containing unconventional superconductivity.

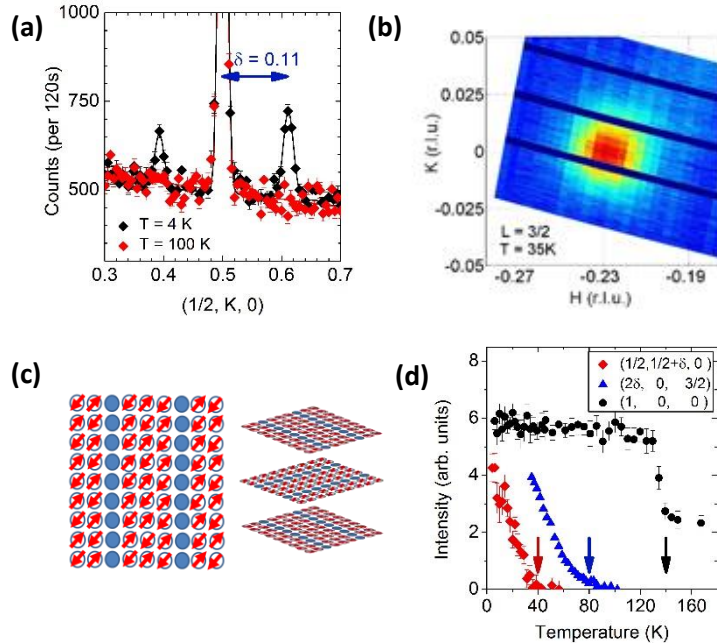
To address these questions in a comprehensive way, our team contains in a complement of experimental techniques. This includes growth of relevant crystals (**MacDougall**) and films (**Van Harlingen**), and exploration with neutron scattering (**MacDougall**), Josephson interferometry (**Van Harlingen**) and Raman scattering (**Cooper**). Close collaboration between our group and **Peter Abbamonte** brings in expertise in x-ray scattering and momentum-resolved electron energy loss spectroscopy (M-EELS). Experimental results are being interpreted in the context of the theoretical framework of **Eduardo Fradkin**, and used by him to develop a more general theory.

Recent Progress

In the past year, our collaboration has perfected the float-zone growth of and performed a series of neutron and resonant x-ray scattering measurements on crystals of $\text{La}_{2-x-y}\text{Eu}_y\text{Sr}_x\text{CuO}_4$ (LESCO), which firmly establish the existence of both spin- and charge-stripe correlations in this cuprate family for the first time. Previously, confirmation of stripe order in LESCO has been confounded by the strong neutron absorption cross-section of natural-abundance europium, which makes neutron scattering experiments virtually impossible. To address this issue, we have grown several centimeter-sized single crystals via the float-zone technique, while enriching with the “neutron-friendly” isotope ^{153}Eu . In January, 2017, we performed the first detailed neutron measurements of magnetism in LESCO at a doping near $x=1/8$ using instruments at the High Flux Isotope Reactor at Oak Ridge National Laboratory (ORNL) to search for signs of spin-stripe order. Parallel resonant x-ray scattering experiments were performed on related crystals at the SLAC National Accelerator Laboratory to search for charge-stripe peaks.

Our scattering data establish for the first time the existence of incommensurate orders at low temperatures, in both spin and charge channels. Neutron scattering data from HFIR (Fig. 1a) reveal the emergence of resolution-limited ordering Bragg peaks at positions $(\frac{1}{2}, \frac{1}{2} \pm \delta, 0)$ and $(\frac{1}{2} \pm \delta, \frac{1}{2}, 0)$, with $\delta \approx 0.11$. X-ray scattering data (Fig. 1b) reveal the emergence of a peak at $(2\delta, 0, 3/2)$, with the same δ . Together, these peaks strongly imply the existence of quasi-1D stripe order running parallel to the Cu-O bond directions (Fig. 1c). The measured value for δ is approximately equal to the hole doping $x=0.115$, as determined from x-ray fluorescence measurements, consistent with the so-called “Yamada relation” observed in inelastic stripe correlation in $\text{La}_{2-x}\text{Sr}_x\text{CuO}_4$ [5].

The temperature dependence of the relevant Bragg peaks (Fig. 1d) gives $T_{\text{charge}}=80\text{K}$, consistent with previous measurements by Fink *et al.*[6], and $T_{\text{spin}}=40\text{K}$, much larger than estimates from earlier μSR measurements [7]. Both neutron and x-ray measurements also observe a known phase transition from high-temperature orthorhombic (HTO) to low-temperature tetragonal (LTT) structures [8], which can be seen in the temperature dependence of the $(1\ 0\ 0)$ Bragg peak and gives $T_{\text{LTT}}=140\text{K}$. The clean separation between charge, spin and LTT transitions makes LESCO distinct from prototypical stripe material, LBCO, where $T_{\text{charge}} \approx T_{\text{LTT}}$ and it is difficult to disentangle the effects of concomitant charge and structural phase transitions.



(a) Neutron and (b) resonant x-ray scattering data revealing the existence of spin and charge peaks, respectively, associated with stripe order in a LESCO crystal with $y=0.2$, $x=0.11$. (c) Sketch of the observed stripe state. (d) Plot of the temperature dependence of Bragg peaks associated with spin order (red), charge order (blue), and the LTT structural transition (black).

In addition to this unambiguous evidence for stripe order, recent magnetization measurements by our group suggest the existence of a quasi-2D superconducting condensate below $T_c=4\text{K}$ - a possible signature of layer-decoupling effects. Collectively, these data establish our internally-grown LESCO crystals as an ideal testbed for theories exploring the interaction between superconducting and stripe orders in the cuprates. Having an internal source of such materials provides our research program with a major competitive advantage as we expand upon our initial results and seek to develop a more complete understanding of the rich and interesting physics associated with intertwined order parameters in unconventional superconductors.

Future Plans

In light of recent developments, current work by our collaboration is seeking to experimentally verify predictions for phase-coherent coupling between superconductivity and stripe order in the LESCO, while simultaneously characterizing this family of materials away from the singular doping $x=1/8$. Specifically, we are pursuing the following sets of experiments:

- 1.) **Measuring current-phase relation (CPR) of junctions made with LESCO.** Work over the last two years by D. Van Harlingen has established the existence of spatially-modulated pair-density-wave (PDW) superconductivity resulting from phase-coherent coupling between charge and superconducting orders in LBCO. As we have now firmly established both stripe order and superconductivity in LESCO, we hope to establish this smoking-gun evidence for PDW order in a second cuprate material in the near future.
- 2.) **Verifying predicted Higgs modes for PDW states in LESCO near $x=1/8$.** In a recent publication, S. L. Cooper and E. Fradkin predicted the emergence of three Higgs-like amplitude modes in materials containing PDW order [A4]. Using the above crystals from G. MacDougall, Cooper is attempting to confirm the existence of these modes with Raman scattering. Crystals will also be provided to P. Abbamonte, to facilitate parallel searches with momentum-resolved EELS and resonant x-ray scattering.
- 3.) **Extending neutron and x-ray scattering of measurements of spin-stripe order away from $x=1/8$.** MacDougall group has recently been awarded neutron beam time from ORNL to follow-up on initial measurements of spin-stripe order in LESCO over a range of dopings. Data obtained by these measurements will be combined with x-ray measurements of P. Abbamonte and magnetization measurements at Illinois to flush out the full temperature-doping phase diagram from LESCO and further understand the complex interaction between spin/charge stripes and superconductivity.

References

- [1] E. Berg, E. Fradkin, and S. A. Kivelson, Theory of the striped superconductor, *Phys. Rev. B* **79**, 064515 (2009)
- [2] E. Berg, E. Fradkin, S. A. Kivelson and J. M. Tranquada, Striped superconductors: how spin, charge, and superconducting orders intertwine in the cuprates, *New Journal of Physics* **11**, 115004 (2009)
- [3] Q. Li, M. Hücker, G.D. Gu, A.M. Tsvelik, and J.M. Tranquada, Two-dimensional superconducting fluctuations in stripe-ordered $\text{La}_{1.875}\text{Ba}_{0.125}\text{CuO}_4$, *Physical Review Letters* **99**, 067001 (2007).
- [4] J.M. Tranquada, G.D. Gu, M. Hücker, Q. Jie, H.-J. Kang, R. Klingeler, Q. Li, N. Tristan, J.S. Wen, G.Y. Xu, Z.J. Xu, J. Zhou, and M.v. Zimmermann, Evidence for unusual superconducting

correlations coexisting with stripe order in $\text{La}_{1.875}\text{Ba}_{0.125}\text{CuO}_4$, *Physical Review B* **78**, 174529 (2008).

[5] K. Yamada, C.H. Lee, K. Kurahashi, J. Wada, S. Wakimoto, S. Ueki, H. Kimura, Y. Endoh, S. Hosoya, G. Shirane, R.J. Birgeneau, M. Greven, M.A. Kastner, and Y.J. Kim. *Phys. Rev. B*, **57**:6165, 1998.

[6] J. Fink, V. Soltwisch, J. Geck, E. Schierle, E. Weschke, and B. Buchner, Phase diagram of charge order in $\text{La}_{1.8-x}\text{Eu}_{0.2}\text{Sr}_x\text{CuO}_4$ from resonant soft x-ray diffraction, *Physical Review B* **83**, 092503 (2011)

[7] H.-H. Klauss, W. Wagener, M. Hillberg, W. Kopmann, H. Walf, F. J. Litterst, M. Hücker, and B. Büchner, From antiferromagnetic order to static magnetic stripes: the phase diagram of $(\text{La,Eu})_{2-x}\text{Sr}_x\text{CuO}_4$, *Physical Review Letters* **85**, 4590 (2000)

[8] J. D. Axe, A.H. Moudden, D. Hohlwein, D.E. Cox, K.M. Mohanty, A.R. Moodenbaugh, and Y. Xu, Structural phase transformations and superconductivity in $\text{La}_{2-x}\text{Ba}_x\text{CuO}_4$, *Physical Review Letters* **62**, 2751 (1989).

Publications

[A1] Kai Sun, Krishna Kumar, **Eduardo Fradkin**, "A discretized Chern-Simons gauge theory on arbitrary graphs", *Physical Review B* **92**, 115148 (2015).

[A2] Yu Gan, Gilberto de la Pena Munoz, Anshul Kogar, Bruno Uchoa, Diego Casa, Thomas Gog, **Eduardo Fradkin**, and Peter Abbamonte, "A reexamination of the effective fine structure constant of graphene, as measured in graphite", *Physical Review B* **93**, 195150 (2016).

[A3] Shichao Yan, Davide Iaia, Emilia Morosan, **Eduardo Fradkin**, Peter Abbamonte, and Vidya Madhavan, "Influence of Domain Walls in the Incommensurate Charge Density Wave State of Cu Intercalated 1T-TiSe₂", *Physical Review Letters* **118**, 106405 (2017).

[A4] Rodrigo Soto-Garrido, Yuxuan Wang, **Eduardo Fradkin**, **S. Lance Cooper**, "Higgs Modes in the Pair Density Wave Superconducting State", *Physical Review B* **95**, 214502 (2017).

[A5] A. Kogar, S. Vig, M. S. Rak, A. A. Husain, F. Flicker, Y. I. Joe, L. Venema, **G. J. MacDougall**, T. C. Chiang, **E. Fradkin**, J. van Wezel and P. Abbamonte, "Exciton condensation in 1T-TiSe₂ observed with meV-resolved electron energy-loss spectroscopy", submitted to *Science* (2016). <https://arxiv.org/abs/1611.04217>

[A6] S. Vig, A. Kogar, V. Mishra, L. Venema, M.S. Rak, A.A. Husain, G.D. Gu, **E. Fradkin**, M.R. Norman and P. Abbamonte, "Fluctuating charge order in the optimally doped high temperature superconductor $\text{Bi}_2\text{Sr}_2\text{CaCu}_2\text{O}_{8+x}$ ", submitted to *Physical Review X* (2017).

[A7] D. Reig-i-Plessis, S. V. Geldern, A. A. Aczel, **G. J. MacDougall**, "Spin ice physics in a new rare-earth selenide spinel MgEr_2Se_4 ", submitted to *Physical Review Letters* (2017). <https://arxiv.org/abs/1703.04267>

Project Title: Superconductivity and magnetism in *d*- and *f*-electron materials

Principal Investigator: M. Brian Maple

Mailing address: Department of Physics, University of California, San Diego, La Jolla, California 92093

Email: mbmaple@ucsd.edu

Program Scope

The general theme of the research carried under this program is the emergence of novel phases and phenomena due to competing interactions in correlated *d*- and *f*-electron materials. Experimental investigations of the physics of several classes of correlated electron materials are currently underway: (1) Superconductivity in layered electron-doped $LnO_{0.5}F_{0.5}BiS_2$ (Ln = lanthanide) compounds, unconventional multiband superconductivity with gap nodes and broken time reversal symmetry in the filled skutterudite compound $PrPt_4Ge_{12}$, and unconventional superconductivity and quantum criticality in $Ce_{1-x}M_xCoIn_5$ ($M = Yb, Sm$) systems; (2) correlated electron phenomena in the “cage-compounds” LnT_2Cd_{20} ($T = Ni, Pd$) whose crystal structure contains two distinct atomic cages, one of which is occupied by a Ln ion and the other a transition metal T ion; and (3) electronic phases that emerge from the “tuning” of competing interactions in the “hidden order” compound URu_2Si_2 via substitution of T ions for Ru (particular Fe and Os) and application of high pressure and high magnetic fields. In the following, we focus on recent progress in the studies of the $URu_{2-x}Fe_xSi_2$ pseudoternary system.

Recent Progress

The correlated *5f*-electron compound URu_2Si_2 undergoes a second order transition at $T_0 = 17.5$ K into an ordered phase whose identity has eluded researchers for more than three decades [R1]. This so-called “hidden order” (HO) phase coexists with an unconventional type of superconductivity (SC) below $T_c \approx 1.5$ K. Features in the electrical resistivity $\rho(T)$, specific heat $C(T)$ and magnetic susceptibility $\chi(T)$ associated with the HO phase transition are reminiscent of a charge or spin density wave that forms a gap over about 40% of the Fermi surface below T_0 , with the remainder of the Fermi surface gapped by the SC below T_c [R2]. The compound URu_2Si_2 has been studied extensively using many experimental techniques (e.g., transport, thermal, magnetic, and spectroscopic measurements), and numerous theoretical models have been proposed for the HO phase [R1]. Competing interactions in URu_2Si_2 can be tuned via the variation of control parameters including substituent composition x , pressure P and magnetic field H . This produces complex phase diagrams of temperature T vs. x , P , and H that contain a multitude of correlated electron phases and phenomena including SC, HO, antiferromagnetic (AFM) order, ferromagnetic order, spin density wave (SDW) order, exotic quantum phases, quantum critical phenomena, and non-Fermi liquid behavior.

Applying pressure to URu_2Si_2 depresses the T_c of the SC'ing phase and induces a transition from the HO phase to a large moment AFM phase at a critical pressure $P_c \approx 1.5$ GPa [R1,R3]. Several years ago, we found that the substitution of isoelectronic Fe for Ru in URu_2Si_2 produces similar behavior – SC is dpressed, a transition from the HO phase to the AFM phase occurs at $x \approx 0.15$, and there is a more than two-fold increase in the temperature of the HO/AFM phase boundary [R4]. This led us to suggest that the HO-AFM phase transition in $URu_{2-x}Fe_xSi_2$ is driven by “chemical pressure” P_{ch} associated with the reduction of the volume of the unit cell upon substitution of smaller Fe atoms for Ru atoms [R4]. We proposed that single crystals of $URu_{2-x}Fe_xSi_2$ could provide an opportunity to study the transition from the HO to the AFM phase at ambient pressure with techniques that cannot be readily performed on URu_2Si_2 under high pressure (e.g., ARPES, STM, neutron scattering, measurements in high magnetic fields, etc.).

During the past several years, we have synthesized a series of $\text{URu}_{2-x}\text{Fe}_x\text{Si}_2$ single crystals by means of the Czochralski method in a tetra-arc furnace. A series of investigations of the physical properties of these crystals are underway in our lab, the labs of our collaborators, and national laboratory facilities. These studies are providing valuable information about the HO and AFM phases in the $\text{URu}_{2-x}\text{Fe}_x\text{Si}_2$ system that will yield a better understanding of the underlying physics and, perhaps, even the identity of the order parameter of the elusive HO phase. The status of the experiments on single crystals of $\text{URu}_{2-x}\text{Fe}_x\text{Si}_2$ and the related system $\text{URu}_{2-x}\text{Os}_x\text{Si}_2$ [R5] that have been completed and are underway are listed below.

Experiments on $\text{URu}_{2-x}\text{Fe}_x\text{Si}_2$ single crystals whose results have been published:

- The T vs. P_{ch} phase diagram of $\text{URu}_{2-x}\text{Fe}_x\text{Si}_2$ was derived from $\rho(T)$, $C(T)$, $\chi(T)$ and thermal expansion measurements and is consistent with the T vs. P phase diagram of URu_2Si_2 [P14].
- Neutron diffraction measurements revealed that the variation of the U magnetic moment μ_{U} with P_{ch} in $\text{URu}_{2-x}\text{Fe}_x\text{Si}_2$ is similar to the variation of μ_{U} with P in URu_2Si_2 [R6].
- The T vs. P phase diagrams for $\text{URu}_{2-x}\text{Fe}_x\text{Si}_2$ determined from measurements of $\rho(T)$ at various values of x and P demonstrated that P_{ch} and P are additive [P20].
- Infrared spectroscopy measurements on $\text{URu}_{2-x}\text{M}_x\text{Si}_2$ ($M = \text{Fe}, \text{Os}$) single crystals yielded values of the energy gaps for charge excitations in the HO and AFM phases [R7].
- Inelastic neutron scattering measurements on $\text{URu}_{2-x}\text{Fe}_x\text{Si}_2$ showed that the commensurate and incommensurate excitations in the HO and AFM phases are consistent with those in URu_2Si_2 under pressure [P5].
- Polarized resolved Raman spectroscopy measurements on $\text{URu}_{2-x}\text{Fe}_x\text{Si}_2$ in the HO and AFM phases are consistent with a chiral density wave scenario for the HO phase [P11].
- The 3D T - x - H phase diagram for $H \leq 45$ T was derived from measurements of $\rho(H)$ isotherms on $\text{URu}_{2-x}\text{Fe}_x\text{Si}_2$ crystals at the NHMFL at FSU, Tallahassee, and LANL [R8].

Experiments on $\text{URu}_{2-x}\text{Fe}_x\text{Si}_2$ single crystals that are currently underway:

- Pump-probe measurements with Prof. Richard Averitt (UCSD).
- ARPES measurements with Prof. Andrés Santander-Syro (CNRS, U. Paris-Sud).
- Scanning tunneling microscopy measurements with Prof. Ali Yazdani (Princeton U.).
- Thermal conductivity, thermopower, and Hall effect measurements.

Future Plans

The following projects are included in future plans:

- Further experiments on $\text{URu}_{2-x}\text{M}_x\text{Si}_2$ ($M = \text{Fe}, \text{Os}$) single crystals and exploratory measurements on $\text{URu}_{2-x}\text{M}'_x\text{Si}_2$ ($M' = \text{Co}, \text{Ir}$) polycrystals.
- Synthesis of $\text{LnT}_2\text{X}_{20}$ ($\text{Ln} = \text{lanthanide}$, $T = \text{Ti}, \text{V}, \text{Ni}, \text{Pd}, \text{Pt}$; $X = \text{Al}, \text{Zn}, \text{Cd}$) single crystals and investigation of correlated electron phenomena in these materials.
- Synthesis and study of unconventional superconductivity and correlated electron phenomena in $\text{PrPt}_4\text{Ge}_{12}$ -based filled skutterudite pseudoternary compounds.
- Synthesis and study of high temperature Fe-based superconductors.

References

- R1. J. A. Mydosh and P. M. Oppeneer, “Colloquium: Hidden order, superconductivity, and magnetism: The unsolved case of URu_2Si_2 ,” *Rev. Mod. Phys.* **83**, 1301 (2011).
- R2. M. B. Maple, J. W. Chen, Y. Dalichaouch, T. Kohara, C. Rossel, M. S. Torikachvili, M. W. McElfresh, and J. D. Thompson, “Partially Gapped Fermi Surface in the Heavy-Electron Superconductor URu_2Si_2 ,” *Phys. Rev. Lett.* **56**, 185 (1986).

- R3. N. P. Butch, J. R. Jeffries, S. Chi, J. B. Leao, J. W. Lynn, and M. B. Maple, “Antiferromagnetic critical pressure in URu₂Si₂ under hydrostatic conditions,” *Phys. Rev. B* **82**, 060408 (2010).
- R4. N. Kanchanavatee, M. Janoschek, R. E. Baumbach, J. J. Hamlin, D. A. Zocco, K. Huang, and M. B. Maple, “Twofold enhancement of the hidden-order/large-moment antiferromagnetic phase boundary in the URu_{2-x}Fe_xSi₂ system,” *Phys. Rev. B* **84**, 245122 (2011).
- R5. N. Kanchanavatee, B. D. White, V. W. Burnett, and M. B. Maple, “Enhancement of the hidden order/large moment antiferromagnetic transition temperature in the URu_{2-x}Os_xSi₂ system,” *Philos. Mag.* **94**, 3681 (2014).
- R6. P. Das, N. Kanchanavatee, J. S. Helton, K. Huang, R. E. Baumbach, E. D. Bauer, B. D. White, V. W. Burnett, M. B. Maple, J. W. Lynn, and M. Janoschek, “Chemical pressure tuning of URu₂Si₂ via isoelectronic substitution of Ru with Fe,” *Phys. Rev. B* **91**, 085122 (2015).
- R7. J. S. Hall, M. Rahimi Movassagh, M. N. Wilson, G. M. Luke, N. Kanchanavatee, K. Huang, M. Janoschek, M. B. Maple, and T. Timusk, “Electrodynamics of the antiferromagnetic phase in URu₂Si₂,” *Phys. Rev. B* **92**, 195111 (2015).
- R8. S. Ran, I. Jeon, N. Pouse, A. J. Breindel, N. Kanchanavatee, K. Huang, A. Gallagher, K.-W. Chen, D. Graf, R. E. Baumbach, J. Singleton, and M. B. Maple, “Phase diagram of URu_{2-x}Fe_xSi₂ in high magnetic fields,” to be published in *PNAS* (2017).

Publications (supported by BES)

- P1. R. E. Baumbach, J. J. Hamlin, M. Janoschek, J. Singleton, and M. B. Maple, “Frustrated magnetism in the spin–chain metal Yb₂Fe₁₂P₇,” *J. Phys.: Cond. Matt.* **28**, 046004 (2016).
- P2. I. Jeon, K. Huang, D. Yazici, N. Kanchanavatee, B. D. White, P.-C. Ho, S. Jang, N. Pouse, and M. B. Maple, “Investigation of superconducting and normal-state properties of the filled-skutterudite system PrPt₄Ge_{12-x}Sb_x,” *Phys. Rev. B* **93**, 104507 (2016).
- P3. K. R. Shirer, A. P. Dioguardi, B.T. Bush, J. Crocker, C. H. Lin, P. Klavins, J. C. Cooley, M. B. Maple, K. B. Chang, K. R. Poeppelmeier, and N. J. Curro, “²⁹Si nuclear magnetic resonance study of URu₂Si₂ under pressure,” *Physica B* **481**, 232 (2016).
- P4. Y. Xu, J. K. Dong, I. K. Lum, J. Zhang, X. C. Hong, L. P. He, K. F. Wang, Y. C. Ma, C. Petrovic, M. B. Maple, L. Shu, and S. Y. Li, “Universal heat conduction in Ce_{1-x}Yb_xCoIn₅: Evidence for robust nodal d-wave superconducting gap,” *Phys. Rev. B* **93**, 064502 (2016).
- P5. N. P. Butch, S. Ran, I. Jeon, N. Kanchanavatee, K. Huang, A. Breindel, M. B. Maple, R. L. Stillwell, Y. Zhao, L. Harriger, and J. W. Lynn, “Distinct magnetic spectra in the hidden order and antiferromagnetic phases in URu_{2-x}Fe_xSi₂,” *Phys. Rev. B* **94**, 201102 (2016).
- P6. P.-C. Ho, J. Singleton, P. A. Goddard, F. F. Balakirev, S. Chikara, T. Yanagisawa, M. B. Maple, D. B. Shrekenhamer, X. Lee, and A. T. Thomas, “Fermi-surface topologies and low-temperature phases of the filled skutterudites compounds CeOs₄Sb₁₂ and NdOs₄Sb₁₂,” *Phys. Rev. B* **94**, 205140 (2016).
- P7. K. Huang, S. Eley, P. F. S. Rosa, L. Civale, E. D. Bauer, R. E. Baumbach, M. B. Maple, and M. Janoschek, “Quantum critical scaling in the disordered itinerant ferromagnet UCo_{1-x}Fe_xGe,” *Phys. Rev. Lett.* **117**, 237202 (2016).
- P8. K. Huang, D. Yazici, B. D. White, I. Jeon, A. J. Briendel, N. Pouse, and M. B. Maple, “Superconducting and normal state properties of the systems La_{1-x}M_xPt₄Ge₁₂ (M = Ce, Th),” *Phys. Rev. B* **94**, 094501 (2016).

- P9. I. Jeon, S. Ran, A. J. Breindel, P.-C. Ho, R. B. Adhikari, C. C. Almasan, B. Luong, and M. B. Maple, “Crossover and coexistence of superconductivity and antiferromagnetism in the filled-skutterudite system $\text{Pr}_{1-x}\text{Eu}_x\text{Pt}_4\text{Ge}_{12}$,” *Phys. Rev. B* **95**, 134517 (2017).
- P10. N. Kanchanavatee, M. Janoschek, K. Huang, B. D. White, P. S. Riseborough, A. V. Balatsky, and M. B. Maple, “Emergence of higher order rotational symmetry in the hidden order phase of URu_2Si_2 ,” *Philos. Mag.* **97**, 144 (2016).
- P11. H.-H. Kung, S. Ran, N. Kanchanavatee, V. Krapivin, A. Lee, J. A. Mydosh, K. Haule, M. B. Maple, and G. Blumberg, “Analogy between the “hidden order” and the orbital antiferromagnetism in $\text{URu}_{2-x}\text{Fe}_x\text{Si}_2$,” *Phys. Rev. Lett.* **117**, 227601 (2016).
- P12. S. Mombetsu, T. Murazumi, H. Hidaka, T. Yanagisawa, H. Amitsuka, P.-C. Ho, and M. B. Maple, “Study of localized character of 4f electrons and ultrasonic dispersions in $\text{SmOs}_4\text{Sb}_{12}$ by high-pressure high-frequency ultrasonic measurements,” *Phys. Rev. B* **94**, 085142 (2016).
- P13. S. Mombetsu, T. Yanagisawa, H. Hidaka, H. Amitsuka, S. Yasin, S. Zherlitsyn, J. Wosnitza, P.-C. Ho, and M. B. Maple, “Crystalline Electric Field and Kondo Effect in $\text{SmOs}_4\text{Sb}_{12}$,” *J. Phys. Soc. Jpn.* **85**, 043704 (2016).
- P14. S. Ran, C. T. Wolowiec, I. Jeon, N. Kanchanavatee, B. D. White, K. Huang, D. Martien, T. DaPron, D. Snow, M. Williamsen, S. Spagna, P. S. Riseborough, and M. B. Maple, “Phase diagram and thermal expansion measurements on the system $\text{URu}_{2-x}\text{Fe}_x\text{Si}_2$,” *PNAS* **113**, 13348 (2016).
- P15. D. J. Scanderbeg, B. J. Taylor, R. E. Baumbach, J. P. Paglione, and M. B. Maple, “Electrical and thermal transport properties of the electron-doped cuprate $\text{Sm}_{2-x}\text{Ce}_x\text{CuO}_{4-y}$ system,” *J. Phys.: Cond. Matt.* **28**, 485702 (2016).
- P16. Y. P. Singh, R. B. Adhikari, S. Zhang, K. Huang, D. Yazici, I. Jeon, M. B. Maple, M. Dzero, and C. C. Almasan, “Multiband superconductivity in the correlated electron filled skutterudites system $\text{Pr}_{1-x}\text{Ce}_x\text{Pt}_4\text{Ge}_{12}$,” *Phys. Rev. B* **94**, 144502 (2016).
- P17. Y. Song, J. Van Dyke, I. K. Lum, B. D. White, S. Jang, D. Yazici, L. Shu, A. Schneidewind, P. Čermák, Y. Qiu, M. B. Maple, D. K. Morr, and P. Dai, “Robust upward dispersion of the neutron spin resonance in the heavy fermion superconductor $\text{Ce}_{1-x}\text{Yb}_x\text{CoIn}_5$,” *Nature* **7**, 12774 (2016).
- P18. B. J. Taylor, T. H. Emery, A. M. Leese de Escobar, I. Jeon, and M. B. Maple, “Examination of the Thermal Annealing Process in Producing $\text{YBa}_2\text{Cu}_3\text{O}_{7-x}$ Films and Characterization of Pressure Stabilized Oxygen Chain States,” *IEEE Trans. Appl. Supercon.* **27**, 7500705 (2017).
- P19. R. Wawryk, O. Zogal, A. Rudenko, T. Cichorek, Z. Henkie, and M. B. Maple, “Electron transport and magnetic properties of the filled skutterudite compound $\text{ThFe}_4\text{As}_{12}$,” *J. Alloys Compds.* **688**, 478 (2016).
- P20. C. T. Wolowiec, N. Kanchanavatee, K. Huang, S. Ran, and M. B. Maple, “Evolution of critical pressure with increasing Fe substitution in the heavy-fermion system $\text{URu}_{2-x}\text{Fe}_x\text{Si}_2$,” *Phys. Rev. B* **94**, 085145 (2016).
- P21. D. Yazici, A. C. Basaran, J. G. Ramirez, I. K. Schuller, and M. B. Maple, “Structure, magnetization, specific heat, and microwave properties of $\text{K}_x\text{Fe}_{2-y}\text{Se}_2$,” *Supercon. Sci. Tech.* **29**, 085015 (2016).
- P22. J. Zhang, K. Huang, Z. F. Ding, D. E. MacLaughlin, O. O. Bernal, P.-C. Ho, C. Tan, X. Liu, D. Yazici, M. B. Maple, and L. Shu, “Superconducting gap structure in ambient-pressure-grown $\text{LaO}_{0.5}\text{F}_{0.5}\text{BiS}_2$,” *Phys. Rev. B* **94**, 244502 (2016).

Program Title: Controlling Superconductivity via Tunable Nanostructure Arrays
Principle Investigator: Nadya Mason; Co-PIs: Raffi Budakian, Taylor Hughes
Mailing Address: Department of Physics, University of Illinois at Urbana-Champaign, Urbana IL 61801
Email: nadya@illinois.edu

Program Scope:

The goal of this program is to use proximity-coupled nanostructure arrays to understand and control how collective behavior emerges in superconducting systems. The outcome of this research has been the discovery and characterization of exotic phases in superconducting systems, a better understanding of how microscopic parameters lead to macroscopic behavior in key materials systems, and an improved ability to control interactions to manipulate the electronic properties of superconductors.

The program is based on the idea that superconducting islands placed on a thin conductor at a separation smaller than the normal metal coherence length can support a finite Josephson coupling between the islands, where the strength of the coupling depends on the length and conductance of the intervening material. By adjusting the size, configuration, and type of islands, the correlated states, as well as the competition between them, can be precisely tuned. This allows for the clear determination of how superconductors' critical properties can be enhanced or diminished. We also aim to determine how controlling these parameters can lead to novel phase regimes, such as pseudogap-like phases and 2D metallic states.

In previous, DOE-supported work, we demonstrated that the array systems behave as 2D superconductors, and showed how junction length controlled the transition [P1]. More significantly, our measurements of these samples [P2] provided evidence of the long sought-after 2D metallic state [P3] as a function of well-understood parameters (e.g., island spacing, a parameter of dissipative coupling). In more recent measurements of superconducting transitions in individual, granular, mesoscopic Nb islands, we observed an anomalous suppression of the superconducting transition temperature T_c at large island diameters (compared to the coherence length), which we can explain as a rare region effect, where superconducting order first appears in unusually large grains [1].

Further, we have recently used the clear vortex signatures in the array system to determine the effects of interactions and dissipation on vortex dynamics. In a joint theoretical and experimental study, we used the current-driven voltage response to demonstrate interactions in the vortex flux creep regime as well as the importance of time-correlated dissipative forces in the transition to vortex flux-flow [2]. We also studied commensurate/incommensurate vortex lattice transitions to examine the effects of disorder on a superconductor [3].

The transport and theoretical studies are complemented by new magnetic force microscopy (MFM) techniques that enable the imaging of both individual and collective vortex *dynamics* at high resolution [4,5]. We developed an MFM-based technique – called Phase-Locked Magnetic Force Microscopy – that is sensitive to the current density flowing in conductors, and more specifically to the spatial variation of the magnetic field induced by this current. We also developed a technique we call Stochastic Resonance Magnetic Force Microscopy (SRMFM), which uses the local field from the MFM tip to reconstruct vortex motion and energy landscapes. MFM images of vortex dynamics in Nb island arrays under various magnetic field and island

configurations were compared to transport results for similar samples, and analyzed using numerical simulations of interacting vortices.

The research combines temperature- and field-dependent transport measurements with magnetic resonance force microscopy measurements of local vortex spatial structure and surface currents, as well as accurate phenomenological modeling, to provide complete characterization of the collective behavior of the samples.

Recent Progress: Unusual dynamics and imaging of vortex transport

Vortex systems provide excellent test-beds for studying the introduction of disorder into crystalline structures. One controlled way of studying disorder is to consider systems of particles in a periodic potential, where disorder is introduced when the particle lattice does not match the potential well. This type of system is described by the 2D Frenkel-Kontorova (FK) model, which exhibits a rich set of structures and modes of motion. We use superconductor-normal-superconductor (SNS) island arrays as an experimental realization of the FK model and examine transitions between ordered and disordered states. SNS arrays provide vortices with a periodic potential defined by array geometry and allow the vortex filling fraction (f) of each potential well to be controlled using magnetic field. The structure of the vortex lattice and type of collective vortex motion at incommensurate fillings has not been well studied previously.

Measurements of dV/dI vs f (which is controlled by magnetic field) show a pattern of peaks and dips that emerge when $f > 0.1$ (Fig. 1a). At special fillings—e.g., $f = 1/12, 1/6, 1/4, 1/2$ —the vortex lattice is commensurate with the array potential wells, resulting in crystalline vortex orderings, strong pinning, and thus dips in dV/dI vs f . However, commensurately and incommensurately filled lattices exhibit different dynamic behavior: Fig. 1b plots dV/dI vs I for the commensurate filling $f=0.25$ alongside the incommensurate filling $f=0.20$. Driven from pinned to flux flow, the commensurate filling undergoes a single transition, while the incommensurate filling undergoes two distinct transitions separated by an intermediate region of constant dV/dI . We can explain the two-step vortex transition as first from pinned to lattice defect motion, then from lattice defect to bulk lattice motion. Comparing our measurements with a dynamic molecular vortex model (Fig. 1c), we show that this two-step transition is indicative of domain wall motion in a polycrystalline vortex lattice. We thus demonstrate that a disordered, interacting vortex system with a sufficiently strong periodic pinning potential can favor interface

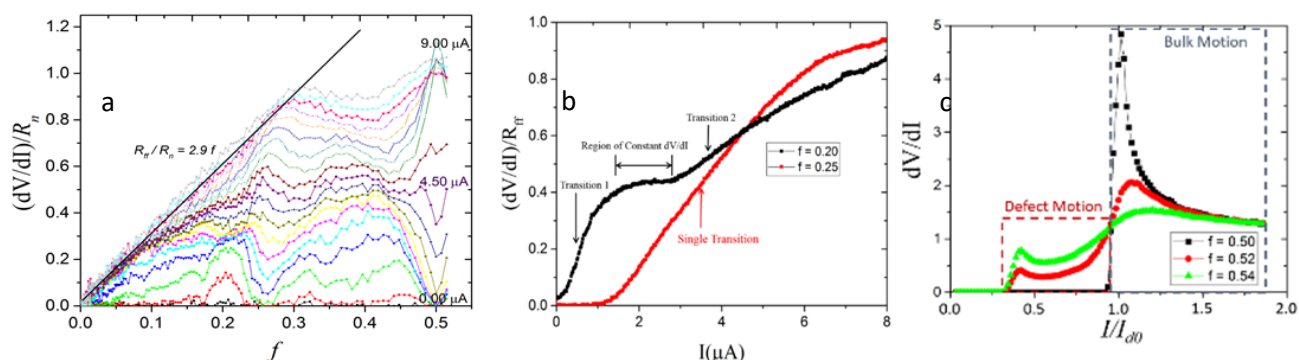


Figure 1 (a) Differential resistance dV/dI at $0.5 \mu\text{A}$ current intervals as a function magnetic filling f . Dips associated with commensurate fillings are visible. (b) dV/dI vs I . The black curve for $f=0.20$ undergoes a two-step transition with an intermediate region of constant dV/dI in between. The red curve for $f=0.25$ undergoes a single transition. (c) Simulated dV/dI showing a two-step transition as is seen experimentally.

physics rather than a quasiperiodic regime. This had been predicted in artificial pinning array structures, but not previously explored in experimental studies.

While it is useful to infer vortex dynamics from collective behavior in transport, an even better understanding can be gained by directly imaging individual vortices. Thus, we developed a magnetic force microscopy (MFM) method for high resolution imaging of the vortex *dynamics* in the Nb-island arrays. This new technique enables the unprecedented ability to model both individual and collective vortex dynamics at high resolution.

For this technique, a micron-size SmCo magnetic particle is attached to the tip of a cantilever (Fig. 2a) and scanned several hundred nanometers over the surface of the array (Fig. 2b). At particular positions of the tip, the energy barrier separating certain vortex configurations is reduced, so that thermal fluctuations can cause the system to rapidly switch between degenerate vortex configurations. The fluctuating surface currents surrounding the vortex cores interact with the magnetic moment on the cantilever, and lower the cantilever frequency. Key features of this experimental platform are the high degree of tunability, and the local nature of the probe.

Applying this technique to lattices of superconductor island arrays on a metal, we obtain a variety of striking spatial patterns that encode information about the energy landscape for vortices in the system. We interpret these patterns in terms of local vortex dynamics, and extract the relative strengths of the characteristic energy scales in the system, such as the vortex-magnetic field and vortex-vortex interaction strengths, as well as the vortex chemical potentials. We also demonstrate that the relative strengths of the interactions can be tuned.

Fig. 2c and 2d shows a set of representative cantilever frequency shift images for two different external field values, where frequency shifts appear as dark lines and indicate boundaries between two stable vortex configurations. A variety of remarkable geometric patterns emerge from these measurements. Numerical simulations of a

simple phenomenological model of vortices shows that the images can be directly understood as specific numbers of vortices moving into their lowest energy configurations as the tip is raster scanned. For example, beneath Figures 2c and 2d are simulations showing frequency shifts and real-space configurations for 5 and 6 vortices, respectively; the simulations have excellent

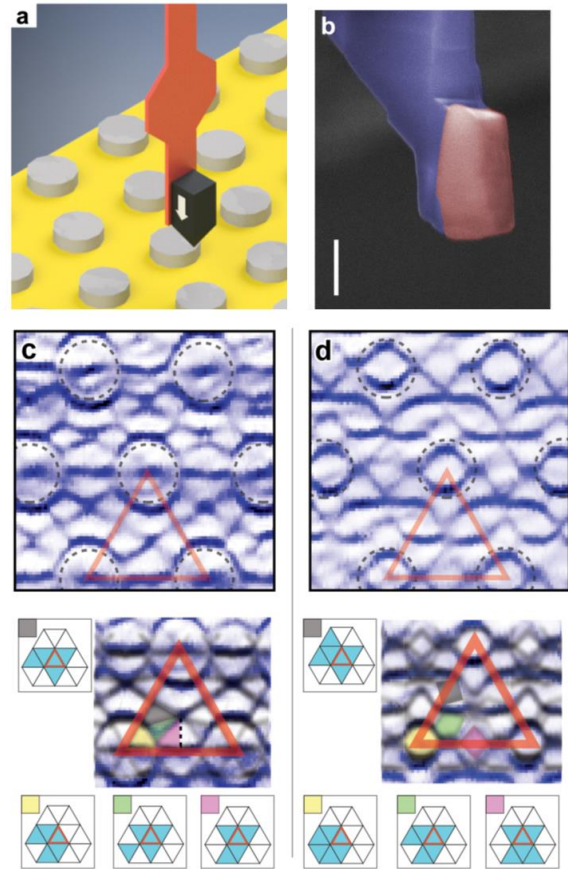


Figure 2 (a) Diagram of cantilever over a triangular array of Nb disks on top of a Au film. (b) SEM image of a SmCo5 magnetic tips White scale bar is 500 nm. (c) and (d) Images of some patterns seen in this experiment (top) and associated vortex configurations (bottom) as determined by simulated annealing. One plaquette (red triangle) and associated islands (dashed circles) are drawn for clarity. Experimental and simulations taken for (c) 5 (80 Oe, 425 nm), and (d) 6 vortices (68 Oe, 425 nm). All images taken at 3.70 K.

correspondence with the experimental data. This robust experimental platform for locally probing and controlling vortex dynamics can be used to better study vortex glasses and liquids, as well as non-standard vortex interactions in unconventional superconductors.

Future Plans

Our future plans for this project include:

1. MFM and transport measurements of current-driven vortex states and transitions.
2. Integrated theoretical, transport, and imaging techniques to study arrays of superconducting and magnetic islands on graphene and topological insulators, for exploring unconventional superconducting states.

References

- P1. S. Eley, S. Gopalakrishnan, P.M. Goldbart, and N. Mason, “Dependence of global superconductivity on inter-island coupling in arrays of long SNS junctions,” *J. Phys.: Condens. Matter* **25**, 445701 (2013).
- P2. S. Eley, S. Gopalakrishnan, P.M. Goldbart, and N. Mason “Approaching zero-temperature metallic states in mesoscopic superconductor-normal-superconductor arrays,” *Nature Physics*, **8**, 59 (2012).
- P3. B. Spivak et al, “Theory of quantum metal to superconductor transitions in highly conducting systems,” *Phys. Rev. B* **77**, 214523 (2008).

Manuscripts from 2015-2017 which acknowledge DOE support

1. M. Durkin, S. Gopalakrishnan, R. Garrido-Menacho, R. Mansbach, J. Zuo, **N. Mason**, “Rare-region onset of superconductivity,” under review, *Nature Communications*, arxiv: 1607.06842 (2017).
2. M. Durkin, I.M. Shem, S. Eley, **T.L. Hughes**, **N. Mason**, “History-dependent dissipative vortex dynamics in superconducting arrays,” *Phys. Rev. B* **94**, 024510 (2016).
3. Malcolm Durkin, Ian Mondragon-Shem, **Taylor L. Hughes**, **Nadya Mason**, “Observation of domain wall motion in a polycrystalline vortex lattice,” under review, *Physical Review Letters* (2017).
4. H. Polshyn, T.R. Naibert, and **R. Budakian**, “Imaging phase slip dynamics in micron-size superconducting rings,” under review, *Phys. Rev. B.*, arxiv: 1703.08184 (2017).
5. T. Naibert, H. Polshyn, M. Durkin, B. Wolin, R. Garrido-Menacho, V. Chua, I. Mondragon-Shem, **T.L. Hughes**, **N. Mason**, and **R. Budakian**, “ Φ_0 -Magnetic force microscopy for imaging and control of vortex dynamics,” under review, *Nature Communications*, arxiv: 1705.08956 (2017).
6. A. Kogar, S. Vig, A. Thaler, M.H. Wong, Y. Xiao, D. Reigi-Plessis, G.Y. Cho, T. Valla, Z. Pan, J. Schneeloch, R. Zhong, G. Gu, **T.L. Hughes**, G.J. MacDougall, T.-C. Chiang, P. Abbamonte, “Surface collective modes in the topological insulators Bi_2Se_3 and $\text{Bi}_{0.5}\text{Sb}_{1.5}\text{Te}_{3-x}\text{Se}_x$,” *Phys. Rev. Lett.* **115**, 257402 (2015).

Exploring superconductivity at the edge of magnetic or structural instabilities

Ni Ni

University of California, Los Angeles, Los Angeles, CA

Program Scope

Modern research of condensed matters devotes in understanding how properties of complex solids are determined by their structural and electronic degrees of freedom. Despite of the complicity in real materials where competing orders often exist, significant progress has been driven by the discovery of new materials with emergent ground states. Of particular interests are the superconductors near the edge of structural/magnetic instabilities and materials with non-trivial topology. The discovery and characterization of materials of the former type can advance our understanding of high T_c superconductivity significantly while bulk materials with nontrivial topology provide a new platform to study the low energy excitations through band engineering. The objective of this research is to discover materials that lie at the edge of structural/magnetic instability and to explore topological semimetals with exotic low energy excitations using solid state reaction and crystal-growth methods, and to characterize them and examine their structure-property relations through thermodynamic, transport, X-ray, and neutron measurements.

Recent Progress

1. We have discovered that $\text{Ca}_{0.73}\text{La}_{0.27}\text{FeAs}_2$, is the "parent" compound of the 112 superconducting family [1]. The breaking of C_4 rotational symmetry even at room temperature makes it unique among all FPS. We first unravel a monoclinic to triclinic phase transition at 58 K, and a paramagnetic to stripe antiferromagnetic (AFM) phase transition at 54 K, below which spins order 45° away from the stripe direction. Furthermore, in addition to the central-hole and corner-electron Fermi pockets usually appearing in Fe pnictide superconductors, angle-resolved photoemission (ARPES) measurements resolve a Fermiology where an extra electron pocket of mainly As chain character exists at the Brillouin zone edge, suggesting the active role of the metallic spacer layers.

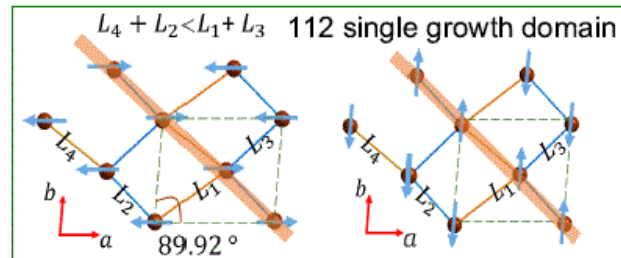


Figure 1: Magnetic structure of $\text{Ca}_{0.73}\text{La}_{0.27}\text{FeAs}_2$.

2. Topological semimetals are characterized by protected crossings between conduction and valence bands. These materials have recently attracted significant interest because of the deep connections to high-energy physics, the novel topological surface states, and the unusual transport phenomena. While Dirac and Weyl semimetals have been extensively studied, the nodal-line semimetal remains largely unexplored due to the lack of an ideal material platform. We found that CaAgAs and CaCdGe provide an ideal platform to perform comparative studies

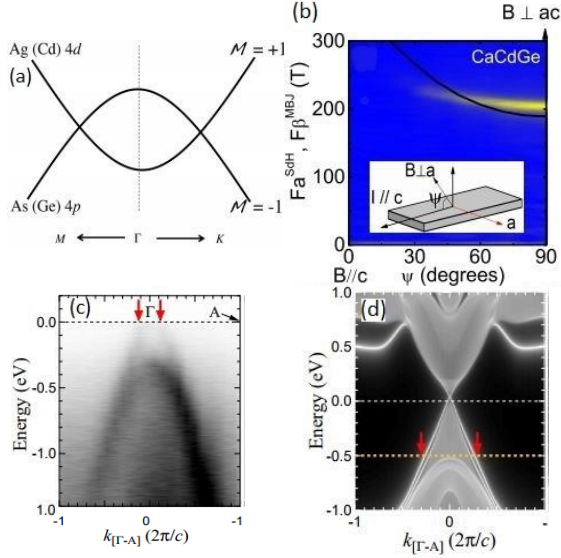


Figure 2: (a) The illustration of the band structure near the Fermi level for CaAgAs/CaCdGe. (b) The SdH QO data for CaCdGe. (c) ARPES and (d) DFT band dispersion along Γ -A directions of CaAgAs. Red arrow points to the surface states.

because the theoretical calculation shows that they feature the same topological nodal line except that CaCdGe has a more complicated Fermiology with irrelevant Fermi pockets. As a result of electron-hole compensation, the magnetoresistance of our CaCdGe sample is more than 100 times larger than that of CaAgAs. Furthermore, ARPES observed a metallic, linear, non-kz-dispersive surface band that coincides with the high-binding-energy part of the theoretical topological surface state, proving the topological nontriviality of the system.

3. Dirac cones have been proposed and observed in non-magnetic materials, including Cd_3As_2 and Na_3Bi . By breaking inversion either symmetry or time-reversal symmetry, Dirac point can be split into pairs of weyl points. To break the time-reversal symmetry, we can either apply an external magnetic field or we can use the spontaneous magnetic moment inside the material. For the latter case, the correlation of spontaneous magnetism and Weyl

fermions has been studied in the 112 compound and half-Heusler compound GdPtBi. Recently, orthorhombic CuMnAs has been proposed to be a magnetic material where Dirac point is robust to the combination of inversion and time-reversal symmetry breaking, providing a system to study the interplay of AFM and Dirac fermions. We first determined the magnetic structure of the orthorhombic $\text{Cu}_{0.95}\text{MnAs}$ and $\text{Cu}_{0.98}\text{Mn}_{0.96}\text{As}$ single crystals (Fig. 2(a)-(b)). While $\text{Cu}_{0.95}\text{MnAs}$ is a commensurate antiferromagnet (C-AFM) below 360 K with a propagation vector of $\mathbf{k} = 0$, $\text{Cu}_{0.98}\text{Mn}_{0.96}\text{As}$ undergoes a second-order paramagnetic to incommensurate antiferromagnetic (IC-AFM) phase transition at 320 K with $\mathbf{k} = (0.1, 0, 0)$, followed by a second-order IC-AFM to C-AFM phase transition at 230 K (Fig 2 (c)). In the C-AFM state, the Mn spins order parallel to the b-axis but antiparallel to their nearest-neighbors

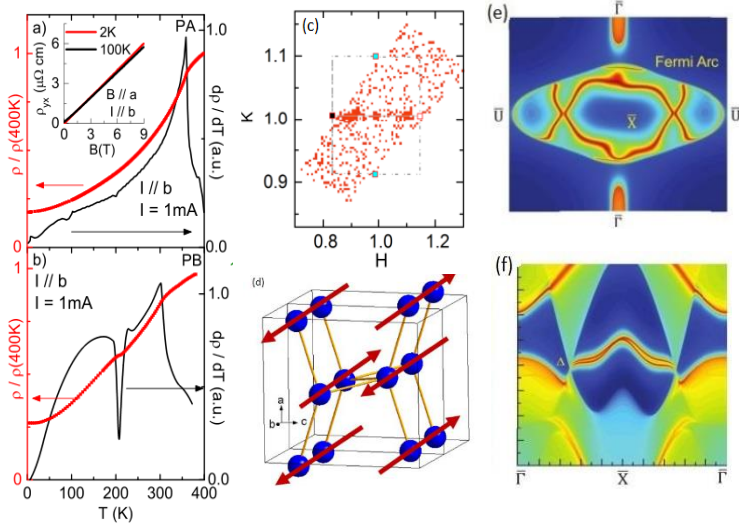


Figure 3: (a) (b) The ρ and derivative vs. T (c): A cut of the neutron scattering of $\text{Cu}_{0.98}\text{Mn}_{0.96}\text{As}$. (d) The magnetic structure in the C-AFM state. (e) The Fermi surface contour on the (010) surface at the Fermi level. (f) The corresponding electronic spectra along $k_z=0$.

with the easy axis along the b axis (Fig. 2(d)). This magnetic order breaks R_y gliding and S_{2z} rotational symmetries, the two crucial for symmetry analysis, resulting in finite band gaps at the crossing point and the disappearance of the massless topological fermions. However, the spin-polarized surface states and signature induced by non-trivial topology still can be observed in this system (Fig. 2 (e)-(f)), which makes orthorhombic CuMnAs promising in antiferromagnetic spintronics.

4. We first mapped out the angular-dependent Shubnikov–de Haas (SdH) of weak topological insulator NbAs₂. Combined with the first-principles calculations, we reveal four types of Fermi-surface pockets, as shown in Fig. Negative longitudinal magnetoresistance is observed which may be linked to novel topological states in this material, although systematic study is necessary to ascertain its origin.

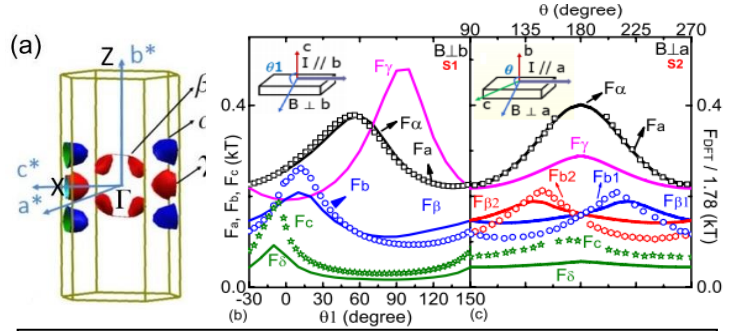


Figure 4: (a) The calculated band structure of NbAs₂. (b) (c) The angular dependence of oscillation frequencies. Solid line is the theoretical value.

5. We have provided high quality of superconducting and topological single crystals to various groups for further investigation, including Weyl semimetal TaAs, type II weyl semimetal TaIrTe₄, CaAgAs, BaFe₂(As_{1-x}P_x)₂, etc. This has led to the understanding of the role of Fermi arcs in the transport by STM [1] and the testing of a single-spin quantum sensor [2].

Future Plans

We will continue our exploration and investigation on topological materials and materials with structural/magnetic instabilities.

1. Along the direction of nonmagnetic and magnetic topological semimetals, especially topological superconductors, we will keep our exploration and focus on arsenides and chalcogenides.

2. Along the direction of superconductors near the edge of structural and magnetic instabilities: (a) Our on-going study on the AAg₄As₂ (A=Sr, Eu) has revealed the existence of charge-density-wave instability. While quantum oscillation has been observed in the SrAg₄As₂, the EuAg₄As₂ shows helical magnetic structure and very interesting behavior of the magnetoresistance, providing a platform to investigate how magnetism affects transport. We will tune their ground state through chemical doping/external pressure.

(b) The recent discovery of increased T_c in KFe₂As₂ under high pressure up to 20 Gpa has been argued to be due to the enhanced superconducting pairing in collapsed tetragonal FeAs phase. On the other hand, the collapsed tetragonal phase has been believed and proved to be harmful for spin fluctuation and thus superconductivity in CaFe₂As₂. Therefore, it is important to clarify the relation between superconductivity in collapsed tetragonal phase. The Na_{1-x}La_xFe₂As₂ system

has the potential to be a chemical-doping analog of the pressure-induced KFe_2As_2 . We will grow single crystals and do systematic study of this series.

References

1. Hiroyuki Inoue, et.al, *Quasiparticle interference of the Fermi arcs and surface-bulk connectivity of a Weyl semimetal*, *Science*, **351**, 1184 (2016)
2. Matthew Pelliccione, et.al, *Scanned Probe Imaging of Nanoscale Magnetism at Cryogenic Temperatures with a Single-Spin Quantum Sensor*, *Nature Nanotechnology*, **11**, 700 (2016)

Publications

1. Eve Emmanouilidou, Huibo Cao, Peizhe Tang, Xin Gui, Chaowei Hu, Bing Shen, Junyi Wu, Shou-Cheng Zhang, Weiwei Xie, Ni Ni, *Magnetic order induces symmetry breaking in the single crystalline orthorhombic CuMnAs semimetal*, [Arxiv: 1708.09340 \(2017\)](https://arxiv.org/abs/1708.09340), *submit to PRL*.
2. Matthew Pelliccione, Alec Jenkins, Preeti Ovarthaiyapong, Christopher Reetz, Eve Emmanuelidu, Ni Ni and Ania C. Bleszynski Jayich, *Scanned Probe Imaging of Nanoscale Magnetism at Cryogenic Temperatures with a Single-Spin Quantum Sensor*, *Nature Nanotechnology*, **11**, 700 (2016)
3. Shan Jiang, Chang Liu, Huibo Cao, Turan Birol, Jared M. Allred, Wei Tian, Lian Liu, Kyuil Cho, Matthew M. Krogstad, Jie Ma, Keith Taddei, Makariy A. Tanatar, Ruslan Prozorov, Stephan Rosenkranz, Yasutomo J. Uemura, Gabriel Kotliar and Ni Ni, *Structural and magnetic phase transitions in $\text{Ca}_{0.73}\text{La}_{0.27}\text{FeAs}_2$ with electron-overdoped FeAs layers*, *Phys. Rev. B* **93**, 054522(2016)
4. Hiroyuki Inoue, András Gyenis, Zhijun Wang, Jian Li, Seong Woo Oh, Shan Jiang, Ni Ni, B. Andrei Bernevig and Ali Yazdani, *Quasiparticle interference of the Fermi arcs and surface-bulk connectivity of a Weyl semimetal*, *Science*, **351**, 1184 (2016)
5. J. W. Harter, H. Chu, S. Jiang, N. Ni, and D. Hsieh, *Nonlinear and time-resolved optical study of the 112-type iron-based superconductor parent $\text{Ca}_{1-x}\text{La}_x\text{FeAs}_2$ across its structural phase transition*, *Phys. Rev. B* **93**, 104506(2016)
6. Bing Shen, Xiaoyu Deng, Gabriel Kotliar, and Ni Ni, *Fermi surface topology and negative longitudinal magnetoresistance observed in NbAs_2 semimetal*, *Phys. Rev. B* **93**, 195119(2016)
7. Andras Gyenis, Hiroyuki Inoue, Sangjun Jeon, Brian B. Zhou, Benjamin E. Feldman, Zhijun Wang, Jian Li, Shan Jiang, Quinn D. Gibson, Satya K. Kushwaha, Jason W. Krizan, Ni Ni, Robert J. Cava, B. Andrei Bernevig, Ali Yazdani, *Imaging electronic states on topological semimetals using scanning tunneling microscopy*, *New J. Phys.* **18**, 105003 (2016)
8. Eve Emmanouilidou, Bing Shen, Xiaoyu Deng, Tay-Rong Chang, Aoshuang Shi, Gabriel Kotliar, Su-Yang Xu, and Ni Ni, *Magnetotransport properties of the single-crystalline nodal-line semimetal candidates CaTX ($T=\text{Ag, Cd}$; $X=\text{As, Ge}$)*, *Phys. Rev. B* **95**, 245113(2017)
9. Xiao-Bo Wang, Xiao-Ming Ma, Eve Emmanouilidou, Bing Shen, Chia-Hsiu Hsu, Chun-Sheng Zhou, Yi Zuo, Rong-Rong Song, Su-Yang Xu, Gan Wang, Li Huang, Ni Ni, Chang Liu, *Topological surface electronic states in candidate nodal-line semimetal CaAgAs* , [Arxiv: 1708.06484 \(2017\)](https://arxiv.org/abs/1708.06484), *submit to PRB*.

Experimental study of novel relativistic Mott insulators in the 2-dimensional limit

PI: Claudia Ojeda-Aristizabal

Department of Physics and Astronomy, California State University Long Beach, CA 90840

Program Scope

The Kitaev-Heisenberg model, a quantum compass model that describes a set of spin-1/2 moments in a honeycomb lattice, yields exciting ground states, such as gapless spin liquids and a variety of spin ordered states [1]. In real materials, the Kitaev-Heisenberg model comes to life assisted by electronic correlations, spin-orbit coupling, crystal field effects and a honeycomb arrangement of ions. Compounds with partially filled 4d and 5d orbitals present important spin-orbit coupling, giving rise to insulating Mott states with spin-orbit coupled moments (despite the extended nature of the electronic wavefunctions in 4d and 5d orbitals). In materials like Sodium iridate (Na_2IrO_3) and Ruthenium Chloride (RuCl_3) (Figure 1), the spin-orbit entangled moments present bond directional interactions thanks to their crystalline structure, where the geometric orientation of their IrO_6 and RuCl_6 octahedra is such that the exchange interaction between the moments is highly anisotropic [2][3]. These features together with the Ir and Ru ions forming a honeycomb lattice, graciously leads to an experimental incarnation of the celebrated Heisenberg-Kitaev model.

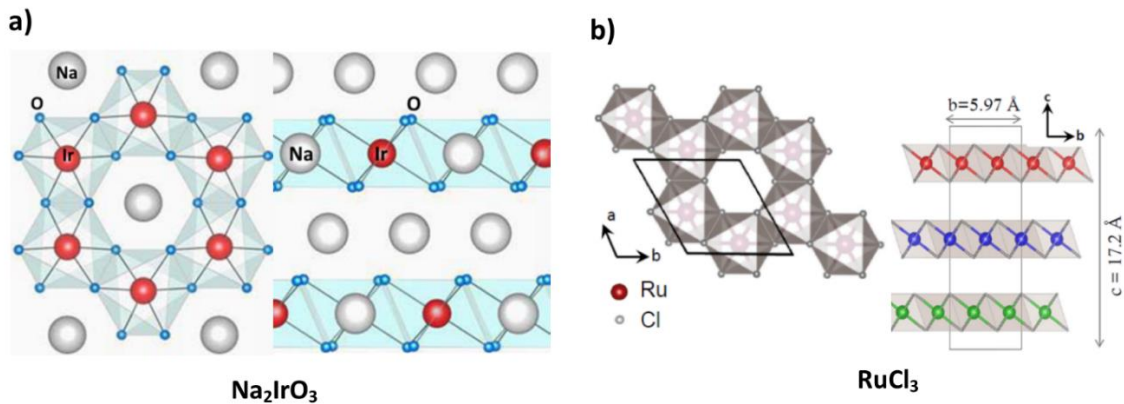


FIG. 1. Schematics of the crystal structure of Na_2IrO_3 (a) and RuCl_3 (b) taken from [4], [5]

Magnetic susceptibility and heat capacity measurements in both of these materials have shown signature of magnetic ordered states [6] [7] [8] [9] and very recent neutron scattering results point towards a spin liquid in RuCl_3 [10].

This project aims to study these exciting compounds in the two dimensional limit, using two different experimental techniques: electronic transport measurements at low temperatures and

angle resolved photoemission spectroscopy (ARPES). Both sodium iridate and ruthenium chloride have weakly bounded layers which allows the isolation of very thin crystals and the use of nanofabrication techniques to integrate them into an electronic device, allowing electronic transport measurements not explored before for their parent crystals. ARPES measurements will allow us to investigate the spin and orbital texture of electrons in these materials as well as the in-situ growth and tailoring of a thin film of RuCl_3 , in order to explore a truly two-dimensional quantum magnet, compatible with an electronic device.

Experimental results from both electronic transport and ARPES will be essential to understand and control emerging phenomena such as long ranged ordered antiferromagnetic states, proximity effects with superconductors and many body effects such as spin and charge density waves, predicted for doped Kitaev-Heisenberg systems.

High quality bulk crystals will be provided by the Analytis group at UC Berkeley through our ongoing collaboration. Sample fabrication and electronic transport measurements will be performed at California State University Long Beach and ARPES measurements will be conducted at the Advanced Light Source (ALS) at the Lawrence Berkeley National Lab (LBNL). Our collaboration with the Lanzara group at LBNL a world expert in ARPES, will give us access to additional state of the art capabilities.

Recent Progress

We have isolated thin crystals of RuCl_3 and Na_2IrO_3 and applied nanofabrication techniques to build electronic devices (Figure 2). Preliminary measurements on Na_2IrO_3 show a variable range hopping of carriers localized by disorder ($R(T) \propto \exp[(\Delta/T)^{1/4}]$) with an energy scale Δ smaller than the one measured for bulk crystals (Figure 2c) indicating a larger localization length and consistent with reported measurements for heteroepitaxial Na_2IrO_3 .

We have observed through ARPES signature of a metallic feature near the Fermi energy, consistent with recent reports [11] and identified as a surface state, given its small dependence in photon energy compared to the bulk (Figure 3). Our ARPES measurements are consistent with our electronic transport measurements, where electrostatic gating induces a dramatic reduction of the resistance of the sample, possibly tuning the Fermi energy into the metallic feature observed by ARPES. ARPES measurements of RuCl_3 indicate an energy gap of at least 1.7eV (Figure 4) which encourages the use of more powerful gating techniques in electronic transport such as ionic liquid gating or the ARPES in-situ growth of a thin film tailored by doping.

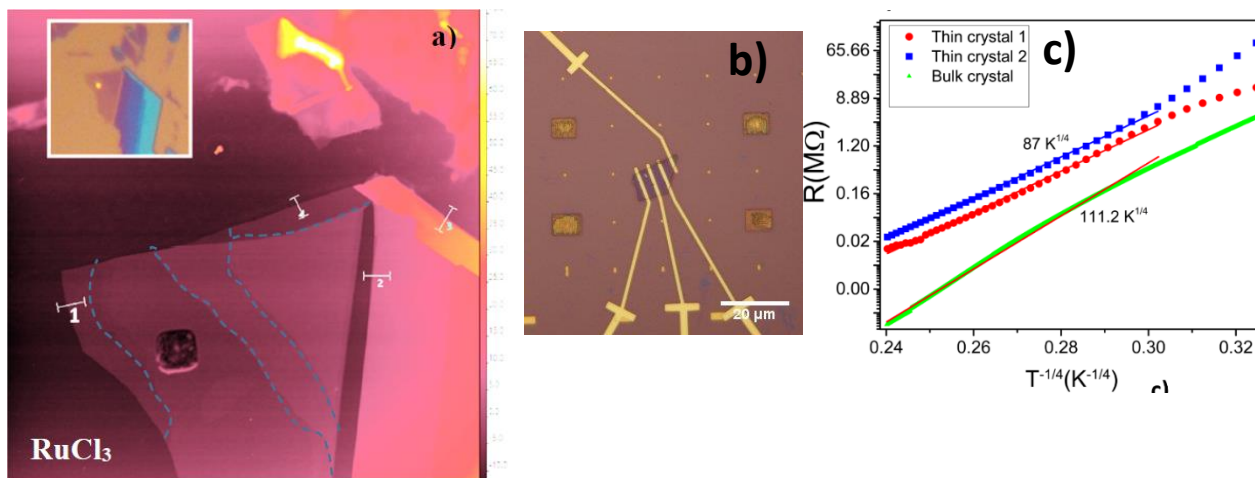


FIG. 2. (a) Atomic force microscopy (AFM) image of mechanically exfoliated RuCl_3 showing a thickness of 3.5nm (region 1). Different crystalline layers can be identified, marked with a pointed line. Inset: optical image of the same crystal. (b) 150nm thick crystal of Na_2IrO_3 . (c) Electronic device of RuCl_3 . Crystals provided by the Analytis group at UC Berkeley

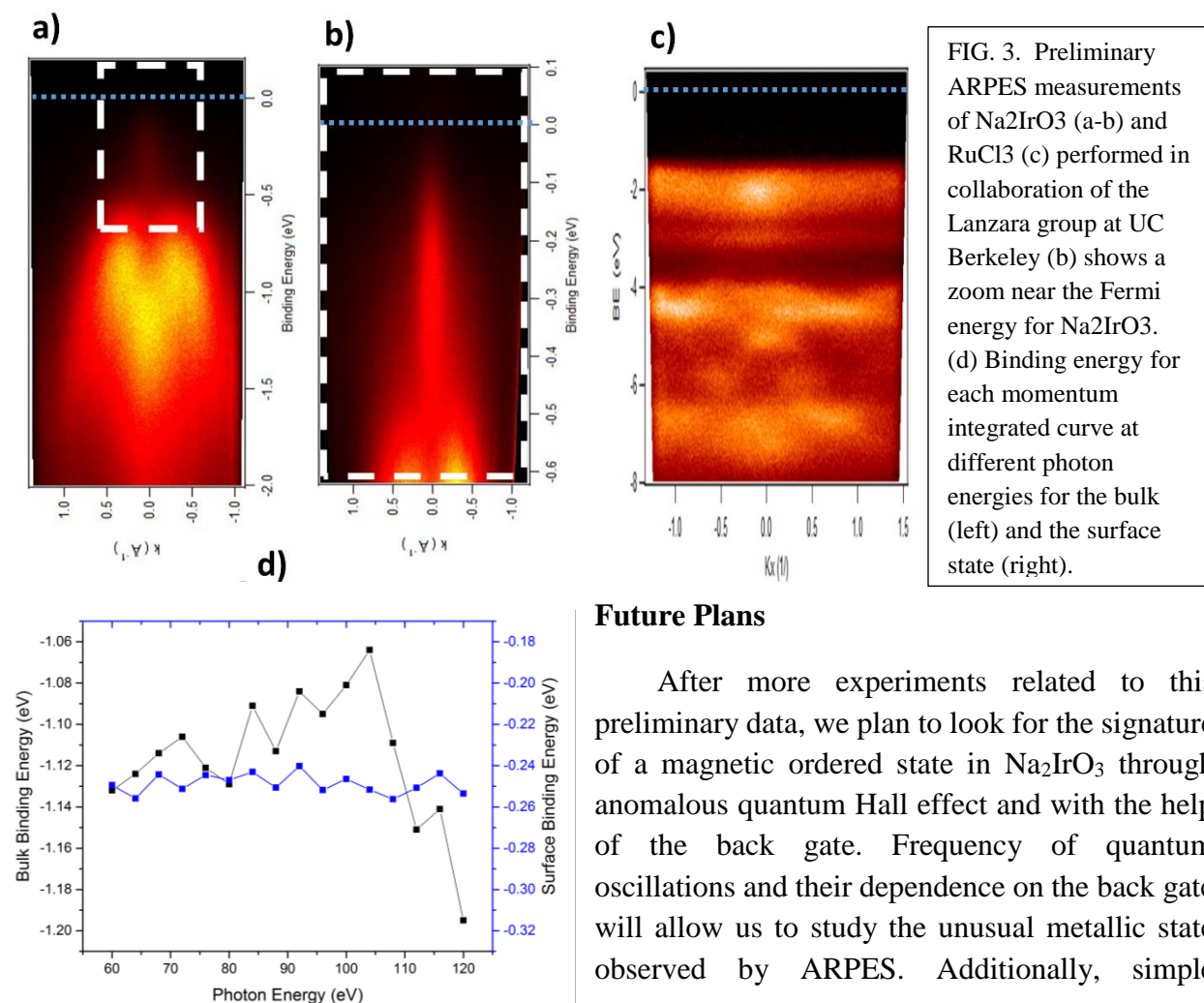


FIG. 3. Preliminary ARPES measurements of Na_2IrO_3 (a-b) and RuCl_3 (c) performed in collaboration of the Lanzara group at UC Berkeley (b) shows a zoom near the Fermi energy for Na_2IrO_3 . (d) Binding energy for each momentum integrated curve at different photon energies for the bulk (left) and the surface state (right).

Future Plans

After more experiments related to this preliminary data, we plan to look for the signature of a magnetic ordered state in Na_2IrO_3 through anomalous quantum Hall effect and with the help of the back gate. Frequency of quantum oscillations and their dependence on the back gate will allow us to study the unusual metallic state observed by ARPES. Additionally, simple

temperature dependence of the resistance of thin crystals of RuCl_3 and Na_2IrO_3 should give us information of the electrons' localization length as the crystals get closer to a two-dimensional regime. ARPES will provide an excellent complementary tool to gauge the electronic properties of these materials. For example, beam-line 4 at the ALS allows to impose different polarizations to the light that when shined on spin-orbit coupled materials like Na_2IrO_3 and RuCl_3 , should result in a spin-dependent differential absorption of left vs right circularly polarized light, called circular dichroism (CD). The study of CD in these materials can give insight on the helicity of their electronic states, in particular the feature observed near the Fermi energy by ARPES. Longer term plans include the study of proximity effects of thin crystals of Na_2IrO_3 and RuCl_3 with a superconductor through electronic transport measurements, the study of many body effects such as superconductivity and charge density waves predicted for the doped Kitaev-Heisenberg model and finally, the in-situ growth and tailoring by ARPES of a thin film of RuCl_3 , with the motivation of reaching a truly two-dimensional quantum magnet.

References

- [1] J. Chaloupka, G. Jackeli, and G. Khaliullin, "Zigzag magnetic order in the iridium oxide Na_2IrO_3 ," *Phys Rev Lett*, **110**, 097204 (2013).
- [2] G. Jackeli and G. Khaliullin, *Phys. Rev. Lett* **102**, 017205 (2009).
- [3] S. Trebst Lecture Notes of the 48th IFF Spring School "Topological Matter – Topological Insulators, Skyrmions and Majoranas" (Forschungszentrum January, 2017). arXiv: 1701.07056.
- [4] Hyun-Jung Kim, Jun-Ho Lee & Jun-Hyung Cho, *Scientific Reports* **4**, 5223 (2014).
- [5] A. Banerjee, C. A. Bridges, J.-Q. Yan, A. A. Aczell, L. P. M. B. Stoner, G. E. Granroth, M. D. Lumsden, Y. Yiu, J. Knolle, S. Bhattacharjee, D. L. Kovrizhin, R. Moessner, D. A. Tennant, D. G. Mandrus and S. E. Naglerill, *Nature Materials* DOI: 10.1038/NMAT4604.
- [6] Y. Singh and P. Gegenwart, *Phys Rev B* **82**, 6 (2010).
- [7] J. A. Sears, M. Songvilay, K. W. Plumb, J. P. Clancy, Y. Qiu, Y. Zhao, D. Parshall and Young-June Kim, *Phys. Rev. B* **91**, 144420 (2015).
- [8] Yogesh Singh and P. Gegenwart, *Phys. Rev. B* **82**, 064412 (2010).
- [9] X. Liu, T. Berlijn, W.-G. Yin, W. Ku, A. Tsvelik, Young-June Kim, H. Gretarsson, Yogesh Singh, P. Gegenwart and J. P. Hill, *Phys Rev. B* **83**, 220403 (2011).
- [10] A. Banerjee, et al. Neutron scattering in the proximate quantum spin liquid α - RuCl_3 . *Science* **356**, 1055-1059 (2017).
- [11] N. Alidoust, C. Liu, S. Xu, I. Belopolski, T. Qi, M. Zeng, D. S. Sanchez, H. Zheng, G. Bian, M. Neupane, Y. Liu, S. D. Wilson, H. Lin, A. Bansil, G. Cao, and Z. M. Hasan, *Phys Rev B*, **93**, 245132 (2016).

Publications

No publications are yet supported by the DOE as the project has just started (08/01/2017)

A gap-protected zero-Hall effect state in the quantum limit of the nonsymmorphic metal KHgSb

N. Phuan Ong, Department of Physics, Princeton University

Program Scope

The research goal is the investigation of nonsymmorphic semimetals to explore novel transport properties associated with their topological states. In addition, the proposed research will investigate microwave absorption of Weyl semimetals to search for signatures of surface Fermi arc states. Possible effects of the appearance of the chiral anomaly in Dirac semimetals on ultrasonic attenuation will also be investigated.

Recent Progress

Nonsymmorphic lattices are distinguished by having glide operations (reflections combined with a fractional lattice translation) which leave the crystal lattice invariant. Recently, much interest has focused on how the glide operations can protect surface states over an extended lines and faces of the surface Brillouin zone (as opposed to just isolated points, e.g. Γ or the corners (π, π) in topological insulators). In the new semimetal KHgSb, the lattice is left invariant if we reflect about the y - z mirror plane (shaded blue in inset in Fig. 1) combined with a translation along z by $c/2$. The glide symmetry has been shown to protect Quantum Spin Hall (QSH) states on the vertical surfaces in the inset of Fig. 1 (but not on the horizontal faces).

We have investigated the Hall effect and magnetoresistance of KHgSb in fields \mathbf{H} up to 63 Tesla. We uncover a novel feature in the Hall response when the chemical potential μ enters the lowest Landau level in large H . At 2 K, with $\mathbf{H} \parallel \mathbf{z}$, the Hall resistivity ρ_{yx} vanishes within our resolution (Fig. 2) while the diagonal conductivity element σ_{xx} settles down to a finite constant value. As shown in Fig. 1, the traces of ρ_{yx} vs. H display very strong dependence on T (temperature), which is rare in metals and semimetals. We have found that this reflects thermal activation across a large gap in the Landau spectrum ($\Delta \sim 14$ mV at 63 T) which opens up when μ enters the lowest Landau level (LLL).

Our results imply that the bulk carriers undergo condensation to become strongly localized, leaving the surface states to carry the injected current. The *ab initio* calculations reveal

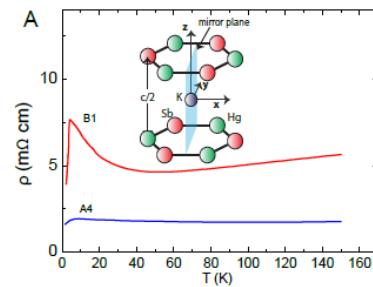


Figure 1: The resistivity ρ vs. T profile of KHgSb. Inset is the crystal lattice.

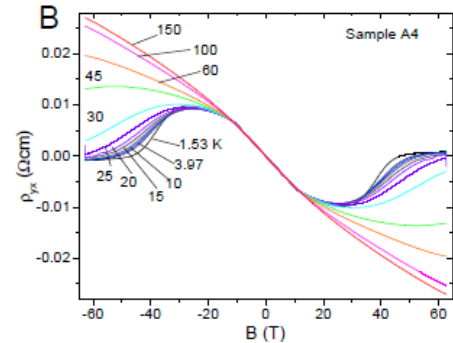


Figure 2: The Hall resistivity ρ_{yx} in KHgSb. At 1.5 K, ρ_{yx} falls sharply to zero above 40 T. The strong T dependence reflects activation across a gap.

that μ intersects 2 “right-moving” and 2 left-moving QSH states. Cancellation between the right and left moving states results in a strictly zero Hall conductance, while the diagonal conductance remains finite. These observations imply that surface QSH states can exist in a bulk crystal that has glide symmetry.

Future Plans

Our plan is to further investigation of the interesting zero-Hall state in KHgSb (and its analogs KHgAs) to determine the nature of the zero Hall state.

References

1. Sihang Liang, Satya Kushwaha, Tong Gao, Max Hirschberger, Jian Li, Zhijun Wang, Karolina Stolze, B. A. Bernevig, R. J. Cava, and N. P. Ong, “A gap-protected zero-Hall effect state in the quantum limit of the nonsymmorphic metal KHgSb,” *in preparation*.

Publications

Understanding and Manipulating Quantum Spin Exchange Interactions in Colloidal Magnet Based Nanostructures by Ultrafast Light

Min Ouyang, University of Maryland- College Park

Program Scope

This awarded DOE program is aimed at exploring a few fundamental spin interactions at the nanoscale by combining both materials development and various optical spectroscopic tools. Ultrafast and single photon optical spectroscopies are applied to probe and to manipulate quantum spin couplings within both pure and hybrid magnetic nanostructures [1-4], which can be chemically synthesized with precisely tailored structural and magnetic properties.

Recent Progress

We have made substantial progress on two themes during our first grant period, including materials development of magnet based zero-dimensional hybrid nanostructures and optical study to understand and manipulate spin dynamics. In particular, we have successfully synthesized different colloidal central spin systems that can allow probing nanoscale magnetic properties and spin interactions. Figure shows one example of colloidal central spin system consisting of one single nitrogen-vacancy (NV) center and its coupled satellite magnetic nanoparticles with controllable structural and magnetic parameters, in which spin dynamics of super-paramagnetic nanoparticles (Fe_3O_4) can be

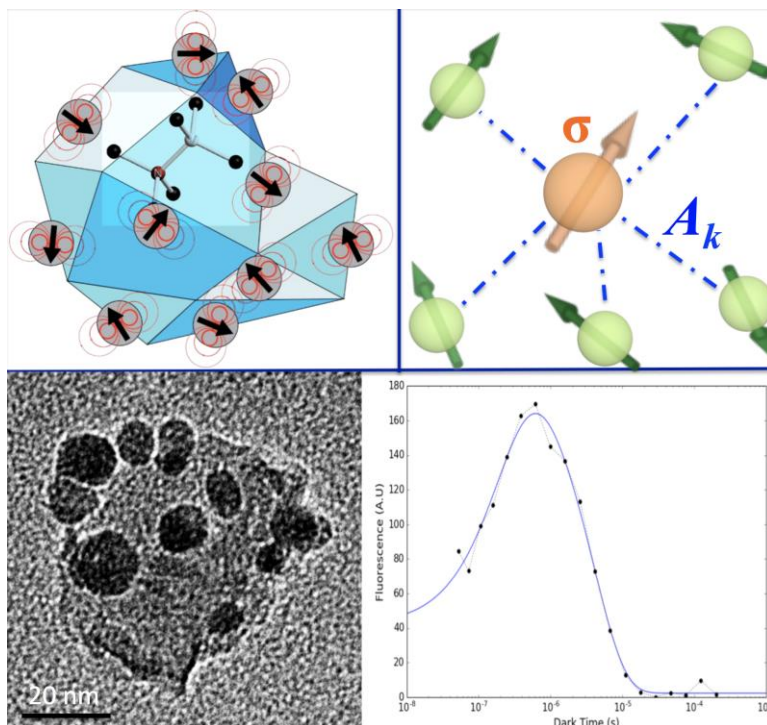


Figure: (Top left) Structural model of a NV center based hybrid magnetic nanostructure; (Top right) Schematic of a central spin system; (Bottom) TEM image of a NV- Fe_3O_4 hybrid nanostructure, and single photon optical measurement of longitudinal spin relaxation of super-paramagnetic Fe_3O_4 nanoparticles by central NV spin.

sensed by the spin of central NV center confined in a nanodiamond. The other major system that we have developed during the grant period is a complex colloidal metal-semiconductor hybrid nanostructures that can allow localized plasmon enhanced all optical spin manipulation and measurement of many body spin physics at the nanoscale by utilizing ultrafast optical spectroscopy.

Future Plans

We will continue our materials development of well-defined colloidal magnet based nanostructures that can serve as model systems for understanding fundamental spin physics. In the mean time, different optics based spin measurement and manipulation methods will be advanced for probing spin dynamics within those colloidal nanostructures.

References

- [1] J. Zhang, Y. Tang, K. Lee and M. Ouyang, Nonepitaxial growth of hybrid core-shell nanostructures with large lattice mismatches, *Science* **327**, 1634 (2010).
- [2] J. Zhang, Y. Tang, K. Lee and M. Ouyang, Tailoring light-matter-spin interactions in colloidal hetero-nanostructures, *Nature* **466**, 91 (2010).
- [3] L. Weng, H. Zhang, A. O. Govorov and M. Ouyang, Hierarchical synthesis of non-centrosymmetric hybrid nanostructures and enabled plasmon-driven photocatalysis. *Nat. Commun.* **5**, 4792 (2014).
- [4] J. Gong, N. Steinsultz and M. Ouyang, Nanodiamond-based nanostructures for coupling nitrogen-vacancy centres to metal nanoparticles and semiconductor quantum dots. *Nat. Commun.* **7**, 11820 (2016).

Publications

1. J. Ren, H. Guo, J. Pan, Y. Zhang, Y.-F. Yang, X. Wu, S. Du, M. Ouyang and H.-J. Gao, Inter-atomic spin coupling in manganese clusters registered on graphene. *Phys.Rev.Lett.* (2017, under review).
2. J. Gong, N. Steinsultz and M. Ouyang, Nanodiamond-based nanostructures for coupling nitrogen-vacancy centres to metal nanoparticles and semiconductor quantum dots. *Nat. Commun.* **7**, 11820 (2016).
3. S. Yu, J. Zhang, Y. Tang & M. Ouyang, Engineering acoustic phonons and electron-phonon coupling by the nanoscale interface. *Nano Lett.* **15**, 6282 (2015).

Investigation of structural and electronic properties of topological Heusler thin films

Chris J. Palmstrøm (PI), Department of Electrical & Computer Engineering and Materials,
University of California, Santa Barbara, Santa Barbara, CA 93106

and

Anderson Janotti (Co-PI), Department of Materials Science & Engineering, University of
Delaware, Newark, DE 19716

Program Scope

Heusler compounds have emerged as an exciting material system where realization of various exotic topological phases is potentially possible [1-2]. This system is of special interest because Heusler compounds provide a large materials basis with over a thousand members with the same basic crystal structure and tunable functional properties including half-metallicity and superconductivity [3]. However, experimental efforts to realize and utilize novel functional properties in the Heusler compounds have remained limited due to the difficulty in fabricating thin film high-quality single crystalline samples. Within the ambit of this program we are harnessing our expertise in molecular beam epitaxy (MBE) and experience with III-V semiconductors to fabricate high quality, phase pure, epitaxial Heusler compounds, for which III-V semiconductors provide ideal atomic templates on which to synthesize such compounds. Furthermore, by combining high quality synthesis with state-of-the-art tools such as angle-resolved photoemission spectroscopy (ARPES), scanning tunneling electron microscopy (STM) and scanning tunneling spectroscopy (STS) along with reflection high energy electron diffraction (RHEED) and transport measurements we are investigating both their electronic and structural properties and their tunability under substrate induced bi-axial strain and chemical doping. Our experimental results along with insights from ab-initio density functional theory calculations will allow us to develop a comprehensive understanding of these materials that we believe would lead to the realization of *engineered* topological properties in *designer* Heusler compounds.

Recent Progress

In the past, we have successfully synthesized high quality, single crystalline, epitaxial (001) oriented PtLuSb thin films by a judicious choice of a buffer layer (InSb) and substrate (GaAs) [4]. Furthermore, by directly visualizing the momentum- and spin-resolved electronic band structure of PtLuSb by ARPES we have found the presence of topologically non-trivial surface states that establish PtLuSb as a topological Half-Heusler semi-metal [5]. Being a surface sensitive technique, ARPES requires access to a pristine sample surface that is preserved by depositing a thick Sb overlayer before taking the samples out of vacuum. Subsequently, the Sb overlayer is desorbed *in-situ* by heating the samples to above 390 °C before transferring them to a measurement chamber for ARPES without breaking vacuum. However, such an approach imposes severe restrictions on the kind of materials that can be investigated as the requirement of

a constituent element with high vapor pressure such as antimony (Sb) is necessary. Furthermore, such an approach invariably degrades the quality of the sample surface and can potentially leave behind unwanted molecular species on the surface. To get around these issues it is imperative to develop capabilities that would allow the transfer of samples between the growth and measurement chambers without breaking vacuum during the process. To that end, we have designed and built a portable vacuum suitcase that can carry as many as 12 samples while

maintaining ultra-high vacuum conditions. The success of the vacuum suitcase was demonstrated using PtLuSb thin films that were synthesized in our MBE lab at UCSB and were transported using the vacuum suitcase to the ARPES beamline 10.0.1.2 at the Advanced Light Source in Berkeley. Our ability to maintain surface quality of our samples during the transportation process is evident in the good quality of the ARPES data taken at the beamline, as shown in Fig. 1. Furthermore, even after more than 3 days in the vacuum suitcase, samples showed no signs of oxygen in their x-ray photoemission (XPS) spectra. This was also the case for ones that had been transferred into the ARPES end chamber and back into the vacuum suitcase. We believe such a technical breakthrough will enable us to elucidate the electronic properties of many other candidate Heusler compounds with predicted exotic properties that have so far remained out of reach of traditional ARPES measurements.

One such system is $\text{Pt}_{1-x}\text{Au}_x\text{LuSb}$. Though, PtLuSb should ideally be a semimetal, the chemical potential was found to lie below the Dirac point of the surface states, consistent with p-type Hall conductivity, both in our thin films [4] and in the reported values for single crystals [6]. The observation of the Fermi level in the valence band of PtLuSb could be explained by native acceptor defects [7] or by a charge transfer between the III-V substrate and the PtLuSb thin film. To gain insights into the origins of such unintentional doping in our thin films we have performed first-principles calculations based on the Density Functional theory that indicate that the conduction-band minimum in bulk PtLuSb is higher than that of InSb on which the PtLuSb thin film is grown. Assuming a Sb-terminated InSb (001) surface and epitaxial growth of PtLuSb on top of it leads to a charge transfer from PtLuSb to InSb, resulting in a hole density of $1.8 \times 10^{20} \text{ cm}^{-3}$ in a 20 nm-thick PtLuSb thin film, this would be consistent with the observed hole concentration. This charge transfer is caused by the polar mismatch at the InSb/PtLuSb interface, as schematically shown in Fig. 2. Transport measurements of PtLuSb thin films with different thicknesses, where the sheet carrier density is expected to *not* change with the film thickness, would be one way to prove the predicted scenario.

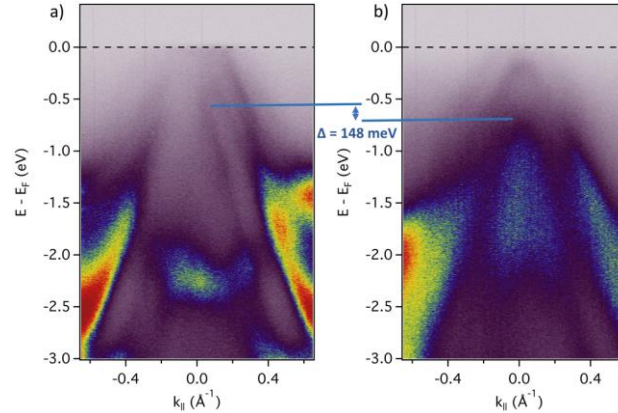


Figure 1. Energy-momentum ($E-k$) spectra of 15 nm thick (001) oriented **a)** PtLuSb **b)** $\text{Pt}_{0.62}\text{Au}_{0.38}\text{LuSb}$ thin film synthesized on InSb buffered GaAs substrate. The spectra were taken at an incident photon energy of 55 eV

One way to shift the chemical potential of the surface state above the Dirac point is to increase the electron density by substituting some of the Pt in PtLuSb with gold (Au), which has one more electron compared to platinum (Pt). We have already successfully grown thin films of Au alloyed PtLuSb with different Au substitution levels, up to 50% (Pt_{0.5}Au_{0.5}LuSb). Transport and *in-situ* STM measurements on these films indicate a shift in chemical potential with doping. By comparing measured electronic band structure of PtLuSb with that of a gold substituted sample (Pt_{0.62}Au_{0.38}LuSb), shown in Fig. 1, we can estimate the shift in chemical potential to be ~ 148 meV. The vacuum suitcase has played an essential role in obtaining these results because the strong reactivity between Au and InSb at the temperature needed to desorb an Sb cap prevents effective desorption of Sb overlayer without destroying the gold doped PtLuSb samples.

Exotic transport and thermodynamic properties expected from topological surface states are often obscured by contributions from trivial bulk carriers. A true bulk gap is an extremely important first step towards realization of other exotic phenomena in these compounds such as quantum anomalous Hall effect [8], axion insulators [9] and topological superconductivity [10] and for possible device applications. PtLuSb being a semi-metal does not possess a bulk band-gap. One way to open a bulk band-gap in PtLuSb is by lifting the degeneracy of the Γ_8 manifold on application of tetragonal distortion, via bi-axial strain.

Our ab-initio calculations confirm this scenario, where a modest in-plane bi-axial compressive strain shows opening of a bulk band gap in a [001] out-of-plane oriented thin film, while maintaining the band inversion, which is consistent with reported predictions for a similar system [11]. Although, this is challenging for single crystal samples, this can be easily achieved by growing thin films on lattice-mismatched substrates. Our PtLuSb thin films are grown on conductive III-V buffered substrates (Si-doped Al_{1-x}In_xSb), which offer great flexibility in terms of the choice of lattice constants and the level of in-plane compressive strain that can be achieved. We have recently successfully synthesized strained PtLuSb thin films where as much as 2% compressive strain can be achieved for 10 nm thick films.

In addition to topological surface states, a Weyl semi-metallic phase, where the topological states occur within the bulk band structure, can also potentially be realized in Heusler compounds [12]. One such candidate compound is Co₂TiGe, where magnetism in Co₂TiGe removes the time-reversal symmetry leading to magnetic Weyl points. Experimental realization of such a phase has not yet been shown in any material system. We have been able to synthesize high quality,

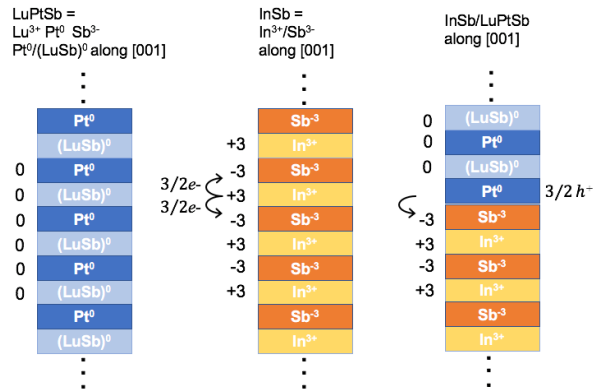


Figure. 2 Origin of the excess charge at the InSb/PtLuSb interface (001). At the interface, there will be a charge transfer from the PtLuSb to the conduction band of InSb due to the polar mismatch and the band alignment

epitaxial thin films of Co_2TiGe , both on (In,Ga)As buffered InP and on MgO substrates [13]. Our thin films have a Curie temperature of 375 K when grown on MgO (001) substrates and 395 K on In(Al,Ga)As buffered InP (001) substrates. A detailed SQUID magnetometry study of our thin films has also allowed us to elucidate the nature of substrate induced magneto-crystalline anisotropy in these thin films.

Future Plans

We plan to 1) bring the chemical potential in PtLuSb to the surface state Dirac point via Au substitution, 2) investigate bi-axial strain to open up a bulk band-gap for $\text{Pt}_{1-x}\text{Au}_x\text{LuSb}$, 3) measure the band structure of Co_2TiGe and other Heusler compounds that are predicted to be topological, 4) verify whether the polarity mismatch drive charge transfer scenario is valid in our Heusler thin films by synthesizing Heusler heterostructures, and 5) determine the origins for atomic surface reconstructions on Heuslers and their electronic structure. ARPES and spin-polarized ARPES measurements will be compared with magnetotransport and magnetic measurements and theory to obtain a better fundamental understanding of these Heusler material systems.

References

1. S. Chadov *et al.*, Nature Mater, 9, 541 (2010)
2. H. Lin *et al.*, Nature Mater, 9, 546 (2010)
3. C. J. Palmstrøm, Prog. Cryst. Growth Charact. Mater,62, 371-397 (2016)
4. S. J. Patel *et al.*, Appl. Phys. Lett, 104, 206103 (2014)
5. J. Logan *et al.*, Nature Commun., 7, 11993 (2016)
6. C. Shekhar *et al.*, Appl. Phys. Lett, 100, 252109 (2012)
7. Y. G. G. Yu *et al.*, Phys. Rev. B 95, 25085201 (2017)
8. C-Z. Chang *et al.*, Science, 340, 167 (2013)
9. L. Wu *et al.*, Science, 354, 1124 (2016)
10. L. Fu and C. Kane, Phys. Rev. Lett,100, 096407 (2008)
11. D. Xiao *et al.*, Phys. Rev. Lett, 105, 096404 (2010)
12. Z. Wang *et al.*, Phys. Rev. Lett., 117, 236401 (2016)
13. J. Logan *et al.*, J. Appl. Phys., 121, 213903 (2017)

Publications

J. A. Logan, S. J. Patel, S. D. Harrington, C. M. Polley, B. D. Schultz, T. Balasubramanian, A. Janotti, A. Mikkelsen, and C. J. Palmstrøm, *Observation of a topologically non-trivial surface state in half-Heusler PtLuSb (001) thin films*, Nature Communications **7**, 11993 (2016)

J. A. Logan, T. L. Brown-Heft, S. D. Harrington, N. S. Wilson, A. P. McFadden, A. D. Rice, M. Pendharkar, and C. J. Palmstrøm, *Growth, structural, and magnetic properties of single-crystal full-Heusler Co_2TiGe thin films*, Journal of Applied Physics 121, 213903 (2017)

Effects of Lateral Broken Crystal Symmetries on Spin-Orbit Torques and Magnetic Anisotropy

Daniel C. Ralph, Cornell University

Program Scope

This new (Sept. 1, 2017) program seeks to answer the question: What is the most efficient and reliable mechanism for manipulating the direction of magnetic moments, for example to drive switching in magnetic memory applications? Recently, several mechanisms have been discovered that are more efficient than using magnetic fields to control magnetism. The most promising is known as spin-orbit torque – electrons flowing within a thin-film material with strong spin-orbit coupling can generate a perpendicularly-flowing spin current that can be absorbed by a neighboring magnetic layer to reorient the magnetization of that layer. However, spin-orbit torques usually suffer from a limitation related to symmetry. For most spin-orbit source materials, the form of the spin-orbit torque that can manipulate magnets most readily (the “antidamping” component) is required to point strictly within the sample plane. Consequently the spin-orbit torque from most materials cannot drive the most efficient form of switching in structures with perpendicular magnetic anisotropy, the geometry which at present is needed to generate uniaxial magnetic anisotropy that is sufficiently strong to stabilize nanoscale magnetic memories against thermal fluctuations. The Ralph group and collaborators have demonstrated recently that this state of affairs is not fundamental, but rather that materials with certain broken crystal symmetries can provide both an out-of-plane antidamping spin-orbit torque and significant in-plane uniaxial magnetic anisotropy.¹ The goal of this program is to understand the fundamental mechanisms by which broken crystal symmetries affect spin-orbit torques and magnetic anisotropy and determine the design principles for selecting materials to best implement these new effects for potential applications.

Recent Progress

This program builds upon measurements of spin-orbit torques by the Ralph group and collaborators on structures consisting of a single-crystal thin film of the transition-metal dichalcogenide (TMD) WTe_2 capped by the magnetic alloy Permalloy. WTe_2 is a semi-metal that possesses both strong spin-orbit coupling and a low crystal symmetry (a T_d structure, a lower symmetry than the 2H structure of more-common TMDs such as MoS_2 or $MoSe_2$). As a consequence, a WTe_2 /Permalloy bilayer has only a single mirror plane and no 2-fold (or higher) rotational symmetry. WTe_2 is also convenient for experiments because flat single crystals without even a single monolayer step can be prepared by exfoliation. The Ralph group performed measurements of the spin-orbit torques in WTe_2 /Permalloy samples by passing an in-

plane charge current through the sample and detecting the resulting changes in the magnetization direction of the Permalloy layer due to the spin-orbit torque. To be careful about experimental artifacts, these measurements were performed using two independent techniques: detecting the Permalloy reorientation (i) by microwave-frequency resistance measurements using spin-torque ferromagnetic resonance (ST-FMR), and (ii) by low-frequency Hall-effect measurements in a second-harmonic Hall technique. Both measurements were performed as a function of changing the angle of an in-plane magnetic field, with quantitatively consistent conclusions.

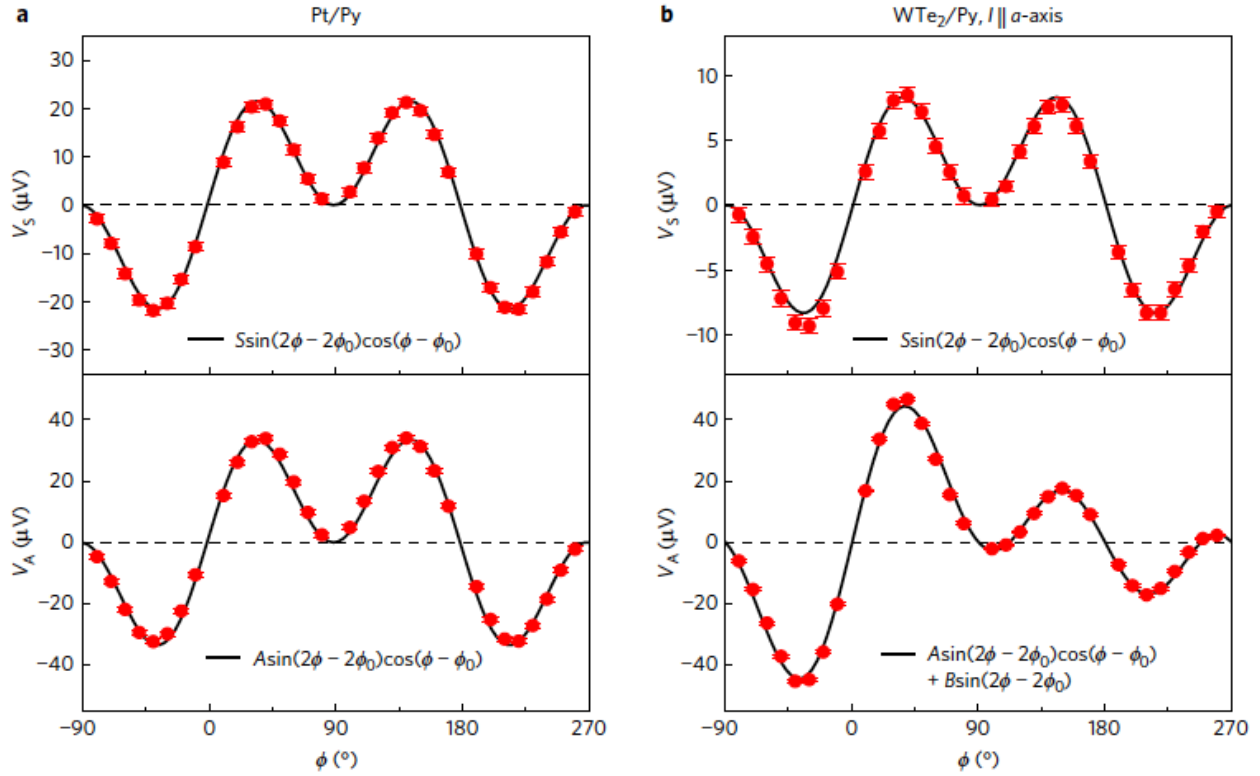


Fig. 1. Amplitude of the symmetric (V_S) and antisymmetric (V_A) components of the ST-FMR resonance as a function of the angle of applied magnetic field for (left) a platinum/Permalloy control sample and (right) a WTe₂/Permalloy sample. The strikingly-different angular dependence in the bottom right reflects the existence an out-of-plane antidamping component of spin-orbit torque that is forbidden by symmetry for Pt/Permalloy.

The results of the ST-FMR measurements are shown in Fig. 1 for current applied perpendicular to the mirror plane of the WTe₂ sample, along with a comparison to a control sample with higher symmetry made from Pt/Permalloy. The quantities plotted are V_S , the symmetric component of the ST-FMR resonance curve that is proportional to the in-plane spin-orbit torque, and V_A , the antisymmetric component of the resonance that is proportional to the out-of-plane torque. Figure 1 shows that for Pt/Permalloy both components have the same functional form for the dependence on magnetic field angle, ϕ ; this form is well-understood. The

symmetric component of the ST-FMR resonance for the WTe₂ sample has the same dependence on \hat{f} as the Pt/Permalloy sample, but the antisymmetric component is strikingly different, in that the signal magnitudes are not the same upon rotating the direction of the magnetic field by 180°. This unusual behavior reflects the broken rotational symmetry in the WTe₂ structure. Based on analysis of the angular dependence, the origin of this new behavior was identified as a new out-of-plane component of anti-damping spin-orbit torque whose existence is normally forbidden in materials with high structural symmetry. The correlation with the WTe₂ crystal structure was further confirmed by making samples in which the applied charge current flows at various angles relative to the WTe₂ mirror plane. As required by symmetry arguments, the out-of-plane anti-damping torque goes to zero when the current is applied parallel to the WTe₂ mirror plane. The magnetic anisotropy of the sample was affected by the broken crystal symmetry as well, with a new component of uniaxial magnetic anisotropy in the sample plane perpendicular to the mirror plane.

This initial experiment showed for the first time that the orientations of spin orbit torques can be modified by the presence of broken crystal symmetries in samples with strong spin-orbit coupling, but the underlying mechanisms were not determined. The Ralph group has in recent months completed a detailed study of the thickness dependence of the spin-orbit torques in WTe₂.² This thickness dependence (Fig. 2) shows that the out-of-plane spin-orbit torque has a field-like component that is quantitatively consistent with expectations for the effect of the Oersted field produced by current flowing in the sample, while the new out-of-plane antidamping torque has only a very weak thickness dependence, with even a single monolayer of WTe₂ producing a strong out-of-plane antidamping torque. This is suggestive that the new out-of-plane antidamping torque arises from an interface-scattering effect rather than from a spin Hall effect within the bulk of the WTe₂. These newer measurements also confirmed that the sign of the out-of-plane antidamping torque is reversed when there is a monolayer step in the WTe₂ at the interface with the Permalloy. This is as required by the crystal structure of WTe₂, because there is a 180° rotation between the structure of neighboring planes in WTe₂.

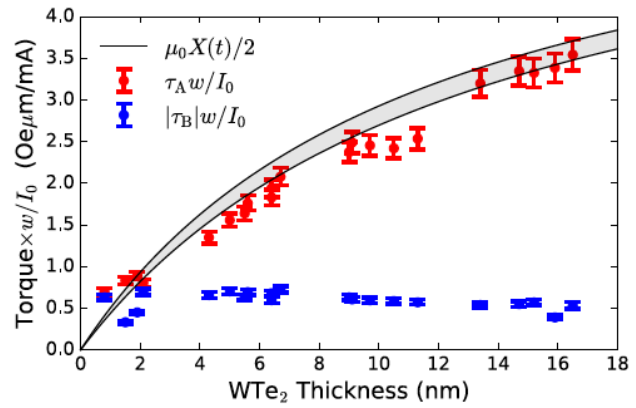


Fig. 2. The out-of-plane field-like torque, t_A , depends on WTe₂ thickness as expected for the contribution from the current-induced Oersted field, but the out-of-plane antidamping torque, t_B , has a much weaker dependence on WTe₂ thickness.

Future Plans

Our plans for the future have not changed from the proposal that was recently approved.

Our first objective is to make measurements of spin-orbit torques and magnetic anisotropy for magnetic layers coupled to a variety of different materials that possess both strong spin-orbit coupling and different types of low crystal symmetry. Our initial targets are TaTe₂, MoTe₂, CdWO₄, 2H-structure TMDs with applied in-plane strain, and doped-HfO₂ ferroelectrics. We have the sample fabrication protocols and measurement methods well in hand. We hope that by comparing the different symmetries of spin-orbit torques generated by these systems, and also the relative strengths of the torques, that we will gain insights into the underlying mechanisms of how broken symmetries affect the torques. We will also seek understanding about how to make both the out-of-plane antidamping torque and the in-plane uniaxial anisotropy as strong as possible.

We plan to perform additional measurements on WTe₂/Permalloy samples with very thin WTe₂ to follow up on experimental hints of an even-odd effect in the strength of the out-of-plane antidamping torque as a function of WTe₂ layer number (in samples to date, 2-layer samples produce a weaker effect than either 1-layer or 3-layer samples). If this is confirmed by future measurements, it may be an important clue as to mechanisms.

We have begun an active collaboration with a new postdoc (Dr. Nikhil Sivadas) in Craig Fennie's group at Cornell to perform ab-initio modeling of the spin-orbit torques and anisotropies in our structures. With him we hope to move beyond symmetry arguments to gain a microscopic understanding about the influence of different electronic orbitals and interface structures. We are discussing ideas for additional experiments with the theorist Paul Haney at NIST. Finally, we have begun a collaboration with Lena Kourkoutis at Cornell to perform detailed STEM characterization of the physical and chemical structure of the interfaces in our samples.

References

1. D. MacNeill, G. M. Stiehl, M. H. D. Guimaraes, R. A. Buhrman, J. Park, and D. C. Ralph, "Control of spin-orbit torques through crystal symmetry in WTe₂/ferromagnet bilayers," *Nature Physics* **13**, 300-305 (2017).
2. D. MacNeill, G. M. Stiehl, M. H. D. Guimaraes, N. D. Reynolds, R. A. Buhrman, and D. C. Ralph, "Thickness dependence of spin-orbit torques generated by WTe₂," accepted and in press, *Phys. Rev. B.* (arXiv:1707.03757).

Publications

No publications yet supported by BES. (new grant)

Tuning Quantum Fluctuations in Low-Dimensional and Geometrically Frustrated Magnets

Arthur P. Ramirez, University of California Santa Cruz

Program Scope

A challenging frontier in many body physics is the search for low-dimensional spin systems that are fully quantum-entangled and have the potential to support fractionalized excitations. Such quantum spin liquids (QSLs) have been proposed for applications in quantum information¹⁻³ but are interesting in their own right as new forms of quantum-entangled topological matter. Such materials incorporate both the suppression of classical long-range ordered (LRO) states via geometrical frustration⁴ and continuous spin-1/2 ions which are most likely to exhibit quantum fluctuations⁵. In such systems, not only is entropy shifted down to low temperatures, but the associated fluctuations should have strong quantum character. Using this approach, a few model spin systems exist that exhibit bulk response – e.g. NMR, neutron scattering, and thermodynamic properties – that is difficult to explain using classical models.⁶

Most claims of QSL behavior have been made for systems possessing the materials attributes mentioned above. An alternative to searching materials phase space for QSL candidates is to develop candidate materials in which quantum fluctuations can be tuned parametrically. Such materials will allow stringent tests of QSL behavior. In addition parametric tunability provides a basis for possible devices. The goal of this project is to develop materials that are amenable to such a tunability paradigm. The work will involve three distinct thrusts. In the **first thrust**, we will explore magnetic field effects on quasi-1D and quasi-2D spin systems, specifically compounds incorporating spin-1/2 Cu^{2+} with molecular ligands. In such systems the large molecules lead to small spin exchange interactions ($1-5k_B$) in the low-D sublattice. These systems should undergo 3D LRO below 1K, allowing interplay of the Zeeman energy with both 3D and low-D energy scales. Our initial work, described below, suggests that magnetic field is an effective tuning parameter to realize quantum entangled states in such systems. In the **second thrust**, we will study two-dimensional (2D) Ising compounds in transverse magnetic fields. These systems, mainly involving Co^{2+} and Dy^{3+} , should be tunable through a quantum critical point, the vicinity in which could be a highly entropic quantum entangled state. This study will extend beyond existing work on 3D and 1D transverse field Ising model (TFIM) systems that demonstrated signs of quantum entanglement. In the **third thrust** we seek to develop new geometrically frustrated compounds with the potential to exhibit QSL ground states and to ultimately feed into the first two thrusts. Our initial work here has identified the so-called “tripod kagome” lattice as a promising materials family. These three thrusts are complementary yet synergistic since all involve a combination of materials exploration and detailed thermodynamic measurements at ultra-low temperatures.

Recent Progress

Initial work was performed on $\text{K}_2\text{PbCu}(\text{NO}_2)_6$, “elpasolite phase”, which adopt an fcc structure at room temperature. This compound displays an incommensurate structural phase between 273 and 281K, driven by the Cu^{2+} JT distortion. Below 273K and down to low temperature, the structure undergoes 2% compression in the c -direction, which favors quasi-1D spin interactions perpendicular to the a - b plane. The 1D behavior is evidenced in the susceptibility, $\chi(T)$, which follows a Bonner-Fisher calculation for AF spin-1/2 chains with exchange coupling of $J = 5.4\text{K}$ (fig. 1, inset). For $H = 0$, Blöte previously reported a single broad ordering peak in $C(T)$ at 0.5K, (fig. 1, inset).⁷ We have measured $C(T)$ as a function of H on crystals grown by T. Siegrist (FSU/NHMFL). At $H = 0$ we now find three sharp transitions, shown in fig. 1, indicative of samples possessing low disorder.⁸ For finite H (parallel to (100)) we see that the lower transition phase boundary terminates above $2T$, indicative of a symmetry-preserving first order transition. The two higher temperature $H = 0$ transitions exhibit $dT_c/dH > 0$ up to $4T$, an effect associated with the reduction of transverse spin fluctuations in ordered spin chains^{9,10}. Measurements of $C(T_{\text{fixed}}, H)$, as shown in fig. 2, show two sharp peaks that continue the phase lines determined in fixed field measurements. The combined height of these peaks levels off below 0.2K , with a magnitude suggestive of a spinon Sommerfeld coefficient, as observed for isolated spin chains in $\text{Cu}(\text{C}_4\text{H}_4\text{N}_2)(\text{NO}_3)_2$.¹¹

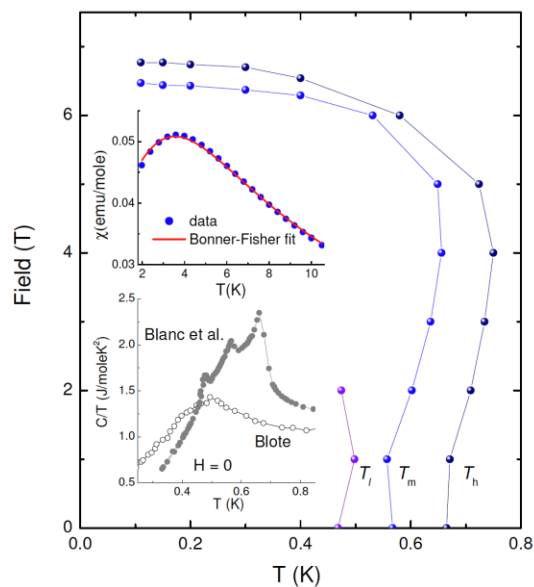


Fig 1. Phase diagram of $\text{K}_2\text{PbCu}(\text{NO}_2)_6$ determined by specific heat peaks⁸. Top inset: susceptibility fit to a finite chain calculation. Bottom inset: Comparison of our $H=0$ data with those of Blöte⁷

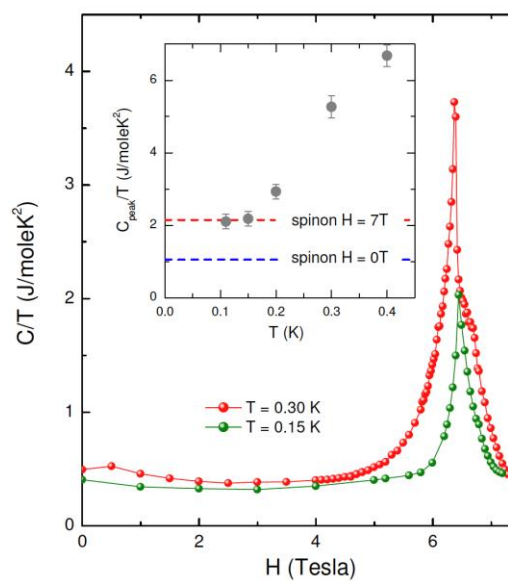


Fig 2. Specific heat versus field for $\text{K}_2\text{PbCu}(\text{NO}_2)_6$. Inset: Maxima of C/T at the peak position vs T , compared to the results of a spinon calculation for two values of H .⁸

Theoretical work is needed to validate the identification of this $C(T,H)$ peak with a spinon origin but the empirical results are novel. First, the value of the critical field, $H_c = 6\text{T}$, is clearly related to the in-chain exchange of 5.4K , rather than the critical temperature at $H = 0$. Second, $C(T, H)$ is suppressed over much of the field range except near the phase boundary. Thus the weak inter-chain interaction suppresses fluctuations responsible for the Sommerfeld coefficient in isolated chains. Second, the large entropy release at the critical field is markedly different from that seen in either 3D antiferromagnets or in spin dimer systems. These observations are likely to result from the approximate singlet state of the 1D spin chain. Lastly, the sharpness of the $C(T, H)$ peaks both at $H = 0$ and $H = 6.5\text{T}$ provide evidence of low disorder in the spin sublattice.

In other recent work with Haidong Zhou (U. Tennessee), we discovered a new class compounds with rare-earth (RE) spins on the sites of a kagome lattice¹². The compound, $\text{Mg}_2\text{RE}_3\text{Sb}_3\text{O}_{14}$, where RE is a rare-earth ion, is a derivative of the pyrochlore structure, but here, Sb^{5+} replaces Ti^{4+} , and the RE sublattice is comprised exclusively of kagome planes. Because the single-ion anisotropy is that of the parent pyrochlore structure, the easy axes are neither uniaxial nor uniplanar – they form a “tripod” for each triangle, as shown in fig. 11.

Initial results, including $C(T)$ and $\chi_{ac}(T)$ on this “tripod Kagome lattice” were obtained for Pr, Nd, Gd, Tb, Dy, Ho, Er, and Yb.^{12,13} where the spin types include Ising (Dy, Ho), XY (Er), Heisenberg (Yb), and singlet (Pr). The Gd spins undergo LRO, consistent with Maleev’s theory of interacting dipoles in 2D¹⁴ and the critical specific heat compares well with a recent numerical result found for classical dipoles on the kagome lattice¹⁵. The Dy compound, unlike its pyrochlore cousin, orders at a temperature consistent with the Weiss constant and our simulations suggest a 120° coplanar state, which is a rare example of ordering on a kagome lattice. The Er compound orders at a temperature two orders of magnitude lower than the Weiss constant, and the simulations suggest the ordered state is projected from the XY planes, the normals of which form a tripod, into a state that is, by coincidence, the same as found for Gd. Finally, the Nd compound has been reported by others to an all-in-all-out state with $T_c = 0.56\text{K}$, possibly stabilized by Dzyaloshinskii-Moriya interactions.¹⁶ We note that, for the systems exhibiting LRO, the $C(T, H=0)$ peaks are very sharp, indicating a high degree of structural order on the magnetic sublattice.

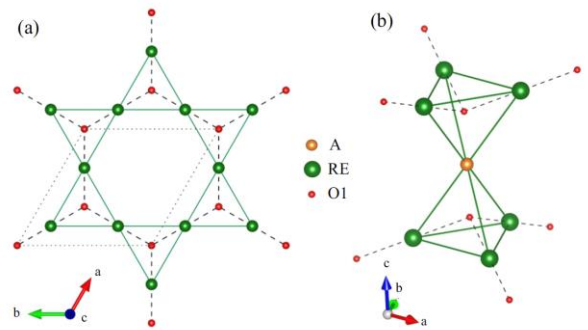


Fig. 3 (a) A single kagome layer with surrounding O1 in the TKL $\text{A}_2\text{RE}_3\text{Sb}_3\text{O}_{14}$. (b) Position of the A^{2+} ion in joining two corner-two tetrahedral. The dashed lines represent the Ising axes.

Future Plans

We will continue to explore the **Thrust 1** work on low-dimensional spin systems at the 3D QCP. In particular, in collaboration with theory colleagues, we will explore quantitatively the influence of quantum fluctuations at the QCP. We will also study 2D compounds where initial work suggests a similar field-induced flow of entropy into the 3D critical region. For **Thrust 2** work we have initiated the development of necessary technology for handling the mechanical strain associated with field-induced torquing of Ising magnets with the application of transverse field. A strategy we will likely adopt is to work with very small samples in order to reduce torquing. This will require the development of ac-calorimetry. In **Thrust 3** work, we continue to explore novel compounds.

References

- 1 Kitaev, A., *Annals of Physics* **321**, 2-111, (2006) 10.1016/j.aop.2005.10.005.
- 2 Kitaev, A. Y., *Annals of Physics* **303**, 2-30, (2003) 10.1016/s0003-4916(02)00018-0.
- 3 Nayak, C., Simon, S. H., Stern, A., Freedman, M. & Das Sarma, S., *Reviews of Modern Physics* **80**, 1083-1159, (2008) 10.1103/RevModPhys.80.1083.
- 4 Ramirez, A. P., *Annual Review of Materials Science* **24**, 453-480, (1994)
- 5 Sachdev, S. *Quantum Phase Transitions*. 2nd edn, (Cambridge University Press, 2011).
- 6 Balents, L., *Nature* **464**, 199-208, (2010) 10.1038/nature08917.
- 7 Blote, H. W. J., *Journal of Applied Physics* **50**, 1825-1827, (1979)
- 8 Blanc, N., Trinh, J., Dong, L., Bai, X., Aczel, A., Mourigal, M., Balents, L., Siegrist, T. & Ramirez, A. P., *manuscript in preparation*, (2016)
- 9 Villain, J. & Loveluck, J. M., *Journal De Physique Lettres* **38**, L77-L80, (1977)
- 10 Hijmans, J., Kopinga, K., Boersma, F. & Dejonge, W. J. M., *Physical Review Letters* **40**, 1108-1111, (1978) 10.1103/PhysRevLett.40.1108.
- 11 Hammar, P. R., Stone, M. B., Reich, D. H., Broholm, C., Gibson, P. J., Turnbull, M. M., Landee, C. P. & Oshikawa, M., *Physical Review B* **59**, 1008-1015, (1999) 10.1103/PhysRevB.59.1008.
- 12 Dun, Z. L., Trinh, J., Li, K., Lee, M., Chen, K. W., Baumbach, R., Hu, Y. F., Wang, Y. X., Choi, E. S., Shastry, B. S., Ramirez, A. P. & Zhou, H. D., *Physical Review Letters* **116**, (2016) 10.1103/PhysRevLett.116.157201.
- 13 Dun, Z. L., Trinh, J., Lee, M., Choi, E. S., Li, K., Hu, Y. F., Wang, Y. X., Blanc, N., Ramirez, A. P. & Zhou, H. D., *Physical Review B* **95**, (2017) 10.1103/PhysRevB.95.104439.
- 14 Maleev, S. V., , *Zhurnal Eksperimentalnoi I Teoreticheskoi Fiziki* **70**, 2374-2389, (1976)
- 15 Maksymenko, M., Chandra, V. R. & Moessner, R., , *Physical Review B* **91**, (2015) 10.1103/PhysRevB.91.184407.
- 16 Scheie, A., Sanders, M., Krizan, J., Qiu, Y., Cava, R. J. & Broholm, C., , *Physical Review B* **93**, (2016) 10.1103/PhysRevB.93.180407.

Publications

No publications have resulted from the D.O.E. project to date.

Program Title: Correlated and Complex Materials

Principle Investigator: B. C. Sales; Co PIs: L. A. Boatner, D. Mandrus, A. F. May, M. A. McGuire, J.-Q. Yan

Materials Science and Technology Division, Oak Ridge National Laboratory, Oak Ridge, TN 37831

Email: salesbc@ornl.gov

Program Scope

This program aims to attain a predictive understanding of the behavior of key correlated and complex materials (CCM). Virtually all of the diverse topics and materials to be investigated involve some aspect of magnetism associated with partially filled d or 4f shells. These include the role of magnetic fluctuations in iron-based superconductors, the behavior of layered and cleavable ferromagnets, the effects of spin orbit coupling in 4d/5d transition metals, the conduction of heat by magnetic excitations and the effects of disorder on quantum critical behavior. Many of the spectacular properties of CCM are believed to result from competing ground states that are close in energy, and hence CCM are often responsive to small changes in composition, temperature, pressure, electric, or magnetic fields. The experimental tools of materials synthesis, compositional tuning, and crystal growth are used to address cutting edge issues in the physics of these systems, with particular focus on the discovery and investigation of novel cooperative phenomena and new forms of order in CCM. A substantial fraction of the effort is devoted to the discovery of innovative materials and the growth of large single crystals of fundamental interest to materials physics. Single crystals are prepared using a variety of techniques, including flux growth, vapor transport, Bridgman, and optical-floating-zone growth, including a new high-pressure optical floating zone furnace. The ability to prepare synthetically challenging and sometimes unique single crystals is a major strength of this project. The program works to identify and synthesize “model compounds” that are complicated enough to exhibit the properties of interest but simple enough to be amenable to both theory and experiment. The composition of these materials is carefully controlled, and the effects of compositional tuning on the basic physics of the materials are studied by measurement of X-ray and neutron diffraction, magnetization, specific heat, electrical and thermal transport, scanning transmission electron microscopy, and electron energy loss spectroscopy. Once the materials have been prepared and a basic understanding of their behaviors has been developed, in-depth experiments such as inelastic neutron scattering, photoemission, and scanning tunneling microscopy are performed (through collaborations) in order to obtain a deeper understanding of the relevant physics. Some of the materials investigated are promising for energy-related applications, such as superconductors for grid applications and thermoelectrics and permanent magnets for energy conversion.

Recent Progress

Cleavable Van der Waals bonded magnets CrI_3 , CrCl_3 , CrTe_3 , RuCl_3 , $\text{Fe}_{3-x}\text{GeTe}_2$

Single crystals of van der Waals bonded magnets are attractive for studying magnetism in the quasi-2D limit, in very thin crystals, and in monolayers. These materials have been used to probe the physics of quantum spin liquids (RuCl_3) [1], and demonstrate ferromagnetism at the monolayer limit (CrI_3) [2,3]. Development of such ultra-thin magnetic materials also may help enable continued advancement in miniaturization and performance enhancement of electronic devices, either as electronically active components themselves, or through interfacing with materials like graphene.

Recently we have grown and characterized several “new” cleavable magnets such as CrCl_3 , CrTe_3 and $\text{Fe}_{3-x}\text{GeTe}_2$ [2-6]. Some results from the CrCl_3 research [4] are illustrated in Fig. 1. Ferromagnetism develops within each layer at T_c 17 K followed by a 3D transition to

antiferromagnetism at 14 K. In the ordered state the spin directions can be easily manipulated using magnetic fields of a few kOe. The ability to cleave CrCl_3 to one monolayer was also demonstrated [4].

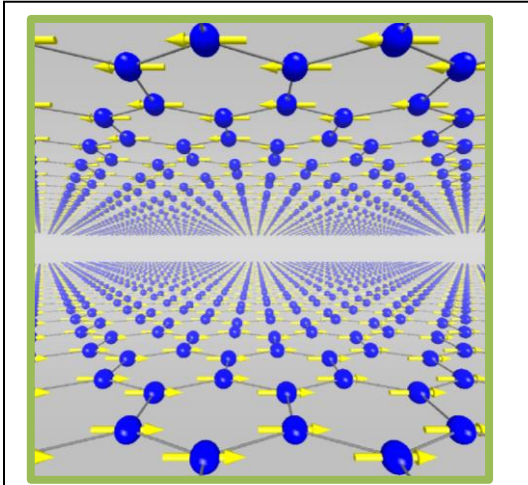


Figure 1. Layers of chromium atoms (blue) in CrCl_3 have ferromagnetic moments (yellow) $T_C=17$ K, with neighboring layers oppositely aligned ($T_N=14$ K). The layers are weakly bound to one another and can be cleaved to one atomic layer. Spin directions can be changed with a few kOe.

Quantum critical behavior and high-entropy alloys

High entropy alloys are concentrated solid solutions typically containing 5 elements in equal concentrations (e.g. CrMnFeCoNi) with extreme chemical disorder but with a simple fcc or bcc crystal structure. Some of these alloys have remarkable structural properties and excellent resistance to radiation damage. Large single crystals can be grown with a typical mosaic spread of 0.4° . During a basic characterization (resistivity, heat capacity, magnetic susceptibility, thermal conductivity) of a series of these alloys we noticed that NiCoCr had very unusual properties; a linear resistivity to at least 0.5 K, and a linear magnetoresistance. Further study showed that NiCoCr is close to the Cr concentration where weak itinerant ferromagnetism disappears [7]. A detailed low temperature thermodynamic study

[8] of crystals very near the critical composition, $\text{NiCoCr}_{0.8}$, showed remarkable agreement with all the predictions of theory in the limit of high disorder [Fig. 2]. To our knowledge this is the best agreement between theory and experiment near a quantum critical point in a metallic system.

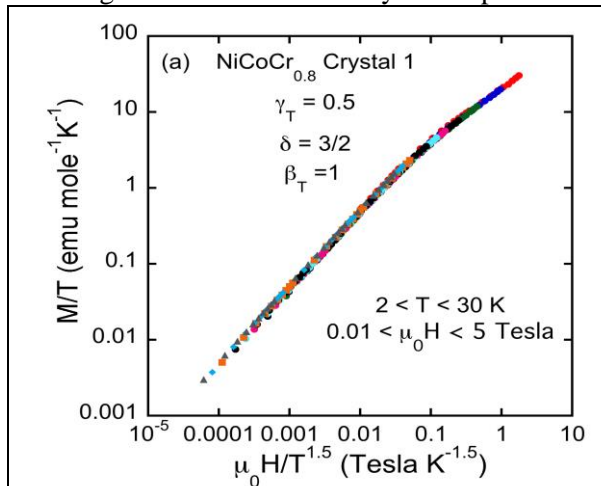


Figure 2. Demonstration of excellent scaling of all magnetization data using experimentally determined values of $\gamma_T \approx 0.5$ and $\beta_T \approx 1$. There are no adjustable parameters. The Widom relationship is also verified [$\gamma_T = \beta_T(\delta-1)$].

First Experimental Evidence for “Kondo Cloud” in $\text{Yb}_{14}\text{MnSb}_{11}$

The magnetic screening cloud or “Kondo Cloud” around a magnetic impurity in a metal has been hypothesized since the explanation of the Kondo effect in 1964. The Kondo effect describes how a localized magnetic atom in a metal interacts with the conduction electrons. If the sign of the interaction is negative, the conduction electrons can effectively screen the magnetic atom resulting in an apparent loss of magnetism. The many-body singlet that forms results in a minimum in the resistivity and is at the heart of heavy fermion physics and some magnetic mechanisms of superconductivity. The compound $\text{Yb}_{14}\text{MnSb}_{11}$ is an ordered dilute magnetic semiconductor with the magnetic Mn atoms separated by at least 1 nm. The

compound is ferromagnetic below 53 K, has a carrier concentration of $\approx 10^{21}$ holes/cm³, and is an underscreened Kondo ferromagnet with $T_K \approx 300$ K. The size of the Kondo cloud is theoretically estimated to be ≈ 0.5 nm, unlike the highly diffuse extent of the cloud expected in most Kondo

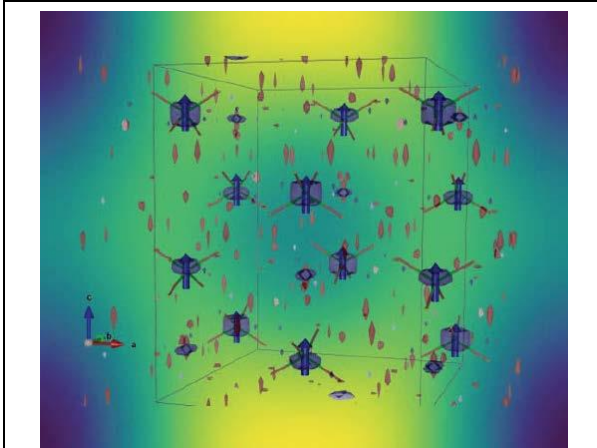


Figure 3. Magnetization density in the underscreened ferromagnetic semiconductor $\text{Yb}_{14}\text{MnSb}_{11}$. The large magnetic moment on the Mn site (blue) is partially screened with a “Kondo cloud” of negative moments (brown) distributed among the other sites. The theoretical size of the cloud $\xi_K = \hbar v_F / 2\pi k_B T_K \approx 0.5$ nm for $\text{Yb}_{14}\text{MnSb}_{11}$, about half of the nearest neighbor distance between Mn atoms.

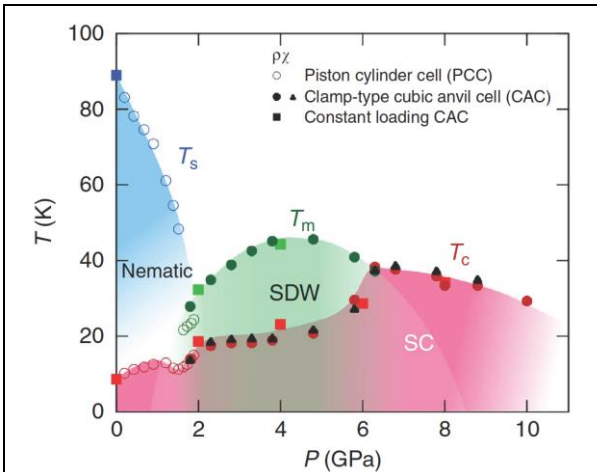


Figure 4. Temperature-pressure phase diagram of bulk FeSe crystals as determined by resistivity and ac susceptibility measurements under pressure. The results were cross-checked using several types of pressure cells [10]

materials. The distribution of negative magnetization in large $\text{Yb}_{14}\text{MnSb}_{11}$ crystals as measured using polarized neutrons [Fig. 3] is consistent with the Kondo cloud scenario [9].

Magnetism and the “simplest” iron-based superconductor

Growth of large high-quality single crystals of FeSe has facilitated in-depth studies of the physics of this unusual superconductor. High-pressure studies with our collaborators have resulted in the most complete T-P phase diagram to date [10] for this material (Fig. 4). This work, Hall data, and input from theory [11], indicate that at high pressures (≈ 6 GPa) the electronic structure and the interplay between magnetism and superconductivity in FeSe are similar to that observed in the other iron-based superconductors.

Future Work

Some of our future efforts will focus on the following questions. It is possible to design/discover a cleavable magnet that magnetically orders above room temperature? Our past work on SrRu_2O_6 and other related compounds [12,13] may provide some guidance. Are there other ternary medium entropy alloys like NiCoCr near a quantum critical point? Will strong spin-orbit coupling significantly modify the physics? Guidance for this work will be provided by theoretical rules that have predicted over 200 similar alloys that should form. [14].

Publications

Since July 2015, this project has fully or partially supported more than 104 refereed publications including 1 Nature, 4 Science, 3 Nat. Mat., 7 Nat. Comm., 2 Nat. Phys, 6 PRL, 2 Nano Letts, 2 Chem. Mat., and 39 PRB. Publications referenced in this abstract and other selected papers with significant input from this project are listed below.

[1] A. Banerjee, J. Q. Yan, *et al.* “Neutron scattering in the proximate quantum spin liquid $\alpha\text{-RuCl}_3$ ”, *Science* **356**, 1055 (2017).

- [2] B. Huang, M. A. McGuire *et al.*. “Layer-dependent ferromagnetism in a van der Waals crystal down to the monolayer limit”, *Nature* **546**, 270 (2017)
- [3] D. Zhong, M. A. McGuire *et al.* ”Van der Waals engineering of ferromagnetic semiconductor heterostructures for spin and valleytronics”, *Science Advances* **3**, e1603113 (2017).
- [4] M. A. McGuire, G. Clark, K C Santosh, W. M. Chance, G. E. Jellison, V. R. Cooper, X. Xu and B. C. Sales, “Magnetic behavior and spin-lattice coupling in cleavable van der Waals layered CrCl₃ crystals”, *Phys. Rev. Mat.* **1**, 014001 (2017).
- [5] M. A. McGuire *et al.* “Antiferromagnetism in the van der Waals layered spin-lozenge semiconductor CrTe₃” *Phys. Rev. B.* **95**, 144421 (2017)
- [6] A. F. May, S. Calder, C. Cantoni, H. B. Cao, and M. A. McGuire “Magnetic structure and phase stability of the van der Waals bonded ferromagnet Fe_{3-x}GeTe₂” *Phys. Rev. B.* **93**, 014411 (2016).
- [7] B. C. Sales *et al.* “Quantum critical behavior in a concentrated ternary solid solution”, *Sci. Rep.* **6**, 26179 (2016).
- [8] B. C. Sales *et al.* “Quantum critical behavior in the asymptotic limit of high disorder in the medium entropy alloy NiCoCr_{0.8}”, *npj Quantum Materials* **2**, 33 (2017)
- [9] M. B. Stone, B. C. Sales *et al.* “Excitations and magnetization distribution density in the dilute ferromagnetic semiconductor Yb₁₄MnSb₁₁”, *Phys. Rev. B.* **95**, 020412 (2017).
- [10] J. P. Sun, B. C. Sales, J. Q. Yan *et al.* “Dome-shaped magnetic order competing with high-temperature superconductivity at high pressures in FeSe”, *Nat. Comm.* **7**, 12146 (2016)
- [11] J. P. Sun, J.-Q. Yan *et al.* “High-T_c Superconductivity in FeSe at High Pressure: Dominant Hole Carriers and Enhanced Spin Fluctuations”, *Phys. Rev. Lett.* **118**, 147004 (2017).
- [12] W. Tian, C. Svoboda, M. Ochi, M. Matsuda, H.B. Cao, J.-G. Cheng, B.C. Sales, D.G. Mandrus, R. ARita, N. Trivedi, J.-Q. Yan, “High antiferromagnetic transition temperature of a honeycomb compound SrRu₂O₆” *Phys. Rev. B.* **92**, 041104(R), 2015.
- [13] Z. Y. Zhao, Y. Wu, H. B. Cao, H. D. Zhou, J.-Q. Yan, “Three dimensional magnetic interactions in quasi-two dimensional PdAs₂O₆”, *J. Phys. Con. Mat.* **29**, 235801 (2017).
- [14] M. C. Tropicovsky, J. R. Morris, P. R. C. Kent, A. R. Lupini, G. M. Stocks, “Criteria for Predicting the Formation of Single-Phase High-Entropy Alloys”, *PRX* **5**, 011041 (2015).
- [15] M.A. McGuire, H. Dixit, V.R. Cooper, and B.C. Sales, “Coupling of Crystal Structure and Magnetism in the Layered, Ferromagnetic Insulator CrI₃,” *Chem. Mater.* **27**, 612 (2015).
- [16] J.-Q. Yan, B. C. Sales, M. A. Susner, and M. A. McGuire, “Flux growth in a horizontal configuration: An analog to vapor transport growth”, *Phys. Rev. Mat.* **1**, 023402 (2017).
- [17] A. Bannerjee, J.-Q. Yan, *et al.* “Proximate Kitaev quantum spin liquid in a honeycomb magnet”, *Nat. Mat.* + cover, **15**, 733 (2016)
- [18] L. Poudel, A. F. May *et al.* “Candidate Elastic Quantum Critical Point in LaCu_{6-x}Au_x”, *Phys. Rev. Lett.* **117**, 235701 (2016).
- [19] G. Z. Ye, J.-Q. Yan, B. C. Sales *et al.* “Competition of superconductivity with the structural transition in Mo₃Sb₇” *Phys. Rev. B.* **94**, 224508 (2016).
- [20] J. G. Rau, A. F. May, *et al.* “Anisotropic exchange within decoupled tetrahedra in the quantum breathing pyrochlore Ba₃Yb₂Zn₅O₁₁,” *Phys. Rev. Lett.* **116**, 257204 (2016).

Title: Nanostructured Materials: From Superlattices to Quantum Dots

Principal Investigator: Prof. Ivan K. Schuller

Physics Department

University of California San Diego

Program Scope

This project is dedicated to the main issues arising when materials, especially magnetic ones, are nanostructured in one, two and three dimensions. The comprehensive approach combines preparation of nanostructures using thin film (Sputtering and MBE) and lithography (electron beam and self assembly) techniques, characterization using surface analytical, scanning probe microscopy, high-resolution scattering (light, X-ray, synchrotron and neutron) and microscopy techniques and measurement of physical properties (magneto-transport, magnetic and magneto-optical) and modeling of the results. All preparation of unique materials and devices and most structural and physical characterization are performed in the PI's laboratory at UCSD. More sophisticated structural and magnetic studies at the nanoscale are performed in collaboration at major facilities of DOE funded national labs.

We aim to investigate general physical phenomena, including exchange bias, effects of confinement on magnetic properties, a variety of proximity effects in magnetic hybrids, and induced phenomena by the application of external driving forces such as time varying electric and magnetic fields, light and other types of radiation. In all cases, a crucial ingredient is the reduction of complex or highly correlated materials to the nanoscale, where fundamental changes may occur in their physical properties. Our studies to date have included fluorides, oxides, borides and organics in addition to many combinations of transition metal elements. We have established a battery of instrumentation and continue expanding our experimental capabilities at UCSD and elsewhere. More recently we have started experiments at fast time scales to investigate the very unusual dynamics present in many hybrid systems.

Recent Progress

In the last year we have focused our attention on a number of hybrid magnetic heterostructures in which the properties of a ferromagnet are affected by the close physical proximity with a dissimilar material (antiferromagnet, metal-insulator oxide). These systems are of great interest because the unique macroscopic magnetic behavior of the hybrid heterostructures are not simple sum of the individual components. Moreover these properties are robust, although they can be manipulated by purposefully introduced disorder. Several of these properties were not predicted a-priori and arose as unexpected discoveries. These discoveries have important implication for the physics of magnetic heterostructured materials and establish the underlying basic aspects of important applications related to transformation and manipulation of energy.

Several important advances have occurred in the last year in different aspects of this project:

- 1) Exchange Bias in (Ferromagnetic/Paramagnetic Metal/ Antiferromagnetic Fluoride) Heterostructures

We have done extensive studies of exchange bias as function of metal thickness separator between a Ferromagnet (FM) and an Antiferromagnet (AFM). In a large series of samples, we

have found a very systematic evolution of the exchange bias as a function of metal (Au) thickness (t_{Au}) and for a variety of field cooling (H_{FC}) as shown in figure 1. We have also developed a theoretical model (solid line), which explains quantitatively the extensive experimental data (dots) only with two adjustable parameters. Unexpectedly the theoretical model only includes classical dipolar interactions. The implications of this result for the understanding of exchange bias are quite substantial, since implies that dipolar interactions are much more important than hitherto realized and must be taken into account and cannot be neglected as is customary in all theoretical treatments of the phenomenon. In addition, this has important implications for the development of (virtually all) devices, which have as an important ingredient exchange bias. The control and understanding of the interfacial microstructure is essential for the development of applications based on Exchange Bias.

2) Dynamics in (Ferromagnet/ Metal-Insulator Oxide) heterostructure.

The proximity between a ferromagnet (FM) and a simple transition metal oxide (TMO) that undergoes a metal-insulator transition has produced a number of very interesting, unexpected results. The transition metal oxide undergoes a first order metal-insulator phase transition concomitant with a structural phase transition. This transition being first order is hysteretic as function of temperature in which the two extreme phases coexist. We have shown the strain at the interface enhances the coercivity of the FM by as much as factor of five in the coexistence region. This phenomenon was explained due to interfacial strain in the heterostructure [2]. Recently we discovered an expected behavior in the evolution of the magnons in the FM as a function of temperature [3]. Fig 2 shows the dependence of the resonant field (H_R) and its width (ΔH_{pp}) as a function of temperature for a Ni film on top of V_2O_3 . The splitting of the magnons and the dependence of their width in the coexistence region, indicates coupling to a yet unidentified collective mode, which only occurs in the coexistence region.

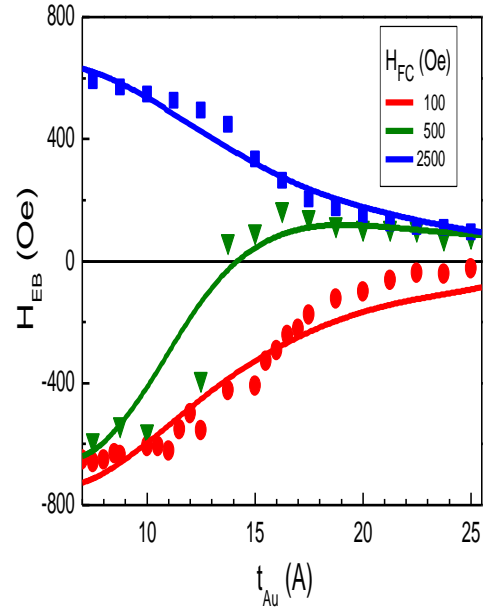


Fig. 1: Experimental (symbols) and calculated (solid line) Exchange Bias (H_{EB}) of a ferromagnetic Ni film at various distances (t_{Au}) from antiferromagnetic FeF_2 .

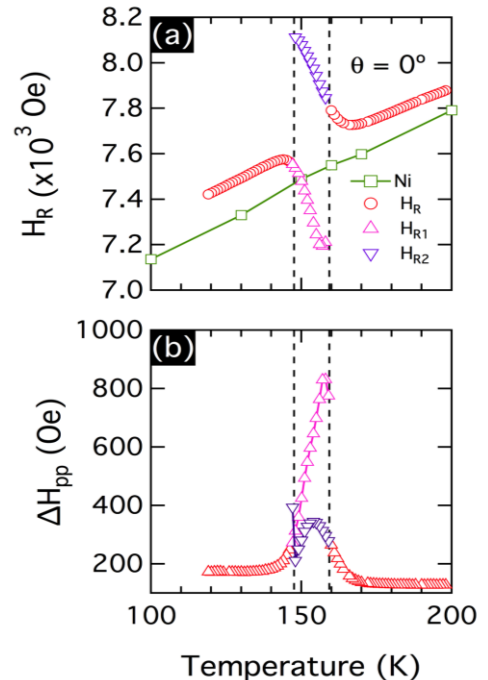


Fig. 2: Comparison of (a) resonant fields (H_R) and (b) resonant widths (ΔH_{pp}) for Ni film on sapphire (green) and on V_2O_3 (in color).

Future Plans

In the next period we will build on the existing results and will initiate research in additional directions outlined in the proposal.

We will perform photoemission electron microscopy (PEEM) using X-ray magnetic circular dichroism (XMCD) to measure the magnetic ordering of Ni films in a V_2O_3 /Ni heterostructure as a function of temperature. Films will be cooled across the V_2O_3 structural phase transition (SPT) temperature to lock-in a uniform magnetization. A small counter-field will be applied as the bilayer is heated through the transition temperature region. Because the coercivity of Ni decreases by a factor of two as the V_2O_3 undergoes the SPT [2], magnetic domains with reverse magnetization will nucleate and eventually percolate throughout the entire film. We will image the counter-field nucleated magnetic domains, their spatial order, characteristic lengths, shapes etc. and compare these with earlier measurements of metallicity in the V_2O_3 alone [4]. This work paves way for the development of nanotextured magnetic materials with sharp temperature dependent properties. In particular, in heat-assisted magnetic recording (HAMR) it is critical to flip the orientation of a targeted magnetic domain without affecting neighbors. By tuning the stripe order self-size in the oxide/ferromagnet heterostructure it might be possible to locally decrease the coercivity of a domain by a factor of two or more while preserving the coercivity of the neighboring domain.

We will study the behavior of one dimensional (1D) ferromagnetic chains as a function of length, temperature, spin, and magnetic field orientation. To accomplish this we will use Metallo-Phthalocyanines (MPc), which incorporate many metal ions (Fe, Cu, Co, Ni, Pd, Zn). This almost flat molecule incorporates a single metal ion (or two H) in between 4 cyanine and 4 benzene rings. Based on extensive studies using Organic Molecular Beam Epitaxy we have been able to control their orientation and structure by appropriate choice of substrate and growth conditions [5,6]. Superlattices of MPc interspaced with H_2Pc allows us to grow metallic (and magnetic) chains of varying lengths. Moreover contrary to other approaches dedicated to the study of 1D magnetism, we can in this fashion control all the relevant parameters of the one dimensional metallic chain and simultaneously produce sufficient material that we can perform conventional magnetic measurements such as; magnetization and Kerr effect.

References

- [1] *From Negative to Positive Exchange-Bias in Dipole Coupled Trilayers: Experiment and Theory*, F. Torres, R. Morales, I.K. Schuller, M. Kiwi, (submitted)
- [2] *Coercivity Enhancement in V_2O_3 /Ni Bilayers Driven by Nanoscale Phase Coexistence*, J. de la Venta, S. Wang, T. Saerbeck, J.G. Ramirez, I. Valmianski and I.K. Schuller, *Appl. Phys. Lett.* **104**, 062410 (2014).
- [3] *Collective Mode Splitting in Hybrid Heterostructures*, J.G. Ramirez, J. de la Venta, S. Wang, T. Saerbeck, A.C. Basaran, X. Batlle and I.K. Schuller, *Phys. Rev. B*, **93**, 214113 (2016)
- [4] *Nanotextured Phase Coexistence in the Correlated Insulator V_2O_3* , A.S. McLeod, E. van Heumen, J.G. Ramirez, S.Wang, T. Saerbeck, S. Guenon, M. Goldflam, L. Andereg, P. Kelly, A. Mueller, M. Liu, I.K. Schuller, D.N. Basov, *Nat. Phys.* **13**, 80 (2017).

[5] *Effect of X-ray Irradiation on Co-phthalocyanine Thin Films Studied by Surface Plasmon Resonance*, A. Serrano, O. Rodríguez de la Fuente, C. Monton, A. Muñoz-Noval, I. Valmianski, J.F. Fernández, G.R. Castro, I.K. Schuller and M.A. García, *J. Phys. D: Appl. Phys.* **49**, 125503, (2016).

[6] *Quadrupolar XMCD at the Fe K-edge in Fe Phthalocyanine Film on Au: Insight into the Magnetic Ground State*, J. Bartolome, F. Bartolome, A.I. Figueroa, O. Bunau, I.K. Schuller, T. Gredig, F. Wilhelm, A. Rogalev, P. Kruger, and C.R. Natoli, *Phys. Rev. B* **91**, 220401(R) (2015).

Publications

1. *From Negative to Positive Exchange-Bias in Dipole Coupled Trilayers: Experiment and Theory*, F. Torres, R. Morales, I.K. Schuller, and M. Kiwi, (submitted).
2. *Role of the Antiferromagnetic Bulk Spins in Exchange Bias*, I.K. Schuller, R. Morales, X. Batlle, U. Nowak, and G. Guntherodt, *J. Magn. Magn. Mat.*, **416**, 2 (2016).
3. *Two State Coercivity Driven by Phase Coexistence in Vanadium Sesquioxide/Nickel Bulk Hybrid Material*, C. Urban, A. Quesada, T. Saerbeck, M.A. Garcia, M.A. de la Rubia, I. Valmianski, J.F. Fernandez and I.K. Schuller, *Appl. Phys. Lett.*, **109**, 112401 (2016).
4. *Control of the Magnetic Configuration of Ferromagnetic Nanostructures Across the Structural Phase Transition of Vanadium Dioxide*, S. Finizio, M. Vafaei, I. Valmianski, R.M. Reeve, R. Lo Conte, A. Kleibert, I.K. Schuller and Mathias Klaui, *IEEE Magnetics Letters*. **7**, 1 (2016).
5. *Collective Mode Splitting in Hybrid Heterostructures*, J.G. Ramírez, J. de la Venta, S. Wang, T. Saerbeck, A.C. Basaran, X. Batlle and I.K. Schuller, *Phys. Rev. B*, **93**, 214113 (2016).
6. *Giant Controllable Magnetization Changes Induced by Structural Phase Transitions in a Metamagnetic Artificial Multiferroic*, S.P. Bennett, A.T. Wong, A. Glavic, A. Herklotz, C. Urban, I. Valmianski, M.D. Biegalski, H.M. Christen, T.Z. Ward and V. Lauter, *Sci. Rep.*, **6**, 22708 (2016).
7. *Effect of X-ray Irradiation on Co-phthalocyanine Thin Films Studied by Surface Plasmon Resonance*, A. Serrano, O. Rodriguez de la Fuente, C. Monton, A. Munoz-Noval, I. Valmianski, J.F. Fernandez, G.R. Castro, I.K. Schuller and M.A. Garcia, *J. Phys. D: Appl. Phys.* **49**, 125503 (2016).
8. *Manipulation of Competing Ferromagnetic and Antiferromagnetic Domains in Exchange Biased Nanostructures*, A.F. Rodriguez, A.C. Basaran, R. Morales, M. Kovylyna, J. Llobet, X. Borrise, M.A. Marcus, A. Scholl, I.K. Schuller, X. Batlle and A. Labarta, *Phys. Rev. B*, **92**, 174417 (2015).
9. *Mesoscopic Magnetism and Superconductivity; Recent Perspectives*, A.C. Basaran, J.E. Villegas, J.S. Jiang, A. Hoffman and I.K. Schuller, *MRS Bulletin* **40**, 925 (2015).

Patent

1. Ivan K. Schuller, J. de la Venta Granda, S. Wang, G. Ramirez, M. Erekhinskiy, A. Sharoni, *Magnetic and Electrical Control of Engineered Materials*, SD2013-022-3, Docket No.: 009062-8244.US02, U.S. Patent Application No. 14/571,015

Dynamics of Emergent Crystallinity in Photonic Quantum Materials

J. Simon

1. Title: ER46317: “Spin-Polarized Scanning Tunneling Microscopy Studies of Nanoscale Magnetic and Spintronic Nitride Systems”

PI: Arthur R. Smith

**Address: Ohio University
Nanoscale & Quantum Phenomena Institute
Department of Physics & Astronomy
Athens, OH 45701**

E-mail: smitha2@ohio.edu

2. Program Scope

The scope of this project is to investigate the structural, electronic, and spin magnetic properties of nitride-related material systems, in particular magnetic nitrides, magnetic gallium nitrides, and related elemental magnetic materials. The project seeks to explore, image, and even manipulate the ferromagnetic, antiferromagnetic, and ferrimagnetic structures of these material systems. An important goal is to develop these materials as advanced spintronic systems which may have future energy-related applications. In order to probe these systems, this project makes use of scanning tunneling microscopy (STM) and especially spin-polarized STM (SP-STM). The latter is a powerful technique which can provide spin information on surfaces with atomic-scale resolution. Combining ultra-high vacuum SP-STM together with *in-situ* molecular beam epitaxial growth, diverse nitride-related material systems can be explored in a pristine state.

3. Recent Progress

- **A Two-dimensional Manganese Gallium Nitride Surface Structure Showing Ferromagnetism at Room Temperature *recently submitted to Nature Materials***

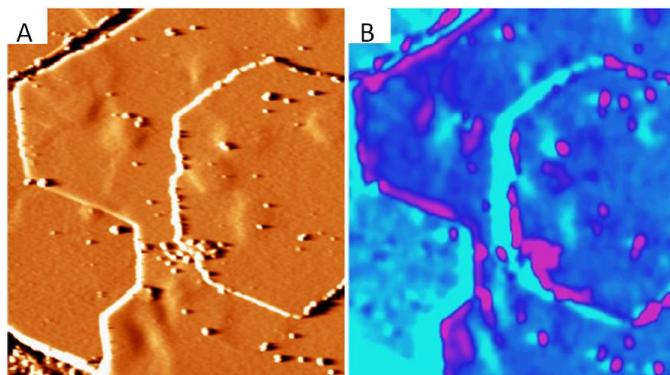


Fig. 1. A) derivative mode STM topographical image where bright lines follow step edges with GaN step height of 2.59 Angstrom and bright patches are impurity atom related effects; B) corresponding dI/dV conductance image revealing light/dark contrast corresponding to spin contrast on adjacent terraces. Images acquired at room temperature.

We have used SP-STM to investigate the formation of an ordered magnetic structure consisting of Mn atoms in the GaN surface with Mn:Ga concentration of 1:3 and a $\sqrt{3}\times\sqrt{3}$ -R30° reconstruction. Manganese atoms are bonded to both Ga and N atoms. Theoretical calculations find this structure to be ferromagnetic with both spin-polarized and spin-split surface states. The images shown in Fig.1 reveal different dI/dV contrast on adjacent terraces. Whereas topographically the adjacent terraces have the same structure (A), the contrast seen cannot be electronic and therefore must be magnetic. Moreover, these results were obtained at room temperature, making

this system a possible candidate for room-temperature spintronic applications.

We have performed extensive verification experiments for these results including obtaining atomic resolution images of the $\sqrt{3}\times\sqrt{3}$ -R30° reconstruction while simultaneously observing

dI/dV contrast in different surface regions which have the same $\sqrt{3}\times\sqrt{3}$ -R30° structure. The contrast can therefore not be ascribed to any electronic effect. We have furthermore observed the spin-splitting by measuring opposite contrast on the same area at opposite voltage biases. And we have observed magnetic hysteresis effects by measuring the dI/dV levels as functions of an applied magnetic field. Magnetic switching effects have also been seen.

Preparation of the sample is however challenging since it requires obtaining a Ga-poor 1×1 structure on N-polar GaN through high temperature annealing prior to Mn deposition. This process can lead to some GaN surface dissociation and some disordered regions. This however creates the opportunity of having small well-ordered, ferromagnetic islands surrounded by disordered areas, as well as large, continuous $\sqrt{3}\times\sqrt{3}$ -R30° areas. And we have obtained magnetic contrast on the $\sqrt{3}\times\sqrt{3}$ -R30° structures in both cases.

- **Relationships Between Surface Structure, Surface Magnetism, and Nitrogen Vacancy Concentrations in θ -MnN *to be submitted to Applied Surface Science***

We have also been exploring the surface properties of θ -MnN(001). The thought-to-be antiferromagnetic θ -phase MnN is the closest to 1:1 stoichiometry for binary manganese nitride.

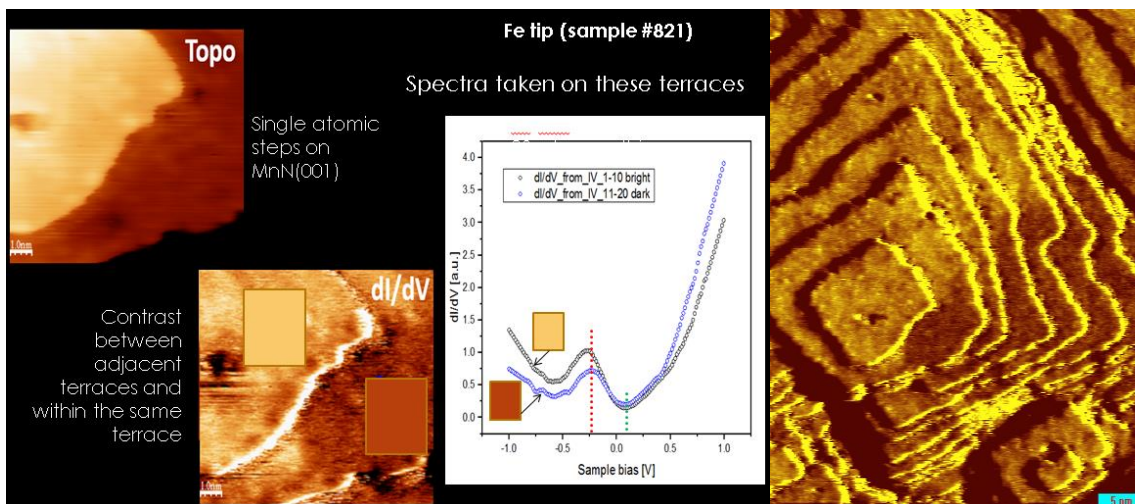


Fig. 2. Topographical and dI/dV mapping of a stepped area on the θ -MnN surface, and additionally spectroscopy taken from the upper and lower terraces. The image at right is a zoomed-out view of the same area. The source of the contrast could be magnetic or it could be electronic, potentially having to do with subsurface N vacancies. Images acquired at room temperature.

A recent paper reported the largest ever observed perpendicular exchange bias using a magnetic bi-layer stack consisting of θ -MnN and ferromagnetic CoFeB.¹ This adds additional interest as well as need to exploring the magnetic properties of θ -MnN.

While the electronic and magnetic properties of θ -MnN surfaces are not yet well known, our STM experiments so far reveal a pyramidal MnN morphology with single atomic steps. The step heights are found to vary from place to place, suggesting electronic or magnetic variations across step edges. At the same time, we have found clear contrasts in dI/dV map images, both across step edges, and within terraces which is shown in Fig. 2. If the sample surface is chemically homogeneous and has a consistent 1×1 structure, then this contrast can only be explained as magnetic. It is also notable that these contrasts have only been seen with magnetic tips.

Complicating the picture however, manganese nitride has other ordered phases (such as η - Mn_3N_2) which leads to triple layer-wise chemical super-periodicities which could give rise to contrast across step edges as well. On the other hand, triple layer periodicities are not actually seen in these θ -phase samples, whereas they are seen in our η - Mn_3N_2 samples. Still, N-vacancies could be having an important effect on the observed dI/dV contrast. Theoretical calculations show that layers of sub-surface N-vacancies depress the density of states at the surface. Since it is never possible to get a fully 1:1 Mn:N, one always has some N-vacancies in the grown samples. While not enough to form triple-ordered periodicities as in η - Mn_3N_2 , N-vacancies could give rise to dI/dV contrast at the surface. At the same time, θ -MnN is fully expected to be magnetically well ordered. And thus magnetic contrast should also be present.

In order to try to unravel the two possible sources of the observed dI/dV contrasts, we are currently performing more experiments using larger out of plane fields of varying magnitude using our LT-SP-STM system. If the observed dI/dV contrast is found to depend on the field, then we can be certain about the magnetic ordering.

- **Perpendicular Magnetic Anisotropy and Surface Spin Polarization in Ferrimagnetic ϵ -phase Mn_4N *SP-STM results to be submitted to JMMM; see also publication #86***

We have investigated the surfaces of ϵ -phase Mn_4N which is a *ferrimagnetic* material. Ultra-thin films (~ 9 nm) of this material are prepared through a combination of manganese nitride MBE growth, annealing, and re-growth. By *ex-situ* magnetometry, it has been found that the samples exhibit perpendicular magnetic anisotropy. SP-STM has been performed under applied magnetic fields, and we have found domain contrast in dI/dV image maps. We have furthermore explored the magnetic field-dependent dI/dV contrast, and full hysteresis behavior has been found.

- **Spin Structure of MBE-grown Cr(001) Surface *Results to be submitted to JMMM***

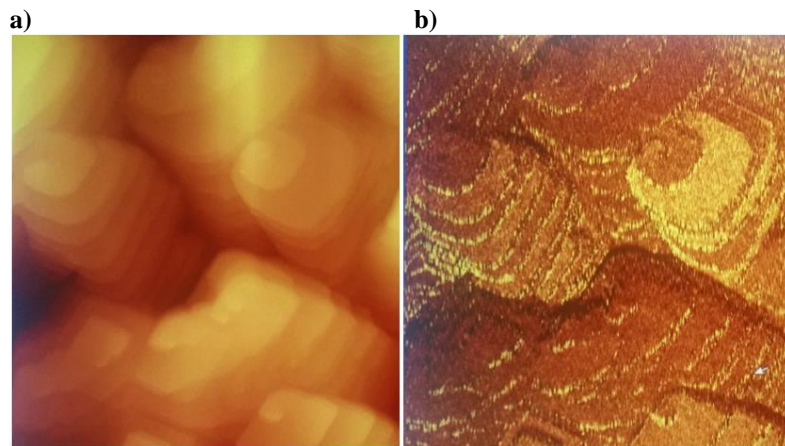


Fig. 3. Topographical and dI/dV mapping of a stepped area on Cr(001) surface showing spin contrast with layer-by-layer antiferromagnetic ordering. Image size is ~ 150 nm. Not everywhere is the contrast so obvious, related to the various possible in-plane sample spin orientations. Images acquired at low (LHe) temperature.

Spin magnetic contrast was obtained on chromium (001) at low temperature using SP-STM. The image at the left in Fig. 3(a) is the topographical image, while the image at right (b) is the dI/dV map image. We can see that there is very clear light-dark-light contrast on the terraces separated by single atomic steps, indicating the antiferromagnetic layering of the Cr(001) surface. For this MBE-grown Cr film however, there are areas also which show very little layer-by-layer contrast, indicating an *in-plane* spin rotation of the sample

spins in those areas, perhaps by 90° . This indicates the various sample spin magnetic anisotropies and is positive confirmation of the spin resolving power of our LT-SP-STM system.

4. Future Plans

In general, each project in our lab should move from the initial growth study, to the structural investigation, and then on to the measurement of electronic and spin magnetic properties. Current and future efforts are therefore to be focused on the use of spectroscopy and SP-STM to obtain the electronic and spin magnetic properties for these nitride-related spintronic materials.

5. References

¹Giant Perpendicular Exchange Bias with Antiferromagnetic MnN, P. Zilske, D. Graulich, M. Dunz, and M. Meinert, *Appl. Phys. Lett.* **110**, 192402 (2017).

6. Publications of DOE sponsored research (2015-2017)

Papers listed below are shown in reverse chronological order, with the numbering defined based on paper #1 = A.R. Smith's first paper. Full publication list can be seen at:

<http://www.phy.ohiou.edu/~asmith/publist.html>.

89. Structural and Magnetic Phase Transitions in Chromium Nitride Thin Films Grown by RF Nitrogen Plasma Molecular Beam Epitaxy, K. Alam, S. M. Disseler, W. D. Ratcliff, J. A. Borchers, R. Ponce-Perez, G. H. Coccoletzi, N. Takeuchi, A. Foley, A. Richard, D. C. Ingram, and A. R. Smith, *Phys Rev B* (accepted 2017).
88. Surface Structures of L10-MnGa (001) By Scanning Tunneling Microscopy and First-Principles Theory, J. P. Corbett, J. Guerrero-Sanchez, A. L. Richard, D. C. Ingram, N. Takeuchi, and A. R. Smith, *Applied Surface Science* 422, 985 (2017).
87. Structural, electronic and magnetic properties of the MnGa(111)-1x2 and 2x2 reconstructions: spin polarized first principles total energy calculations, R. Garcia-Diaz, G. H. Coccoletzi, A.-O. Mandru, K. Wang; A. R. Smith; and N. Takeuchi, *Applied Surface Science* 419, 286 (2017).
86. Contribution from Ising domains overlapping out-of-plane to perpendicular magnetic anisotropy in Mn₄N thin films on MgO(001), Andrew Foley, Joseph Corbett, Khan Alam, Andrea L. Richard, David C. Ingram, Arthur R. Smith, Lianshui Zhao, James C. Gallagher, and Fengyuan Yang, *Journal of Magnetism and Magnetic Materials* 439, 236 (2017).
84. Structural and Magnetic Properties of Ferrimagnetic Epsilon-phase Mn₄N and Antiferromagnetic Zeta-phase Mn₁₀N Thin Films on MgO(001), A. Foley, J. Corbett, A. L. Richard, K. Alam, D. C. Ingram, and A. R. Smith, *Journal of Crystal Growth* 446, 60 (2016).
83. Structure and Magnetism in Ga-rich MnGa/GaN Thin Films and Unexpected Giant Perpendicular Anisotropy in the Ultra-Thin Film Limit, A.-O. Mandru, J.P. Corbett, J. Lucy, A.L. Richard, F.Y. Yang, D.C. Ingram, and A.R. Smith, *Appl. Surf. Sci.* 367, 312 (2016).
81. Structural, Electronic, and Magnetic Properties of Mn₃N₂(001) Surfaces, Jonathan Guerrero-Sanchez, Andrada-Oana Mandru, Kangkang Wang, Noboru Takeuchi, Gregorio H. Coccoletzi, and Arthur R. Smith, *Appl. Surf. Sci.* 355, 623 (2015).
80. Molecular Beam Epitaxial Growth and Scanning Tunneling Microscopy Studies of the Gallium Rich Trench Line Structure on N-polar w-GaN(000-1), Z. Alhashem, Andrada-Oana Mandru, Jeongihm Pak, and Arthur R. Smith, *J. Vac. Sci. Technol. A* 33, 061404 (2015).
79. Surface Structure of Manganese Gallium Quantum Height Islands on Wurtzite GaN(0001) Studied by Scanning Tunneling Microscopy, Jeongihm Pak, Andrada-Oana Mandru, Abhijit Chinchore, and Arthur R. Smith, *Applied Physics A* 120, 1027 (2015).
77. Native Gallium Adatoms Discovered on Atomically-Smooth Gallium Nitride Surfaces at Low Temperature, K. Alam, A. Foley, and A. R. Smith, *Nano Letters* 15, 2079 (2015).

Understanding and Controlling Conductivity Transitions in Correlated Solids: Spectroscopic Studies of Electronic Structure in Vanadates.

Kevin E. Smith, Department of Physics, Boston University.

Program Scope

There is enormous scientific and technological interest in understanding and controlling solid state electronic conductivity transitions. The switching of the electrical properties of a material between those of a metal and those of a non-metal is the very basis of the electronics industry. Conductivity transitions can be driven by many external and internal mechanisms, including electric and magnetic fields, chemical doping, defects, disorder, pressure, dimensionality, and temperature. The significance of these transitions can be gauged from the fact that a substantial fraction of all research in solid state physics is directed at understanding such transitions, and ultimately controlling their properties.

Vanadium oxides (vanadates) display particularly complex and fascinating electronic phenomena. Whether as simple binary oxides or as ternary compounds with substituted metal cations, vanadates are replete with complex conductivity transitions, as well as charge ordering transitions, structural phase transitions, frustrated spin structures, superconductivity, and unusual magnetic properties. As such, vanadates are a prototypical class of correlated material, where fundamentally important physical themes can be explored, both experimentally and theoretically. Key to understanding the origin of the properties of vanadates is the accurate determination of their electronic structure.

This program is focused on measuring the electronic properties of a selection of vanadates, and to use the knowledge gained to provide a deeper understanding of the origins of conductivity transitions in correlated materials. This in turn facilitates the control of these transitions. The experimental tools used are soft x-ray emission spectroscopy (XES), soft x-ray absorption spectroscopy (XAS), resonant inelastic soft x ray scattering (RIXS), x-ray photoemission spectroscopy (XPS), angle resolved photoemission spectroscopy (ARPES), and spectroscopic photoemission low energy electron microscopy (SPELEEM). The use of this diverse suite of electron and photon techniques enables a very wide range of physically important vanadates to be studied, since we can measure electronic structure in samples that are electrical conductors or electrical insulators, and in samples that are single crystals, thin films, polycrystalline powders, or nanoparticles. This degree of flexibility is unusual and highly advantageous. In this ambitious program we measure (and test against theory), vanadate band structures, densities of states, Fermi surfaces, many body correlations, cation charge states, valence band hybridization, low energy valence excitations, and most importantly, the changes in electronic structure during vanadate conductivity transitions.

Recent Progress

The scientific highlights of our program include the following:

- The observation of a *striped electronic and structural phase* during the metal-to-insulator transition in VO₂;¹
- The observation of a *decoupling of the electronic and structural phase transitions* in VO₂;¹
- The discovery of *surface enhanced electron correlation* in Sr_xCa_{1-x}VO₃;^{2,3}
- The determination of the electronic structure of β -Na_xV₂O₅ ($x \approx 0.33$);⁴
- The observation low-energy *t_{2g} orbital excitations* in NdVO₃;⁵
- Exploration of the effects of *rare-earth atomic size* on the electronic structure of La_{1-x}Lu_xVO₃;⁶
- Definitive studies of the electronic properties of *BiVO₄*;^{7,8}
- A study of the surfaces of *V₂O₅ films* grown by thermal evaporation and sol-gel methods;⁹
- Also, given our access to various synchrotron radiation sources, a selection of other spectroscopic electronic structure studies were performed and subsequently published. These studies provided important complimentary information to our vanadate results. The progress made in these experiments include: the observation using ARPES of surface states in the *superconducting topological insulator*, indium doped SnTe(111);¹⁰ a RIXS/XAS study of the first *lithiation cycle* of the Li-ion battery cathode material Li_{2-x}MnSiO₄;¹¹ a study of the origin of the *bipolar doping* behavior of SnO;¹² exploration of the nature of *pseudo Jahn-Teller distortions* in Li_xMnPO₄;¹³ determination of the *k-resolved susceptibility function* for 2H-TaSe₂ from ARPES,¹⁴ and finally, a study of visible-light-active Sn(II)-TiO₂ *photocatalysts*.¹⁵

Future Plans

Our future focus will be to understand the effect of reduced dimensionality on many body electronic properties in these prototypical correlated materials. Understanding how electron correlation in metal oxides can be controlled by the dimensionality of the solid is a crucially important issue if these materials are to be used in next-generation electronic and magnetic devices. We intend to explore this issue by reducing sample dimensionality in two distinct ways: by varying the thickness and repeat units of vanadate superlattices, and by varying the size of vanadate nanoparticles.

References

1. J. Laverock, S. Kittiwatanakul, A.A. Zakharov, Y.R. Niu, B. Chen, S.A. Wolf, J.W. Lu, and K.E. Smith, "Direct Observation of Decoupled Structural and Electronic Transitions and an Ambient Pressure Monocliniclike Metallic Phase of VO₂", Phys. Rev. Lett. **113**, 216402 (2014).

2. J. Laverock, J. Kuyyalil, B. Chen, R.P. Singh, B. Karlin, J.C. Woicik, G. Balakrishnan, and K.E. Smith, "Enhanced electron correlations at the $\text{Sr}_x\text{Ca}_{1-x}\text{VO}_3$ surface", *Phys. Rev. B* **91**, 165123 (2015).
3. J. Laverock, B. Chen, K.E. Smith, R.P. Singh, G. Balakrishnan, M. Gu, J.W. Lu, S.A. Wolf, R.M. Qiao, W. Yang, and J. Adell, "Resonant soft x-ray emission as a bulk probe of correlated electron behavior in metallic $\text{Sr}_x\text{Ca}_{1-x}\text{VO}_3$ ", *Phys. Rev. Lett.* **111**, 047402 (2013).
4. B. Chen, J. Laverock, D. Newby, T.-Y. Su, K.E. Smith, W. Wu, L.H. Doerr, N.F. Quackenbush, S. Sallis, L.F.J. Piper, D.A. Fischer, and J.C. Woicik, "Electronic Structure of $\beta\text{-Na}_x\text{V}_2\text{O}_5$ ($x \approx 0.33$) Polycrystalline Films: Growth, Spectroscopy, and Theory", *J. Phys. Chem. C* **118**, 1081 (2014).
5. J. Laverock, B. Chen, A.R.H. Preston, D. Newby, L.F.J. Piper, L.D. Tung, G. Balakrishnan, P.A. Glans, J.H. Guo, and K.E. Smith, "Low-energy V t_{2g} orbital excitations in NdVO_3 ", *J. Phys. Cond. Mat.* **26**, 455603 (2014).
6. B. Chen, J. Laverock, J. D. Newby, J.F. McNulty, K.E. Smith, P.A. Glans, J.H. Guo, R.M. Qiao, W.L. Yang, M.R. Lees, L.D. Tung, R.P. Singh, and G. Balakrishnan, "Effects of rare-earth size on the electronic structure of $\text{La}_{1-x}\text{Lu}_x\text{VO}_3$ ", *J. Phys. Cond. Mat.* **27**, 105503 (2015).
7. V. Jovic, J. Laverock, A.J.E. Rettie, J.S. Zhou, C.B. Mullins, V.R. Singh, B. Lamoureux, D. Wilson, T.Y. Su, B. Jovic, H. Bluhm, T. Soehnel, and K.E. Smith, "Soft X-ray spectroscopic studies of the electronic structure of $\text{M}:\text{BiVO}_4$ ($\text{M} = \text{Mo}, \text{W}$) single crystals", *Journal of Materials Chemistry A* **3**, 23743 (2015).
8. V. Jovic, A.J.E. Rettie, V.R. Singh, J.-S. Zhou, B. Lamoureux, C.B. Mullins, H. Bluhm, J. Laverock, and K.E. Smith, "An x-ray spectroscopic perspective of electron localization and transport in $\text{W}:\text{BiVO}_4$ single crystals", *Chem. Mat.* (*submitted*) (2016).
9. B. Lamoureux, V.R. Singh, V. Jovic, J. Kuyyalil, T.-Y. Su, and K.E. Smith, "Structural and Electronic Properties of Thermally Evaporated V_2O_5 Epitaxial Thin Films", *Thin Solid Films* **615**, 409 (2016).
10. C.M. Polley, V. Jovic, T.Y. Su, M. Saghir, D. Newby, B.J. Kowalski, R. Jakiela, A. Barcz, M. Guziewicz, T. Balasubramanian, G. Balakrishnan, J. Laverock, and K.E. Smith, "Observation of surface states on heavily indium-doped $\text{SnTe}(111)$, a superconducting topological crystalline insulator", *Phys. Rev. B* **93**, 075132 (2016).
11. P.T. Kristiansen, M. Dahbi, T. Gustafsson, K. Edstrom, D. Newby, K.E. Smith, and L.C. Duda, "X-ray absorption spectroscopy and resonant inelastic scattering study of the first lithiation cycle of the Li-ion battery cathode $\text{Li}_{2-x}\text{MnSiO}_4$ ", *Phys. Chem. Chem. Phys.* **16**, 3846 (2014).
12. N.F. Quackenbush, J.P. Allen, D.O. Scanlon, S. Sallis, J.A. Hewlett, A.S. Nandur, B. Chen, K.E. Smith, C. Weiland, D.A. Fischer, J.C. Woicik, B.E. White, G.W. Watson, and L.F.J. Piper, "Origin of the Bipolar Doping Behavior of SnO from X-ray Spectroscopy and Density Functional Theory", *Chem. Mat.* **25**, 3114 (2013).
13. L.F.J. Piper, N.F. Quackenbush, S. Sallis, D.O. Scanlon, G.W. Watson, K.W. Nam, X.Q. Yang, K.E. Smith, F. Omenya, N.A. Chernova, and M.S. Whittingham, "Elucidating the nature of pseudo Jahn-Teller distortions in Li_xMnPO_4 : Combining density functional theory with soft and hard x-ray spectroscopy", *J. Phys. Chem. C* **117**, 10383 (2013).
14. J. Laverock, D. Newby Jr., E. Abreu, R.D. Averitt, K.E. Smith, R.P. Singh, G. Balakrishnan, J. Adell, and T. Balasubramanian, "Determination of the k -resolved

- susceptibility function of 2H-TaSe₂ from angle-resolved photoemission measurements", Phys. Rev. B **88**, 035108 (2013).
15. V.B.R. Boppana, F. Jiao, D. Newby, J. Laverock, K.E. Smith, J.C. Jumas, G. Hutchings, and R.F. Lobo, "Analysis of Visible-Light-Active Sn(II)-TiO₂ Photocatalysts", Phys. Chem. Chem. Phys. **15**, 6185 (2013).

Publications

1. "***Orbital orientation mapping of V₂O₅***",
B. Lamoureux, V. Jovic, V.R. Singh, and K.E. Smith, J. App. Phys. **122**, 045305 (2017)
2. "***Large-Area 2D/3D MoS₂-MoO₂ Heterostructures with Thermally Stable Exciton and Intriguing Electrical Transport Behaviors***",
D.W. Li, Z.Y. Xiao, H.R. Golgir, L. Jiang, V.R. Singh, K. Keramatnejad, K.E. Smith, X. Hong, L. Jiang, J.-F. Silvain, and Y.F. Lu, Adv. Elec. Mater. 1600335 (2017)
3. "***Structural and Electronic Properties of Thermally Evaporated V₂O₅ Epitaxial Thin Films***",
B. Lamoureux, V.R. Singh, V. Jovic, J. Kuyyalil, T.-Y. Su, K.E. Smith, Thin Solid Films **615**, 409 (2016)
4. "***An X-Ray Spectroscopic Perspective of Electron Localization and Transport in Tungsten Doped Bismuth Vanadate Single Crystals***", V. Jovic, A.J. Rettie, V.R. Singh, J.-S. Zhou, C.B. Mullins, T.-Y. Su, B. Lamoureux, H. Bluhm, J. Laverock, K.E. Smith, Phys. Chem. Chem. Phys. **18**, 31958 (2016)
5. "***Observation of Surface States on Heavily Indium Doped SnTe(111), a Superconducting Topological Crystalline Insulator***",
C.M. Polley, V. Jovic, T.-Y. Su, M. Saghir, T. Balasubramanian, G. Balakrishnan, J. Laverock, and K.E. Smith, Phys. Rev. B **93**, 075132 (2016)

Understanding (Mostly) Iron Based Superconductors

G. R. Stewart, Department of Physics, University of Florida, Gainesville FL 32611

Program Scope

This work addresses several key questions important for understanding superconductivity (and its origin) in Iron Based Superconductors ('**IBS**' hereafter), which are potentially technologically useful materials. Techniques we are developing are applicable to other superconductors, including cuprates, as well. In addition, a new collaborative effort in 2 dimensional properties using cleavable superconductors is underway. We are focused primarily on the following areas of research:

a.) investigate the effect of strain in IBS. Small differences in strain have been found (by our work and others) to be surprisingly important for T_c and transition width. Our recent work (see publication #1 in the 2 year list) found a strong dependence of superconductivity in a 122 structure IBS on the strain (implying non-conventional superconductivity). We propose to investigate the influence of strain on T_c and the transition width ΔT_c in several IBS, including KFe_2As_2 (which has a known broad ΔT_c as measured in the specific heat even in high residual resistivity ratio (i. e. supposedly high quality) samples) and further study strain relief in $BaFe_{2-x}Co_xAs_2$ to determine T_c vs strain for very low strain.

b.) investigate, using our recently adapted-for-IBS technique of scaling in the specific heat, if line nodes/deep minima appear to be present:

Such line nodes/deep minima can come in IBS either from d-wave pairing or from s_{\pm} pairing where the nodes are accidental, rather than symmetry driven. These nodes can morph into deep minima in the presence of disorder/defects. Using a method previously used¹ for proving the existence of line nodes/deep minima in d-wave YBCO, we first investigated (publication #4) the possibility of line nodes in overdoped $Ba_{1-x}K_xFe_2As_2$.

c.) We continue to investigate the behavior of the **discontinuity in the specific heat, ΔC , at T_c** in the IBS. This work is based on a discovery² of a correlation in the specific heat with T_c that the discontinuity in the specific heat at T_c , ΔC , varies as T_c^3 . This is quite different than the standard BCS superconductors, where the pairing involves phonons and ΔC varies approximately as T_c^2 . Secondly, we propose, in the Co-doped $BaFe_2As_2$ in which we have experience in sample preparation, to study the details of the $\Delta C \sim T_c^3$ trend with extended strain-relieving annealing to minimize possible impurity scattering. Thirdly, the question of what causes the residual γ value in the superconducting state as $T \rightarrow 0$ (which impacts the calculation of ΔC) will be investigated in light of our recent results where strain seriously affects ΔT_c . Is strain also a deciding influence for $\gamma_{residual}$?

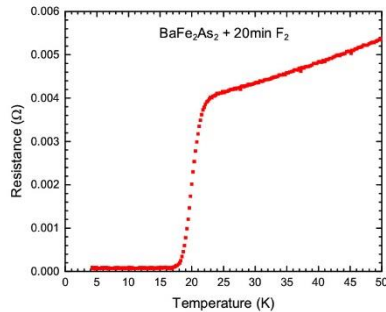
d.) Continue our work (graduate student thesis) reacting **$BaFe_2As_2$ with fluorine** and extend this work to (less reactive) chlorine.

e.) Investigate if Be, with which our lab has special expertise, can be inserted into several IBS including $LiFeAs$ and doped $BaFe_2As_2$ and measure its effects on the properties. From an atomic radius and valency point of view, Be would be expected to substitute for Fe. Fe and Be form numerous binary compounds, while Ba and Be form $BaBe_{13}$.

f.) Prepare high T_c BiSSCO and TaS₂, which are **cleavable** down to **monolayer** thicknesses, for research collaborations (Centre for Advanced 2D Materials in Singapore and University of Florida) exploring 2-dimensional behavior.

Recent Progress

1. Reaction of undoped BaFe₂As₂ and SrFe₂As₂ with fluorine and chlorine to cause **superconductivity at $T_c \sim 22$ K**. Recent progress includes determination via careful x-



ray photoemission that F is replacing As in the lattice; the diffusion depth of F after 20 minutes is up to 10 microns; Cl is much less (at least a factor of 20 in exposure time) reactive than F. We have begun a collaboration on this project with the group of Prof. Juan Nino in Materials Science at the University of Florida for both experimental and theoretical support.

Fig. 1: Resistance vs temperature of BaFe₂As₂ exposed to fluorine gas (5%) for 20 minutes.

2. We have built a new strain apparatus in our Physics Dept. machine shop using a pure Titanium strain-induction part to approximately match the strain of our proposed samples with the thermal strain introduced by cooling, and finished wiring the new rig with 9 piezoelectric stacks installed, with a strain gauge to measure the applied strain. We have begun measurements, as a first test of the apparatus, on URu₂Si₂ which has a so-called “hidden order” transition at 17 K. We have overcome initial problems with small cracks in the samples appearing under strain, and are now able to measure the hysteresis (like in the magnetization of ferromagnets) in the resistivity of the sample (predicted to provide evidence of possible nematic order) between ramping down the strain from the maximum (+0.0002) vs ramping up the strain from the minimum (-0.0002). We are receiving theoretical support on this project from Rafael Fernandes, University of Minnesota, who has a recent publication³ on the subject.
3. Two publications (see list) resulted with the supplying of thin, cleavable high quality single crystals of BiSSCO and TaS₂ to the group of Art Hebard, University of Florida.

Future Plans

1. Reaction of undoped BaFe₂As₂ and SrFe₂As₂ with fluorine and chlorine to cause **superconductivity at $T_c \sim 22$ K**: We propose to finish this project in the coming year with one major remaining goal to investigate: Can addition of FeF₂ to the self-flux mixture of Ba:Fe:As components result in a more bulk superconductivity? Or is this type of superconductivity inherently non-bulk?
2. Continue strain work on the hidden order transition in URu₂Si₂. Investigate the effect of strain on T_c and ΔT_c of single crystals of BaFe_{2-x}Co_xAs₂ using our strain rig and resistivity as the characterization technique.
3. Investigate the residual γ in single crystals of BaFe_{2-x}Co_xAs₂ as a function of strain, using pellets of ground powder.
4. Investigate Be as a dopant in IBS.

References

1. Y. X. Wang, B. Revaz, A. Erb, and A. Junod, Phys.Rev.B **63**, 094508 (2001).
2. S. Bud'ko, N. Ni, and P. C. Canfield, Phys. Rev. B **79**, 220516 (2009).
3. J. Kang and R. M. Fernandes, Phys. Rev. B **92**, 054504 (2015).

Publications

1. J. S. Kim, G. N. Tam, and G. R. Stewart, "Unusual Sensitivity of Superconductivity to Strain in Iron-Based 122 Superconductors," Phys. Rev. B **91**, 144512 (2015).
2. G. R. Stewart, "Ted Geballe: A Lifetime of Contributions To Superconductivity," Physica C **514**, 435-436 (2015).
3. G. R. Stewart, "Superconductivity in the A15 Structure," invited review in Physica C **514**, 28-35 (2015).
4. J. S. Kim, G. R. Stewart, Yong Liu, and Thomas A. Lograsso, "Specific Heat Evidence for Line Nodes in Heavily Overdoped $Ba_{1-x}K_xFe_2As_2$," Phys. Rev. B **91**, 214506 (2015).
5. L. Li, H. Cao, M.A. McGuire, J.S. Kim, G.R. Stewart, and A.S. Sefat, "Role of Magnetism in Superconductivity of $BaFe_2As_2$: Study of $5d$ Au-doped $BaFe_2As_2$ Crystals," Phys. Rev. B **92**, 094504 (2015).
6. J. S. Kim, G. N. Tam, and G. R. Stewart, "Universal Scaling Law for the Condensation Energy, U , Across a Broad Range of Superconductor Classes," Phys. Rev. B **92**, 224509 (2015).
7. Y. Bang and G. R. Stewart, "Anomalous scaling of the specific-heat jump ΔC vs. T_c in the Fe-based superconductors: the $\pm s$ -wave pairing state model," New J. Phys. **18**, 023017 (2016).
8. Y. Bang and G. R. Stewart, "Superconducting Properties of the s_{\pm} State: Fe-Based Superconductors," topical review in J. Phys.: Cond. Matter. **29**, 123003 (2017).
9. D. VanGennep, A. Linscheid, D. E. Jackson, S. T. Weir, Y. K. Vohra, H. Berger, G. R. Stewart, R. G. Hennig, P. J. Hirschfeld, and J. J. Hamlin, "Pressure-induced superconductivity in the giant Rashba system BiTeI," J. Phys.: Cond. Matter. **29**, 09LT02 (2017).
10. G. R. Stewart, "Unconventional Superconductivity," Advances in Physics **66**, 75-196 (2017).
11. Ang J. Li, Xiaochen Zhu, Gregory R. Stewart and Arthur F. Hebard, "Bi-2212/1T-TaS₂ Van der Waals junctions: Interplay of proximity induced high- T_c superconductivity and CDW order," Scientific Reports **7**, 4639 (2017).
12. Xiaochen Zhu, Ang J. Li, G. R. Stewart, Arthur F. Hebard, "Detection of charge density waves at 1T-TaS₂/GaAs interfaces," Appl. Phys. Lett. **110**, 181603 (2017).

Nanoscale Electrical Transfer and Coherent Transport Between Atomically-Thin Materials

Douglas R. Strachan, Department of Physics and Astronomy, University of Kentucky

Program Scope

The working paradigm of the electronics field over the last 50 years has been the steady reduction in size of their components, yet as the size of electronics are reduced towards nanoscale dimensions electrical contacts are increasingly important, and their resistances are major obstacles to achieving faster and more efficient devices. It is widely expected that this steady reduction in size will soon involve the incorporation of the new class of atomically-thin materials (such as, graphene, nanotubes, and the dichalcogenides) into future electronics. At this extreme limit of miniaturization, the interfaces to electrical contacts will likely become the critical barriers to improved performances and energy efficiencies. The case in which both the device material and the contact comprise an atomically-thin material is particularly exciting, however, as this nanostructure has the potential to realize controlled coherent transport at the electrode-channel interface, enabling very high conductivities over extremely short length scales; in essence pushing the limit of miniaturization of the electrode thickness can in this situation be exploited as an advantage rather than being an obstacle.

The objective of this project is to utilize highly-ordered atomically-thin commensurate nanoscale electrodes to probe and control the coherent electron transfer to another atomically-thin material. To fulfill the objective, two aims will be pursued to determine the electron transport between commensurate electrodes through channel materials comprising two prototypical atomically-thin materials with different dimensionalities; one-dimensional nanotubes, and atomically-thin 2D materials. This two-aim research effort will provide fundamental complementary understanding of coherent transfer processes as the dimensionality of the electrical interface is varied.

Recent Progress

Towards the first-year goals of this program, we have so far prepared more than 30 crystallographically-aligned carbon nanotube (CNT) samples^{1,2} over few-layer graphene films that have been etched into two electrically isolated electrodes.^{3,4} An atomic-force microscopy image of representative selection of these CNTs over graphene etch tracks is shown in Figs. 1. Lithography is currently being performed on these samples in order to make the relevant transport measurements of these extremely small nanoscale structures.

In the sample preparation work we have obtained two related results for which we have manuscripts in preparation. One of these related results is the discovery of crystallographic etching of boron nitride.⁵ The second result is the discovery of a method for the crystallographic growth of carbon nanotubes (CNTs) on hexagonal boron nitride (hBN) surfaces.⁶ This result is shown in Fig. 8 in the attached file. Figure 9 of this file shows an AFM image of the same

sample with nano-lithography electrodes placed on the nanotubes for electrical measurements (which are currently underway in our lab).

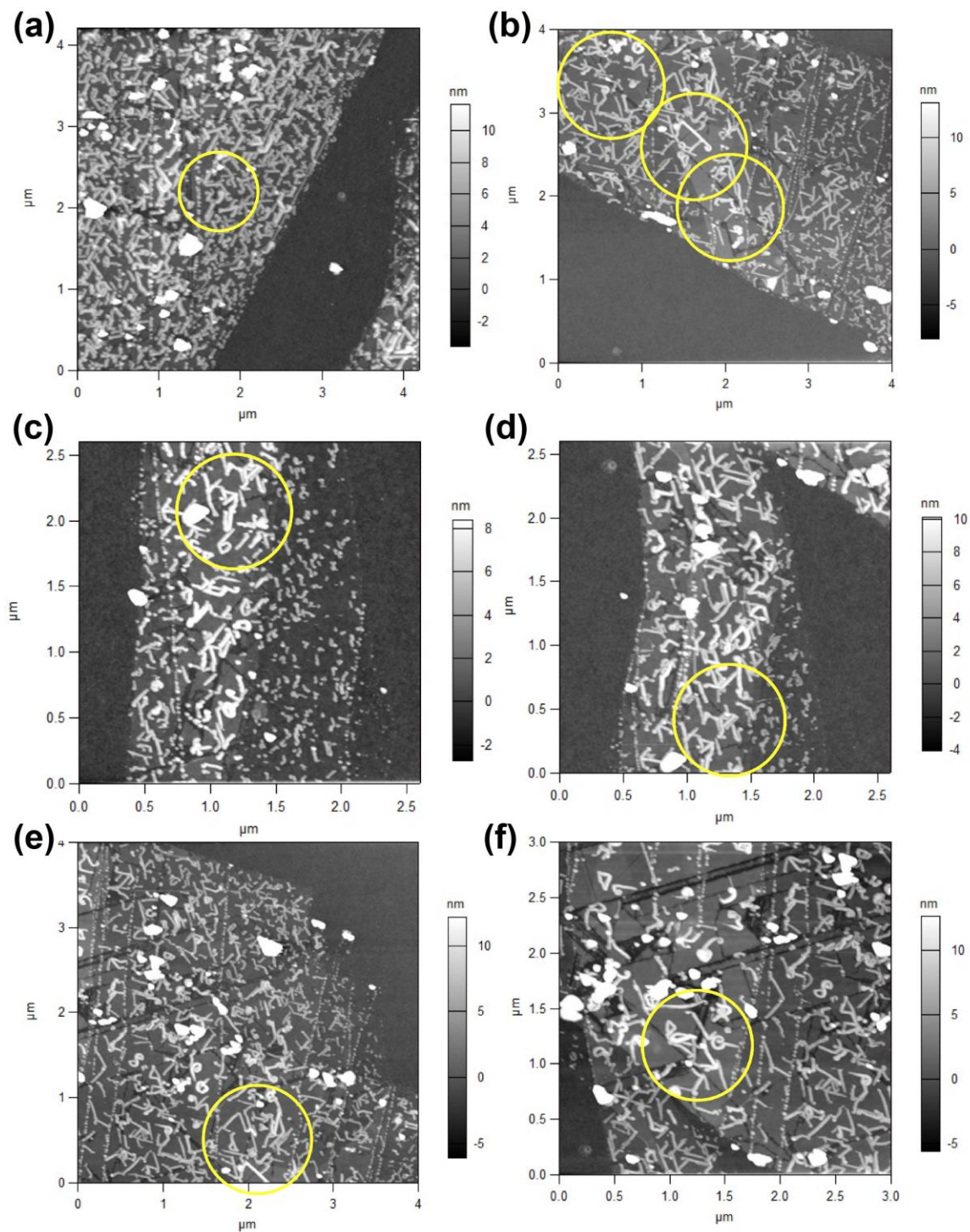


Figure 1. An assortment of recently prepared crystallographically-aligned carbon nanotubes grown over insulating few-layer graphene etch tracks.

Related to the two-dimensional channel materials and the atomic-resolution imaging, we have developed a dry transfer and placement technique of atomically-thin materials that does not require solvents. These samples are currently being imaged at ORNL using in-situ scanning transmission electron microscopy (STEM). Our initial results indicate that the surfaces are clear of any residue due to sample preparation. We are also using this technique for preparing the two-dimensional channels over the crystallographic electrodes.

We have also recently performed multi-terminal nanoscale electrical measurements on organic composite films that are similar to those we will perform on the ultra-short 2D materials.⁷

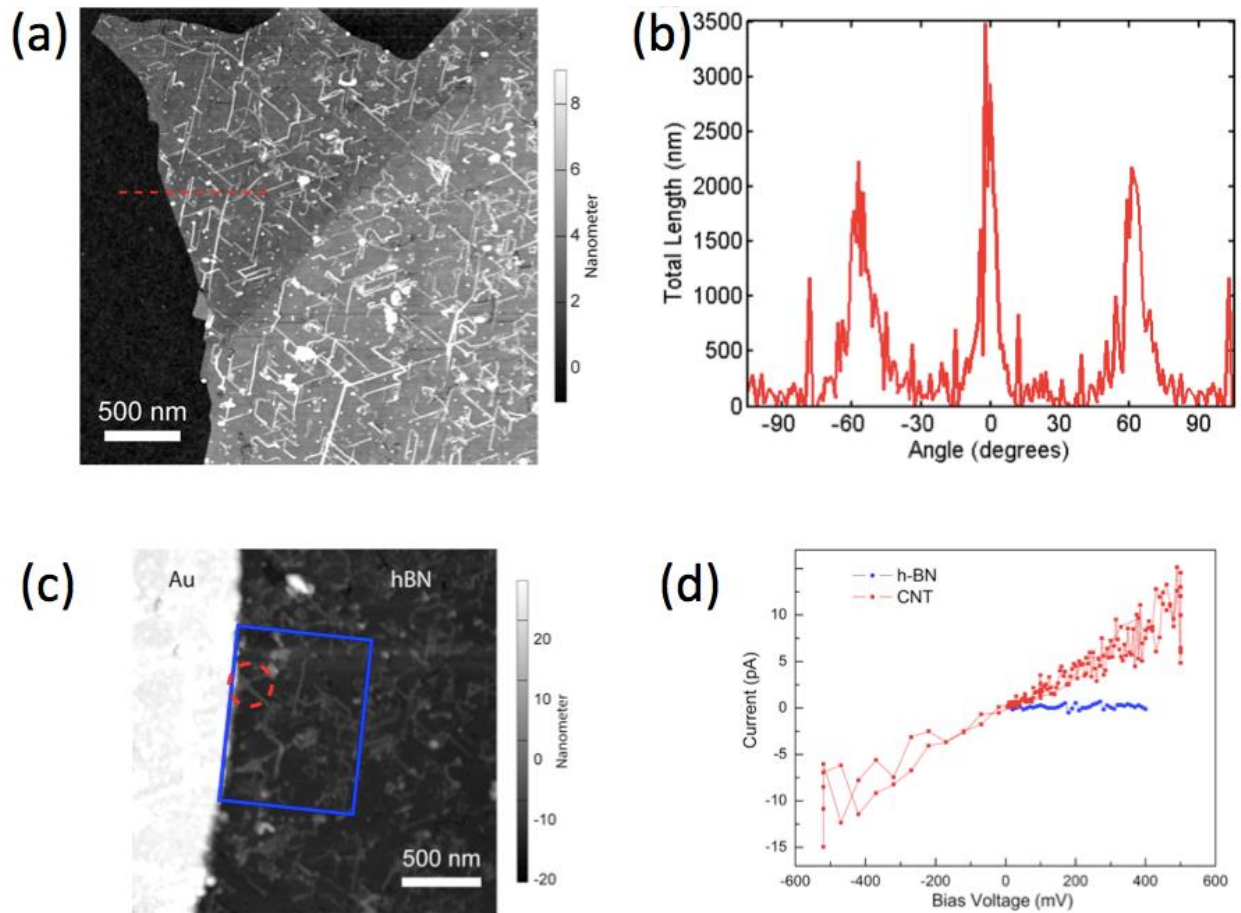


Figure 2. (a) Crystallographically-aligned nanotubes on boron nitride (hBN) surface and (b) histogram showing alignment. (c-d) Electrical measurements of aligned nanotubes on hBN.

Future Plans

Our upcoming future work on this program will include extensive electrical transport measurement on the ultra-short atomically-thin test devices, and their atomic-scale imaging at ORNL.

References

- ¹ Hunley, D. P., Johnson, S. L., Stieha, J. K., Sundararajan, A., Meacham, A. T., Ivanov, I. N. & Strachan, D. R. Crystallographically Aligned Carbon Nanotubes Grown on Few-Layer Graphene Films. *ACS Nano* **5**, 6403–6409 (2011).
- ² Nasserri, M., Hunley, D. P., Sundararajan, A., Boland, M. J. & Strachan, D. R. Tuning between crystallographically aligned carbon nanotube growth and graphene etching. *Carbon* **77**, 958-963 (2014).
- ³ Hunley, D. P., Sundararajan, A., Boland, M. J. & Strachan, D. R. Electrostatic Force Microscopy and Electrical Isolation of Etched Few-Layer Graphene Nano-Domains. *Appl. Phys. Lett.* **105**, 243109 (2014).
- ⁴ Hunley, D. P., Boland, M. J. & Strachan, D. R. Integrated Nanotubes, Etch Tracks, and Nanoribbons in Crystallographic Alignment to a Graphene Lattice. *Adv Mater* **27**, 813-818 (2015).
- ⁵ Ansary, A., Nasserri, M., Boland, M. J., Guiton, B. S. & Strachan, D. R. Boron Nitride One-Dimensional Crystallographic Catalytic Etching and Nanoribbons. *In preparation*.
- ⁶ Nasserri, M., Ansary, A., Boland, M. J. & Strachan, D. R. Carbon Nanotubes on Boron Nitride with Crystallographic Orientation. *In preparation*.
- ⁷ Liang, Z. M., Boland, M. J., Butrouna, K., Strachan, D. R. & Graham, K. R. Increased power factors of organic-inorganic nanocomposite thermoelectric materials and the role of energy filtering. *J. Mater. Chem. A* **5**, 15891-15900 (2017).

Publications

- ¹ Ansary, A., Nasserri, M., Boland, M. J., Guiton, B. S. & Strachan, D. R. Boron Nitride One-Dimensional Crystallographic Catalytic Etching and Nanoribbons. *In preparation*.
- ² Nasserri, M., Ansary, A., Boland, M. J. & Strachan, D. R. Carbon Nanotubes on Boron Nitride with Crystallographic Orientation. *In preparation*.
- ³ Liang, Z. M., Boland, M. J., Butrouna, K., Strachan, D. R. & Graham, K. R. Increased power factors of organic-inorganic nanocomposite thermoelectric materials and the role of energy filtering. *J. Mater. Chem. A* **5**, 15891-15900 (2017).

Fermi Gases in Bichromatic Superlattices

John E. Thomas

Physics Department, North Carolina State University, Raleigh, NC 27695

Program Scope

The purpose of the proposed program is the broad study of designer materials made of ultra-cold atoms and light, which provides new paradigms for emulating exotic layered systems. Of particular interest are bichromatic superlattices, which enable precise control of the band structure for mixtures of spin-up and spin-down atoms. Exploiting magnetically tunable two-body interactions near a Feshbach resonance, this system enables study of dimensionality, dispersion, and pairing in layered, strongly correlated Fermi gases, to model high-temperature superfluidity/superconductivity.

Recent Progress

1) 2D to Quasi-2D Crossover

We made the first studies of the crossover from a nearly two-dimensional (2D) Fermi gas to a quasi-2D gas, resolving a controversy in previously measured pairing spectra by our group¹ and those obtained by the Cavendish lab group of Michael Kohl² and the MIT group of Martin Zwierlein³.

In the 2D regime, the measured pairing energies by all groups are consistent with confinement-induced dimers, as predicted by 2D-BCS mean-field theory. These results suggested that a mean field description might be applicable in this 2D system, despite theoretical expectations that mean field theory cannot describe 2D systems, due to enhanced fluctuations in the confined geometry. For the quasi-2D regime, the measured pairing energies are in strong disagreement with confinement-induced dimers, and can be understood using a (beyond mean field) polaron model. No previous experiment has continuously tuned between these regimes, to shed light on the connection between them.

To explore this problem, we use a 1064 nm (red) standing wave to tightly confine the atoms in periodic pancake-shaped potentials $V(z)$. A focused CO₂ laser beam is superimposed on this lattice to provide tunable confinement in the radial r direction of the pancakes. With weak confinement, the potential is nearly 2D, with atoms residing the ground z -vibrational state. With tight confinement, the increase in the radial Fermi energy accesses higher z -vibrational states. For the first time, we measured *both* the radio-frequency pairing spectra and the radial cloud size in the same experiments, enabling a stringent test of predictions.

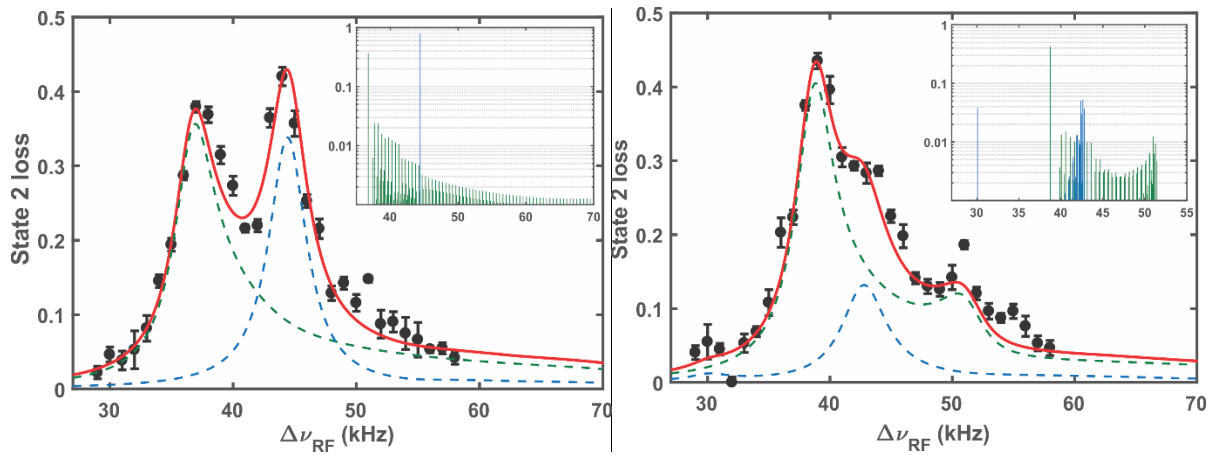
We find that while the dimer-2D-BCS model can predict the 2D spectra, the measured cloud radii are much smaller than 2D-BCS prediction, showing that the mean-field model is not valid

in this 2D system, despite apparent agreement with the spectra. In the quasi-2D regime, explaining both the spectra and the cloud profiles requires a beyond mean field treatment.

Our results clearly confirm theoretical predictions that a beyond mean field description is required throughout the 2D to quasi-2D crossover. Further, we find that for binding energy small compared to the Fermi energy, the measured cloud radii approach predictions for a Fermi liquid.

2) Pairing in a Bichromatic Superlattice

In the past year, our primary focus has been on comprehensive experimental and theoretical studies of atom pairing in a bichromatic superlattice, which will enable new studies of superfluidity, nonequilibrium dynamics, and exotic phases of matter in the strongly interacting regime near a Feshbach resonance. For these experiments, we combine 1064 nm (red) and 532 nm (green) standing wave lattices, which are superimposed on ${}^6\text{Li}$ atoms confined in a CO_2 laser trap in a mixture of the two lowest hyperfine states (denoted 1,2). With control of both the amplitudes and relative phase ϕ of the green and red lattices, we are able to create periodic double-well potentials of arbitrary shape and symmetry. Using radio-frequency spectroscopy to induce transitions from state 2 to an initially unoccupied state 3, we have observed a rich spectral structure, strongly dependent on the relative phase between the red and green lattices, posing new questions about the entanglement between the dimer center of mass motion and the relative motion within the dimer pair. Spectra for symmetric periodic double wells (left for $\phi = 0$) and tilted periodic double wells (right for $\phi = \pi/35$) are shown below.



The observed spectra suggest multiple dimer pairing mechanisms, perhaps with two atoms in the first band or for one atom in each of the first two bands. However, without a comprehensive theory, the origin of the complex spectral structure and its sensitivity to the relative phase of the lattice remained unclear.

To interpret the data, we succeeded in developing a rigorous theory of atom pairing in a bichromatic superlattice, using a 9-band model and including finite harmonic confinement in the radial direction. For tight radial confinement in a single lattice, our model reduces to the well-known Hubbard model, which is often employed as a simple approximation. For the weak radial confinement employed in our experiments, our model predicts a nontrivial spectral structure, consisting of hundreds of transitions from the initially populated dimer states to a dense, but discrete set of bound states and “trap” states with energies near the bare two-atom lattice states. We have computed all of the transition probabilities (insets in the figures), the corresponding spectra arising from each initial state (green-dashed and blue-dashed curves), and the Boltzmann factor weighted total spectra (red curves), in excellent agreement with the measurements.

By comparing our predictions to experimental spectra, we are now able to clearly identify the two initial 1-2 dimer states that contribute the spectrum. For $\phi = 0$, with symmetric, periodic double well potentials, the two initial states are delocalized, symmetric or antisymmetric in the CM coordinate, and closely spaced in total energy. Increasing ϕ to $\pi/35$ produces tilted double wells, for which the two initial states are localized, left or right well states, with a larger energy separation. By altering the energy difference, the choice of phase strongly affects the Boltzmann factor and hence the initial state populations. Further, the change in the symmetry of the initial 1-2 dimer states greatly affects the strengths of the radio frequency transitions to the final 1-3 dimer states as observed in the spectra.

Future Plans

We will complete our measurements of pairing spectra, as a function of interaction strength, relative phase and amplitudes of the green and red lattices.

We have installed an electro-optic modulator to enable dynamical control of the relative phase of the red and green lattices. This has already improved our measurement method and enables new studies of the non-equilibrium dynamics of multiple pairing mechanisms in the superlattice.

References

- 1) Y. Zhang, W. Ong, I. Arakelyan, and J. E. Thomas, Phys. Rev. Lett. **108**, 235302 (2012).
- 2) B. Frohlich, M. Feld, E. Vogt, M. Koschorreck, W. Zwerger, and M. Kohl, Phys. Rev. Lett. **106**, 105301 (2011).
- 3) A. T. Sommer, L. W. Cheuk, M. J. H. Ku, W. S. Bakr, and M. W. Zwierlein, Phys. Rev. Lett. **108**, 045302 (2012).

Publications

- 1) Chingyun Cheng, J. Kangara, I. Arakelyan, and J. E. Thomas, “Fermi Gases in the Two-Dimensional to Quasi-Two-Dimensional Crossover,” Phys. Rev. A **94**, 031606(R) (2016).

Designing Metastability: Coercing Materials to Phase Boundaries

T. Zac Ward, Oak Ridge National Laboratory

Program Scope

Crystalline materials are defined by their highly ordered microscopic arrangement of atoms. Functionality is then dictated by how the constituent atoms and their spatial relationship to one another affects the electrons in the material. The often strong coupling between spin, charge, orbital, and lattice degrees of freedom in transition metal oxides (TMOs) creates a particularly high sensitivity to slight variations in the crystal composition and structure. The crystal lattice—including the coupled effects of lattice parameter, symmetry, strain state, and octahedral rotations—is thus one of the most important degrees of freedom in these materials. Effective control over lattice parameters not only facilitates the understanding of multiple interactions in strongly correlated systems, but also creates new phases and emergent behaviors: ranging from metal-insulator transitions to superconductivity to multiferroicity. Lattice engineering through epitaxy and/or chemical pressure induced by isovalent substitution are widely used methods of controlling lattice parameters in TMOs and have demonstrated great functional importance. However, these routes can be a tedious trial and error process that requires multiple samples to be grown while only allowing discrete symmetry configurations dictated by available substrate and the Poisson effect. These methods also rule out the ability to continuously and/or locally control a material's structure and resulting function. In other words, we have many technologically important materials which are highly sensitive to small structural perturbations but no means of applying these structural perturbations systematically to explore and ultimately design explicit structure-driven functionalities. Recent work has shown that low energy He ion implantation is a viable means to bypass these limitations by allowing continuous, post-synthesis modification of structure in crystalline films through a "strain doping" process¹⁻⁴.

This project is aimed at creating, understanding, and utilizing previously inaccessible structural distortions in transition metal oxides by means of strain doping, with the goal of obtaining new and highly controllable functional properties. We examine how global structural changes induce emergent local inhomogeneities arising from metastabilities using a top-down approach. The area of implantation can also be applied at the nanometers scale which allows comparative bottom-up studies where we intentionally create local distortions to observe their impact on meso- and macroscopic phenomena. The specific aims of this project are: (1) to design metastable ferroic states, (2) to understand local inhomogeneity's role in emergent functionalities, and (3) to understand the mechanisms of structural distortions under strain doping. This work will provide previously hidden insights into the structure-function relationship of transition metal oxides while providing a means of designing competing nanoscale functionalities locally in a single crystal wafer. Together, these aims will provide significant insight into the role of strain and of defects in determining properties of TMO systems.

Recent Progress

The central challenge of this proposal is to create, understand, and utilize previously inaccessible structural distortions in transition metal oxides with the goal of obtaining enhanced functional properties. Our effort is motivated by the ability to exert unprecedented control over crystal symmetries related to single axis lattice expansion and octahedra rotation through strain doping; the availability of exceptional tools to analyze materials across multiple length scales; and the need for a fundamental understanding of how the strain doping process modifies crystal structure. Selected highlights of recent progress are listed as follows:

Strain Doping: A new approach to controlling orbital populations and crystal anisotropy

Interstitial helium atoms can be used to control the length of a single axis in a crystal lattice, allowing for delicate manipulations of complex behavior¹. Crystal structure is of central importance to understanding and controlling complex materials that offers great potential functionality in high-temperature superconductors, multiferroics, and colossal magnetoresistors. However, current methods of controlling lattice structure are limited to methods that cannot be continuously controlled in a single direction. These restrictions can be overcome by implanting helium atoms into a crystal, providing a means to finely control electron orbits and lattice-anisotropy-dependent electronic and magnetic behaviors (**Fig. 1**). This approach can be applied to any epitaxially locked thin film across a wide spectrum of materials. This new ability is critical to fundamental studies and promises to accelerate commercial deployment of complex materials by providing a way to tune material properties using wafer-scale processing that can be implemented using existing ion-implantation infrastructure. Ultimately, strain doping may become an important means to tune tomorrow's complex materials, similar to how electron/hole doping engineers today's semiconducting materials.

Controlling optical bandgap in semiconducting oxide

This study demonstrated that helium implantation allows for continuous control of optical band gaps in semiconducting oxide films through the resultant strain — an impossibility with traditional strain engineering^{2,3} (**Fig.**

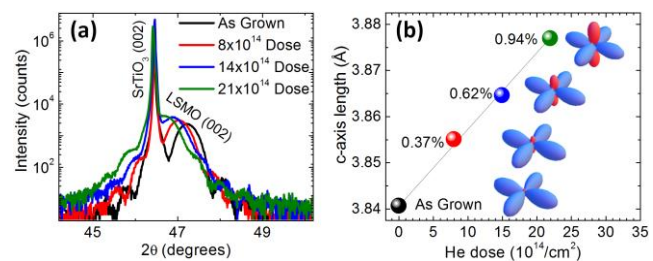


Fig. 1 X-ray data on helium implanted La_{0.7}Sr_{0.3}MnO₃ films. (a) θ - 2θ scans of LSMO thin films on SrTiO₃ substrates under different helium dosage. (b) The out-of-plane lattice constant changes as a function of helium dose where percentages note the change in the c -axis relative to the undosed state. *Inset*: calculated orbital populations of the x^2-y^2 (blue) and $3z^2-r^2$ (red) for related strain state.

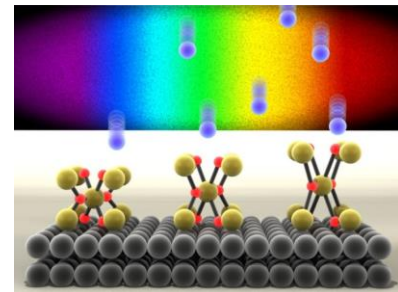


Fig. 2 Inserting helium atoms into a SnO₂ crystalline film allows for fine control over the elongation of the out-of-plane axis which drives a reduction in optical bandgap (represented here as a red-shift with increased doping).

2). This critical advance allows a direct approach to tuning material properties which may significantly impact several alternative energy technologies. While traditional epitaxy results in multi-directional lattice changes that only allow discrete increases in bandgap, this work showed that a downward shift in the band gap can be linearly dictated as a function of out-of-plane lattice expansion. Density functional theory calculations showed that uniaxial strain provides a fundamentally different effect on the band structure than traditional multi-axes strain effects. Charge density calculations provided further explanation by showing that uniaxial strain drives orbital hybridization inaccessible to traditional strain engineering techniques. Importantly, the use of noble ions may allow for bandgap tuning without inducing charge trap sites.

Manipulating octahedral rotation

In this work, helium implantation is used to control the octahedral rotation pattern in a single crystal perovskite SrRuO₃ film⁴. The perovskite unit cell is the fundamental building block of many functional materials. The manipulation of this crystal structure is known to be of central importance to controlling many technologically promising phenomena related to superconductivity, multiferroicity, magnetoresistivity, and photovoltaics. The broad range of properties that this structure can exhibit is in part due to the centrally coordinated octahedra bond flexibility, which allows for a multitude of distortions from the ideal highly symmetric structure. Continuous and fine manipulation of these distortions is not possible with traditional techniques. We showed that controlled insertion of He atoms into an epitaxial perovskite film can be used to finely tune the lattice symmetry by modifying the local distortions, i.e., octahedral bonding angle and length (Fig. 3). Implanted He atoms induced out-of-plane strain, thereby providing the ability to controllably shift the bulk-like orthorhombically distorted SrRuO₃ film to a tetragonal structure by shifting the oxygen octahedra rotation pattern. The ability to finely control octahedral rotations across any material class is expected to greatly enhance our ability to explore fundamental properties and generate novel functionality.

Future Plans

Great initial strides with strain doping have been made, demonstrating that we can tune crystal structures in a manner never before possible. We may now begin to exploit this through directed studies across a wide range of transition metal oxides. This new ability to continuously control lattice symmetry allows for the fine structural manipulations needed to address many pressing questions regarding structure–function relationships while opening new unexplored structural geometries for fundamental investigation. Further, the ability to “write” different magnetic, ferroelectric, and electronic behaviors at the nanoscale into a single crystal wafer opens the door to designing truly revolutionary multifunctional devices. Employing the same ion implantation infrastructure that is currently used in the semiconductor industry, we can envision

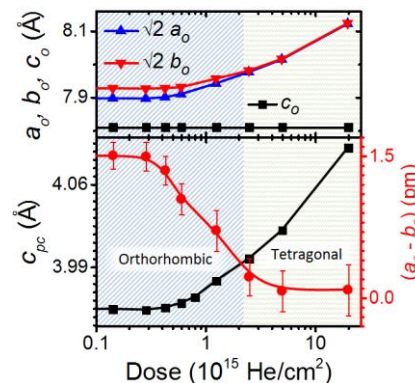


Fig. 3 Helium implantation allows for continuous control over octahedral rotation patterns and crystal symmetry.

a future in which the flexibility of locally strain-doped correlated materials could be used to design next generation multistimulus-multiresponse characteristics far beyond what is currently possible by electron/hole doping of simple semiconducting materials.

References

1. Guo, H. *et al.* Strain Doping: Reversible Single-Axis Control of a Complex Oxide Lattice via Helium Implantation. *Phys. Rev. Lett.* **114**, 256801 (2015).
2. Herklotz, A., Rus, S. F. & Ward, T. Z. Continuously Controlled Optical Band Gap in Oxide Semiconductor Thin Films. *Nano Lett.* **16**, 1782–1786 (2016).
3. Herklotz, A. *et al.* Symmetry driven control of optical properties in WO₃ films. *APL Mater.* **5**, 066106 (2017).
4. Herklotz, A. *et al.* Controlling Octahedral Rotations in a Perovskite via Strain Doping. *Sci. Rep.* **6**, 26491 (2016).

Publications

N/A: New Project

Charge inhomogeneity in correlated electron systems: charge order or not

PI: Barrett O. Wells

Department of Physics and Institute of Materials Science

University of Connecticut, Storrs, CT 06269-3046

barrett.wells@uconn.edu

Program Scope

The goal of this program is to develop an understanding of how and why conduction electrons arrange themselves in correlated electron systems, with particular emphasis on superconducting and closely related materials. Our strategy is to explore materials in which dopants can be controlled in a manner that leads to interesting properties. A primary path towards this goal is to compare the properties of similar compounds doped with highly mobile oxygen defects versus static cation substitutions. While charge and spin order are common in both, doping via oxygen defects often leads to electronic phase separation. In the cases we study, oxygen can be incorporated topotactically, at lower temperatures within an already formed crystalline network.

Our group both synthesizes materials and performs advanced measurements. Synthesis capabilities include the growth of epitaxial films using laser deposition and control of oxygen concentration with a variety of techniques including electrochemical oxidation, ozone treatment, and oxygen annealing. We pursue advanced measurements such as magnetic neutron scattering, resonant x-ray scattering and μ SR, and look to partner with experts in other techniques.

The systems we study include unconventional superconductors and related materials, mostly transition metal oxides. We have a long running interest in the unique cuprate superconductor $\text{La}_{2-x}\text{Sr}_x\text{CuO}_{4+y}$, co-doped with both Sr on La sites and excess oxygen. Samples with adequate excess oxygen spontaneously phase separate into lower doped, stripe-like magnetic phases and non-magnetic high T_C superconducting phases. In some sense, the separated regions are notably pure examples of each phase making an interesting test-bed for new developments on the cuprates. We have pushed lately to investigate related compounds, looking for universal properties in doped Mott insulators and related strongly correlated metals. This has led to studies of 214 nickelates, 113-perovskite cobaltates, and similar compounds that also can be charge doped through either cation substitution or oxygen defect formation. The oxygen doped version often self-segregate into regions with different effective charge density, with the stable phases characterized by particular charge order.

Recent Progress

Charge order in electronically phase separated $\text{La}_{2-x}\text{Sr}_x\text{CuO}_{4+y}$

Over the past few years charge order (CO) has been found in most cuprate superconductors doped to have $1/8^{\text{th}}$ hole per planar Cu site. [1] An important exception has been $\text{La}_2\text{CuO}_{4+y}$, doped with large amounts of excess oxygen. As noted above, this material spontaneously phase separates into non-superconducting regions with stripe-like magnetism and optimally doped superconducting regions. [2] The magnetic regions ought to also have well-developed charge order if the stripe picture holds, but several searches failed to find CO.

Through a careful study of freshly cleaved samples, we have been able to find charge order peaks in a sample of $\text{La}_2\text{CuO}_{4+y}$, whose near surface regions was doped close to an overall hole concentration near $1/8^{\text{th}}$ hole per Cu. Samples whose near surface region was doped nearer to 0.16 holes per Cu showed no such charge order peak. The behavior of this peak matches

expectations for intertwined charge and spin order. Fig. 1 shows a basic q-scan over the peak and the temperature dependence of the intensity.

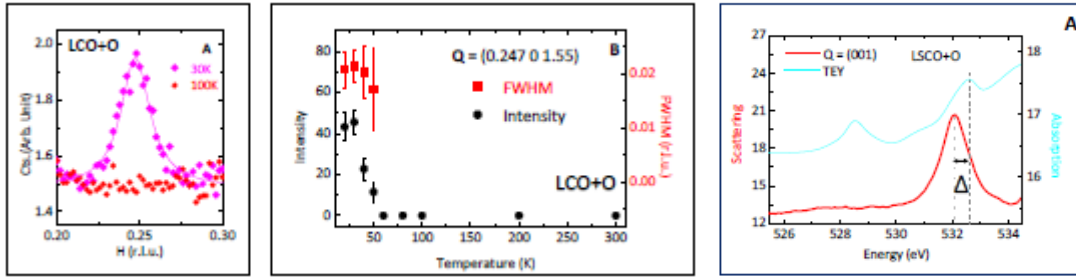


Fig. 1. Left: Q scan over the charge order peak at two temperatures (background subtracted). Center: temperature dependence of the charge order peak intensity and peak width. Right: Bottom trace is the energy dependence of the resonantly allowed (001) peak for a sample doped to have near 0.16 holes per Cu (no charge order). Top trace is the x-ray absorption measured in total electron yield for comparison.

Another peak which may appear on resonance in the 214 family of cuprates is the nominally disallowed (001) reflection. When resonant at energies associated with the apical oxygen or lathanide, the peak reflects the presence of the low temperature tetragonal structural phase. [3] When resonant at energies associated with the copper and in-plane oxygen, this peak has been proposed as a direct measure of electronic nematicity. [4] For the super-oxygenated compounds, we found no (001) peak at any resonance energy, though were able to find it in higher doped samples at energies associated with the LTT phase. The lack of such a peak in the charge-spin stripe phase is curious as it is hard to envision the charge-stripe phase without x/y anisotropy. Further, the lack of this peak at the LTT-related energies firmly establishes that charge/spin stripes do not require pinning by the LTT tilt pattern.

Electronic phase separation and charge order in related compounds.

At least two other transition metal oxide systems exhibit electronic phase separation when charge doped using mobile oxygen defects but not when doped using cation substitution: 214-nickelates and 113-cobaltates. Both sets of compounds have many parallels to the cuprates. Here we recap some recent work on the cobaltates, the lesser known of these compounds.

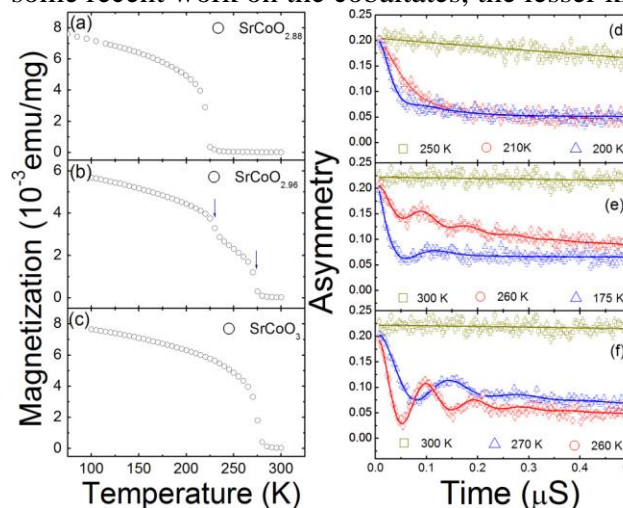


Fig. 2. A comparison for three samples of the bulk magnetization and the zero-field μ SR asymmetry profile: top panels for $\text{SrCoO}_{2.88}$, middle for $\text{SrCoO}_{2.96}$ (mixed phase), bottom for SrCoO_3 . Panels (a)-(c) are bulk magnetization. Panels (d)-(f) are muon profiles, with solid lines representing model fits. The intermediate and low temperature muon profiles for $\text{SrCoO}_{2.96}$ (panel e), can only be fit by a composite model.

Hole doping LaCoO_3 through substitution of Sr^{2+} for La^{3+} leads to a spin glass and short length scale charge variations [5]. Controlling the charge doping of $\text{SrCoO}_{2.5}$ - SrCoO_3 with mobile oxygen defects leads to the coexistence of multiple magnetic transitions. For example, $\text{SrCoO}_{2.88}$ is ferromagnetic with $T_C = 220$ K and SrCoO_3 is ferromagnetic with $T_C = 280$ K. For intermediate oxygen concentrations a double transition appears with characteristic temperatures of 220 and 280 K, despite the fact that the crystal structure is intermediate between $\text{SrCoO}_{2.88}$ and SrCoO_3 and not a sum of these end point structures. We conducted mSR experiments, a local probe of magnetism, to determine that the multiple magnetic transitions in SrCOO_x ($2.88 < x < 3$) represent different magnetic phases in separate regions of the sample. However, the low-temperature muon asymmetry needs a third, damped component for a good fit, indicating that inter-domain regions are substantial and the phase separated regions are smaller than in $\text{La}_2\text{CuO}_{4+y}$.

The unique phases in SrCOO_x ($2.88 < x < 3$) are both ferromagnetic, and thus do not provide any obvious driving force for phase separation. Since the missing oxygen in the stable phases constitute a simple fraction, we used resonant scattering to look for some commensurate ordering. For the $\text{SrCoO}_{2.88}$ phase alone, we found strongly resonant peaks at the $(\frac{1}{4}, \frac{1}{4}, \frac{1}{4})$ position relative to the simple perovskite unit cell. These peaks appear to represent combined charge and orbital ordering, with an example of the resonant behavior in Fig. 4. Among transition metal oxide samples we know to electronically phase-separate, there does not appear to be a common thread in the electronic ground states of the stable phases. However, the presence of charge order in at least one of the stable phases does appear to be universal – perhaps indicating the source of the tendency to phase separate is to accommodate charge order.

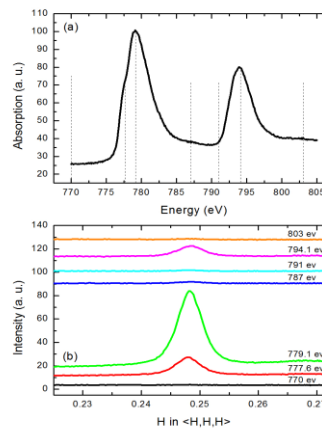


Fig. 3. (a) Absorption of a film of $\text{SrCoO}_{2.88}$ taken at $T = 250$ K ($T_C = 220$ K). (b) An X-ray diffraction scan in the longitudinal direction through the $(\frac{1}{4}, \frac{1}{4}, \frac{1}{4})$ position at several different photon energies. The photon energies used are indicated by dashed lines in part (a). The peak is strongest at the L_2 edge, visible at the L_2 edge, and not measurable otherwise.

Future Plans

Our future plans are to pursue a line of continuing work on charge order and electronic phase separation and to begin a new effort studying unconventional superconductivity in electron doped SrTiO_3 .

For the studies of charge order and electronic phase separation we will pursue several follow-up studies to those above. In the cuprates we wish to explore an apparent connection between the mix of cation (Sr for La) and anion (O) dopants and the size of the charge and spin ordered regions as measured by the scattering peak widths. This may give insight in the role of disorder on the electronic properties. In the cobaltates, we are studying samples at the same electron concentration, but doped with cation substitution rather than oxygen vacancies, for example $\text{Sr}_{0.75}\text{La}_{0.25}\text{CoO}_3$ in comparison to $\text{SrCoO}_{2.88}$. This type of study can disentangle features inherently driven by the charge state from chemistry associated with the particular stoichiometry.

We are very excited for building a new research thrust on strain effects and the interplay between polar phases and unconventional superconductivity in electron-doped SrTiO_3 . SrTiO_3 has long been a playground for new concepts in condensed matter physics, and a series of recent

works have revisited unconventional superconductivity in the material at extremely low carrier concentration. A recent theory by Balatsky et al. postulates that superconductivity is due to proximity to a quantum phase transition between ferroelectric and paraelectric states. That transition can be driven by several tuning parameters, including oxygen isotope substitution, cation substitution for Sr, or biaxial strain in films. Our group has expertise both in the growth of highly strained films and charge doping via oxygen control, and thus are well positioned to produce film samples tuned via strain. The project takes advantage of recent expansion of the condensed matter program at the University of Connecticut, where we have hired Dr. Balatsky who will provide theory support, Dr. Sochnikov who will lead low temperature measurements and scanning SQUID microscopy to find phase variation, and Dr. Hancock who will lead optical measurements of phonon spectra as a function of strain and the connection to superconductivity.

References

1. S. Blanco-Canosa, *Phys. Rev. B* **90**, 054513 (2014); J. Fink et al, *Phys. Rev. B* **79**, 100502 (2009). ; E. H. da Silva Neto et al., *Science* **343**, 393 (2014); R. Comin et al., *Science* **343**, 390 (2014); E. H. da Silva Neto et al., *Science* **347**, 282 (2015).
2. Hashini E. Mohottala, et al, “Phase Separation in Superoxygenated $\text{La}_{2-x}\text{Sr}_x\text{CuO}_{4+y}$ ” *Nature Materials* **5**, 377 (2006)
3. Jörg Fink et al., “Phase diagram of charge order in $\text{La}_{1.8-x}\text{Eu}_{0.2}\text{Sr}_x\text{CuO}_4$ from resonant soft x-ray diffraction” *Phys. Rev. B* **83**, 092503 (2011).
4. A. Achkar et al., “Nematicity in stripe-ordered cuprates probed via resonant x-ray scattering” *Science* **351**, 576 (2016).
5. C. He et al., “Doping fluctuation-driven magneto-electronic phase separation in $\text{La}_{1-x}\text{Sr}_x\text{CoO}_3$ single crystals” *Europhys. Lett.* **87**, 27006 (2009).
6. Jonathan M. Edge et al., “Quantum Critical Origin of the Superconducting Dome in SrTiO_3 ” *Phys. Rev. Lett.* **115**, 247002 (2015).

Publications

1. Zhiwei Zhang, R. Sutarto, F. He, F. C. Chou, L. Udby, S. L. Holm, Z. H. Zhu, W. A. Hines, J. I. Budnick, and B. O. Wells, “On Charge Order and Nematicity in Superoxygenated $\text{La}_{2-x}\text{Sr}_x\text{CuO}_{4+y}$ ” submitted to *Phys. Rev. Lett.* <https://arxiv.org/abs/1707.04367>
2. Zhiwei Zhang, Z.H. Zhu, A. Jayakody, J.I. Budnick, W.A. Hines, and B.O. Wells, “Structural and Magnetic Properties of Cobalt Telluride Thin Films” submitted to *Journal of Applied Physics*. <https://arxiv.org/abs/1707.06963>
3. F.J. Rueckert, F. Z. He, B. Dabrowski, W. A. Hines, J. I. Budnick, and B. O. Wells “Charge order in SrCoO_3 investigated through resonant soft x-ray scattering” submitted to *Phys. Rev. B* <https://arxiv.org/abs/1707.04336>
4. P. J. Ray, N. H. Andersen, T. B. S. Jensen, H. E. Mohottala, Ch. Niedermayer, K. Lefmann, B. O. Wells, M. v. Zimmermann, F. C. Chou, and L. Udby, “Staging superstructures in high-Tc Sr/O co-doped $\text{La}_{2-x}\text{Sr}_x\text{CuO}_{4+y}$ ” submitted to *Phys. Rev. Lett.* <https://arxiv.org/abs/1707.08871>
5. H. Jacobsen, S.L. Holm, M.-E. Lacatus, A. T. Roemer, M. Bertelsen, P.G. Freemany, M. Boehm, M. Skoulatos, R. Toft-Petersen, J.-C- Grivel, D. Prabhakaran, L. Udby, B.O. Wells, K. Lefmann, “Static and dynamic magnetic stripes in phase-separated high-temperature superconductors” submitted to *Phys. Rev. Lett.* <https://arxiv.org/abs/1704.08528v3>
6. Z. H. Zhu, F. J. Rueckert, J. I. Budnick, Ch. Niedermayer, L. Keller, Luetkens, B. Dabrowski, O. Wells, “Distinct Local Magnetic Structures in Single Crystalline SrCoO_{3-y} ,” *Phys. Rev. B* **93**, 224412 (2016). <https://doi.org/10.1103/PhysRevB.93.224412>

Title: Imaging Electrons in Atomically Layered Materials
PI: Robert M. Westervelt
Collaborator: Philip Kim
Address: School of Engineering and Applied Sciences, Harvard University
29 Oxford Street, Cambridge MA 02138
Email: westervelt@seas.harvard.edu

Program Scope

Atomically layered materials offer a dramatically new approach to electronics and photonics. Electrons in graphene have very long mean free paths that open the way to ballistic electronics [1, 2] as well as the ability to pass through potential barriers *via* Klein tunneling [3, 4], while a single sheet of hexagonal boron nitride (hBN) provides an insulating layer [5]. Andreev reflection transfers electrons and holes in graphene into Cooper pairs in a superconducting contact [6,7]. Transition metal dichalcogenides (TMDs) such as MoS₂ provide conventional semiconductors and optoelectronic materials that also can be cleaved into layers that are just a few quantum layers thick [8, 9]. By stacking different materials together, a new class of atomic-layer heterostructures with new properties can be created.

Imaging electron flow with a cooled scanning probe microscope (SPM) shows how electrons move through these new materials and provides the understanding we need make new types of devices [10-13, Bhandari et al. 2016].

Recent Progress

The past year has been quite successful. Sagar Bhandari has made oral presentations at four major international conferences: EDISON 20 held at the University of Buffalo on July 17-21, 2017; Electronic Properties of Two Dimensional Systems (EP2DS-22) held at Penn State University on July 31 - Aug 4, 2017; Mesoscopic Transport and Quantum Coherence held in Helsinki, Finland on Aug 5-8, 2017; and Low Temperature Physics (LT28) held in Gothenburg, Sweden on Aug 9-15, 2017.

In the past year, we have completed two imaging projects on hBN encased graphene devices using our cooled SPM described below: *Imaging Electron Flow in Graphene from a Collimating Contact*, and *Imaging Andreev Reflection in Graphene from a Superconducting Contact*.

Imaging Electron Flow in Graphene from a Collimating Contact

Graphene opens exciting opportunities for ballistic devices. A narrow electron beam is desirable, to understand and control electron flow. Figure 1(a) is an SEM image of a hBN-encased graphene sample with four collimating contacts, defined by etch. The end contact emits electrons while the zig-zag contacts on either side can absorb electrons travelling in the wrong direction. Collimation is turned on by grounding the zig-zag contacts, so they form an electron beam (Fig. 1(b)). Collimation can be turned off by floating the zig-zag contacts.

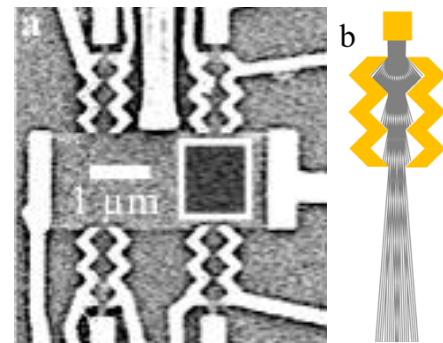


Fig. 1 (a) SEM image of hBN encased graphene device with 4 side contacts. (b) Ray tracing simulation of a collimating contact.

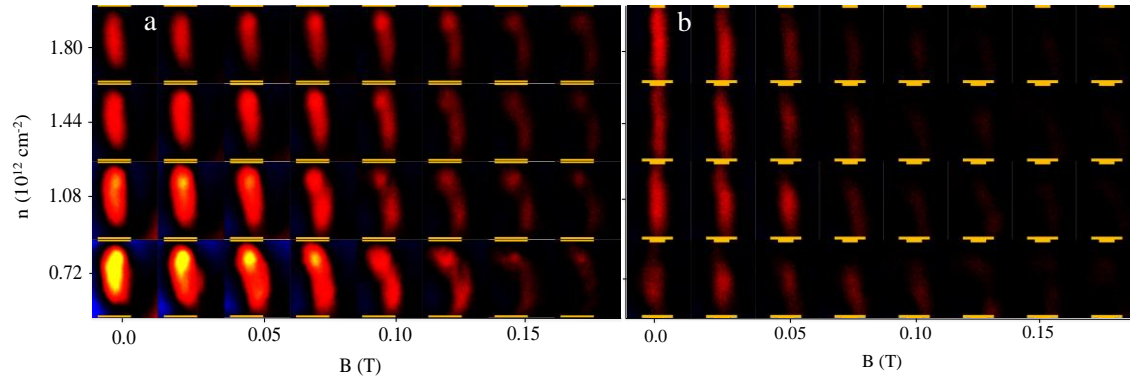


Fig. 2 Cooled SPM images of electron flow between the top and bottom contacts at 4.2K (white box in Fig. 1(a)). The top contact is a collimated electron emitter when the zig-zag side contacts are grounded. A perpendicular magnetic field B bends electron orbits; the electron density is n . (a) Broad flow without collimation, (b) narrow flow with collimation turned on.

A cooled SPM was used to image the pattern of electron flow between the emitting contact at the top right of Fig. 1(a) and collecting contact at the lower right. Collimation can be turned on for the top contact by grounding the zig-zag side contacts. The SPM tip creates a capacitive image charge in the graphene below that deflects electrons away from their original orbits, changing the transmission between the emitting and collecting contacts. An image of flow is created by displaying the change in transmission as the tip is raster scanned at a fixed height above the sample.

Comparison of the SPM images of collimated flow (Fig. 2(b)) with uncollimated flow (Fig. 2(a)) show that the collimating contact narrows the width of the electron beam when it is turned on. To measure the angular width of the electron beam emitted by the top contact, we applied a perpendicular magnetic field B that bends electron trajectories into cyclotron orbits so that they can miss the collecting contact, reducing the intensity of the SPM image. For the collimated contact (Fig. 2(b)) which produces an electron beam perpendicular to the sample side, the loss of intensity is significant. However, when the electrons enter over a larger range of angles for an uncollimated contact (Fig. 2(a)), the intensity if the image is maintained over a larger range of B , and the curvature of the cyclotron orbits is visible. By fitting the measured drop in the magnitude with B by ray-tracing simulations, we find that the half-width at half-maximum (HWHM) angular width is quite narrow $\Delta\theta = 9.2^\circ$ for the collimating contact, considerably narrower than the width $\Delta\theta = 54^\circ$ when collimation is turned off.

Imaging Andreev Reflection in Graphene from a Superconducting Contact

Andreev reflection from a superconducting contact provides a way to introduce the coherence associated with superconductivity into graphene [6,7]. Figure 3 is an SEM image of a hBN-encased graphene device with

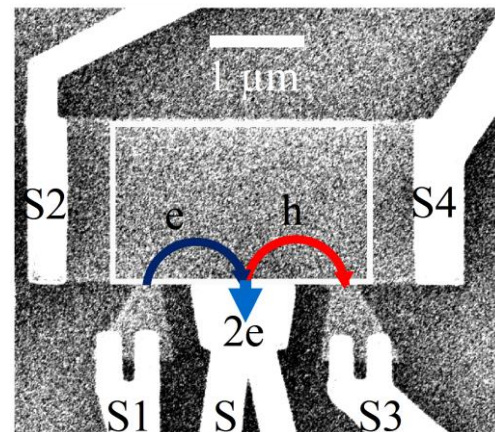


Fig. 3 SEM sample of hBN-encased graphene sample with superconducting contacts. Andreev reflection occurs when an electron (blue) and hole (red) in graphene convert to a Cooper pair in the superconductor.

superconducting contacts. In a perpendicular magnetic field B , magnetic focusing of electron and hole orbits occurs when the cyclotron diameter is equal to the contact spacing, as indicated by the schematic electron (blue) and hole (red) orbits in the inset to Fig. 3. Andreev reflection occurs when an electron hits the superconductor contact: a hole is reflected, traveling in the same direction along the sample wall, and a Cooper pair passes into the superconductor. The superconductor electron and hole are both in the conduction band: the electron is slightly above the Fermi level E_F and the hole is slightly below.

Figure 4 shows SPM images of flow in the magnetic focusing regime that visualize how Andreev reflection occurs. The top image shows electrons flowing along a cyclotron orbit between the two outer contacts, as indicated in the schematic diagram. The transmission of electrons is reduced (red) because the tip scatters them away from their original paths. The bottom image on the second magnetic focusing peak shows two cyclotron orbits: one between the left and center contacts, and one between the center and right contacts. The transmission between the two outer contacts is displayed in image. When Andreev reflection occurs, the image changes sign: scattering of holes by the SPM tip now increases the transmission of electrons and the image changes from red to blue.

Future Plans

In the coming year, we plan to pursue a number of projects: 1) The experiments to image the formation of a narrow electron beam in graphene by collimating contacts worked well. We plan to extend these measurements to from a beam of holes in the valance band. 2) The Andreev reflection imaging experiments were a first step. In collaboration with Philip Kim, we plan to image new geometries of graphene with superconducting contacts, to develop ways to make coherent electron and hole channels to transmit information. 3) A new student Mary Keenan is making etch-defined quantum point contacts (QPCs) for SPM imaging experiments. Unlike GaAs, graphene QPCs do not typically show well defined conductance steps at multiples of e^2/h . Possible causes could be nonuniformity due to edge roughness, strain, and electrostatic charge buildup. SPM imaging can clear up the situation by imaging electron flow and the possible formation of quantum dots [13]. 4) In collaboration with Kim, we plan to image MoS_2 quantum dots. SPM images provide detailed information about the location of electronic charge, and can do Coulomb blockade spectroscopy of energy states [13].

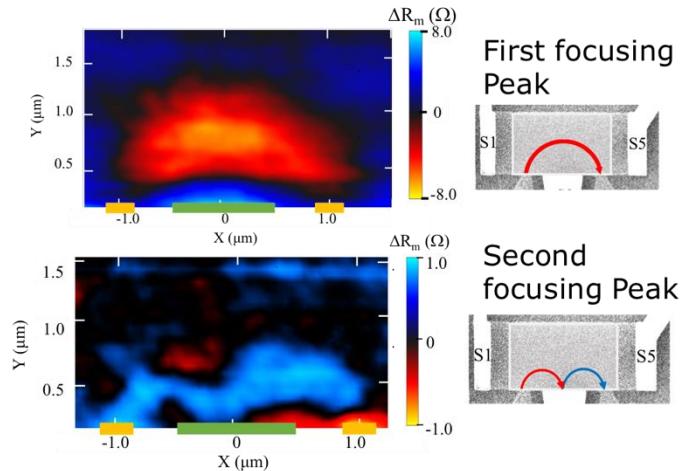


Fig. 4 (top) SPM image of electron flow on the first magnetic focusing peak that shows a cyclotron orbit connecting the two outer contacts. The tip reduces the transmission (red) by scattering electrons. (bottom) SPM image of flow between the outer contacts on the second focusing peak, where Andreev reflection has converted the electrons into holes. The tip now increases transmission of electrons (blue) by scattering holes.

References

- [1] A Geim, K Novoselov, *Nat. Mater.* **6**, 183–191 (2007).
- [2] AH Castro Neto, F Guinea, NMR Peres, KS Novoselov, A Geim, *Rev. Mod. Phys.* **81**, 109 (2009).
- [3] MI Katsnelson, KS Novoselov, A Geim, *Nat. Phys.* **2**, 620–625 (2006).
- [4] AF Young, P Kim, *Nat. Phys.* **5**, 222–226 (2009).
- [5] CR Dean, AF Young, I Meric, C Lee, L Wang, S Sorgenfrei, K Watanabe, T Taniguchi, P Kim, KL Shepard, J Hone *Nat. Nanotechnol.* **5**, 722–726 (2010).
- [6] CWJ Beenakker, *Phys. Rev. Lett.* **97**, 067007 (2006).
- [7] DK Efetov, L Wang, C Handschin, KB Efetov, J Shuang, R Cava, T Taniguchi, K Watanabe, J Hone, CR Dean, P Kim, *Nature Physics* **12**, 328-332 (2016).
- [8] S Kim, W-S Hwang, JH Lee, J Lee, J Yang, C Jung, H Kim, J-B Yoo, J-Y Choi YW Jin, SY Lee, D Jena, W Choi, and K. Kim, *Nature Comm* **3** 1011 (2012).
- [9] KF Mak, KL McGill, J Park and PL McEuen, *Science* **344**, 1489-1492 (2014).
- [10] MA Topinka, BJ LeRoy, RM Westervelt, SEJ Shaw, R Fleischmann, EJ Heller, KD Maranowski, AC Gossard, *Nature* **410**, 183 (2001).
- [11] BJ LeRoy, AC Bleszynski, KE Aidala, RM Westervelt, A Kalben, EJ Heller, KD Maranowski, AC Gossard, "Imaging electron interferometer", *Phys. Rev. Lett.* **94**, 126801 (2005).
- [12] Kathy E Aidala, RE Parrott, T Kramer, RM Westervelt, EJ Heller, MP Hanson, AC Gossard, "Imaging Magnetic Focusing of Coherent Electron Waves", *Nature Physics* **3**, 464 (2007).
- [13] Ania C Bleszynski, F Zwanenburg, R Westervelt, A Roest, E Bakkers, L Kouwenhoven, "Scanned Probe Imaging of Quantum Dots in InAs Nanowires", *Nano Lett* **7**, 2559 (2007).

Publications (last 2 years)

- Sagar Bhandari, G-H Lee, A Klales, K Watanabe, T Taniguchi, E Heller, P Kim, and RM Westervelt, "Imaging cyclotron orbits of electrons in graphene," *Nano Lett.* 16(3), 1690-1694 (2016), doi:10.1021/acs.nanolett.5b04609.
- Sagar Bhandari and RM Westervelt, "Imaging Electron Motion in Graphene," Special Issue *Hybrid Quantum Materials and Devices*, Semiconductor Science and Technology, volume 32 number 2 (IOP Science, 2017) doi:10.1088/1361-6641/32/2/024001.
- Sagar Bhandari, Gil-Ho Lee, P Kim, RM Westervelt, "Analysis of Scanned Probe Images of Magnetic Focusing in Graphene," *Proc IC Superlattices, Nanostructures and Nanodevices (ICSNN 2016)*, *J Elect. Materials*, (2017), arXiv:1608.02248, doi: 10.1007/s11664-017-5350-y
- Sagar Bhandari, Andrew Lin, RM Westervelt, "Investigating the Transition Region in Scanned Probe Microscope Images of the Cyclotron Orbit in Graphene," *Proc. IC Nanoscience and Technology (ICN+T)*, Busan, Korea, *J. Nanoelectronics and Optoelectronics* **12**, 1-4 (2017), doi: 10.1166/jno.2017.2158.
- Sagar Bhandari, K Wang, K Watanabe, T Taniguchi, P Kim, and RM Westervelt, "Imaging Electron Motion in a Few Layer MoS₂ Device," *Proc Int. Conf. Physics of Semiconductors*, Beijing, China, 2016, *IOP Conference Series*, in press (2017), arXiv:1608.02250
- Sagar Bhandari, G-H Lee, K Watanabe, T Taniguchi, P Kim, R M Westervelt, "Imaging Electron Flow in a Graphene Device with Superconducting Contacts," *Proc. Int. Conf. Low Temperature Physics (LT28)*, Gothenburg, Sweden, in review (2017).

Quantum Hall Systems In and Out of Equilibrium

Michael Zudov, University of Minnesota – Twin Cities

Program Scope

This program deals with quantum transport phenomena in semiconductor nanostructures focusing on the roles of microwave radiation, dc electric field, in-plane magnetic field, and disorder. The research expands upon the area originated by discoveries of integer and fractional quantum Hall effects [1], followed by other phenomena, such as quantum Hall stripes (QHS) [2-5], bubbles and associated reentrant quantum Hall states, microwave- and Hall field-induced resistance oscillations, etc. The proposal is aimed to address issues of contemporary interest related to both nonequilibrium and equilibrium physics in quantum Hall systems.

Recent Progress (on QHS)

1. Reorientation of QHS within a partially filled Landau level [6] – We have investigated the effect of the partial filling factor on the stripe reorientation by in-plane magnetic fields. In Fig. 1 we present resistances measured along two orthogonal directions, R_{xx} (solid line) and R_{yy} (dotted line), versus filling factor ν at different tilt angles θ , as marked. At $\theta = 0$, the data reveal strong anisotropy near $\nu = 9/2$ with $R_{xx} \gg R_{yy}$ [see Fig. 1(a)]; i.e., stripes are oriented along the y direction. At finite θ [Fig. 1(b)], stripes of orthogonal orientation (e.g., along the x direction) develop away from half filling, as manifested by $R_{xx} \gg R_{yy}$. These regions of orthogonal orientation propagate towards $\nu = 9/2$ [Fig. 1(c,d)] and eventually take over the whole range of ν at which the native stripes exist [Fig. 1(e)]. This behavior is generic and is readily observed in both spin-up and spin-down branches and in different Landau levels. We thus conclude that the stripes orientation can be controlled by the filling factor within a given Landau level. This switching of the anisotropy axes within a single Landau level can be attributed to a strong dependence of the native symmetry-breaking potential on the filling factor.

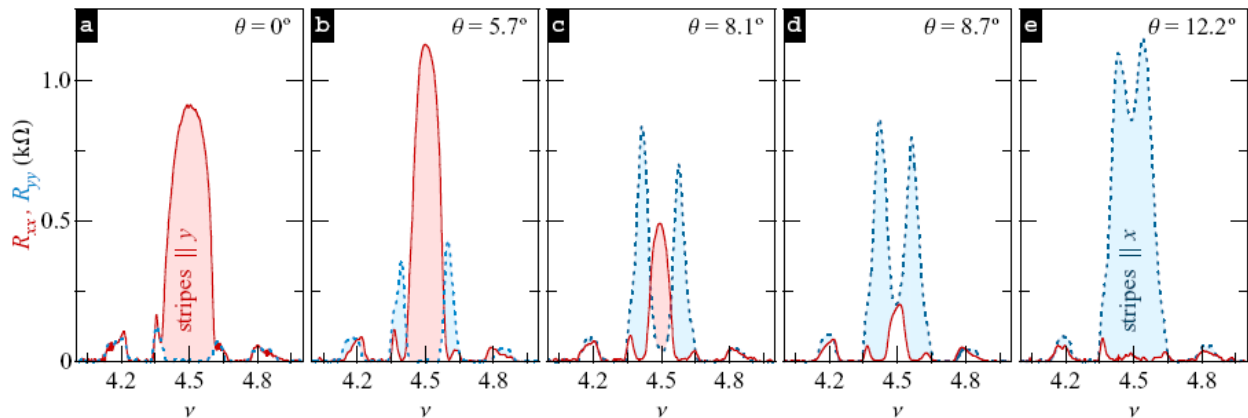


Fig. 1. R_{xx} (solid line) and R_{yy} (dotted line) vs filling factor ν at $B_{||} = B_y$ and different tilt angles θ , as marked.

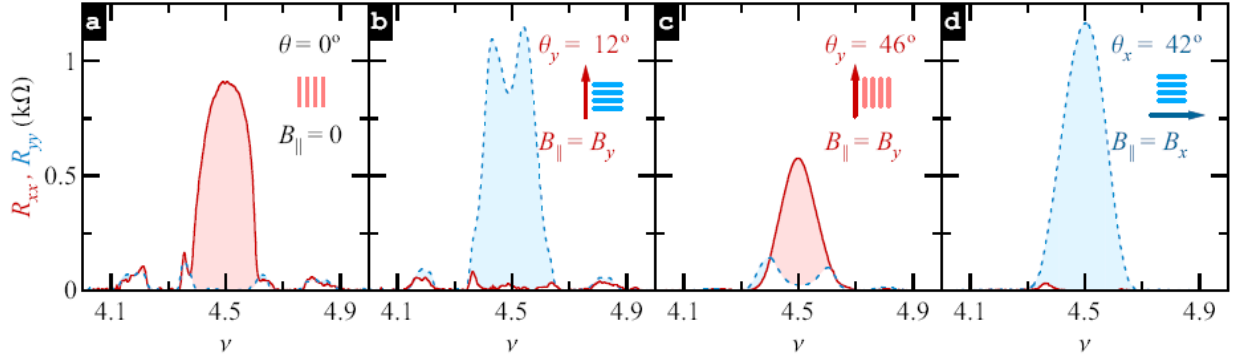


Fig. 2. R_{xx} (solid line) and R_{yy} (dotted line) vs ν at (a) $B_{\parallel} = 0$, (b-c) $B_{\parallel} = B_y$ and (d) $B_{\parallel} = B_x$.

2. Evidence for a new symmetry breaking mechanism reorienting QHS [7] – We have studied the effect of in-plane magnetic field B_{\parallel} on quantum Hall stripes [Fig. 2(a)]. In accord with previous studies [4,5], a modest B_{\parallel} applied parallel to the native stripes aligned them perpendicular to it [Fig. 2(b)]. However, upon further increase of B_{\parallel} , stripes were reoriented back to their native direction [Fig. 2(c)]. Remarkably, applying B_{\parallel} perpendicular to the native stripes also aligned stripes parallel to it [Fig. 2(d)], i.e., regardless of the initial orientation of stripes with respect to B_{\parallel} , stripes are ultimately aligned parallel to B_{\parallel} . These findings provide evidence for a new B_{\parallel} -induced symmetry-breaking mechanism which challenge our current understanding of the role of B_{\parallel} and should be taken into account when determining the strength of the native symmetry-breaking potential. Finally, our results indicate nontrivial coupling between the native and external symmetry-breaking fields, which has not yet been theoretically considered.

3. Effect of density on QHS orientation in tilted magnetic fields [8] – We have studied QHS in a variable-density sample. At $\nu = 9/2$, we observed one, two, and zero B_{\parallel} -induced reorientations at low, intermediate, and high densities, respectively [Fig.3]. The appearance of these distinct regimes is due to a strong density dependence of the B_{\parallel} -induced orienting mechanism which triggers the second reorientation, rendering stripes parallel to B_{\parallel} . Measurements at $\nu = 9/2$ and $11/2$ at the same, tilted magnetic field allowed us to rule out the density dependence of the native symmetry-breaking field as a dominant factor. These findings suggest that screening plays an important role in determining stripe orientation, providing guidance to theories aimed at describing native and B_{\parallel} -induced symmetry-breaking fields.

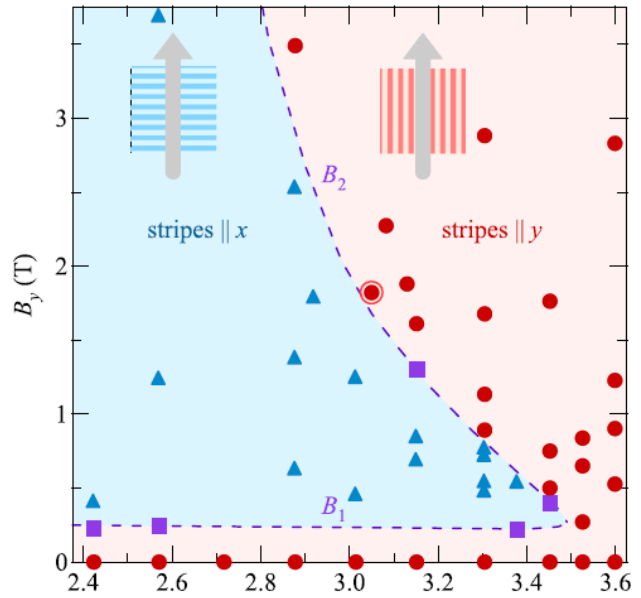


Fig. 3. Stripe orientation vs n_e and $B_{\parallel}=B_y$ at $\nu = 9/2$.

4. Temperature-induced reorientation of QHS in tilted magnetic fields [9] – We have found that the orientation of QHS can be changed by temperature T [Fig. 4]. Field-cooling/warming measurements and observation of a hysteresis at intermediate T allowed us to conclude that the T -induced reorientation of QHS signals the existence of two distinct minima in the symmetry-breaking potential. We also found that the native symmetry-breaking field does not depend on T and that low- T magnetotransport might not reveal the ground state even in the absence of hysteresis.

Future Plans (on QHS)

We next plan to perform the following studies:

- (i). Role of alloy disorder on QHS reorientation.
- (ii). Reorientation of QHS with abnormal native orientation in high density samples.
- (iii). Filling factor dependence of the second reorientation and with in-plane field applied perpendicular to the native stripes.
- (iv). Search for multiple reorientations in the first excited Landau level.
- (v). Role of density when the in-plane field applied perpendicular to the native stripes.
- (vi). QHS in two-subband systems in tilted magnetic fields.
- (vii). Relaxation dynamics from metastable QHS orientation.

References

- [1] K. von Klitzing, G. Dorda, and M. Pepper, Phys. Rev. Lett. **45**, 494 (1980); D.C. Tsui, H. L. Stormer, and A. C. Gossard, Phys. Rev. Lett. **48**, 1559 (1982).
- [2] A. A. Koulakov, M. M. Fogler, and B. I. Shklovskii, Phys. Rev. Lett. **76**, 499 (1996)
- [3] M. P. Lilly, K. B. Cooper, J. P. Eisenstein, L. N. Pfeiffer, and K. W. West, Phys. Rev. Lett. **82**, 394 (1999); R. R. Du, D. C. Tsui, H. L. Stormer, L. N. Pfeiffer, K. W. Baldwin, and K. W. West, Solid State Commun. **109**, 389 (1999).
- [4] M. P. Lilly, K. B. Cooper, J. P. Eisenstein, L. N. Pfeiffer, and K. W. West, Phys. Rev. Lett. **83**, 824 (1999); W. Pan, R. R. Du, H. L. Stormer, D. C. Tsui, L. N. Pfeiffer, K. W. Baldwin, and K. W. West, Phys. Rev. Lett. **83**, 820 (1999).
- [5] T. Jungwirth, A. H. MacDonald, L. Smrčka, and S. M. Girvin, Phys. Rev. B **60**, 15574 (1999); T. D. Stanescu, I. Martin, and P. Phillips, Phys. Rev. Lett. **84**, 1288 (2000).

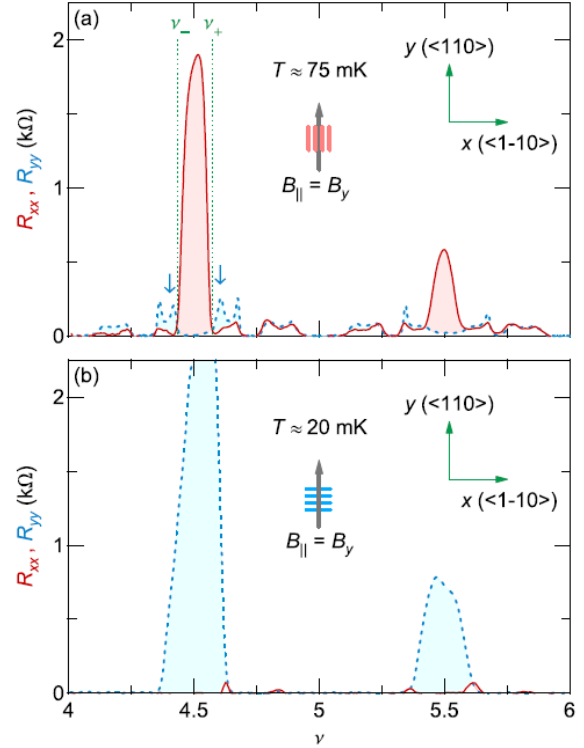


Fig. 4. R_{xx} (solid line) and R_{yy} (dotted line) vs ν measured at (a) $T \approx 75$ mK and (b) $T \approx 20$ mK.

- [6] Q. Shi, M. A. Zudov, J. D. Watson, G. C. Gardner and M. J. Manfra, Phys. Rev. B **93**, 121404(R) (2016)
- [7] Q. Shi, M. A. Zudov, J. D. Watson, G. C. Gardner and M. J. Manfra, Phys. Rev. B **93**, 121411(R) (2016)
- [8] Q. Shi, M. A. Zudov, J. D. Watson, Q. Qian, and M. J. Manfra, Phys. Rev. B **95**, 161303(R) (2017)
- [9] Q. Shi, M. A. Zudov, B. Friess, J. Smet, J. D. Watson, G. C. Gardner, and M. J. Manfra, Physical Review **95**, 161404(R) (2017)

Publications (2016-2017)

1. Q. Shi, M. A. Zudov, J. Falson, Y. Kozuka, A. Tsukazaki, M. Kawasaki, and J. Smet, “Nonlinear response of a MgZnO/ZnO heterostructure close to zero bias”, submitted to Physical Review B (2017)
2. M. A. Zudov, Q. Shi, I. A. Dmitriev, B. Friess, V. Umansky, K. von Klitzing, and J. Smet, “Hall field-induced resistance oscillations in a wide GaAs quantum well with tunable density”, submitted to Physical Review B – Rapid Communications (2017)
3. X. Fu, Q. A. Ebner, Q. Shi, M. A. Zudov, Q. Qian, and M. J. Manfra, “Microwave-induced resistance oscillations in a backgated GaAs quantum well”, Physical Review B **95**, 235415 (2017)
4. Q. Shi, M. A. Zudov, B. Friess, J. Smet, J. D. Watson, G. C. Gardner, and M. J. Manfra “Apparent temperature-induced reorientation of quantum Hall stripes”, Physical Review B – Rapid Communications **95**, 161404(R) (2017)
5. Q. Shi, M. A. Zudov, J. D. Watson, Q. Qian, and M. J. Manfra, “Effect of density on quantum Hall stripe orientation in tilted magnetic fields”, Physical Review B – Rapid Communications **95**, 161303(R) (2017)
6. Q. Shi, M. A. Zudov, J. Falson, Y. Kozuka, A. Tsukazaki, M. Kawasaki, K. von Klitzing, and J. Smet, “Hall field-induced resistance oscillations in MgZnO/ZnO heterostructures”, Physical Review B – Rapid Communications **95**, 041411(R) (2017)
7. Q. Shi, M. A. Zudov, L. N. Pfeiffer, K. W. West, J. D. Watson and M. J. Manfra “Resistively detected high-order magnetoplasmons in a high-quality two-dimensional electron gas”, Physical Review B **93**, 165438 (2016)
8. Q. Shi, M. A. Zudov, J. D. Watson, G. C. Gardner and M. J. Manfra, “Evidence for a new symmetry breaking mechanism reorienting quantum Hall nematics”, Physical Review B – Rapid Communications **93**, 121411(R) (2016)
9. Q. Shi, M. A. Zudov, J. D. Watson, G. C. Gardner and M. J. Manfra, “Reorientation of quantum Hall stripes within a partially filled Landau level”, Physical Review B – Rapid Communications **93**, 121404(R) (2016) [editor’s suggestion]

Author Index

Abbamonte, P.....	293	Geballe, Theodore H.....	51
Adams, Philip W.....	211	Hadjipanayis, George.....	256
Analytis, James.....	82	Halperin, William P.....	199
Andrei, Eva Y.....	165	Harrison, Neil.....	187
Ashoori, Raymond.....	25	Hellman, Frances.....	260
Balicas, Luis.....	55	Heremans, Jean J.....	264
Basov, D. N.....	11	Hikita, Y.....	125
Bawendi, Mounqi G.....	158	Hla, Saw Wai.....	177
Beach, Geoffrey.....	73	Hodapp, Theodore.....	268
Bhattacharya, Anand.....	215	Hoffmann, A.....	74
Bird, Jonathan.....	18	Holcomb, Mikel.....	133
Birgeneau, R. J.....	183	Homes, Chris.....	67
Blumberg, Girsh.....	219	Hone, James.....	146
Boatner, L. A.....	329	Hsieh, David.....	99
Bockrath, Marc.....	3	Hughes, Taylor.....	301
Bokor, Jeff.....	260	Hunt, Ben.....	271
Bourret, E.....	183	Hupalo, M.....	41
Broholm, Collin.....	47	Hwang, H. Y.....	125
Budakian, Raffi.....	301	Irvin, Patrick.....	285
Bud'ko, Sergey.....	223	Janotti, Anderson.....	317
Butov, Leonid.....	227	Jiang, J. S.....	74
Canfield, Paul.....	223	Jiang, Zhigang.....	195
Cha, Judy J.....	107	Jin, R.....	239
Cho, Kyuil.....	41	John, V. T.....	239
Christen, H. M.....	121	Johnson, Peter D.....	67
Civale, Leonardo.....	230	Johnston, David.....	223
Cohen, Marvin.....	173	Johnston-Halperin, Ezekiel.....	137
Cooper, S. L.....	293	Kaminski, Adam.....	223
Crommie, Michael.....	173	Kapitulnik, Aharon.....	51
Csathy, Gabor.....	33	Ke, Liqin.....	41
Davidovic, Dragomir.....	235	Ketterson, J. B.....	272
Dean, Cory.....	146	Kevan, Steve.....	260
Dessau, Dan.....	63	Khonsari, M.....	239
DiTusa, J. F.....	239	Kim, Philip.....	7, 364
Doty, Matt.....	91	Kivelson, Steven A.....	51
Drew, H. Dennis.....	248	Kogan, Vladimir.....	223
Engel, Lloyd W.....	252	Kono, Junichiro.....	273
Eom, Chang-Beom.....	129	Koshelev, A. E.....	281
Eres, G.....	121	Krivorotov, Ilya.....	277
Fang, F.....	289	Kumar, R.....	239
Finkelstein, Gleb.....	169	Kwok, W.-K.....	281
Fischer, Peter.....	260	Lanzara, Alessandra.....	173, 183
Fisher, Ian R.....	51	Lau, Chun Ning (Jeanie).....	3
Fradkin, E.....	293	Law, Stephanie.....	91
Furukawa, Yuji.....	223	Lee, D. H.....	183
Gai, Zheng.....	191	Lee, Ho Nyung.....	121

Lee, J.-S.....	125	Rosenbaum, Thomas F.....	78
Lee, Y.....	41	Rouleau, C. M.	121
Levy, Jeremy.....	285	Salahuddin, Sayeef.....	260
Li, Qi.....	103, 289	Sales, B. C.....	329
Louie, Steven.....	173	Samarth, Nitin.....	87
Lüpke, G.....	289	Schiffer, Peter.....	87
MacDougall, G. J.	293	Schneider, G. J.	239
Maiorov, Boris.....	230	Schuller, Ivan K.	333
Mak, Kin Fai.....	145	Sefat, Athena S.....	191
Mandrus, D.....	329	Sellmyer, David J.....	256
Manfra, Michael.....	33	Shayegan, M.....	29
Mao, Z.....	239	Shelton, W. A.....	239
Maple, M. Brian.....	297	Simon, J.....	337
Mason, Nadya.....	301	Skomski, Ralph.....	256
May, A. F.....	329	Smirnov, Dmitry.....	195
McGuire, M. A.....	329	Smith, Arthur R.....	338
Mitchell, John F.....	59	Smith, Kevin E.....	342
Mkhitarian, V.....	41	Sprunger, P. T.....	239
Moler, Kathryn A.....	51	Stewart, G. R.....	346
Moore, J. E.....	183	Strachan, Douglas R.....	349
Musfeldt, Janice L.....	154	Sushkov, Andrei.....	248
Natelson, Douglas.....	115	Tanatar, M. A.....	41, 223
Nesterov, E.....	239	Thomas, John E.....	353
Ni, Ni.....	305	Tringides, M.....	41
Nikolic, Branislav.....	91	Vaknin, D.....	41
Novosad, V.....	74	Valla, Tonica.....	67
Nusran, N. M.....	41	Valls, Oriol T.....	277
Ojeda-Aristizabal, Claudia.....	309	Van Harlingen, D.....	293
Ong, N. Phuan.....	313	Vlasko-Vlasov, V.....	281
Orenstein, Joseph.....	183	Wang, Feng.....	150
Ouyang, Min.....	315	Wang, J.....	41
Paglione, Johnpierre.....	111	Wang, Lin-Wang.....	260
Palmstrøm, Chris J.....	317	Wang, Y. L.....	281
Pan, Wei.....	14	Ward, T. Zac.....	121, 356
Parker, David.....	191	Wells, Barrett O.....	360
Pearson, J. E.....	74	Welp, U.....	281
Phelan, D.....	59	Westervelt, Robert M.....	364
Plummer, E. W.....	239	Xiao, John Q.....	91
Prozorov, Ruslan.....	41, 223	Xiao, Z. L.....	281
Raghu, S.....	125	Yan, J.-Q.....	329
Ralph, Daniel C.....	321	Yang, Fengyuan.....	137
Ramesh, R.....	183	Yin, Y. W.....	289
Ramirez, Arthur P.....	325	Young, D. P.....	239
Rick, S. W.....	239	Zettl, Alex.....	173
Rokhinson, Leonid P.....	37	Zhang, D.....	239
Romero, Aldo.....	133	Zhang, J.....	239

Zheng, H.....59
Zudov, Michael368

Participant List

Name	Organization	Email
Adams, Philip	Louisiana State University	pwadams9@gmail.com
Analytis, James	University of California, Berkeley	analytis@berkeley.edu
Andrei, Eva	Rutgers University	eandrei@physics.rutgers.edu
Ashoori, Raymond	Massachusetts Institute of Technology	ashoori@mit.edu
Balicas, Luis	National High Magnetic Field Laboratory	balicas@magnet.fsu.edu
Basov, Dmitri	Columbia University	db3056@columbia.edu
Bawendi, Moungi	Massachusetts Institute of Technology	mgb@mit.edu
Beach, Geoffrey	Massachusetts Institute of Technology	gbeach@mit.edu
Bery, Joseph	US Department of Energy	joe.berry@nrel.gov
Bhattacharya, Anand	Argonne National Laboratory	anand@anl.gov
Bird, Jonathan	University at Buffalo	jbird@buffalo.edu
Blumberg, Girsh	Rutgers University	girsh@physics.rutgers.edu
Bud'ko, Sergey	AMES Laboratory	budko@ameslab.gov
Butov, Leonid	University of California, San Diego	lvbutov@physics.ucsd.edu
Cha, Judy	Yale University	judy.cha@yale.edu
Chan, Mun	Los Alamos National Laboratory	mkchan@lanl.gov
Civale, Leonardo	Los Alamos National Laboratory	lcivale@lanl.gov
Csathy, Gabor	Purdue University	gcsathy@purdue.edu
Davenport, Jim	US Department of Energy	james.davenport@science.doe.gov
Davidovic, Dragomir	Georgia Institute of Technology	dragomir.davidovic@physics.gatech.edu
Dessau, Dan	University of Colorado	dessau@colorado.edu
Engel, Lloyd	Florida State University	engel@magnet.fsu.edu
Eom, Chang-Beom	University of Wisconsin, Madison	eom@engr.wisc.edu
Finkelstein, Gleb	Duke University	gleb@phy.duke.edu
Fitzsimmons, Tim	US Department of Energy	tim.fitzsimmons@science.doe.gov
Gersten, Bonnie	US Department of Energy	Bonnie.Gersten@science.doe.gov
Graf, Matthias	US Department of Energy	matthias.graf@science.doe.gov
Hadjipanayis, George	University of Delaware	hadji@udel.edu
Halperin, William	Northwestern University	w-halperin@northwestern.edu
Harrison, Neil	Los Alamos National Laboratory	nharrison@lanl.gov
Hellman, Frances	University of California, Berkeley	fhellman@berkeley.edu
Heremans, Jean	Virginia Tech	heremans@vt.edu
Hla, Saw Wai	The Ohio State University	hla@ohio.edu
Hodapp, Theodore	American Physical Society	hodapp@aps.org
Hoffmann, Axel	Argonne National Laboratory	hoffmann@anl.gov
Holcomb, Mikel	West Virginia University	mikel.holcomb@mail.wvu.edu
Hone, James	Columbia University	jh2228@columbia.edu
Horwitz, James	US Department of Energy	james.horwitz@science.doe.gov
Hsieh, David	California Institute of Technology	dhsieh@caltech.edu
Hunt, Benjamin	Carnegie Mellon University	bmhunt@andrew.cmu.edu
Hwang, Harold	SLAC National Accelerator Laboratory	hyhwang@stanford.edu
Janotti, Anderson	University of Delaware	janotti@udel.edu
Jiang, Zhigang	Georgia Institute of Technology	zhigang.jiang@physics.gatech.edu

Johnson, Peter	Brookhaven National Laboratory	pdj@bnl.gov
Kapitulnik, Aharon	Stanford University	aharonk@stanford.edu
Ketterson, John	Northwestern University	j-ketterson@northwestern.edu
Kim, Philip	Harvard University	pkim@physics.harvard.edu
Krivorotov, Ilya	University of California, Irvine	ikrivoro@uci.edu
Kwok, Wai-Kwong	Argonne National Laboratory	wkwok@anl.gov
Lau, Jeanie	The Ohio State University	lau.232@osu.edu
Lee, Honyung	Oak Ridge National Laboratory	hnlee@ornl.gov
Levy, Jeremy	University of Pittsburgh	jlevy@pitt.edu
Li, Qi	Pennsylvania State University	qil1@psu.edu
Luepke, Gunter	The College of William and Mary	luepke@wm.edu
MacDougall, Gregory	University of Illinois	gmacdoug@illinois.edu
Mak, Kin Fai	Pennsylvania State University	kzm11@psu.edu
Manfra, Michael	Purdue University	mmanfra@purdue.edu
Maple, M. Brian	University of California, San Diego	mbmaple@ucsd.edu
Mason, Nadya	University of Illinois, Urbana-Champaign	nadya@illinois.edu
Mitchell, John	Argonne National Laboratory	mitchell@anl.gov
Musfeldt, Janice	University of Tennessee	musfeldt@utk.edu
Natelson, Douglas	Rice University	natelson@rice.edu
Ni, Ni	University of California, Los Angeles	nini@physics.ucla.edu
Noe, Gary Tim	Rice University	as115@rice.edu
Ojeda-Aristizabal, Claudia	California State University, Long Beach	Claudia.Ojeda-Aristizabal@csulb.edu
Ong, Nai Phuan	Princeton University	npo@princeton.edu
Orenstein, Joseph	University of California, Berkeley/LBNL	jworenstein@lbl.gov
Ouyang, Min	University of Maryland	mouyang@umd.edu
Paglione, Johnpierre	University of Maryland	paglione@umd.edu
Palmstrom, Chris	University of California, Santa Barbara	cpalmstrom@ece.ucsb.edu
Pan, Wei	Sandia National Laboratories	wpan@sandia.gov
Pechan, Michael	US Department of Energy	michael.pechan@science.doe.gov
Prozorov, Ruslan	AMES Laboratory	prozorov@ameslab.gov
Ralph, Daniel	Cornell University	dcr14@cornell.edu
Ramirez, Arthur	University of California, Santa Cruz	apr@ucsc.edu
Rhyne, Jim	US Department of Energy	james.rhyne@science.doe.gov
Rokhinson, Leonid	Purdue University	leonid@purdue.edu
Rosenbaum, Thomas	California Institute of Technology	tfr@caltech.edu
Rustad, Jim	US Department of Energy	James.Rustad@science.doe.gov
Sales, Brian	Oak Ridge National Laboratory	salesbc@ornl.gov
Schiffer, Peter	University of Illinois, Urbana-Champaign	chamber1@illinois.edu
Schuller, Ivan	University of California, San Diego	ischuller@ucsd.edu
Schwartz, Andy	US Department of Energy	andrew.schwartz@science.doe.gov
Sefat, Athena	Oak Ridge National Laboratory	sefata@ornl.gov
Shayegan, Mansour	Princeton University	shayegan@princeton.edu
Simon, Jonathan	University of Chicago	simonjon@uchicago.edu
Smirnov, Dmitry	National High Magnetic Field Laboratory	smirnov@magnet.fsu.edu

Smith, Kevin	Boston University	ksmith@bu.edu
Smith, Arthur	The Ohio State University	ohiousmith@gmail.com
Stewart, Greg	University of Florida	stewart@phys.ufl.edu
Strachan, Douglas	University of Kentucky	doug.strachan@uky.edu
Sushkov, Andrei	University of Maryland College Park	sushkov@umd.edu
Thiyagarajan, Pappannan	US Department of Energy	p.thiyagarajan@science.doe.gov
Thomas, John	North Carolina State University	jethoma7@ncsu.edu
Wang, Feng	Lawrence Berkeley National Laboratory	fengwang76@berkeley.edu
Wells, Barrett	University of Connecticut	barrett.wells@uconn.edu
Westervelt, Robert	Harvard University	westervelt@seas.harvard.edu
Xiao, John	University of Delaware	jqx@udel.edu
Yang, Fengyuan	The Ohio State University	yang.1006@osu.edu
Zudov, Michael	University of Minnesota	zudov@physics.umn.edu